UFS 3-220-10
16 January 2026

UNIFIED FACILITIES SUPPLEMENT (UFS)

SOIL MECHANICS (DM 7.1)

APPROVED FOR PUBLIC RELEASE; DISTRIBUTION UNLIMITED

FOREWORD

Unified Facilities Supplements (UFS) provide non-mandatory, supplemental information in support of Unified Facilities Criteria (UFC). Only UFC establish enforceable criteria. UFS are For Information Only (FIO) and exist to help users understand and apply UFC requirements.

The purpose of UFS is to offer procedural guidance, best practices, lessons learned, examples, and explanatory materials that clarify how to meet UFC criteria. They may include step-by-step procedures, checklists, illustrations, or decision aids, but they do not create new requirements or modify UFC content.

UFS are developed by Discipline Working Groups (DWGs) and published by the Military Services under MIL-STD-3007. Because they are not criteria, they do not require Coordinating Panel (CP) or Engineering Senior Executive Panel (ESEP) approval.

UFS content may be referenced or incorporated into project documents at the discretion of project delivery teams but are not binding unless explicitly included in contract requirements. For Service-specific supplemental guidance, refer to Facilities Supplements (FS).

UNIFIED FACILITIES SUPPLEMENT (UFS)

SOIL MECHANICS (DM 7.1)

TABLE OF CONTENTS

INTRODUCTION 1
I-1 REISSUES AND CANCELS. 1
I-2 PURPOSE AND SCOPE. 1
I-3 APPLICABILITY. 1
I-4 GENERAL BUILDING REQUIREMENTS 1
I-5 GLOSSARY. 1
I-6 REFERENCES. 1
CHAPTER 1 IDENTIFICATION AND CLASSIFICATION OF SOIL AND ROCK 3
1-1 INTRODUCTION. 3
1-1.1 Scope. 3
1-2 SOIL DEPOSITS 3
1-2.1 Geologic Origin and Mode of Occurrence. 3
1-3 SOIL VISUAL DESCRIPTION, IDENTIFICATION, AND CLASSIFICATION. 7
1-3.1 Definitions. 7
1-3.2 Visual Description and Identification (ASTM D2488). 8
1-3.3 Unified Soil Classification System (ASTM D2487). 13
1-3.4 Soil Classification for Highways (AASHTO). 17
1-3.5 Other Classification Systems. 18
1-3.6 Common Soil and Rock Names. 20
1-4 ROCK VISUAL DESCRIPTION, AND CLASSIFICATION. 25
1-4.1 Definitions. 25
1-4.2 Visual Classification. 26
1-4.3 Classification by Field and Laboratory Measurements. 31
1-4.4 Rock Mass Classification Systems 32
1-5 SPECIAL MATERIALS 37
1-5.1 Expansive Soils. 37
1-5.2 Collapsing Soils. 41
1-5.3 Frost Susceptibility and Permafrost 43
1-5.4 Limestone and Related Materials. 46
1-5.5 Coral and Coral Formation. 49

1-5.6 Quick Clays. 50
1-5.7 Other Materials and Considerations. 50
1-6 SUGGESTED READING. 54
1-7 NOTATION. 54
CHAPTER 2 FIELD EXPLORATION, TESTING, AND INSTRUMENTATION 56
2-1 INTRODUCTION. 56
2-1.1 Scope. 56
2-1.2 Planning for Field Investigations. 56
2-2 PUBLISHED REFERENCE MATERIALS. 58
2-2.1 Previous Investigations. 58
2-2.2 Published Geologic and Hydrogeologic Maps. 59
2-3 REMOTE SENSING DATA METHODS. 59
2-3.1 Sources. 59
2-3.2 Utilization. 59
2-4 GEOPHYSICAL METHODS. 62
2-4.1 Utilization and Applications. 62
2-4.2 Advantages and Limitations. 63
2-5 SOIL AND ROCK EXPLORATION METHODS. 64
2-5.1 Drilling and Boring Methods. 64
2-5.2 Test Pits and Test Trenches. 70
2-5.3 Other Exploratory Techniques. 70
2-6 SAMPLING. 71
2-6.1 Soil Sampling. 72
2-6.2 Rock Sampling 75
2-6.3 Offshore Sampling. 78
2-6.4 Field Logging and Boring Logs. 78
2-7 PENETRATION RESISTANCE TESTS. 81
2-7.1 Standard Penetration Test (SPT). 81
2-7.2 Cone Penetrometer Tests (CPT). 83
2-7.3 Flat Plate Dilatometer. 86
2-7.4 Dynamic Cone Penetrometer. 89
2-8 GROUNDWATER MEASUREMENTS. 91
2-8.1 Types of Standpipe Piezometer. 91
2-8.2 Multiple or Nested Installations. 94

2-8.3 Measurement of Groundwater Levels. 94
2-8.4 Detection of Combustible Gases....95
2-9 MEASUREMENT OF SOIL AND ROCK PROPERTIES *IN SITU.* 96
2-9.1 Strength and Deformation Properties of Soil. 96
2-9.2 Hydraulic Conductivity of Soil....103
2-9.3 Engineered Fill and Earthworks. 104
2-9.4 Rock Properties. 112
2-10 FIELD INSTRUMENTATION AND MONITORING. 116
2-10.1 Operating Concepts for Geotechnical Monitoring Instruments. 116
2-10.2 Linear Deformation Measurements. 117
2-10.3 Angular Displacement Measurements. 122
2-10.4 Pore Pressure and Water Pressure Measurements. 122
2-10.5 Earth Pressure Measurements. 126
2-10.6 Load Measurements. 126
2-10.7 Temperature Measurements. 126
2-10.8 Vibration Measurements. 127
2-10.9 Field Applications for Instrumentation. 128
2-11 SUGGESTED READING. 130
2-12 NOTATION. 130
CHAPTER 3 LABORATORY TESTING 132
3-1 INTRODUCTION. 132
3-1.1 Scope. 132
3-1.2 Evolution of Laboratory Test Procedures. 132
3-1.3 Laboratory Certification. 133
3-2 LABORATORY TESTS ON SOILS. 134
3-2.1 Sample Selection. 134
3-2.2 Index Property Tests. 137
3-2.3 Compaction Tests. 141
3-2.4 Strength Tests. 143
3-2.5 Dynamic Tests. 159
3-2.6 Compressibility Tests. 162
3-2.7 Hydraulic Conductivity (Permeability) Tests. 168
3-3 LABORATORY TESTS ON ROCK....170
3-3.1 Unconfined Compression Test (ASTM D7012). 171

3-3.2 Split Cylinder Test (ASTM D3967). 171
3-3.3 Rock Direct Shear Test (ASTM D5607). 171
3-3.4 Point Load Test (ASTM D5731). 173
3-4 OTHER SOIL AND ROCK TESTS. 174
3-5 SUGGESTED READING. 175
3-6 NOTATION. 175
CHAPTER 4 DISTRIBUTION OF STRESSES 178
4-1 INTRODUCTION. 178
4-1.1 Scope. 178
4-1.2 State of Stress. 178
4-2 STRESS CONDITIONS AT A POINT 178
4-2.1 Stress Conditions in Soil. 178
4-2.2 Mohr Circle of Stress. 183
4-3 ELASTIC SOLUTIONS FOR STRESSES DUE TO APPLIED LOADS. 183
4-3.1 Use and Applicability 183
4-3.2 Semi-Infinite Elastic Conditions. 183
4-3.3 Layered or Anisotropic Foundations. 193
4-4 SHALLOW PIPES AND CONDUITS. 195
4-4.1 General. 195
4-4.2 Vertical Loads on Rigid Pipe. 195
4-4.3 Vertical Loads on Flexible Pipe. 196
4-4.4 Long Span Metal Culverts. 198
4-5 DEEP UNDERGROUND OPENINGS. 198
4-5.1 General Factors. 198
4-5.2 Openings in Rock. 199
4-5.3 Loads on Underground Openings in Rock. 200
4-5.4 Openings in Soft Ground (Soil). 203
4-5.5 Pressure on Vertical Shafts 208
4-6 NUMERICAL SOLUTIONS FOR STRESSES IN SOIL 211
4-6.1 Numerical Analysis Types. 211
4-6.2 Linear Elastic Stress Analysis. 212
4-6.3 Nonlinear Elastic Stress Analysis. 212
4-6.4 Numerical Modeling Best Practice. 213
4-6.5 Evaluation of Stress Due to Applied Loads. 215

4-6.6 Evaluation of Stress within Embankments and Slopes. 215
4-7 SUGGESTED READING. 216
4-8 NOTATION. 216
CHAPTER 5 ANALYSIS OF SETTLEMENT AND VOLUME EXPANSION 220
5-1 INTRODUCTION. 220
5-1.1 Scope. 220
5-1.2 Occurrence of Settlement. 220
5-1.3 Occurrence of Heave. 221
5-1.4 Applicability. 221
5-2 MECHANICS OF CONSOLIDATION. 222
5-2.1 Consolidation Process. 222
5-2.2 Initial Vertical Stress State. 223
5-2.3 Stress History. 223
5-2.4 Evaluation of Existing Conditions. 225
5-2.5 Change in Vertical Stress. 227
5-3 SETTLEMENT CALCULATIONS. 227
5-3.1 Basic Formulation. 227
5-3.2 Soil Layers in Settlement Calculations. 227
5-4 SETTLEMENT OF COARSE-GRAINED SOILS. 228
5-4.1 Short Term Settlement of Coarse-Grained Soil. 229
5-4.2 Long-Term Settlement of Coarse-Grained Soil. 235
5-5 SETTLEMENT OF FINE-GRAINED SOILS. 236
5-5.1 Immediate Settlement of Fine-Grained Soils. 236
5-5.2 Primary Consolidation Settlement of Fine-Grained Soils. 237
5-5.3 Time Rate of Primary Consolidation. 244
5-5.4 Secondary Compression of Fine-Grained Soils. 254
5-5.5 Organic Soils and Peat. 255
5-6 DIFFERENTIAL AND TOLERABLE SETTLEMENT. 256
5-6.1 Differential Settlement. 256
5-6.2 Tolerable Settlement. 257
5-6.3 Differential Settlement of Mat Foundations. 259
5-7 METHODS OF CONTROLLING SETTLEMENT. 260
5-7.1 Removal or Displacement of Compressible Soils. 260
5-7.2 Balancing Load by Excavation. 262

5-7.3 Preconsolidation by Surcharge. 262
5-7.4 Vertical Drains. 265
5-8 VOLUME EXPANSION. 272
5-8.1 Mechanics of Volume Expansion. 272
5-8.2 Effects of Volume Expansion. 274
5-8.3 Estimates of Heave or Swell Pressure. 274
5-8.4 Design in Expansive Soils. 276
5-8.5 Construction Practices in Expansive Soils. 278
5-9 HYDROCOMPRESSION. 278
5-10 SUGGESTED READING. 279
5-11 NOTATION. 279
CHAPTER 6 SEEPAGE AND DRAINAGE 283
6-1 INTRODUCTION. 283
6-1.1 Scope. 283
6-1.2 Background. 283
6-2 SEEPAGE ANALYSES. 283
6-2.1 Hydraulic Head. 283
6-2.2 Darcy's Law and One-Dimensional Flow 285
6-2.3 Two-Dimensional Seepage. 287
6-2.4 Flow Nets 287
6-2.5 Closed-Form Equations. 291
6-2.6 Numerical Seepage Analysis. 292
6-3 HYDRAULIC CONDUCTIVITY (COEFFICIENT OF PERMEABILTY). 296
6-3.1 Laboratory Testing. 297
6-3.2 Field Testing. 297
6-3.3 Empirical Relationships for Hydraulic Conductivity. 297
6-3.4 Anisotropy 301
6-4 INTERNAL EROSION. 302
6-4.1 Heave. 303
6-4.2 Erosion and Stoping. 304
6-4.3 Internal Instability. 306
6-5 SEEPAGE AND INTERNAL EROSION MITIGATION METHODS. 306
6-5.1 Problems and General Strategies. 306
6-5.2 Seepage Barriers. 308

6-5.3 Filters and Drains....318
6-6 DEWATERING....338
6-6.1 Collection and Sump....338
6-6.2 Wellpoint Systems....338
6-6.3 Extraction Wells....340
6-7 SUGGESTED READING....343
6-8 NOTATION....343
CHAPTER 7 SLOPE STABILITY....346
7-1 INTRODUCTION....346
7-2 TYPES OF SLOPES AND MODES OF FAILURE....346
7-3 DEFINITION OF FACTOR OF SAFETY....349
7-4 METHODS OF ANALYSIS OF SOIL SLOPES....349
7-4.1 Limit Equilibrium Analysis....350
7-4.2 Finite Element Analysis of Slopes....352
7-4.3 Limit Analysis....352
7-5 WATER PRESSURE EFFECTS....355
7-5.1 Incorporating Water Pressures in Computer Analyses....355
7-5.2 Seepage Forces....357
7-6 STRENGTH MODELS AND ANALYSIS CASES....357
7-6.1 End of Construction (Short Term)....358
7-6.2 Cut Slope in Clay....358
7-6.3 Steady State Seepage in Dams....358
7-6.4 Stabilizing Berm for Failed Slope....360
7-6.5 Other Analysis Cases....360
7-6.6 Back-Analysis of Slopes....361
7-6.7 Evaluation of Slope Stability Results....361
7-6.8 Slope Stability Charts....362
7-7 SLOPE STABILIZATION....364
7-8 REQUIRED FACTOR OF SAFETY FOR SOIL SLOPES....365
7-9 MECHANICALLY STABILIZED EARTH SLOPES....366
7-9.1 Applications of MSE....367
7-9.2 Reinforced Slope Materials....368
7-9.3 Geosynthetic Reinforcement Strength....370
7-9.4 Soil-Geosynthetic Interaction....372

7-9.5 Analysis and Design of Reinforced Slopes....373
7-9.6 Required Factor of Safety for MSE Slopes....375
7-10 ROCK SLOPE STABILITY....375
7-10.1 Modes of Rock Slope Failure....376
7-10.2 Mechanics of a Sliding Block....378
7-10.3 Plane Failure....379
7-10.4 Plane Failure Analyses....380
7-10.5 Wedge Failure....381
7-10.6 Toppling Failure....383
7-10.7 Circular Failure....383
7-10.8 Rock Slope Stabilization and Protection....384
7-11 SUGGESTED READING....390
7-12 NOTATION....391
CHAPTER 8 CORRELATIONS FOR SOIL AND ROCK....393
8-1 INTRODUCTION....393
8-2 EFFECTIVE STRESS (DRAINED) SHEAR STRENGTH....394
8-2.1 Coarse-Grained Soils....394
8-2.2 Fine-Grained Soils....406
8-3 UNDRAINED SHEAR STRENGTH....419
8-3.1 Correlations with Index Properties....419
8-3.2 Correlations with Stress History....422
8-3.3 Correlations with Cone Penetration Test....426
8-3.4 Correlations with Standard Penetration Test....427
8-3.5 Correlations with Dilatometer....429
8-4 CONSOLIDATION PARAMETERS....430
8-4.1 Compression and Recompression Indices – Fine-Grained....430
8-4.2 Compression and Recompression Indices – Coarse-Grained....441
8-4.3 Constrained Modulus....442
8-4.4 Coefficient of Secondary Compression....446
8-4.5 Coefficient of Consolidation....448
8-5 ELASTIC PARAMETERS....448
8-5.1 Definitions....448
8-5.2 Undrained Young's Modulus of Fine-Grained Soils....449
8-5.3 Drained Young's Modulus of Coarse-Grained Soils....453

8-6 CALIFORNIA BEARING RATIO (*CBR*).....454
8-6.1 Correlations with Index and Compaction Properties.....454
8-6.2 Correlations with Dynamic Cone Penetration.....456
8-6.3 Correlations with Standard Penetration Test.....457
8-7 HYDRAULIC CONDUCTIVITY.....458
8-7.1 Typical Values.....458
8-7.2 Correlations for Coarse-Grained Soils.....458
8-7.3 Correlations for Fine-Grained Soils.....462
8-8 SHEAR WAVE VELOCITY.....464
8-8.1 Correlations with Standard Penetration Test.....464
8-8.2 Correlations with Cone Penetration Test.....466
8-9 SUGGESTED READING.....468
8-10 NOTATION.....468
APPENDIX A. REFERENCES.....473
APPENDIX B. LIST OF COMPUTER PROGRAMS.....497
APPENDIX C. SYMBOLS USED IN GEOTECHNICAL ENGINEERING.....512
APPENDIX D. GLOSSARY.....528

LIST OF FIGURES

Figure 1-1 Typical Angularity of Bulky Grains (after Sowers 1979)..... 10
Figure 1-2 Plasticity Chart 14
Figure 1-3 Soil Property Variation with Liquid Limit and Plasticity 15
Figure 1-4 Rock Strength Characterization (after Broch and Franklin 1972) 33
Figure 1-5 *GSI* Selection Chart for Jointed Rock (after Marinos et al. 2007)..... 35
Figure 1-6 *GSI* Selection Chart for Heterogeneous Rock (after Marinos et al. 2007) 36
Figure 1-7 Expansive Soils in the United States (Nelson and Miller 1992)..... 38
Figure 1-8 Soil Expansion Prediction (after Holtz et al. 2011) 39
Figure 1-9 Collapsibility Based on *In situ* Dry Density and Liquid Limit (after Holtz et al. 2011) 42
Figure 1-10 Design Charts for Predicting Collapse Behavior of Soils (after Ayadat and Hanna 2007b)..... 42
Figure 1-11 Maximum Depths (in meters) of Frost Penetration in the Continental United States (NOAA 1978) 44
Figure 1-12 Rates of Heave in Laboratory Freezing Tests on Remolded Soils (U.S. Department of the Army 1984) 44
Figure 1-13 Karst and Potential Karst Areas in Soluble Rocks in the Contiguous United States (USGS 2014) 48
Figure 2-1 Schematic of Various Drilling Techniques for Soil and Rock (after NCHRP 2018 and Mayne 2012)..... 67
Figure 2-2 Cross Section of Split Barrel Sampler 73
Figure 2-3 Cross Section of Shelby Tube Sampler with Ball-check Valve Head.. 73
Figure 2-4 Cross Section of a Stationary or Fixed Piston Sampler..... 75
Figure 2-5 Rock Core Samplers (after NCHRP 2018) 77
Figure 2-6 Example Geotechnical Boring Log 80
Figure 2-7 Standard Penetration Test (after NCHRP 2018 and Mayne 2012)..... 82
Figure 2-8 CPT - Example Test Record and Equipment..... 85
Figure 2-9 Nine Zone (Normalized) Soil Behavioral Chart for CPT (after Robertson 2009 and NCHRP 2018)..... 86
Figure 2-10 Flat Plate Dilatometer Test Schematic (after NCHRP 2018 and Mayne 2012) 87

Figure 2-11 Flat Plate Dilatometer and Control Unit (Marchetti et al. 2006) 88
Figure 2-12 Schematic of Dynamic Cone Penetrometer (DCP) Equipment (after Webster et al. 1992) 90
Figure 2-13 Open Piezometers 92
Figure 2-14 Schematic of Pressuremeter Test (after NCHR 2018 and Mayne 2012) 98
Figure 2-15 Typical Result and Characteristic Pressures from Pressuremeter Test (after FHWA 2002) 99
Figure 2-16 Example Result from Self-boring Pressuremeter Test in Clay (after Windle and Wroth 1977) 100
Figure 2-17 Schematic of Vane Shear Test (after Mayne 2012) 102
Figure 2-18 Schematic of Equipment and Process to Perform a Sand Cone Test (after Dunn 2017) 106
Figure 2-19 Schematic of Equipment to Perform Water Balloon Test (after Dunn 2017) 107
Figure 2-20 Schematic of Drive Cylinder (after ASTM D2937) 107
Figure 2-21 Schematic of Nuclear Gauge in Direct Transmission Mode (after NRC 1996) 108
Figure 2-22 Example Plate Load Test Result on Intact Limestone (after NCHRP 2017) 113
Figure 2-23 Double Packer Set-up to Conduct Five-step Lugeon test (after Clayton et al. 1995) 115
Figure 2-24 Electrical Crack Gauge and Reference Pins (after Dunnicliff 1993) . 119
Figure 2-25 Surface Settlement (a) Plate or (b) Platform (after Dunnicliff 1993) . 120
Figure 2-26 Liquid Level System to Continuously Profile Settlements (after Dunnicliff 1993) 121
Figure 2-27 Borehole Extensometer (after Dunnicliff 1993) 121
Figure 2-28 Slope Inclinometers – (a) Manual System, (b) Measurement Principle, and (c) In-Place Inclinometer System (after Dunnicliff 1993) 123
Figure 2-29 Dual-tube Hydraulic Piezometer in Embankment Dam (after Dunnicliff 1993) 124
Figure 2-30 Example of Electrical Diaphragm Piezometer Transducer (after Dunnicliff 1993) 125
Figure 2-31 Estimated Hydrodynamic Lag Time for Various Piezometers and Wells (after Dunnicliff 1993) 125

Figure 3-1 Basic Elements for a Consolidated Drained Direct Shear Test Along with Example Data Collected for One Test Specimen 146
Figure 3-2 Basic Elements of a Consolidated Drained Triaxial Test Along with Example Data Collected for One Test Specimen 147
Figure 3-3 Basic Elements of a Consolidated Undrained Triaxial Test Along with Example Data Collected for One Test Specimen 148
Figure 3-4 Basic Elements of a Ring Shear Test Along with Sample Data 150
Figure 3-5 Undrained Shear Strength Envelopes for Saturated and Partially Saturated Soils 151
Figure 3-6 Example Distribution of Undrained Strength Versus Depth Relationship for a Hypothetical Saturated Clay 152
Figure 3-7 Basic elements of a UU Test Apparatus with Sample Data for a Single Test 154
Figure 3-8 Basic Elements of the Direct Simple Shear Test (ASTM D6528) 156
Figure 3-9 Laboratory Miniature Vane Shear Apparatus 157
Figure 3-10 Fall Cone Apparatus 159
Figure 3-11 Loading Function and Stresses Applied for a Cycle of Loading in a Cyclic Triaxial Test for a Cyclic Stress Ratio of 0.2 161
Figure 3-12 Basic Information Obtained from a Consolidation Test 164
Figure 3-13 Fixed-Ring and Floating-Ring Consolidometers 165
Figure 3-14 Basic Elements of a Constant Rate of Strain Consolidation Test 167
Figure 3-15 Volume Change of Soil as a Function of Stress at Inundation 168
Figure 3-16 Specimen Container for Rock Direct Shear Test (after ASTM D5607) 172
Figure 3-17 Rock Direct Shear Apparatus for High Normal and Shear Loads 173
Figure 3-18 Point Load Apparatus for Rock Index Testing 174
Figure 4-1 Calculation of Vertical Stresses for Hydrostatic Conditions 180
Figure 4-2 Variation in Contact Pressure – a) Rigid Foundation and b) Completely Flexible Foundation 182
Figure 4-3 Mohr Circle Relationships 184
Figure 4-4 Vertical Stress Contours from Strip and Square Loaded Areas – Boussinesq 187
Figure 4-5 Influence Factors for a Rectangular Loaded Area – Boussinesq 188

Figure 4-6 Influence Factors for a Circular Loaded Area – Boussinesq (after Ahlvin and Ulery 1962, Poulos and Davis 1974) 189
Figure 4-7 Influence Factors for Embankment Loading – Boussinesq (after Poulos and Davis 1974) 190
Figure 4-8 Use of Superposition to Determine Change in Vertical Stress 191
Figure 4-9 Stress Distribution Examples..... 192
Figure 4-10 Influence Factors for a Rectangular Loaded Area – Westergaard.... 194
Figure 4-11 Loading Mechanisms for Soft Ground Tunneling 207
Figure 4-12 Radial Stress at the Sides of a Vertical Shaft in Sand (based on Cheng et al. 2007)..... 210
Figure 4-13 Parameters Used in Duncan-Chang Model..... 213
Figure 5-1 Initial Vertical Stresses for a) Hydrostatic and b) Artesian Pore Water Pressure Conditions 223
Figure 5-2 Vertical Stress History Examples..... 224
Figure 5-3 Vertical Stress Profile Cases – Transient 225
Figure 5-4 Example Evaluation of Existing Conditions 227
Figure 5-5 Three Possible Methods to Define Layers for Homogeneous Conditions 228
Figure 5-6 Elastic Influence Factors for $\nu = 0.5$ for (a) μ_1 (after Giroud 1972) and (b) μ_0 (after Burland 1970)..... 230
Figure 5-7 Influence Diagram and Modulus Correlation for Schmertmann CPT Method (Schmertmann 1970, Schmertmann et al. 1978)..... 233
Figure 5-8 Comparison of Settlement Calculation Methods for Coarse-Grained Soils based on SPT Blow Count (after Tan and Duncan 1991)..... 235
Figure 5-9 Creep Factors for Settlement of Coarse-Grained Soils (t_0 = 0.1 year and q_0 in same units as P_a) (after Schmertmann 1970, Terzaghi et al. 1996) 236
Figure 5-10 Correlation of Normalized Undrained Modulus and Overconsolidation Ratio (after Duncan and Buchignani 1987)..... 237
Figure 5-11 Consolidation Behavior based on (a) Void Ratio and (b) Vertical Strain 238
Figure 5-12 Common Compression Index Correlations..... 240
Figure 5-13 Primary Consolidation Example 242
Figure 5-14 Vertical Movements during a Typical Construction Process..... 243

Figure 5-15 Correction Factor for Overconsolidated Clays and Loads of Limited Lateral Extent (after Leonards 1976) 244
Figure 5-16 Degree of Consolidation for Instantaneous Uniform Loading and One-Dimensional Flow 245
Figure 5-17 Degree of Compression and Excess Pore Pressure (Contours Indicate the Time Factor) 246
Figure 5-18 Effect of Load Geometry on Time Rate of Consolidation (after Davis and Poulos 1972) 248
Figure 5-19 Effect of Anisotropy on Time Rate of Consolidation (after Davis and Poulos 1972) 248
Figure 5-20 Degree of Consolidation for Gradual Load Application for Vertical Drainage (after Olson 1977) 249
Figure 5-21 Determination of Coefficient of Consolidation from Laboratory Data (Note: the y-axis can also be plotted as volume or void ratio) 250
Figure 5-22 Determination of c_v from Lab and Field Data 252
Figure 5-23 Multi-layer Consolidation Example 253
Figure 5-24 Calculation of Secondary Compression 255
Figure 5-25 Components of Settlement (after Duncan and Buchignani 1987, Ricceri and Soranzo 1985) 256
Figure 5-26 Allowable Deflection Ratios Related to Structural Proportions (after Burland and Wroth 1974, Wahls 1981) 259
Figure 5-27 Surcharge Load and Consolidation Required to Eliminate Settlement under Final Load 264
Figure 5-28 Surcharge Loading Example 265
Figure 5-29 Vertical Drains – (a) Triangular Pattern, (b) Rectangular Pattern, and (c) Equivalent Cylinder for Theoretical Solutions 266
Figure 5-30 Degree of Radial Consolidation 269
Figure 5-31 Radial Consolidation with Gradual Loading (after Olson 1977) 270
Figure 5-32 Design Chart for Radial Drainage 271
Figure 5-33 Radial Consolidation Example 272
Figure 6-1 Example of the Components of Hydraulic Head 284
Figure 6-2 One-Dimensional Flow through Soil 285
Figure 6-3 Flow Net for Seepage Through an Isotropic Soil Layer Beneath an Impermeable Dam 288

Figure 6-4 Deflection of Flow at a Boundary with Changed Permeability 290
Figure 6-5 Flow Net Example Calculations 292
Figure 6-6 Variation of Hydraulic Conductivity with Soil Type for Various Unit Systems (after Freeze and Cherry 1979) 298
Figure 6-7 Variation of Hydraulic Conductivity with Fines Content (after California Department of Water Resources 2013) 301
Figure 6-8 Heave – (a) Effective Stress and (b) Total Stress 304
Figure 6-9 Erosion and Stoping Mechanisms 306
Figure 6-10 Internal Instability – (a) Suffusion and (b) Suffosion 306
Figure 6-11 Required Depth of Penetration of Cutoff Wall-Supported Excavations in Homogenous Isotropic Sand (after Marsland 1953) 313
Figure 6-12 Corrections to Required Depth of Penetration of Cutoff Wall-Supported Excavations for Stratified Sand (after Marsland 1953) 314
Figure 6-13 Corrections to Required Depth of Penetration of Cutoff Wall-Supported Excavations in Sand Containing Fine-Grained Layers (after Marsland 1953) 315
Figure 6-14 Seepage Blankets and Berms 316
Figure 6-15 Example Base Soil and Filter Gradations 319
Figure 6-16 Example Filter Design 322
Figure 6-17 Subsurface Drain Constructed of Filter Fabric, Drainage Rock, and a Slotted Pipe 323
Figure 6-18 Linear Coefficient of Uniformity (after Giroud 2010) 324
Figure 6-19 Use of Subsurface Interceptor Drains and Blanket Drains for Roadway Drainage 327
Figure 6-20 Subsurface Drain with a Two-Stage Filter and a Slotted Pipe 328
Figure 6-21 Drainage of an Aggregate Base Course (after Barber 1959) 329
Figure 6-22 Retaining Wall Drainage Alternatives 330
Figure 6-23 Seepage into Drainage Trenches Used for Draining Ponded Areas (after Kirkham 1950 and 1960) 331
Figure 6-24 Embankment Fill Subdrains 332
Figure 6-25 Toe, Blanket, and Chimney Drains 334
Figure 6-26 Outlet Filter Collars 335

Figure 6-27 Relief Trench Used to Relieve Pressure from Beneath a Blanket Layer with Low Hydraulic Conductivity (not to scale) 336
Figure 6-28 Relief Well Used to Relieve Pressure from Beneath a Blanket Layer with Low Hydraulic Conductivity (not to scale) 337
Figure 6-29 Typical Relief Well Construction 337
Figure 6-30 Calculation of Relief Well Discharge and Spacing (after USACE 1952) 339
Figure 6-31 Staged Installation of Wellpoints to Lower the Groundwater Table for a Deep Excavation 340
Figure 6-32 Drawdown and Pumping Quantities for Single Extraction Wells and Groups of Extraction Wells (after USACE 1952) 342
Figure 7-1 Failure Conditions for Cross-sections through Natural Slopes 347
Figure 7-2 Failure Conditions in Embankment Foundations and Cut Slopes..... 348
Figure 7-3 Examples of Limit Equilibrium Analysis 351
Figure 7-4 Example Slope Stability Analysis using Bishop's Simplified Method for an Effective Stress Analysis 353
Figure 7-5 Examples of Internal and External Water Pressures in Slope Stability Analyses..... 355
Figure 7-6 Approximate Flow Net for Seepage into a Drain Showing the Difference between the Piezometric Surface and the Phreatic Surface 356
Figure 7-7 Analysis Cases for (a) End of Construction for Embankment on Clay, (b) Cut Slope in Clay, and (c) Levee or Dam in a Condition of Steady State Seepage..... 359
Figure 7-8 Stabilizing Berm Used to Increase the Factor of Safety of a Failed Slope 360
Figure 7-9 Chart Solution for Infinite Slope Analysis (after Duncan et al. 2014) 363
Figure 7-10 Methods of Stabilizing Slopes 364
Figure 7-11 Typical Cross-Section of an MSE Slope..... 367
Figure 7-12 Difference in Usable Land for Walls and Slopes 368
Figure 7-13 Rock Discontinuity Conditions (after FHWA 1998)..... 376
Figure 7-14 Weathering and Weak Rock Conditions (after FHWA 1998)..... 377
Figure 7-15 Rock Slope with Sliding Block 378
Figure 7-16 Definition of Sloped Surface Orientation Terms 379

Figure 7-17 Geometry for Plane Failure (after Hoek and Bray 1981) 380
Figure 7-18 Rock Slopes with Tension Cracks (after Hoek and Bray 1981) 381
Figure 7-19 Rock Slope with Sliding Wedge (after Hoek and Bray 1981) 382
Figure 7-20 View of Wedge Geometry (after Hoek and Bray 1981) 383
Figure 7-21 Rock Slope Subject to Toppling Failure 384
Figure 7-22 Rock Slope Stabilization and Protection Measures (after FHWA 1998) 385
Figure 8-1 Approximate Relationship between the Effective Stress Friction Angle and Dry Unit Weight for Various Relative Densities and Types of Soil 395
Figure 8-2 Relationship between Effective Stress Friction Angle of Coarse-Grained Soils and SPT N_{60} Value 397
Figure 8-3 Relationship between Peak Effective Stress Friction Angle, Overburden Pressure, and SPT Blow Count for Sands (top) after Parry (1977) and (bottom) after DeMello (1971) and Schmertmann (1975) 398
Figure 8-4 Variation of Effective Stress Friction Angle with $N_{1,60}$ (after Peck at al. 1974, and Hatanaka and Uchida 1996) 399
Figure 8-5 Relationship between Effective Stress Friction Angle and Cone Tip Resistance (after Kerisel 1961, Kahl et al. 1968, Melzer 1968, Muhs and Weiss 1971, and Meyerhof 1976) 401
Figure 8-6 Estimation of ϕ' from a Cone Resistance Profile (after Duncan et al. 1989) 401
Figure 8-7 Relationship between Bearing Capacity Number N_q and Peak Effective Stress Friction Angle from Large Calibration Tests (after Duncan et al. 1989) 402
Figure 8-8 Variation of Peak Effective Stress Friction Angle with σ'_v and Cone Resistance for Normally Consolidated, Uncemented, Quartz Sands (after Robertson and Campanella 1983) 403
Figure 8-9 Estimation of Relative Density for Normally Consolidated Sands from Cone Penetration Resistance (after Schmertmann 1978) 404
Figure 8-10 Relationship between Friction Angle and Relative Density based on Triaxial Compression Tests on North Sea Sands (after Schmertmann 1975, and Lunne and Kleven 1982) 405

Figure 8-11 Correction for Effects of Overconsolidation on Cone Penetration Tip Resistance in Sand (after Lunne and Christoffersen 1985, and Duncan et al. 1989) 405

Figure 8-12 Range of Effective Stress Friction Angle for Clean Sands based on the Horizontal Stress Index from the Dilatometer Test (after Marchetti 1997, and Ricceri et al. 2002) 407

Figure 8-13 Relationship between the Effective Stress Friction Angle of Fine-Grained Soil and Plasticity Index (after Gibson 1953, Carter and Bentley 2016) 408

Figure 8-14 Correlation between ϕ'_{FS} and *PI* based on Triaxial Tests on NC Clays (after Kenney 1959, Bjerrum and Simons 1960, Ladd et al. 1977) ... 408

Figure 8-15 Relationship between ϕ'_{FS} and PI (after Terzaghi et al. 1996) 409

Figure 8-16 Variation of the Fully Softened Friction Angle with Plasticity Index (after Tiwari and Ajmera 2011) 410

Figure 8-17 Fully Softened Friction Angle based on Mineral Composition (after Tiwari and Ajmera 2011) 410

Figure 8-18 Correlation between Power Function Parameters a_{FS} and b_{FS} and Plasticity Index (after Castellanos et al. 2021) 412

Figure 8-19 Correlation between Power Function Parameters a_{FS} and b_{FS} and $CF \times PI$ (after Castellanos et al. 2021) 412

Figure 8-20 Correlation between the Residual Friction Angle and Clay-sized Fraction (after Skempton 1964, 1985) 414

Figure 8-21 Residual Friction Angle vs. Plasticity Index – (top) Data Collected by Voight (1973), and (bottom) Measurements by Bovis (1985) 415

Figure 8-22 Drained Residual Secant Friction Angle as a Function of LL and CF (after Stark and Hussain 2013) 416

Figure 8-23 Residual Shear Strength Power Function Parameters Related to Plasticity Index (after Castellanos et al. 2021) 418

Figure 8-24 Residual Shear Strength Power Function Parameters Related to Plasticity Index and Clay Fraction (after Castellanos et al. 2021) 418

Figure 8-25 Relation between Liquidity Index and Undrained Shear Strength of Remolded Clays (after Skempton and Northey 1952) 419

Figure 8-26 Relationship between Remolded Undrained Shear Strength and Liquidity Index (after Terzaghi et al. 1996) 420

Figure 8-27 Correlation between Undrained Strength Ratio and Plasticity Index – Field Vane (after Robertson and Campanella 1984) 421

Figure 8-28 Correlation between Undrained Strength Ratio and Plasticity Index – Laboratory Testing (after Ladd and DeGroot 2004) 421

Figure 8-29 Variation of the Undrained Strength Ratio with Liquid Limit (after Larson 1980) 422

Figure 8-30 Normalized Undrained Strength Ratio vs. OCR (after Schmertmann 1978) 424

Figure 8-31 Correlation between Undrained Shear Strength, SPT N Value, and Plasticity Index for Overconsolidated Clays (after Stroud and Butler 1975) 428

Figure 8-32 Relationship between Undrained Shear Strength and SPT N (after Terzaghi and Peck 1967, Hara et al. 1974, and Sowers 1979) 429

Figure 8-33 Range of Compression Index based on Liquid Limit Predicted by Correlations 435

Figure 8-34 Range of Compression Index based on Initial Void Ratio Predicted by Correlations 435

Figure 8-35 Range of Compression Index based on Natural Water Content Predicted by Correlations 436

Figure 8-36 Correlations for Recompression Index based on Liquid Limit 436

Figure 8-37 Range of Recompression Index based on Initial Void Ratio Predicted by Correlations 437

Figure 8-38 Range of Recompression Index based on Natural Water Content Predicted by Correlations 437

Figure 8-39 Sensitivity (S_t), *In situ* Void Ratio, and Compression Index Relationship (after Leroueil et al. 1983) 438

Figure 8-40 Correlation between Modified Compression Index and Water Content (after Lambe and Whitman 1969) 438

Figure 8-41 Sedimentation and Intrinsic Compression Lines (after Burland 1990) 440

Figure 8-42 Example NC Compression Curves based on a) Intrinsic Compression Line and b) Sedimentation Compression Line 440

Figure 8-43 Relationship between Modulus Number and Void Ratio for NC Soils (after Janbu 1963) 443

Figure 8-44 Modulus Number for NC Clays (after Janbu 1985) 443

Figure 8-45 Modulus Number for NC Silts and Sands (after Janbu 1985) 444

Figure 8-46 Variation of Empirical Coefficient f used for Calculating Constrained Modulus with PI (after Stroud 1974) 444

Figure 8-47 Correlation between Normalized Constrained Modulus and Normalized q_t from CPTu for Clays (after Kulhawy and Mayne 1990) 445

Figure 8-48 Correlation between Modified Secondary Compression Index and Natural Water Content for Normally Consolidated Clays (after Mesri 1973, Holtz and Kovacs 1981) 446

Figure 8-49 Secondary Compression Index for Silts and Clays 447

Figure 8-50 Approximate Relationship between Coefficient of Consolidation and Liquid Limit 448

Figure 8-51 Correlation of Undrained Modulus Normalized by Undrained Shear Strength to Overconsolidation Ratio (after Duncan and Buchignani 1987) 450

Figure 8-52 Correlation between PMT Modulus for Clays and SPT N (after Ohya et al. 1982) 451

Figure 8-53 Undrained Modulus for Deep Foundations in Compression (after Poulos and Davis 1980) 452

Figure 8-54 Undrained Modulus for (left) Drilled Shafts in Compression and Uplift and (right) Spread Foundations in Uplift (after Callanan and Kulhawy 1985) 452

Figure 8-55 Correlations for Drained Young's Modulus of Granular Soils 454

Figure 8-56 Range of CBR based on DCP Predicted by Correlations 457

Figure 8-57 Correlation for CBR in Terms of SPT N Value (Livneh 1989) 458

Figure 8-58 Horizontal Hydraulic Conductivity based on D_{10} (after USACE 1993) 459

Figure 8-59 Hydraulic Conductivity based on D_5 (after Kenney et al. 1984) 460

Figure 8-60 Hydraulic Conductivity of Sands and Sand-Gravel Mixtures as a Function of D_5, D_{10}, C_u, and e 461

Figure 8-61 Range of Shear Wave Velocities based on SPT N Value Predicted by Correlations 464

LIST OF TABLES

Table 1-1 Principal Soil Deposits in Terms of Origin 4
Table 1-2 Principal Soil Deposits by Mode of Occurrence 5
Table 1-3 Classification of Fine-grained Soils 12
Table 1-4 Other Soil Classification Systems 18
Table 1-5 AASHTO Soil Classification System 19
Table 1-6 Simplified Rock Classification - Common Igneous Rocks 26
Table 1-7 Simplified Rock Classification - Common Metamorphic Rocks 27
Table 1-8 Simplified Rock Classification – Common Sedimentary Rocks 27
Table 1-9 Rock Color Descriptors (Geological Society of London 1977) 28
Table 1-10 Grain-Size Descriptors for Rock 28
Table 1-11 Criteria for Defining Rock Grain Size (after FHWA 2017) 29
Table 1-12 Weathering Classification 29
Table 1-13 Discontinuity Spacing 30
Table 1-14 Hardness Classification of Intact Rock (Hough 1969) 30
Table 1-15 Criteria and Descriptions for Relative Rock Strength (after FHWA 2017) 31
Table 1-16 Engineering Classification for *In situ* Rock Quality (Merritt and Coon 1970) 31
Table 1-17 Other Rock Classification Systems 34
Table 1-18 Swelling Potential (Dakshanamurthy and Raman 1973) 38
Table 1-19 Expansion Potential from Classification Test Data (Holtz et al. 2011) 38
Table 1-20 Classification of Potential Expansion of Soils using EI (ASTM D4829) 40
Table 1-21 U.S. Army Corps of Engineers Frost Design Soil Classification 45
Table 1-22 Selection of Geophysical Method (after ASTM D6429) 49
Table 1-23 Corrosive Soil Environments (FHWA 2009) 51
Table 2-1 Items that can be Evaluated During Field Reconnaissance (NCHRP 2018 and FHWA 2002) 57
Table 2-2 Sources of Readily Available Subsurface Information (after NCHRP 2018, FHWA 2002, and FHWA 2016) 60
Table 2-3 Historic Remote Sensing Data Sources 61

Table 2-4 Current Remote Sensing Data Sources 62

Table 2-5 Surface Geophysical Methods and Investigation Objectives (after NCHRP 2018, Fenning and Hasan 1995, USACE 1995a, Sirles 2006, FHWA 2006, and Anderson et al. 2008)..... 63

Table 2-6 Methods of Advancing an Exploration Hole in Soil (NCHRP 2018 and Day 1999)..... 65

Table 2-7 Rock Core Drilling Methods (NCHRP 2018 and Day 1999)..... 66

Table 2-8 Soil and Rock Investigation Equipment and Their Applications (NCHRP 2018 and Australian Drilling Industry Training Committee 2015)..... 67

Table 2-9 Selecting Number, Locations, and Depths of Investigation (after NCHRP 2018, FHWA 2002, FHWA 2016, NYDOT 2013, and SCDOT 2010) 68

Table 2-10 Use and Limitations of Test Pits and Test Trenches (after NCHRP 2018) 71

Table 2-11 Samplers to Collect Disturbed Soil Samples 72

Table 2-12 Samplers Used to Collect Intact Soil Samples 74

Table 2-13 Standard Size of Rock Casing, Drill Rods, Core Barrels, and Coreholes (after ASTM D2113) 76

Table 2-14 Common Samplers for Rock Cores (after NCHRP 2018)..... 76

Table 2-15 Common Underwater Samplers (after NCHRP 2018) 79

Table 2-16 Factors Affecting the Standard Penetration Test and SPT results (after Kulhawy and Mayne 1990)..... 83

Table 2-17 Types of Standpipe Piezometers..... 93

Table 2-18 *In situ* Testing Methods Used in Soil for Strength and Deformation (after FHWA 2002) 97

Table 2-19 Summary of *In situ* Test Procedures for Measuring Hydraulic Conductivity of Soil Deposits 104

Table 2-20 Comparison of Non-nuclear Technologies for Assessing Soil Density (Berney et al. 2013, 2016)..... 109

Table 2-21 Gravimetric Testing Methods for Moisture Content (after Berney et al. 2013) 110

Table 2-22 Indirect Testing Methods to Assess As-compacted Moisture Content (after Berney et al. 2012)..... 111

Table 2-23 Bias, Accuracy, and Precision of Test Methods for the As-Compacted Measurement of Moisture Content (after Berney et al. 2012, 2013). 111

Table 2-24 Interpretation of Lugeon Test Results (after Tunbridge 2017) 115
Table 2-25 Types of Geotechnical Monitoring Instruments 117
Table 2-26 Methods of Determining Linear Deformation 118
Table 2-27 Angular Displacement Instruments 122
Table 2-28 Piezometer Types 124
Table 2-29 Instruments for Measuring Load 127
Table 2-30 Example Questions for Instrumentation Decisions 129
Table 3-1 Amount of Soil Needed for Common ASTM Tests 134
Table 3-2 Summary of Phase Relationship Calculations 139
Table 3-3 Index Property Tests and Engineering Parameters Obtained 140
Table 3-4 Laboratory Strength Tests with ASTM Standards 144
Table 3-5 Dynamic Tests for Soils 159
Table 3-6 Tests for Volume Change with ASTM Standards 163
Table 3-7 Potential Expansion for EI Values 168
Table 3-8 Laboratory Rock Strength Tests with ASTM Standards 170
Table 4-1 Lateral Earth Pressure Coefficients 181
Table 4-2 Equations for the Calculation of Change in Vertical Stress Below Various Loading Conditions 185
Table 4-3 Recommended Values for Trench Load Coefficient (after Moser 1990) 195
Table 4-4 Impact Factors for Live Loading of Buried Pipe (from American Lifelines Alliance 2001) 196
Table 4-5 Live Load Pressures from Various Vehicle Loading (after American Lifelines Alliance 2001) 197
Table 4-6 Approximate Overburden Rock Load Carried by Roof Support 201
Table 4-7 Approximate Relationship Between Rock Quality Indices (after Deere et al. 1970, Barton et al. 1974, Bieniawski 1990, Hemphill 2012) 202
Table 4-8 Types of Ground Behavior 204
Table 4-9 Ground Behavior for Clayey Fine-Grained Soils and Silty Sand (after FHWA 2009) 205
Table 4-10 Ground Behavior for Coarse-Grained Soils (after FHWA 2009) 205
Table 4-11 Simplified Tunnel Support Loads based on Ground Behavior (FHWA 2009) 208

Table 4-12 Soft Ground Tunnel Support Loads for $H > 1.5 \cdot (B+H_t)$ 209
Table 4-13 Summary of Model Parameters for Duncan-Chang Model 213
Table 5-1 Settlement Calculation Methods for Different Soil Types (after Coduto et al. 2011, Salgado 2008) 221
Table 5-2 Approximate Modulus Values for Coarse-Grained Soil (after Bowles 1996, Duncan and Mokwa 2001) 231
Table 5-3 Estimates of E_s based on SPT N_{60} values. 232
Table 5-4 Empirical Equations for Settlement of Coarse-Grained Soils 234
Table 5-5 Correlations for Compression Indices 240
Table 5-6 Typical Values of C_α / C_c (after Terzaghi et al. 1996) 254
Table 5-7 Angular Distortion Limits for Various Structures (after Skempton and MacDonald 1956, Polshin and Tokar 1957, Duncan and Buchignani 1987, and Day 1990) 257
Table 5-8 Relative Mat Stiffness and Behavior (after Brown 1969, Frazer and Wardle 1976) 260
Table 5-9 Methods to Reduce, Accelerate, or Prevent Excess Settlement (after FHWA 2017) 261
Table 5-10 Empirical Correlations to 1D Heave and Swell Pressure and Required Input Parameters (after Rao et al. 2011, Vanapalli and Lu 2012) 275
Table 5-11 Foundation Design Approaches in Expansive Soil (after Bowles 1996) 277
Table 6-1 Common Finite Element Analysis Boundary Conditions 294
Table 6-2 Examples of Boundary Condition Usage 295
Table 6-3 Typical Ranges of Horizontal Hydraulic Conductivity for Natural Soil and Unfractured Rock Deposits (after USBR 2014) 298
Table 6-4 Typical Range of Vertical Hydraulic Conductivity for Compacted Soil in Embankments (after USBR 2014) 298
Table 6-5 Estimating Hydraulic Conductivity based on Effective Grain Size 299
Table 6-6 Typical Values of Anisotropy in Natural Soils (after USBR 2014) 302
Table 6-7 Typical Values of Anisotropy in Engineered Fill (after USBR 2014) 302
Table 6-8 Seepage Severity Categories (after Duncan et al. 2011, USACE 1956) 307
Table 6-9 Construction Methods for Vertical Seepage Barriers (Cutoff Walls) 309

Table 6-10 Backfill Material Description and Characteristics for Vertical Seepage Barriers (Cutoff Walls) 311
Table 6-11 Base Soil Categories for Mineral Filter Design (after FEMA 2011)... 320
Table 6-12 Restraint Criteria for Mineral Filter Design (after FEMA 2011) 320
Table 6-13 Flow Criteria for Mineral Filter Design (after FEMA 2011)..... 321
Table 6-14 Segregation Criteria for Mineral Filter Design (after FEMA 2011) 321
Table 6-15 Geotextile Opening Size Criteria for Soils with Less than 10% Fines (after Luettich et al. 1992)..... 325
Table 7-1 Strength Models for Different Soil Types and Drainage Conditions.. 350
Table 7-2 Factors of Safety for New Earth and Rockfill Dams (USACE 2003) . 365
Table 7-3 Factor of Safety for Dams using Spencer's Method for Dams (USBR 2011) 365
Table 7-4 Recommendations for Reinforced Fill Soil in MSE Slopes Based on Geometry..... 368
Table 7-5 Summary of Applications and Materials for Reinforced Soil Slopes . 369
Table 7-6 Methods of Incorporating Geosynthetic Reinforcement Strength in Factor of Safety Equation 373
Table 7-7 Steps for Designing an MSE Slope 374
Table 7-8 Recommended Limits of Electrochemical Properties for Reinforced Fill with Steel Reinforcement (after FHWA 2009b)..... 387
Table 8-1 Typical Values of the Effective Stress Friction Angle for Coarse-grained Soils (Carter and Bentley 2016)..... 394
Table 8-2 Typical Values of the Effective Stress Friction Angle for Compacted Coarse-grained Soils (Carter and Bentley 2016)..... 394
Table 8-3 Relationship between SPT N Value, Relative Density and Effective Stress Friction Angle (Meyerhof 1956) 396
Table 8-4 Relationship between SPT N Value, Relative Density, and Angle of Internal Resistance (after Mitchell 1981) 396
Table 8-5 Relationship between Relative Density, Cone Tip Resistance, and Effective Stress Friction Angle (after Bergdahl et al. 1993, and Ameratunga et al. 2016) 400
Table 8-6 Coefficients for Stark and Hussain (2013) Residual Friction Angle Correlation 417
Table 8-7 Typical Normally Consolidated Undrained Strength Ratios 423

Table 8-8 Approximate Relation of Undrained Strength Ratio and OCR (after Schmertmann 1978) 423
Table 8-9 Typical Values of m 425
Table 8-10 Approximate Undrained Shear Strength for Cohesive Soils Based on SPT N 428
Table 8-11 Undrained Shear Strength Correlations to Dilatometer 429
Table 8-12 Typical Values for C_c for Undisturbed Clays 430
Table 8-13 Compression Index Correlations 431
Table 8-14 Recompression Index Correlations 434
Table 8-15 Modified Compression Indices for Saturated, Normally Consolidated Sands (after Burmister 1962, Coduto et al. 2011) 441
Table 8-16 Compressibility Data for Six Sands (Been et al. 1987) 441
Table 8-17 Typical Values of C_α / C_c for Natural Soils (after Mesri and Godlewski 1977) 447
Table 8-18 Relationships between Common Elastic Parameters 449
Table 8-19 Typical Range of Undrained Young's Modulus for Clays 450
Table 8-20 Typical Ranges of Drained Young's Modulus for Coarse-Grained Soils 453
Table 8-21 Correlations for Drained Young's Modulus of Coarse-Grained Soils using SPT N Values 453
Table 8-22 CBR Correlations with Grain Size, Atterberg Limits, and Unit Weight 455
Table 8-23 CBR Correlations to Index and Compaction Properties (after Singh et al. 2011) 455
Table 8-24 CBR Correlations with DCP 456
Table 8-25 Typical Ranges of Hydraulic Conductivity based on Soil Type (after Terzaghi et al. 1996) 459
Table 8-26 Shear Wave Velocity Correlated to SPT N Value and Depth 465
Table 8-27 Shear Wave Velocity Correlated to SPT N Value 465
Table 8-28 Correlations for Shear Wave Velocity with CPT results 467

INTRODUCTION

I-1 REISSUES AND CANCELS.

This UFS supersedes UFC 3-220-10 dated 1 February, 2022, and all subsequent changes.

I-2 PURPOSE AND SCOPE.

This UFS provides technical guidance on contemporary soil mechanics principles and the practice of geotechnical engineering used in planning, design, construction, evaluation and maintenance of Government facilities for the Department of Defense (DoD). Where other criteria, contractual, statutory or regulatory requirements are referenced, the more stringent requirement must be met.

I-3 APPLICABILITY.

This UFS follows the same applicability as UFC 1-200-01, paragraph 1-3, as it pertains to soil mechanics and the practice of geotechnical engineering.

I-4 GENERAL BUILDING REQUIREMENTS.

Comply with UFC 1-200-01, *DoD Building Code*. UFC 1-200-01 provides applicability of model building codes and government unique criteria for typical design disciplines and building systems, as well as for accessibility, antiterrorism, security, high performance and sustainability requirements, and safety. Use this UFS in addition to UFC 1-200-01 and the UFCs and government criteria referenced therein.

I-5 GLOSSARY.

APPENDIX C contains a list of symbols used in geotechnical engineering. APPENDIX D contains definitions of terms.

I-6 REFERENCES.

APPENDIX A contains a list of references used in this document.

This Page Intentionally Left Blank

CHAPTER 1 IDENTIFICATION AND CLASSIFICATION OF SOIL AND ROCK

1-1 INTRODUCTION.

1-1.1 Scope.

This chapter presents criteria for *soil* and *rock* identification and classification based on internationally accepted standards as well as information on their physical engineering properties. Common soils and rocks are discussed as well as special materials, such as expansive and collapsing soils, permafrost, limestone and related materials, coral and coral formations, quick clays, and other materials (i.e., man-made fills, chemically reactive and lateritic soils, calcareous sands, and submarine soils).

1-2 SOIL DEPOSITS.

1-2.1 Geologic Origin and Mode of Occurrence.

Soils are masses of solid particles along with the materials within the voids between the particles. The solid particles typically are a mixture of sediments or other accumulated, unconsolidated[1] material produced by the chemical and physical disintegration of rocks. Soils can contain organic materials. From a geologic standpoint, soils can be classified in terms of origin (e.g., transported, *pyroclastic*, *residual*, and *organic*), and mode of occurrence (e.g., *aeolian*, *alluvial*, *colluvial*, *glacial*, and *marine*). A geologic description can assist in correlating experiences between several sites, and in a general sense, can indicate the pattern of strata to be expected prior to making a field investigation (test borings, etc.).

Soils with similar origin and mode of occurrence are expected to have comparable, if not similar, engineering properties. For quantitative foundation analysis, a geological description is inadequate and a more specific classification and testing is required. A study of references on local geology should precede a major subsurface exploration program as this will help with planning the exploration and also with identifying possible challenges for the project. Also, information on known projects near the site should be obtained, if available, to give specific details about the soils and conditions that will likely be encountered. Table 1-1 describes the principal soil deposits grouped in terms of origin, and Table 1-2 describes the principal soil deposits by mode of occurrence.

[1] In this context, unconsolidated means that the particles have not lithified into rock. It does not imply a particular state of consolidation as described in Chapter 5.

Table 1-1 Principal Soil Deposits in Terms of Origin

Major Division	Principal Soil Deposits	Pertinent Engineering Characteristics
Organic: Accumulation of highly organic material formed in place by the growth and subsequent decay of plant life	*Peats*: Somewhat fibrous aggregate of decayed and decaying vegetation matter having a dark color and odor of decay	Very compressible; entirely unsuitable for supporting building foundations
	Mucks: Peat deposits which have advanced in stage of decomposition to such extent that the botanical character is no longer evident	
Pyroclastic: Material ejected from volcanoes and transported by gravity, wind and air	*Ejecta*: Loose deposits of volcanic ash, lapilli, bombs, etc.	Typically, shard-like particles of *silt* size with larger volcanic debris; weathering and redeposition produce high plasticity, compressible *clay*; unusual and difficult foundation conditions
	Pumice: Highly porous volcanic rock that is frequently associated with lava flows and mud flows, or may be mixed with nonvolcanic sediments	
Residual: Material formed by disintegration of underlying parent rock or partially indurated material	Residual sands and fragments of gravel-sized material formed by dissolution and leaching of cementing material, leaving behind the more resistant particles, commonly quartz	Generally favorable foundation conditions
	Residual clays formed by the decomposition of silicate rocks, disintegration of shales, and solution of carbonates in limestone; with few exceptions, becomes more compact, rockier and less weathered with increasing depth; at intermediate stage may reflect composition, structure and stratification of parent rock	Variable properties requiring detailed investigation; deposits present favorable foundation conditions except in humid and tropical climates, where depth and rate of weathering are very great
	Transported soils: See Table 1-2	

Table 1-2 Principal Soil Deposits by Mode of Occurrence

Major Division	Principal Soil Deposits	Pertinent Engineering Characteristics
Aeolian: Material transported and deposited by wind.	*Loess*: A calcareous unstratified deposit of silts or sandy or clayey silt traversed by a network of tubes formed by root fibers now decayed	Relatively uniform deposits characterized by ability to stand in vertical cuts; collapsible structure; deep weathering or saturation can modify characteristics
	Dune sands: Mounds, ridges, and hills of uniform fine sand characteristically exhibiting rounded grains	Very uniform grain size; may exist in relatively loose condition
Alluvial: Materials transported and deposited by running water.	*Floodplain:* Low-lying stream or river deposits that are subject to inundation by floodwaters	
	Point bar: Alternating deposits of arcuate ridges and swales (lows) formed on the inside or convex bank of mitigating river bends; ridge deposits consist primarily of silt and sand, swales are clay filled	Generally favorable foundation conditions; however, detailed investigations are necessary to locate discontinuities; flow slides may be a problem along riverbanks; soils are quite pervious
	Channel fill: Deposits laid down in abandoned meander loops isolated when rivers shorten their courses; composed primarily of clay; however, silty and sandy soils are found at the upstream and downstream ends	Fine-grained soils are usually compressible; portions may be very heterogeneous; silty soils generally present favorable foundation conditions
	Backswamp: The prolonged accumulation of floodwater sediments in flood basins bordering a river; materials are generally clays but tend to become siltier near riverbank	Relatively uniform in a horizontal direction; clays are usually subjected to seasonal volume changes
	Terrace: Relatively narrow, flat-surfaced, river-flanking remnants of floodplain deposits formed by entrenchment of rivers and associated processes	Usually drained and oxidized; generally favorable foundation conditions
	Estuarine: Mixed deposits of marine and alluvial origin laid down in widened channels at mouths of rivers and influenced by tide of body of water into which they are deposited	Generally fine grained and compressible; many local variations in soil conditions
	Lacustrine: Material deposited within lakes (other than those associated with glaciation) by waves, currents, and organo-chemical processes; deposits consist of unstratified organic clay or clay in central portions of the lake and typically grade to *stratified* silts and sands in peripheral zones	Usually very uniform in horizontal direction; fine-grained soils generally compressible
	Deltaic: Deposits formed at the mouths of rivers, which result in extension of the shoreline	Generally fine-grained and compressible; many local variations in soil condition
	Piedmont: Alluvial deposits at foot of hills or mountains; extensive plains or alluvial fans	Generally favorable foundation conditions

Table 1-2 (cont.) Principal Soil Deposits by Mode of Occurrence

Major Division	Principal Soil Deposits	Pertinent Engineering Characteristics
Colluvial: Material transported and deposited by gravity	*Talus*: Deposits created by gradual accumulation of unsorted rock fragments and debris at base of cliffs	Previous movement indicates possible future difficulties; generally unstable foundation conditions
	Hillwash: Fine colluvium consisting of clayey sand, sand silt, or clay	
	Landslide deposits: Considerable masses of soil or rock that have slipped down, more or less as units, from their former position on steep slopes	
Glacial: Material transported and deposited by glaciers, or by meltwater from the glacier.	*Glacial till*: An accumulation of debris, deposited beneath, at the side (lateral moraines), or at the lower limit of a glacier (terminal moraine); material lowered to ground surface in an irregular sheet by a melting glacier is known as a ground moraine.	Consists of material from *boulder* and *gravel* to clay; deposits are unstratified; present generally favorable foundation conditions but rapid changes in conditions are common.
	Glacio-fluvial deposits: Coarse and fine-grained material deposited by streams of meltwater from glaciers; material deposited on ground surface beyond terminal edge of a glacier is known as an outwash plain; gravel ridges known as kames and eskers; depressions known as kettles can be filled with peat	Many local variations; generally present favorable foundation conditions
	Glacio-lacustrine deposits: Material deposited within lakes by meltwater from glaciers; consisting of clay in central portions of lake and alternate layers of silty clay or silt and clay (varved clay) in peripheral zones	Very uniform in the horizontal direction
Marine: Material transported and deposited by ocean waves and currents in shores and offshore areas.	*Shore deposits*: Deposits of sands and/or gravels formed by the transporting, destructive, and sorting action of waves on the shoreline	Relatively uniform and of moderate to high density
	Marine clays: Organic and inorganic deposits of fine-grained material	Generally, very uniform, compressible and usually very sensitive to remolding

1-3 SOIL VISUAL DESCRIPTION, IDENTIFICATION, AND CLASSIFICATION.

Standardized procedures for visual description, identification, and formal classification of a soil specimen are presented in this section. These procedures follow the corresponding ASTM standard available for this purpose. Visual description entails describing the characteristics of the soil that can be perceived with the senses (e.g. vision, touch, and smell). The identification of the soil refers to knowing the soil type without having to use specialized equipment to do so. The visual description and identification of soils are normally done in the field and the procedures are based on ASTM D2488. The classification of the soils involves using specialized equipment and tests to classify the soil using a standard classification system.

1-3.1 Definitions.

The definitions used in this chapter agree with the Unified Soil Classification system presented in ASTM D2487.

Boulders: Rock particles will not pass a 12-inch square opening.

Clay: Soil particles passing a No. 200 (75-µm) sieve that exhibit plasticity (putty-like properties) within a range of water contents, and considerable strength when air dried. For classification of clayey soils, refer to Section 1-3.3.

Coarse-grained soils: Soils that contain 50% or more particles retained on a No. 200 (75 µm) sieve.

Cobbles: Rock particles that pass through a 12-inch square opening sieve but are retained on a 3-inch square opening sieve.

Fine-grained soils: Soils that contain 50% or more particles passing a No. 200 (75 µm) sieve.

Gravel: Soil particles that pass through a 3-inch square opening sieve but are retained on a No. 4 (4.75 mm) sieve. Gravels can be divided into: (1) coarse gravels, gravel particles that are retained on a ¾-inch square opening sieve, and (2) fine gravels, gravel particles that pass through a ¾-inch square opening sieve.

Sand: Soil particles that pass through a No. 4 (4.75 mm) sieve and are retained on a No. 200 (75 µm) sieve. Sands can be divided into: (1) coarse sands, sand particles that are retained on a No. 10 (2.00 mm) sieve, (2) medium sands, sand particles that pass through a No. 10 (2.00 mm) sieve and are retained on a No. 40 (425 µm) sieve, and (3) fine sands, sand particles that pass through a No. 40 (425 µm) sieve.

Silt: Nonplastic or very slightly plastic soil particles passing a No. 200 (75-μm) sieve that exhibit little or no strength when air dried. For classification of silty soils, refer to Section 1-3.3.

1-3.2 Visual Description and Identification (ASTM D2488).

Visual description of soil samples is commonly performed in the field during the drilling process and consists of a visual description of the soil accompanied by an identification of the type of soil. This should be done by an engineer or a qualified person and should include as much information as possible regarding the observed conditions of the soil *in situ*. The visual description of the soil, along with the drilling logs, can provide very useful qualitative information to the engineer if done correctly. One of the most widely used standards for this purpose is ASTM D2488, which uses visual examination and simple manual tests to describe and identify soils.

1-3.2.1 Visual Description.

The descriptors for soils consist of properties and qualitative information of the soil that can be perceived with our senses. This information can be very valuable to the engineer. Below are some guidelines on what should be observed based on ASTM D2488.

1-3.2.1.1 Descriptors for All Soils.

Color: Use the color or colors that best describes the sample. Color is an important property that can help in identifying organic soils. Within a given locality, it may also be useful in identifying materials of similar geologic origin. Layers or patches of different colors should also be noted. The color described should be that of a moist sample. If the color represents a dry condition, this should be stated in the report. A Munsell color chart is a useful tool to help describing the color.

HCl reaction: Diluted hydrochloric acid (HCl) (one part of HCl to three parts of distilled water) can be used to identify the presence of calcium carbonate. The HCl reaction should be described as: (1) none, for no visible reaction, (2) weak, for some reaction with bubbles forming slowly, or (3) strong, for violent reaction with bubbles forming immediately.

Moisture condition: The moisture condition of the soil should be described as follows: (1) dry, for soils with absence of moisture, dusty, or dry to the touch, (2) moist, for damp soils with no visible water, or (3) wet, for soils with visible free water.

Odor: The odor of the soils should be described if the soil is organic or has an unusual odor.

Others: Additional comments like the presence of roots or root holes, difficulty in drilling the hole, caving of the trench or hole, or the presence of mica should be included. In addition, a local or commercial name, or a geologic interpretation of the soil could be added to help identifying the soil.

1-3.2.1.2 Descriptors for Fine-Grained Soils.

Consistency: The consistency of intact fine-grained soils should be described as: (1) very soft, if the thumb will penetrate soil more than 1 inch (25 mm); (2) soft, if the thumb will penetrate soil about 1 inch (25 mm); (3) firm, if the thumb will indent soil about 1⁄4 inch (6 mm); (4) hard, if the thumb will not indent soil but readily indented with thumbnail; or (5) very hard, if the thumbnail will not indent soil.

Structure: The structure for intact soils should be described using the following terms:

1) *Stratified*: Use for soils with layers of different material or color of at least ¼ inch in thickness. The layer thickness should be noted.
2) *Laminated*: Use for soils with layers of different material or color of less than ¼ inch in thickness. The layer thickness should be noted.
3) *Fissured*: Use for soils that break along predetermined planes with little resistance.
4) *Slickensided*: Apply to fissured soils that show polished, glossy, or sometimes striated fracture planes.
5) *Blocky*: Describes soils that can be broken down into small angular lumps which are hard to break down further.
6) *Lensed*: Use for soils with inclusions of small pockets of different soils scattered through the mass of the clay. The lens thickness should be noted.
7) *Homogenous*: Use for soils with the same color and appearance throughout.

1-3.2.1.3 Descriptors for Coarse-Grained Soils.

Angularity: Describe the angularity of coarse-grained soils as: (1) angular, if the particles have sharp edges and relatively plane sides with unpolished surfaces, (2) subangular, if the particles are angular but with rounded edges, (3) subrounded, if particles have nearly plane sides but well-rounded corners and edges, or (4) rounded, if particles have smoothly curved sides and no edges. Figure 1-1 shows examples of these four terms.

Cementation: Describe the cementation of intact coarse-grained soils as: (1) weak, if the soil crumbles or breaks with handling or little pressure, (2) moderate, if the soil crumbles or breaks with considerable finger pressure, or (3) strong, if the soil will not crumble or break with finger pressure.

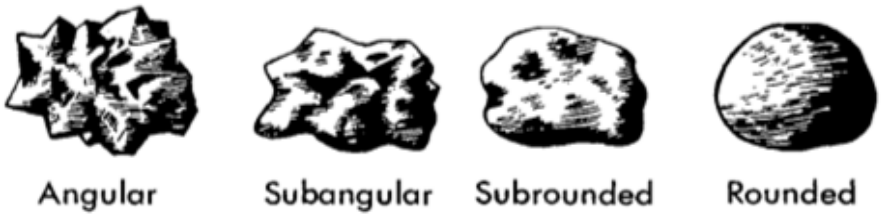

Figure 1-1 Typical Angularity of Bulky Grains (after Sowers 1979)

Hardness: Describe the hardness of coarse-grained soils as hard if the particles do not crack, fracture, or crumble when struck by a hammer, or state what happens to the particles when hit by a hammer.

Maximum particle size: Describe the maximum particle size. For sands, describe it as coarse, medium, or fine. For gravels, the maximum particle size is the smallest sieve opening that the particle will pass. For cobbles and boulders, the maximum particle size is the maximum dimension of the largest particle.

Range of particle size: Describe the range of particle sizes within each component. For example, about 15% of coarse gravel and about 45% of fine to coarse sand.

Shape: Describe the shape as: (1) flat, for particles with width/thickness > 3, (2) elongated, for particles with length/width > 3, or (3) flat and elongated, for particles that meet both criteria.

1-3.2.2 Identification.

The identification method presented in this section follows ASTM D2488. The identification should be performed on a sample that excludes cobbles and boulders. These large particles should be manually removed from disturbed samples and ignored for intact samples. The percentage of cobbles and boulders from the total samples should be estimated by volume and noted. Estimate the percentage, by dry mass, of gravel, sand and fines. The percentages should be estimated to the closest 5% and all the percentages should add to 100%. If one type of soil is encountered but the amount is less than 5% the term trace should be used to indicate its presence. A component described as trace should not be included in the 100%.

1-3.2.2.1 Identification of Fine-Grained Soils.

The identification of fine-grained soils is based upon the results of the dry strength, dilatancy, toughness, and plasticity tests.

Dry strength test: This test should be performed using a 0.5-inch diameter ball of soil. The ball needs to be air-dried or dried by artificial means at a temperature not exceeding 140°F. After drying, the ball is crushed between the fingers and the strength is classified as:

1) None, if the dry specimen crumbles into powder with the mere pressure of handling,
2) Low, if the dry specimen crumbles into powder with some finger pressure,
3) Medium, if the dry specimen breaks into pieces or crumbles with considerable finger pressure,
4) High, if the dry specimen cannot be broken with finger pressure but will break into pieces between thumb and a hard surface, or
5) Very high, if the dry specimen cannot be broken between the thumb and a hard surface.

Dilatancy: This test is performed using a 0.5-inch diameter ball molded to a soft but not sticky consistency. The ball is smoothed in the palm of one hand using the blade of a knife or a small spatula. The hand is then shaken horizontally and vigorously struck against the other hand several times. The reaction of water appearing on the surface should be noted. The soil is then squeezed by closing the hand or pinched between the fingers and the reaction of water is noted. The dilatancy is classified as:

1) None, if no visible change in the specimen was observed,
2) Slow, if water appears slowly on the surface of the specimen during shaking and does not disappear or disappear slowly upon squeezing, or
3) Rapid, if water appears quickly on the surface of the specimen during shaking and disappears quickly upon squeezing.

Toughness: This test is performed after the dilatancy test is completed and using the same specimen. The test specimen is rolled by hand on a smooth surface into a thread of about 1/8 inches in diameter. The sample is folded, mixed again, and rerolled until the threads break at a diameter of about 1/8 inches, which means the soil is near the plastic limit. The toughness of the soil is classified as:

1) Low, if only slight pressure is required to roll the thread near the plastic limit and the thread and the lump are weak and soft,
2) Medium, if medium pressure is required to roll the thread to near the plastic limit and the thread and the lump have medium stiffness, or
3) High, if considerable pressure is required to roll the thread to near the plastic limit and the thread and the lump have very high stiffness.

Plasticity: The plasticity of the soil is classified based on observations made during the toughness test as:

1) Nonplastic, if a 1/8-in-diameter thread cannot be rolled at any water content,
2) Low, if the thread can barely be rolled and the lump cannot be formed when drier than the plastic limit,

3) Medium, if the thread is easy to roll and not much time is required to reach the plastic limit, if it cannot be rolled after reaching the plastic limit, and the lump crumbles when drier than the plastic limit, or
4) High, if it takes considerable time rolling and kneading to reach the plastic limit, if the thread can be rerolled several times after reaching the plastic limit, and the lump can be formed without crumbling when drier than the plastic limit.

After these tests are performed, classify inorganic-fine-grained soils using the information in Table 1-2. If the soil contains enough organic matter, identify the soil as organic soil, OL/OH. Normally organic soils have a brown to black color and some organic odor. Normally organic soils will not have a high toughness or plasticity and the threads for the toughness test will be spongy.

Table 1-3 Classification of Fine-grained Soils

Soil Symbol	Dry Strength	Dilatancy	Toughness and Plasticity
ML	None to low	Slow to rapid	Low or thread cannot be formed
CL	Medium to high	None to slow	Medium
MH	Low to medium	None to slow	Low to medium
CH	High to very high	None	High

For fine-grained soils with an estimated percentage of sand, gravel or both the term “with sand” or “with gravel” depending on which one is more predominant should be added to the group name. If the percentage of sand and gravel is the same, use the term “with sand.” For fine-grained soils with an estimated percentage of sand, gravel or both above 30%, the words “sandy” or “gravelly” should be added to the group name depending on which one is more predominant. If the percentage of sand and gravel is the same, use the word “sandy.”

1-3.2.2.2 Identification of Coarse-Grained Soils.

For coarse-grained soils, the identification is only based on visual observations. Classify the soil as gravel or sand depending on which soil type is more predominant. The soil is considered a clean gravel or a clean sand if the percentage of particles that pass the #200 (75 µm) sieve is less than 5%. If the soil has a wide range of particle sizes and considerable amount of the intermediate particle sizes, the soil is considered to be a well-graded gravel or sand (GW or SW, respectively). If not, the soil is considered a poorly-graded gravel or sand (GP or SP, respectively).

For soils with 10% fines, a dual classification should be used. The first set of symbols consist of the clean gravel or sand symbols (GW, GP, SW, or SP) followed by the gravel

or sand with fines symbols (GC, GM, SC, or SM). The group name should consist of the name of the first set of symbols followed by the words “with clay” or “with silt” to identify the fines.

If the soil has 15% or more fine-grained particles, the soil shall be identified as clayey gravel (GC) or clayey sand (SC), if the fines are clay as determined in the previous section, or silty gravel (GM) or silty sand (SM) if the fines are silty.

For gravels or sands with an estimated 15% or more of other coarse-grained particles, the words “with gravel” or “with sand” should be added. If the sample contains cobbles, boulders, or both the words “with cobbles,” “with boulders,” or “with cobbles and boulders” should be added to the group name.

1-3.2.3 Examples.

Below are a few examples of visual descriptions and identifications (ASTM D2488):

1) Poorly-Graded Gravel with Sand (GW): About 80% medium to coarse, hard, angular gravel; about 20% fine to coarse, hard, subangular sand; trace of fines; maximum size, 70 mm, gray, moist; no reaction with HCl.
2) Silty Sand with Gravel (SM): About 65% predominantly medium to fine sand; about 20% silty fines with low plasticity, low dry strength, low dilatancy, and low toughness, about 15% fine, hard, rounded gravel, a few gravel-size particles fractured with hammer blow; maximum size, 1.5 inch (38 mm); weak reaction with HCl.
3) Organic Soil (OL/OH): About 100% fines with low plasticity, slow dilatancy, low dry strength, and low toughness; wet, black, organic odor; strong reaction with HCl.
4) Well-Graded Gravel with Clay, Sand, Cobbles and Boulders (GW-GC): About 70% medium to coarse, hard, rounded to subangular gravel; about 20% fine, hard, rounded to subangular sand; about 10% clay low plasticity fines; moist, dark grey; no reaction with HCl; original field sample had about 5% (by volume) hard, rounded cobbles and a trace of hard, rounded boulders, with a maximum dimension of 18 inches (450 mm).

1-3.3 Unified Soil Classification System (ASTM D2487).

The unified soil classification system (USCS) is the most common classification system used for soils in the engineering community. This section is based on the USCS as presented in ASTM D2487. This classification system consists of three major soil divisions: coarse-grained soils, fine-grained soils, and highly organic soils, which are further subdivided into 15 soil groups. To use this soil classification system the grain-size distribution (ASTM D6913) of the minus 3-inch (75-mm) material, and the liquid limit and plasticity index (ASTM D4318) of the minus No. 40 (425-µm) sieve material

should be known. The various groups used in this classification system have been divided to correlate in a general way with the engineering behavior of soils.

The grain-size distribution is needed for soils with 10% or more coarse-grained particles and it can be estimated for soils with less than 10% coarse-grained particles. The liquid limit and plasticity index are required for soils with 15% or more fines and the plasticity can be estimated for soils with 5% to less than 15% fines as described in Section 1-3.2.2.1. For soils with less than 5% fines, the plasticity is not needed.

1-3.3.1 Classification of Fine-Grained Soils.

Using the liquid limit and plasticity index, classify inorganic soils as lean clay (CL), fat clay (CH), silt (ML), elastic silt (MH), or silty clay (CL-ML) using Figure 1-2. For dark soils with organic odor, two liquid limit tests should be performed on the soil. One test is performed before drying, and a second test is completed after oven drying the soil at 110 ± 5°C. The soil is considered an organic silt or clay if the liquid limit of the oven-dried material is less than 75% of that of the material before oven drying. Classify the organic soil as organic silt or clay OL or OH depending on where the liquid limit and plasticity index of the non-oven-dried material plot in Figure 1-2.

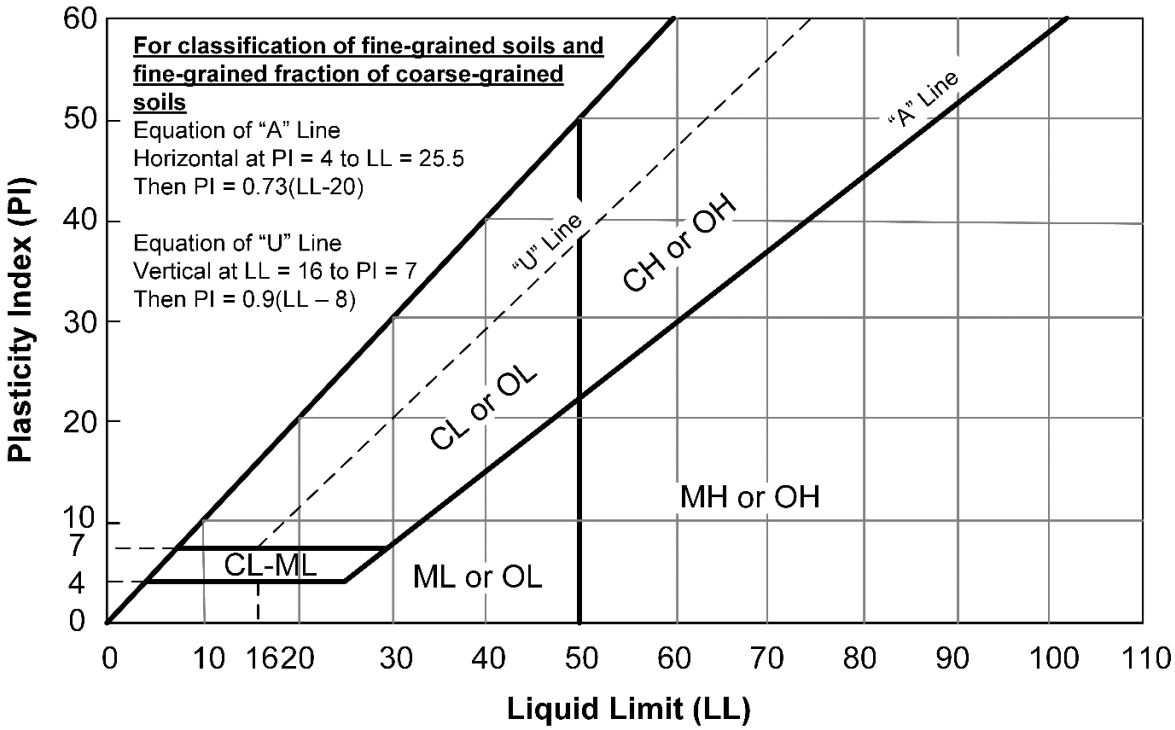

Figure 1-2 Plasticity Chart

If the fine-grained soil contains 30% or more retained in the No. 200 (75 µm) sieve the words "gravelly" or "sandy" should be added to the group name based on the type of particle that is predominant in the coarse-grained portion. For soils with equal

percentage of sand and gravel, use “sandy.” If the coarse-grained portion is less than 30% but greater or equal than 15%, the words “with gravel” or “with sand” should be added to the group name depending whichever is predominant. For soils with equal percentage of sand and gravel, use “with sand.”

Some properties of fine-grained soils are usually related to the plasticity characteristics of the soil. Figure 1-3 describes how the liquid limit and plasticity index affect the compressibility, permeability, toughness at the plastic limit, and the dry strength of fine-grained soils.

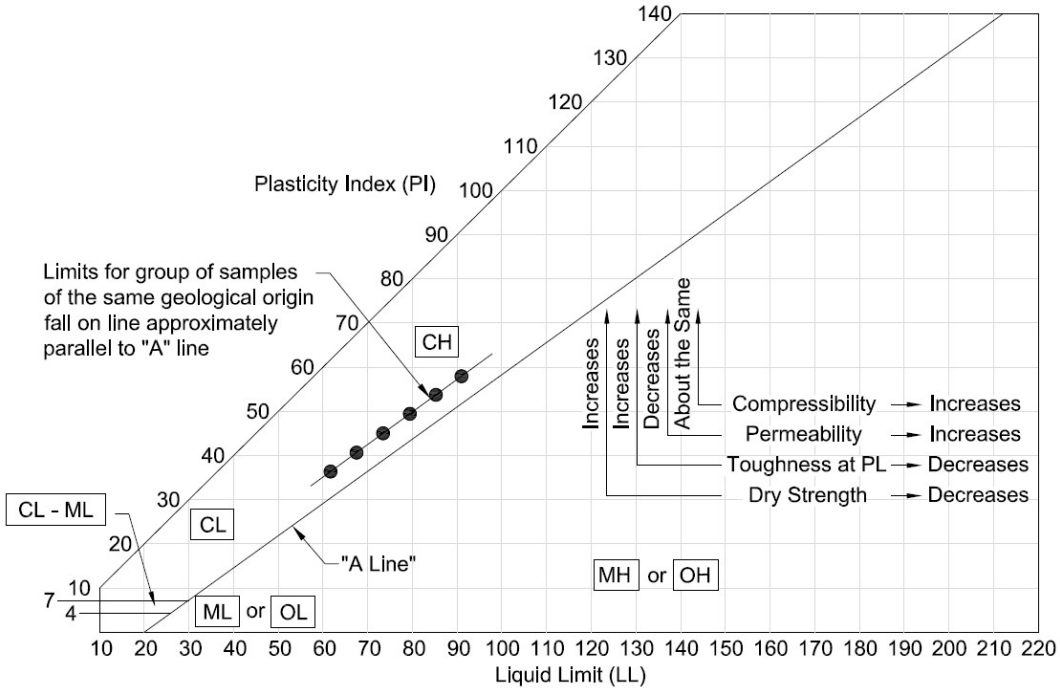

Figure 1-3 Soil Property Variation with Liquid Limit and Plasticity

1-3.3.2 Classification of Coarse-Grained Soils.

Coarse-grained soils that contain more than 50% of the coarse-grained fraction retained on the No. 4 (4.75-mm) sieve should be classified as gravel, and as sand otherwise. Using the information on the grain-size distribution curve, calculate the following to define whether the soil is well-graded or poorly-graded:

$$C_u = \frac{D_{60}}{D_{10}} \quad \textbf{(1-1)}$$

and

$$C_c = \frac{D_{30}^2}{D_{60} \times D_{10}} \quad \textbf{(1-2)}$$

where:
D_{60}, D_{30}, and D_{10} = particle-size diameters corresponding to 60%, 30%, and 10%, respectively, passing on the cumulative particle-size distribution curve,
C_u = coefficient of uniformity, and
C_c = coefficient of curvature.

Coarse-grained soils are classified as well-graded if C_u is greater than or equal to 4.0 for gravels or greater than 6.0 for sands, and C_c is at least 1.0 but not more than 3.0. Otherwise, the soil is poorly-graded.

Coarse-grained soils with less than 5% passing the No.200 (75-µm) sieve are considered *clean* and are classified as well-graded gravel (GW), well-graded sand (SW), poorly-graded gravel (GP), or poorly-graded sand (SP).

For coarse-grained soils with more than 12% fines, the classification of the fines needs to be determined using the plasticity chart presented in Figure 1-2. If insufficient fines are available to run plasticity tests, the classification of the fines shall be completed as described in Section 1-3.2.2.1. Classify the soil as silty gravel or sand (GM or SM, respectively) if the fines are silt or clayey gravel or sand (GC or SC, respectively) if the fines classify as clay. If the fines plot as silty clay (CL-ML) classify the soil as a silty, clayey gravel (GC-GM) or a silty, clayey sand (SC-SM).

Coarse-grained soils with a fine content between 5% and 12% require the use of a dual classification. The first group symbol corresponds to that for a gravel or sand having less than 5% fines (GW, GP, SW, or SP), and the second symbol correspond to a gravel or sand having more than 12% fines (GC, GM, SC, or SM). The group name is formed by the name of the first group symbol following the words “with clay” or “with silt” depending on the characteristics of the fines. If the fines plot as a silty clay, CL-ML, the second group symbol would be either GC or SC and the words “with silty clay” will be used in the name.

If the soil is mainly sand or gravel but contains 15% or more of the other coarse-grained constituent, the words “with gravel” or “with sand” shall be added to the group name. Soils with cobbles and boulders should have the words “with cobbles,” “with boulders,” or “with cobbles and boulders” added to the group name.

1-3.3.3 Examples.

Below are a few examples of visual descriptions and identifications accompanied by the proper USCS classification (ASTM D2487):

1) Well-Graded Gravel with Sand (GW): 71% fine to coarse, hard, angular gravel; 25% fine to coarse, hard, angular sand; 4% fines; C_c = 2.7, C_u = 12.4.
2) Silty Sand with Gravel (SM): 62% predominantly medium sand; 22% silty fines, LL = 32, PI = 6; 16% fine, hard, rounded gravel; no reaction with HCl.
3) Poorly-Graded Gravel with Silt, Sand, Cobbles and Boulders (GP-GM): 75% medium to coarse, hard, rounded to subangular gravel; 19% fine to medium, hard, rounded to subangular sand; 6% silty (estimated) fines; moist, brown; no reaction with HCl; original field sample had 7% hard, subrounded cobbles and 2% hard, subrounded boulders with a maximum dimension of 18 inches.

1-3.4 Soil Classification for Highways (AASHTO).

The American Association of State Highway and Transportation Officials (AASHTO) developed their soil classification system, which is mainly used for highway design and construction purposes. This system classifies the soils in 12 divisions based on the grain-size distribution, the liquid limit, and the plasticity index, using only the soil particles that pass through a 3-inch sieve. This section is based on the classification system as detailed in ASTM D3282.

An important distinction between this classification system and the USCS is the threshold used between the different types of soils. Coarse-grained or granular materials are considered to be any soil that has 35% or less passing a No. 200 (75 μm) sieve. Gravel is any material passing a 3-inch sieve and retained on a No. 10 (2.00 mm) sieve. Coarse sand is considered any soil that passes a No. 10 (2.00 mm) sieve and is retained on a No. 40 (0.425 mm) sieve. Fine sand is any material passing a No. 40 (0.425 mm) sieve and retained on a No. 200 (75 μm) sieve. Silts and clays are anything passing a No. 200 (75 μm) sieve, silts being materials with plasticity indices of 10 or less and clays being materials with plasticity indices above 10.

Soils are classified using Table 1-5 below from left to right. Highly organic soils (peat or muck) may be classified in Group A-8. Classification of organic soils is based on visual inspection and is not dependent on the percentage passing the 75-μm (No. 200) sieve, liquid limit, or plasticity index. Organic material is composed primarily of partially decayed organic matter, generally has a fibrous texture, a dark brown or black color, and an odor of decay. These organic materials are unsuitable for use in embankments and subgrades. They are highly compressible and have low strength.

The classification obtained with the table above might be modified by adding a group-index value that will be shown in parenthesis after the group symbol. The group index is calculated using the empirical equation shown below:

$$GI = (F - 35)[0.2 + 0.005(LL - 40)] + [0.01(F - 15)(PI - 10)] \quad \textbf{(1-3)}$$

where:

GI = group index,
F = percentage passing a No. 200 (75 μm) sieve (only considering the particles passing a 3-inch sieve),
LL = liquid limit of the soil, and
PI = plasticity index of the soil.

The group index should be reported as zero if calculated to be negative, if the soil is nonplastic, and when the liquid limit cannot be determined. For soils in the A-2-6 and A-2-7 subgroups, the group index should be calculated using the second part of the equation only (the part that contains the PI).

1-3.5 Other Classification Systems.

Different regions in the United States and countries around the world have their own soil classification systems. Below is a list containing the name of the country or region in the United States and the reference to the standard used. This list is not intended to be exhaustive but to show some examples. For the countries who are member of the European Union, all the local standards are superseded by the ISO standards which have the same numbers as European Norms (EN). Each country is allowed to further refine the ISO/EN standards by adding appendices as long as the appendices do not contradict the main standard. Each local standard will have the same number as the ISO standard but will have the country designation at the beginning (e.g. BS for British standards). When working on different projects in different parts of the United States or the world the engineer should investigate the standards and norms that are used in that particular area.

Table 1-4 Other Soil Classification Systems

Country / Region of USA / Agency	Reference / Name
Australia	AS 1726
Canada	Canadian System of Soil Classification
International Organization for Standardization (ISO)	ISO 14688
Occupational Safety and Health Administration (OSHA)	1926 Subpart P App A
New Orleans	USACE New Orleans District Internal Document
USDA	USDA Soil Taxonomy

Table 1-5 AASHTO Soil Classification System

Instructions: Work from left to right checking each column. The classification is the first one that matches all the criteria in the column.													
General Classification	Coarse-grained (granular) Materials (35% or less passing No. 200 sieve)							Fine-grained (Silt-Clay) Materials (more than 35% passing No. 200 sieve)					Highly Organic
Group Classification	A-1		A-3	A-2				A-4	A-5	A-6	A-7[b]		A-8
	A-1-a	A-1-b		A-2-4	A-2-5	A-2-6	A-2-7				A-7-5	A-7-6	
Sieve analysis Percent passing:													
#10 (2 mm)	≤ 50												
#40 (0.4 mm)	≤ 30	≤ 50	≥ 51										
#200 (0.075 mm)	≤ 15	≤ 25	≤ 10	≤ 35	≤ 35	≤ 35	≤ 35	≥ 36	≥ 36	≥ 36	≥ 36	≥ 36	
Characteristics of fraction passing #40													
Liquid Limit				≤ 40	≥ 41	≤ 40	≥ 41	≤ 40	≥ 41	≤ 40	≥ 41	≥ 41	
Plasticity Index	≤ 6	≤ 6	NP[a]	≤ 10	≤ 10	≥ 11	≥ 11	≤ 10	≤ 10	≥ 11	≥ 11	≥ 11	
Usual types of significant constituent materials	Stone fragments; gravel and sand		Fine sand	Silty or clayey gravel and sand				Silty soils	Clayey soils				Peat or muck
General rating as subgrade	Excellent to good							Fair to poor					Unsuitable

Notes:

[a]NP indicates that the soil is "non-plastic." NP soils have $LL = PL$, $LL < PL$, or PL that cannot be determined.

[b]Use the following criteria to divide A-7: A-7-5 has $PI \le (LL - 30)$ and A-7-6 has $PI > (LL - 30)$.

Group Index, GI

$$GI = (F - 35)\left[0.2 + 0.005(LL - 40)\right] + 0.01(F - 15)(PI - 10)$$

Calculate the group index as:

where: F= %fines = P#200, LL = liquid limit, and PI = plasticity index.

If a negative value is calculated for GI, then report GI = 0.

Note: Use only the second term in the GI equation for A-2-6 and A-2-7 soils.

1-3.6 Common Soil and Rock Names.

In practice, some areas have specific names for different types of soils. Some of these names can be considered colloquialisms within the geotechnical engineering community. Below is a list with definitions of the most common soil names used in practice.

Adobe: Refers to sandy clays and silts of medium plasticity usually found in the semiarid regions of the southwestern United States. These soils were commonly used to make sun-dried bricks. The name is also applied to some high plasticity clays with high clay content and high swell and shrink potential usually found in the western part of the United States.

Baby poop: Refers to a very soft clay located just above limestone in karst. Frequently orange and formed by dissolution.

Back-packing: Refers to any material (commonly granular) that is used to fill the empty space between the lagging of a wall system and the rock surface.

Bank-run sand and gravel: Refers to the raw material excavated from a borrow pit, but not sorted or separated into specific grades.

Beachrock: See reefrock.

Bentonite: Refers to a high plasticity clay consisting of mostly montmorillonite, resulting from the weathering of volcanic ash mainly in the presence of water. It is normally hard when dry but swells considerably when wet. This clay is commonly used with water as drilling mud and as liner in landfills.

Black cotton soil: Refers to a black expansive soil commonly encountered in India. The name comes because this soil is common in areas where the main crop is cotton.

Blow sand: Term normally used for wind-driven or drifted sands.

Blue Marl: Name given to a bluish-green clay from the Miocene that can be found along the fall line from Richmond into Maryland. This soil is considered to be acidic, usually with a pH less than 4.0, which can affect water quality and prevent plant or aquatic life.

Bog: Refers to a wetland covered with peat with a high water table that accumulates dead plants, such as sphagnum. It is generally nutrient poor and acidic.

Boney ground: Ground containing significant amounts of large gravel, cobbles and boulders.

Boulder clay: Geological term used to designate clays formed from glacial drift that have not been subjected to the sorting action of water and therefore contains particles from boulders to clay sizes. Boulder clays are also called tills.

Breaker run: Crushed rock with large particles refers to large broken stone obtained as part of quarrying or mining activities.

Buckshot: Term applied to clays of the southern and southwestern United States that cracks into small, hard, relatively uniform-sized lumps on drying. The lumps are usually the size of buckshot and the soil is very sticky when wet.

Bull's liver: Name given to an inorganic silt or silty sand usually encountered in the New York City area. The name Bull's liver comes from its red color and jelly-like behavior when it is subjected to vibration.

Bull's Tallow or Bull Tallow clay: Refers to a tan or gray high plasticity clay typically found in relatively thin layers directly above partially weathered rock or rock in the Charlotte, NC area. This clay normally has high shrink and swelling potential.

Caliche: Refers to a sedimentary rock from arid and semiarid climate in which soil particles, such as gravel, sand, clay, and silt, are cemented and coated by carbonate (often calcium or magnesium carbonate). The level of cementation varies significantly within a deposit. The soil has light coloration often exhibits light colored concretions of various sizes depending on the level of development of the soil profile. The consistency of caliche varies from soft rock to firm soil.

Chip: Name given to crushed angular rock fragments smaller than a few centimeters.

Coffee grounds: Soil formed from freshwater marshes that has been dry for decades and has decomposed to the point that is black and inert with no plasticity. It is black and granular even when wet.

Colluvium: Loose soil deposited at the bottom of a slope.

Coquina: Soft, porous sedimentary rock, mainly limestone, composed largely of shells, coral, and fossils cemented together with particles averaging 0.079 inch (2 mm) or greater in size.

Desert varnish: Also called patina, rock varnish or rock rust. Consists of a thin, dark red to black mineral coating found on pebbles and rocks surfaces in arid regions.

Diatomaceous earth: Soft, siliceous sedimentary rock that usually crumbles into powder. When crumbled, the particles are silty and contain large amounts of diatoms, the siliceous skeletons of minute marine or freshwater organisms.

Dispersive clays: These clays contain a high percentage of dissolved sodium in the pore water. When these soils are exposed to water, the clay particles deflocculate (i.e., separate) making these soils very susceptible to erosion.

Fibric peat: Peat in which the original plant fibers are slightly decomposed and contain 67% or more of fibers.

Fill: Any man-made soil deposit. It can range from soils that are free of organic matter and that are carefully compacted to heterogeneous accumulations of rubbish and debris.

Fuller's earths: Soils having the ability to absorb fats or dyes. These soils have the capability to decolorize oil or other liquids without chemical treatment. They are usually high plasticity sedimentary clays.

Glacial till: See boulder clay.

Glassified sand: Term used to name the ground surface after a big forest fire.

Goonies: Name given to the cobbles found floating in a soil matrix.

Grove sand: See sugar sand.

Gumbo: Refers to a fine-grained, high plasticity clay of the Mississippi Valley according to Sowers (1979). It has a sticky, greasy feel and forms large shrinkage cracks on drying.

Gyp or gip soil: Refers to gypsum soil (or soil containing gypsum) or caliche soil.

Hardpan: Normally refers to a soil layers that has become hard as rock due to cementing minerals, does not become plastic when mixed with water and is relatively impervious. The name has also been applied to any hard or overconsolidated layer that is hard to excavate. Because of this ambiguity, Sower (1979) recommends that engineers should avoid this term because many lawsuits have centered about the meaning of it. The name implies a condition of the soil rather than a type of soil.

Humus: Refers to a brown or black material formed by the partial decomposition of vegetable or animal matter. It is the organic portion of soil.

Kaolin: Refers to a white or pink clay of low plasticity. It is composed largely of minerals of the kaolinite family.

Laterites: Refers to residual soils rich in iron formed in hot and humid climates (tropical regions). The cementing action of iron oxides and hydrated aluminum oxides makes

dry laterites extremely hard. The high iron oxide content makes nearly all laterites to be rusty-red. These are usually developed after significant weathering of the parent rock.

Ledge: Name used for bedrock in Vermont, and sometimes in New Hampshire.

Loam: Refers to a low plasticity sandy silt or silty sand mixed with organic matter that is well suited to tilling. Mainly applies to the uppermost soil layer and should not be used to describe deep deposits of parent materials. Major soil type in the USDA system.

Marl: Refers to a calcium carbonate or lime-rich sedimentary rock. It is mainly composed of a mixture of sand, silt, or clay. Marls are often light to dark gray or greenish in color and sometimes contain colloidal organic matter.

Montmorillonite: A group of very fine clay minerals with extreme swelling and shrinking properties. Normally results from volcanic or hydrothermal activities. Bentonite is a form of montmorillonite.

Muskeg: Refers to peat found in North America. According to Sowers (1979) the bogs in which the peat forms are often termed muskegs.

Peat: Refers to a fibrous, partially decomposed and highly compressible organic soil. Peats are dark brown or black.

Pit-run sand and gravel: See bank run.

Pluff mud: Refers to an odoriferous and very soft mud usually encountered in South Carolina.

Recycled concrete aggregate (RCA): Recycled road or structural concrete. The concrete is usually processed and screened. The processing consists of crushing the concrete into smaller pieces. Any leftover steel is removed using a magnet. This type of material is very popular as a replacement for natural stone aggregates.

Recycled or reclaimed asphalt pavement (RAP): Term used to describe the removed asphalt layer. When properly processed, it consists of high-quality and well-graded aggregates coated by asphalt cement.

Recycled or reclaimed asphalt shingles (RAS): Recycled shingles that are used as aggregate for hot mix asphalt. Depending on the quality, this can reduce the cost of the new asphalt mix and the amount of fine aggregate used in the mix.

Recycled pavement material (RPM): Pulverized mixture of asphalt and base course material usually forming a broadly-graded material.

Reefrock: Cemented coralline deposits.

Riprap: Boulder-size material normally placed to strengthen structures against scour, wave action, and ice erosion.

Riverjack: Name usually given to alluvial cobbles and boulders.

Rock dirt combination (RDC): Local term used in the Harrisonburg, VA area to describe material from a quarry consisting of a mixture of overburden soil and rock.

Rock flour: Fine-grained soil with silt-sized particles formed by the grinding of bedrock by glaciers.

Shale: Refers to a fine-grained sedimentary rock made of silt and clay particles. This rock usually breaks along thin laminates and can slake when subjected to wet-dry cycles.

Shot rock: Refers to the material from a rock quarry that has not been sorted. It includes everything that can be picked up (from fine sand to small boulders) after a quarry blast. It is also a name given to riprap, although riprap is typically sorted and graded.

Slickensided clay: Name given to a clay that has experienced repeated or enough displacement along a fissure or a failure plane causing the surface to be smooth and shiny.

Stone: Gravel size-particles manufactured by crushing rock.

Sugar sand: Local name for a type of fine sandy soil found in New Jersey. In Kansas, the term refers to a type of granular calcite found in Ness and Hodgeman counties. In addition, the term may refer to a fine sand usually found in Florida that does not hold water or nutrients very well. It is normally windblown medium and/or fine sand, poorly-graded, nonplastic. It often contains nonplastic silt.

Till: See boulder clay.

Tire derived aggregate (TDA): Refers to a lightweight construction material obtained by shredding or chipping scrap tires. The particle size usually ranges from 0.5 inches to 12 inches. TDA has been used in a wide range of projects, including lightweight embankment fill, landslide repair or stabilization, landfills, retaining wall backfill, roads, vibration mitigation, among others.

Topsoil: Upper and outermost layer of soil that support plant life. Usually contains considerable organic matter.

Trap: Includes any dark-colored, fine-grained, non-granitic intrusive rock. The most common trap rock is basalt, but also includes peridotite, diabase, and gabbro.

Tuff: Refers to a soft porous rock made from consolidated volcanic ash.

Varved clays: Sedimentary deposits consisting of alternate thin layers of silt and clay. According to Sowers (1979), each pair of silt and clay layers is from 1/8 inch to 1/2 inch thick. These soils result from deposition in lakes during periods of alternately high and low water in the in flowing streams and are often formed in glacial lakes.

1-4 ROCK VISUAL DESCRIPTION, AND CLASSIFICATION.

1-4.1 Definitions.

Azimuth: Angle of a feature measured from North at 0° in a spherical coordinate system.

Bedding: Planes of dissimilar materials caused by deposition normally encountered in sedimentary rocks.

Dip: Angle that the surface of the rock forms with a horizontal plane.

Flow banding: Refers to the layering that is normally seen in rocks formed from magma.

Foliation: Refers to the laminated structure of the minerals in a rock created by the deformation.

Igneous rocks: Rocks formed from the cooling and solidification of magma.

Lamination: Sequence of fine layers in a small scale (usually less than one centimeter in thickness) normally observed in sedimentary rocks.

Metamorphic rocks: Rocks formed from the transformation by heat, pressure, or both of existing rocks. This transformation can alter the physical and chemical properties of the rock.

Rock: Natural solid mineral or aggregate of minerals which is normally classified by the way it was formed.

Rock mass: A large body containing rock in intact and weathered conditions accompanied by structural discontinuities like fault, joints, etc., which can be interbedded with soil material.

Sedimentary rocks: Rocks formed by the accumulation and cementation of smaller particles.

Strike: Is the line representing the intersection of the rock surface with a horizontal plane.

1-4.2 Visual Classification.

Rock samples and exposures can be visually classified by weathering, discontinuities, color and grain size, hardness, and geological origin.

1-4.2.1 Geological Name and Origin.

The first step in visually classifying a rock is to identify the type of rock (e.g., igneous, metamorphic, or sedimentary). Then, the geologic name and local name (if any) is identified based on characteristics, such as texture and mineralogy. Igneous rocks are normally classified by their mineralogical composition, texture, and color as can be seen in Table 1-6.

Metamorphic rocks are normally classified by their texture and structure, as can be seen in Table 1-7. Sedimentary rocks are normally classified by whether they are derived from clastic sediments or chemical precipitates/organisms, as can be seen in Table 1-8. Subordinate constituents in rock samples, such as seams or bands of other type of minerals, should also be identified (e.g., dolomitic limestone, calcareous sandstone, sandy limestone, mica schist).

Table 1-6 Simplified Rock Classification - Common Igneous Rocks

Color		Light		Intermediate	Dark	
Principal Mineral		Quartz and Feldspar Few other minerals	Feldspar	Feldspar and Hornblende	Augite and Feldspar	Augite, Hornblende, Olivine
Texture	Coarse, Irregular Crystalline	Pegmatite	Syenite Pegmatite	Diorite Pegmatite	Gabbro Pegmatite	
	Coarse and Medium Crystalline	Granite	Syenite	Diorite Dolerite	Gabbro Dolerite	Peridotite Dolerite
	Fine Crystalline	Aplite			Diabase	
	Aphanitic	Felsite			Basalt	
	Glassy	Volcanic Glass			Obsidian	
	Porous (Gas Openings)	Pumice		Scoria or vesicular basalt		
	Fragmental	Tuff (fine), Breccia (coarse), cinders (variable)				

Table 1-7 Simplified Rock Classification - Common Metamorphic Rocks

Texture	Structure		
	Foliated		Massive
Coarse Crystalline	Gneiss		Metaquartzite
Medium Crystalline	Schist	Sericite	Marble
		Mica	Quartzite
		Talc	Serpentine
		Chlorite	Soapstone
Fine to Microscopic	Phyllite		Hornfels
	Slate		Anthracite Coal

Table 1-8 Simplified Rock Classification – Common Sedimentary Rocks

Group	Grain Size	Composition		Name
Clastic	Mostly coarse grains	Rounded pebbles in medium-grained matrix		Conglomerate
		Angular coarse-grained fragments, often quite variable		Breccia
	More than 50% medium grains	Medium coarse grains	Less than 10% of other minerals	Siliceous sandstone
			Appreciable quantity of clay minerals	Argillaceous sandstone
			Appreciable quantity of calcite	Calcareous sandstone
			Over 25% feldspar	Arkose
			25%-50% feldspar and darker minerals	Graywacke
	More than 50% fine grains	Fine to very fine quartz grains with clay minerals		Siltstone (if laminated, Shale)
		Microscopic clay minerals	<10% other minerals	Shale
			Appreciable calcite	Calcareous Shale
			Appreciable carbon / carbonaceous material	Carbonaceous Shale
			Appreciable iron oxide cement	Ferruginous Shale
Organic	Variable	Calcite and fossils		Fossiliferous Limestone
	Medium to microscopic	Calcite and appreciable dolomite		Dolomite Limestone or Dolomite
	Variable	Carbonaceous material		Bituminous coal
Chemical	Microscopic	Calcite		Limestone
		Dolomite		Dolomite
		Quartz		Chert, Flint, etc.
		Iron compounds with Quartz		Iron Formation
		Halite		Rock Salt
		Gypsum		Rock Gypsum

1-4.2.2 Color and Grain Size.

Rock can be described with respect to basic colors on a rock color chart. The most common chart used for this purpose in the United States is the Munsell rock color chart

which includes 115 color chips and works with both wet and dry specimens. Another commonly used system is the one published by the Geological Society of London (1977). This system is based on three descriptors as can be seen in Table 1-9.

Grain size for rock refers to the sizes of the small grains that comprise the rock. Because of the nature of some rocks, a 10X hand lens can be used, if necessary, to examine rock sample. Various grain-size criteria have been established, and no single criteria is standard or used most often. An example of grain-size descriptors for different types of rock are found in Table 1-10. Another criterion presented by FHWA (2017) is also included here in Table 1-11 which is similar to that presented by the Geological Society of London (1977).

Table 1-9 Rock Color Descriptors (Geological Society of London 1977)

1st Descriptor	2nd Descriptor	3rd Descriptor
Light Dark	Yellowish Buff Orangish Brownish Pinkish Purplish Orange Olive Greenish Greyish	White Yellow Buff Orange Brown Pink Red Blue Green Purple Olive Grey Black

Table 1-10 Grain-Size Descriptors for Rock

Igneous and Metamorphic		Sedimentary Rocks	
Description	**Grain Diameter**	**Description**	**Grain Diameter**
Coarse-grained	> 5 mm	Coarse-grained	> 2 mm
Medium-grained	1 to 5 mm	Medium-grained	0.06 to 2 mm
Fine-grained	< 1 mm	Fine-grained	0.002 to 0.06 mm
Aphantic	Too small to be perceived by eye	Very fine-grained	< 0.002 mm
Glassy	No grain form distinguishable		

Table 1-11 Criteria for Defining Rock Grain Size (after FHWA 2017)

Grain Size	Description	Criteria
< 0.003 in. (< 0.075 mm)	Very Fine-Grained	Cannot be distinguished by unaided eye. Few to no mineral grains are visible with a hand lens.
0.003 – 0.02 in. (0.075 – 0.425 mm)	Fine-Grained	Few crystal boundaries are visible; grains can be distinguished with difficulty by the unaided eye but can be somewhat distinguished by hand lens.
0.02 – 0.8 in. (0.425 – 2 mm)	Medium-Grained	Most crystal boundaries are visible; grains distinguishable by eye and with hand lens.
0.8 – 2 in. (2 – 4.75 mm)	Coarse-Grained	Crystal boundaries are visible; grains distinguishable with naked eye.
2 in. (> 4.75 mm)	Very Coarse-Grained	Crystal boundaries are clearly visible; grains are distinguishable with the naked eye.

1-4.2.3 Weathering.

Weathering is the mechanical or chemical deterioration of rock properties by the exposure to water, temperature changes, among other factors. Rock can be described as fresh, slightly weathered, etc. in accordance with Table 1-12 as indicated by the International Society of Rock Mechanics (ISRM). As the degree of weathering increases, usually the strength, stiffness, and quality of the rock decrease.

Table 1-12 Weathering Classification

Grade	Symbol	Weathering Grade[1]	Diagnostic Features
Fresh	F	I	No visible sign of decomposition or discoloration; rings under hammer impact
Slightly Weathered	WS	II	Slight discoloration inwards from open fractures, otherwise similar to F
Moderately Weathered	WM	III	Discoloration throughout; weaker minerals such as feldspar decomposed; strength somewhat less than fresh rock but cores cannot be broken by hand or scraped by knife; texture preserved
Highly Weathered	WH	IV	Most minerals somewhat decomposed; specimens can be broken by hand with effort or shaved with knife; core stones present in rock mass; texture becoming indistinct but fabric preserved
Completely Weathered	WC	V	Minerals decomposed to soil but fabric and structure preserved (saprolite); specimens easily crumbled or penetrated
Residual Soil	RS	V	Advanced state of decomposition resulting in plastic soils; rock fabric and structure completely destroyed; large volume change.

[1] After FHWA (2017).

1-4.2.4 Discontinuities.

The spacing of discontinuities in the rock can be described as close, wide, etc., in accordance with Table 1-13. The structural features of a rock mass can be described as thickly bedded or thinly bedded, in accordance with Table 1-13. Depending on project requirements, the form of joint should be identified as stepped, smooth, undulating, planar, etc. In addition, the dip (in degrees), surface condition (rough,

smooth, slickensided), opening size (giving width), and filling (none, sand, clay, breccia, etc.) should also be recorded.

1-4.2.5 Hardness.

The hardness of rock can be estimated by field tests using a geologic hammer or knife and, in the laboratory, using the point load test in accordance with Table 1-14. The corresponding range of strength values for intact rock is also provided. A more recent grading system presented by the ISRM is presented in Table 1-15.

Table 1-13 Discontinuity Spacing

Type of Feature	Description	Spacing	Description for Joints, Faults, or Other Fractures
Macrostructural: Bedding, Foliation, or Flow Banding	Very thickly (bedded, foliated, or banded)	> 6 feet	Very widely (fractured or jointed)
	Thickly	2 to 6 feet	Widely
	Medium	8 to 24 inches	Medium
	Thinly	2.5 to 8 inches	Closely
	Very Thinly	0.75 to 2.5 inches	Very Closely
Microstructural: Lamination, Foliation, or Cleavage	Intensely (laminated, foliated, or cleavage)	0.25 to 0.75 inch	Extremely close
	Very Intensely	< 0.25 inch	

Table 1-14 Hardness Classification of Intact Rock (Hough 1969)

Class	Hardness	Field Test	Approximate compressive strength (kg/cm^2 or tsf)
I	Extremely hard	Many blows with geologic hammer required to break intact specimen	>2000
II	Very hard	Handheld specimen breaks with hammer end of pick under more than one blow	1000 - 2000
III	Hard	Cannot be scraped or peeled with knife, hand held specimen can be broken with a single moderate blow with pick	500 - 1000
IV	Soft	Can just be scraped or peeled with knife. Indentations of 1 mm to 3 mm show in specimen with moderate blow with pick	250 - 500
V	Very soft	Material crumbles under moderate blow with sharp end of pick and can be peeled with a knife, but is too hard to hand trim for triaxial test specimen	10 – 250

Table 1-15 Criteria and Descriptions for Relative Rock Strength (after FHWA 2017)

Grade	Description	Field Identification	Approximate Compressive Strength (kg/cm^2 or tsf)
R0	Extremely Weak Rock	Specimen can be indented by thumbnail	2.5 – 10.8
R1	Very Weak Rock	Specimen crumbles under sharp blow with point of geological hammer and can be peeled with a pocket knife	10.8 – 52.2
R2	Weak Rock	Shallow cuts or scrapes can be made in a specimen with a pocket knife; a firm blow with a geological hammer creates shallow indents	52.2 – 252
R3	Medium Strong Rock	Specimen cannot be scraped or cut with a pocket knife; specimen can be fractured with a single firm blow with a geological hammer point	252 – 522
R4	Strong Rock	Specimen requires more than one firm blow of the point of a geological hammer to fracture	522 – 1,044
R5	Very Strong Rock	Specimen requires many firm blows from the hammer end of a geological hammer to fracture	1,044 – 2,610
R6	Extremely Strong Rock	Specimen can only be chipped with firm blows from the hammer end of a geological hammer	> 2,610

1-4.3 Classification by Field and Laboratory Measurements.

1-4.3.1 Rock Quality Designation.

The Rock Quality Designation (RQD) is only for NX size core samples and is computed by summing the lengths of all pieces of core equal to or longer than 4 inches and dividing by the total length of the coring run. The resultant is multiplied by 100 to get RQD in percent. It is necessary to distinguish between natural fractures and those caused by the drilling or recovery operations. The fresh, irregular breaks should be ignored and the pieces counted as intact lengths. Depending on the engineering requirements of the project, breaks induced along highly anisotropic planes, such as foliation or bedding, may be counted as natural fractures. A qualitative relationship between RQD, velocity index, and rock mass quality is presented in Table 1-16. The velocity index is defined as the square of the ratio of the *in situ* to laboratory or intact compressional wave velocities.

Table 1-16 Engineering Classification for *In situ* Rock Quality (Merritt and Coon 1970)

RQD	Velocity Index	Rock Mass Quality
90-100	0.80-1.00	Excellent
75-90	0.60-0.80	Good
50-75	0.40-0.60	Fair
25-50	0.20-0.40	Poor
0-25	0.00-0.20	Very Poor

1-4.3.2 Classification by Strength.

The uniaxial compressive strength and modulus ratio can be used to classify rock using the results of ASTM D7012. The strength of intact sample can be used with Figure 1-4 to assign a classification as weak, strong, etc.

The point load strength can also be used to classify rock as indicated in Figure 1-4. Point load strength tests, described in ASTM D5731, are sometimes performed in the field for larger projects where rippability and rock strength are critical design factors. This simple field test can be performed on core samples and irregular rock specimens. The point load strength index, $I_{s(50)}$, is defined as:

$$I_{s(50)} = F \cdot \frac{P}{d^2} \quad \textbf{(1-4)}$$

$$F = \sqrt{\frac{D_e}{50}} \quad \textbf{(1-5)}$$

where:
F = size correction factor,
P = the applied force at failure,
d = the distance between the loaded points, and
D_e = equivalent core diameter.

This index is related to the direct tensile strength of the rock by a proportionality constant F depending on the size of sample. Useful relationships of point load tensile strength index to other parameters such as specific gravity, seismic velocity, elastic modulus, and compressive strength are readily available in the literature.

1-4.3.3 Classification by Durability.

Short-term weathering of rocks, particularly shales, and mudstones, can have a considerable effect on their engineering performance. The weatherability of these materials is extremely variable, and rocks that are likely to degrade on exposure should be further characterized by use of tests for durability under standard drying and wetting cycles. The slake durability test is a standardized procedure, described in ASTM D4644, used for this purpose. For example, if wetting and drying cycles reduces the grain size of shale, then rapid slaking and erosion in the field is probable when the rock is exposed. Another method used for this purpose is the jar slake test described by Santi (1998).

1-4.4 Rock Mass Classification Systems.

Various classification systems have been developed for classifying rock mass for engineering projects. Three of the main systems are described in this section. The

reader is encouraged to check for the classification system used in the region of practice and that most applies to the project in question.

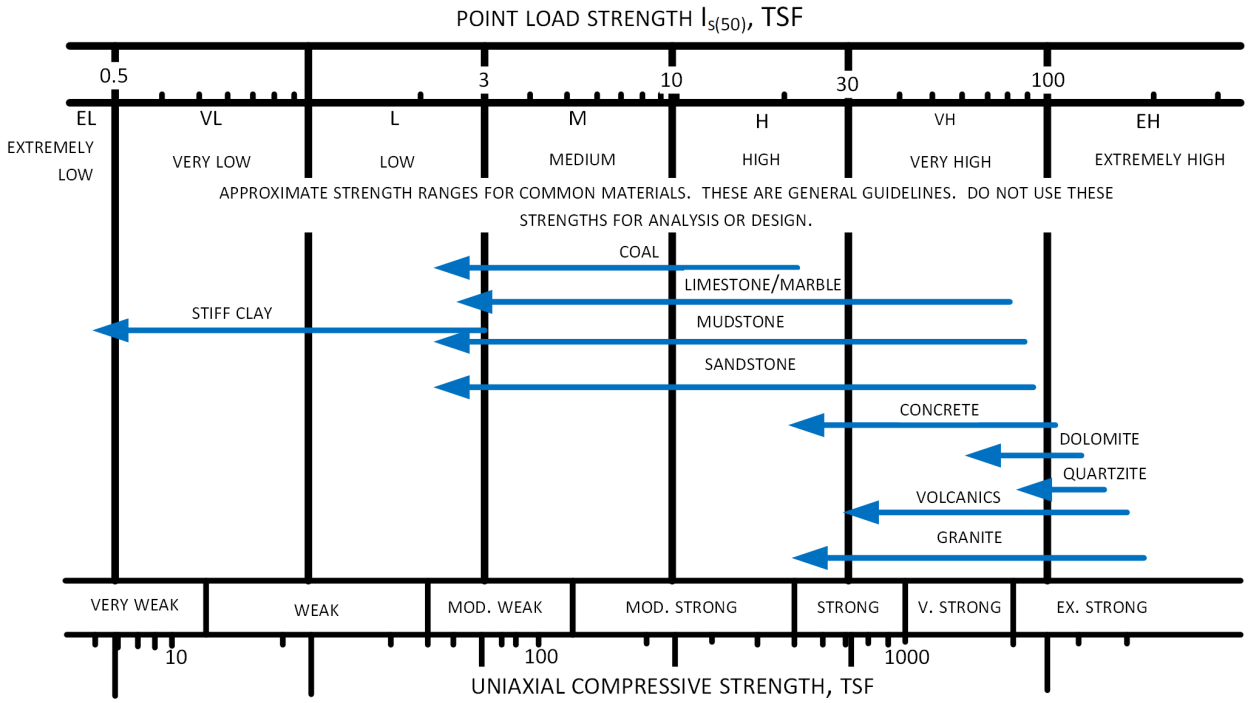

Figure 1-4 Rock Strength Characterization (after Broch and Franklin 1972)

The classification of the rock mass using some of these systems is useful to estimate physical and engineering properties using published values and charts. Also, some design methodologies rely on the classification of the rock mass.

1-4.4.1 *Q* System.

Barton et al. (1974) defines the value of Q in terms of RQD, the number of joint sets, the joint properties, and a stress reduction factor. Extensive tables are provided to guide the engineer in the selection of appropriate values. The roof pressure and support requirements for tunnels can be estimated from the value of Q, as well as some of the joint properties.

1-4.4.2 Rock Mass Rating System.

The rock mass rating system (RMR), also known as the Geomechanics classification, by Bieniawski (1973) classifies rock based on the uniaxial compressive strength, RQD, the spacing and properties of the joints, and groundwater conditions. While not solely intended for tunneling applications, the RMR can be related to stand-up time, unsupported active span length, and roof pressure.

1-4.4.3 Geological Strength Index.

The Geological Strength Index (GSI) has become a commonly used approach to describe rock mass quality in a qualitative manner (Marinos et al. 2007). Because it is closely linked to rock strength, GSI is most useful as a tool to help estimate rock properties for stability analysis. The GSI can be quantified as indicated in Figure 1-5; however, a range of values should always be used. Such values of GSI may be used as input for empirical equations for the shear strength of a rock mass.

The GSI is most useful for rock masses with many discontinuities that cannot be effectively modeled in direct fashion. According to Marinos et al. (2007), GSI should not be used for (1) rocks with clear discontinuities and well-defined dominant structure, (2) excavated faces in strong, hard rock with discontinuities spaced at similar dimensions to the tunnel or slope, or (3) low strength “young” rocks such as marls, claystones, siltstones, and weak sandstones. Marinos et al. (2007) developed a modified GSI system for heterogeneous rocks, such as layered shales and sandstones, as shown in Figure 1-6. The application of GSI to these rocks should account for their tendency to behave differently at depth compared to near the ground surface.

1-4.4.4 Other Classification Systems.

Some other classification systems have been proposed depending on the region, purpose, and needs. Some of these systems are summarized in Table 1-17.

Table 1-17 Other Rock Classification Systems

Rock Mass Classification System	Main Uses	Reference
Rock Structure Rating	Tunnel support and excavation and other ground support work in mining and construction	Skinner (1988)
Unified Rock Classification	Foundations, methods of excavation, slope stability, uses of earth materials, blasting characteristics of earth materials, and transmission of groundwater	Williamson and Kuhn (1988)
Rock Material Field Classification	Shallow excavation, particularly with regard to hydraulic erodibility in earth spillways, excavatability, construction quality of rock, fluid transmission, and rock-mass stability	NRCS (2002)
New Austrian Tunneling Method	Conventional (cyclical, such as drill and-blast) and continuous (tunnel-boring machine or TBM) tunneling; this is a tunneling procedure in which design is extended into the construction phase by continued monitoring of rock displacement; support requirements are revised to achieve stability	Lauffer (1997)
Coal Mine Roof Rating	bedded coal-measure rocks, in particular with regard to their structural competence as influenced by discontinuities in the rock mass	Molinda and Mark (1994)

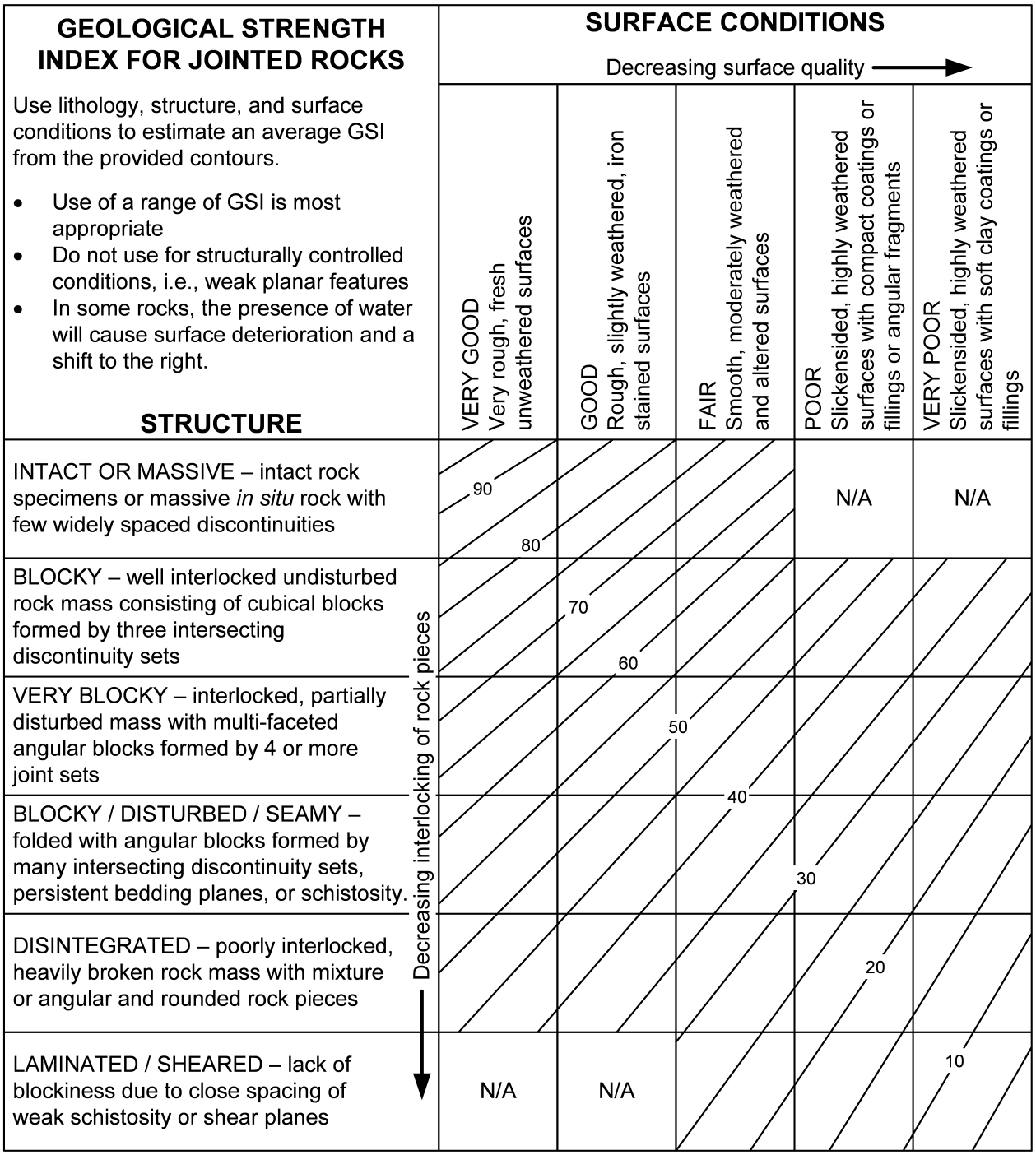

Figure 1-5 *GSI* Selection Chart for Jointed Rock (after Marinos et al. 2007)

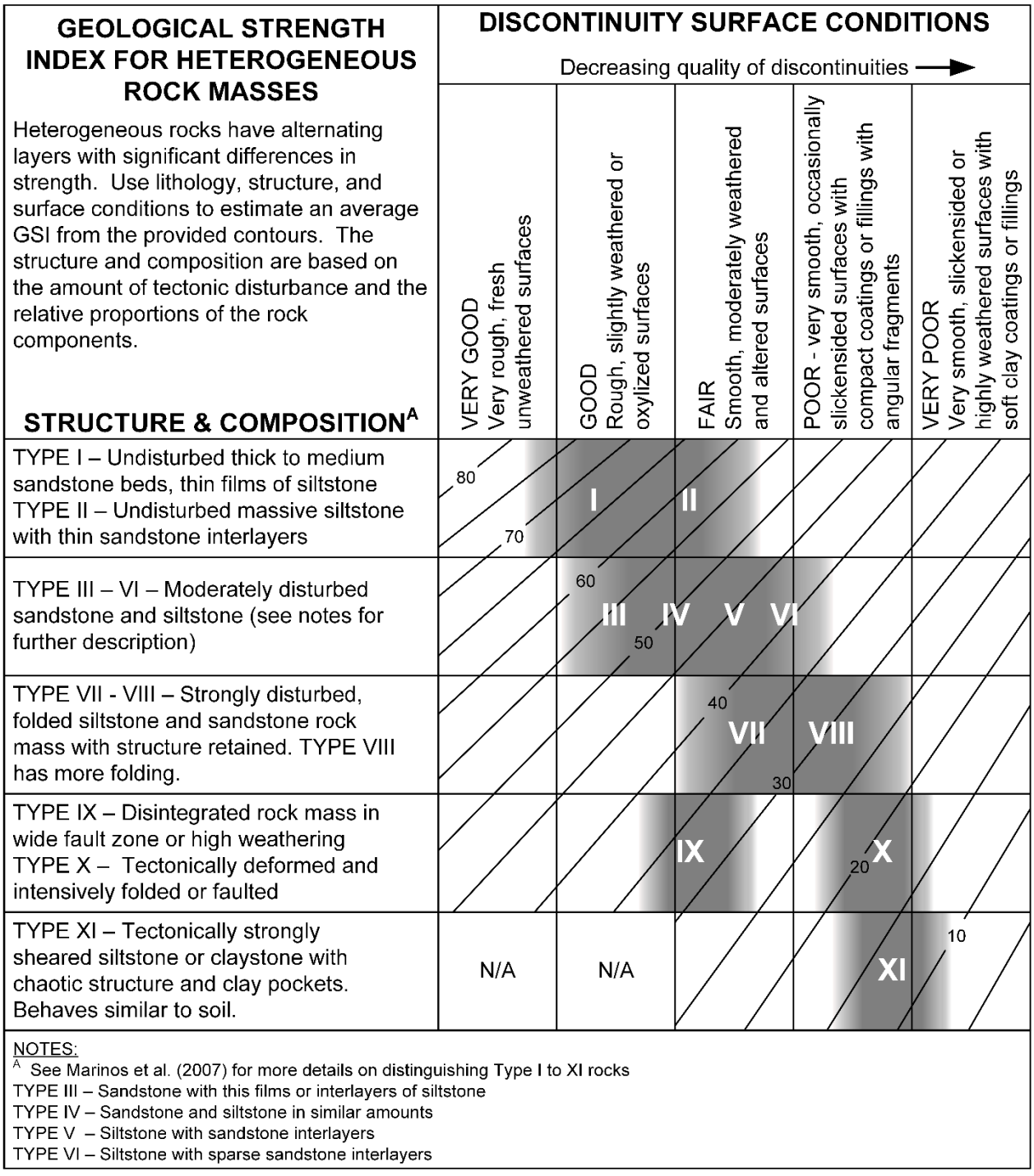

Figure 1-6 *GSI* Selection Chart for Heterogeneous Rock (after Marinos et al. 2007)

1-5 SPECIAL MATERIALS.

1-5.1 Expansive Soils.

1-5.1.1 Characteristics.

Expansive soils are distinguished by their potential for excessive volume increase upon access to moisture. The swelling potential and the magnitude of the swelling pressure are controlled by the clay minerals contained in the soil, the structure and fabric of the soil, overburden pressure, and other physical-chemical aspects of the soil (Holtz et al. 2011). These soils usually contain montmorillonite and vermiculite clay minerals. Expansive soils are characterized by a very high dry strength and high plasticity, are often shiny when cut with a knife, and are very weak when wet (Holtz et al. 2011). These soils usually form deep cracks during the dry season and expand closing the gaps creating a homogenous appearance during the wet season.

Even though expansive soils can be encountered at great depth, they are mainly a problem at shallow depths were the effect of variations in water content is greater (FHWA 2017). The zone affected by seasonal variation in water content is also called the *active zone* for expansive soils. This is very important when designing foundations, roads, etc.

According to Holtz et al. (2011) expansive soils can be found around the world. In the United States, the regions with the greatest occurrence of highly expansive soils are North and South Dakota, Montana, eastern Wyoming, eastern Colorado, the Four Corners Region, California, and east Texas. Figure 1-7 illustrates the distribution of expansive soils throughout the United States.

1-5.1.2 Identification and Classification.

Expansive soils can be identified in various ways, and their swelling potential can be nominally predicted. Expansive soils can sometimes be identified during visits to a project site by looking for cracks in nearby structures or desiccation cracks in the soil surface. Another method is identifying the clay minerals in the soil. If the soil has highly expansive clay minerals (e.g. montmorillonite), that is a good indication that the soil could be expansive. Some of the methods that can be used to identify clay minerals are x-ray diffraction, differential thermal analyses, cation exchange capacity, and electron microscopy.

Soil plasticity is often used to identify expansive soils. As the plasticity index or liquid limit of the soils increases, the potential for swelling upon contact with water also tend to increase. Dakshanamurthy and Raman (1973) presented the method shown in Table 1-18 to infer the swelling potential based on the liquid limit. The information presented in Table 1-19 and Figure 1-8 provides another method of assessing the potential for volume change of a given soil.

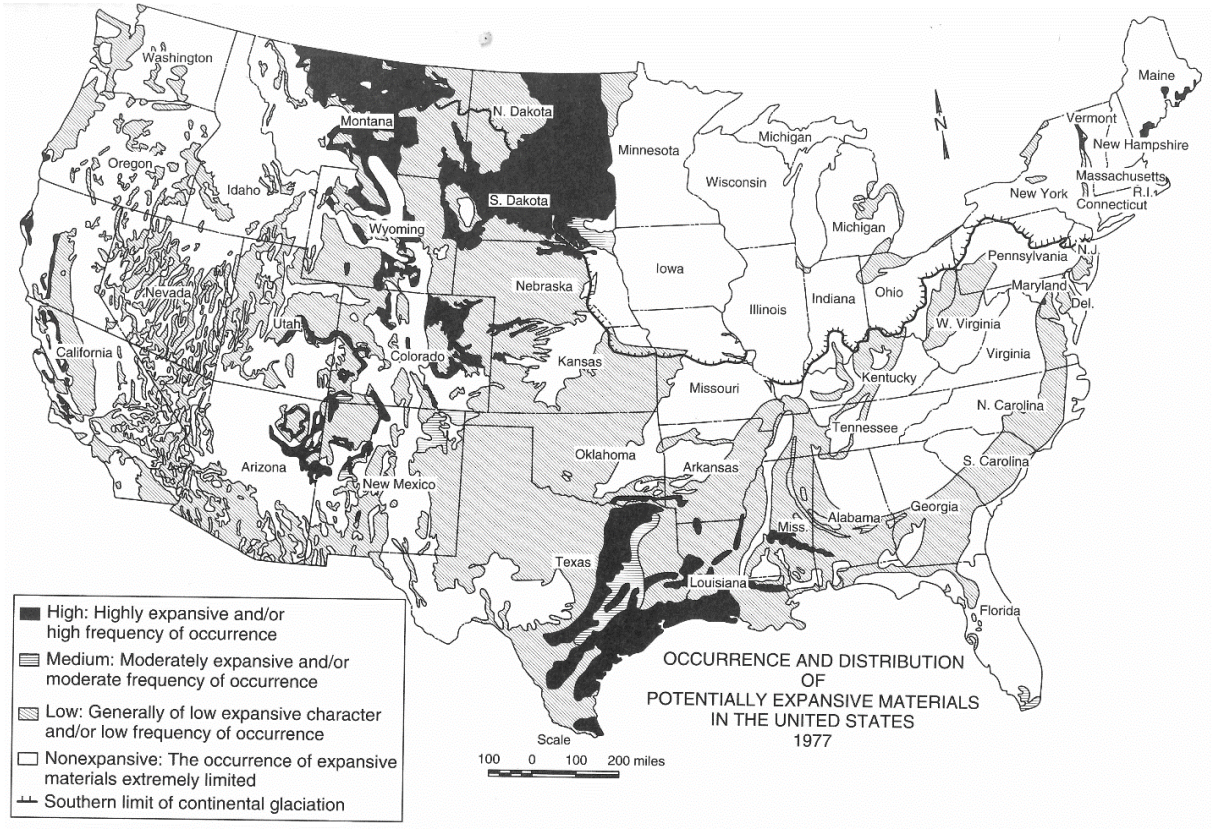

Figure 1-7 Expansive Soils in the United States (Nelson and Miller 1992)

Table 1-18 Swelling Potential (Dakshanamurthy and Raman 1973)

Liquid Limit	Classification
0 to 20	Non-Swelling
20 to 35	Low-Swelling
35 to 50	Medium-Swelling
50 to 70	High Swelling
70 to 90	Very High Swelling
> 90	Extra High Swelling

Table 1-19 Expansion Potential from Classification Test Data (Holtz et al. 2011)

Degree of Expansion	Probable Expansion as a Percent of Total Volume Change (Dry to Saturated Condition)[1]	Colloidal Content (% < 1μm)	Plasticity Index	Shrinkage Limit
Very high	>30	> 28	>35	<11
High	20-30	20-31	25-41	7-12
Medium	10-20	13-23	15-28	10-16
Low	<10	<15	<18	>15

[1]Under a surcharge of 1 psi.

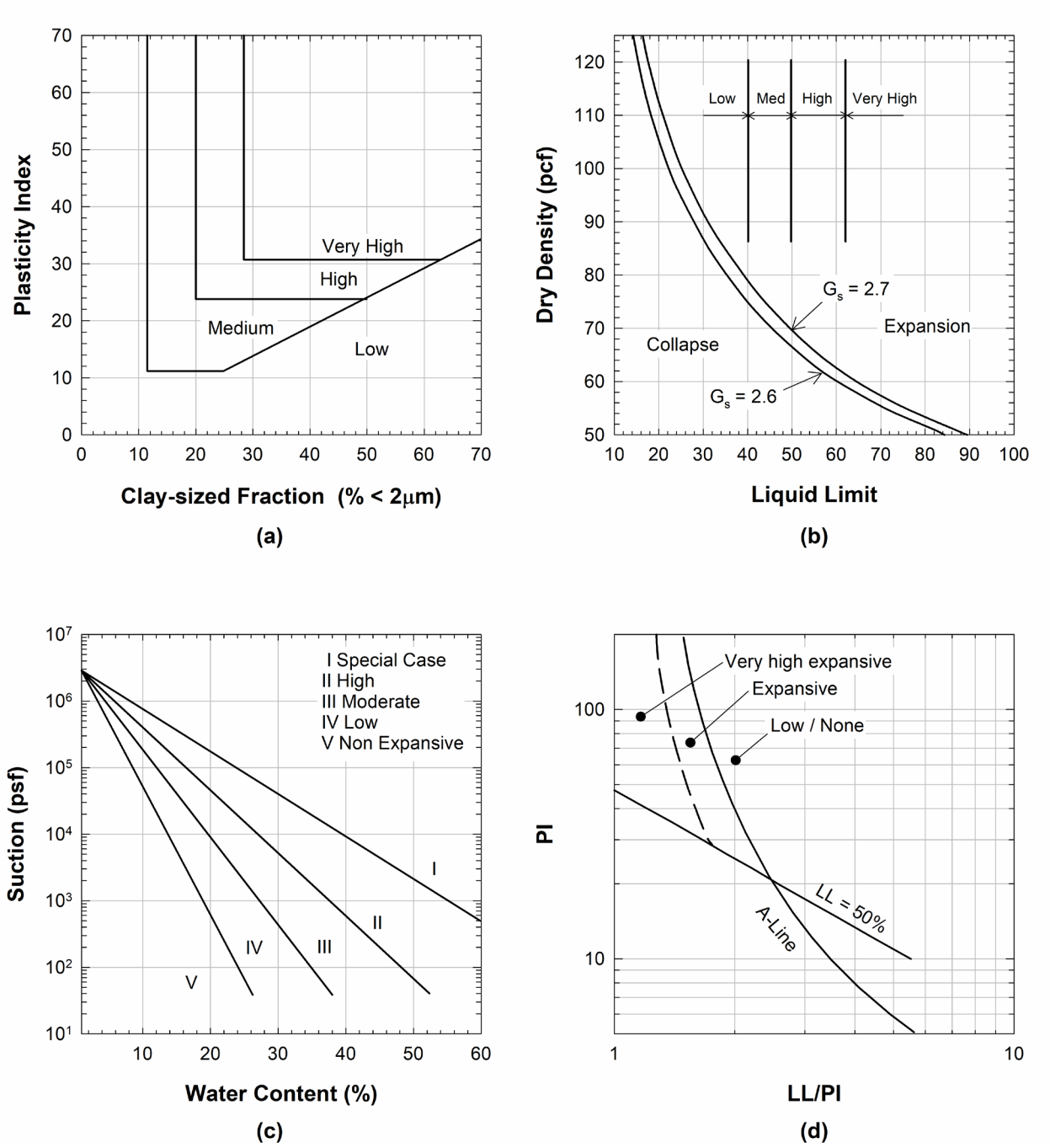

Figure 1-8 Soil Expansion Prediction (after Holtz et al. 2011)

The International Building Code 2018 (ICC 2018) considers a soil to be expansive if these four criteria are met:

1) Plasticity index equal or greater than 15 as determined using ASTM D4318,
2) More than 10% of soil particles passing a No. 200 (75 μm) sieve, as determined using ASTM D6913 or D1140,
3) More than 10% of soil particles are less than 5 μm in size, as determined using ASTM D7928, and
4) Expansion index is greater than 20, as determined using ASTM D4829 (described below).

If the soil shows compliance with Item 4, it is not necessary to show compliance with Items 1 through 3.

Two laboratory tests have standardized procedures to measure the swelling potential of soils. In the *Expansion Index test* (ASTM D4829), the soil is compacted in a rigid mold at a water content and unit weight that gives a degree of saturation of 50% ± 2%. A vertical confining pressure of 1 psi is applied to the specimen before the specimen is submerged in distilled water, and the deformation of the specimen is recorded for 24 hours or until the rate of deformation is below 0.0002 inch/hour, whichever occur first with a minimum recording time of 3 hours. This test is used to obtain the expansion index of the soil, defined as follows:

$$EI = \frac{\Delta H}{H_i} \times 1000 \qquad \textbf{(1-6)}$$

where,
EI = expansion index,
ΔH = change in height during the test, and
H_i = initial height of the test specimen.

According to ASTM D4829, the expansion index can be used to estimate the swelling potential of soils as described in Table 1-20.

Table 1-20 Classification of Potential Expansion of Soils using EI (ASTM D4829)

Expansion Index, EI	Potential Expansion
0-20	Very low
21-50	Low
51-90	Medium
91-130	High
>130	Very High

The one-dimensional swell or collapse test (ASTM D4546) can also be used to measure expansion potential. This test method allows intact samples and samples compacted at different water contents and compactive effort to be tested. In addition, this test allows different loading conditions, wetting and drying schedules, and reading intervals to be used.

1-5.2 Collapsing Soils.

1-5.2.1 Characteristics.

Collapsing soils are distinguished by their potential to undergo large decrease in volume upon increase in moisture content without an increase in external loading. When dry, these soils are stable and able to support significant structural loads. Examples of soils exhibiting this behavior are loess, weakly cemented sands and silts where cementing agent is soluble (e.g., soluble gypsum, halite, etc.), and certain granite residual soils. A common feature of collapsible soils is loose bulky grains held together by capillary stresses. Collapsible soils are also characterized by loss of strength when wetted, low density, moisture sensitivity, and the presence of gypsum or anhydrite. Deposits of collapsible soils are usually associated with regions of moisture deficiency (arid or semi-arid regions). According to FHWA (2017), the following conditions are necessary for collapse to occur:

1) an open, and partially saturated and unstable fabric,
2) enough total stress to make the soil structure metastable,
3) existence of a bonding agent or negative pore pressures to create a metastable structure, and
4) addition of water to destroy the metastable structure.

The collapse of soils supporting structures can cause significant damage as a result of total and differential settlement. The magnitude of the collapse depends on factors, such as the soil composition, dry density, water content, confining stress, and the agent causing the metastable structure. For this reason, it is important to identify collapsible soils during the subsurface investigation so they can be remediated or considered in the design phase.

1-5.2.2 Identification and Classification.

One method to identify the potential of soils to collapse is presented by Holtz et al. (2011) using data from the USBR and is shown in Figure 1-9. From this figure, the potential for collapse increases with decreasing liquid limit and *in situ* dry density.

Ayadat and Hanna (2007b) presented a detailed study on the potential of collapse of soil. In this study, they investigated the effect of the uniformity coefficient, water content, and dry unit weight on the collapse potential. Figure 1-10 was presented as a method to assess the potential for a soil to be collapsible along with a detailed method

to estimate the strain caused by collapsing for different soils. Ayadat and Hanna (2007a) also presented a method to assess the potential for a soil to be collapsible using the fall cone apparatus (Section 3-2.4.2.6).

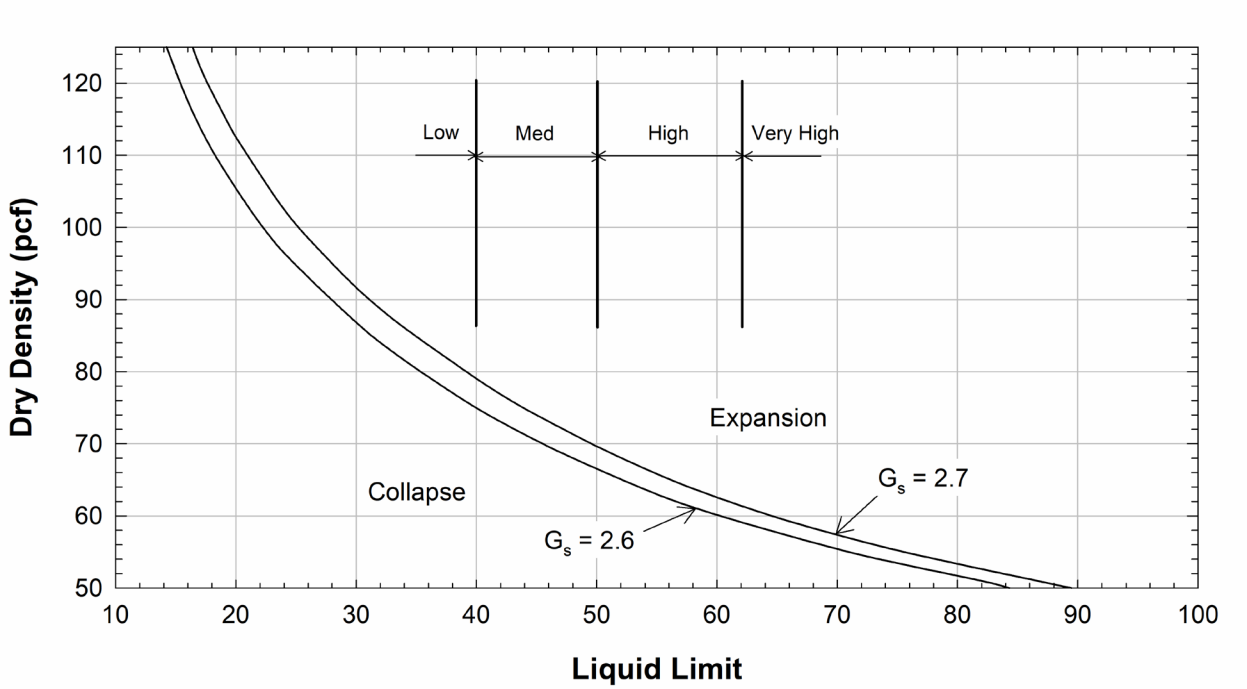

Figure 1-9 Collapsibility Based on *In situ* Dry Density and Liquid Limit (after Holtz et al. 2011)

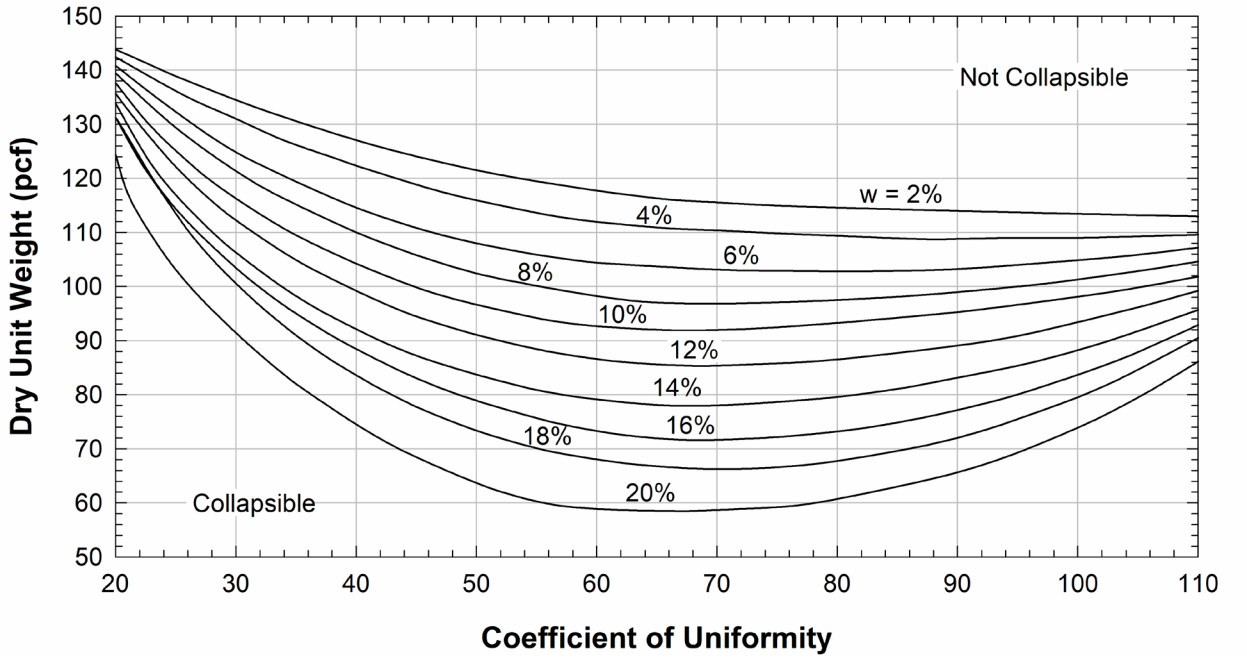

Figure 1-10 Design Charts for Predicting Collapse Behavior of Soils (after Ayadat and Hanna 2007b)

A method for quantifying the collapse potential of soils is presented in ASTM D4546. This test method allows intact samples and samples compacted at different water contents and compactive effort to be tested in a one-dimensional apparatus. In this test, the specimen is loaded to a desired normal stress using any loading sequence, water is added, and the vertical displacement is monitored.

1-5.3 Frost Susceptibility and Permafrost.

1-5.3.1 Characteristics.

In non-frost susceptible soil, a typical volume increase due to ground freezing is about 4%. This volume increase is caused by the increase in water volume as it freezes. In soils susceptible to frost, soil heave is much greater as water flows to colder zones forming ice lenses. The formation of ice lenses typically is not uniform, meaning that the increase in volume is not evenly distributed throughout a site and can cause distress to structures. During warmer weather, the soil and ice lenses will tend to thaw from the top down. Water can become trapped in the soil near the surface, leading to an increase in water content and softening of the soil. The associated loss of support can be even more detrimental to structures than the frost heave itself. This is specially a problem for pavement structures and structures supported on shallow foundations, as well as utilities, if not buried well below the depth of freezing.

Permafrost refers to a thick top later of soil that stays frozen throughout the year. Permafrost particularly occurs in the Northern Hemisphere, including Canada and Alaska. Construction in permafrost is very challenging and requires special considerations during design and construction.

1-5.3.2 Identification and Classification.

Problematic frost action requires both frost penetration into the ground and frost susceptible soils. According to Holtz et al. (2011), if the frost penetration during the worst part of the winter is less than about 0.30 m, frost heave should not be of concern to structures. The maximum depths of frost penetration in the United States are shown in Figure 1-11. These depths are for extremely cold winters without much snow cover. Snow cover, especially early in the winter, will decrease the frost depth significantly.

Silts are the most susceptible to frost heave, but most soils with some fines content have also some susceptibility to freezing. This includes soils classifying as SM, ML, GM, SC, GC, and CL. Holtz et al. (2011) presented the information shown in Table 1-21 summarizing a design classification system for frost susceptible soils. This system uses the soil classification system and the percent of soil finer than 0.02 mm ($8x10^{-4}$ inches) to assess the susceptibility to freezing.

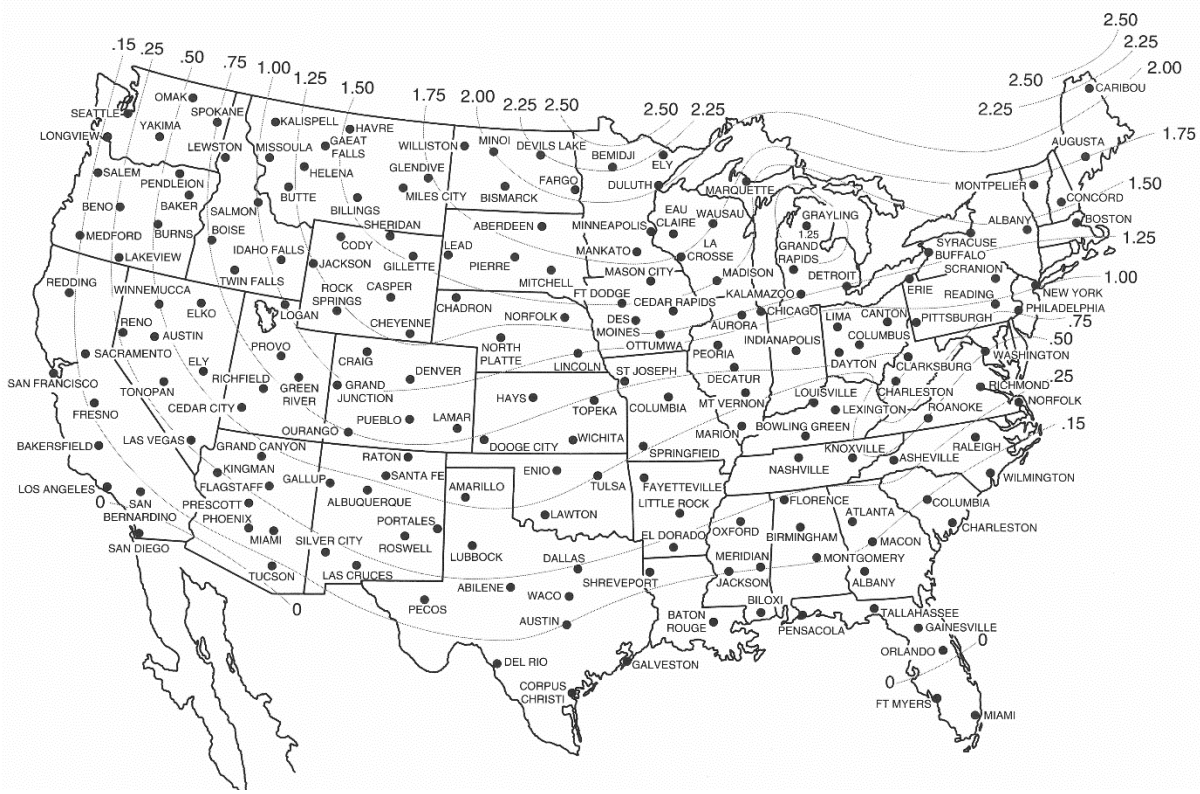

Figure 1-11 Maximum Depths (in meters) of Frost Penetration in the Continental United States (NOAA 1978)

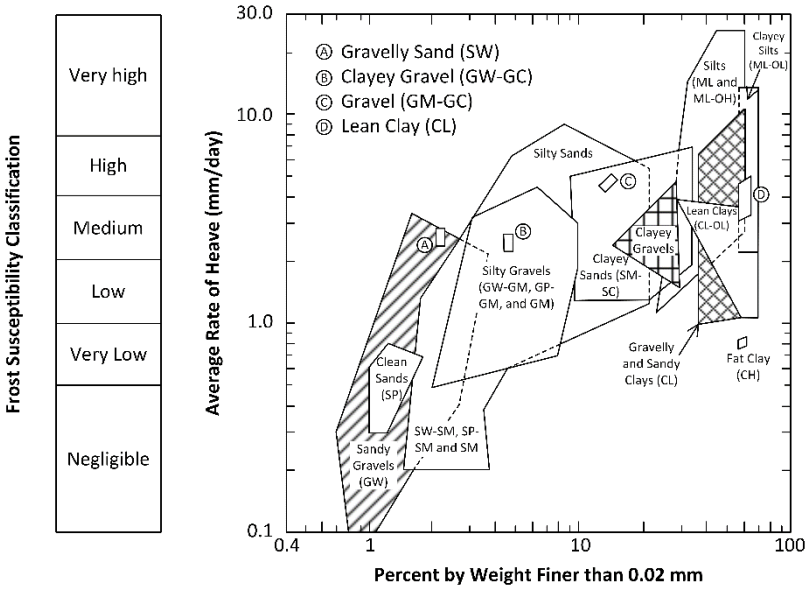

Figure 1-12 Rates of Heave in Laboratory Freezing Tests on Remolded Soils (U.S. Department of the Army 1984)

Table 1-21 U.S. Army Corps of Engineers Frost Design Soil Classification

Frost Group	Frost Susceptibility	Soil Type	Percent Finer than 0.02 mm	Typical USCS Classification
Not frost-susceptible (NFS)	Negligible to low	Gravels, crushed stone and rock	0-1.5	GW, GP
		Sands	0-3	SW, SP
Possibly frost-susceptible (PFS)	Possibly	Gravels, crushed stone and rock	1.5-3	GW, GP
		Sands	3-10	SW, SP
S1	Very low to medium	Gravelly soils	3-6	GW, GP, GW-GM, GP-GM
S2	Very low to medium	Sandy soils	3-6	SW, SP, SW-SM, SP-SM
F1	Very low to high	Gravelly soils	6-10	GM, GW-GM, GP-GM
F2	Medium to high	Gravelly soils	10-20	GM, GM-GC, GW-GM, GP-GM
		Sands	6-15	SM, SW-SM, SP-SM
F3	Medium to very high	Gravelly soils	>20	GM, GC
		Sands except very fine silty sands	>15	SM, SC
	Low	Clays, PI >12		CL, CH
F4	Low to very high	All silts		ML, MH
		Very fine silty sands	>15	SM
	Low to high	Clays, PI <12		CL, CL-ML
	Very low to very high	Varved clays and other fine-grained banded sediments		CL and ML; CL, ML, and SM; CL, CH, and ML; CL, CH, ML and SM.

Figure 1-12 relates the rate of frost heave to the percent of particles finer than 0.02 mm ($8x10^{-4}$ inches) based on USCS classification. This figure also includes the susceptibility classification for each type of soil. The information presented in this figure is based on laboratory testing by the U.S. Department of the Army (1984). According to Holtz et al. (2011), these rates are higher than those expected in the field, and soils with a laboratory rate of frost heave of up to 1 mm/day (0.04 inches/day) can be used under pavements, unless severe conditions are expected, but some frost heave should be expected.

1-5.4 Limestone and Related Materials.

1-5.4.1 Characteristics.

Limestone, dolomite, gypsum, and anhydrite are characterized by their solubility and thus the potential for the presence and/or development of cavities. Limestones are defined as those rocks composed of more than 50% carbonate minerals of which 50% or more consist of calcite and/or aragonite. Some near-shore carbonate sediments (also called limestone, marl, and chalk) could fit this description. Such sediments are noted for erratic degrees of induration, and thus variability in load supporting capacity and uncertainty in their long-term performance under sustained loads. The most significant limestone feature is its solubility. An extremely soluble limestone can contain many solution caves, channels, or other open, water, or clay-filled features. These features are often referred to as *karst* geology or topography.

Karst features that present important engineering challenges include vertical and horizontal fissures and joints, pinnacles, and sinkholes. Fissures and joints may contain very weak soil and also provide conduits for the flow of water, which are particularly problematic for water retaining structures. *Pinnacles* are spires or spines of rock left behind by the dissolution process and result in very uneven foundation support. *Sinkholes* are the result of soil erosion into karst voids or the sudden collapse of voids. Structures and pavements can be catastrophically damaged by sinkholes.

1-5.4.2 Identification and Classification.

The identification of karstic areas should start by desk studies and site visits to look for surface expressions of solution features. Sinkholes are the surface expression of rock dissolution and can be used to infer that karstic rocks are found in the area. Aerial photos, local geology maps, LIDAR data, etc. are also a useful source of information to identify features that are caused by karstic rocks. A map of the karst and potential karst areas in the United States presented by USGS (2014) is shown here in Figure 1-13.

A subsurface investigation program is very important in karstic areas to better characterize the possible caverns, sinkholes, pinnacles, etc. Drilling is a very powerful tool for this purpose and should be done more extensively in this type of terrain (FHWA 2017). Geophysical techniques, including shallow seismic refraction, resistivity, and gravimetry, are often found to be valuable supplements. The suggested methods by ASTM D6429 to estimate the depth to bedrock and the occurrence of sinkholes and voids is presented in Table 1-22.

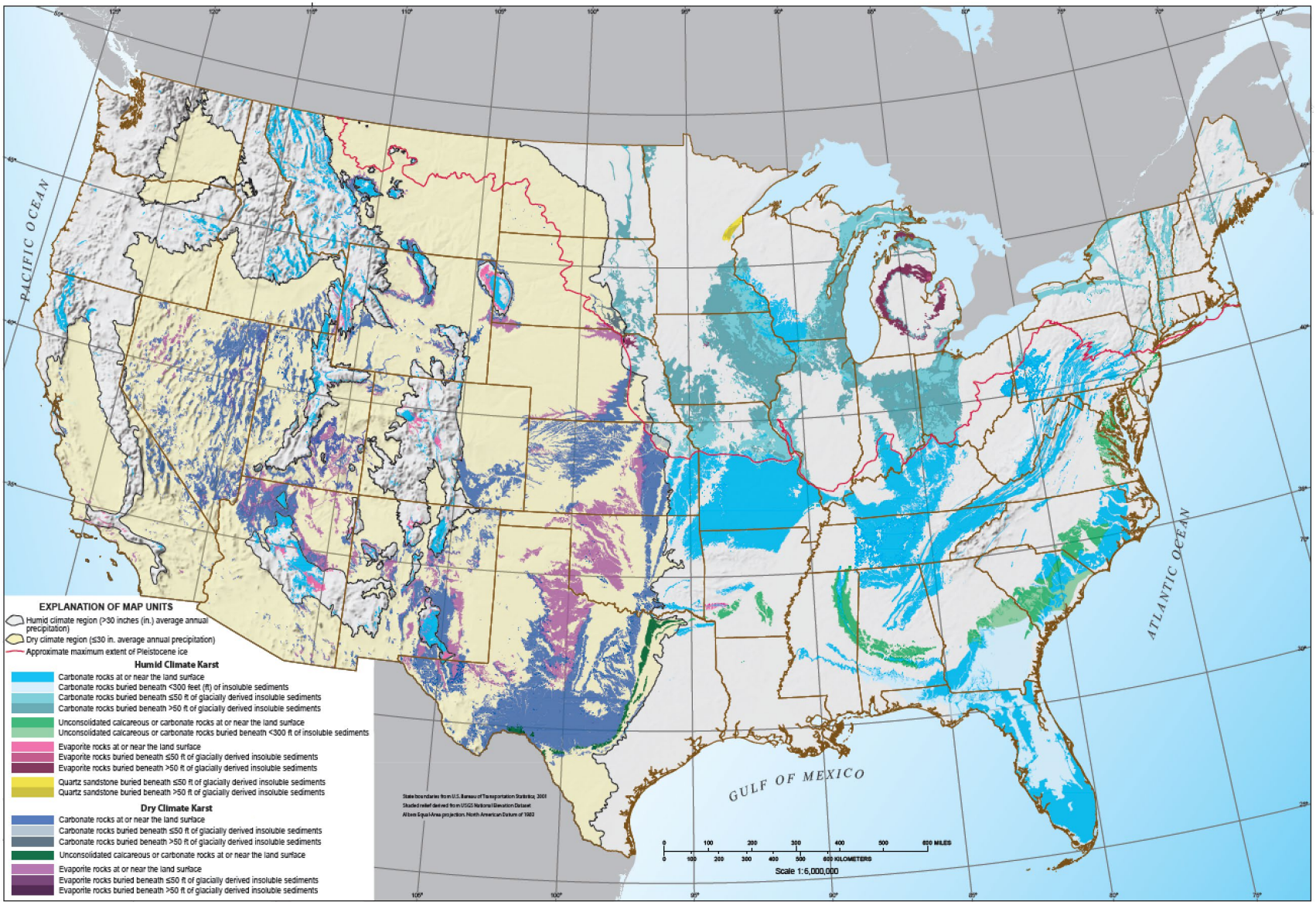
PACIFIC OCEAN
ATLANTIC OCEAN
GULF OF MEXICO
EXPLANATION OF MAP UNITS
Humid climate region (>30 inches (in.) average annual precipitation)
Dry climate region (≤30 in. average annual precipitation)
Approximate maximum extent of Pleistocene ice
Humid Climate Karst
Carbonate rocks at or near the land surface
Carbonate rocks buried beneath <300 feet (ft) of insoluble sediments
Carbonate rocks buried beneath ≤50 ft of glacially derived insoluble sediments
Carbonate rocks buried beneath >50 ft of glacially derived insoluble sediments
Unconsolidated calcareous or carbonate rocks at or near the land surface
Unconsolidated calcareous or carbonate rocks buried beneath <300 ft of insoluble sediments
Evaporite rocks at or near the land surface
Evaporite rocks buried beneath ≤50 ft of glacially derived insoluble sediments
Evaporite rocks buried beneath >50 ft of glacially derived insoluble sediments
Quartz sandstone buried beneath ≤50 ft of glacially derived insoluble sediments
Quartz sandstone buried beneath >50 ft of glacially derived insoluble sediments
Dry Climate Karst
Carbonate rocks at or near the land surface
Carbonate rocks buried beneath ≤50 ft of glacially derived insoluble sediments
Carbonate rocks buried beneath >50 ft of glacially derived insoluble sediments
Unconsolidated calcareous or carbonate rocks at or near the land surface
Evaporite rocks at or near the land surface
Evaporite rocks buried beneath ≤50 ft of glacially derived insoluble sediments
Evaporite rocks buried beneath >50 ft of glacially derived insoluble sediments
State boundaries from U.S. Bureau of Transportation Statistics, 2005
Shaded relief derived from USGS National Elevation Dataset
Albers Equal-Area projection, North American Datum of 1983
0 100 200 300 400 500 600 MILES
0 100 200 300 400 500 600 KILOMETERS
Scale 1:6,000,000

Figure 1-13 Karst and Potential Karst Areas in Soluble Rocks in the Contiguous United States (USGS 2014)

Table 1-22 Selection of Geophysical Method (after ASTM D6429)

Application or Method	Seismic		Electrical	Electromagnetic				
	Refraction or Reflection	MASW	DC Resistivity	Freq. Domain	Time Domain	Very Low Frequencies	Ground Penetrating Radar	Gravity
Depth to rock	A	A	B	B	B	B	A	B
Voids and sinkholes	B	A	B	B	B		A	A

Notes: “A” means preferred method and “B” alternate method based on the 2020 version of the standard.

1-5.5 Coral and Coral Formation.

1-5.5.1 Characteristics.

Living coral and coralline debris are generally found in tropical regions where the water temperature exceeds 20°C. Coral is a term commonly used for the group of animals which secrete an outer skeleton composed of calcium carbonate, and which generally grow in colonies. The term *coral reef* is often applied to large concentrations of such colonies which form extensive submerged tracts around tropical coasts and islands. In general, coralline soils deposited after the breakdown of the reef, typically by wave action, are thin (a few meters thick) and form a veneer upon cemented materials (limestones, sandstones, etc.).

Coralline deposits are generally poor foundation materials in their natural state because of their variability and susceptibility to solution by percolating waters, and their generally brittle nature. Coralline materials are often used for compacted fill for roads and light structures. Under loads, compaction occurs as the brittle carbonate grains fracture and consolidate. They can provide a firm support for mats or spread footings bearing light loads, but it is necessary to thoroughly compact the material before using it as a supporting surface. Heavy structures in coral areas are generally supported on pile foundations because of the erratic induration. Predrilling frequently is required.

Because of extreme variability in engineering properties of natural coral formations, it is not prudent to make preliminary engineering decisions on the basis of "typical properties." Unconfined compression strengths of intact specimens may range from 50 tsf to 300 tsf.

1-5.5.2 Identification and Classification.

Because the granular coralline and algal materials are derived from organisms which vary in size from microscopic shells to large coral heads several meters in diameter, the fragments are broadly graded and range in size from boulders to fine-grained muds. Similarly, the shape of these materials varies from sharp, irregular fragments to well-rounded particles. Coralline deposits are generally referred to as "biogenic materials"

by geologists. When cemented, they may be termed "reefrock," or "beachrock," or other names which imply an origin through cementation of particles into a hard, coherent material.

1-5.6 Quick Clays.

1-5.6.1 Characteristics.

Quick clays are clays from marine origin that are characterized by their very high sensitivity or strength reduction upon disturbance. Quick clays are formed when the formation water containing salts is replaced with fresh water. Disturbance of these clays can be caused by construction activities or seismic ground shaking. In their undisturbed state, they are relatively strong. Following disturbance, they become very weak and possibly liquid. Because of their brittle nature, collapse occurs at relatively small strains. This type of clay is normally found in Norway, Canada, Sweden, Finland, Russia, the United States and other locations around the world. The Leda clay and Champlain Sea clay in Canada are examples of quick materials.

1-5.6.2 Identification and Classification.

Quick clays are readily recognized by measured sensitivities greater than about 15 and by the distinctive, strain-softening shape of their stress-strain curves from strength or compressibility tests. The sensitivity of clays is defined as the ratio of the undrained shear strength in the undisturbed state to that in the disturbed state. The *in situ* liquidity index of quick clays is typically above one, which means the water content is in excess of the liquid limit.

1-5.7 Other Materials and Considerations.

1-5.7.1 Man-made Fills.

Man-made fills can be divided into engineered fills and uncontrolled fills. Engineered fills are fills that were properly compacted to a specified density within a specified range of water contents. These fills are normally strong, have low compressibility, and are very favorable for building foundations. More detail on engineered fill can be found in NAVFAC DM 7.2 (NAVFAC 1982).

Uncontrolled fills are very problematic because these fills were placed under conditions that were not controlled and/or the materials that compose these fills were not controlled. These fills can be made from uncompacted soils and may contain deleterious building debris, old pavement, or concrete. Because of the variability of the materials and uncontrolled placement conditions, the engineering properties are very unpredictable and should be analyzed on a case-by-case basis.

1-5.7.2 Chemically Reactive Soils.

For foundation construction, the main concerns related to chemically reactive soils are usually are corrosion and gas generation. Corrosive soils can be problematic when dealing with foundations, especially steel foundation systems. Potential for corrosion must be considered in the design of foundations compared to the design life of the structure. Protection systems can be used to reduce the corrosion rate. For concrete foundations, increasing the cover thickness over the steel, the use of additive treated concrete, or a specialized cement for this purpose can help mitigate the effect of corrosion on the reinforcement.

Corrosion potential is determined in terms of pH, resistivity, stray current activity, groundwater position, chemical analysis, etc. Based on this information, a compatible foundation treatment, (e.g., sulfate resistant concrete, lacquers, creosote, cathodic protection, etc.) can be prescribed. According to AASHTO (2017), a soil is considered have high corrosion potential if: (1) the resistivity is less than 2,000 ohm-cm, (2) the pH less than 5.5, (3) pH between 5.5 and 8.5 for soils with high organic content, (4) the sulfate concentration is greater than 1,000 ppm, (5) is subjected to mine or industrial drainage, or (6) the chloride concentration is greater than 500 ppm.

The location of the water table also influences the corrosion rate. Decker et al. (2008) observed higher corrosion rate on steel piles in the section located above the water table in the fluctuation zone.

FHWA (2009) presents an extensive study on the corrosion potential of soils focused on MSE walls. Table 1-23 indicates regions in the United States with soils with high potential for corrosion.

Table 1-23 Corrosive Soil Environments (FHWA 2009)

Environment	Prevalence	Characteristics
Acid-Sulfate Soils	Appalachian Regions	Pyritic, pH < 4.5, SO_4 (1000 to 9000 ppm), Cl^- (200 to 600 ppm)
Sodic Soils	Western States	pH > 9, high in salts including SO_4 and Cl^-
Calcareous Soils	FL, TX, NM and Western States	High in carbonates, alkaline but pH<8.5, mildly corrosive
Organic Soils	FL (Everglades), GA, NC, MI, WI, MN	Contain organic material in excess of 1% facilitating microbial induced corrosion
Coastal Environments	Eastern, Southern and Western Seaboard States and Utah	Atmospheric salts and salt laden soils in marine environments
Road Deicing Salts	Northern States	Deicing liquid contain salts that can infiltrate into soils
Industrial Fills	Slag, cinders, fly ash, mine tailings	Either acidic or alkaline and may have high sulfate and chloride content

For gas concentration, organic matter content and field testing for gas are usually performed. If gas generation is expected, some form of venting system is designed. The potential presence of noxious or explosive gases should be considered during the construction excavations and tunneling.

1-5.7.3 Lateritic Soils.

Lateritic soils are found in tropical climates throughout the world. These soils are rich in iron and aluminum. Because of the high iron content, most of these soils have a rusty-red color. Extensive weathering of the parent rock normally develops these soils. These soils can be problematic because of their loss in strength with time, high void ratio and permeability, aggregate deterioration, and shrinkage cracks. These soils tend to have shear strength characteristics between those of sands and silts. They are prone to cause landslides, have highly variable moisture content, and provide erratic conditions for foundations.

1-5.7.4 Calcareous Sands.

Calcareous sands are composed mainly of the skeletal remains of marine organism having high carbonate content. These sands have significant intra-particle voids created by shells that have not broken yet and by the cavities in the corals. These sands are also characterized by having angular particles. The engineering properties of these sands vary over a wide range and are controlled by the cementation and the structure of the sand. More information on calcareous sands can be found in an ASTM Special Technical Publication on the topic (ASTM International 1981).

1-5.7.5 Submarine Soils.

Ocean environments contains the following main topographic features: (1) the continental margin including the continental shelf fringing the coast and the continental slope; (2) the continental rise; and (3) the abyssal plains with local seamounts and trenches (Randolph and Gourvenec 2011). The distribution of marine sediments along those geomorphological regions varies with thickest sediment deposits being mostly near continents and thinnest on recently formed mid-oceanic ridges. Continental margins contain almost 75% of marine sediments, while only representing 20% of the seabed area. The continental rise is also considered a depositional feature with sediment thickness reaching locally up to 1.6 km (Randolph and Gourvenec 2011).

Marine sediments are either terrigenous (i.e., transported from land to the ocean), or pelagic (i.e., settled through the water column). Coastal and nearshore zones are dominated by terrigenous sediments. Terrigenous sediments are often granular silicate minerals formed from erosion (lithogenous). Pelagic sediments are often finer and derived from insoluble remains of marine organisms. Poulos (1988) presented samples from abyssal plain and hill environments and found that most samples from abyssal

plains and hills characterized as clayey silt to clay. Ocean sediment mapping also revealed that deep ocean floors are widely covered with calcareous ooze that classified as mostly silty clay (Poulos 1988).

Marine sediments that were deposited slowly and remained undisturbed from physical, chemical, benthic biogenic, and/or anthropogenic processes are commonly normally consolidated. Overconsolidated sediments can result from glaciation, recent sediment erosion, or submarine landslides. Underconsolidated marine sediments can follow from rapid sedimentation events and recent sediment dynamics, as well as from benthic biogenic processes, amongst others. More information on the stress states of marine sediments can be found in Randolph and Gourvenec (2011).

The following key differences between marine and terrestrial sediments can be listed:

- Environmental conditions cover a wider range of pressures (depending on water depth) and temperature and can affect the engineering behavior of marine sediments, particularly in deep ocean environments.
- Oceans feature saline water. Local salinity may affect the engineering behavior, particularly of clays.
- Hydrodynamic conditions (i.e., waves, tides, currents) vary on spatial and temporal scales, particularly in nearshore environments and on the continental shelf. Hydrodynamic forcing can exert stresses onto the seabed and change pore pressures. It also drives sediment dynamics, potentially leading to complex sediment dynamics including erosion, transport, and deposition, and resulting in geomorphodynamics including the formation, destruction, and migration of bedforms on scales of centimeters to hundreds of meters. These processes affect sediment composition, texture, and thus, engineering properties.

1-6 SUGGESTED READING.

Topic	Reference
Soil Classification	Holtz, R. D., Kovacs, W. D., and Sheehan, T. C. (2011). *An Introduction to Geotechnical Engineering*. Pearson.
	FHWA. (2017). *Geotechnical Engineering Circular No. 5 - Geotechnical Site Characterization*. U.S. Department of Transportation - Federal Highway Administration, Washington, DC.
Rock Description and Classification	Hoek, E. (2007). *Practical Rock Engineering*.
	ASTM. (1988). *Rock Classification Systems for Engineering Purposes - STP984*. ASTM International.
Expansive and Collapsing Soils	Holtz, R. D., Kovacs, W. D., and Sheehan, T. C. (2011). *An Introduction to Geotechnical Engineering*. Pearson.
	FHWA. (2017). *Geotechnical Engineering Circular No. 5 - Geotechnical Site Characterization*. U.S. Department of Transportation - Federal Highway Administration, Washington, DC.
Frost Susceptibility	U.S. Department of the Army. 1984. *Engineering and Design - Pavement Criteria for Seasonal Frost Conditions - Mobilization Construction - EM 1110-3-138*.
Limestone / Karst	FHWA. (2017). *Geotechnical Engineering Circular No. 5 - Geotechnical Site Characterization*. U.S. Department of Transportation - Federal Highway Administration, Washington, DC.
	Veress, M. (2020). “Karst Types and Their Karstification.” *Journal of Earth Science*, 31(3), 621–634.
	Waltham, A. C., and Fookes, P. G. (2003). “Engineering Classification of Karst Ground Conditions.” *Quarterly Journal of Engineering Geology and Hydrogeology*, 36, 101–118.
Lateritic Soils	Wesley, L. D. (2010). *Geotechnical Engineering in Residual Soils*. John Wiley & Sons, Ltd.
Submarine Soils	Randolph, M., and Gourvenec, S. (2011). *Offshore Geotechnical Engineering*. CRC Press.

1-7 NOTATION.

Symbol	Description
C_u	Coefficient of uniformity
C_c	Coefficient of curvature
d	Distance between the loaded points in rock point load test
D_e	Equivalent core diameter
D_{10}	Particle size diameter corresponding to 10% passing
D_{30}	Particle-size diameter corresponding to 30% passing
D_{60}	Particle-size diameter corresponding to 60% passing
EI	Expansion index

Symbol	Description
F	Percentage passing a No. 200 (75 µm) sieve (only considering the particles passing a 3-inch sieve)
F	Size correction factor for rock point load test
GI	Group index
GSI	Geological strength index
H_i	Initial height of the test specimen in the expansion index test
LL	Liquid limit of the soil
P	Applied force at failure
PI	Plasticity index of the soil
PL	Plastic limit of the soil
RMR	Rock mass rating
RQD	Rock quality designation
ΔH	Change in height during the expansion index test

CHAPTER 2 FIELD EXPLORATION, TESTING, AND INSTRUMENTATION

2-1 INTRODUCTION.

2-1.1 Scope.

This chapter contains information on exploration methods including use of geologic maps, air photos, and remote sensing; geophysical methods; test borings and test pits, and penetration resistance tests. Also presented is information on methods of drilling and sampling, obtaining groundwater measurements, measuring *in situ* properties of soil and rock, selecting field instrumentation and geotechnical performance monitoring equipment.

2-1.2 Planning for Field Investigations.

The initial phase of field investigations should commence with a thoughtful assessment of the data needs for the specific project, which will help define the objectives of the subsequent field investigation. Prior to mobilizing to the field, readily available information should be located that is relatively inexpensive and often invaluable. In cases where the new project is adjacent to an existing project (e.g., highway widening, lateral expansion of an existing levee, etc.), the initial research should focus on information and data that have previously been collected and/or compiled for the project. For a new project, the initial effort should include a detailed review of geological conditions at the site and within the region where the site is located. This should then be followed by a “desk top” study, utilizing sources of available data, including historical and current aerial photography, remote sensing imagery, and (whenever possible) a field reconnaissance. The collective information obtained from these activities should be used as a guide in planning the project-specific field exploration.

To the extent possible as dictated by project data needs, individual test borings should be supplemented by lower cost exploration techniques that include test pits, test probes, and geophysical surveys. This is particularly true for remote sites, sites exhibiting wide variability in subsurface conditions, projects occupying a large footprint, linear projects (e.g., roadways, pipelines, etc.), and projects in the offshore environment where mobilizations and test borings can be exceptionally expensive.

Project explorations generally have three distinct phases: (1) reconnaissance/feasibility exploration; (2) preliminary exploration; and (3) detailed/final exploration. These phases usually have different objectives. A fourth phase of exploration that involves additional sampling and/or *in situ* testing may be desired and/or required during or after construction to confirm conditions. Frequently (and most common for relatively small projects), these three phases are combined into a single exploration effort.

Reconnaissance includes a review of available topographic, geologic, and hydrogeologic information; aerial photographs; data from previous investigations and

projects; and a site visit. Geophysical methods may prove to be helpful in many cases, particularly for large projects where subsurface conditions are variable and for linear projects (e.g., levees, highways, etc.). Reconnaissance/feasibility exploration frequently reveals difficulties which may be expected in later exploration phases and assists in determining the type, number and locations of borings required. Examples of information that can be obtained from field reconnaissance activities are presented in Table 2-1.

Table 2-1 Items that can be Evaluated During Field Reconnaissance (NCHRP 2018 and FHWA 2002)

Item	Things to Note	Comments
Access	Rank access using one of the following criteria: (1) easy, (2) accessible by four-wheel drive, (3) dozer and grading required, and (4) inaccessible.	Evaluating access helps determine the types of equipment that will be required.
Utilities	Existing overhead lines, marked gas lines, manholes, sewer outfalls, and power substations.	Utilities information helps select appropriate *in situ* testing, drilling, and sampling locations.
Surface soils	Presence of fill, debris, pollutants, slope instabilities, heave, subsidence, and scour	Evaluating surface soils can reveal evidence of abandoned landfills, historic landslides, contamination, subsidence, and flooding.
Shallow subsurface materials	Visual soil and rock classifications, loose cobbles, boulders, rock outcrops, rock joint patterns, faults, discontinuities, weathering, planes of weakness, talus, karst features	Subsurface materials can provide evidence for subsidence, landslide activity, unstable soil and rock, and stratigraphy.
Surface drainage	Swamps, ponds, lakes, streams, and rivers	Surface drainage information provides indications of the depth to groundwater level, hydraulic conductivity of the underlying materials, and potential for flooding.
Subsurface drainage	Major aquifers, water wells, and pumping from deep wells	Subsurface drainage information provides indication of groundwater level, natural springs, and potential artesian conditions.
Terrain	Rank terrain in terms of (1) level ground, (2) sloping, (3) hummocky, (4) rolling hills, and (5) mountainous.	Evaluating terrain helps with selecting appropriate exploration and construction equipment, assessing the need for slope stability investigations, and site access.
Past investigations	Existing test pits, boreholes, coreholes, and past blasting operations	Past investigations can provide information regarding stratigraphy, types of soil and rock, and groundwater levels.

Preliminary exploration may include borings and/or penetration soundings to identify specific features (e.g., top of rock, etc.) and/or to recover samples. The collected samples are generally used for index testing only. Penetration sounding test results are

often used to help identify the location of strata or formations where detailed exploration activities will be advanced.

The detailed investigation phase typically includes subsurface borings, disturbed and intact sampling for laboratory testing, standard penetration resistances, cone penetration test soundings, and other *in situ* measurements. At critical sites it may also include test pits, piezometer installation and measurements, pumping tests, etc. Following completion of this phase and the associated testing, the site conditions and soil/rock properties should be sufficiently known to design the project.

Monitoring of the site or structure is recommended throughout the construction and the post-construction phases. Performance monitoring instrumentation (e.g., piezometers and/or settlement plates to assess consolidation during staged loading) may need to be installed. In some cases, further evaluation of foundation conditions may be required during the construction phase. This is particularly true when foundation conditions have the potential to vary widely across the project site (e.g., when using deep foundations for project sites underlain by karst).

2-2 PUBLISHED REFERENCE MATERIALS.

When starting an investigation, the first step is to identify sources of readily available and pertinent information. In general, this information comes from two sources: (1) previous investigations; and (2) published literature in the public domain.

2-2.1 Previous Investigations.

For studies in developed areas, subsurface conditions and selected foundation recommendations may be available from previous work for surrounding projects. Earlier site-specific data may be “dated” and while the underlying geology is unchanged, the site-specific information may have been superseded by recent activities. For example, industrialized waterfront areas near major cities may undergo cycles of expansion and reconstruction, causing subsurface conditions to change. Often old foundations and wharf structures remain buried in place. Records of former construction may contain information on borings, field tests, groundwater conditions, and potential or actual sources of construction difficulties. Note that explorations from state departments of transportation (DOT), the United States Geological Survey (USGS), and United States Environmental Protection Agency (USEPA) may be publicly available.

Review of data from previous work should receive the greatest attention of any phase in a reconnaissance investigation because it is likely very relevant. Additionally, this information generally comes at relatively little cost and allows the project team to quickly become familiar with the project location and noted problems related to geology and construction.

2-2.2 Published Geologic and Hydrogeologic Maps.

Data on the physical geology and topography of the United States (and foreign countries) are available in maps and reports by government agencies, universities, and professional societies. An example of documents and sources of available information is provided in Table 2-2. While providing excellent regional and general information, the information from these sources may not be entirely "site-specific." However, this information often can be used to identify specific data gaps that need to be addressed during subsequent phases.

2-3 REMOTE SENSING DATA METHODS.

2-3.1 Sources.

Aerial photographs are a common type of remote sensing, including older printed images (scales from 1:12,000 to 1:80,000) and reasonably high-resolution digital images for most of the United States (scale of 1:1000 or better). Some regions possess a wealth of "historic" imagery that may extend before the current site was developed. Photos are useful for topographic and/or geologic mapping in addition to identifying drainage patterns, locations of existing structures, vegetation, access routes and site locations for planned explorations. Remote sensing also refers to non-photographic data gathering satellites, from which data, such as vegetation development, water sources, etc., are available. Table 2-3 summarizes sources and types of remote sensing data that have been historically (i.e., pre-2019) used by geotechnical engineers. The technologies identified in Table 2-3 generally require the purchase of images from the entities that generated the images.

Table 2-4 provides a summary of more recent remote sensing technologies. Data from some of these are free to the user and are often available on the internet. Data from remote sensing technology can be incorporated into developing augmented reality (AR) platforms, which provide an interactive experience where objects are projected into a perceived real-world environment. This requires computer-generated information presented in a geospatial environment through the use of special lenses and headsets.

2-3.2 Utilization.

Remote sensing represents a well-adopted resource by geotechnical engineers. The emergence of internet-based mapping tools coupled with the cross-section profiling capabilities using geographic information system (GIS) tools currently exceed the capabilities and functionality of earlier tools.

Table 2-2 Sources of Readily Available Subsurface Information (after NCHRP 2018, FHWA 2002, and FHWA 2016)

Types of Documents	Sources of Information	Type of Available Information	Comments
Topographic maps	USGS and state geological survey agencies	Site topography, physical features, and index map of site area	Maps can be used to evaluate access issues for field equipment and identify areas susceptible to slope instability.
Soil survey reports	National Resource Conservation Service, Web Soil Survey, and local soil conservation agencies	AASHTO and USCS classifications, moisture contents, Atterberg limits, organic contents, chemical properties (e.g., pH), permeability of soils, climate, stratigraphy, and groundwater level	Available information is for shallow depths (6 ft. or less) and is useful for identifying near-surface problematic soils (e.g., soils susceptible to swelling and shrinkage) or identifying potential borrow sources.
Geologic maps and reports, including sinkhole and karst maps	USGS and state geological survey agencies	Soil and rock formations (rock types, fracture, orientation and approximate age), groundwater flow patterns, and bedrock contours that provide approximate estimates of rock depths, and potential geologic hazards	These documents can be used to identify areas susceptible to sinkholes, landslides, subsidence, and other hazards.
Aerial photographs	Internet mapping sites, National Agriculture Imagery Program (NAIP), and aerial survey companies	Man-made structures, geologic and hydrogeologic information, current and past land use, borrow sources, and potential geologic and man-made hazards	Photographs can track site changes over time to identify potential problematic past land use activities or geologic events, including landslides.
Hydrological and well maps and well logs	USGS, state natural resources and soil survey agencies	Hydrogeological features (e.g., springs), groundwater hazards, stratigraphy, and groundwater depths	Well maps and logs can be useful to evaluate the need for construction dewatering and permanent groundwater control.
Utility maps	Utility companies and local government agencies	Locations of buried utilities	Very useful to identify locations for *in situ* testing, drilling, and sampling, useful to map equipment access routes
Flood insurance maps	FEMA, USACE, USGS, State and local government agencies	100- and 500-year floodplains, data for evaluating scour potential	This information can be used to ensure that the site isn't in the 100- and 500-year floodplains.
Sanborn fire insurance maps	Library of Congress, state and university libraries, and Sanborn Company	Environmental hazards and historical land use	Sanborn maps are available for urban areas.
Agencies: United States Geological Service (USGS), American Association of State Highway and Transportation Officials (AASHTO), Unified Soil Classification System (USCS) , Federal Emergency Management Agency (FEMA), United States Army Corps of Engineers (USACE)			

Table 2-3 Historic Remote Sensing Data Sources

Type	Description and General Use	Availability
Aerial photography	Available in 9-inch frames with overlap for stereoscopic viewing. Valuable because of high resolution and available scales could range from 1:12,000 (or larger) to 1:80,000.	USGS, NCIC, NCRS, USFS, BLM, TVA
	Satellite imagery with repetitive coverage every 18 days in four spectral bands: • BAND 4: emphasizes movement of sediment-laden water and delineates areas of shallow water and useful in differentiating lithology • BAND 6: emphasizes cultural features, such as metropolitan areas • BAND 7: emphasizes vegetation, the boundary between land and water, landforms and useful in structural interpretation of geology; • BAND 8: provides the best penetration of atmospheric haze, the best band for detecting faults, lineaments, mega-joint patterns or other structural features, and also emphasizes vegetation, the boundary between land and water, and landforms.	EROS
Skylab	High-quality photography of Earth's surface useful for regional planning, environmental studies, and geologic analyses. Images cover an area of 100 x 100 miles or 70 x 70 miles depending on the camera used. Images are from 1973-74 and do not provide full coverage.	EROS
NASA	Black and white, color, or false-color infrared aerial photography produced from NASA Earth Resources Aircraft Program with scales ranging from 1:120,000 to 1:60,000. Coverage not available for all areas. Useful for planning, environmental and site-oriented studies, and fault/lineament evaluation (color IR).	EROS
SLAR	Side-looking airborne radar (SLAR) is a valuable complement to photos for regional studies especially applicable in areas of persistent cloud cover. Scales range from 1:2,000,000 to 1:250,000. Best imagery for identifying regional faults/lineaments.	NCIC, Goodyear Aerospace Corporation and Motorola, Westinghouse Electric Corp.,
Thermal IR	Thermal infrared (IR) imagery can be useful where temperature contrasts are significant. Useful for special projects or as a complement to other remote sensing data Useful in fault detection in covered alluvial areas, geothermal exploration, location of seepage, location of near surface peat deposits, covered meander scars, and heat loss studies.	Obtained as needed by aerial survey firms. Images may be available from an HCMM.
Agencies: United States Geological Service (USGS), National Information Center (NCIC), National Resources Conservation Service (NCRS), U.S. Forest Service (USFS), U.S. Bureau of Land Management (BLM), Tennessee Valley Authority (TVA), Earth Resources Observation System (EROS), Heat Capacity Mapping Mission (HCMM) by National Space Science Data Center Goddard Space Flight Center		

For project sites where limited information is available, aerial images greatly aid in planning and layout of an appropriate boring program and currently be considered a minimal requirement for projects. For large engineering studies, including highway and airfield work, a three-dimensional (3D) visualization may be beneficial. Individual users can develop digital terrain model (DTM) files using data from UAVs data, and commercial companies can economically develop local 3D topography with the use of UAVs.

Table 2-4 Current Remote Sensing Data Sources

Type	Description and General Use	Availability
Aerial Photography	Recent and historical aerial maps (including approximate topography) for most of the United States. Generally, very good resolution at <1:1000 scale. Excellent to see regional and site-specific topography, roads, drainage features. In many areas, it is possible to get a relatively recent "street view" 3D image to depict observations from the ground surface.	Various internet map tools are available, with some databases updated quarterly. Most images are generally less than 3 years old.
LIDAR	Light Detection and Ranging (LIDAR) uses a pulsed laser light whose signal is reflected back to a sensor to record distance. The signal source is usually positioned on a moving vehicle and recovered data can be used to generate 3D images of terrain.	Usually provided by commercial vendors as a specialized commodity due to high equipment and processing costs.
SAR	Synthetic Aperture Radar (SAR) is an advanced form of SLAR that uses radio waves from a moving platform. Data can be used for high resolution 2D and 3D images, with the larger aperture (or larger antennae) providing higher resolution.	Provided by commercial vendors with specialized electronic equipment for data capture and processing, Images may be available to the general public at reasonable cost in the future.
UAV	Unmanned Aerial Vehicles (UAVs) or drones are increasingly useful for project aerial imagery. UAVs can carry digital and infrared cameras and other sensors. High resolution is possible. Overlapping passes allows for generation of 3D imagery and topography. Excellent resource for tracking construction progress.	Equipment is readily available at low cost for individual users. Commercial services are also widely available.

Interpretation of information from aerial photographs and other remote sensed data requires experience and skill. The interpretation process combined with other information from the published reference material often informs the interpretation of what features may be present at the project site. Spot checking in the field is an essential element in the interpretation of geologic features from aerial photographs. Aerial photographs are most helpful when assessing similarities and differences between areas. Use of these images in urbanized and develop areas is of limited quantitative subsurface informational value. As with any aerial image, whether photographic or remote data, vegetation and cloud cover can often obscure the underlying topography. Recently, computer enhancements of multi-spectral imagery have made LANDSAT data compatible with conventional aerial photography.

2-4 GEOPHYSICAL METHODS.

2-4.1 Utilization and Applications.

With increasing regularity, geophysical investigations are being used to estimate subsurface conditions because of improved interpretation techniques and the overall acceptance within the professional community of the geophysical characterization

techniques. Table 2-5 provides a summary of the common geophysical testing techniques and the objectives/characterizations that are obtained from these techniques. Information regarding the selection of appropriate surface geophysical testing techniques is also presented in ASTM D6429.

Geophysical methods are best suited when investigating relatively large and/or linear sites, including dams, reservoirs, tunnels, highways, and large groups of structures. Techniques are available for both onshore and offshore exploration. Geophysics have been used to locate gravel deposits and sources of other construction materials, particularly for stratified materials where properties differ substantially from adjacent soil/rock. As shown in Table 2-5, many of the geophysical testing methods are helpful in identifying different subsurface strata and anomalies in the subsurface.

Table 2-5 Surface Geophysical Methods and Investigation Objectives (after NCHRP 2018, Fenning and Hasan 1995, USACE 1995a, Sirles 2006, FHWA 2006, and Anderson et al. 2008)

	Seismic		Electrical and Electromagnetic				Potential Field	
Information Obtained	Refraction and Reflection	Surface Wave	Resistivity	Electromagnetic	Ground-Penetrating Radar	Microgravity	Magnetometry	Self-Potential
Lithology and stratigraphy	✓	✓	✓	✓	✓			
Bedrock topography	✓	✓	✓	✓	✓	✓	✓	
Water table	✓		✓		✓			
Rippability of rock	✓							
Shear wave velocity profile		✓						
Fault detection	✓		✓	✓	✓	✓		
Void and cavity detection	✓	✓	✓	✓	✓	✓		
Subsurface fluid flow				✓				✓
Ferrous anomalies			✓		✓		✓	
Conductive anomalies			✓	✓	✓			✓
Corrosion potential			✓					

2-4.2 Advantages and Limitations.

In contrast to borings, geophysical surveys explore large areas rapidly and economically. Because they evaluate conditions over a large area, the results reflect average conditions in an area rather than a specific result that one would obtain from a series of vertically advanced borings. Geophysical testing can prove most

advantageous in geologic conditions that display a strong contrast between adjacent strata (i.e., rock beneath soil, interface between hard and soft rock, water- or air-filled voids in soil or rock, etc.). Geophysical testing can often detect irregularities of bedrock surface and the interface between soil and rock strata, and may be particularly useful in karst topography.

Geophysical surveys can often distinguish boundaries between strata, but most methods can only indicate approximate soil properties. These “approximate” properties should be considered the average properties within the subsurface, as delineation of specific properties of specific strata are generally not possible.

Interpretation of geophysical testing results is often difficult and subjective to the experience of the operator or interpreter. In many cases, there are no definite criteria for the interpretation of geophysical testing techniques. Some techniques are highly specialized and almost all techniques require experienced operators and interpreters for each application. Spot checks of “interpreted” versus “actual” conditions are strongly recommended for each site using boring methods. Previously successful techniques and an experienced interpreter should be used.

Differences in degree of saturation, presence of mineral salts in groundwater, or similarities of strata that effect transmission of seismic waves may lead to vague or inaccurate conclusions. These limitations notwithstanding, geophysical testing is anticipated to see more widespread use and acceptance in the future. Further reference and extensive discussion are found in FHWA (2003) and NCHRP (2018).

2-5 SOIL AND ROCK EXPLORATION METHODS.

Soil borings are the most commonly used method for subsurface soil exploration in the field. They allow a vertical profile of soil to be established at a specific location and for the collection of samples at selected vertical intervals at specific locations. Rock drilling and coring techniques are more specialized than those used for soils and are used less frequently.

2-5.1 Drilling and Boring Methods.

Most geotechnical borings in soils have historically utilized either hollow-stem augers or rotary wash techniques, where numerous variations technologies are available. Recent advancements that are gaining popularity and acceptance include the use of direct-push and sonic boring techniques. Table 2-6 identifies the applicability of the several methods for advancing soil borings. Table 2-7 provides similar information for rock.

The drilling equipment used for geotechnical investigation is selected based on a combination of: (1) ground conditions encountered at the site (i.e., soft ground, steep terrain, over water, etc.) and (2) the type of drilling that is selected (i.e., auger, rotary,

percussion, etc.). Table 2-8 provides a summary of various types of drilling equipment and their application. Figure 2-1 provides a schematic of the various drilling methods.

Table 2-6 Methods of Advancing an Exploration Hole in Soil (NCHRP 2018 and Day 1999)

Method	Procedure	Applications	Limitations / Remarks
Auger boring (ASTM D1452)	Dry hole drilled with hand or power auger; samples recovered from auger flights	Identify geologic units and water content above water table in soil and soft rock	Stratification destroyed; sample mixed with water below the water table.
Hollow-stem auger boring	Hole advanced by hollow-stem auger; soil sampled with auger in place	Typically used in soils that would require casing to maintain an open hole for sampling.	Sample limited by larger gravel; maintaining hydrostatic balance in hole below water table is difficult.
Wash-type boring	Light chopping and strong jetting of soil; cuttings removed by circulating fluid and discharged into settling tub	Soft to stiff cohesive materials and many granular soils.	Coarse material tends to settle to bottom of hole; Should not be used in boreholes above water table where intact samples are desired.
Becker hammer penetration test (BPT)	Hole advanced using double acting diesel hammer to drive a 168 mm double-walled casing into the ground.	Typically used in soils with gravel and cobbles; casing driven open-ended if sampling of materials is desired.	Skin friction of casing difficult to account for; repeatability of test unclear.
Bucket auger boring	Rotates and advances a 600- to 1200-mm diameter drilling bucket with cutting teeth; bucket retrieved and emptied on the ground.	Most soils above water table; can penetrate harder soils than above types; can penetrate soils with cobbles and boulders if equipped with a rock bucket.	Not applicable in running sands; used for obtaining large volumes of disturbed samples; used to provide access to enter a boring for observations.
Direct push	Static weight and percussion used to advance a 90- to 115-mm diameter casing;	Most cohesive and granular soils; near-continuous sample	Recovered samples are generally disturbed
Sonic drilling	High-frequency resonant vertical oscillations advance a 75- to 300-mm diameter core barrel; recovers a continuous 3.3-m long core; after sample is retrieved, overcore barrel advanced to bottom of core barrel by similar technique and process is repeated	Applicable in nearly all soils and much bedrock; returns continuous stratigraphy; applicable for conditions both above and below the water table; process does not require drilling fluids	Not cost effective in very dense and hard rock where coring is desired; recovered samples are disturbed

Table 2-7 Rock Core Drilling Methods (NCHRP 2018 and Day 1999)

Method	Procedure	Type of sample	Applications	Limitations / Remarks
Rotary coring of rock (ASTM D2113)	Outer tube with diamond (or tungsten carbide) bit rotated to cut annular hole in rock; core protected by stationary inner tube; cuttings flushed by drill fluid	Rock cylinder 22 to 100 mm wide and as long as 3 m, depending on rock soundness; standard size is 54 mm diameter.	Obtain continuous core in sound rock (percent of core recovered depends on fractures, rock variability, equipment, and driller skill)	Core loss in fractured or variable rock; blockage prevents drilling in badly fractured rock; dip of bedding and joint evident but not strike
Rotary coring of rock, wire line	Same as ASTM D2113, but core and stationary inner tube retrieved from outer core barrel by lifting device or “overshot” suspended on thin cable (wire line) through large-diameter drill rods and outer core barrel	Rock cylinder 28 to 85 mm wide and 1.5 to 3 m long	Better core recovery in fractured rock; much faster cycle of core recovery and efficiency in deep holes	Core loss in fractured or variable rock; blockage prevents drilling in badly fractured rock; dip of bedding and joint evident but not strike
Rotary coring of swelling clay, soft rock	Similar to rotary coring of rock; swelling core retained by third inner plastic liner	Soil cylinder 28.5 to 53.2 mm wide and 600 to 1500 mm long encased in plastic tube	Soils and soft rocks that swell or disintegrate rapidly in air (protected by plastic tube)	Small sample; equipment more complex than other soil sampling techniques
Sonic drilling	High-frequency resonant vertical oscillations advance a 75- to 300-mm diameter core barrel; recovers a continuous 3.3-m long core	Continuous core sample when overcore barrel is advanced	Applicable most bedrock; applicable for conditions both above and below the water table; process does not require drilling fluids	Not cost effective in hard rock where coring is desired; recovered rock cores may be disturbed in fractured rock, provides good recovery and continuous stratigraphy
Percussive Method	Impact drill used; cuttings removed by compressed air	Rock dust and chips	To locate rock, soft seams, or cavities in sound rock; advance through boulders	Drill may become plugged by wet soil

Table 2-8 Soil and Rock Investigation Equipment and Their Applications (NCHRP 2018 and Australian Drilling Industry Training Committee 2015)

Rig Type	Application
Truck-mounted drill rigs	Areas with easy access
All-terrain vehicles drill rigs	Sites with soft ground and rugged terrain
Track-mounted drill rigs	Sites with swampy and very soft ground
Skid drill rigs	Sites with steep terrain
Wireline drill rigs	Rock sampling
Hydraulic direct-push rigs	Fast, continuous sampling, cleaner (no spoils)
Sonic rigs	Continuous sampling of soil and rock
Barges – regular	Over water drilling for shallow water depths (10 ft. [3 m] or less)
Jack up platforms	Over water drilling for areas with deep water (up to 40 ft. [12 m])

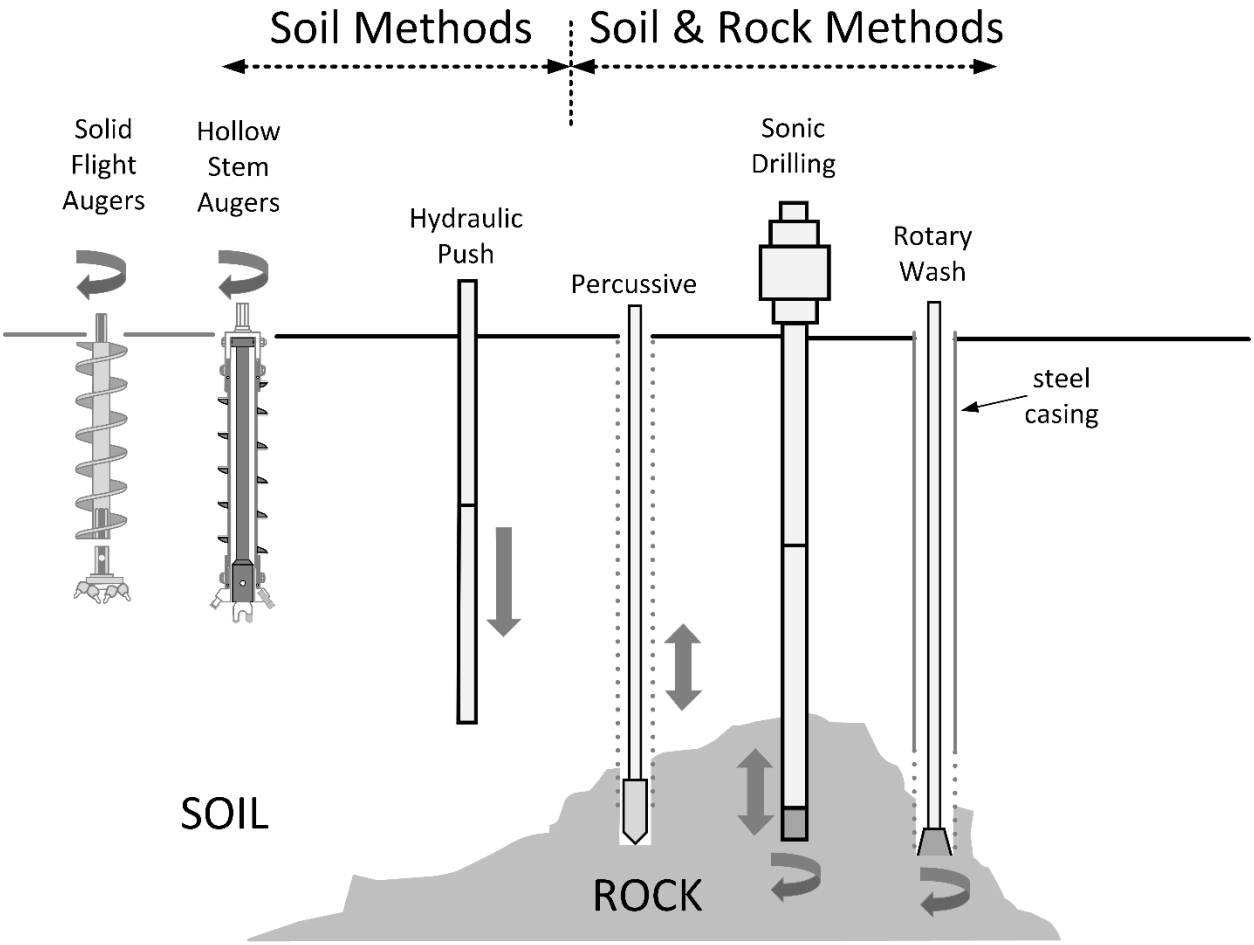

Figure 2-1 Schematic of Various Drilling Techniques for Soil and Rock (after NCHRP 2018 and Mayne 2012)

2-5.1.1 Boring Layout and Depth.

General guidance for preliminary and final boring layout (i.e., location and number of borings) and the depth of the borings is presented in Table 2-9 according to the type of structure and/or problem being investigated. Additional discussion of the spacing and number of borings is presented in FHWA (2002). In addition to structure type, boring layout and depth are strongly dependent on past experience in the region (or at the site) and the site/region geology. When a project is in an unfamiliar area, at least one boring should extend well below the zone necessary for apparent stability to verify that the site conditions are consistent with the anticipated geology and to assure no unusual or unanticipated condition exist at depth.

The site geology is an important factor in developing the boring layout and should influence the arrangement of borings so that geological sections may be viewed in the context of the final design. This requires review of geologic maps of the area and compilation of the information in a format that allows the geology, existing topography, current site plans, and boring locations to be presented at similar scales on the same figure/drawing.

In cases where detailed settlement, slope stability, or seepage analyses are required, the boring plan should include a minimum of two borings in each critical stratum to obtain intact samples (if applicable). For some site investigation programs this may mean that preliminary sample borings and/or cone penetration soundings may be needed to determine the most representative location and depth for intact sample borings.

Table 2-9 Selecting Number, Locations, and Depths of Investigation (after NCHRP 2018, FHWA 2002, FHWA 2016, NYDOT 2013, and SCDOT 2010)

Project	Minimum Number of Investigation Locations	Minimum Depth of Investigation[a]
Bridge - shallow foundations	• One location per pier if width of foundation is less than 100 ft. • Two locations per pier if width of foundation is greater than 100 ft. • Additional investigation locations should be included if uncertain or highly variable subsurface conditions are encountered.	• For $L \leq 2B$, use depth of $2B$ • For $2B \leq L \leq 5B$, use depth of $3B$ • For $L \geq 5B$, use depth of $4B$ • Extend below any soft compressible material into competent material • Extend 10 ft. into competent rock if encountered before the above are met.
Bridge - deep foundations	• One location per pier if width of foundation is less than 100 ft. • Two locations per pier if width of foundation is greater than 100 ft. • Additional investigation locations should be included if uncertain or highly variable subsurface conditions are encountered • At each shaft location for rock sockets	• In soil, extend below the anticipated tip or base elevation the greater of 20 ft. or 2x the maximum group dimension. • In rock, extend below anticipated tip or base elevation a minimum of 10 ft. or 3x shaft diameter for isolated piles/shafts or 2x maximum group dimension, whichever is greater.

[a] B = footing width and L = footing length

Table 2-9 (cont.) Selecting Number, Locations, and Depths of Investigation (after NCHRP 2018, FHWA 2002, FHWA 2016, NYDOT 2013, and SCDOT 2010)

Project	Minimum Number of Investigation Locations	Minimum Depth of Investigation[a]
Retaining structures	• A minimum of one location for each wall. If the wall is greater than 100 ft. long, spacing should be 100 to 200 ft. with locations alternating in front to behind the wall. • Anchored walls: Additional locations in the anchorage zone spaced at 100 to 200 ft. • Soil nail walls: Additional locations behind the wall at a distance of 1 to 1.5x the wall height; spacing should be at intervals of 100 to 200 ft	• Extend below bottom of the wall 2x the wall height or 10 ft. into hard rock. • Should extend below any soft compressible material into competent material.
Roadway - embankment foundations	• Along embankment centerline: spacing of 200 ft. in uncertain or highly variable conditions to 400 ft. in uniform conditions • At critical locations (maximum height or maximum depth of soft strata): a minimum of three locations along the transverse direction • Bridge approach embankment: a minimum of one location per abutment	• Depth of 2x the embankment height unless a hard stratum is encountered above this depth. • If soft strata are encountered extending to a depth greater than 2x embankment height, extend below the soft strata into competent material.
Roadway cuts	• Along centerline of cut: spacing of 200 ft. in uncertain or highly variable conditions to 400 ft. in uniform conditions • At critical locations (maximum cut depth or maximum depth of soft strata): a minimum of three locations along the transverse direction • For cut slopes in rock: perform geologic mapping along the length of the cut slope.	• Minimum depth of 15 ft. (4.5 m) below lowest cut elevation unless a hard stratum is encountered before the minimum depth is achieved. • If soft strata are encountered, extend investigation to a competent layer. • If base of cut extends below groundwater level, extend depth of investigation to determine the depth of the underlying pervious strata.
Pavements	• Spacing of 100 to 300 ft. depending on the subsurface conditions. Closer spacing for uncertain or highly variable conditions and longer spacing for uniform conditions.	• Minimum depth of 10 ft. from the proposed top of subgrade elevation.
Culverts and pipes	• One boring at each end of the culvert. • Additional borings between the end of culvert spaced at 100 to 300 ft. depending on the variability of the subsurface conditions • For culvert extensions: one boring every 50 to 100 ft. with a minimum of one boring	• Large culverts: same criteria as for bridge foundations • Small culverts: Minimum of 10 ft. below anticipated invert elevation
Poles, masts and towers	• One boring at each foundation location	• 30 ft. below the anticipated top of foundation in soil or 10 ft. of rock coring whichever is shallower.

[a] B = footing width and L = footing length

2-5.1.2 Abandoning or Sealing Boreholes.

Boreholes should be backfilled. Often, backfilling with the drill cuttings is sufficient. However, boreholes must be sealed with grout in cases where the borings are advanced below groundwater, in all cases where artesian pressures are encountered, and whenever environmental borings are advanced. Under these conditions, boreholes may be left temporarily unfilled to use for water-level observations after the initial field investigation drilling is completed. In boreholes for groundwater observations, the casings should be placed in tight contact with walls of boreholes or the annular space between the standpipe and borehole should be backfilled using the appropriately graded sand or gravel. Many agencies, such as the USACE and state DOTs have specific guidelines for sealing boreholes, and these are part of the project specifications. Additional discussion of details regarding groundwater investigation is presented in Section 2-8.

2-5.2 Test Pits and Test Trenches.

Test pits are commonly used to examine and sample soils *in situ* at relatively shallow depths. Test pits can be used to determine the depth to shallow groundwater, thickness of topsoil or surficial deposits, and/or to assess near surface conditions. Test pits are often used to determine sources of construction materials for earthwork projects, such as dams and embankments. Test pits range from shallow, hand-excavated pits or (more commonly) machine-advanced excavations.

Test trenches are essentially long test pits and are particularly useful for exploration in very heterogeneous deposits (e.g., rubble fills) where borings may be misleading, meaningless, or not feasible. Test trenches are used commonly for detection of fault traces in seismicity investigations and for investigating conditions near a slide plane in a landslide investigation. Safety precautions need to be recognized when working in and around test pits and trenches.

Table 2-10 provides guidance for the use and limitations of test pits and trenches. Hand-cut, block samples are frequently obtained from these explorations and may be necessary for sensitive soils, brittle and weathered rock, and soil formations exhibiting a honeycomb structure.

2-5.3 Other Exploratory Techniques.

Once a hole is advanced in either soil or rock, downhole tools can be placed in the open hole to make specific measurements or serve as carriers for geophysical testing instruments. Borehole cameras are commonly used for open holes in rock to assess stratigraphy, as well as strike and dip of the formation. Geotechnical performance monitoring instruments (i.e., slope inclinometers, water pressure transducers, borehole extensometers, etc.) can also be placed in the advanced borehole.

2-6 SAMPLING.

Recovery of representative samples of the subsurface soil and rock for testing is perhaps the most common goal of the techniques in Section 2-5. These samples are commonly referenced as *disturbed* or *undisturbed* depending on how well the recovered sample maintains the structure of the *in situ* material. Disturbance is initiated by the process of removing the soil/rock from the confined conditions in the subsurface. Thus, an "undisturbed" sample is actually a misnomer, as it (hopefully) represents a *minimally* (or *nominally*) *disturbed* sample. The term *intact sample* has largely replaced *undisturbed sample* in geotechnical engineering vernacular.

Table 2-10 Use and Limitations of Test Pits and Test Trenches (after NCHRP 2018)

Exploration Method	General Use	Capabilities	Limitations
Hand-excavated test pits and shafts	Bulk sampling, *in situ* testing, visual inspection	Provides data in inaccessible areas, less mechanical disturbance of surrounding ground.	Expensive, time-consuming, limited to depths above groundwater level.
Backhoe excavated test pits and trenches	Bulk sampling, block sampling, *in situ* testing, visual inspection, depth of bedrock and groundwater.	Fast and economical, generally less than 15-feet deep, can be up to 30-feet deep	Equipment access, generally limited to depths above groundwater level, limited intact sampling.
Drilled shafts	Pre-excavation for piles and shafts, landslide investigations, drainage wells.	Fast, more economical than hand excavated, min. 30-inches dia., max. 6-feet dia.	Equipment access, difficult to obtain intact samples, casing obscured visual inspection.
Dozer cuts	Bedrock characteristics, depth of bedrock and groundwater level, rippability, used in conjunction with backhoes for deeper excavations, used to level areas for other exploration equipment.	Relatively low cost, create exposures for geologic mapping.	Exploration limited to depth above groundwater level.
Trenches for fault investigations	Evaluation of presence and activity of faulting and sometimes landslide features.	Definitive location of faulting, subsurface observation up to 30 feet.	Costly, time-consuming, requires shoring, only useful where dateable materials are present, depth limited to zone above groundwater level. Specialized application.

Disturbed samples are primarily used for index tests that are performed for classification. A disturbed sample needs only to be representative of the soil composition and moisture because the soil structure is disturbed. Intact samples are obtained primarily for laboratory strength, compressibility, and permeability tests. The *in situ* structure and composition significantly influence the strength, compressibility and

permeability (i.e., engineering) properties of the soil. Most of the discussion in this section focuses on sampling from terrestrial or shallow-water locations. Offshore samplers are specialized and are treated separately in Section 2-6.3.

The number and type of samples depend on the stratification of the subsurface, the type of material encountered, the quantity needed for testing, and the criticality of the application. For most projects, both disturbed and intact samples are obtained for testing.

2-6.1 Soil Sampling.

2-6.1.1 Disturbed Soil Samples.

In general, representative disturbed samples are obtained at vertical intervals of no less than 5 feet and at every change in strata. Continuous samples are occasionally required or justified. This may be the case when a relatively thin layer of critical material is anticipated. Table 2-11 lists common types of disturbed samples and samplers. Recommended procedures for obtaining disturbed samples are provided in ASTM D1586. The split barrel (a.k.a., split spoon) sampler, depicted in Figure 2-2**,** is the most commonly used sampler.

Table 2-11 Samplers to Collect Disturbed Soil Samples

Sampler (Method of Penetration)	Typical Dimensions	Soils that Give Best Results	Cause of Low Recovery	Remarks
Split Barrel (140-lb hammer driven)	2.0-inch outside diameter (OD), 1.375-inch inside diameter (ID)	All soils finer than gravel-size particles; gravels invalidate drive data; soil retainer may be used in coarse-grained soils	Gravel-sized particles and larger	Standard Penetration Test (SPT) performed using this hammer and sampler and hammer; samples are extremely disturbed
Continuous helical-flight auger (Rotation)	3- to 16-inch diameter; penetration to depths exceeding 50 ft.	Most soils above water table; will not penetrate hard soils or those containing cobbles or boulders	Hard soils, cobbles, boulders	Method of determining soil profile, bag samples can be obtained; log and sample depths must account for lag time between penetration of bit and arrival of sample at surface
Bucket auger (Rotation)	Up to 48-inch diameter common; with extensions, depth over 80 ft. are possible	Most soils above water table; can penetrate harder soils than above types, can penetrate cobbles and boulders with a rock bucket	Soil too hard to penetrate	Several bucket types available, including those with ripper teeth and chopping tools; progress is slow when extensions are used
Large Penetration Test (LPT) (Up to 300-lb hammer driven)	2- to 3-inch ID, 2.5- to 3.5-inch OD samplers, (e.g., Converse and California samplers)	Sandy to gravelly soils	Particles large than coarse gravel	Sample is intact but very disturbed; A resistance can be recorded during penetration, but is not equivalent to the SPT N value and is more variable due to no standard equipment and methods

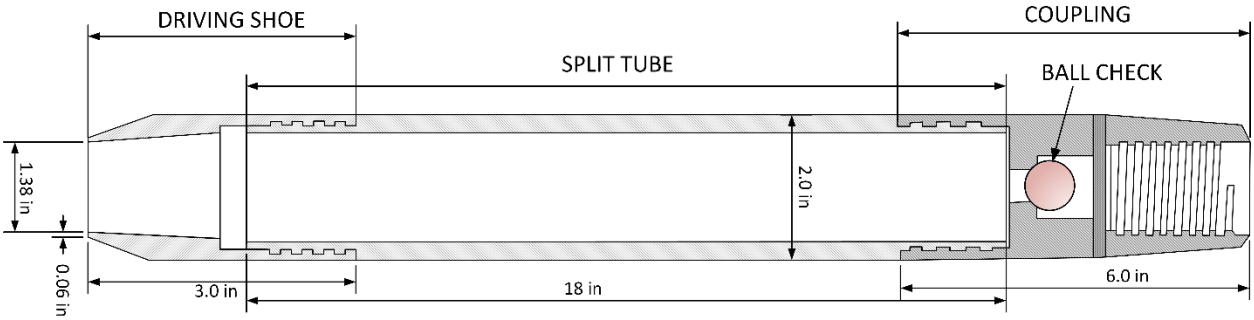

Figure 2-2 Cross Section of Split Barrel Sampler

2-6.1.2 Intact Soil Samples.

Intact (or "undisturbed") samples are most commonly obtained using a thin-walled steel tube (Shelby tube) that is pushed at a relatively rapid and constant rate following procedures in accordance with ASTM D1587. Intact sampling and samplers should provide samples that comply with the following criteria: (1) show no visible distortion of strata, (2) include no visible openings or softened material, (3) exhibit a recovery ratio (i.e., sample length divided by distance of sample push) that exceeds 95 percent, (4) have an area ratio (i.e., area displaced by the sampler tube divided by the area of the sample) of less than 15 percent, and (5) have a clearance ratio (i.e., the difference between the diameter of inside of the tube and the diameter of the opening at the bottom of the tube divided by the diameter of the opening at the bottom of the tube) as small as possible but less than 3 percent. A schematic and photograph of a thin-walled Shelby tube that meets these criteria is presented in Figure 2-3.

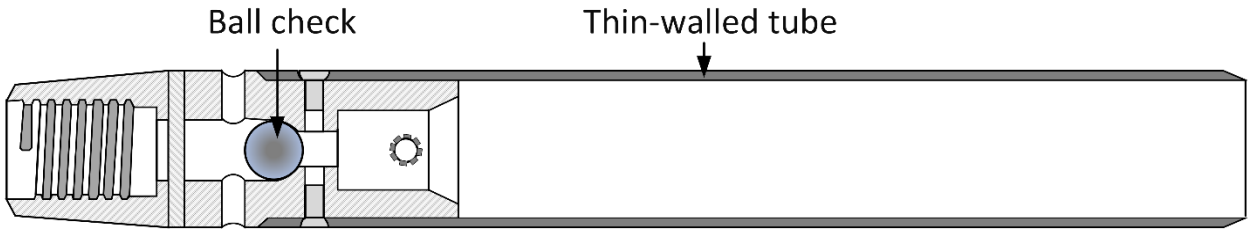

Figure 2-3 Cross Section of Shelby Tube Sampler with Ball-check Valve Head

In general, intact samples of clean sands and gravels cannot be obtained, even when using thin-walled samplers. For this reason, *in situ* testing methods are commonly used in these soils, and intact sampling focuses on silts, clays, and coarse-grained soils with a significant amount of silty and clayey fines. Because fine-grained soils can vary from very soft to very hard, different types of samplers have been developed to facilitate the

recovery of intact samples. Table 2-12 summarizes common types of samplers used for intact soil samples.

Table 2-12 Samplers Used to Collect Intact Soil Samples

Sampler	Typical Dimensions	Method of Penetration
Shelby tube (ASTM D1587)	3.0-inch OD and 2.87-inch inside diameter (ID) most common; available from 2- to 5-inch OD; 30-inch sampler length standard	Pressing with relatively rapid, smooth stroke; can be carefully hammer driven but this will induce additional disturbance
Fixed or Stationary piston	3-inch OD most common; available from 2- to 5-inch OD; 30-inch sampler length standard	Pressing with continuous, steady stroke
Foil Sampler	Continuous samples with 2-inch ID; up to 65 ft. long	Pushed into the ground with steady stroke; Pauses occur to add segments to sampler
Hydraulic piston (Osterberg)	3-inch OD is most common; available from 2- to 4-inch OD; 36-inch length standard	Hydraulic or compressed air pressure
Denison	3.5- to 7-inch OD, producing samples 2.4 to 6.3 inches; 24-inch sampler length standard	Rotation and hydraulic pressure
Pitcher sampler	4-inch OD; uses 3-inch diameter Shelby tubes; sample length 24 inches	Same as Denison

Sampler	Soils that Give Best Results	Cause of Disturbance or Low Recovery	Remarks
Shelby tube (ASTM D1587)	Cohesive fine-grained or soft soils; gravelly / very stiff soils will crimp tube	Erratic sampling pressure, hammering, gravel particles, crimping of tube edge, improper soil types, pressing more than 80% of tube length	Simplest device for undisturbed samples; clean boring before sampler is lowered; little waste area in sampler; not suitable for hard, dense or gravelly soils
Fixed or Stationary piston	Soft to medium clays and fine silts; not for hard, dense, sandy, or gravelly soil	Erratic pressure during sampling, allowing piston rod to move during press, improper soil types for sampler	Piston at end of sampler prevents entry of fluid and contaminating material, requires heavy drill rig with hydraulic drill head; less disturbance than Shelby tube
Foil sampler	Soft sensitive clays, silts, and varved clays	Samplers should not be used in soils containing fragments or shells	Samples surrounded by thin strips of stainless steel, stored above cutter, to prevent contact of soil with tube
Hydraulic piston (Osterberg)	Silts and clays, some sandy soils	Inadequate clamping of drill rods, erratic pressure	Needs only standard drill rods; requires adequate hydraulic or air capacity to activate sampler; samples generally less disturbed compared with Shelby tube; not suitable for hard, dense, or gravelly soil
Denison	Stiff to hard clay, silt, and sands with some cementation, soft rock	Improper operation of sampler; poor drilling procedures	Inner tube face projects beyond outer tube, which rotates; amount of projection can be adjusted; generally good samples; not suitable for loose sands and soft clays
Pitcher sampler	Same as Denison	Same as Denison	Differs from Denison in that inner tube projection is spring controlled; often ineffective in cohesionless soils

For soft soils, a stationary (or fixed-piston) sampler (Figure 2-4) or hydraulic piston sampler is commonly deployed. For very soft soils and varved clays, a foil sampler may be deployed, although limited in use in the United States.

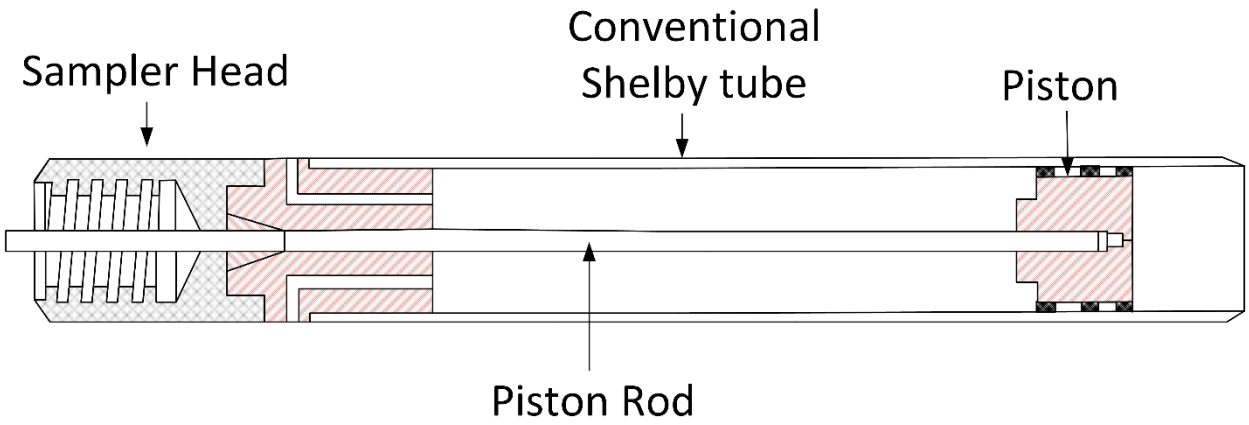

Figure 2-4 Cross Section of a Stationary or Fixed Piston Sampler

For stiff fine-grained soils, or for layers of soft and hard materials, special samplers have been developed that have the ability to "core" around the recovered stiff materials while capturing the softer materials in the same thin-walled tube. The Denison sampler and the Pitcher sampler are two types of common samples for these subsurface conditions.

2-6.1.3 Intact Samples from Test Pits and Test Trenches.

One of the advantages of test pits and test trenches is that hand-trimmed (i.e., block) samples may be obtained from the bottom or the sidewalls of the test pits and test trenches. These block samples are potentially the least disturbed of all types of samples. Unfortunately, the test pits and trenches are only feasible to a limited depth.

To obtain a block sample, a column of soil is trimmed the same size or slightly smaller than the container that will be used for transporting the sample. The container should be placed over the top of the sample and should provide as small an annular space as possible. This annular space ideally would be filled using wax. A tight fit in a stiff container that can be sealed provides the ideal conditions for retrieving and transporting block samples with least disturbance.

2-6.2 Rock Sampling.

Rock is sampled with core barrels that have either tungsten carbide or diamond core bits at the cutting face. Drill rods and core barrels come in a variety of standard sizes (see Table 2-13), depending on the size of the recovered rock core.

Table 2-13 Standard Size of Rock Casing, Drill Rods, Core Barrels, and Coreholes (after ASTM D2113)

Casing, Core Barrel	Drill Rod	Casing OD (in.)	Casing Bit OD (in.)	Core Barrel Bit OD (in.)	Drill Rod OD (in.)	Approx. Diameter of Corehole (in.)	Approx. Diameter of Core (in.)
EX	E	1-13/16	1-7/8	1-7/16	1-5/16	1-1/2	7/8
AX	A	2-1/4	2-11/32	1-27/32	1-5/8	1-7/8	1-3/16
BX	B	2-7/8	2-31/32	2-5/16	1-29/32	2-3/8	1-5/8
NX	N	3-1/2	3-5/8	2-15/16	2-3/8	3	2-1/8

For hard and massive rock, relatively undisturbed rock samples may be obtained using just the core barrel to recover the sample. More commonly, a tube (or series of tubes) is used to contain the rock core and the tube is isolated from the core barrel to minimize disturbance. Inner tubes must be used for undisturbed rock sampling whenever the rock includes discontinuities. Table 2-14 lists summarizes techniques for recovery of relatively undisturbed samples of rock.

Table 2-14 Common Samplers for Rock Cores (after NCHRP 2018)

Diamond Core Barrels			
Dimensions		**Best Results in Soil or Rock Types**	**Methods of Penetration**
Standard sizes: 1-1/2” to 3” OD, 7/8” to 2-1/8” core. Barrel lengths 5 to 10 feet for exploration.		Hard rock. All barrels can be fitted with insert bits for coring soft rock or hard soil.	Rotary drilling using water or slurry
Details for tube sampling			
Type	**Causes of Disturbance or Low Recovery**	**Best Results in Soil or Rock Types**	**Remarks**
Single Tube	Fractured rock. Rock too soft.	Primarily for strong, sound and uniform rock.	Drill fluid must circulate around core – rock must not be subject to erosion. Single tube not often used for exploration.
Double Tube	Improper rotation or feed rate in fractured or soft rock.	Non-uniform, fractured, friable and soft rock.	Has inner barrel or swivel which does not rotate with outer tube. For soft, erodible rock. Best with bottom discharge bit.
Triple Tube	Same as Double Tube	Same as Double Tube.	Differs from Double Tube by having an inner split tube liner. Intensely fractured rock core best preserved in this barrel.

Double tube core barrels are the most commonly used in practice. Depending on the number of discontinuities in the rock, the recovered sample may be considered either disturbed or undisturbed. Schematics of single and double tube rock core samplers are provided in Figure 2-5(a) and (b), respectively.

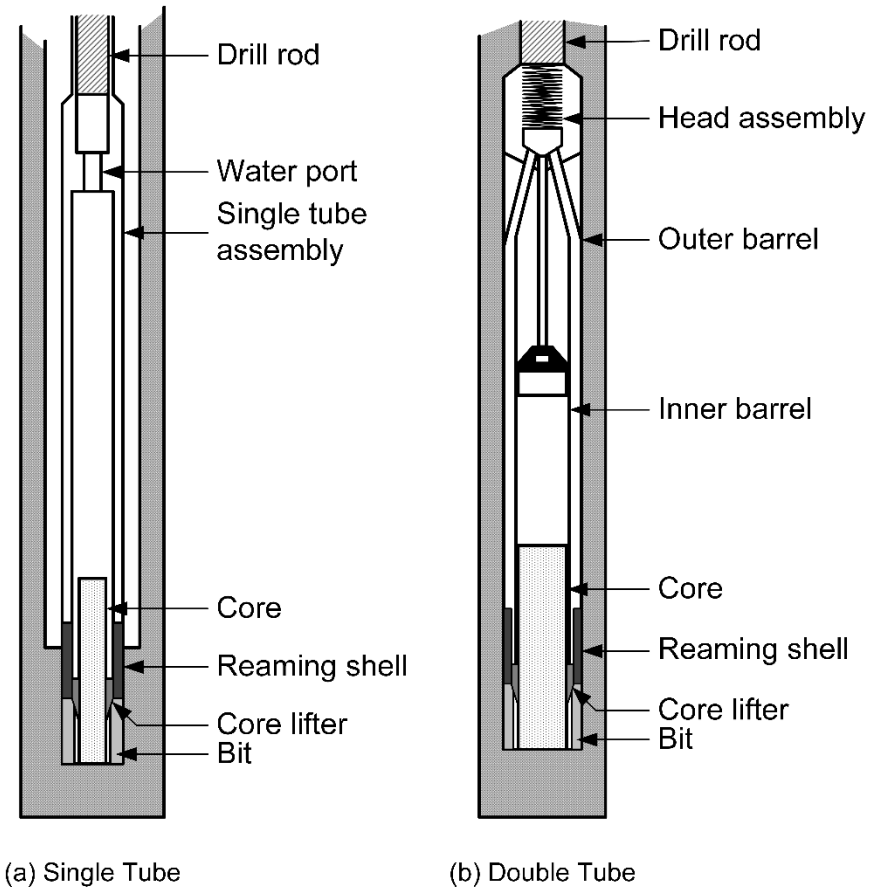

Figure 2-5 Rock Core Samplers (after NCHRP 2018)

The suitability of rock cores for structural property tests depends on the quality of individual recovered samples. If the properties of the intact rock are desired, then smaller diameter cores are recommended because large-diameter rock cores likely include more discontinuities than small-diameter rock cores.

The percentage of core recovery (i.e., recovered core length divided by the recorded core run) provides an indication of soundness and degree of weathering of rock. The Rock Quality Designation, RQD, (i.e., total length of recovered core pieces greater than 4 inches in length divided by the recorded core run) provide a better indication of the soundness and degree of rock weathering because it essentially disallows the consideration of the fractured and weathered rock intervals. The RQD is also a major factor in assessing the behavior of the *in situ* rock mass, as defined by the Rock Mass Rating (RMR) of the rock. The engineer and geologist should carefully examine rock core samples exhibiting low recovery and/or low RQD to assess the reasons for low recovery and the interpreted poor rock quality. Details regarding on rock classification and rock properties are presented in Chapter 1 and in NCHRP (2018).

Sampling of highly (or partially) weathered, fractured, or disintegrated rock is extremely difficult. These materials often occur near the interface between soil and rock and represent the transition between these two materials, especially in the case of residual soils. The best samples of these materials are obtained by experienced drillers using double- or triple-core barrel samplers.

2-6.3 Offshore Sampling.

In some cases, samples of soil and rock must be obtained from the bottom of rivers, lakes, or the ocean. For water depths less than about 60 feet, the conventional soil and rock boring equipment can be used on small jack-up platforms, small barges, or barrel floats. The challenge is that floating equipment requires suitable anchoring and is limited to fairly calm water, although tidal fluctuations can be easily accommodated. For deep water sites and/or extreme ocean settings, large dedicated drill ships, specialized equipment, and experience are required to obtain quality intact samples. Table 2-15 identifies some of the specialized equipment used for underwater sampling.

Numerous types of oceanographic samplers, both open-tube and piston types, are available for use when drilling from ships. Some of these depend upon free-fall penetration and are limited in the depth of exploration. Drilling and sampling from the ocean floor can be accomplished using specialized equipment deployed remotely from portable equipment that is deployed in underwater vessels or on underwater platforms operating on the ocean floor. The quality of samples obtained by most oceanographic samplers is not high because of their large length to diameter ratio and because air/gas in the dissolved state in the underwater environment comes out of solution when the sample is recovered at the ground surface. For detailed information on underwater sampling equipment, refer to ASTM STP 501 (ASTM 1972).

2-6.4 Field Logging and Boring Logs.

While monitoring drilling and sampling activities, an engineer, geologist, or experienced driller prepares a *field boring log* to document the findings and observations. This field logging is an important part of documenting the soil and rock conditions that exist at the project site. A typical field log includes all the relevant information for the boring that was completed, including a unique boring identification number, date of drilling, personnel on-site, boring advancement method (i.e., auger, rotary wash, direct push, sonic), depths where samples were obtained, type of samples (i.e., split-barrel and Shelby tube), hammer type, raw SPT N values, water level observations, and preliminary estimates of stratigraphy. If available, the global positioning system (GPS) coordinates should be included. The field log provides a unique designation of each recovered sample, whether disturbed or intact, as well as a field visual classification of the sample in accordance with ASTM D2488.

Table 2-15 Common Underwater Samplers (after NCHRP 2018)

Sampler	Size of Sample	Length of Sample	Water Depth Limitations	Method of Penetration	Remarks
Peterson Dredge	Grab	± 6-inch depth	To 200 ft. and more with additional weight	Clam shell jaw	Reliable grab sampler; intact samples may be obtained with jaws that precisely mate
Open Barrel Gravity Corer	2.5- to 6-inch diameter	Core barrels length from 6 to 30 ft	No limit on depth but required weight, amount of line or size of vessel may control	Spooled freely off the winch drum	
Pflueger Corer	About 1.5-inch diameter	Core barrels available in 12, 24 and 36 in. length	From 25 to 200 ft	Free fall from 10 to 20 ft. above bottom	Relatively light weight core for upper 1 to 3 ft. of bottom sediments; usually not suitable for strength tests
Piston Gravity Corer	Standard corer has 2.5-in. barrel	Standard barrel is 10 ft. Additional 10 ft. sections can be added	No depth limit except that available weight, amount of line, or size of vessel may control	Free fall from calibrated height above bottom such that piston does not penetrate sediments	Capable of obtaining samples suitable for strength tests with experienced crew; samples may be seriously disturbed
Vibratory Corer	Sample is 3.5-in. diameter	20 ft. standard, can be lengthened to 40 ft.	Minimum depth limited by draft of support vessel; maximum depth about 200 ft.	Pneumatic impacting vibratory hammer	Samples are disturbed because of vibration and large area ratio; not suitable for strength testing; Penetration resistance can be measured; obtains continuous samples in marine soils

The field log, the recovered samples, and lab/field testing results are used to produce the *final boring log*, which represents the official engineering record of the drilling and sampling efforts. The boring log provides the permanent, technical documentation of the materials encountered during drilling, sampling, and coring. The geotechnical engineer or geologist uses the results from the field and their training/experience to group samples/records together based on color, soil type, and SPT N values and identify layers or strata, which may be consistently found in the adjacent companion borings from the site. An example of the engineering boring log is shown as Figure 2-6. In the final engineering boring logs, soil types are categorized according to a user- or agency-specified soil classification system. The most common soil classification systems in the United States include the Unified Soil Classification System (USCS) (ASTM D2487 or D2488), the AASHTO system, and the United States Department of Agriculture (USDA) system.

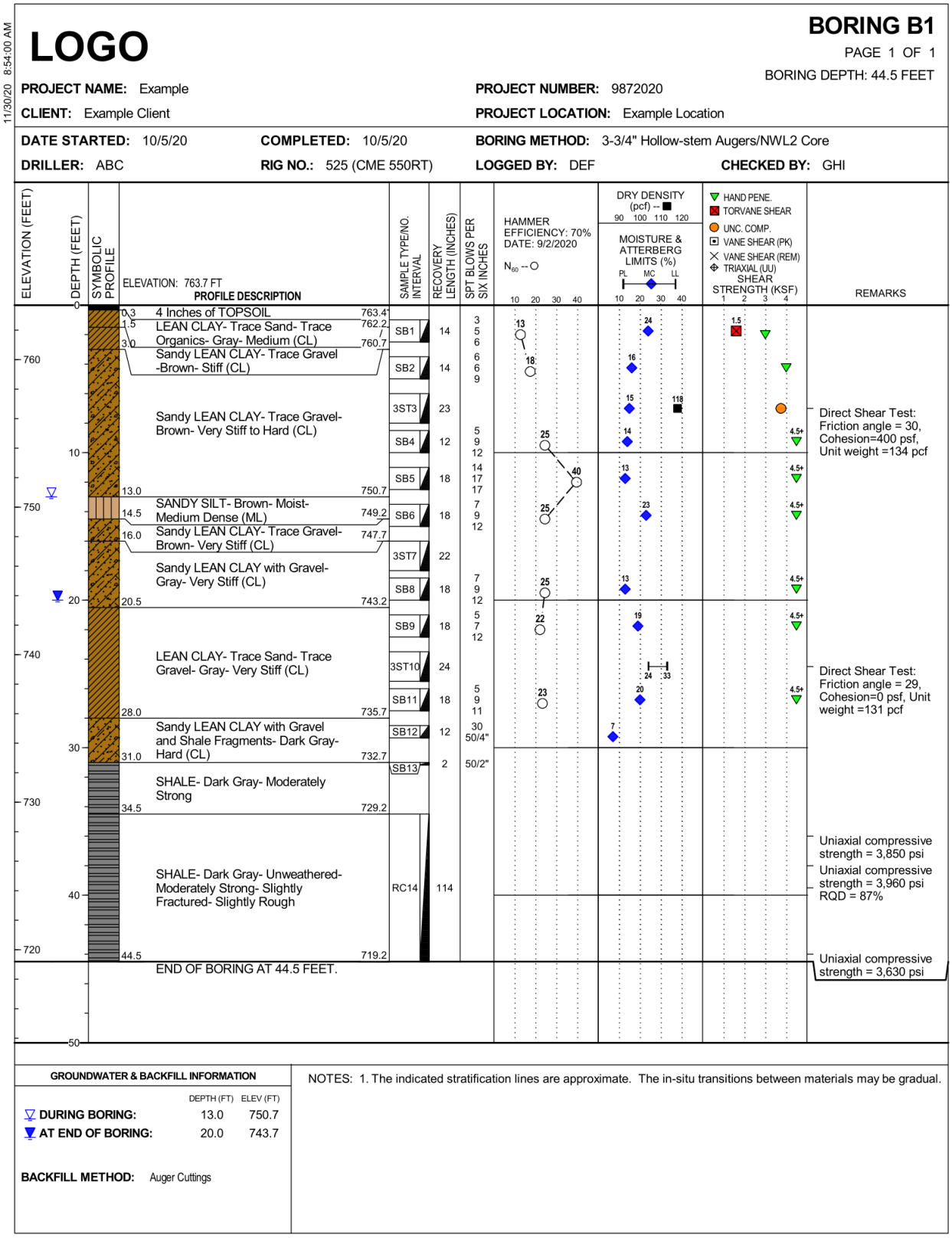

Figure 2-6 Example Geotechnical Boring Log

In addition to the soil classification, the boring log description should also include color, relative density (e.g., loose, dense, etc.) or consistency (e.g., soft, medium, hard, etc.), and the presence of organics, shells, peat and/or manmade materials. Identification of these additional features may impact engineering performance and may prove beneficial in subsequent construction/excavation phases of the project.

2-7 PENETRATION RESISTANCE TESTS.

Penetration resistance tests are the most common *in situ* testing techniques for characterizing subsurface conditions. The most common field penetration test remains the *Standard Penetration Test* (SPT), which measures resistance to the penetration of a standard, thick-walled drive sampler in an open borehole using a drop hammer. A more controlled and increasingly popular test is the *Cone Penetration Test* (CPT), which utilizes a standard cone-shaped instrument that is pushed at a standard constant rate from the ground surface. Another common test is the *flat plate dilatometer* (DMT). This device utilizes a robust steel blade that is pushed into the ground at a constant rate and then periodically stopped to allow the controlled measured inflation of a flexible steel membrane. In many parts of the United States, particularly when stiff soils and//or granular soils are encounters, a *dynamic cone penetration* (DCP) test is performed by driving a standard sized cone into the ground using a drop hammer. This section provides information regarding these four penetration tests. Section 2-9 will address other common *in situ* testing methods.

2-7.1 Standard Penetration Test (SPT).

The SPT was originally developed in the 1900s and proceeds by driving a thick-walled, split-barrel (a.k.a., “split spoon”) sampler into the ground using incremental blows from a drop hammer. The sampler is driven a total of 18 inches into the ground. The number of blows required to drive the sampler the 12-inch vertical interval between 6 and 18 inches is referred to as an N value or the *blow count*. The procedure is presented in ASTM D1586, and a schematic of the SPT is presented in Figure 2-7.

The SPT provides a disturbed sample of the tested material and generates useful data that can be used to correlate to many engineering properties. Many factors can affect the SPT results, and there are several vastly superior *in situ* testing methods. Nevertheless, the test is still almost universally referenced and often required in the United States. One reason for this is the large amount of historical (i.e., legacy) data available. Numerous correlations have been published (see Chapter 8) and their use along with SPT represents the Standard of Practice in many parts of the country.

2-7.1.1 Corrections to Field Blow Counts.

As an improvement on older donut and safety hammers, most current SPT programs use an automatic hammer that does not rely on an operator-dependent cathead and

rope to establish the drop height of the hammer. Modern automatic deliver consistent energy to the sampler, which should be measured periodically. The field-recorded N values may be adjusted to reflect the energy of the specific hammer. The adjustments are intended to correct the N value to the 60 percent hammer efficiency that is assumed for the older equipment and historic correlations. The energy corrected value (N_{60}) can also be normalized to an equivalent value at a vertical stress of one atmosphere. The "overburden corrected" or "normalized" blow count is labeled $(N_1)_{60}$ or $N_{1,60}$. Several correlations to normalized blow count are presented in Chapter 8 and in McGregor and Duncan (1998).

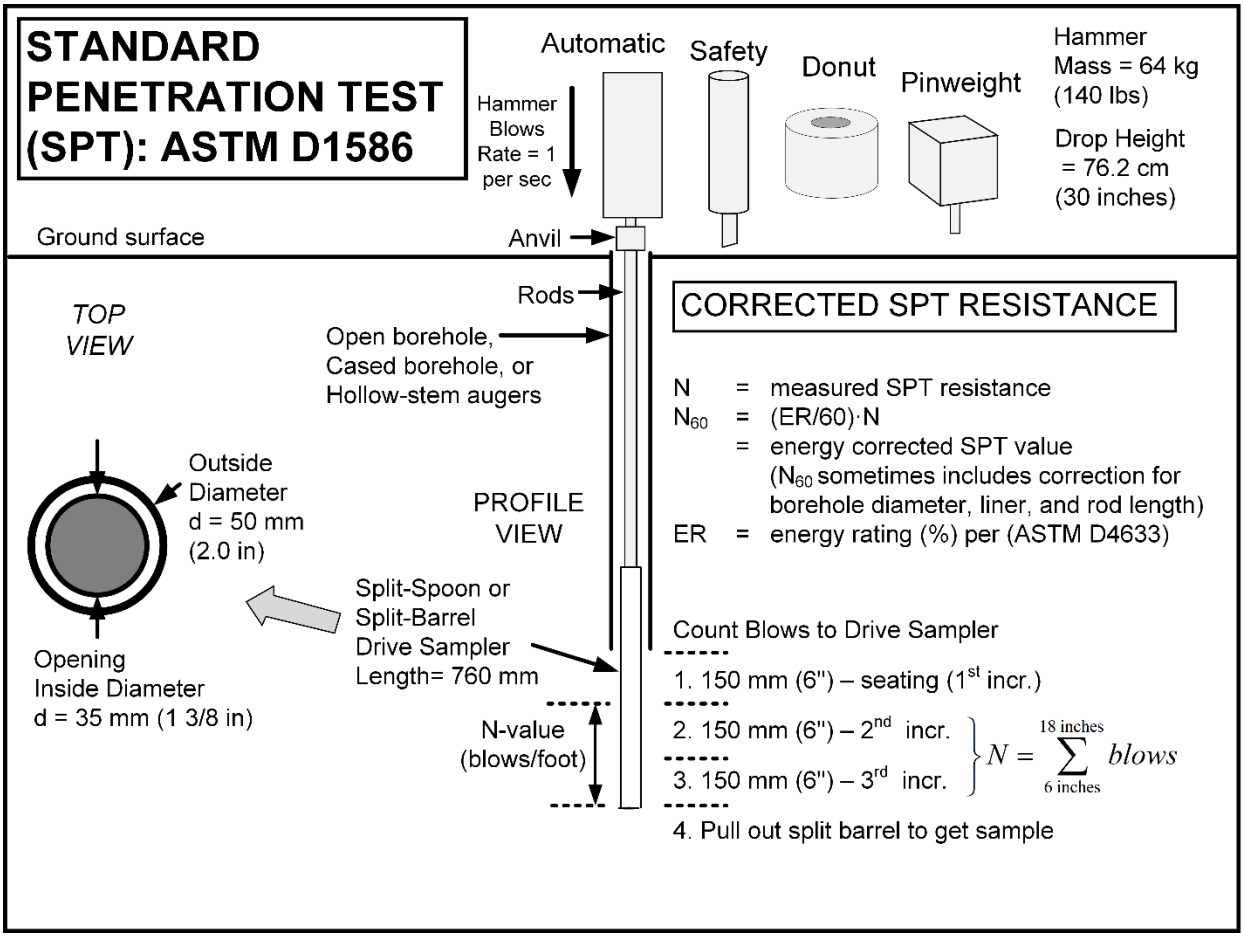

Figure 2-7 Standard Penetration Test (after NCHRP 2018 and Mayne 2012)

2-7.1.2 Advantages and Limitations.

The biggest advantage to the SPT is its near-universal acceptance and use in the United States. As a result, there is a large data set that can be used for correlation.

However, SPT blow counts are affected by many operational procedures, the presence of gravel, and by cementation between the particle grains. In clays, the blow count does not reflect the influence of fractures or slickensides. Table 2-16 presents a

summary of the many operational factors that are known to influence the N value measured in the field.

Table 2-16 Factors Affecting the Standard Penetration Test and SPT results (after Kulhawy and Mayne 1990)

Cause	Effects	Influence on SPT N Value
Sampler driven above bottom of casing	Sampler driven in disturbed, artificially densified soil	Increases greatly
Inadequate cleaning of base of borehole	Test not performed in original *in situ* soil; soil may become trapped in sampler and may be compressed as sampler is driven, recovery reduced	Increases
Careless measure of drop	Hammer energy varies (generally variations cluster on low side)	Increases
Hammer strikes drill rod collar eccentrically	Hammer energy reduced	Increases
Lack of hammer free fall because of ungreased sheaves, new stiff rope on weight, more than two turns on cathead, incomplete release of rope each drop	Hammer energy reduced	Increases
Coarse gravel or cobbles in soil	Sampler becomes clogged or impeded	Increases
Use of bent drill rods	Inhibited transfer of energy of sampler	Increases
Hammer weight inaccurate	Hammer energy varies (driller supplies weight; variations of 5 – 7% common)	Increases or decreases
Careless blow count	Inaccurate results	Increases or decreases
Use of non-standard sampler	Correlations with standard sampler invalid	Increases or decreases
Failure to maintain adequate head of water in borehole	Bottom of borehole may become quick	Decreases

2-7.2 Cone Penetrometer Tests (CPT).

The CPT involves hydraulically pushing an instrumented steel probe at a constant rate to obtain a continuous record of the penetration resistance of the cone tip and the frictional resistance of the soil. The CPT does not produce a borehole, samples, or drill cuttings. The original test involved a mechanically operated cone, referenced as a “Dutch” cone (DPT). The original equipment has been superseded, modified, and improved to allow electronic measurements.

Most modern instruments also include a piezometer near the tip. When equipped with the proper sensors and instruments, the routine performance of the CPT also allows the measurement of temperature, vertical alignment, electrical resistivity, acoustic emissions, and shear wave velocity.

Testing is currently conducted in accordance with ASTM D5778. The test can be conducted without the use of a pore pressure measurement and is referenced simply as

the CPT. Alternatively (and commonly) the test is performed using a device to measure pore pressures behind the tip of the probe while pushing. This is referred to as the *piezocone test* (CPTu). Recent advances have allowed the ability to measure the propagation of shear waves using a seismic piezocone, which is referred to as a *seismic CPT* (SCPTu).

2-7.2.1 Equipment and Testing Procedure.

The cone penetration test requires continuous hydraulic advancement of the probe and the simultaneous recording of multiple electronic instruments. Specific equipment and procedures necessary for performing a CPT are summarized as follows:

- Cone Penetrometer: A standard cone penetrometer is a 1.4-inch (35.7-mm) diameter cylindrical probe with a 60^o apex at the tip, which results in a projected tip area of 1.55 in^2 (10 cm^2) and a 23.3 in^2 (150 cm^2) instrumented sleeve surface area. Other sizes (both smaller and larger) are available. The size of a cone is typically identified by the projected tip area (i.e., 10-cm^2 cone or a 15-cm^2 cone). A variety of tip load capacities (i.e., 2-ton, 15-ton, etc.) are available.
- Drill Rig/CPT Truck and Cone Rods: A hydraulic actuator is attached to a truck or drill rig that can provide sufficient reaction mass to advance the penetrometer at a constant rate of 2 cm/second. This reaction can be provided using a conventional drilling rig, but dedicated CPT trucks typically weighing 20 to 25 tons have become the standard.
- Water Pressure Transducer: Valuable information can be provided by measuring the pore water pressure behind the cone tip during penetration. For a CPTu, the water pressures are monitored using a transducer and porous filter element.
- Geophone: For the SCPTu, a geophone is located along the drill string at a distance of approximately 20 inches (500 mm) above the cone tip. The geophone detects shear waves generated at the ground surface at specific vertical intervals. During advancement of the seismic cone, a shear wave is generated at the ground surface. An average shear wave velocity of the soils between the ground surface and the geophone can be calculated.

An example record from a CPT sounding is shown in Figure 2-8. This shows a schematic of the CPT probe and the near-continuous vertical profile of cone tip resistance (q_t), sleeve friction (f_s), and pore pressure at the u_2 position (behind the tip).

2-7.2.2 Soil Classification with CPT.

Regardless of the specific type of cone penetration test probe (i.e., CPT CPTu, SCPTu), the testing concept has gained near universal acceptance and interest. As shown in Figure 2-8, a near-continuous vertical profile of the stratigraphic variations is obtained. A variety of engineering parameters can be estimated from CPT results. Many

correlations of CPT data to strength, compressibility, modulus, hydraulic conductivity, and other properties are available, some of which are provided in Chapter 8.

The CPT is able to estimate the soil type of the deposit penetrated. A common method for doing this is shown in Figure 2-9, which relates soil behavior type (SBT) to specific CPT results. This type of correlation is extremely useful for site characterization and subsurface stratigraphy. Other soil type correlations are available.

2-7.2.3 Advantages and Limitations.

The CPT provides numerous advantages, due to its popularity in engineering practice and proliferation of useful correlations to other engineering parameters. The test can be performed quickly. The speed of operation allows considerable data to be obtained in a short period of time, resulting in a continuous record of soil conditions. It is particularly helpful in assessing variability in subsurface conditions across a site.

The major limitation of all cone penetration tests is that discrete samples are not recovered for physical observation and companion testing. The cone can be difficult to advance in dense or stiff to hard soils, and if the operator is not experienced, the probe can be damaged (or destroyed) when encountering these materials. The specialized equipment and the reliance on electronic instrumentation usually requires the services of a specialty vendor to perform the tests.

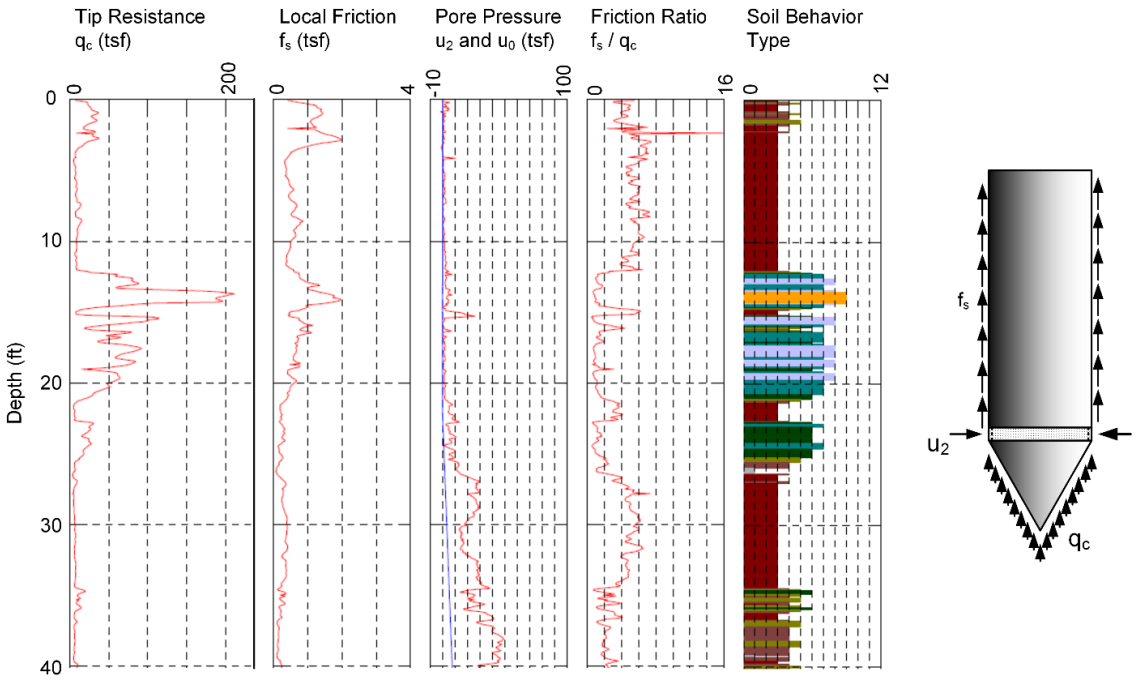

Figure 2-8 CPT - Example Test Record and Equipment

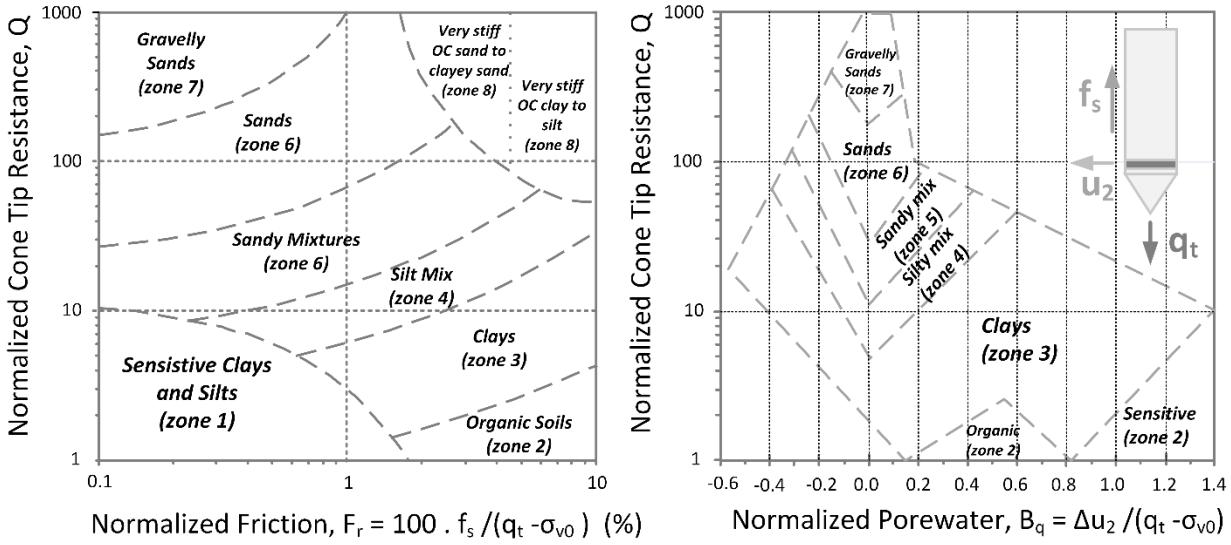

Figure 2-9 Nine Zone (Normalized) Soil Behavioral Chart for CPT (after Robertson 2009 and NCHRP 2018)

2-7.3 Flat Plate Dilatometer.

The flat plate dilatometer test (DMT) was developed in Italy and introduced to the United States practice in the 1980s (Marchetti et al. 2006). It has been widely adopted worldwide and the testing procedures have been standardized in ASTM D6635. The test involves pushing a relatively long and thin flat plate into the ground, generally in 9- to 12-inch vertical increments and then inflating a flexible steel diaphragm while making two or three specific measurements (i.e., A, B, and C). The A reading is the pressure required to lift off the membrane from the face of the blade. The B reading is the pressure required to move the center of the membrane a distance of 0.04 inch (1.1 mm) into the soil. The C reading is an optional reading that can be taken by deflating the membrane until the center of the membrane again contacts the face of the blade. Many practitioners perform the DMT using the same specialized equipment for performing a CPT. In most cases, the test is run without an excavated borehole, so no samples or drill cuttings are produced. However, in some cases, the DMT is lowered into a sampled borehole, advanced approximately 12 inches past the base of the borehole and then inflated as described above. A schematic representation of the test is presented in Figure 2-10.

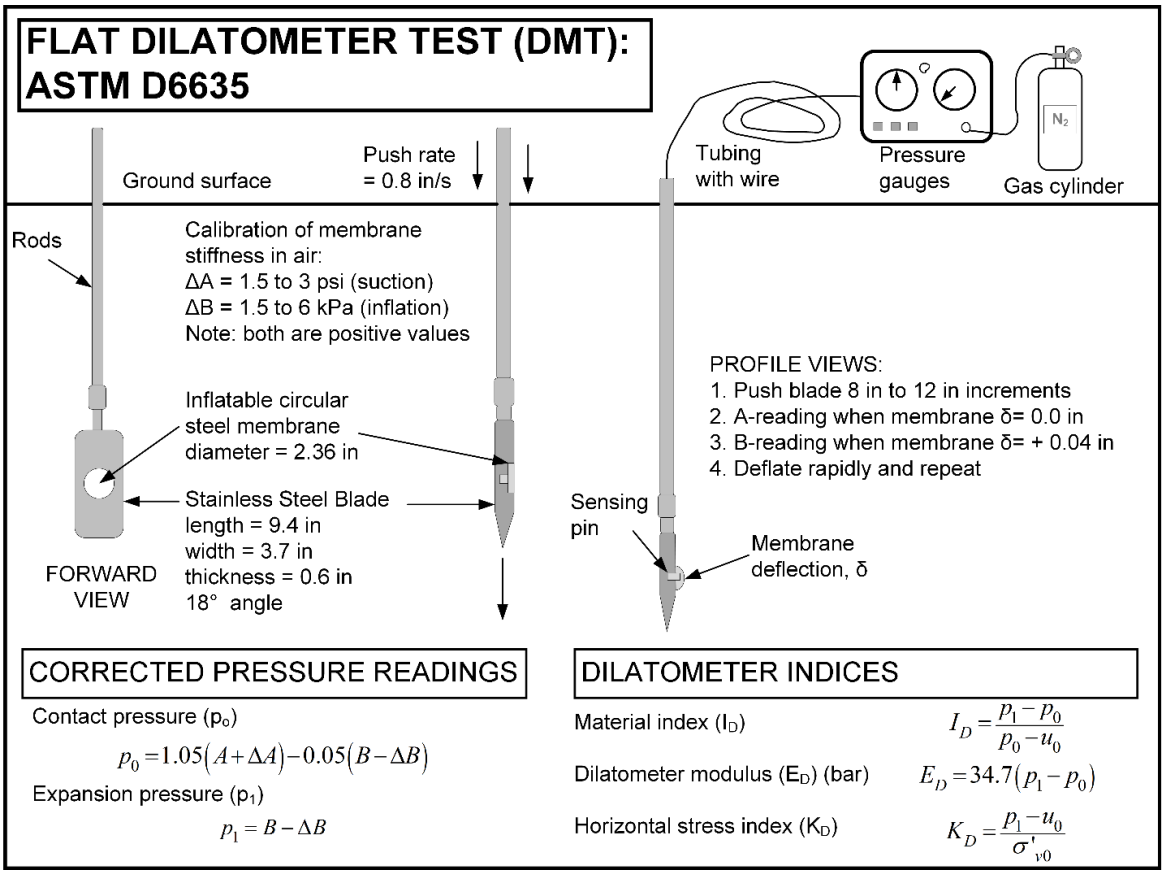

Figure 2-10 Flat Plate Dilatometer Test Schematic (after NCHRP 2018 and Mayne 2012)

2-7.3.1 Equipment, Procedure, and Results.

A photograph of the flat plate dilatometer is presented in Figure 2-11(a), and the control unit used to perform the test (i.e., control inflation and deflation of the membrane) is shown in Figure 2-11(b). The dilatometer blade is nominally 3.75-inches (95-mm) wide, 0.60-inches (15-mm) thick, and 7.5-inches (190-mm) tall with a 30° apex angle at the tip. A 2.4-inch (60-mm) diameter stainless steel membrane is used. The membrane is typically 0.008-inches (0.20-mm) thick and requires careful calibration. The control unit uses bottled gas (nitrogen) supply. A CPT rig is often used to push the dilatometer at a rate of about 0.4 to 1.2 inches/second (1 to 3 cm/s). The vertical thrust is typically monitored and recorded during the test.

(a) Flat plate dilatometer (b) Control unit

Figure 2-11 Flat Plate Dilatometer and Control Unit (Marchetti et al. 2006)

The DMT method and calculations are summarized in Figure 2-10. For more details about the test procedure, refer to NCHRP (2018). The reduced DMT test results produces three values, p_0, p_1, and u_0, from which the following DMT index values are directly calculated for each test depth:

- Material Index, $I_D = (p_1 - p_0) / (p_0 - u_0)$, which is used to identify soil type;
- Dilatometer Modulus, $E_D = 34.7 \times (p_1 - p_0)$ in units of atmospheres, which is a measure of soil stiffness; and
- Horizontal Stress Index, $K_D = (p_1 - p_0) / \sigma'_{v0}$, which is used to assess stress history.

These three indices are typically plotted with respect to test depth to develop a near-continuous vertical profile. Similar to the techniques used for the CPT, these directly calculated values are used to estimate important engineering parameters, including strength, compressibility, modulus, lateral earth pressure) by semi-empirical correlations. A summary of correlations to the DMT results is presented Chapter 8.

2-7.3.2 Advantages and Limitations.

The DMT provides multiple advantages. The test can be performed relatively quickly using a variety of insertion equipment. The probe itself is relatively simple to maintain and training is not particularly onerous. It provides some information regarding horizontal stress and stiffness, which the SPT and CPT are unable to provide.

A major limitation of the dilatometer is that the thin blade and particularly, the diaphragm, can be easily damaged when penetrating soil with particles the size of coarse sand or larger. The diaphragm can be replaced, but the break-in and calibration procedures must be performed, and that can often be difficult to do in the field. The specialized equipment needs to be maintained and properly cleaned between tests, as erratic electric signaling has been experienced when humid conditions exist beneath the membrane. Caution should be used when using dilatometer correlations directly for engineering design parameters.

2-7.4 Dynamic Cone Penetrometer.

Like the CPT, the dynamic cone penetrometer (DCP) has seen a historical evolution. In the United States, the device was developed in the late 1950s in the southeastern United States, primarily to confirm near-surface conditions for spread footings and as a potential surrogate for the SPT. This original, heavier DCP correlate closely with the SPT blow count but was not formally standardized. The United States Army Corps of Engineers (USACE) developed a lightweight DCP that correlates to SPT N values and California Bearing Ratio, CBR (Webster et al. 1992). This lightweight device has seen more widespread use and is standardized in ASTM D6951.

2-7.4.1 Equipment, Procedure, and Results.

A schematic of the lightweight DCP equipment and details of the cone tip are presented in Figure 2-12. A drop hammer (either 17.4 or 10.1 pounds) strikes the anvil to drive in the cone tip. The upper and lower shaft guide the hammer and transmit the driving force to the cone tip. The 60° apex angle cone is at the bottom of the lower shaft. Both fixed and disposable cone tips are available. An extraction jack may be needed to remove the cone and shaft.

The DCP is normally conduct by two people. After seating the cone tip about 1.0 inch, the cone is advanced incrementally by successive drops of the hammer, while holding the device vertical. After each hammer blow, the penetration of the cone is measured and recorded to the nearest 0.1 inch. The test is terminated when a target depth is achieved, when the full length of the lower shaft is embedded, or when the total penetration is less than 0.1 inch/blow for 10 successive hammer blows. The extraction jack is then used to retrieve the embedded shaft/cone.

From the recorded test results, the DCP Penetration Index (DPI) is calculated, and tabulated versus depth. A plot can be developed of the *incremental* values of DPI versus the *cumulative* penetration depth, providing an indication of relative stiffness/strength versus depth. Correlations to DCP are found in Chapter 8.[2]

[2] DCP is often used to represent the DCP Index in equations. This convention is followed in Chapter 8.

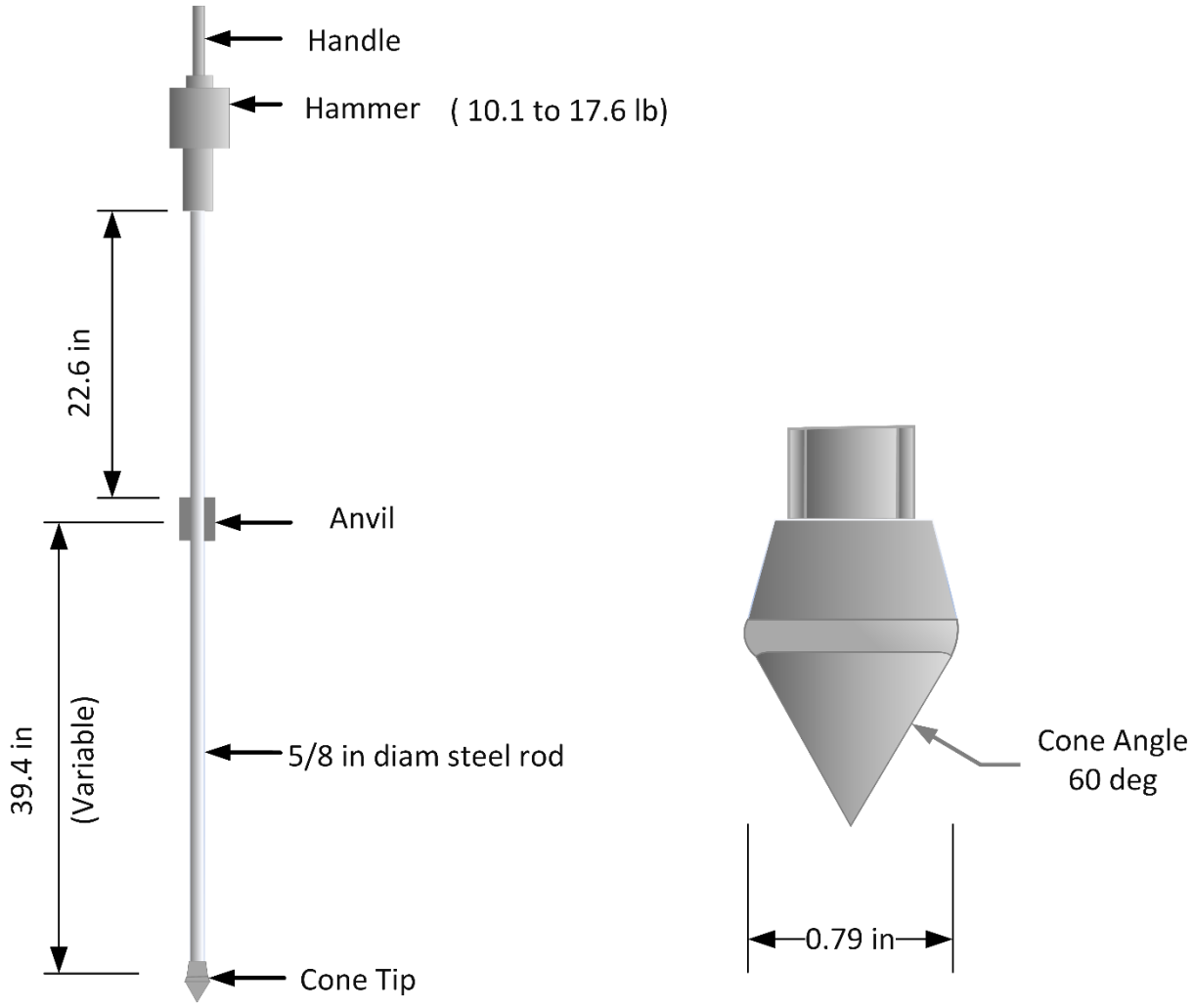

Figure 2-12 Schematic of Dynamic Cone Penetrometer (DCP) Equipment (after Webster et al. 1992)

2-7.4.2 Advantages and Limitations.

The DCP is a simple, low-cost, easy-to-use tool, which is ideal for quick or very low-cost results, or when site access is limited. The results of the DCP can be used as compaction acceptance criteria. It can easily assess stratigraphy, particularly in the delineation of soft and hard layers. The equipment is easy to maintain. Perhaps the biggest advantage is that local and regional correlations can be easily developed and updated as needed.

A significant limitation of the test is the shallow depth of penetration. Verticality of the shafts when driving is critical, and operator experience is valuable. Because a donut-style drop hammer is used, the operator (and helper) need to be avoid “pinch points” between the hammer and anvil.

2-8 GROUNDWATER MEASUREMENTS.

Because of its importance in geotechnical analysis, location of the groundwater table is a key element of a subsurface investigation. During drilling, depths are typically recorded at which the water is first encountered in the borehole and at which the water level stabilizes after drilling. The latter is often recorded after the borehole remains open for approximately 24 hours. In some soils, the sidewalls will collapse unless they are confined or supported (e.g., sands beneath the water table). In these cases, perforated pipe may be used as a temporary casing to protect against borehole collapse while allowing water to flow through the perforations. Knowledge of the seasonal groundwater fluctuation is important, and long-term measurements can be made by converting borings to piezometers, which can vary from open wells to electronic transducers.

Knowledge of the local groundwater regime is required to correctly interpret groundwater measurements, especially those from piezometers. Groundwater can occur at different elevations in the subsurface. It may be *perched* in isolated zones, or it may be confined between different low-permeability strata. In addition, groundwater flow can affect the interpretation of water levels. Where gradients are low and the groundwater table is relatively horizontal, groundwater depths can be directly inferred from piezometer measurements. However, where large gradients are present, the water pressure measured at a point in the ground cannot be directly used to calculate the vertical depth of water above that point. Knowledge of the seepage conditions is required (see Chapter 7-6) to make this determination. Finally, a distinction must be made between steady state and transient conditions. Steady state conditions can be effectively monitored using all types of piezometers. However, under transient conditions (e.g., rapid drawdown in dams, consolidation or swell in fine-grained soils), pore pressures may be changing significantly with time and require instrumentation with a fast response time, such as diaphragm type transducers.

2-8.1 Types of Standpipe Piezometer.

Groundwater level monitoring involves direct measurement of water levels within open well, open standpipe piezometer, or porous element piezometers. The common types of standpipe piezometer for monitoring groundwater levels are depicted in Figure 2-13 and summarized in Table 2-17. The type of standpipe that is selected depends on preferences, regulations (if applicable), and the type of subsurface soils in which the groundwater level will be measured.

The three basic components of a standpipe piezometer include: (1) the tip or well screen; (2) the standpipe itself; and (3) the standpipe seal. These can be installed by hand at shallow depths, but in most cases are installed using a drill rig after the completion of a boring in the soil or rock.

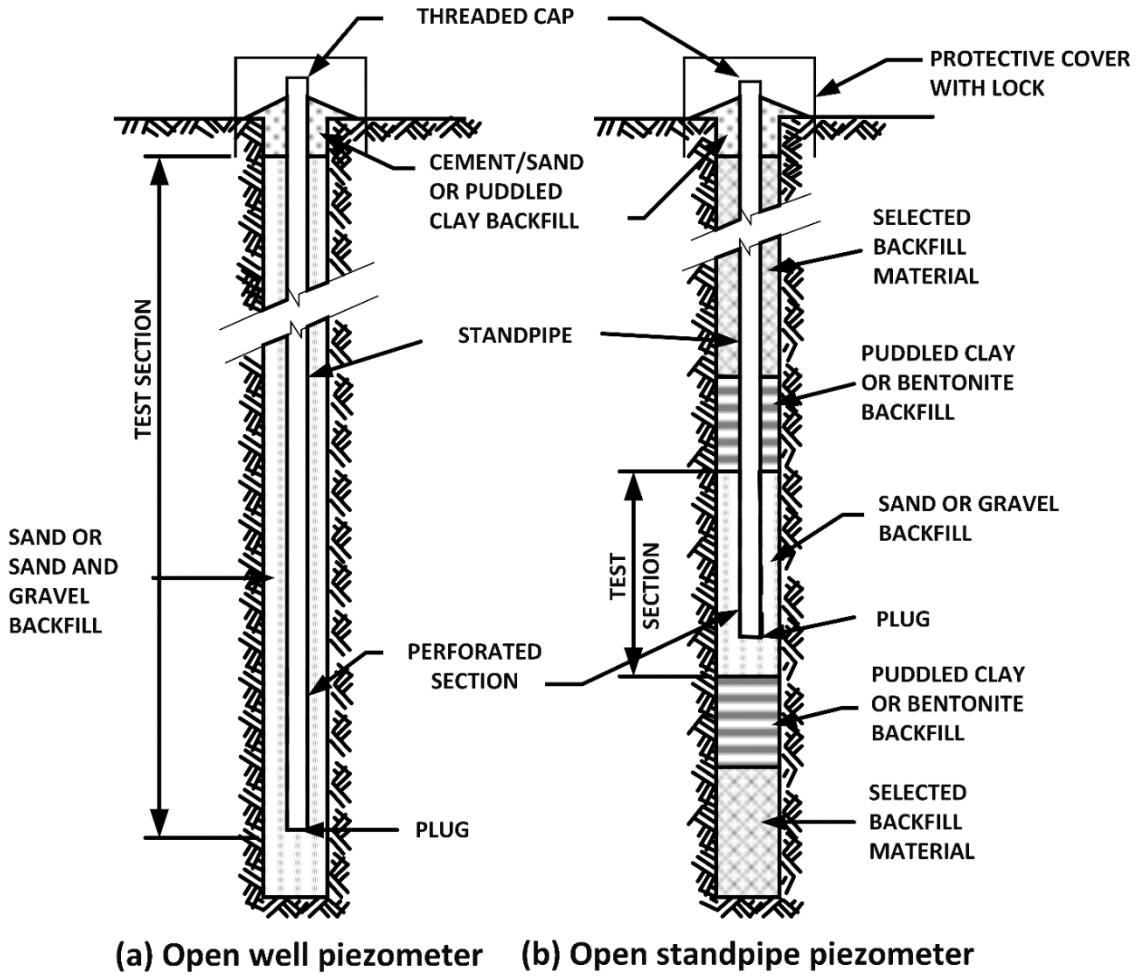

Figure 2-13 Open Piezometers

2-8.1.1 Open Well Piezometer.

A common groundwater monitoring technique is to install a *standpipe*, or water tight pipe, within an open boring as shown in Figure 2-13(a). The standpipe has a perforated tip or screen that allows water to enter are usually small-diameter (e.g., less than 2 inches) PVC plastic pipe but may be larger for environmental sampling applications. In an open well, the annular space between the pipe and borehole wall is filled with filter sand or gravel almost to the ground surface. At the ground surface, a seal of cement grout, bentonite slurry, or other low permeability material is placed above the filter sand to isolate the well from surface water flow. Open wells are often called groundwater monitoring wells and are commonly used for environmental applications when samples of the groundwater are required.

Table 2-17 Types of Standpipe Piezometers

Piezometer Type	Advantages	Disadvantages
Open well piezometer	Simple and reliable; long experience record; good for coarse-grained soils; large diameter may be required/needed for environmental monitoring and groundwater sampling	Slow response time, particularly in fine grained soils; unable to monitor distinct stratum exhibiting different groundwater levels; freezing potential in winter
Open standpipe piezometer	Simple and reliable; long experience record; able to monitor distinct stratum exhibiting different groundwater levels; good for coarse-grained soils	Slow response time in low permeability soils
Porous element piezometer (hydraulic)	Rapid response time; good for soils exhibiting medium permeability; good for applications impacted by electrical interference	Humid air entering tubing may impact readings; time consuming to make measurements.
Porous element piezometer (electronic)	Rapid response; high sensitivity; suitable for automatic readout	Relatively expensive; temperature and barometric pressure correction may be required; zero drift errors can arise

Because an open well has a full-length screen or a full depth filter zone, it is best suited for measuring water levels in relatively homogeneous deposits with high permeability. When multiple strata are crossed, the groundwater level corresponds the stratum with the highest total head. A significant advantage of an open well piezometer is that it can be cleaned and "developed" by flushing water from the standpipe into the formation, which is critical for open well piezometers used for environmental applications.

2-8.1.2 Open Standpipe Piezometer.

An *open standpipe piezometer* is similar to an open well, except that the screen extends only across a specific stratum of interest. Seals are installed above and below this zone to only allow water to enter from the stratum of interest. An open standpipe piezometer is shown in Figure 2-13(b). Outside of the screened test section, select backfill materials are used but not necessarily filter sand. A seal is typically placed around the open standpipe at the ground surface.

Multiple open standpipe piezometers can be installed to measurement groundwater levels in multiple strata within a single borehole through careful installation of multiple seals. This approach is sometimes referred to as a nested piezometer. The vertical location (i.e., depth, thickness, and elevation) of each seal must be accurately measured and recorded on the well log.

A major disadvantage of open well and open standpipe piezometers is the long equalization time that may be required for water to flow from the formation and fill the piezometer. Until the groundwater level stabilizes in this manner, the readings are inaccurate. To reduce the equalization time, the diameter of the standpipe can be reduced to less than 0.5 inches, which decreases the volume of water needed.

2-8.1.3 Porous Element Piezometers.

The primary disadvantage of open well and open standpipe piezometers is the potentially long equalization time for the groundwater level to stabilize since the riser pipe must fill with a considerable volume of water from the formation. Porous element or hydraulic piezometers have a ceramic or porous metal tip attached to a small-diameter riser pipe (i.e., standpipe). Modern versions use a porous element with pore sizes of <50 microns, so that the tip can be used in direct contact with fine-grained soils. One of the primary advantages of the porous element piezometer is the relatively short equalization time periods in fine-grained soils exhibiting low permeability. However, water must still flow from the formation through the porous element and into the standpipe to obtain accurate groundwater level measurements.

2-8.2 Multiple or Nested Installations.

Several standpipe piezometers may be installed in a single boring with an impervious seal separating the different measuring zones. These are called *nested* piezometers. This concept represents a cost advantage, as it reduces the number of borings (but increases the difficulties/challenges of installing seals and specific elevations) and the number of “obstacles” during for the contractor during construction. However, if measurements are needed in zones with 10 feet or less of vertical separation, piezometers should be installed in separate borings.

2-8.3 Measurement of Groundwater Levels.

Groundwater levels/elevations can be obtained by either direct or indirect methods. The direct method includes: (1) surveying the elevation of the top of the riser pipe and/or the ground surface; (2) measuring or calculating the “stick-up” of the riser pipe above the ground surface; and (3) measuring the distance depth from the top of the riser pipe to the water surface inside the open pipe or the standpipe. The elevation of the groundwater can then be easily calculated. There are several methods to measure the distance from the water surface to the top of the riser pipe; including a plumb bob, cloth or metal surveyors' tapes coated with chalk, or commercially available electrical indicators. Using these direct measurements, the water level can be established generally within a tolerance of about 0.5 inch.

An indirect, but more accurate, method for measuring the depth of water in an open well uses an electrical transducer capable of measuring water pressure. The transducer is attached to a hoisting cable and an electrical cable. Markings on the electrical cable are used to measure the length of the cable in the open pipe. Commercially, these portable systems are called *water level indicators*. The transducer is lowered to a depth typically near the bottom of the open hole such that the transducer is submerged. The electrical cable is attached at the surface to a readout unit that measures the pressure due to water column above the tip of the transducer. From the unit weight of water

(i.e., 62.4 pcf or 9.81 kN/m^3), the depth of water above the tip of the transducer is calculated, which combined with the length of cable in the open pipe can be used to calculate the groundwater level in the pipe. This type of transducer can be connected to a data collection unit and groundwater levels can be automatically collected over time. This capability is often quite efficient and is, in fact, a requirement when groundwater pumping tests are performed and the time-dependent groundwater elevation as a function of pumping rate is necessary for subsequent calculations of *in situ* permeability of a formation (see Section 2-9.2). The indirect method can also be used with pore pressure transducers that are grouted or sealed directly in boreholes without a standpipe. More information on the transducers used with this type of piezometer is provided in Section 2-10.4.

While being simple in concept, the techniques for measuring groundwater levels have some inherent limitations. First, standpipe piezometers require access to the top of the vertical riser pipe, which usually extends above the ground surface and may be easily damaged during construction. If the riser is extended vertically during construction (e.g., installed in a constructed embankment), the extension activities must be carefully coordinated with the earthwork contractor. Manual or direct measurement of water levels is time consuming and may adversely impact construction. The largest source of error for standpipe piezometers is the lag time required for the piezometer to respond to changing groundwater levels because water must flow from the formation into the piezometer. For this reason, groundwater piezometers are intended to measure hydrostatic groundwater levels and are inappropriate for time-dependent pore pressures. Other sources of error that impact piezometer readings include the possibility of direct introduction of precipitation into the riser pipe due to a missing or vandalized cap, infiltration of surface water into the borehole, and the formation of gas bubbles within the pipe. Indirect groundwater measurements by porous element piezometers without a standpipe or pore pressure transducers can alleviate many of these limitations.

2-8.4 Detection of Combustible Gases

Gas bubbles in groundwater can influence the measurement of groundwater levels. Gas can exist in subsurface soils and pose other hazards. Specifically, methane (CH_4) and other combustible gases may be present in subsurface soils and rock, particularly in sites near municipal solid waste (MSW) landfills, or at sites near or over peat bogs, marshes, and swamp deposits. Methane is a dominating combustible gas in the subsurface because it is one of the primary by-products of the anaerobic decomposition of organic material. The other dominant gas is carbon dioxide (CO_2). Commercially available portable instruments, referenced as landfill gas analyzers, are used to detect the presence and concentration of combustible methane gas in landfill gas wells and monitoring probes. These instruments sample the air/gas from the confined space in wells and borings above the water table. The instrument generally detector indicates

the concentration of gases in the collected gas sample. The critical concentration limits for methane is between 5 and 17 percent by volume. A concentration of less than 5 percent methane is considered too “lean” to burn or ignite and is referenced as the lower explosive limit (LEL). A concentration of more than 17 percent methane is considered too “rich” to ignite and cause a flash fire (i.e., explosion) and is referenced as the upper explosive limit (UEL). If methane concentrations are measured within the 5 to 17 percent range, all possibilities of spark generation (e.g., pile driving, grinding, welding, smoking) should be eliminated and a venting system should be considered, to provide worker protection.

2-9 MEASUREMENT OF SOIL AND ROCK PROPERTIES *IN SITU.*

Field sampling and laboratory testing can sometimes be complemented or replaced by *in situ* testing, which refers to measurements conducted on soil and rock “in place.” As a general rule, an *in situ* testing program can be performed faster and in many cases at a lower cost than most laboratory testing programs. As a result, this alternative has seen growing popularity since the 1980s. The SPT, CPT, DMT, and DCP are four of the most popular *in situ* testing methods, which are often correlated to engineering parameters. This section discusses other *in situ* tests that measure strength, stiffness/modulus, and permeability of existing soils, as well as the as compacted properties of earthwork. Methods for *in situ* testing of rock are also discussed.

Although not universally adopted, many practitioners find that the pocket penetrometer and the field torvane provide useful correlations to the shear strength as measured in the laboratory. These tests may be performed on the soil exposed at the bottom of a recovered Shelby tube sample. Practitioners who use these tests often correlate the results to results from laboratory strength tests, to increase the value of the field test. Although these tests are often used in practice, the results are very inexact and should not be used for design.

2-9.1 Strength and Deformation Properties of Soil.

The pressuremeter test, vane shear test, and the plate load test are the most commonly used *in situ* testing methods for assessing strength and stiffness of soils. A summary and comparison of these tests is presented in Table 2-18. Where ASTM standards are available, they have been included in the table.

Table 2-18 *In situ* Testing Methods Used in Soil for Strength and Deformation (after FHWA 2002)

Method and ASTM No.	Procedure	Applicable Soil Types	Applicable Soil Properties	Limitations / Remarks
Pre-bored Pressuremeter (PMT) ASTM D4719	Borehole drilled and the bottom is carefully prepared. The pressure required to expand the cylindrical membrane to a certain volumetric or radial strain is recorded	Clays, silts, and peat; marginal response in some sands and gravels	E, G, m_v, s_u	Preparation of the borehole most important step to obtain good results; good test for calculation of lateral deformation characteristics
Full Displacement Pressuremeter (PMT)	Cylindrical probe with a pressuremeter attached behind a conical tip is hydraulically pushed through the soil and paused at select intervals for testing. The pressure required to expand the cylindrical membrane to a certain volume or radial strain is recorded	Clays, silts, and peat	E, G, m_v, s_u	Disturbance during advancement of the probe will lead to stiffer initial modulus and mask liftoff pressure $\left(p_0\right)$; good test for calculation of lateral deformation characteristics
Vane Shear Test (VST) ASTM D2573	Four- blade vane is pushed into the bottom of a borehole. The vane is slowly rotated until the maximum torque required for rotation is recorded. The vane is rapidly rotated for 10 turns, and the residual torque is recorded.	Clays, some silts and peats if undrained conditions can be assumed. Not for use in granular soils	s_u, S_t, σ'_p	Disturbance may occur in soft sensitive clays, reducing measured shear strength; partial drainage may occur in fissured clays and silty materials, leading to errors in calculated strength; rod friction needs to be accounted for in calculation of strength; vane diameter and torque wrench capacity need to be properly sized for adequate measurements in various clay deposits
Plate Load Test (PLT) ASTM D1196	A circular, rigid steel plate is hydraulically pushed into the soil and the relationship between bearing stress and vertical settlement is recorded	All soils and rock, particularly helpful in unbounded base aggregate for pavements	q_{ult}, k_s	Limited depth of influence; short-term test will not capture consolidation impacts; not typically used as part of geotechnical site investigation

Note: E = elastic modulus; G = shear modulus; m_v = coefficient of volume compressibility; s_u = undrained shear strength; S_t = sensitivity; σ'_p = preconsolidation stress, q_{ult} = ultimate bearing capacity; k_s = modulus of subgrade reaction

2-9.1.1 Pressuremeter Test.

The pressuremeter test (PMT) was first developed in about 1955. In the PMT, a membrane is inflated from a cylindrical probe against the sidewalls of an open borehole. The radial expansion is measured, and this response is used to calculate specific strength and deformation properties of the subsurface soils. PMT can be performed in a wide range of materials, including sands, residual soil, tills, and soft rock, that are usually difficult to sample. The "traditional" is called the "pre-bored" or "Menard" pressuremeter. Other types include the self-boring pressuremeter (SBPMT) that includes its own cutting shoe and does not require an existing borehole and the full-displacement or cone pressuremeter (CPMT) that is pushed into the ground, usually behind a piezocone. A schematic of the PMT equipment and test is shown in Figure 2-14.

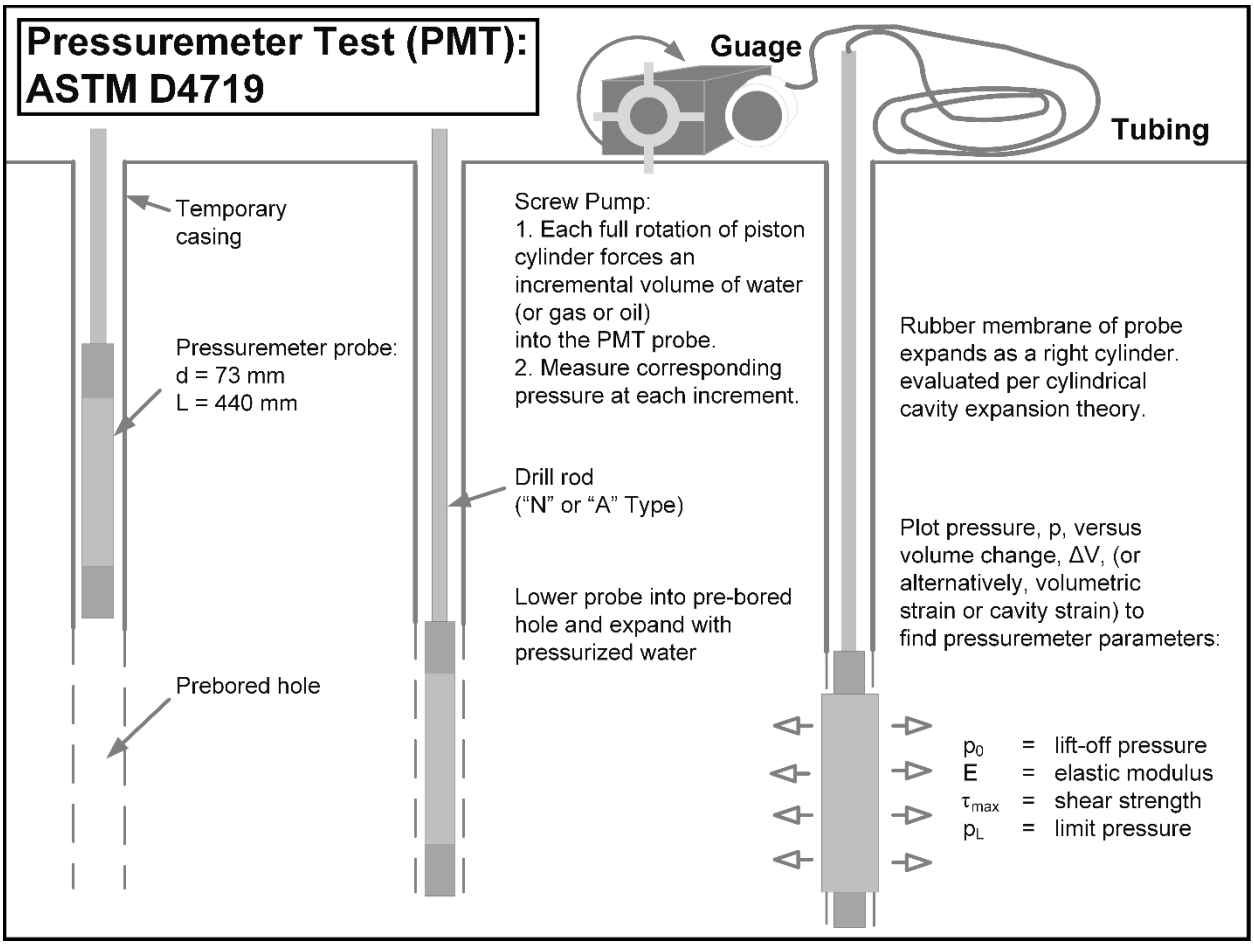

Figure 2-14 Schematic of Pressuremeter Test (after NCHR 2018 and Mayne 2012)

As shown in Figure 2-14, the equipment needed to perform a PMT includes of an expandable cylindrical probe, rubber membrane, outer slotted sleeve, pressure lines, and control unit. The PMT procedures are defined in ASTM D4719 and can be

consulted for further details on the test method. The inner membrane is hydraulically expanded to obtain an expansion pressure versus volume curve. During loading, disturbed soil in the borehole wall first compresses, followed by a pseudo-elastic response and then plastic yielding. After plastic yielding is induced, a creep test is performed by holding pressure constant until the lateral expansion falls below a threshold. The PMT concludes with an unload-reload cycle to better define the elastic properties.

Typical PMT pressure vs. volume change results are shown in Figure 2-15 along with definitions of the characteristic pressures. For comparison, a typical SBPMT test result is presented in Figure 2-16.

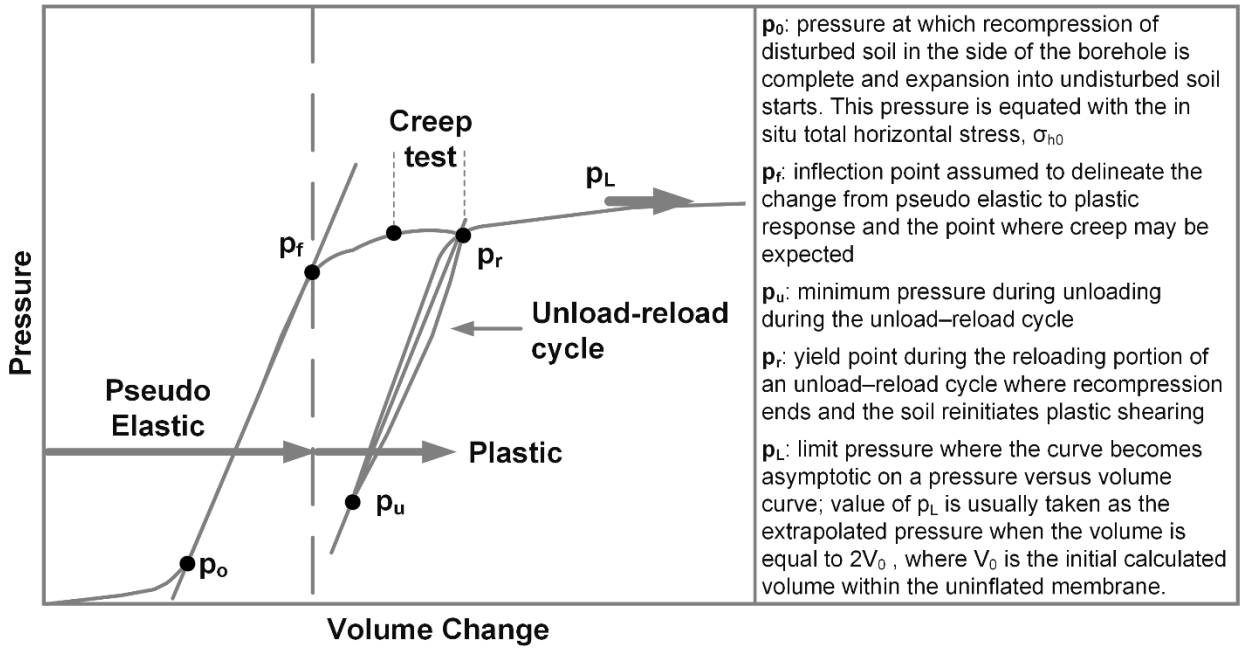

Figure 2-15 Typical Result and Characteristic Pressures from Pressuremeter Test (after FHWA 2002)

2-9.1.1.1 Test Interpretation.

Pressuremeter tests have been used to estimate the coefficient of lateral earth pressure at rest (K_0), the soil stiffness; and undrained shear strength (s_u).

- Coefficient of Lateral Earth Pressure at Rest (K_0): Upon initial inflation, the membrane will expand to contact the borehole sidewalls. In the PMT, p_0 is related to the *in situ* total horizontal stress, which combined with the vertical stress allows K_0 to be calculated. Due to unloading effects and disturbance during drilling the borehole, the accuracy of this calculation is questionable. To

accurately assess the *in situ* lateral stress and K_0, a self-boring pressuremeter should be considered. Point A in Figure 2-16 is a relatively accurate representation of the total horizontal stress in the ground.

- Stiffness: The elastic stiffness of the soil can be estimated by the slope of the unload-reload pressuremeter curve where the response is assumed to be nearly elastic. One technique calculates the pressuremeter modulus (E_p), while another uses cavity expansion theory to calculate shear modulus, G (Gibson and Anderson 1961, Windle and Wroth 1977).
- Undrained Shear Strength (s_u): Methods exist to estimate the undrained shear strength from pressuremeter results, but the resulting values are less reliable than those from other *in situ* tests, such as the cone penetration test or the vane shear test.

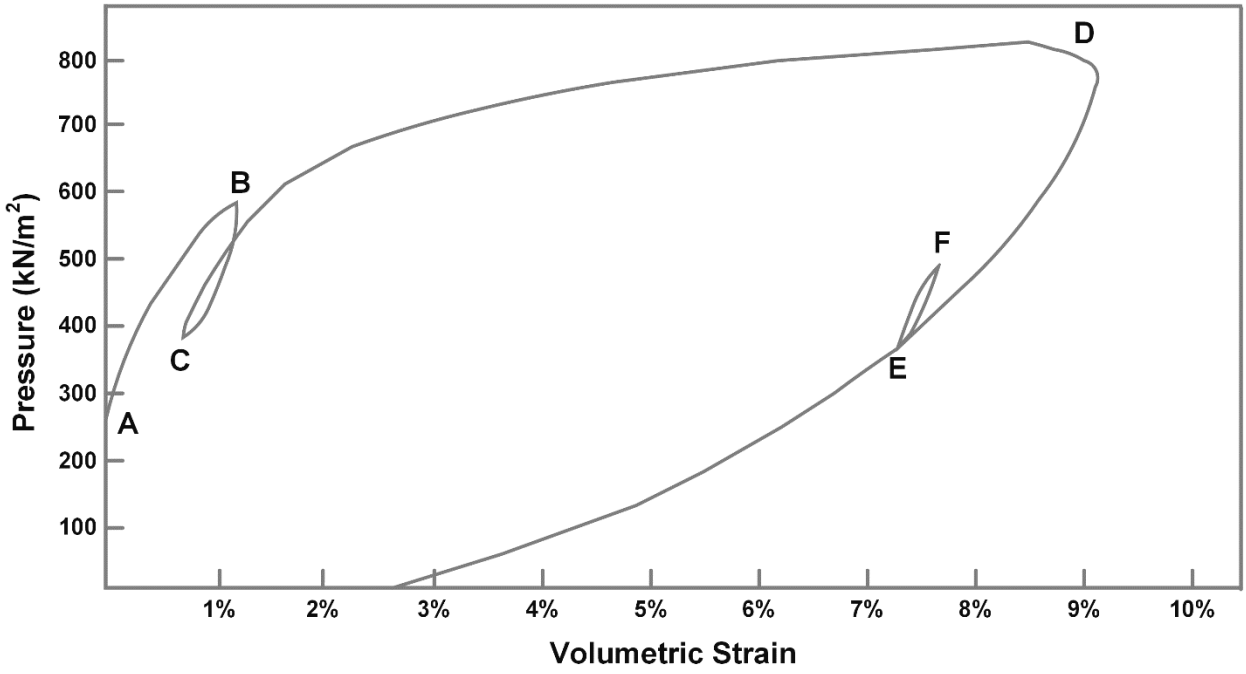

Figure 2-16 Example Result from Self-boring Pressuremeter Test in Clay (after Windle and Wroth 1977)

2-9.1.1.2 Limitations.

Pressuremeter testing is sensitive to test procedures. In very soft soils and in sands, it may be difficult to maintain borehole stability before the probe is inserted. In these cases, a self-boring pressuremeter may be necessary. Irregularities in the wall of the borehole wall also affects test results, and the self-boring pressuremeter eliminates some of this disadvantage. The SBPMT usually requires a specialist familiar with the test and the instrument. Pressuremeter test interpretation has a theoretical basis and,

therefore, either drained or undrained conditions need to be maintained. The pressuremeter is relatively long (i.e., generally greater than 2 feet in length) and results reflect an averaging of the soils over this length. For this reason, the PMT in best used in relatively homogenous deposits, and it not expected to provide reliable parameters in stratified soil. Pressuremeter equipment has many moving parts and requires maintenance and careful handling.

2-9.1.2 Vane Shear Test.

The vane shear test (VST) is a popular and reliable *in situ* test that has been in use since the 1940s. The VST involves the use of a simple four-sided blade (i.e., vane) that is pushed into the ground and then rotated to evaluate the undrained shear strength and sensitivity of soft to stiff clays and silts. The use of the VST should be limited to soils in which slow (i.e., ~6° / min) rotation of the vane represents undrained shearing. A schematic of the VST equipment and operation is presented in Figure 2-17. At failure, the vane will cut a "cylinder" of soil equivalent to the outside dimensions of the vane and the torque will reduce. The vane is often rotated 10 more revolutions, and the residual torque is measured.

The undrained shear strength ($s_{u,fv}$), the remolded undrained shear strength ($s_{ur,fv}$), and the sensitivity ($S_{t,fv}$), can be obtained from the VST. During rotation, the maximum net torque (T_{max}) is measured and the undrained shear strength for a "standard" rectangular vane with an H/D ratio of 2 is as follows:

$$s_{u,fv} = \frac{6T_{max}}{7\pi D^3} \quad \textbf{(2-1)}$$

where:
D = diameter of the vane.

To measure the remolded undrained shear strength, the torque reading (T_{res}) is taken during rotation of the vane following five to ten rapid turns of the vane. The remolded strength is calculated by replacing T_{max} with T_{res} in Equation 2-1. With knowledge of the peak and remolded values for undrained shear strength, the sensitivity of the soil from vane shear tests can be calculated by:

$$S_{t,fv} = \frac{s_{u,fv}}{s_{ur,fv}} \quad \textbf{(2-2)}$$

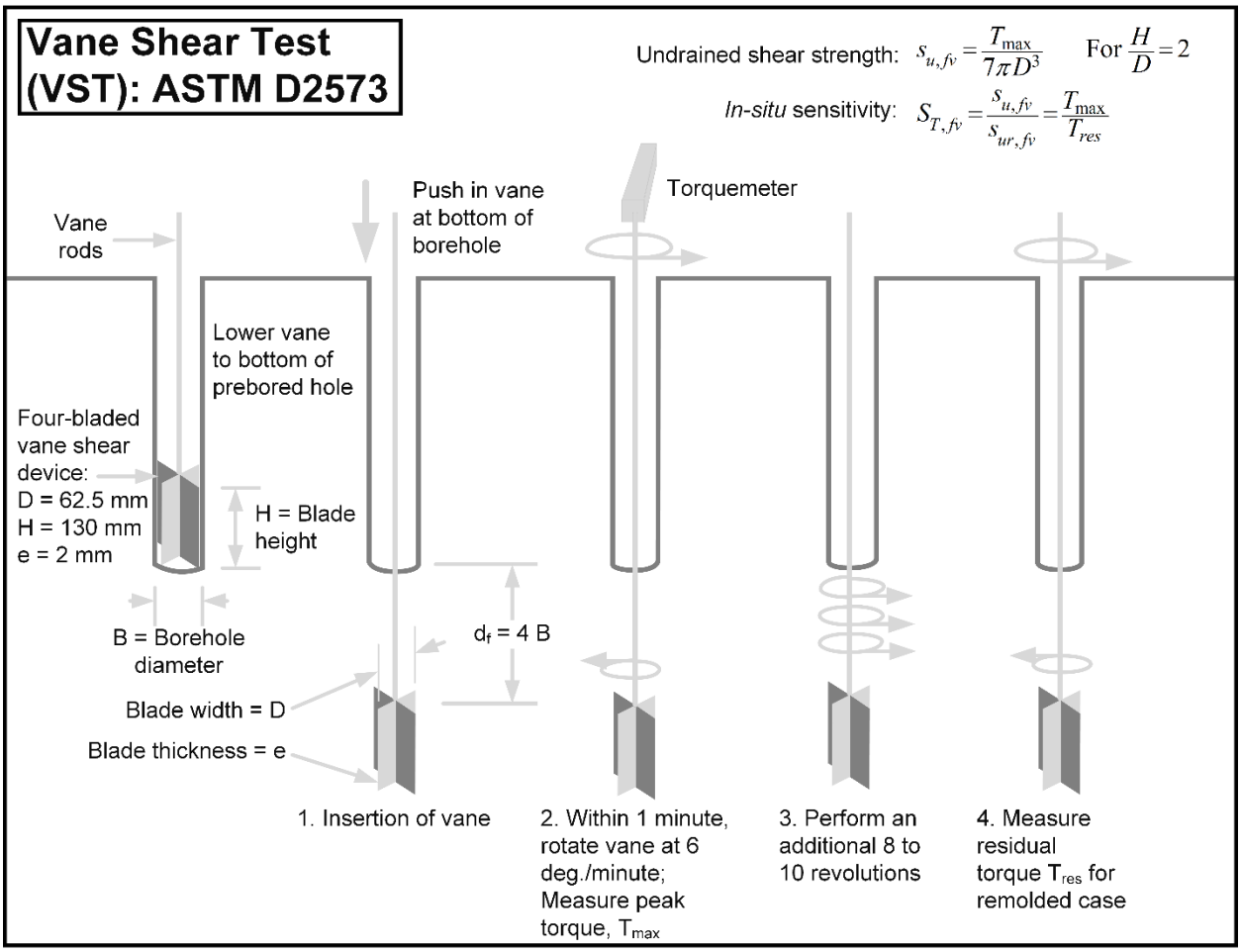

Figure 2-17 Schematic of Vane Shear Test (after Mayne 2012)

The undrained shear strength from the VST overpredicts the shear strength mobilized in failures of embankments, shallow footings, and slopes constructed on soft clay. In order to account for this, $s_{u,fv}$ should be adjusted by a correction factor (μ_R), which is a function of the PI of the soil tested. Three different vane correction methods are given in the ASTM specification. The corrected shear strength can be calculated by:

$$s_{u,field} = s_{u,fv} \times \mu_R \quad \textbf{(2-3)}$$

where:
μ_R = vane correction factor.

The VST has proven to be a very reliable and repeatable *in situ* test and enjoys widespread popularity due to cost and efficiency. It is perhaps the best device to measure the *in situ* strength of soft to medium clays (s_u < 2000 psf). The biggest limitation of the VST is the types of soil where it can be used. The VST cannot

accurately assess the strength of fissured clays, clays with significant amounts of sand or gravel, and soils with relatively thin laminations. The data for the VST is reduced based on the assumption of undrained conditions. Therefore, soils that might allow partial drainage during shear are problematic.

2-9.2 Hydraulic Conductivity of Soil.

Hydraulic conductivity is the most variable of all the material properties commonly measured and used in geotechnical analysis, with the range extending to more than ten orders of magnitude. Accurate measurement of hydraulic conductivity is very sensitive to the type of soil, the disturbance of the soil, site stratigraphy, and the variability of the soil deposit across the site. Laboratory testing of the hydraulic conductivity of soil, even on samples of minimally disturbed recovered samples, may not reflect the hydraulic conductivity of the natural deposit because the lab sample is quite small and certainly not representative of a geologically placed and weathered material. If the soils at the site are relatively uniform and can be sampled with minimal disturbance (i.e., uniform clay soils), laboratory testing may be sufficient and adequate. However, for deposits of coarse-grained materials, intact sample are nearly impossible to obtain, and *in situ* hydraulic conductivity tests are commonly used. In particular, *in situ* tests are important for uniform coarse-grained deposits. Correlations based on grain-size distribution are also very common for coarse-grained deposits (see Chapter 8).

The following five physical characteristics influence the performance and applicability of *in situ* hydraulic conductivity tests: (1) water level position, (2) type of soil or rock, (3) depth of the test zone, (4) hydraulic conductivity of the test zone, and (5) heterogeneity and anisotropy of the test zone.

The difficulties inherent with *in situ* hydraulic conductivity testing require that great care be taken to minimize sources of error and to correctly interpret and compensate for deviations from ideal test conditions. Many of these difficulties can be overcome by planning tests to isolate specific zones of material assumed to be uniform.

In situ hydraulic conductivity tests are most commonly used in geotechnical engineering investigations for dams, hydraulic barriers, geo-environmental projects, and project with a strong hydrogeologic component. For strictly geotechnical applications, steady-state testing is much more common than transient state testing. In addition, saturated hydraulic conductivity testing is more common than *in situ* testing for unsaturated conditions. A brief summary of the four most common types of *in situ* hydraulic conductivity tests is presented in Table 2-19.

A considerable amount of skill is necessary to correctly measured the hydraulic conductivity of soil *in situ*. Specialty firms will likely provide more accurate and prompt results compare with the personnel used for routine drilling and sampling. Specialty

firms are staffed by geotechnical and hydrogeologists who routinely conduct *in situ* permeability tests.

Table 2-19 Summary of *In situ* Test Procedures for Measuring Hydraulic Conductivity of Soil Deposits

Type of Test	Description	Advantages and Disadvantages
Constant Head Test	Water is added to an open-ended pipe (cased borehole) at a constant rate. Water level in hole maintained at a constant level.	Can be performed in saturated and partially saturated soils. Difficult to perform on soils with a very high or very low k. Only a small zone of soil is tested (if unscreened).
Variable Head Rising Head and Falling Head Tests (ASTM D4044)	An interval of a borehole is screened. A "slug" of water removed from or added to the borehole. Elevation of the water level recorded over time.	Construction and development of the well is more difficult than constant head test. Data reduction can be complex.
Pressure Tests	Borehole section isolated by or sealed off with "packers." Elevated pressure can be applied to achieve increased flow.	Best for deep explorations. Can be conducted above or below the water table. Can be used to measure the hydraulic conductivity of fractured rock.
Pumping Tests	Install pumped well and observations wells radially from the pumped well. Record the amount of water pumped and the elevation of water in the wells is over time. Use analytical or numerical analysis to determine the hydraulic parameters of the soil deposit.	More expensive than other methods. Hard to justify increased cost for common geotechnical projects. Provides addition information regarding aquifer transmissivity and storativity. Tests a larger volume of soil than other methods. Long testing times.

2-9.3 Engineered Fill and Earthworks.

The *as-compacted* moisture/water content and unit weight (often referred to as density) of compacted soils is a significant component of geotechnical practice involving constructed engineered fill or earthworks (e.g., dams, embankments, etc.). For purposes of this discussion, the terms moisture content and unit weight will be used. Geotechnical engineers have long recognized that many of the desired engineering properties of both fine- and coarse-grained compacted materials depend on the compaction moisture content and/or unit weight. The compaction water content is much more important for fine-grained as opposed to coarse-grained soils. This section focuses on the use and limitations of the numerous techniques used in practice for these important measurements.

It should be noted that compactors are current available that can measure the stiffness of soils "on-the-fly" during compaction (McGuire et al. 2009). These special compactors are becoming very popular in earthwork construction, and their use has supplanted many of the older methods of compaction quality control incorporated into earthwork specifications.

2-9.3.1 Measurement of As-Compacted Soil Unit Weight.

Four general strategies can be used to assess the as-compacted unit weight of soils: (1) displacement methods; (2) drive-cylinder methods; and (3) nuclear gauge methods; and (4) non-nuclear gauge methods. All of these methods use measurements from the ground surface to assess the near-surface characteristics of the soil. This section provides a discussion of each of these strategies and methods.

2-9.3.1.1 Displacement Methods.

Of the displacement methods, the sand displacement and water balloon displacement techniques are the most widely used because of their simplicity, applicability to a wide range of material types, and their historical performance and record of accuracy. In both cases, a known weight of soil is excavated from the ground. Either sand or water of a known unit weight is used to measure the volume of the excavated hole. The results are more accurate when a large volume is measured. Displacement methods measure the total unit weight of the soil. The water content of the excavated soil must be determined to calculate the dry unit weight.

The sand displacement method, usually referenced as the “sand cone” method, is the most frequently used displacement test to assess *in situ* dry unit weight. A schematic of the sand cone apparatus is shown in Figure 2-18. Originally standardized in 1958 (ASTM D1556), the sand cone method remains the recognized reference test for all other methods used to assess *in situ* soil unit weight. Consistent results strongly depend on operator experience and care in performing the test.

The water balloon displacement test (ASTM D2167) uses the same principle as the sand cone. The excavated hole in the soil is lined with a balloon (i.e., watertight, thin membrane), which is filled with pressurized water from a volume-calibrated container as shown in Figure 2-19. The water balloon method should not be used in soils that contain significant amounts of gravel that can potentially puncture the balloon. The water balloon method generally provides consistent and accurate results when performed correctly, although not as consistent as the sand cone (Berney et al. 2013).

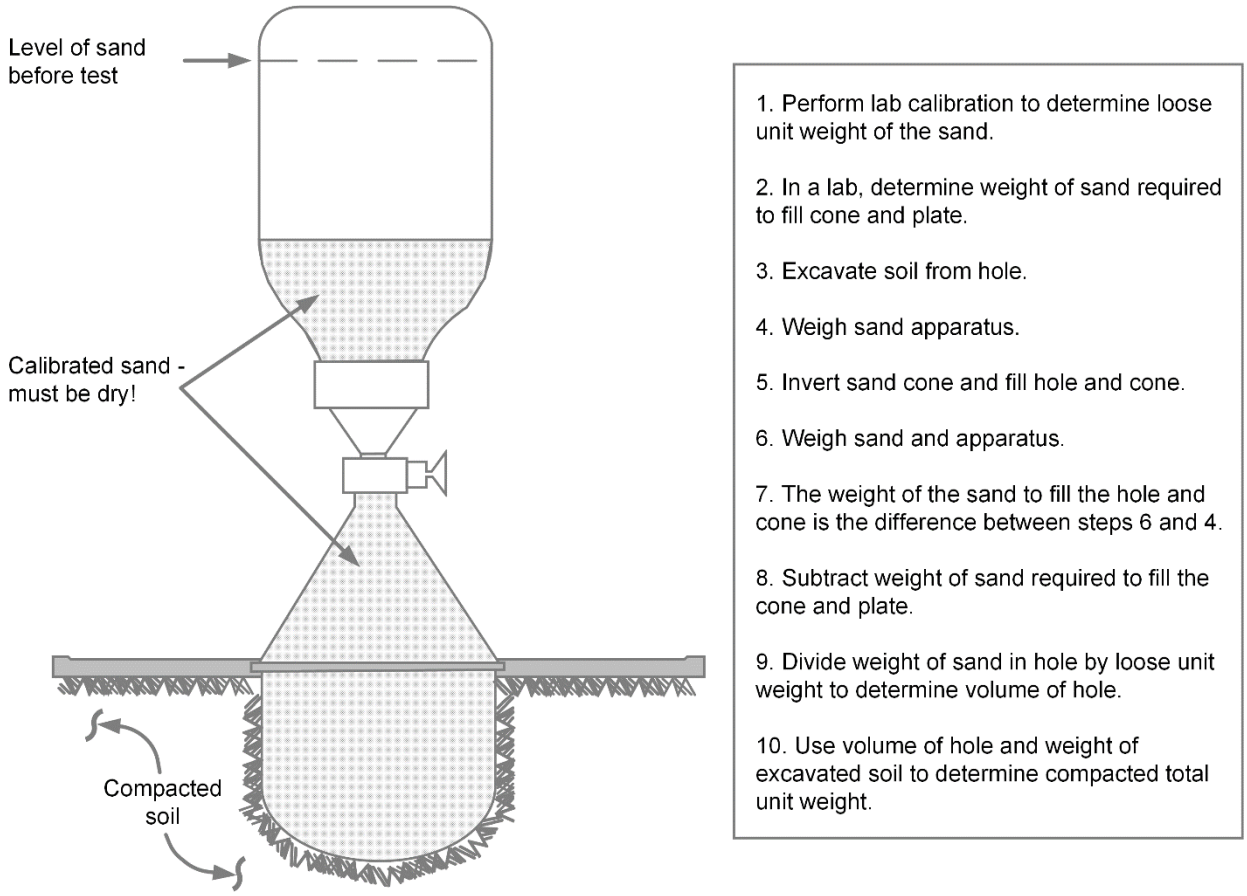

Figure 2-18 Schematic of Equipment and Process to Perform a Sand Cone Test (after Dunn 2017)

2-9.3.1.2 Drive-Cylinder Method.

The drive cylinder method (ASTM D2937) is a convenient and rapid technique to obtain the as-compacted total unit weight of soil. A slide hammer is used to drive a relatively short thin-walled tube (e.g., shortened Shelby tube) into the ground to obtain a sample. After the cylinder is driven, the soil-filled cylinder is carefully dug out of the ground, and the top and bottom of the sample is trimmed flush with the ends of the tube. The inside volume of the tube is the volume of the sample. A conventional drive cylinder is shown in Figure 2-20. This method can be used as long as the soil will remain in the cylinder, most notably fine-grained soils containing little or no gravel and moist, fine sands that exhibit apparent cohesion. The method cannot be used in soils that contain gravel, as the cylinder can be easily damaged. The drive cylinder measures the total unit weight, and the water content must be determined by drying the soil sample.

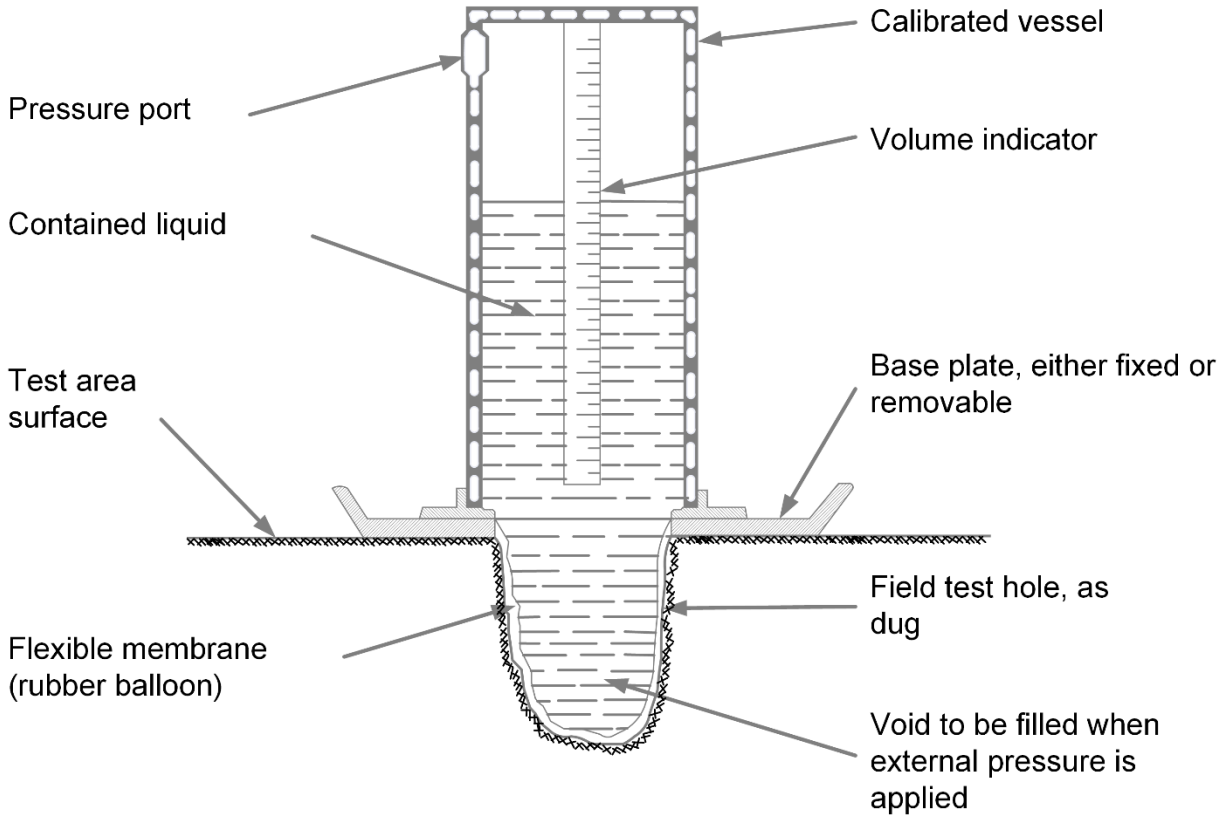

Figure 2-19 Schematic of Equipment to Perform Water Balloon Test (after Dunn 2017)

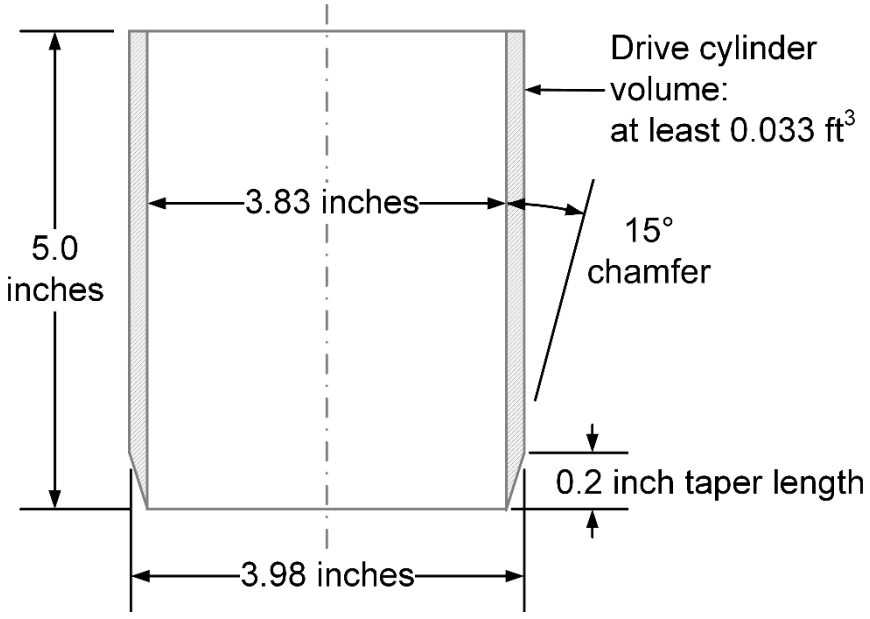

Figure 2-20 Schematic of Drive Cylinder (after ASTM D2937)

2-9.3.1.3 Nuclear Gauge Method.

The use of nuclear technology to assess soil unit weight and moisture content commenced in the early 1950s (Burgers and Yoder 1962). As shown in Figure 2-21, the nuclear source (usually Cesium-231) is housed near the tip of a rod that is inserted in a prepared hole at the test location. A low-power nuclear source is used to emit gamma rays through the soil to detectors in the gauge, and the detection rate is correlated to total unit weight of the soil. When not in use for testing, the nuclear source is protected inside of the shielded gauge. Procedures for using a nuclear gauge to measure unit weight and water content can be found in ASTM D6938. Proper, regular calibration of nuclear gauges is essential to obtain consistent and accurate results.

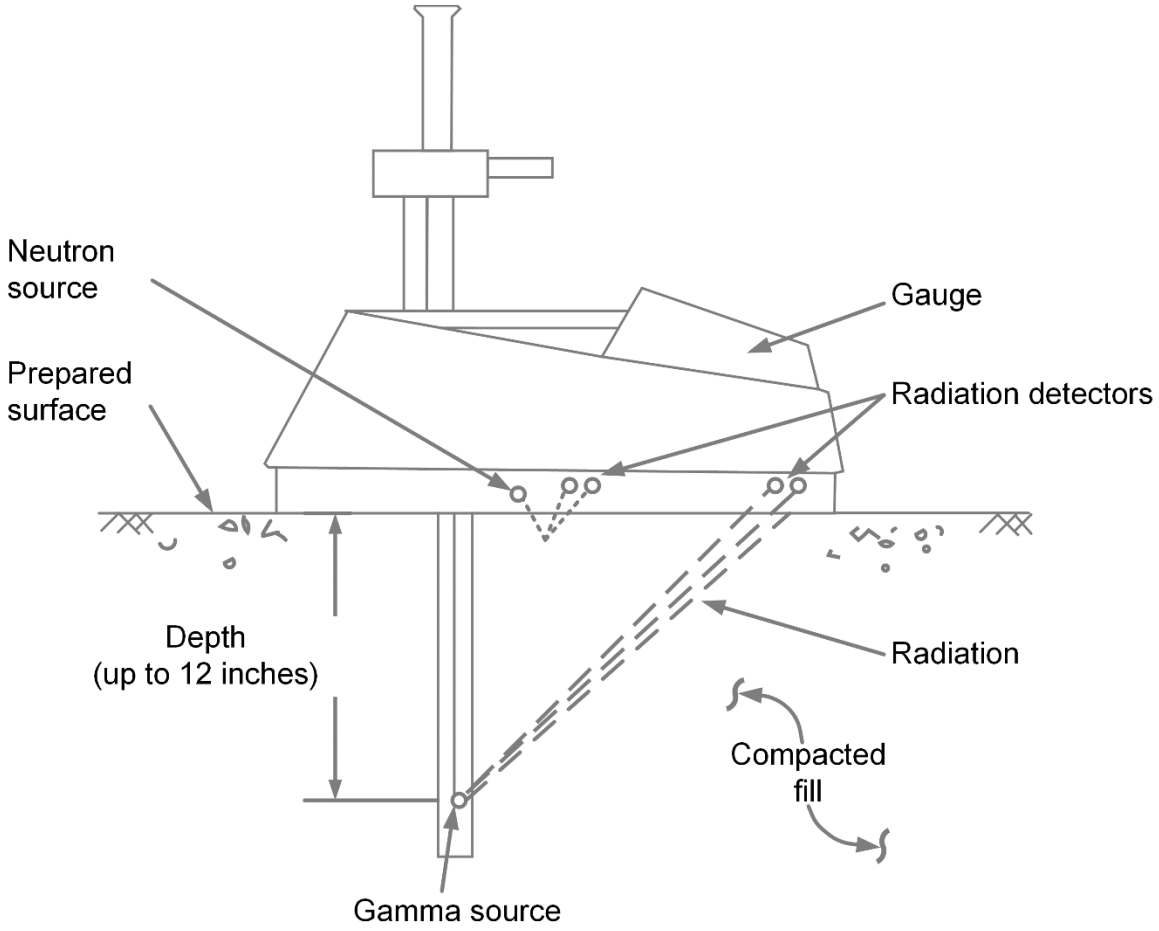

Figure 2-21 Schematic of Nuclear Gauge in Direct Transmission Mode (after NRC 1996)

Guidelines for the safe operation and licensing are provided by the Nuclear Regulatory Commission (NRC) in NUREG/BR-0133, *Working Safely with Nuclear Gauges* (NRC 1996). Technicians working with nuclear gauges should be trained in the safe operation and handling of the gauge. They also need to wear a dosimeter that is periodically

tested to confirm no unexpected exposure, although the risks are relatively minor due to the low energy emitted and the safety precautions built into the gauge.

2-9.3.1.4 Non-nuclear Gauge Methods.

Because of the NRC requirements regarding licensing and transportation of nuclear gauges, several agencies (including the U.S. military) have been researching reliable alternatives to the nuclear gauge. Interestingly, these groups are also assessing direct measurement of the *in situ* strength and/or stiffness to replace the traditional density-moisture content specification for compacted soil. Table 2-20 provides a summary of various techniques and their performance compared to the "traditional" nuclear gauge based on field assessments by Berney et al. (2013, 2016). These devices are commercially available and operate using different principles.

Table 2-20 Comparison of Non-nuclear Technologies for Assessing Soil Density (Berney et al. 2013, 2016)

Non-nuclear Device	Measuring Technology	Field Performance
Moisture-Density Indicator (M-DI)	Electromagnetic pulses and time domain reflectometry used to determine total unit weight and moisture content	Requires third-party software, difficult installation without causing disturbance
Electrical Density Gauge (EDG)	High radio frequency waves measure the soil's dielectric constant, capacitance, impedance, total unit weight, and moisture content are calculated	Highest precision, but average accuracy, requires extensive calibration to site-specific soil to establish accuracy
Soil Density Gauge (SDG)	Electrical impedance spectroscopy (EIS) used for non-contact measurement of total unit weight and moisture content	Accurate but imprecise measurement of density, requires calibration with site specific soil, (i.e., grain size and Atterberg limits)
License-exempt soil density gauge	Low level nuclear source (Cesium-127) used to measure total unit weight, exempt from NRC licensing because of source size	High correlation to results from traditional nuclear gauge
Lightweight Falling Deflectometer (LFD); Dynamic Cone Penetrometer (DCP); Impact Soil Tester (IST), Surface Stiffness (SS)	Various methods used to assess soil stiffness and/or strength, results can be correlated to unit weight and moisture content	None of the devices directly provide unit weight or moisture content, poor correlation to unit weight and moisture content.

2-9.3.2 Measurement of As-Compacted Soil Moisture Content.

The standard method to measure moisture content is the laboratory oven and is the appropriate basis of comparison for all other methods. Unfortunately, drying in the oven requires a 24-hour time period at a temperature of 110°C ± 5°C (ASTM D2216), which is too slow for quality control of engineered fill. At least ten alternative methods have been developed for *in situ* moisture content evaluation. These methods can be classified either as: (1) gravimetric, in which the soil is actually heated and dried; or (2)

indirect, in which the moisture content is correlated to another parameter, as the soil is not physically dried.

Gravimetric methods for field measurement of moisture content are compared to ASTM D2216 in Table 2-21. In all four cases, the soil is physically dried to obtain total mass and dry mass measurements from which moisture content is calculated.

Table 2-21 Gravimetric Testing Methods for Moisture Content (after Berney et al. 2013)

Technique (Standard)	Summary	Comments
Laboratory Oven (ASTM D2216)	Sample dried in conventional oven at temperature of 110°C for 24 hours	Standard by which all other methods are compared, requires long testing time period (about 24 hours)
Standard (700-Watt) Microwave (ASTM D4643)	Sample heated and weighed repeatedly in 1-minute intervals until dry weight is constant	Results sensitive to specific microwave and type of soil, use of 1-minute cycles minimizes chance of overheating, requires electricity, relatively rapid testing time (≈ minutes)
Field Microwave (low power) (ASTM D4643)	Sample heated and weighed repeatedly in 1-minute intervals until dry weight is constant, more heating cycles are required compared to standard microwave	Same as standard microwave
Direct Heating (ASTM D4959)	Sample heated in a container exposed to direct flame from a field stove, heating and cooling cycles are used until specimen achieves constant weight	Heating time periods will vary depending on size of test specimen
Moisture Analyzer (N/A)	Sample dried under halogen lights or infrared heating elements on a dedicated laboratory-scale, internal controls periodically weigh specimen and terminate test automatically	Not traditionally used in geotechnical applications due to small size of test specimen (i.e., <50 gm)

A number of indirect methods have been developed to assess moisture content without physically drying the soil. As summarized in Table 2-22, these methods use a surrogate for temperature (i.e., gas pressure, dielectric constant changes, electrical impedance, etc.). Moisture content has a benchmark test that can and should be used - the laboratory oven. Each method has specific advantages and disadvantages, which can be expressed in statistical terms of bias, accuracy, and precision. Table 2-23 summarizes of comparison of the techniques (Berney et al. 2012, 2013).

Table 2-22 Indirect Testing Methods to Assess As-compacted Moisture Content (after Berney et al. 2012)

Technique (Standard)	Summary	Comments
Nuclear Density Gauge (NDG) (ASTM D6938)	A neutron source is used to determine hydrogen ion concentration by "backscatter" method, hydrogen is assumed to be in form of water in soil, measures upper 4 inches	Most common method used in compaction quality control, results can be affected by chemical composition of the soil, results biased by the soil closest to the surface.
Electrical Density Gauge (EDG) (ASTM D7698)	High-frequency radio waves are used to measure the dielectric constant of soil, which is correlated to moisture content	Very dependent on type of soil and requires calibration of the equipment to the site-specific soil, calculates average moisture content in a relatively large block of soil
Soil Density Gauge (SDG) (N/A)	Non-contact test uses electrical impedance spectroscopy (EIS) to assess dielectric constant of the soil	Similar to EDG because both measure dielectric constant, results in average estimate of moisture content, affected by near-surface moisture conditions.
Gas Pressure Moisture Tester (a.k.a., Speedy) (ASTM D4944)	A calcium carbide reagent reacts with water to produce acetylene gas within a sealed pressure vessel, gas pressure is proportional to the moisture content	Uses a small sample size that must be carefully selected, the acetylene gas by-product must be carefully vented, reagent must be kept dry, rapid test results
Electromagnetic Gauge (N/A)	An electromagnetic probe is used to measure the dielectric constant by "fringing field capacitance"	May be part of a license-exempt soil density gauge, similar comments to EDG

Table 2-23 Bias, Accuracy, and Precision of Test Methods for the As-Compacted Measurement of Moisture Content (after Berney et al. 2012, 2013)

Method	Bias (Slope)	Accuracy (R^2)	Precision (Standard deviation)
Lab Oven	1.00	0.995	0.087
Standard Microwave	1.11	0.973	0.109
Field Microwave	0.924	0.976	0.145
Direct Heating	1.027	0.964	0.159
Moisture Analyzer	0.731	0.915	0.044
Nuclear Density Gauge	0.922	0.970	0.091
Electrical Density Gauge	1.01	0.866	0.253
Soil Density Gauge	0.979	0.936	0.175
Gas Pressure Tester	1.405	0.867	0.056
Electromagnetic Probe	1.096	0.857	~0.10 (similar to NDG)
Explanation (for comparison of field and oven measurements of moisture content)	Slope of trend: slope > 1 indicates over-prediction, slope < 1 indicates under-prediction	Measure of scatter about trend, R^2=1 for results with no scatter	Scatter about the average value, standard deviation approaches 0 for more precise results

2-9.4 Rock Properties.

Strength and stiffness tests on rock core tend to reflect the characteristics of the “intact” rock, while the engineering performance of rock in the field is governed by the rock discontinuities (Deere and Deere 1988; Bieniawski 1989). Therefore, *in situ* tests that include rock discontinuities and assess their impact are useful. The following tests are discussed in this section: plate load, flat jack, rock dilatometer, rock borehole shear, field direct shear, and rock joint hydraulic conductivity. Because of the specialized nature of this testing and the cost of the equipment, many of these *in situ* testing methods for rock are subcontracted to a specialty contractor.

2-9.4.1 Strength and Stiffness Tests on Rock Masses.

Plate load testing (ASTM D4394, D4395) on rock is an *in situ* test method for that evaluates the rock mass stiffness (Goodman 1989, George et al. 1999). The test can also assess the strength of medium to low strength rock. The results from rock plate load tests are presented in terms of stress vs. displacement (Figure 2-22). Tests often include a series of loading and unloading cycles to help isolate the influence of fractures and discontinuities. Generally, the results are analyzed using solutions based on elastic theory to calculate an equivalent modulus, E' (Hoek 2007, Goodman 1989).

The plate bearing test requires a large reaction system to apply the required force. As an alternative, the flat jack concept uses a relatively thin (i.e., ~0.25 inches thick), flat, hydraulic jack that is inserted into a slot in the rock, thus allowing the rock to provide its own reaction. The flat jack test (ASTM D4729) is performed to assess the *in situ* state of stress in the rock and the rock mass stiffness.

For a geotechnical engineer who is familiar with *in situ* soil testing, a rock dilatometer is a misnomer, because it is actually a high-capacity pressuremeter (see Section 2-9.1.1). Operating procedures for a rock dilatometer are generally similar to those identified in ASTM D4719. The rock dilatometer test involves placing a long, cylindrical probe into a rock corehole and inflating a membrane on the probe. The membrane is expanded laterally while measuring the radial deformation. The results are used to evaluate rock mass stiffness.

The rock dilatometer may not be able to sufficiently stress the rock without rupturing the membrane. The *borehole jack*, commonly called a *Goodman jack*, overcomes this problem using small internal hydraulic jacks to induce lateral force across opposing curved steel platens that each stress a 90°sector of the borehole wall over a length of 8 inches. Equipment description and operating procedures are presented in ASTM D4971. The borehole jack can be used in boreholes core with NX-size coring equipment. The hydraulic system used for the borehole jack can generate up to 10,000 psi, so it can be used on virtually any rock. The borehole jack is a common *in situ* rock test that does not require extensive experience to perform and obtain reliable results.

The interpretation of the results presents some unique challenges, but also provides some insight regarding the *in situ* response of rock.

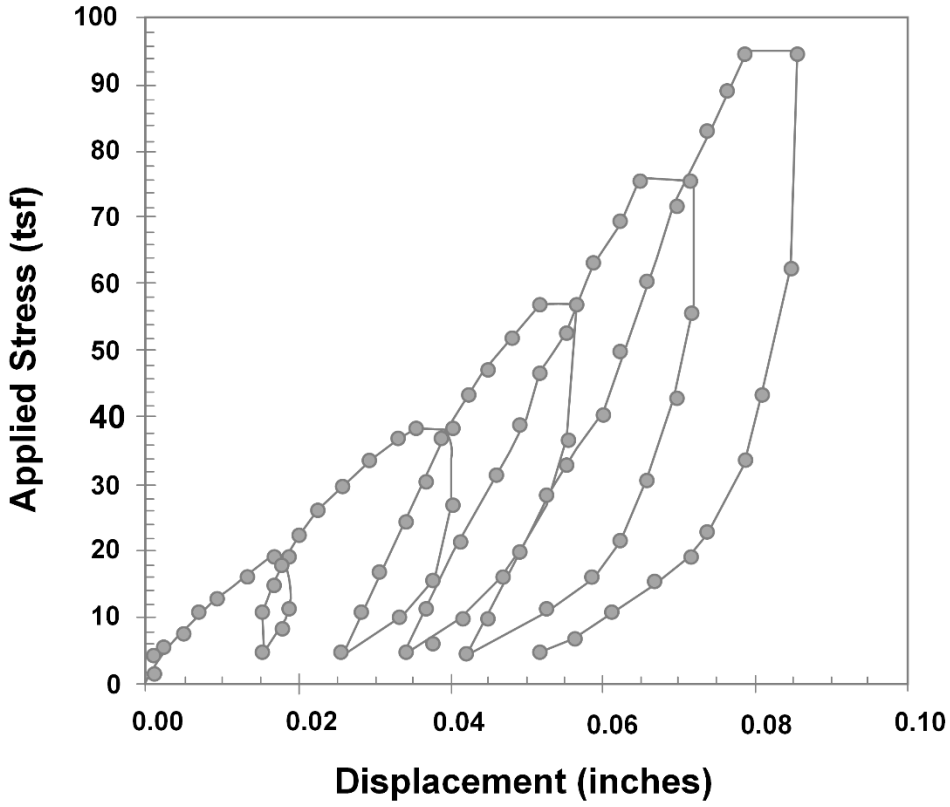

Figure 2-22 Example Plate Load Test Result on Intact Limestone (after NCHRP 2017)

The *rock borehole shear test* is an alternative *in situ* borehole method for relatively weak rock or rock that is easily disturbed upon drilling and coring (e.g., weathered rock, fractured rock, shale, etc.). This test is a modification of the Iowa borehole shear test originally developed for soil (Yang et al. 2006). The rock borehole shear test measures the shear strength of rock. While there is no recognized testing standard, guidelines for the rock borehole shear test are presented in Lutenegger and Hallberg (1981). The device is lowered down the hole to the desired test elevation. Hydraulic pressure is applied to shear plates to obtain the desired normal stress, and a tether is pulled to create a shear force on the plates. The normal stress and shear stress are recorded. The calculated shear stress values for each of three or four normal stresses provide the data points to construct a strength envelope.

2-9.4.2 Direct Shear Tests on Rock Discontinuities.

Rock mass behavior governs the engineering performance, as dictated by discontinuities, which can vary from clean fractures with a certain surface roughness caused by asperities to weathered rock joints to clay-filled fractures. Many field

applications load those discontinuities in shear (e.g., rock slopes, tunnel side walls and crown). Undisturbed, representative samples of discontinuities can be difficult to obtain.

Direct shear testing of rock discontinuities has been developed similar to direct shear testing for soils. The test equipment is highly specialized and quite large. Large-scale *in situ* direct shear tests on rock are performed on exposed from natural rock outcrops, in tunnels, or in excavations. In almost all cases, the test is performed to evaluate the strength of the discontinuity.

A description and discussion of the use of large-scale direct shear testing of rock by USACE is presented in Zeigler (1972). Standardized testing procedures are presented in ASTM D4554. A confining ring is place around the *in situ* rock specimen such that the discontinuity is parallel to the ring. The specimen is encased in the ring using plaster of Paris or hydrostone. Normal and shear loads are applied perpendicular and parallel to the discontinuity, and displacements are measured.

While the performance of large-scale *in situ* direct shear tests on rock discontinuities can be daunting and difficult, the interpretation is similar to the conventional direct shear test performed on soil specimens. Pairs of normal and shear stress are plotted to define the failure envelope and shear strength parameters. In rock and along rock discontinuities, it is possible to measure the peak and residual strength of the discontinuities (Goodman 1970).

2-9.4.3 Hydraulic Conductivity of Rock Discontinuities.

Water flows through rocks occurs mostly in open voids, fractures, joints, and other discontinuities, which contribute to the “primary” porosity of the rock. Water flow in this regime may be turbulent instead of laminar and may not be governed by Darcy’s law, making quantification of water flow in rock discontinuities challenging. In the 1930s, the *lugeon* was introduced to quantify water flow in jointed rock (Houlsby 1976). A lugeon is defined as the flow of one liter of water per meter per minute under a pressure of 10 bars (145 psi) in a constant head double packer test as shown in Figure 2-23. For this situation, a lugeon is approximately 1×10^{-5} cm/s for laminar flow conditions.

To assess the flow regime for water in rock joints, the five-step test method summarized in Figure 2-23 was developed. Based on the five-step test results, the rock is characterized as being in one of five groups (Houlsby 1976).

- Group A – Laminar Flow: Lugeon values relatively constant through all five steps
- Group B – Turbulent: Lowest lugeon occurs at highest pressure
- Group C – Dilation: Highest lugeon occurs at highest pressure
- Group D – Wash-out: Lugeon increases as test progresses
- Group E – Void Filing: Lugeon decreases as test progresses

These characterizations are commonly used to select the appropriate grouting strategy for hydraulic barriers in jointed rock. The interpretation of the lugeon test and physical characterization of the jointed rock is shown in Table 2-24.

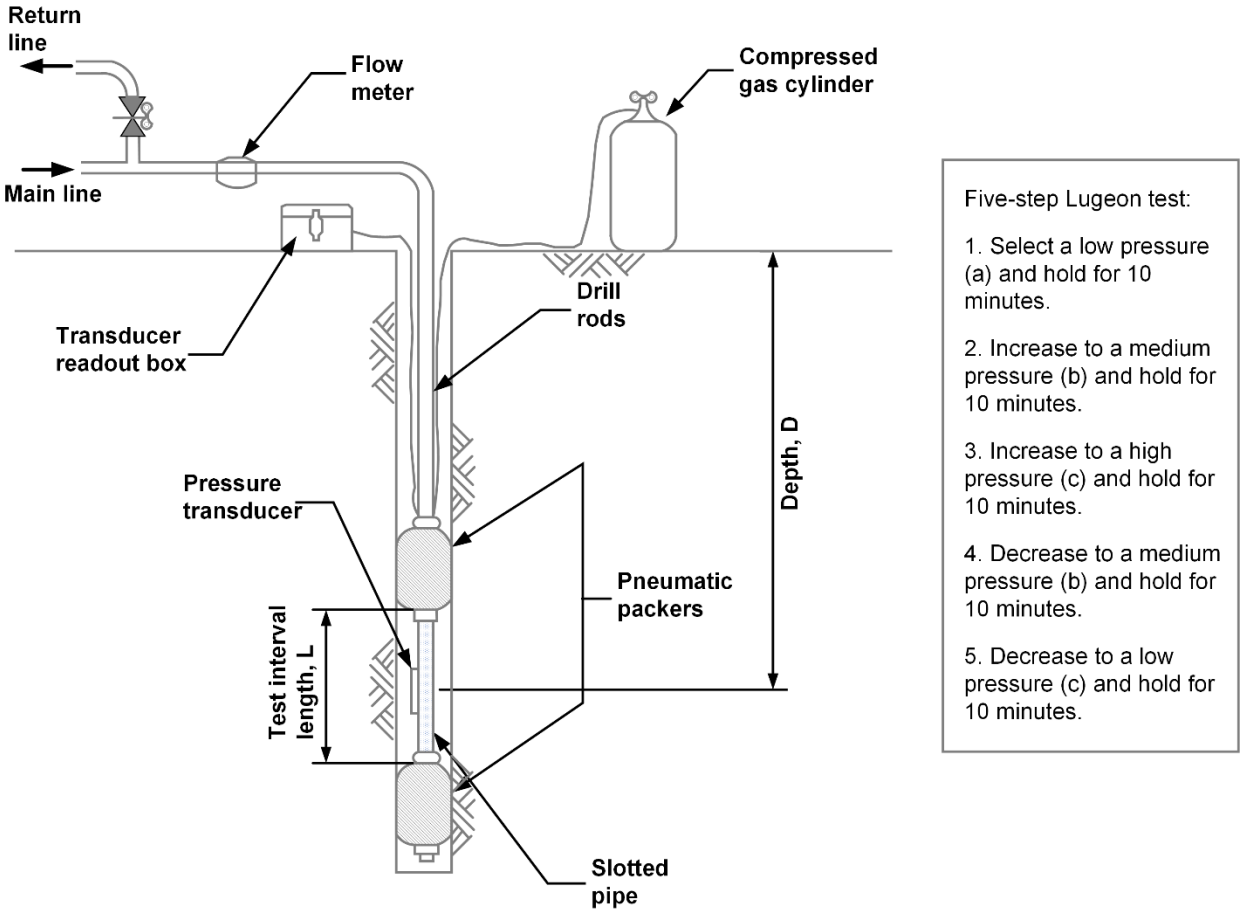

Figure 2-23 Double Packer Set-up to Conduct Five-step Lugeon test (after Clayton et al. 1995)

Table 2-24 Interpretation of Lugeon Test Results (after Tunbridge 2017)

Lugeon Range	Classification	Approx. Hydraulic Conductivity (cm/s)	Condition of Rock Mass Discontinuities	Report Precision (lugeons)
<1	Very Low	$< 1 \times 10^{-5}$	Very Tight	<1
1-5	Low	1×10^{-5} - 6×10^{-5}	Tight	±0
5-15	Moderate	6×10^{-5} - 2×10^{-4}	Few partly open	±1
15-50	Medium	2×10^{-4} - 6×10^{-4}	Some open	±5
50-100	High	6×10^{-4} - 1×10^{-3}	Many open	±10
>100	Very High	$> 1 \times 10^{-3}$	Open closely spaced or voids	>100

2-10 FIELD INSTRUMENTATION AND MONITORING.

Monitoring the performance of geotechnical structures is a vital consideration for individual projects and has helped guide the evolution of the practice (Peck 1969). Monitoring field performance starts with an assessment of what “performance” is anticipated. Once this is established, instruments may need to be installed before, during, and/or after construction or after a failure as part of the forensic investigation to understand the failure mechanisms. Finally, certain instruments may be integral components of early warning systems for sensitive structures. This section summarizes the types of geotechnical instrumentation and their operations to help guide the geotechnical engineer in selecting the most appropriate instrument for a given project. In-depth details regarding geotechnical instrumentation can be found in USACE (1987, 1995b), Bartholomew et al. (1987, 1987a), FHWA (1988) and most notably Dunnicliff (1993). The rapid evolution of the various measurement technologies and the recognition of the importance of performance monitoring will undoubtedly result in further expansion and utility of geotechnical instrumentation over the coming years.

2-10.1 Operating Concepts for Geotechnical Monitoring Instruments.

Making a measurement of engineering performance involves using some type of instrument or transducer for obtaining the measurement. The major types of instruments are summarized in Table 2-25. The transducers introduced in this table are incorporated into instruments that are used to make specific measurements. These measurements may include: (1) deformations (e.g., horizontal movement of a landslide, vertical settlement, tilt of retaining wall), (2) pore pressures in soil (e.g., excess pore pressure due to consolidation or static water levels in wells), (3) earth pressures (e.g., pressures acting on earth retaining structures), (4) loads (e.g., strut loads in braced excavations, anchor loads on tiebacks, vertical loads for plate load tests), (5) temperature (e.g., frost penetration, thermal-induced stress/deformation), and (6) vibration (e.g., geophysical testing, blast monitoring, seismic activity).

Regardless of the type, selection of monitoring instruments must consider the instrument range, accuracy, and precision as well as the required calibration procedures. Geotechnical instruments have a specific measurement range, which must encompass the values anticipated in the field application. Instruments also have a precision, which refers to the smallest recordable unit that can be measured. For example, a 1,000 lb. capacity load cell that records to the nearest 0.1 lb. has a precision of 0.01% of its full range or *full scale*. The accuracy of an instrument refers to the ability to obtain a correct and repeatable measurement of the desire quantity. Instruments with a large range are not always sufficiently accurate at values near the lower end of the range. Many instruments require calibration to convert the measured property into the desired engineering property. While typically provided by the manufacturer, the calibration should be confirmed and repeated on a regular basis.

Table 2-25 Types of Geotechnical Monitoring Instruments

Instrument Type	Examples	Advantages	Disadvantages
Mechanical	Plumb bob, tape measure, micrometer	Low cost, simple and direct measurement, readings in engineering units, external power not required	Continuous readings are not possible, manual recording
Pneumatic – use air pressure	Piezometers, earth pressure cells	Relatively rugged, and portable electrical supply not required, not impacted by electrical signals, relatively good for long-term measurements	Difficulty of reading systems, time-consuming manual effort
Hydraulic – use water or hydraulic fluid	Piezometers, earth pressure cells	Similar to pneumatic but with higher pressures available	Similar to pneumatic
Electrical – sensing element bonded to surface expected to strain	Bonded strain gauge, piezoelectrics, vibrating wire devices	Very stable and reliable, can be automated and remotely accessed, low voltage and portable power supplies are available	Higher cost, require a controlled power supply, signal processing is required to obtain data in engineering units
Micro-electro-mechanical (MEMS)	Tiltmeter, piezometer, load cell	Combine microscopic mechanical parts with electric signals, can be automated	Require a controlled power supply, signal processing is required to obtain data in engineering units
Fiber optics – measurements of strain along an embedded or bonded fiber	Strain gauge (distributed or discrete), temperature	Can measure strain along the entire length of a structure, sensor cost is low, potential for automation and dynamic analysis	Requires external power, relatively high cost for readout and signal processing, data interpretation is required

2-10.2 Linear Deformation Measurements.

There are many applications where deformation monitoring is either imperative or, at least beneficial (see Section 2-10.9 below). The deformation could involve vertical movement from consolidation adjacent to a deep excavation, horizontal and rotational movements from a landslide, or outward tilt of a retaining wall. Methods for determining linear deformation are summarized in Table 2-26 and can range from simple to relatively complex.

Table 2-26 Methods of Determining Linear Deformation

Instrument Type	Operation	Comments
Human eyes	Observe conditions within the subsurface and effects on structures	Readily available at no cost, helps develop observational method, often overlooked
Crack pins and tape measure	Measure cracking by distance between pins on either side of a crack in soil or rock	Simple solution, can be automated using electrical displacement sensors
Grid crack gauges	Used to monitor cracks in structures, two-piece plastic gauge attached to structure on opposite sides of crack	Simple solution, requires manual readings
Displacement gauge – e.g., dial gauge or LVDT (Figure 2-24)	Use to measure displacement over relatively short time or in a protected environment	Very accurate, electrical instruments can be automated, sensitive to environmental disturbance, more expensive
Field survey	Use conventional surveying to locate position and elevation of points	Requires a common benchmark, survey must be “closed,” precision should be established by completion of two surveys, including equipment tear-down, on the same day
Automated total station (AMTS)	Use an AMTS set up in a secure location to take measurements of targets at selected time interval	Excellent for construction-induced movements, more repeatable than conventional survey, near real-time readings, can be included in online monitoring sites
Surface settlement plates or platforms (Figure 2-25)	Plate with riser pipe is installed on or within the ground and surveyed over time to track settlement, riser extensions can be used for deep fills	Good long-term measurement technique, accurate and relatively inexpensive, riser pipes must be protected during construction, benchmark must be outside of area impacted by construction
Liquid level settlement gauge (Figure 2-25)	Similar to surface settlement plate with a pressure transducer and without risers, changes in pressure from an external reservoir are converted to settlement	Higher initial cost than surface settlement plates, construction is much easier without risers, potential for leakage, reservoir and tubing must be protected from freezing
Liquid level settlement profiler (Figure 2-26)	Install a flexible pipe below the embankment, pull transducer and water line through the pipe, measure pressure at intervals, calculate settlement from pressure	Can use a water filled pipe and a standalone pressure transducer, provides distributed measurement of settlement, time intensive manual measurements
Borehole extensometer (Figure 2-27)	Measures relative position of two or more points along the axis of a borehole, anchor the rod at the base or point of measurement	Requires a borehole, can monitor movements at multiple points

Simple methods for deformation monitoring should not be overlooked. Peck (1972) notes that the human eye is too often overlooked and “can detect most of what we need to know about subsurface construction.” Measurements by crack pins and tape measure can be used to monitor observed cracks in soils adjacent to slopes or cracks in rock. If conditions warrant, distances can be continuously monitored using a displacement transducer as shown in Figure 2-24. When considering instruments for

monitoring observed cracks in the walls of buildings, a mechanical grid crack gauge can be monitored to show magnitude and direction of movement over time. This gauge is simply attached across the crack using epoxy or pins though the mounting holes.

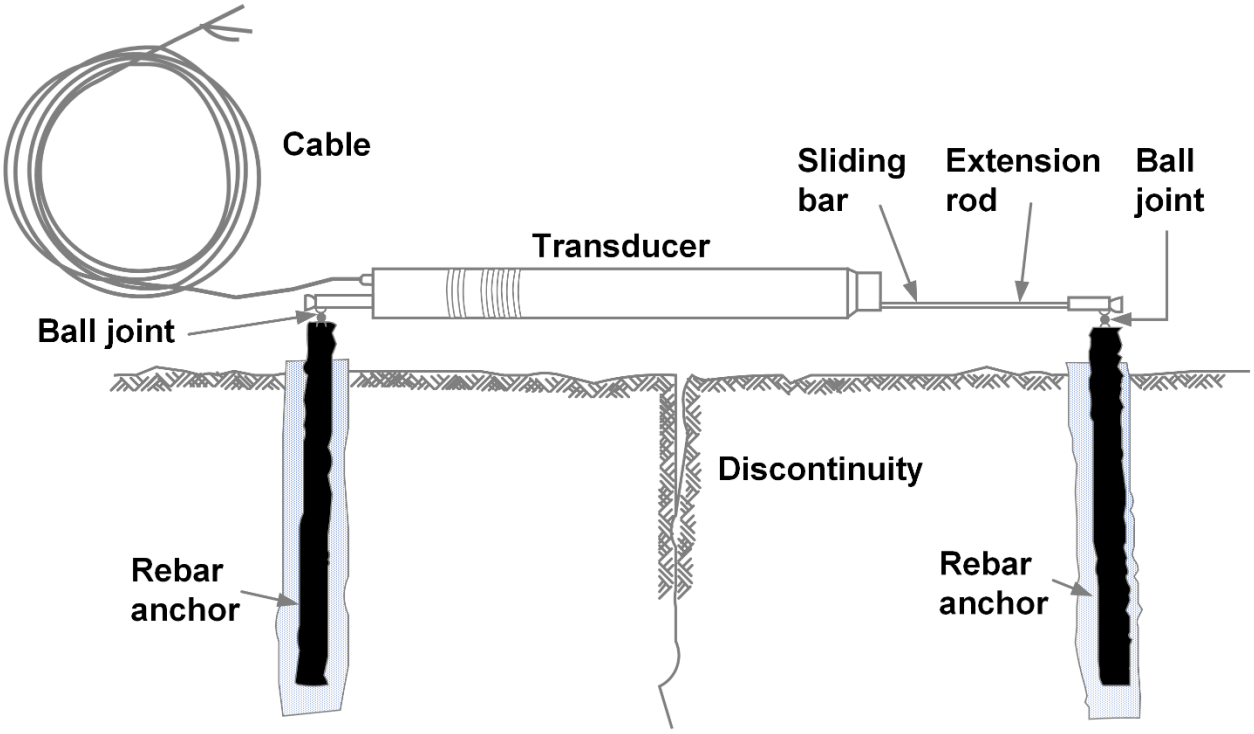

Figure 2-24 Electrical Crack Gauge and Reference Pins (after Dunnicliff 1993)

Where needed, more precise deformation measurements can be made using transducers. When monitoring deformations over relatively short time periods or when the instrument is protected, a simple dial gauge may be used. For automated readings, an electrical transducer (i.e., linear variable displacement transformer (LVDT), direct current LVDT, or linear potentiometer) provides a precise and potentially highly accurate alternative.

Conventional field survey equipment can be used to monitor deformations of several points over large distances and often over long time periods, based on a common benchmark. Such surveys must be “closed” by shooting the benchmark before and after the survey. Automated total stations (AMTS) can provide accurate near real-time monitoring for multiple points and are especially useful for monitoring construction-induced movements. The accuracy of the AMTS is inversely proportional to the distance from instrument to prism (or object), but can be used at distances greater than 1,000 feet. As with any surveying option, it is always desired to include a benchmark point during each reading cycle. The AMTS uses a laser for finding and monitoring the target so it can be used day or night.

The magnitude and time-rate of consolidation *settlements* during construction are often used to direct certain construction activities (i.e., fill placement rate). Monitoring long-term settlement is often desired. Surface settlement plates (often referred to as platforms) are monitored using conventional surveying instruments and provide an accurate and relatively inexpensive technique. The settlement plate is placed on the original ground surface before fill placement commences. A figure showing a typical set-up is provided in Figure 2-25a. It is necessary to protect the pipe from being damaged or tilted during construction by either vehicle impact or differential fill placement around the riser pipe. As with all survey measurements, a non-moving benchmark is to be shot during each cycle of readings. More advanced systems use liquid pressure to measure change in height below a fixed reservoir (Figure 2-25b) or probes to measure the profile of settlement in a buried tube (Figure 2-26).

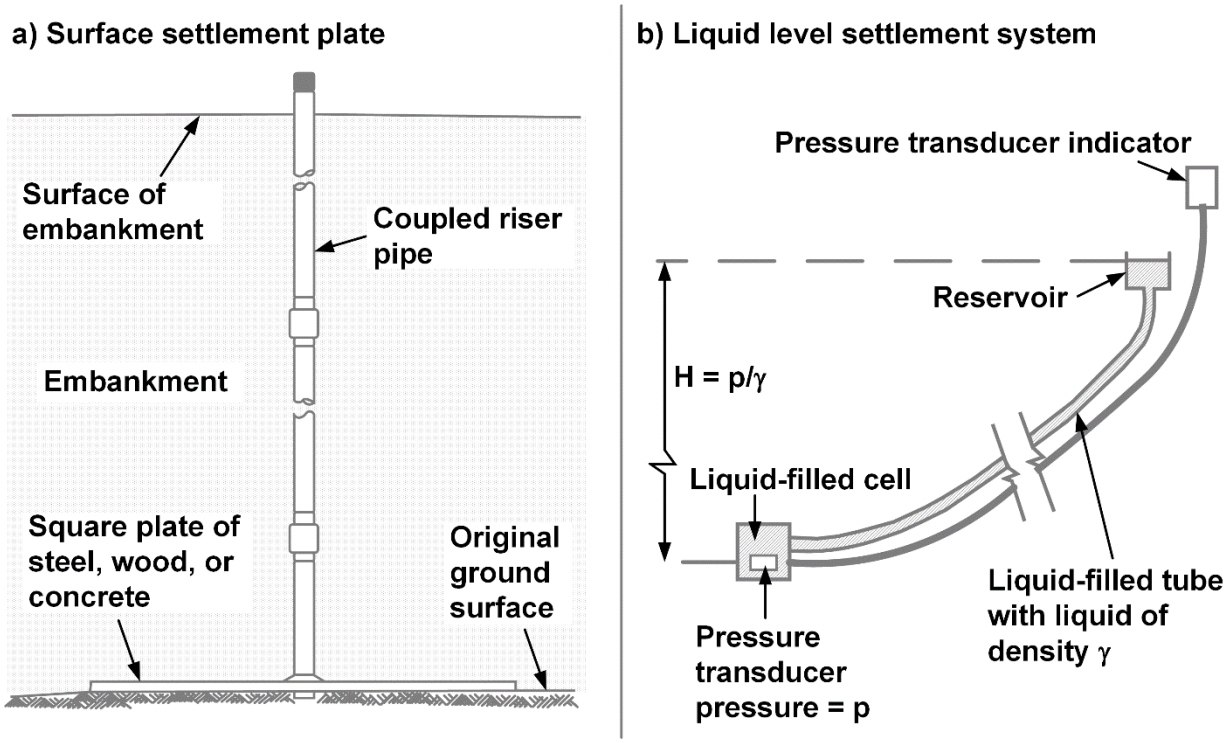

Figure 2-25 Surface Settlement (a) Plate or (b) Platform (after Dunnicliff 1993)

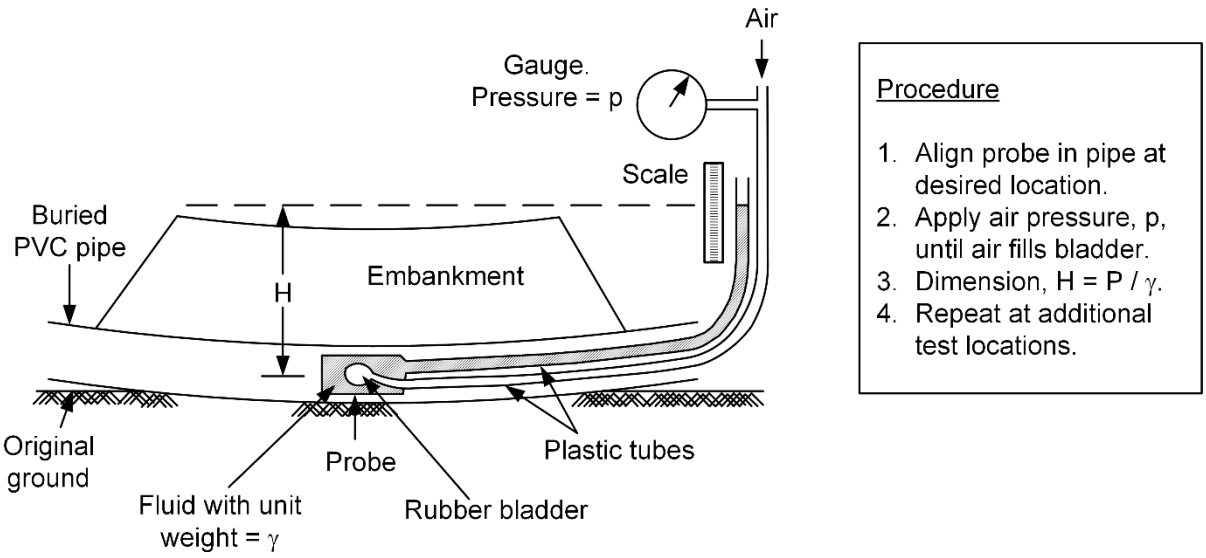

Figure 2-26 Liquid Level System to Continuously Profile Settlements (after Dunnicliff 1993)

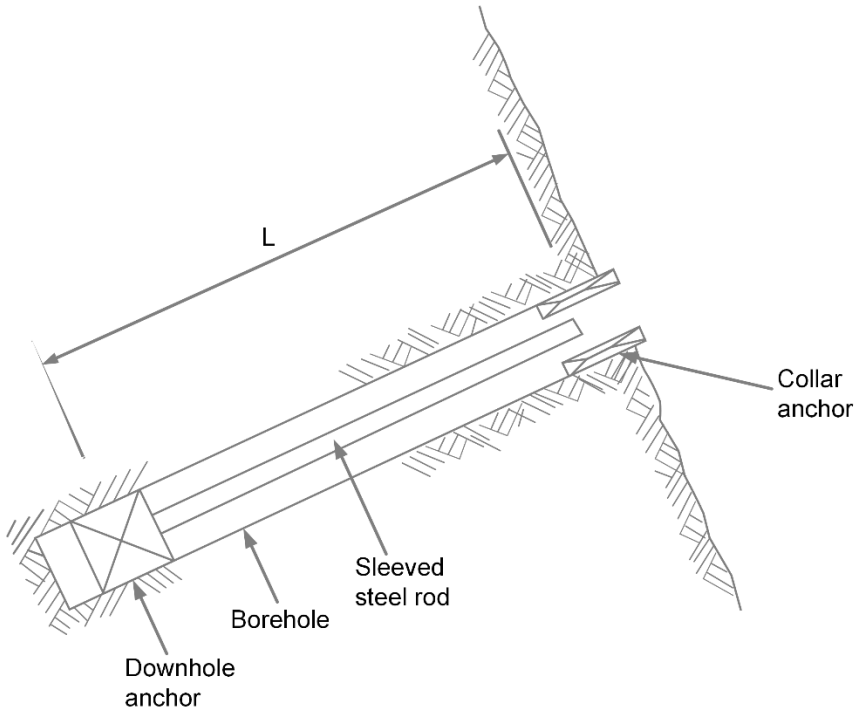

Figure 2-27 Borehole Extensometer (after Dunnicliff 1993)

2-10.3 Angular Displacement Measurements.

Angular displacement measurements are used to measure relative displacements of slopes or tilting of structures, such as retaining walls. These instruments can be used to determine the location of planes of sliding and to give warnings when structures become out-of-vertical. Types of angular displacement instruments are summarized in Table 2-27.

Table 2-27 Angular Displacement Instruments

Instrument Type	Operation	Comments
Tiltmeter	Uses accelerometer to determine inclination with respect to vertical, typical operating range of a few degrees, affixed to a structure or used as integral part of inclinometers	MEMS tiltmeters may have range up to 40 arc minutes and precision of 1 arc second
Slope inclinometer (Figure 2-28)	Special grooving casing grouted into a borehole, inclinometer probe with biaxial accelerometer is pulled through the casing, measures inclination of casing at regular intervals, integration of tilt provides deformed shape of casing	Frequently used to assess movement for landslides, can be used for vertical structures and deep excavations, initial baseline reading obtained after grout is set, casing should extend into a stable stratum, two passes through the casing are required for quality data, time-consuming manual process, bias correction must be completed in data processing, excessive deformation prevents ongoing use of casing
In-place inclinometer (Figure 2-28)	Same principle as conventional inclinometer except that the instrument has multiple segments with multiple accelerometers, the instrument remains at same location within casing	Can be automated, less time-consuming, much higher equipment cost compared to conventional inclinometer, MEMS accelerometers can be used that are cheaper and do not require special casing

2-10.4 Pore Pressure and Water Pressure Measurements.

Transducers that are capable of measuring transient water pressures are commonly relied upon for pore pressure measurements. These transducers are often generically referenced as *piezometers*. This is in contrast to the use of the term *standpipe piezometer* in Section 2-8 to describe a specific type of well. As described above, the same basic technology can be used for measuring both static and transient water pressures, and the transducer types include pneumatic, hydraulic, electrical, and MEMS devices. Operation and application of these piezometers are summarized in Table 2-28. All of these methods measure positive water pressures in saturated soil.

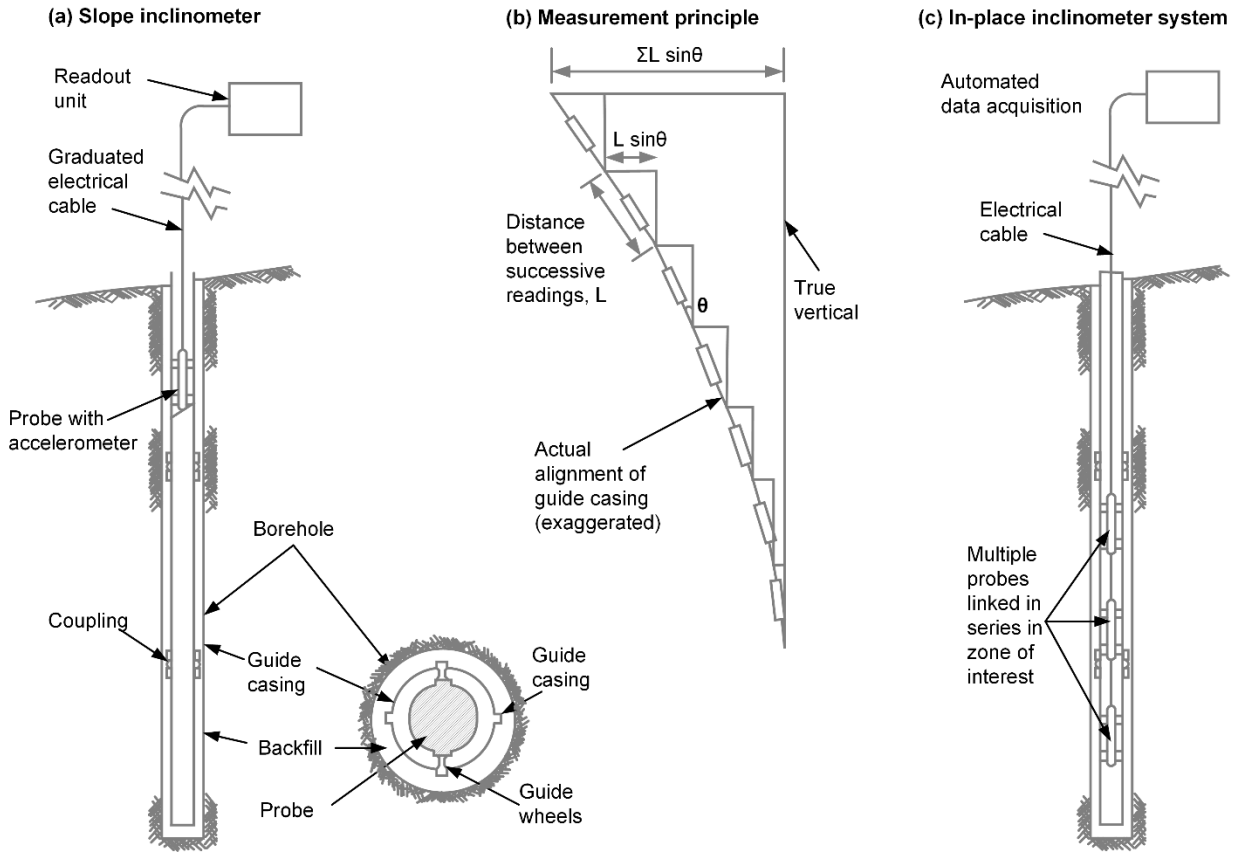

Figure 2-28 Slope Inclinometers – (a) Manual System, (b) Measurement Principle, and (c) In-Place Inclinometer System (after Dunnicliff 1993)

Hydrodynamic lag time or simply *lag time* refers to the time required for an instrument to respond to a change in pressure. Figure 2-31 plots the estimated lag time (in terms of time for 90% response) for various types of wells and piezometers compared to the hydraulic conductivity of the soil. Note the short lag time for diaphragm transducers and the extended time lag for open piezometer wells. As indicated by the figure, open wells cannot effectively measure hydrodynamic water pressures for transient flow situations.

Table 2-28 Piezometer Types

Piezometer Type	Operation	Comments
Pneumatic	Device pushed or grouted in-place at location of interest, air pressure is used to measure water pressure on opposite side of a diaphragm	Good choice for long-term monitoring, can be flushed and cycled to increase confidence, power source not required, insensitive to stray electrical signals, time-consuming manual readings
Hydraulic, a.k.a., twin-tube (Figure 2-29)	Similar operation to pneumatic except water pressure is used instead of air, pressure lines are filled with deaired fluid, pressure is measured with mechanical or electrical gauges	Period flushing is required for long-term monitoring
Electrical and MEMS (Figure 2-30)	Strain gauge, piezoelectric, or vibrating wire transducer attached to a diaphragm to measure pressure, transducer output is proportional to pressure, use high-air-entry saturated filters to accurately measure changes in pore pressure during transient conditions	Very common, can be automated and remotely monitored, very little water flow required to move the diaphragm resulting in rapid response to transient conditions (i.e., short lag time), requires power source (can be low voltage), MEMS sensors experience electrical drift in the signal, can recalibrate MEMS if sensor is accessible

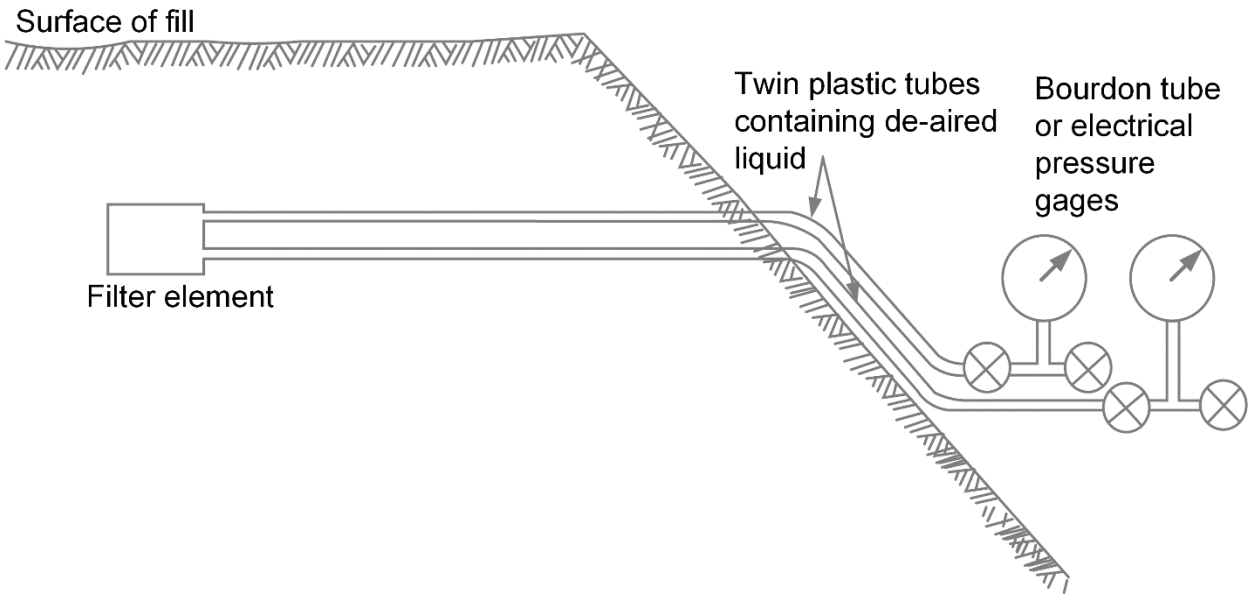

Figure 2-29 Dual-tube Hydraulic Piezometer in Embankment Dam (after Dunnicliff 1993)

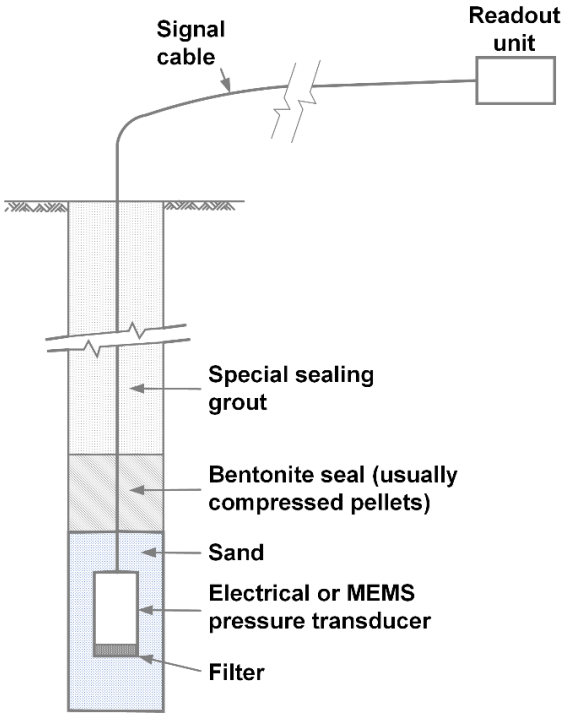

Figure 2-30 Example of Electrical Diaphragm Piezometer Transducer (after Dunnicliff 1993)

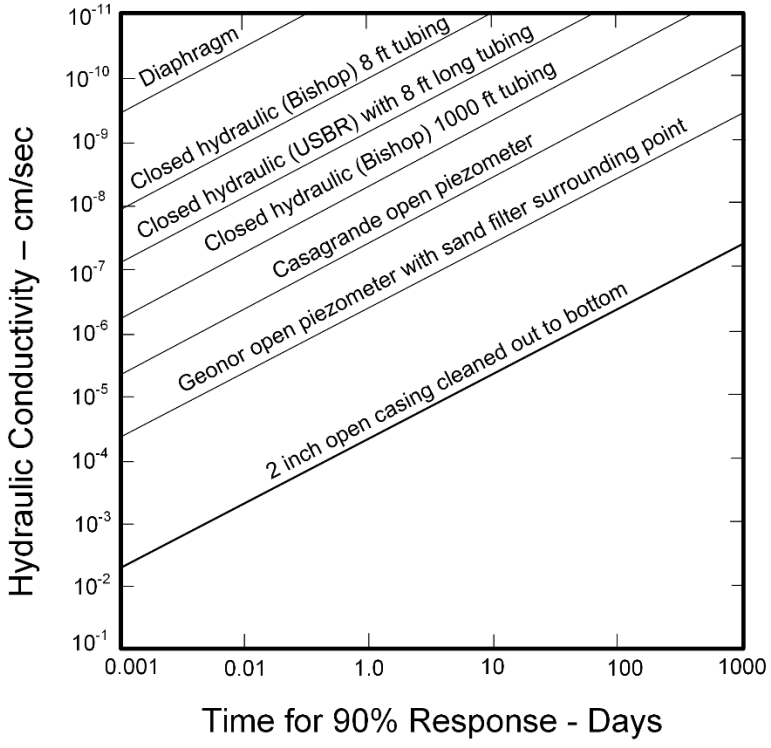

Figure 2-31 Estimated Hydrodynamic Lag Time for Various Piezometers and Wells (after Dunnicliff 1993)

2-10.5 Earth Pressure Measurements.

Although uncommon, measurement of the actual vertical and/or horizontal stress in the ground is sometimes desired. The concept for making these measurements is easy, while the interpretation of the results can be challenging. An earth pressure cell (a.k.a., total stress cell) measures stress by deformations of a thin diaphragm or transfer of pressure to a hydraulic cell. Deformations of the diaphragm-type cell can be measured by a strain gauge, vibrating wire transducer, or MEMS gauge. Earth pressure cells make an internal measurement compared with most of other transducers that monitor soil response externally. The presence of the cell alters the stresses in the soil due to differences between the stiffness of the cell and the soil. Good summaries of the influence of installation and type of earth pressure cells can be found in Filz and Brandon (1994) and Sehn (1990). As an alternative to earth pressure cells, tactile pressure sensors are thin, flexible polymer sheets with many embedded strain sensors that allow stress to be measured (Paikowsky et al. 2006).

From experience, earth pressure cells should be relatively large (i.e., 9 to 12 inches) in diameter and thin, resulting in a ratio of thickness to diameter of less than 1:10. The cell must be in intimate contact with the soil and is generally surrounded (i.e., bedded) using fine sand to minimize potential for stress concentrations from large particles in the soil.

2-10.6 Load Measurements.

Many applications in geotechnical projects require the measurement of load. A summary of the common load measuring instruments is provided in Table 2-29.

2-10.7 Temperature Measurements.

As described in Dunnicliff (1993), temperature measurements in geotechnical engineering are typically obtained for one of three specific reasons. The appropriate instrument for the specific application should be selected and used accordingly.

- Direct Measurement: Temperature measurements may be required for projects, such as depth of frost penetration, soil temperature beneath industrial furnaces, temperatures of thermal piles. Thermocouples and resistance temperature devices (RTDs) are the most common devices for these applications.
- Measurement of Temperatures that Induce Loads: Temperature changes cause thermal expansion and contraction of materials. The loads in structural members (e.g., struts for excavation support, tunnel support systems) will be impacted when subjected to temperature fluctuations. Again, thermocouple or RTDs are commonly used for these applications.
- Measurement of Temperatures that Influence Transducer Performance: Transducer temperatures can also have significant impacts on the response of geotechnical instruments themselves. For example, in closed hydraulic systems,

temperature can change the viscosity of the fluid and can cause expansion and/or contraction of the fluid and the hoses. These changes will influence the interpreted response unless appropriate corrections are made. Instrument manufacturers will report the necessary corrections. Monitoring temperature changes for transducers requires accurate measurement of small temperature changes. The thermistors used for this purpose are usually built directly into the transducer by the manufacturer.

Table 2-29 Instruments for Measuring Load

Instrument Type	Operation	Comments
Hydraulic Load Cell	Load is applied to a sealed hydraulic chamber, increase in pressure is measured and converted to load	Passive system that responds to load by internal pressure increase, relatively robust, capable of measuring loads >500 tons with about 0.1% accuracy, no external power required for cell with mechanical pressure transducer
Calibrated Hydraulic Jack	An external pressure transducer to measures pressure induced by a hydraulic jack, pressure over a known area is converted to load	Same advantages and capacities as hydraulic load cells, Osterberg Cell (O Cell) is an example used for load testing of drilled shafts
Electric Load Cell	Load applied to metal gauge, bonded strain gauges or vibrating wire transducers measure strain, which is converted to load via calibration	Commonly used in laboratory and field applications, wide range of capacities and physical sizes, can be custom made, robust and reliable, require external power supply, signal conditioning and data processing required to determine load
Embedded and surface-mounted strain gauges	Strain gauge attached to surface of metal structural members, stresses in structure are determined from strain and can be converted to load via section size	Can be bonded strain gauges attached to surface of structure or pre-attached (sister bars) gauges welded to the structural member or reinforcing cage, gauges must be correctly located to measure the desired strain and typically are installed in sets, must be protected during construction and operation

2-10.8 Vibration Measurements.

In some specialty cases, the measurement of vibrations may be a component of a performance monitoring program. Both steady state vibrations and transient vibrations may be of interest.

- Steady State Vibrations: Oscillating machinery that can induce vibratory loads to the foundation and foundation soils. These vibrations may induce cracks concrete floors, walls, masonry, or finishes. Vibration transducers use accelerometers (often MEMS based) to assess the magnitude and frequency of the vibration. These transducers may be included in portable handheld meters that are effective at capturing the induced vibrations from the machinery. Modern smartphones use MEMS accelerometers and can be used to assess vibrations.

- Transient Vibrations: Transient vibrations may be induced by construction activity, such as equipment traffic, pile driving, dynamic compaction, or blasting; machinery; or seismic activity. Transient vibration monitoring is an integral part of many of the geophysical tests discussed in Section 2-4. Transient vibrations are captured by accelerometers and require high sampling rates in order to capture vibrations that may occur over a few seconds. Of particular interest for the transient vibrations are the magnitude, duration, and frequency content.

Capturing and storing vibration data for detailed analysis usually requires dedicated hardware, specifically portable (or permanent) seismographs. This equipment may include geophones to measure ground velocity or accelerometers to measure ground acceleration. The equipment usually has a user-defined threshold limit for the device to trigger its recording and the ability to capture data a few seconds before the triggering event. A brief discussion of the equipment to measure and capture ground vibrations is presents in NCHRP (2018). There are engineering firms that specialize in measuring transient vibrations.

2-10.9 Field Applications for Instrumentation.

Every instrument used to monitor geotechnical projects should be selected to answer a particular performance question. This approach opposes the tendency to adopt a philosophy of "*if you can monitor it, you should monitor it,*" which is not recommended. Table 2-30 provides example performance questions that might be appropriate for various project types. Significant forethought should be given before an instrumentation plan is developed and the program should be organized around addressing specific questions. Additional discussion on these topics is provided in Dunnicliff (1993) and NCHRP (2018).

Table 2-30 Example Questions for Instrumentation Decisions

Project Category	Example Project Types	Potential Questions
Braced or Anchored Excavations	• Deep excavations in urban areas and/or near historical structures • Excavation support system that uses high strength anchors	• What is the lateral extent and magnitude of ground surface deformations? • Would an instrumented test anchor load test benefit the final design?
Embankments on Soft Ground	• Strength gain and staged construction are part of the design • Significant settlement or long-term movements are anticipated	• What rate of strength gain is required to not impact the construction schedule? • What is the confidence of predicted long-term settlement?
Embankment Dams	• Excavation for rehabilitation is anticipated near the downstream toe • Cutoff structure is part of the rehabilitation	• During rehabilitation, how much movement is anticipated at specific locations? • What measurements can be made to increase confidence of cutoff performance?
Excavated and Natural Slopes	• Existing slopes that have to be steepened • Seepage appears to be impacting slope stability	• What is the anticipated movement or impact of slope steepening? • What is the confidence that the design accurately accounts for groundwater levels?
Underground Construction	• Tunnel will be advanced below groundwater • Fractured rock conditions are anticipated • Seams of weak materials are anticipated	• What is the confidence in the ability to control water? • What is the confidence of the variation in rock structure along alignment?
Driven Piles	• Deep foundation system new to the area is being considered • Driven piles in urban environments	• What is the confidence of pile driving acceptance criteria? • What is level of vibration for structures in close proximity?
Drilled Shafts	• Larger loads than had previously been used in area are included in the design • Drilled shaft will be located below groundwater	• What is the confidence in lateral load capacity and location of bending moments? • What is the impact of excavation below the groundwater table?
Earth Retaining Structures	• Earth retaining structures not previously been used in area • Wall height exceeds heights previously constructed in the region	• What is the estimated settlement of the wall? • What is the estimated tilt of the wall? • What is the confidence in anchors loads and long-term creep?
Dewatering	• Dewatering in urban areas • Dewatering is considered on the critical path of construction	• Will the drawdown be uniform? • What is the confidence in pumping rate and drawdown?
Grouting	• Uncertainty regarding grout take • Grouting in fractured rock and karst • Grouting is initiated to minimize potential for settlement of critical structures	• What is the confidence in predicted grout take? • Will post-construction verification provide useful verification data?
Ground Improvement	• Techniques have previously been untried in region • Ground improvement is implemented to strengthen or stiffen the existing soil	• What is the confidence in long-term performance? • What is the confidence in ability to predict settlement and strength gain?
Liability Control	• Litigation is anticipated • Client may be implicated based on conditions encountered in the field during a forensic investigation	• How closely do original design assumptions match as-constructed conditions? • Will additional monitoring benefit the client? What type?

2-11 SUGGESTED READING.

Topic	Reference
Subsurface Exploration	NCHRP. (2018). *Manual on Subsurface Investigations. National Cooperative Highway Research Program. Publication No. CRP Project 21-20.* Transportation Research Board, National Academies of Science Engineering, and Medicine, Washington, DC.
Cone Penetration Test	Cone Penetration Testing (CPT) Design Manual for State Geotechnical Engineers. Report No. 2018-32, Minnesota Department of Transportation, St. Paul, MN, 2018.
In situ Measurements	*Geotechnical Site Characterization. Geotechnical Engineering Circular No. 5. Publication No. NHI-16-072.*, Federal Highway Administration, U.S. Department of Transportation, Washington, D.C., 2016.
Groundwater Measurements	*Ground Water Manual*, Water Resources Technical Publication, United States Department of the Interior, Bureau of Reclamation, Washington, D.C., 1995.
Field Instrumentation	*Geotechnical Instrumentation for Monitoring Field Performance.* by J. Dunnicliff, John Wiley & Sons, New York, NY, 1993.

2-12 NOTATION.

Symbol	Description
D	Diameter of the vane - VST
E_D	Dilatometer modulus - DMT
E_p	Pressuremeter modulus - PMT
E'	Equivalent modulus
f_s	Sleeve friction - CPT
G	Shear modulus
I_D	Material index
K_D	Horizontal stress index - DMT
K_0	Coefficient of lateral earth pressure at rest
k_s	Modulus of subgrade reaction
q_t	Normalized tip resistance - CPT
q_u	Tip resistance - CPT
RQD	Rock Quality Designation
$S_{t,fv}$	Sensitivity in undrained shear strength from vane shear test
s_u	Undrained shear strength
$s_{u,fv}$	Undrained shear strength from vane shear test

Symbol	Description
$s_{ur,fv}$	Remolded undrained shear strength from vane shear test
T_{max}	Maximum net torque for vane shear test
T_{res}	Residual torque for vane shear test
V_0	Initial calculated volume within the uninflated membrane in PMT
μ_R	Vane correction factor
p_f	Inflection point assumed to delineate the change from pseudo elastic to plastic response and the point where creep may be expected in PMT
p_0	Pressure at which recompression of disturbed soil in the side of the borehole is complete and expansion into undisturbed soil starts in PMT, also referred to as liftoff pressure
p_r	Yield point during the reloading portion of a PMT unload–reload cycle where recompression ends and the soil reinitiates plastic shearing
p_t	Limit pressure in PMT where the curve becomes asymptotic on a pressure versus volume curve
p_u	Minimum pressure during unloading during the PMT unload–reload cycle
σ_{h0}	Total horizontal stress

CHAPTER 3 LABORATORY TESTING

3-1 INTRODUCTION.

3-1.1 Scope.

This chapter discusses the common laboratory tests that are used in geotechnical engineering practice. The chapter has been written assuming that the reader will not personally be conducting the tests, but will be engaging a commercial laboratory to do the tests. The discussion considers the types of test that can be conducted for different engineering parameters and important factors influencing the values obtained.

3-1.2 Evolution of Laboratory Test Procedures.

Geotechnical laboratory testing began in the early part of the last century. The test apparatuses and procedures were developed by a variety of organizations. Certain index tests used in geotechnical engineering were originally used in soil science and agronomy. Many of the compression and strength tests were initially developed by universities in the United States and Europe. An important early study published in 1946 was “The Use of the Triaxial Test in Engineering Practice” which was the summary report for a 10-year study sponsored by the Corps of Engineers. In this study, Professors Arthur Casagrande of Harvard, Don Taylor of MIT, and P. Rutledge of Northwestern, developed the major categories for triaxial testing of soils which are still used today.

During the next 40 years, testing procedures and specifications were developed by organizations involved in constructing dams and highways. The U.S. Bureau of Reclamation first published the *Earth Manual* in 1951, and newer editions were released in subsequent years. The U.S. Army Corps of Engineers developed EM 1110-2-1906 *Laboratory Soils Testing*, which provided procedures for conducting and presenting the results of a variety of geotechnical tests. AASHTO has published over thirty editions of *Standard Specifications for Transportation Materials and Methods of Sampling and Testing*, which contains many geotechnical tests. In addition, some state departments of transportation have developed their own test specifications. The testing procedures for all of these organizations have coalesced to procedures standardized by ASTM International.

ASTM was initially named the American Society of Testing Materials in 1902, and the first specifications focused on tests related to the railway industry. The organization has expanded to manage the specifications for testing a variety of engineering materials and consumer products. ASTM has been very active in developing standards for soil and rock testing, and these standards have been widely adopted in U.S. and international engineering practice. Committee D18 oversees the standards for soil and rock testing, and dozens of subcommittees covering a wide array of special areas in laboratory

testing. The name of the organization was changed to ASTM International to reflect that the test standards are used internationally as opposed just in the United States. ASTM International provides standards for hundreds of soil and rock tests and these standards have been adopted by most of the organizations that once produced their own standards.

ASTM standards for soil and rock testing usually begin with a “C” or “D” followed by a three or four digit number. In geotechnical engineering practice, engineers often refer to specific tests by the ASTM number as opposed to the test name itself. As an example, engineers will often say “ASTM D698” as opposed to “standard Proctor compaction test.” The letter and test number are also followed by a dash and a two digit number reflecting the year that the standard was adopted or last reviewed. For example, ASTM D698-12 indicates that the standard was last approved in 2012. In this manual, the date portion of the ASTM standard is omitted since these will change during the useful life of the manual.

ASTM standards are not static. Each standard is reviewed every five years. During review, the standard may be reapproved, modified, or withdrawn. Individuals who are actively engaged in soil and rock testing need to ensure that tests are conducted to the most recent approved version of the standard.

3-1.3 Laboratory Certification.

The specifications and guidelines for laboratory tests are often quite complex. It takes a considerable investment of time and money for a laboratory to competently conduct many geotechnical tests and obtain reliable and repeatable results. It is often difficult for an engineer to know the competency of a laboratory to conduct high quality tests without conducting an assessment of the laboratory’s past performance. Two organizations conduct routine assessments of a laboratory’s ability to conduct standardized tests to a minimum level of competency.

The Materials Testing Center (MTC) of the U.S. Army Corps of Engineers inspects laboratories and validates their ability to conduct tests that follow ASTM standards. They see if the laboratory has a quality manual, certified technicians, functional equipment, and calibration procedures. Their inspection is done for specific tests, and they maintain an online register of validated labs and the tests that they are able to perform.

AASHTO also has a laboratory accreditation program. They perform on-site assessments of a laboratory’s prowess in conducting tests to AASHTO and ASTM standards. The laboratory must demonstrate the specific tests on the apparatuses where they will be performed. They also review the laboratory’s quality management program, technician training, and calibration procedures. AASHTO maintains a register of accredited labs online.

When planning to engage a private testing firm to conduct tests for a project, it is prudent to examine the validation or accreditation of the proposed laboratory for the specific tests that will be conducted. Even though a laboratory has been validated, it is still necessary to carefully review the test results to ensure that the tests were conducted properly and that the test results are reasonable.

3-2 LABORATORY TESTS ON SOILS.

There are hundreds of ASTM standardized tests used in geotechnical engineering. A small subset of those, perhaps 40 tests, are routinely used in geotechnical practice. It the following discussion, the tests will be categorized as: (1) index tests, (2) strength tests, (3) compression tests, (4) dynamic tests, and (5) permeability tests.

3-2.1 Sample Selection.

Soil samples normally can be categorized as *disturbed* or "undisturbed." As explained in Chapter 2, disturbed samples can be obtained by drive samplers, cuttings generated by an auger, materials excavated in test pits, etc. "Undisturbed" or *intact* samples are those obtained from thin-walled samplers or excavated block samples.

Remolded samples are a form of disturbed sample, and this term is normally reserved for fine-grained soils. Clays can be remolded by mixing them with a spatula or other stirring device at a high water content. A remolded sample has lost the structure of the parent material. A *reconstituted* sample is also a form of disturbed sample, and that term is normally reserved for coarse-grained soils. *Compacted* samples, which can be formed from either fine-trained or coarse-grained soils, can also be considered disturbed samples.

The amount of material needed to conduct a given test can vary greatly. Over 100 pounds of soil may be required for compaction tests (ASTM D698 or ASTM D1557), and only a few ounces of soil may be needed for ring shear tests (ASTM D6467). The individual ASTM test procedures often state the amount of material needed for a test series. Table 3-1 provides a summary of the amount of material needed for common soil tests.

As a general rule, fine-grained soils should not be allowed to dry out prior to testing unless the test procedures specifically require drying the sample. In particular, oven drying of a fine-grained soil can cause irreversible changes in mechanical properties. Correct methods of sample storage for soils is provided in ASTM D3213 (Standard Practices for Handling, Storing, and Preparing Soft Intact Marine Soil) and ASTM D4220 (Standard Practices for Preserving and Transporting Soil Samples).

Table 3-1 Amount of Soil Needed for Common ASTM Tests

ASTM #	Description	Sample Size[A]	Comments

D698	Laboratory Compaction Characteristics of Soil Using Standard Effort (12,400 ft-lbf/ft^3 (600 kN-m/m^3))	23 kg (Methods A and B) 45 kg (Method C)	16 kg dry (Methods A and B), 29 kg dry (Method C). If the sample has material larger than the No. 4 sieve (Methods A and B) or greater than ¾" (Method C), much more material may be needed.
D854	Specific Gravity of Soil Solids by Water Pycnometer	100 g dry	The test can be conducted with less material if the small (250 ml) pycnometer is used.
D1140	Determining the Amount of Material Finer than 75 µm (No. 200) Sieve in Soils by Washing	200 g	This value is for a sample where 100% passes the No. 4 sieve. Considerably more material is needed for accurate results of coarser soils.
D1557	Laboratory Compaction Characteristics of Soil Using Modified Effort (56,000 ft-lbf/ft^3 (2,700 kN-m/m^3))	23 kg (Methods A and B) 45 kg (Method C)	16 kg dry (Methods A and B), 29 kg dry (Method C). If the sample has material larger than the No. 4 sieve (Methods A and B) or greater than ¾" (Method C), much more material may be needed.
D2166	Unconfined Compressive Strength of Cohesive Soil	250 - 300 g	Around 150 g for test specimen and 50-70 g for trimmings
D2216	Laboratory Determination of Water (Moisture) Content of Soil and Rock by Mass	Depends on particle size: 20 g – 5 kg (Method A)	For maximum particle size: 75 mm: 5 kg required 37.5 mm: 1 kg 19 mm: 250 g 9.5 mm: 50 g 4.75 mm: 20 g 2 mm: 20 g
D2435	One-Dimensional Consolidation Properties of Soils Using Incremental Loading	300 g	Assuming 2.5-in. diameter sample with height 1 in. Also including weight of trimmings.
D2487	Classification of Soils for Engineering Purposes (Unified Soil Classification System)	Exact mass not provided in ASTM	
D2488	Description and Identification of Soils (Visual-Manual Procedures)	Depends on particle size: 110 g – 60 kg	For maximum particle size: 75 mm: 60 kg required 38.1 mm: 8 kg 19 mm: 1 kg 9.5 mm: 220 g 4.75 mm: 110 g
D2850	for Unconsolidated Undrained Triaxial Compression Test on Cohesive Soils	250 - 300 g	150 g -170 g for specimen loaded into cell for test and 50-70 g for trimmings. Minimum diameter is 1.3 in. and H / D ratio is 2 to 2.5. Considering a sample with 1.4-in. diameter and 3-in. height.

[A] Moist sample size unless indicated otherwise

Table 3-1 (cont.) Amount of Soil Needed for Common ASTM Tests

ASTM #	Description	Sample Size[A]	Comments

D3080	Direct Shear Test of Soils Under Consolidated Drained Conditions	250 – 300 g	Minimum specimen diameter for circular specimens, or width for square specimens, is 2 in. and minimum thickness 0.5 in. Considering 2.5-in. diameter and 1-in. height.
D3967	Splitting Tensile Strength of Intact Rock Core Specimens	200 g each (10 specimens required of this mass)	Circular specimen with $_D$ = 54 mm (2 in.) $_t/_D$ = 0.2 to 0.75. Considering $_D$ = 54 mm, thickness = 27 mm, G_S = 2.7, approximate weight for each sample is 167 g. 10 specimens required.
D3999	Determination of the Modulus and Damping Properties of Soils Using the Cyclic Triaxial Apparatus	200 g	Cylindrical specimens with a minimum diameter of 36 mm [1.4 in.]. The height-to-diameter ratio shall be between 2 and 2.5. Considering $_D$ = 1.4 in. and $_H$ = 3 in.
D4015	Modulus and Damping of Soils by Fixed-Base Resonant Column Devices	650 - 700 g	$_D$ = 7.1 cm, $_L$ = 14.2 cm. Average mass required is 609 g.
D4186	One- Dimensional Consolidation Properties of Saturated Cohesive Soils Using Controlled- Strain Loading	300 g	Around 150 g for specimen loaded into cell for test and 50-70 g for trimmings
D4253	Maximum Index Density and Unit Weight of Soils Using a Vibratory Table	11 - 34 kg	Mass of specimen depends on Maximum particle size: 3 in: 34 kg required 1.5 in: 34 kg 0.75 in. or less: 11 kg
D4254	Minimum Index Density and Unit Weight of Soils and Calculation of Relative Density	11 - 34 kg	Mass of specimen depends on Maximum particle size: 75 mm: 34 kg required 38.1 mm: 34 kg 19 mm: 11 kg 9.5 mm or less: 11 kg
D4318	Liquid Limit, Plastic Limit, and Plasticity Index of Soils	150 - 200 g	Sample should be passing No 40 sieve.
D4427	Classification of Peat Samples by Laboratory Testing	Representative samples of the peat should be used.	The size and type of sample needed is dependent on the tests to be performed and the coarseness and moisture content of the peat.
D4546	One-Dimensional Swell or Collapse of Soils	250 - 300 g	Considering 2.5-in. diameter and 1-in. height
D4643	Determination of Water Content of Soil and Rock by Microwave Oven Heating	100 - 1000 g	Percentage retained not more than 10 % of sieve: No 10: 100 – 200 g required No 4: 300 – 500 g required ¾ in: 500 -1000 g Rock/gravel samples: 500 g
D4648	Laboratory Miniature Vane Shear Test for Saturated Fine- Grained Clayey Soil	200 - 250 g	For vane of diameter 0.5 in. and height 1 in., Minimum Sample required has diameter 2 in. and height 2 in.
D4767	Consolidated Undrained Triaxial Compression Test for Cohesive Soils	200 – 250 g	Considering 1.4-in. diameter samples with height around 3 in. Including weight of trimmings.

[A] Moist sample size unless indicated otherwise

Table 3-1 (cont.) Amount of Soil Needed for Common ASTM Tests

ASTM #	Description	Sample Size[A]	Comments

D4829	Expansion Index of Soils	1 kg (dry)	Sample is first air dried or oven dried.
D5084	Measurement of Hydraulic Conductivity of Saturated Porous Materials Using a Flexible Wall Permeameter	200 g	Considering 2-in. diameter and 2-in. height. Minimum height and diameter are 1 in.
D5311	Load Controlled Cyclic Triaxial Strength of Soil	750 - 800 g	Cylindrical specimens with min Diameter of 2 in. and ratio H / D = 2-2.5.
D5607	Performing Laboratory Direct Shear Strength Tests of Rock Specimens Under Constant Normal Force	Exact mass not provided in ASTM	The height of each specimen shall be greater than the thickness of the shear (test) zone and sufficient to embed the specimen in the holding rings. Specimens may have any shape such that the cross-sectional areas can be determined.
D5731	Determination of the Point Load Strength Index of Rock and Application to Rock Strength Classifications	700 - 800 g each	Preferred diameter/width of 50 mm (2 in). Average Length = 4 to 5 in. 10 samples required
D6467	Torsional Ring Shear Test to Determine Drained Residual Shear Strength of Cohesive Soils	100 g	Soil passing through No. 40 sieve. Including soil for water content. Around 40-45 g needed for test specimen.
D6528	Consolidated Undrained Direct Simple Shear Testing of Fine Grain Soils	400 – 450 g	Considering 30 mm height and 78 cm^2 cross sectional area.
D6913	Particle-Size Distribution (Gradation) of Soils Using Sieve Analysis	50 g – 70 kg (depends on particle size)	For maximum particle size (99% passing): 0.425 mm: 50 g required 2 mm: 50 g 4.75 mm: 75 g 9.5 mm: 165 g 19 mm: 1.3 kg 25.4 mm: 3 kg 38.1 mm: 10 kg 50.8 mm: 25 kg 76.2 mm: 70 kg
D7181	Consolidated Drained Triaxial Compression Test for Soils	250 – 300 g	Cylindrical sample, including trimmings
D7263	Laboratory Determination of Density (Unit Weight) of Soil Specimens	500 - 600 g	Considering 2.8-in. specimens on all sides.
D7928	Particle- Size Distribution (Gradation) of Fine-Grained Soils Using the Sedimentation (Hydrometer) Analysis	50 g (dry)	Passing No. 10 sieve and retained on No. 200 sieve

[A] Moist sample size unless indicated otherwise

Tests conducted to determine important strength or compressibility parameters for *in situ* soil conditions require high-quality intact or undisturbed samples. It has become common practice to X-ray soil samples while still in the tube (prior to extrusion) to select the best portions for test assignments. ASTM D4452 (Standard Practice for X-Ray Radiography of Soil Samples) provides guidance for X-raying soil samples.

3-2.2 Index Property Tests.

Index properties are used to classify soils and to group soils in major strata. In general, soils with similar index properties behave similarly, so index properties are often used in

empirical correlations. Index property tests are normally much more inexpensive than other types of tests, so they are conducted in greater numbers than the more complex tests. Index property tests can be conducted on both disturbed and intact samples. However, it is prudent to save intact samples for tests that specifically require them, and to use disturbed samples for index property tests. One of the simplest and least expensive index property tests is ASTM D2216 (Standard Test Methods for Laboratory Determination of Water (Moisture) Content of Soil and Rock by Mass). This test requires a relatively small sample, and it is good practice to conduct this test on every disturbed sample that is taken, particularly of fine-grained soils. Important engineering information can be gleaned from plots of water content versus depth.

Other index tests are essential to obtain the parameters required for soil classification. As discussed in Chapter 1, the most common classification scheme used in U.S. geotechnical engineering practice is ASTM D2487 (Standard Practice for Classification of Soils for Engineering Purposes (Unified Soil Classification System)). In order to correctly classify fine-grained and coarse-grained soils, ASTM D4318 (Standard Test Methods for Liquid Limit, Plastic Limit, and Plasticity Index of Soils) and ASTM D6913 (Standard Test Methods for Particle-Size Distribution (Gradation) of Soils Using Sieve Analysis) must be conducted. Determination of the Atterberg limits for fine-grained soils (ASTM D4318) is especially important because they are used in many of the correlations developed for strength and compressibility properties. The parameters from the gradation curve (ASTM D6913) are frequently used in correlations with fluid flow properties of granular soils.

Index tests provide the information necessary to calculate the phase relationship parameters used to characterize various aspects of densities and saturation conditions of soils. The phase relationship parameters are import parts of almost all soil tests. A summary of the phase relationship calculations for soils and rock is given in Table 3-2.

Some index tests are required for specific purposes. As an example, the specific gravity of soils (ASTM D854 - Standard Test Methods for Specific Gravity of Soil Solids by Water Pycnometer) is necessary to calculate the void ratio and porosity of a soil or rock. It is also needed as part of a hydrometer test (ASTM D7928 Standard Test Method for Particle-Size Distribution (Gradation) of Fine-Grained Soils Using the Sedimentation (Hydrometer) Analysis) in the data reduction procedure.

Table 3-2 Summary of Phase Relationship Calculations

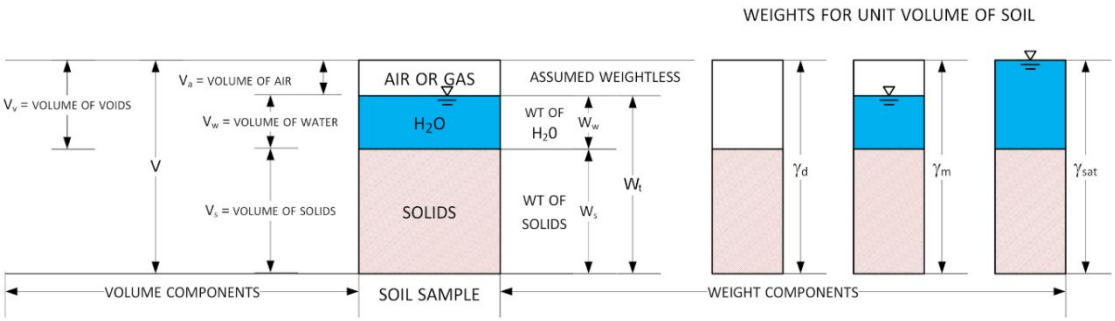

	Property	Saturated: W_s, W_w, G_s are known	Unsaturated: W_s, W_w, G_s, V are known	Supplementary Formulae Relating Measured and Computed Parameters			
Volume Components	V_s = Volume of solids	$\frac{W_s}{G_s \cdot \gamma_w}$		$V-(V_a+V_w)$	$V\cdot(1-n)$	$\frac{V}{1+e}$	$\frac{V_v}{e}$
	V_w = Volume of water	$\frac{W_w}{\gamma_w}$		V_v-V_a	$S\cdot V_v$	$\frac{S\cdot V_a}{1+e}$	$S\cdot V_s\cdot e$
	V_a = Volume of air	zero	$V-(V_s+V_w)$	V_v-V_w	$(1-S)\cdot V_v$	$\frac{(1-S)\cdot V_a}{1+e}$	
	V_v = Volume of voids	$\frac{W_w}{\gamma_w}$	$V-\frac{W_s}{G_s\cdot\gamma_w}$	$V-V_s$	$\frac{V_s\cdot n}{1-n}$	$\frac{V\cdot e}{1+e}$	$V_s\cdot e$
	V = Total volume	V_s+V_w	Measured	$V_s+V_w+V_a$	$\frac{V_s}{1-n}$	$V_s\cdot(1+e)$	$\frac{V_v\cdot(1+e)}{e}$
	n = porosity	$\frac{V_v}{V}$		$1-\frac{V_s}{V}$	$1-\frac{W_s}{G_s\cdot V\cdot\gamma_w}$	$\frac{e}{1+e}$	
	e = Void ratio	$\frac{V_v}{V_s}$		$\frac{V}{V_s}-1$	$\frac{G_s\cdot V\cdot\gamma_w}{W_s}-1$	$\frac{G_s\cdot w}{S}$	$\frac{n}{1-n}$
Weights for Specific Sample	W_s = Weight of solids	Measured		$\frac{W_t}{1+w}$	$G_s\cdot V\cdot\gamma_w\cdot(1+n)$	$\frac{W_w\cdot G_s}{S\cdot e}$	
	W_w = Weight of water	Measured		$w\cdot W_s$	$S\cdot\gamma_w\cdot V_v$	$\frac{e\cdot W_s\cdot S}{G_s}$	
	W_t = Total weight	W_s+W_w		$W_s\cdot(1+w)$			
Weights for Sample of Unit Volume	γ_d = Dry unit weight	$\frac{W_s}{V_s+V_w}$	$\frac{W_s}{V}$	$\frac{W_t}{V\cdot(1+w)}$	$\frac{G_s\cdot\gamma_w}{1+e}$	$\frac{G_s\cdot\gamma_w}{1+w\cdot G_s/S}$	
	γ_t = Total (wet) unit weight	$\frac{W_s+W_w}{V_s+V_w}$	$\frac{W_s+W_w}{V}$	$\frac{W_t}{V}$	$\frac{(G_s+S\cdot e)\cdot\gamma_w}{1+e}$	$\frac{(1+w)\cdot\gamma_w}{w/S+1/G_s}$	
	γ_{sat} = Sat. unit weight	$\frac{W_s+W_w}{V_s+V_w}$	$\frac{W_s+V_v\cdot\gamma_w}{V}$	$\frac{W_s}{V}+\left(\frac{e}{1+e}\right)\cdot\gamma_w$	$\frac{(G_s+e)\cdot\gamma_w}{1+e}$	$\frac{(1+w)\cdot\gamma_w}{w+1/G_s}$	
	γ_b = Buoyant unit weight or submerged unit weight	$\gamma_{sat}-\gamma_w$		$\frac{W_s}{V}-\left(\frac{1}{1+e}\right)\cdot\gamma_w$	$\left(\frac{G_s+e}{1+e}-1\right)\cdot\gamma_w$	$\left(\frac{1-1/G_s}{w+1/G_s}\right)\cdot\gamma_w$	
Combined Relations	w = water content	$\frac{W_w}{W_s}$		$\frac{W_t}{W_s}-1$	$\frac{S\cdot e}{G_s}$	$S\cdot\left(\frac{\gamma_w}{\gamma_d}-\frac{1}{G_s}\right)$	
	S = Degree of saturation	1.00	$\frac{V_w}{V_v}$	$\frac{W_w}{V_v\cdot\gamma_w}$	$\frac{G_s\cdot w}{e}$	$\frac{w}{\gamma_w/\gamma_d-1/G_s}$	
	G_s = Specific gravity	$\frac{W_s}{V_s\cdot\gamma_w}$		$\frac{S\cdot e}{w}$			

Some commercial laboratories may include the cost of conducting certain index tests within the cost of the more elaborate strength and compressibility tests. For example, a laboratory may include a specific gravity test (ASTM D854) automatically as part of a consolidation test (ASTM D2435 Standard Test Methods for One-Dimensional Consolidation Properties of Soil Using Incremental Loading). The water content test (ASTM D2216) is normally automatically performed in many other tests. There is a separate test to measure the unit weight of soils (ASTM D7263 – Standard Test Methods for Laboratory Determination of Density (Unit Weight) of Soil Specimens), but determination of the unit weight is a by-product of most of the strength and compressibility tests on intact soil specimens.

Table 3-3 includes a list of the common ASTM index tests that are available and the associated parameters that are determined.

Table 3-3 Index Property Tests and Engineering Parameters Obtained

ASTM #	Description	Parameters	Comments
D698	Laboratory Compaction Characteristics of Soil Using Standard Effort (12,400 ft-lbf/ft^3 (600 kN-m/m^3))	$\gamma_{d\text{-}max}$, w_{opt}	Sometimes it is useful to conduct compaction tests at an effort less than D698. This can be done by using 15 to 20 tamps per lift.
D854	Specific Gravity of Soil Solids by Water Pycnometer	G_s	Required when void ratios are to be calculated or when hydrometer tests are performed.
D1140	Determining the Amount of Material Finer than 75 µm (No. 200) Sieve in Soils by Washing	% Fines	Useful when classifying a soil in lieu of conducting a complete gradation.
D1557	Laboratory Compaction Characteristics of Soil Using Modified Effort (56,000 ft-lbf/ft^3 (2,700 kN-m/m^3))	w_{opt}	The normal maximum mold diameter is 6 inches. If larger molds are to be used, calculations are necessary to guarantee the correct compactive effort.
D2216	Laboratory Determination of Water (Moisture) Content of Soil and Rock by Mass	$w\%$	Note that lower oven temperatures are used for organics. Oven drying can cause irreversible changes in the mechanical behavior of clay soils. Specimens which have been oven dried should not be used for other tests.
D2487	Classification of Soils for Engineering Purposes (Unified Soil Classification System)	Classification Symbol	Classification of peat (Pt) is in D4427
D2488	Description and Identification of Soils (Visual-Manual Procedures)	Classification Symbol Description	Visual classification is used on boring logs and most laboratory test reports.
D4221	Dispersive Characteristics of Clay Soil by Double Hydrometer	% Dispersion	Important when examining erosion potential of fine-grained soils for use in levees and dams.
D4253	Maximum Index Density and Unit Weight of Soils Using a Vibratory Table	e_{min}	A vibratory compactor standard for maximum density may be available. Concerns exist on proper calibration of the vibratory table.
D4254	Minimum Index Density and Unit Weight of Soils and Calculation of Relative Density	$\gamma_{d\text{-}min}$	

Table 3-3 (cont.) Index Property Tests and Engineering Parameters Obtained

ASTM #	Description	Parameters	Comments
D4318	Liquid Limit, Plastic Limit, and Plasticity Index of Soils	PL LL PI	In international practice, the fall-cone device is often used for LL and sometimes PL.
D4427	Classification of Peat Samples by Laboratory Testing	Ash content Fiber content Acidity	
D4643	Determination of Water Content of Soil and Rock by Microwave Oven Heating	$w\%$	This normally is used for field compaction control tests. D2216 is normally used in standard laboratory practice.
D4647	Identification and Classification of Dispersive Clay Soils by the Pinhole Test	Dispersive classification	Important when examining erosion potential of fine-grained soils for use in levees and dams.
D4972	pH of Soils	pH	Important when examining the compatibility of steel and other engineering materials in contact with soil.
D6572	Determining Dispersive Characteristics of Clayey Soils by the Crumb Test	Dispersive classification	Important when examining erosion potential of fine-grained soils for use in levees and dams.
D6913	Particle-Size Distribution (Gradation) of Soils Using Sieve Analysis	C_u, C_c, D_{xx}	
D7263	Laboratory Determination of Density (Unit Weight) of Soil Specimens	γ_d, γ_t, $w\%$	
D7928	Particle- Size Distribution (Gradation) of Fine-Grained Soils Using the Sedimentation (Hydrometer) Analysis	% > 2μm	

3-2.3 Compaction Tests.

Two types of compaction tests are available for determining the compaction characteristics of soils. For soils having greater than 15% fines, impact compaction tests are the most appropriate. Impact compaction tests provide a compaction curve for the soil, and the maximum dry density ($\gamma_{d\text{-}max}$) and optimum water content (w_{opt}) can be determined from the curve. The as-compacted density of the soil can be characterized by relative compaction (RC). Relative compaction is defined as:

$$RC = \frac{\gamma_d}{\gamma_{d-\max}} \cdot 100\% \quad \textbf{(3-1)}$$

where:
γ_d = dry density of the soil to be characterized, and
$\gamma_{d\text{-}max}$ = maximum dry density from the compaction curve for a particular effort.

For soils having less than 15% fines, the density of a soil can be characterized by *relative density* (D_r). Relative density is defined as:

$$D_r = \frac{e_{\max} - e}{e_{\max} - e_{\min}} \cdot 100\% = \frac{\gamma_{d-\max}}{\gamma_d}\left[\frac{\gamma_d - \gamma_{d-\max}}{\gamma_{d-\max} - \gamma_{d-\min}}\right] \cdot 100\% \quad \textbf{(3-2)}$$

where:
e = void ratio of soil to be characterized,
e_{max} = maximum index void ratio,
e_{min} = minimum index void ratio,
γ_d = dry density of soil to be characterized (corresponding to e),
$\gamma_{d\text{-}max}$ = maximum index dry density (corresponding to e_{min}), and
$\gamma_{d\text{-}min}$ = minimum index dry density (corresponding to e_{max}).

Soils in their loosest states have a relative density equal to 0% and soils in their densest state have a relative density equal to 100%. For these soils, tests must be conducted to determine the maximum and minimum index void ratios and index densities. These tests are not "compaction tests" in the strictest sense of the term, but are index values corresponding to the loosest and densest states of the soil. The maximum dry density used in relative density calculations is not necessarily the same as that obtained in ASTM D1557 that is described below.

3-2.3.1 Impact Compaction Tests.

ASTM D698 (Standard Test Methods for Laboratory Compaction Characteristics of Soil Using Standard Effort (12,400 ft-lbf/ft^3)) and ASTM D1557 (Standard Test Methods for Laboratory Compaction Characteristics of Soil Using Modified Effort (56,000 ft-lbf/ft^3)). These tests differ by the amount of effort that is applied to compact the soil. The ASTM standards provide test procedures for compaction molds having diameters of 4 inches and 6 inches. Following the specifications, both of these impact compaction tests should be limited to soils having no more than 30% retained on the 3/4-inch sieve, although corrections exist for materials having as much as 70% retained on the 3/4-inch sieve. However, if impact compaction test results are required for larger grain-size materials, the mold diameters and hammer weights should be scaled up to keep the compactive effort the same.

3-2.3.2 Index Density Determination.

For soils having less than 15% fines, there are specific tests that can be conducted to determine the maximum and minimum index densities so that the soil can be characterized in terms of relative density. ASTM D4254 (Standard Test Methods for Minimum Index Density and Unit Weight of Soils and Calculation of Relative Density) provides three methods to determine e_{max} and $\gamma_{d\text{-}min}$ depending on the grain size of the soil tested. Methods are available for soils have a maximum grain size of 3 inches or less. ASTM D4253 (Test Methods for Maximum Index Density and Unit Weight of Soil Using a Vibratory Table) is used to determine e_{min} and $\gamma_{d\text{-}max}$.[3] The apparatus used to

[3] Some engineers use the dry density obtained from ASTM D4253 for calculating relative compaction for a soil deposit in the same manner as done using the maximum dry density from impact compaction tests.

perform this test is expensive and many commercial laboratories are not able to perform this test.

3-2.4 Strength Tests.

There are a variety of strength tests that have ASTM specifications for both drained (effective stress) strength parameters and undrained (total stress) strength parameters. The most common drained shear strength parameters are the effective stress cohesion (c') and the effective stress friction angle (ϕ'). Total stress shear strength parameters are s_u (undrained shear strength for a $\phi = 0$ envelope) for saturated soils, and total stress cohesion (c) and total stress friction angle (ϕ) for partially saturated soils.

The shear strength parameters listed above are for linear failure envelopes. It also is possible to determine parameters for non-linear failure envelopes for many of the strength tests.

Shear strength parameters are often needed for undisturbed or intact specimens, compacted specimens, remolded specimens, and reconstituted specimens. The different strength tests will be assessed based on their ability to accommodate these different types of test specimens. Table 3-4 lists the ASTM strength tests and the parameters obtained.

3-2.4.1 Drained or Effective Stress Strength Tests.

There are four recommended tests listed in the ASTM specifications for measuring drained or effective stress strength parameters: (1) Direct Shear Test, (2) Consolidated Drained Triaxial Test, (3) Consolidated Undrained Triaxial Test, and (4) Ring Shear Test.

3-2.4.1.1 Direct Shear Test (ASTM D3080).

The direct shear test (ASTM D3080 – Standard Test Method for Direct Shear Test of Soils Under Consolidated Drained Conditions) is one of the oldest and most common strength tests. Figure 3-1 shows the basic elements of a direct shear tests and the data collected. In U.S. engineering practice, the most common specimen cross-sections are 2 inch × 2 inch and 4 inch × 4 inch square specimens and 2.5-inch diameter circular specimens. A few commercial laboratories have direct shear apparatuses that can accommodate 12 inch × 12 inch specimens. The 2.5-inch diameter cylindrical shear box is very popular since intact specimens can be easily trimmed from the common 3-inch diameter Shelby tubes. It is also easier to compact test specimens in a cylindrical specimen container than a square specimen container. The direct shear apparatus can use intact, compacted, or remolded test specimens.

The direct shear test is most often used for clay soils and for some sandy soils. ASTM D3080 requires that the maximum grain size of the test specimen be no greater than

1/10 of the shear box width and no greater than 1/6 of the specimen height. Based on the common sizes of the shear box, it is not appropriate to test materials larger than medium sands.

Table 3-4 Laboratory Strength Tests with ASTM Standards

ASTM #	Description	Parameters	Comments
D2166	Unconfined Compressive Strength of Cohesive Soil	q_u	Best used as an index test as opposed to obtaining shear strength for design.
D2573	Field Vane Shear Test in Saturated Fine-Grained Soils	s_u, S_t strength anisotropy	Perhaps the best all-around tests for undrained strengths of soft, saturated clays.
D2850	Unconsolidated Undrained Triaxial Compression Test on Cohesive Soils	c-ϕ, s_u	Best results are obtained when all samples come from the same depth, which can be obtained using 5-in. diameter sampling tubes.
D3080	Direct Shear Test of Soils Under Consolidated Drained Conditions	c'-ϕ'	Good test for measuring fully softened shear strength.
D3967	Splitting Tensile Strength of Intact Rock Core Specimens	σ_t	Indirect measurement of tensile strength.
D4648	Laboratory Miniature Vane Shear Test for Saturated Fine- Grained Clayey Soil	s_u, S_t strength anisotropy	Very good test for soft clay samples that are not trimmable for UU triaxial tests.
D4767	Consolidated Undrained Triaxial Compression Test for Cohesive Soils	c'-ϕ' s_u for σ'_{3con}	Good for effective stress strength parameters of sands and clays. Use caution when using total stress strength parameters for stability analyses.
D5607	Laboratory Direct Shear Strength Tests of Rock Specimens Under Constant Normal Force	c'-ϕ' joint roughness coefficient	
D5731	Determination of the Point Load Strength Index of Rock and Application to Rock Strength Classifications	I_s, $I_{s(50)}$	Used for rock classification and other applications.
D6467	Torsional Ring Shear Test to Determine Drained Residual Shear Strength of Cohesive Soils	ϕ'_r	Best test for residual shear strength for clays. Staged tests can save a lot of time. Very small test specimen.
D6528	Consolidated Undrained Direct Simple Shear Testing of Fine Grain Soils	s_u, G	The undrained strength measured is a conservative approximation of the maximum shear stress at failure.
D7181	Consolidated Drained Triaxial Compression Test for Soils	c'-ϕ'	Tests on CL and CH clays may take a very long time to complete. D3080 may be a better choice.

Direct shear tests are relatively easy to conduct. A consolidation stress is first applied to the test specimen. After all excess pore water pressures are dissipated, the sample is sheared at a constant displacement rate very slowly to ensure drained conditions are maintained. Direct shear tests do not produce stress-strain results, but rather stress-displacement results. Moduli cannot be determined from direct shear tests.

Since the failure plane in a direct shear test is constrained to the horizontal plane, then the shear strength parameters measured might be lower than those measured in other tests that have an inclined shear plane for soils that exhibit horizontal layering (Duncan et al. 2014). Soils that are deposited in water; such as lacustrine, alluvial, and marine soils; may exhibit this *inherent anisotropy* whereby the shear strength is a function of

the orientation of the failure plane. This issue of the failure plane orientation is insignificant for remolded and compacted soils. Direct shear tests also may suffer from progressive failure, whereby the shear strength is not fully mobilized on the entire failure plane at the same instant. This can also result in lower peak shear strength parameters for materials that exhibit brittle stress-displacement curves, such as heavily overconsolidated clay.

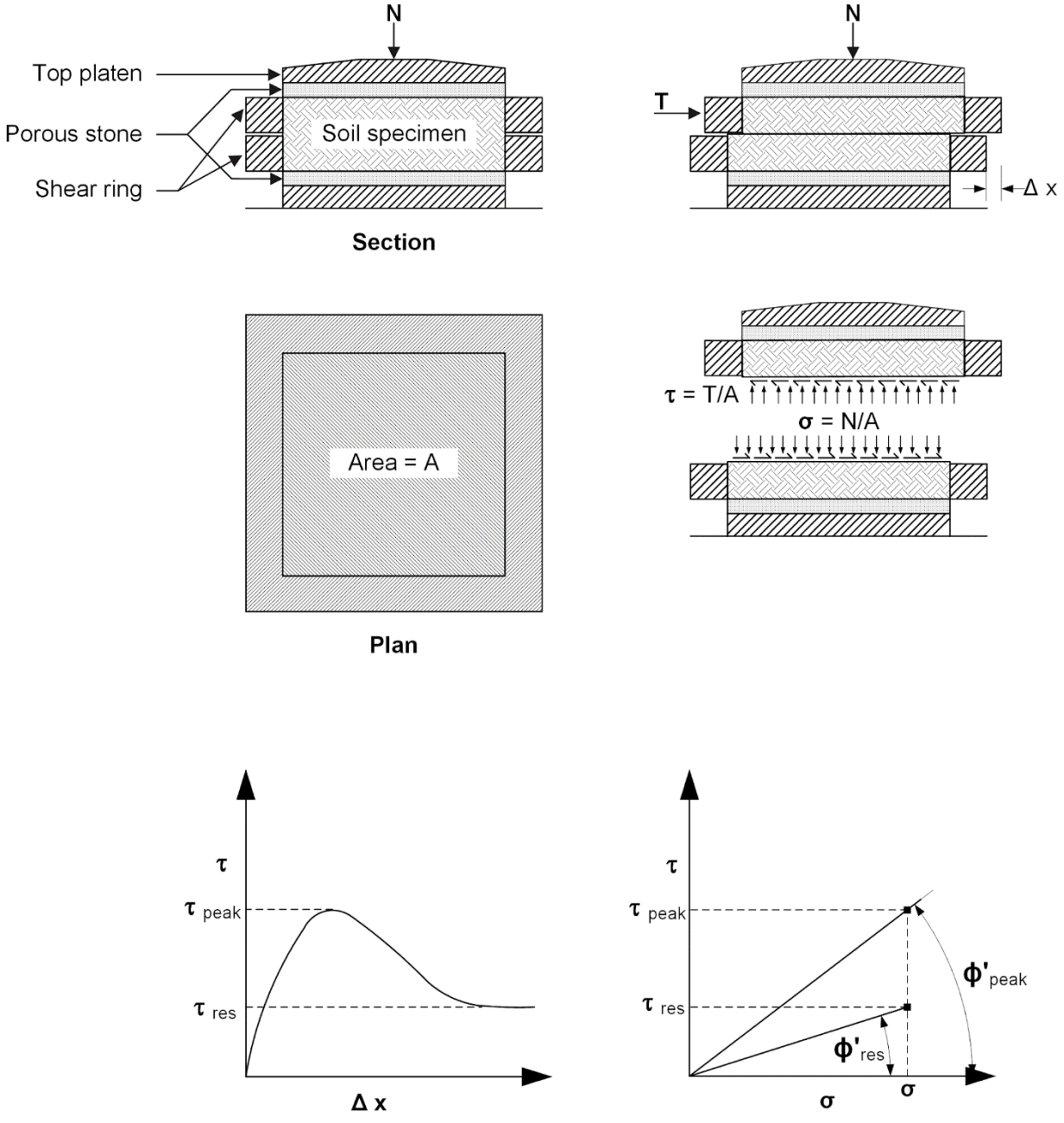

Figure 3-1 Basic Elements for a Consolidated Drained Direct Shear Test Along with Example Data Collected for One Test Specimen

Direct shear tests are especially well-suited for testing remolded clays. It is easy to form test specimens in the shear box and the device allows the application of small consolidation stresses. It is the best test available for measuring the *fully softened shear strength*, which is the peak shear strength of remolded, normally consolidated clays.

3-2.4.1.2 Consolidated Drained (CD) Triaxial Test (ASTM D7181).

The consolidated drained (CD) triaxial test (ASTM D7181 – Standard Test Method for Consolidated Drained Triaxial Testing of Soil) is one of the oldest types of triaxial test. The procedure was defined in the Army Corps of Engineers 1930s study. This type of triaxial tests was also called an *S* triaxial, with S denoting slow, since this test has the slowest shear phase of the major categories of triaxial tests.

Common specimen sizes in U.S. practice are 1.4-inch diameter for fine-grained soils and 2.8-inch diameter for sandy soils or for test specimens directly extruded from Shelby tubes without trimming[4]. Many laboratories can test 2-inch diameter and 4-inch diameter specimens as well. The larger 6-inch diameter and 12-inch diameter apparatuses are rarer in commercial laboratories. ASTM D7181 requires that the maximum grain size of the soil tested should be 1/6 of the test specimen diameter, so the diameter of the test specimen should be selected based on the grain-size distribution of the soil.

Figure 3-2 shows the basic elements of a manual CD triaxial test. The test specimen is consolidated by applying a cell pressure. Most tests specimens are consolidated to isotropic stress conditions, but anisotropic consolidation is also possible. The sample is back-pressure saturated by using an elevated pore pressure (back pressure), and the final consolidation stress is the cell pressure minus the back pressure. The sample is sheared very slowly, so that excess pore pressures are not developed, by increasing the vertical stress at a constant displacement rate. The volume change of the test specimen is measured by recording the level of the burette as the load is applied. These tests require considerable skill to perform correctly.

CD triaxial tests are more applicable to sandy soils because a high permeability allows the test specimen to be sheared in a reasonable time. If clayey soils are tested, the sample must be sheared very slowly, and the test may take weeks to months to complete. Some laboratories will not agree to conduct these tests on clay soils.

[4] Although ASTM D7181 allows directly extruded samples to be tested, it is better practice to trim samples to a smaller diameter to reduce the disturbance caused by sampling.

Triaxial tests can be used to test intact, compacted, and remolded test specimens. There is some difficulty in testing very soft remolded test specimens since the soil needs to have sufficient strength to allow trimming and mounting in the triaxial cell. Remolded soils often need to be consolidated outside of the triaxial cell to allow a strength gain prior to trimming. This procedure can limit the consolidation stress that can be applied to the test specimen if normally consolidated conditions are desired.

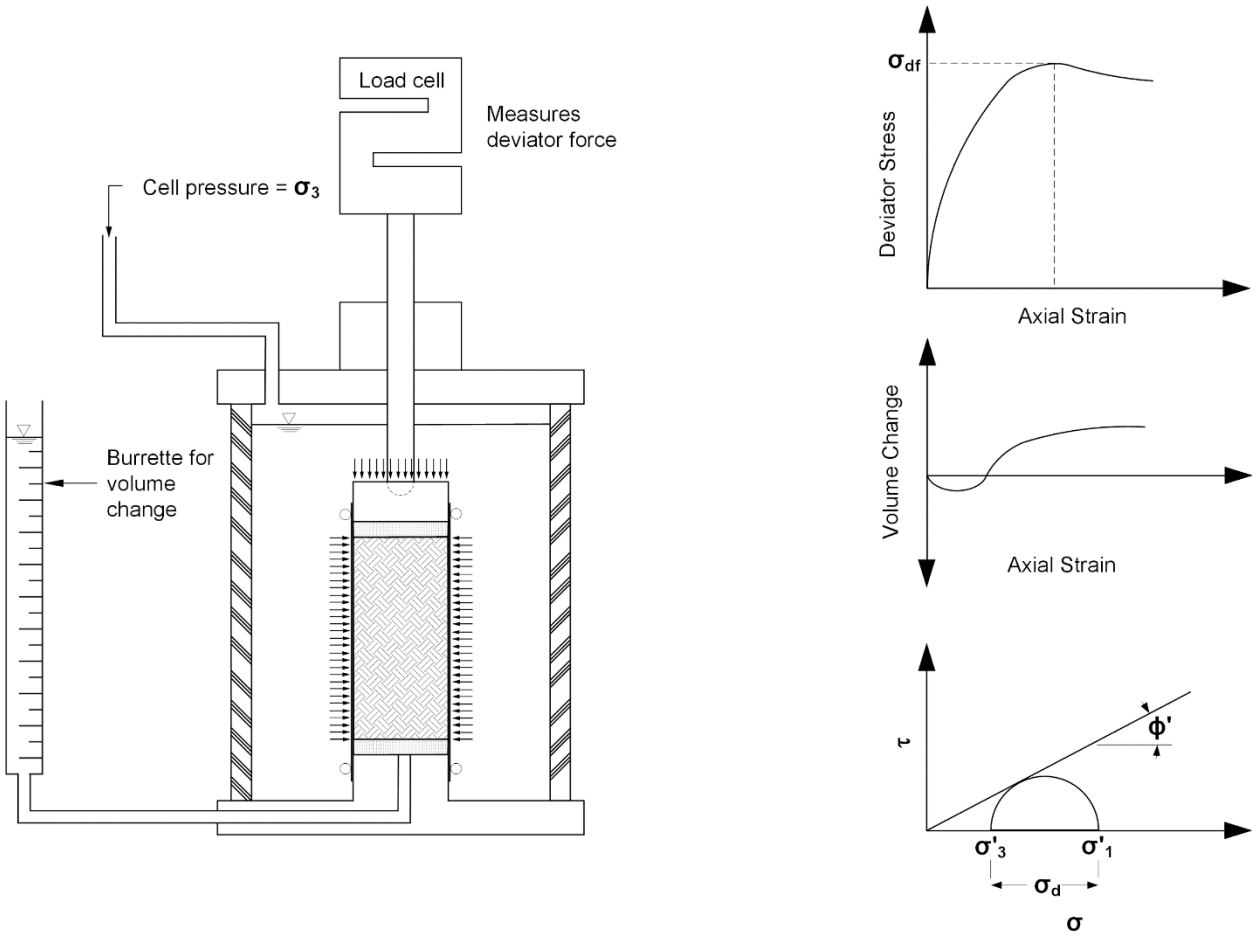

Figure 3-2 Basic Elements of a Consolidated Drained Triaxial Test Along with Example Data Collected for One Test Specimen

3-2.4.1.3 Consolidated Undrained (CU) Triaxial Test (ASTM D4767).

The consolidated undrained (CU) triaxial test (ASTM D4767 – Standard Test Method for Consolidated Undrained Triaxial Compression Test for Cohesive Soil) is another of the three major types of triaxial tests defined by the U.S. Army Corps of Engineers' 1946 study. This test was also called an *R* test if pore pressures are not measured and an $\bar{R}$

if pore pressures are measured.[5] The R test has become obsolete and it is difficult to justify a case where this test should be conducted. Figure 3-3 shows the basic elements of a CU triaxial test and example data.

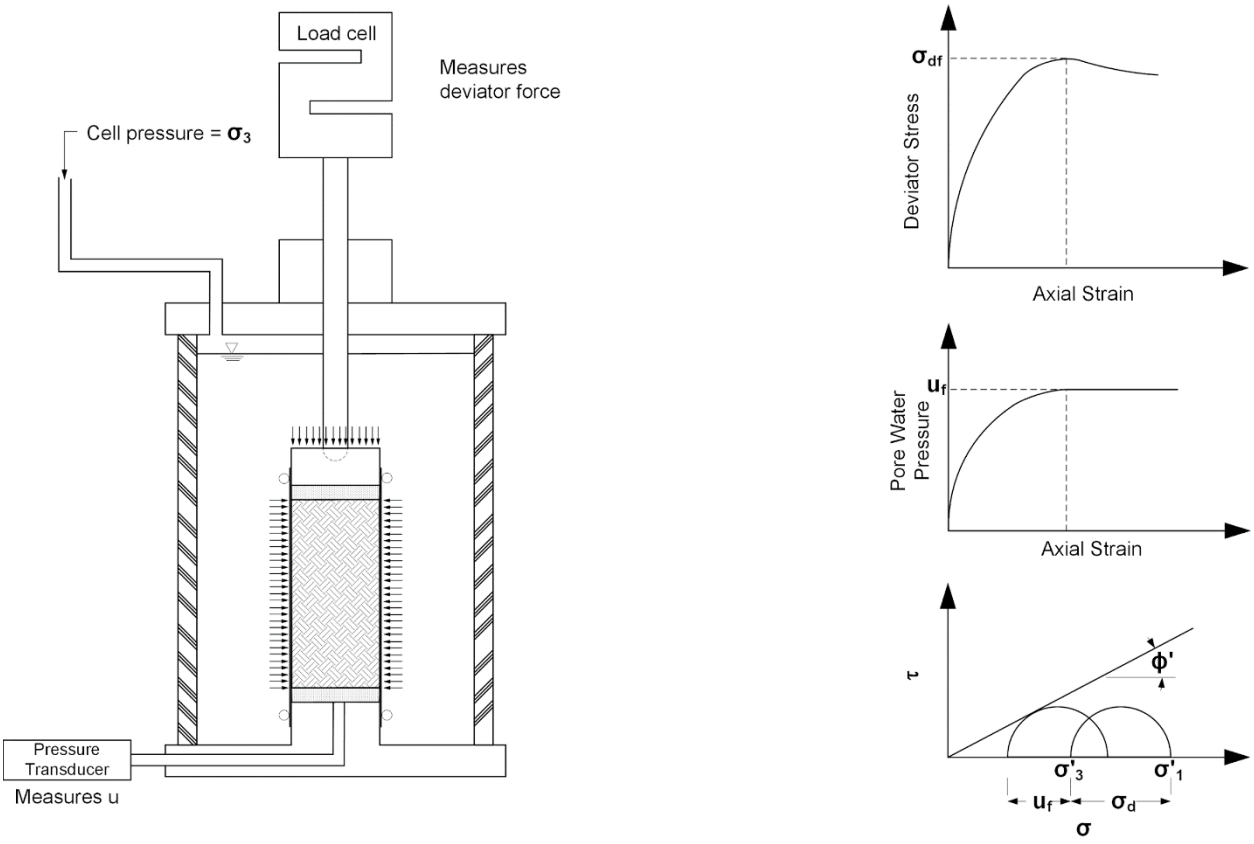

Figure 3-3 Basic Elements of a Consolidated Undrained Triaxial Test Along with Example Data Collected for One Test Specimen

The CU triaxial test is very similar to the CD triaxial test, and most of the information provided for the CD test is also true for the CU test. The test procedures are identical until it is time to shear the test specimen. In the CD test, the drainage valve is open during shear, and in the CU test, the drainage valve is closed during shear. Volume change is measured during a CD test, and pore pressure is measured during a CU test. In a CD test, the strain rate ($\dot{\varepsilon}$) is very slow because the pore pressured generated during shear must *dissipate* throughout the test specimen. In the CU tests, the strain rate is considerably greater since the goal is to allow *equalization* of pore pressures as

[5] It is not clear why the letter R is used for this test. It may be that the other tests are referred to Q and S tests, and R is the letter in the alphabet that falls between these. In the past, engineers would refer to the QRS triaxial test types.

opposed to dissipation. In other words, CU test specimens can be sheared much faster that CD tests test specimens, and this is a big advantage in clay soils.

Pore pressures are measured during shear during CU triaxial tests, and this allows the effective stresses in the sample to be determined. Since effective stress values are available, drained or effective stress strength parameters (c' and ϕ') can be determined. However, there is an important difference in the volume change of the test specimen in CU and CD tests and this can influence the shear strength parameters determined. In the CD test, volume change is allowed, and the void ratio of the test specimen can change during shear. In the CU test, there is not volume change during shear, so the test specimen has the same void ratio at failure as it did prior to shear (after consolidation). The void ratios of CU and CD test specimens can be different at failure, even though they may have started at the same consolidation pressure and void ratio, and this may cause differences in the effective stress shear strength parameters. In engineering practice, this difference is usually neglected, and results from CU and CD tests are often used interchangeably.

3-2.4.1.4 Ring Shear Test (ASTM D6467).

The ring shear test (ASTM D6467 – Standard Test Method for Torsional Ring Shear Test to Determine Drained Residual Shear Strength of Soil) is similar to a direct shear test in that it is a consolidated drained test with shearing occurring on a horizontal plane. A ring shear test should be only used to determine the *residual shear strength*, which is the shear strength of a soil at very high strains or displacements. Residual shear strength is used in geotechnical designs for situations where a failure has already occurred and considerable movement has taken place.

The ring shear apparatus uses an annular test specimen. The specimen size used the most in the U.S. has an inside diameter of 2.8 inches, and outside diameter of 4 inches, and a thickness of 0.2 inches. The basic elements of a ring shear tests are shown in Figure 3-4. The specimen tested is markedly smaller than the other strength tests discussed. The specimen volume is equivalent to about 4 teaspoons. Only remolded clay samples are tested in common ring shear apparatuses, and these are placed in the apparatus in the form of a paste.

The ring shear apparatus allows *staged* tests to be conducted[6]. A single test specimen can be reconsolidated and sheared multiple times. The normal test procedure is to place a specimen in the apparatus and consolidate it to the lowest vertical stress. The specimen is then sheared until the residual strength is achieved. Next, a higher

[6] Although some older testing manuals provide instructions for conducting staged CU and CD triaxial tests, the results of these tests are very unreliable. These types of tests should not be specified and the data from these tests should not be used.

consolidation pressure is applied, and the sample is sheared again. Normally, three different normal stresses can be used for one test specimens.

It is possible to measure residual shear strength properties using a direct shear apparatus if the direction of shear is reversed so that enough shear displacement can be accumulated to obtain residual conditions. Although this test is reported in geotechnical literature, there is not an ASTM procedure for conducting repeated direct shear tests. The ring shear tests is a better test for measuring the residual friction angle since the direction of shear does not need to be reversed during the test, and the area of the shear surface remains constant.

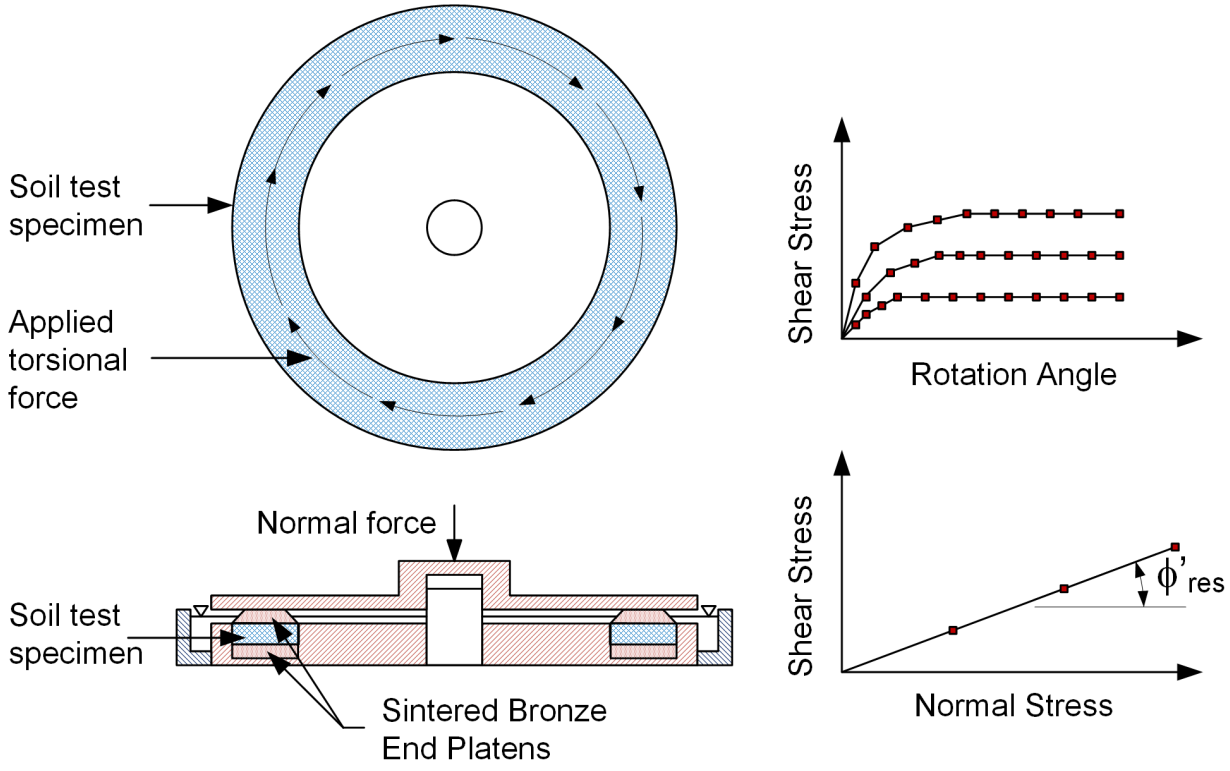

Figure 3-4 Basic Elements of a Ring Shear Test Along with Sample Data

3-2.4.2 Undrained or Total Stress Strength Tests.

There are five laboratory tests with ASTM standards for measuring the undrained shear strength of soils. Since undrained strengths are normally used for fine-grained soils, owing to their low permeability, these tests mainly address clayey and silty soils. The value of undrained shear strength can vary considerably from test to test. The two fundamental undrained strength envelopes that are used for fine-grained soils are shown in Figure 3-5.

For saturated soils undergoing undrained loading, the shear strength *is not* a function of the normal stress on the failure plane, thus $\phi = 0$. For partially saturated soils undergoing undrained loading, the shear strength *is* a function of the normal stress on the failure plane, thus $\phi > 0$. The envelope for the partially saturated soil usually deviates from a straight line, but a linear interpretation over the appropriate range of normal stress if often used in engineering analysis.[7]

The undrained strength of a soil can depend on many different factors. Primary factors include the major effective consolidation stress prior to undrained loading and the overconsolidation ratio (OCR). There are many secondary factors, including the orientation of the failure plane, the rate of loading, the amount of sample disturbance, the system of stresses imposed by the field loading condition or the laboratory test, etc. For the envelopes shown in the figure, only one of the ASTM tests (D2850) provides multiple points to define the envelopes. The other ASTM tests only provide one point to define the shear strength envelope.

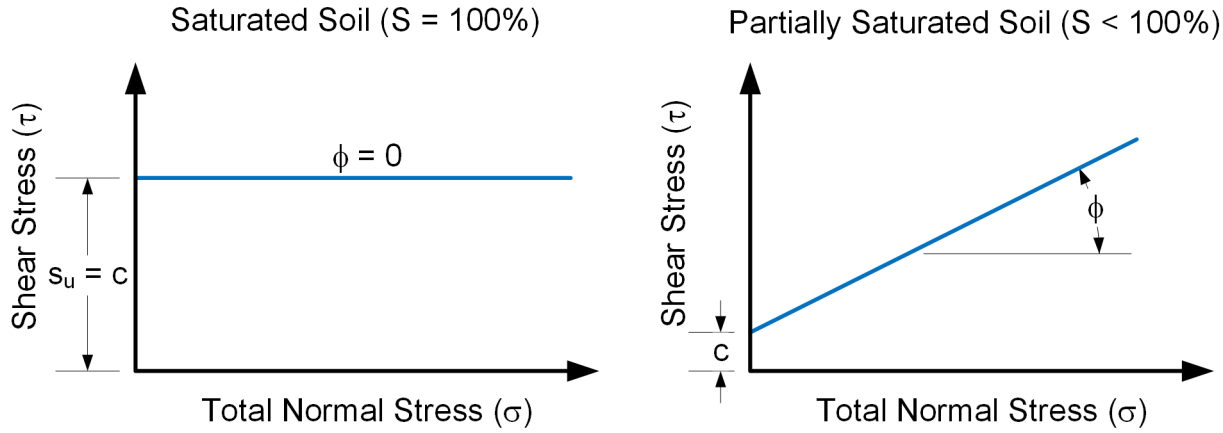

Figure 3-5 Undrained Shear Strength Envelopes for Saturated and Partially Saturated Soils

For layers of saturated fine-grained soils, the goal of an undrained strength testing program is often to determine the variation of undrained strength with depth, such as shown in Figure 3-6. For these cases, enough *in situ* or laboratory tests should be conducted so that the undrained shear strength values, shown as the squares, are determined in order that the variation with strength with depth can be estimated, shown as the dashed line.

[7] A saturated soil is often called a "$\phi = 0$ soil" and a partially saturated soil is called a "c-ϕ soil" by geotechnical engineers.

3-2.4.2.1 Unconfined Compression Test (ASTM D2116).

Unconfined compression tests, UCTs, (ASTM D2166) are one of the oldest and simplest strength tests. The quality and care in conducting the test can vary greatly from specimens being tested using portable load frames in the field to testing the specimen in a membrane in a temperature-controlled laboratory. The basic premise of the test is that if the soil is saturated, the undrained shear strength (s_u) should be the same if the soil is tested with zero confining pressure (σ_3) as it would be with an elevated confining pressure. This assumption might be valid for high quality test specimens carefully tested, but actual test results can deviate from this assumption considerably. In general, UCTs provide lower strengths than would be determined from higher quality tests.

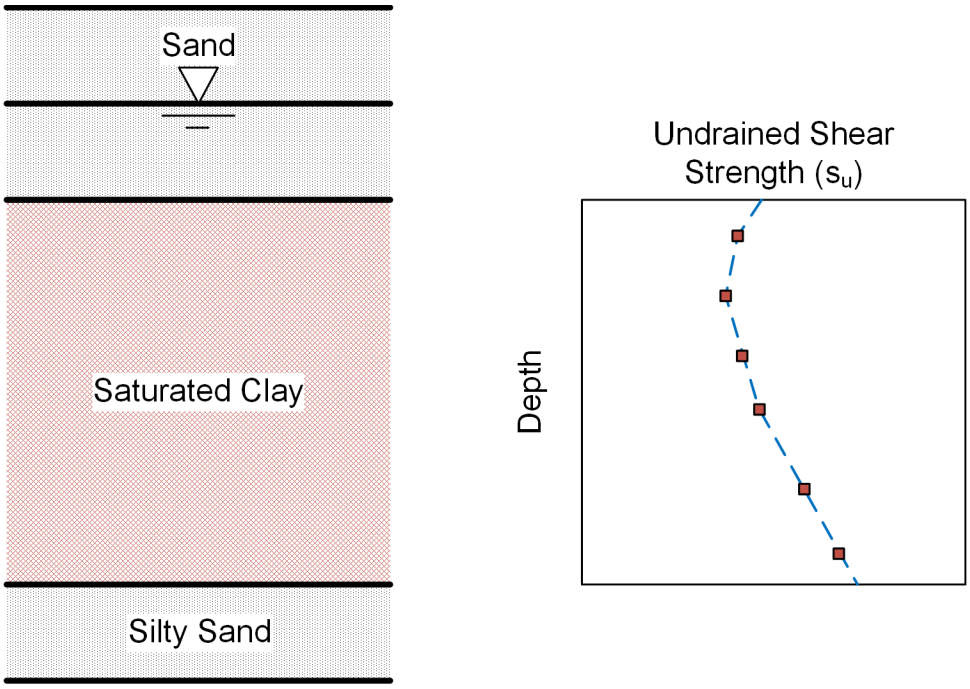

Figure 3-6 Example Distribution of Undrained Strength Versus Depth Relationship for a Hypothetical Saturated Clay

In practice, UCTs are also conducted on partially saturated soils. These tests are difficult to correctly interpret since the results would represent one shear strength value on a c-ϕ envelope, and one point cannot define the envelope. Shortcomings of the UCT have been recognized for over 70 years, and this test should be considered as an index test as opposed to a viable method to measure reliable shear strengths.

3-2.4.2.2 Unconsolidated Undrained (UU) Triaxial Test (ASTM D2850).

The unconsolidated undrained triaxial test (ASTM 2850 – Standard Test Method for Unconsolidated-Undrained Triaxial Compression Tests on Cohesive Soil) has been the

most popular test for measuring undrained shear strength in U.S. geotechnical engineering practice. The basic procedure for this test was outlined in the Corps of Engineers Triaxial Test report in 1946. This test is often called a *Q* triaxial, with Q standing for "quick" since this is the fastest triaxial test. The test specimen is sheared at a strain rate of 1% axial strain per minute, so the shearing phase of the test only lasts about 20 minutes.[8]

UU tests on saturated fine-grained soils are normally conducted using three test specimens to define an envelope. All three test specimens should come from the same depth, with all three having the same *in situ* consolidation pressure and OCR. All three specimens should have the same shear strength, which would verify the $\phi = 0$ failure envelope. UU tests on saturated soil should always be interpreted with a $\phi = 0$ failure envelope, regardless of any slope implied by the tests.

A schematic of the basic test apparatus is shown in Figure 3-7. The sample is sealed in thin rubber membranes, but there are not any porous stones or drainage lines. Special triaxial cells are commercially available just for UU tests. UU tests are most often conducted on 1.4-inch and 2.0-inch diameter trimmed specimens or 2.8-inch directly extruded specimens.

[8] ASTM D2850 suggests using a strain rate of 0.3% for brittle soils, but most laboratories use 1% per minute for all soils.

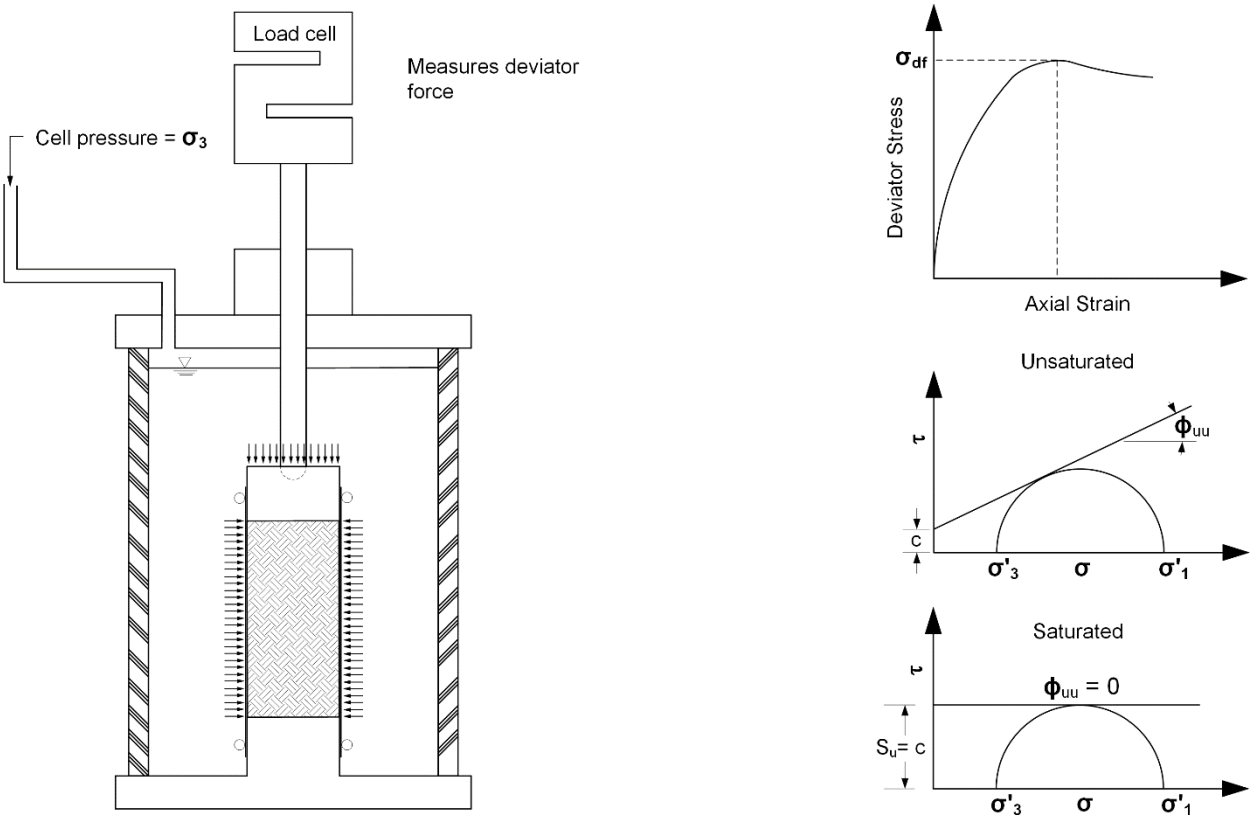

Figure 3-7 Basic elements of a UU Test Apparatus with Sample Data for a Single Test

One deficiency of the UU test is that it is challenging to test very soft soils. For soils that have an undrained shear strength less than about 250 psf, it can be very difficult to trim a test specimen, to mount the specimen in a triaxial cell, and to place a membrane over the specimen. It is very easy to disturb the specimen, and that tends to lower the shear strength even more. For very soft materials, it is best to use the laboratory miniature vane shear test (discussed below) or a fall cone test.

UU tests can also be conducted on partially saturated soils, and have often been used to determine the shear strength parameters for compacted clays. UU tests are the only viable test to determine the values of c and ϕ for partially saturated soils for use in end-of-construction analyses. Special compaction equipment is available to form triaxial test specimens of compacted soils.[9]

There are critics of the UU test, and many of the criticisms are valid (Ladd 1991). However, strengths resulting from UU tests have been validated by back analysis of

[9] There are test apparatuses available for conducting triaxial tests on partially saturated soils, but few commercial labs are equipped to perform these tests.

failed slopes and found to be representative, and it remains a very popular test in engineering practice.

3-2.4.2.3 Consolidated Undrained (CU) Triaxial Test (ASTM D4767).

Since the CU triaxial test is sheared undrained, it is possible to obtain undrained or total stress strength parameters. However, this test has been misused for undrained strength determination in the past. It is not possible to determine viable values of c and ϕ from this test, yet these values are commonly reported by commercial laboratories. The correct way to use the CU test for undrained analyses is to associate the value of s_u (half the deviator stress at failure) with the isotropic consolidation stress. The CU triaxial test provides undrained shear strength values that are normally too high to be used in most analyses. Details of the use of the CU test for undrained strength determination is presented by Duncan and Wong (1983).

3-2.4.2.4 Consolidated Undrained Direct Simple Shear Test (ASTM D6528).

The direct simple shear (DSS) test (ASTM D6528 – Standard Test Method for Consolidated Undrained Direct Simple Shear Testing of Fine Grain Soils) was developed in the 1950s. Commercially-available apparatuses test a cylindrical specimen that is nominally 2.5 inches in diameter and up to 1 inch tall. A schematic of the basic elements of the DSS test is shown in Figure 3-8. The specimen is confined with a wire-reinforced membrane or a set of thin, stacked rings, often coated with Teflon, located outside of an unreinforced latex membrane. The intent of the confining rings is to prevent lateral strain from occurring when the vertical consolidation stress is applied, and to allow the test specimen to deform in the manner of pure shear. After the test specimen is consolidated, it is sheared undrained (technically at constant volume) by translation of the top platen relative to the bottom platen. The undrained shear strength (s_u) is assumed to be the maximum value of shear stress applied to the horizontal plane of the test specimen.

The DSS test was not a common test in geotechnical engineering for fifty years after its development. Few commercial laboratories were able to conduct the test. There are valid criticisms of the DSS test (Saada and Townsend 1981). However, the popularity of this test has increased in recent years, and many more laboratories are able to run the test. The DSS apparatus provides an undrained shear strength that is comparable to that obtained with the field vane shear test (for the same vertical consolidation stress and OCR) and is appropriate for many engineering design cases. This test can only be conducted on saturated soils, and the ASTM standard only addresses fine-grained soils.

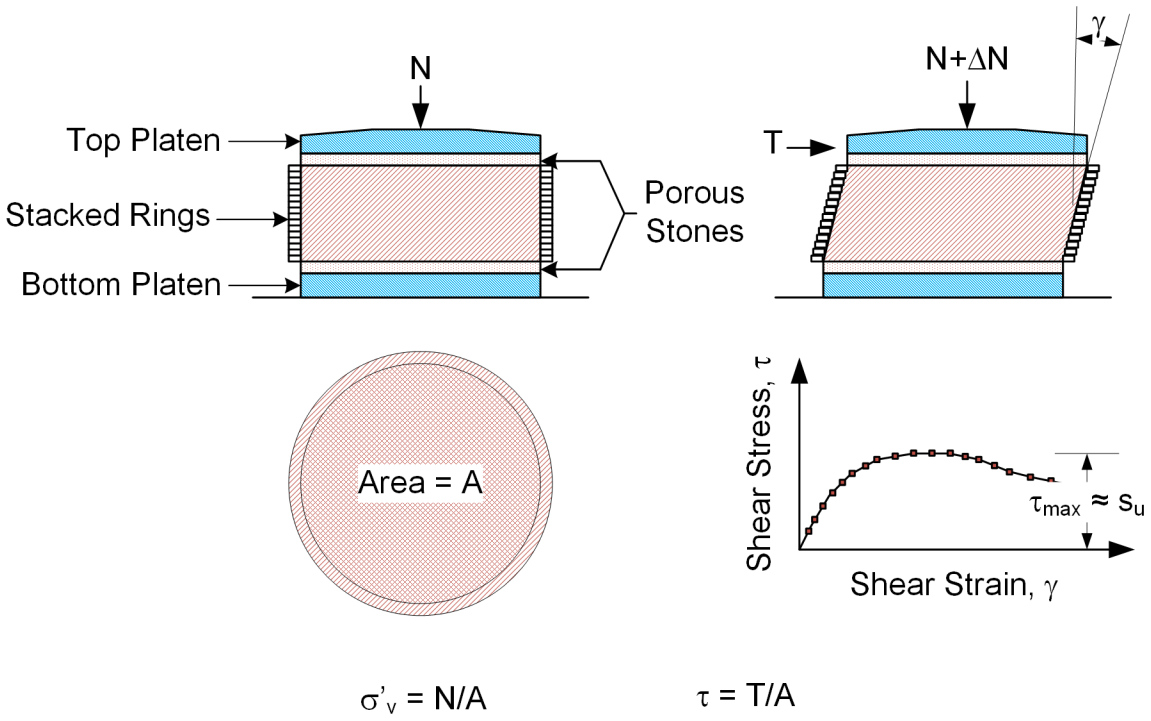

Figure 3-8 Basic Elements of the Direct Simple Shear Test (ASTM D6528)

3-2.4.2.5 Laboratory Miniature Vane Shear Apparatus (ASTM D4648).

The laboratory miniature vane shear apparatus (ASTM D4648 – Standard Test Methods for Laboratory Miniature Vane Shear Test for Saturated Fine-Grained Clayey Soil) is a scaled-down version of the field vane shear test. The vane sizes range from 0.5 inch × 0.5 inch to 1.0 inch × 1.0 inch. Vanes having a smaller diameter than the length can also be obtained to aid in determining anisotropic strengths. A photograph of a vane shear apparatus is shown in Figure 3-9. The vane is inserted into an intact or remolded test specimen and rotated at a constant rate while the torque is measured. The vane can be rotated by a hand crank or an electric drive unit. The torque can be measured by calibrated springs or by electronic load cells. Most legacy data for the miniature vane apparatus has been collected using the calibrated springs, and this is the preferred method.

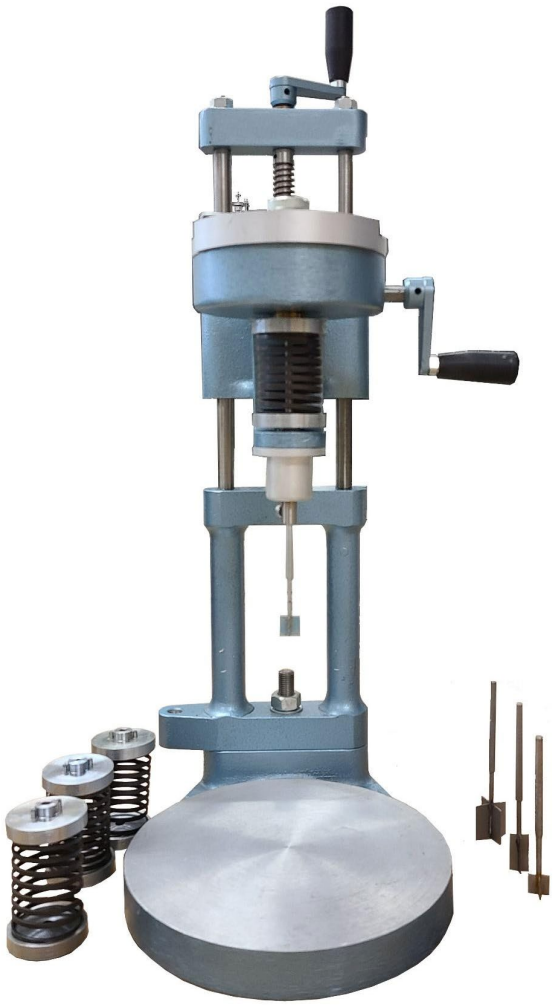

Figure 3-9 Laboratory Miniature Vane Shear Apparatus

Lab vane shear tests are not very common in geotechnical engineering practice, but this type of test can be especially useful in very soft clays. If a clay sample is too soft to be trimmed for a UU triaxial test, then a laboratory miniature vane test is a viable alternative.

3-2.4.2.6 Other Strength Tests.

There are other tests available to measure the laboratory undrained shear strength of soils that do not have specific ASTM standards available, or they are variations of the conventional ASTM tests.

There are two variations of the CU triaxial test that have limited use in geotechnical practice. The conventional CU triaxial test is normally conducted on test specimens that have been *isotropically* consolidated (vertical stress = horizontal stress during consolidation). These are often referred to as *ICU* triaxial tests. It is possible to anisotropically consolidate test specimens where the vertical stress is different than

(usually greater) the horizontal stress. These are called *ACU* triaxial tests. The ASTM specifications address the basic components of ACU tests. ACU tests produce essentially the same effective stress strength parameters as ICU tests. ACU tests normally provide different undrained shear strengths than ICU tests, so the main usefulness of the test would be for projects where special undrained strengths are required.

A separate type of ACU test can be conducted where the ratio of the effective stresses during consolidation (minor effective stress/major effective stress) is equal to the at-rest earth pressure coefficient (K_0). These tests are sometimes called CK_0U triaxial compression tests. For these tests, the exact stresses are not specified, but determined to be the stresses necessary for no lateral strain to occur during consolidation. It is difficult to conduct these tests on manual triaxial apparatuses, but they can be easily conducted on fully-automatic apparatuses. These tests also provide essentially the same effective stress shear strength parameters as conventional ICU triaxial tests. Their main utility would be when undrained strengths are needed for special projects.

Another special type of triaxial test that is occasionally used in engineering practice is the *stress path triaxial test*. While most triaxial tests involve loading a test specimen axially while the cell pressure is constant, stress path tests vary both the vertical stress and the horizontal stress simultaneously to follow prescribed loading paths. The loading path is often selected to match field loading conditions. In some cases, the intent is to measure the strains obtained in the test specimen after the loading path has been applied. In other cases, the intent is to measure the strength of the test specimen for a specified system of stress changes. Fully-automated triaxial test apparatus are normally required to conduct these types of tests.

An alternative to the miniature laboratory vane shear test (ASTM D4648) for measuring the shear strength of very soft clay is the fall cone test. Although there currently is not an ASTM standard for this test, it is very popular in Europe, and there are standards in Norway, Germany, the U.K., and other countries. A photograph for the Norwegian apparatus is shown in Figure 3-10. This test involves dropping a weight cone onto the surface on an intact or remolded soil specimen and measuring the penetration. Cones are available with different weights for different penetration depths for soils having various consistencies. This test is also used to determine the liquid limit of soils in international geotechnical engineering practice.

Figure 3-10 Fall Cone Apparatus

3-2.5 Dynamic Tests.

Geotechnical earthquake engineering is a specialty area within geotechnical engineering. The methods of analysis used to predict the performance of structures during earthquakes can often be quite complex, and the tests to measure soil properties for use in these analyses can likewise be complex. Only a few geotechnical laboratories have the equipment to conduct these tests. Table 3-5 lists the common dynamic tests for soils.

Table 3-5 Dynamic Tests for Soils

ASTM #	Description	Parameters	Comments
D3999	Determination of the Modulus and Damping Properties of Soils Using the Cyclic Triaxial Apparatus	E, D, ε_{DA}, ε_{SA}	Can be used for secant modulus and damping coefficients. Tests can be stress or strain controlled.
D4015	Modulus and Damping of Soils by Fixed-Base Resonant Column Devices	D, G, γ	Some apparatuses can allow anisotropic consolidation and large torsional strains.
D5311	Load Controlled Cyclic Triaxial Strength of Soil	multiple plots	Multiple tests should be conducted to determine the number of cycles to failure for different cyclic stress ratios.
D8296	Consolidated Undrained Cyclic Direct Simple Shear Test under Constant Volume with Load Control or Displacement Control	$G, \gamma_{DA}, \gamma_{SA}$	Multiple tests should be conducted to determine the number of cycles to failure for different cyclic stress ratios. Tests can be stress or displacement controlled.

3-2.5.1 Cyclic Triaxial Test (ASTM D5311).

The cyclic triaxial test (ASTM D5311 – Standard Test Method for Load Controlled Cyclic Strength of Soil) is the most common of the dynamic tests, and it is one of the oldest, first being run since the 1960s or before. The cyclic triaxial test is a consolidated undrained (CU) test, and the initial portion of the test is the same as the static CU test (ASTM D4767). The back-pressure saturation and consolidation phases are essentially the same. The difference is in the manner of loading. Cyclic triaxial tests are normally loaded with a sinusoidal loading function, with the maximum stress difference specified by a *cyclic stress ratio* (CSR). The CSR is one-half of the applied deviator stress divided by the isotropic consolidation stress. An example of the loading function is shown in Figure 3-11. The loading frequency is ideally 1 Hz, but slower frequencies are often used owing to the difficulty of many commercial apparatuses in maintaining a constant 1 Hz throughout the test. The ASTM standard allows frequencies as slow as 0.1 Hz. Tests are normally conducted at three or four different values of CSR to determine the number of cycles until failure. A plot of the applied CSR versus the number of cycles until failure is used to define the cyclic strength of the soil.

Failure in a cyclic triaxial test can be defined in several different ways. The conventional definition of cyclic tests conducted on clean sands was when a 100% pore pressure ratio was achieved (pore pressure = confining stress). Soils with a significant amount of fines may not achieve failure by this definition, so it has become common to define failure based on axial strain. Strain values of ±2.5%, ±5% and ±10% axial strain have been used to define failure.

3-2.5.1.1 Cyclic Direct Simple Shear Test.

The cyclic direct simple shear test (CYCDSS) is popular in geotechnical earthquake engineering, and an ASTM standard is available (D8296). The test specimen can be loaded by either a cyclic stress or a prescribed displacement. These tests are normally performed using constant volume conditions where the height of the test specimen is not allowed to change during the test. A sinusoidal loading function is applied to the test specimen as a horizontal force to the top or bottom platen for a load-controlled test. A loading frequency of 1 Hz is desired, but some tests are conducted much slower frequencies, particularly for fine-grained soils.

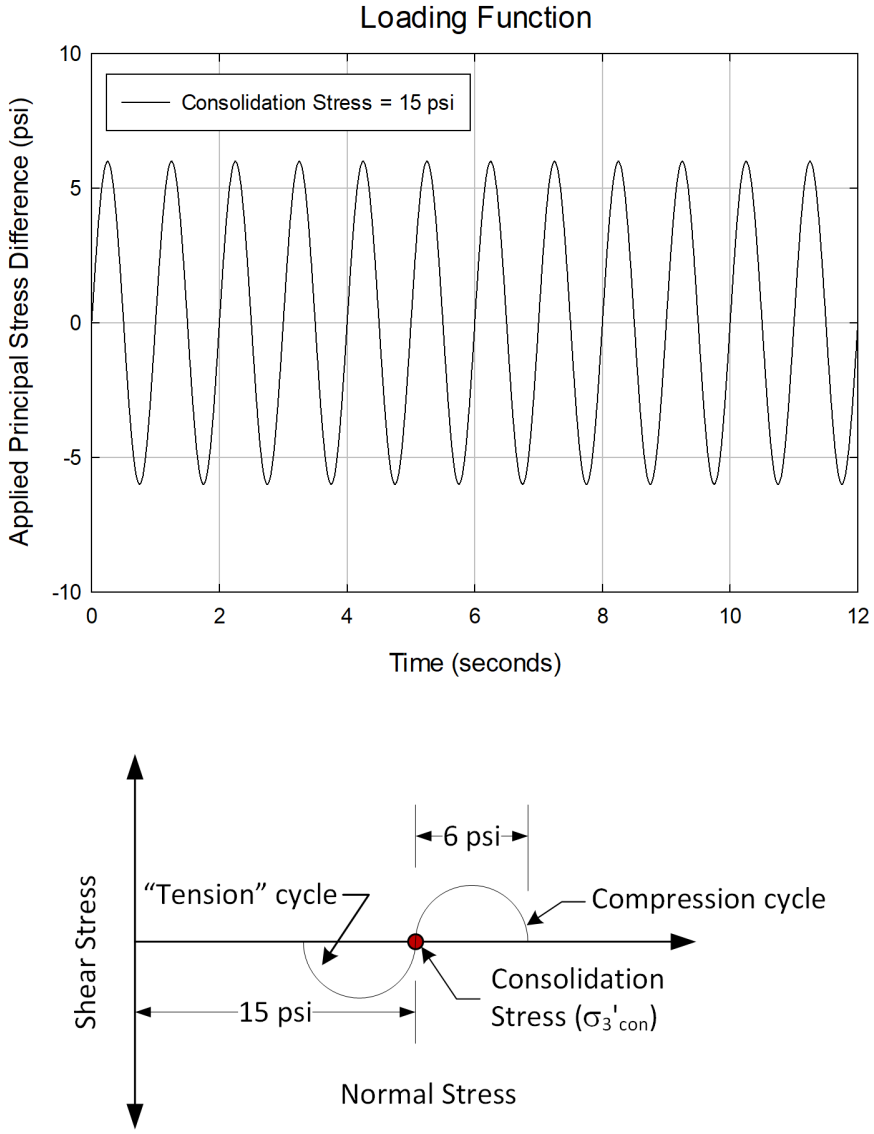

Figure 3-11 Loading Function and Stresses Applied for a Cycle of Loading in a Cyclic Triaxial Test for a Cyclic Stress Ratio of 0.2

CYCDSS tests are also specified in terms of cyclic stress ratio. The cyclic stress ratio is defined as:

$$CSR = \frac{\tau_{cyc}}{\sigma'_v} \quad \textbf{(3-3)}$$

where:
τ_{cyc} = applied peak cyclic shear stress, and
σ'_v = vertical effective consolidation stress.

Failure is defined as a pore pressure ratio of 100% or a limiting cyclic shear strain. As with the cyclic triaxial test, the cyclic strength is normally represented as a plot of the applied cyclic stress ratio versus the logarithm of the number of cycles until failure.

3-2.5.1.2 Resonant Column Test (ASTM D4015).

The resonant column test (ASTM D4015 – Standard Test Methods for Modulus and Damping of Soils by Fixed-Base Resonant Column Devices) is a dynamic test that provides values of shear modulus for low shear strain amplitudes. The test is conducted in a modified triaxial cell and can be conducted on intact and remolded test specimens. A cylindrical test specimen is loaded by applying a cyclic torque to the top of the specimen while the resulting angular displacement is measured. The cyclic load normally follows a sinusoidal function, and the frequency of the load is varied until the resonant frequency of the test specimen is determined. This is a complex test and the results are used in specialized earthquake engineering analyses.

3-2.5.1.3 Cyclic Triaxial Test for Modulus and Damping (ASTM D3999).

A different version of the cyclic triaxial test can be used for determining the secant Young's Modulus and Damping Coefficients (ASTM D3999 - Standard Test Methods for the Determination of the Modulus and Damping Properties of Soils Using the Cyclic Triaxial Apparatus). This test can be conducted on intact or reconstituted saturated and partially saturated test specimens. Both fine-grained and coarse-grained soils can be tested. The main purpose of this test is to determine the dynamic properties for strains ranging from about 0.01% to 0.5%. The test specimen may be back-pressure saturated, or it may be tested in a partially saturated condition.

3-2.6 Compressibility Tests.

There are four ASTM tests used to measure the volume change of soils, which are summarized in Table 3-6. Two of these are categorized as *consolidation tests*, where the volume change of the soil is determined for a change in applied stress. The basic information obtained from a consolidation test is shown in Figure 3-12. The remaining two tests can be categorized as *response to wetting tests*, where the volume change of the soil is measured if the soil is given access to water or if the water content is reduced.

Table 3-6 Tests for Volume Change with ASTM Standards

ASTM #	Description	Parameters	Comments
D2435	One-Dimensional Consolidation Properties of Soils Using Incremental Loading	c_v, m_v, a_v, C_c, C_r, σ'_p, C_a	Can be performed on samples that are initially partially saturated.
D4186	One- Dimensional Consolidation Properties of Saturated Cohesive Soils Using Controlled- Strain Loading	c_v, m_v, a_v, C_c, C_r, σ'_p, C_a	Provides a good compression curve for determination of σ'_p Fast, compared to D2435. Test specimens must be saturated.
D4546	One-Dimensional Swell or Collapse of Soils	ε_s, ε_c	Used to determine the "response to wetting" of compacted or intact soils.
D4829	Expansion Index of Soils	EI	Often cited in building codes.

3-2.6.1 Incremental Loading Consolidation Test (ASTM D2435).

The incremental loading or incremental stress consolidation test (ASTM D2435 – Standard Test Methods for One-Dimensional Consolidation Properties of Soil Using Incremental Loading) is over 80 years old and is a very common test in geotechnical engineering practice. Figure 3-13 shows the basic elements of the fixed-ring and floating-ring consolidometers. The test is normally conducted on saturated fine-grained test specimens, but it may also be conducted on partially-saturated soils, compacted soils, and remolded soils. The most common test specimen size in U.S. geotechnical engineering practice is a cylindrical specimen with a 2.5-inch diameter and 1-inch height, although other size apparatuses are commercially available. The test specimen is contained in a rigid ring that prevents lateral expansion of the soil during loading, thus all displacement is vertical. This type of test is also called a *one-dimensional compression test*. A porous stone is usually located above and below the test specimen to allow for *double drainage*. The fixed-ring consolidometer is the most common in geotechnical engineering practice, but the floating-ring consolidometer can be used if high friction between the ring and soil is anticipated (e.g. sandy clay).

As loads are applied to the test specimen, the displacement of the top platen is measured over time. Each load is normally applied for a specific time period (i.e., 24 hours) or until the *end of primary consolidation* (EOP) is achieved. An example *time-deformation curve* or *time curve* for one load increment is shown in Figure 3-12. The time curve is important in that the value of the coefficient of consolidation (c_v) is determined from this curve. Details on calculating the value of c_v from the time curve can be found in Chapter 5 or ASTM D2435.

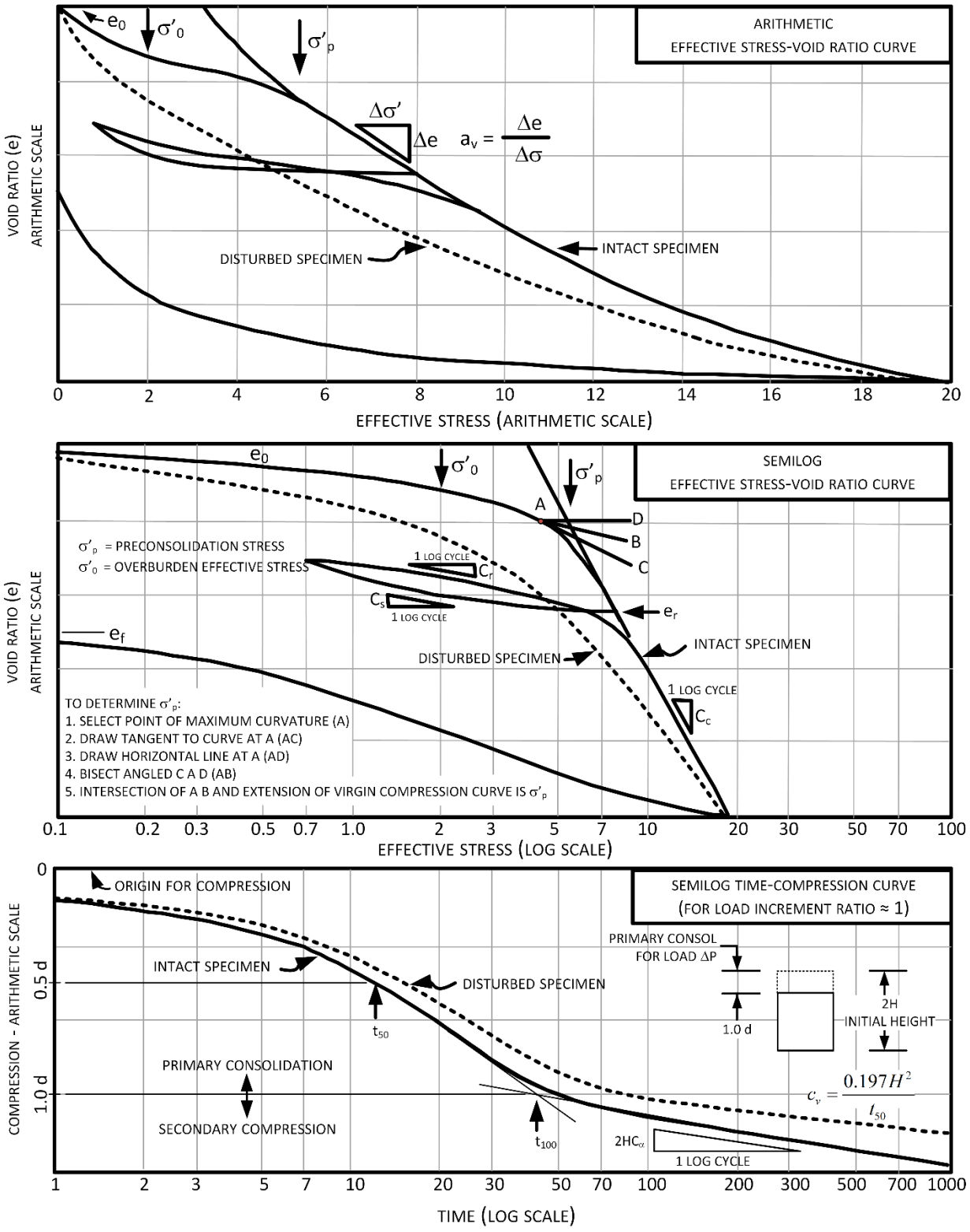

Figure 3-12 Basic Information Obtained from a Consolidation Test

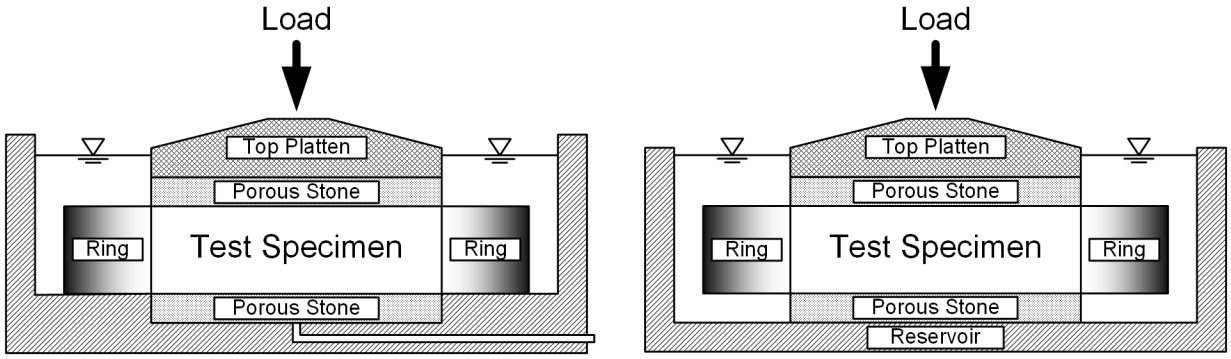

a) Fixed ring consolidometer b) Floating ring consolidometer

Figure 3-13 Fixed-Ring and Floating-Ring Consolidometers

The load applied to the test specimen is usually doubled for each load increment. The *Load Increment Ratio* (LIR) is used to quantify the change in load to the test specimen, and is defined below:

$$LIR = \frac{\Delta\sigma}{\sigma_0} \quad \textbf{(3-4)}$$

where:
$\Delta\sigma$ = change in applied stress, and
σ_0 = initial total stress.

An LIR = 1 corresponds to doubling the load on the test specimen. For unloading, an LIR = -0.75 is often used, which means the immediately previous load is skipped. For reloading, an LIR = 4 is used, which follows the same stresses as the unloading cycle until the past load has been reached.

Each load applied to the test specimen; for unloading, rebound, and reloading cycles; provides a data point for the *compression curve*. An example compression curve is shown in Figure 3-12. The conventional method used to plot the compression curve is using void ratio (y-axis) and the logarithm of the effective vertical stress (x-axis).[10] The compression curve is used to determine the *preconsolidation pressure* or *maximum past pressure* (σ'_p or P_p) and the compression index (C_c) and the recompression index (C_r). The compression curve can also be plotted using axial strain instead of void ratio. For plots using strain, the compression parameters are $C_{\varepsilon c}$ and $C_{\varepsilon r}$ (instead of C_c and C_r). The strain or void ratio used in plotting the compression curve can either be the

[10] The compression curve is often called the “e-log p” curve in older geotechnical publications.

value at the end of the time increment or the value at the end of primary consolidation. It is important that the method used is indicated for the plot.

If a 24-hour load cycle is used for the incremental stress consolidation test, the test can take two to three weeks to complete, depending on the value of the maximum stress and the number of unload-reload loops. Laboratories often try to decrease the amount of time required by reloading the test specimen at the end of primary (EOP) consolidation as opposed to constant time intervals. If the test is conducted using an automated apparatus, the time corresponding to EOP is often determined by a computer program. The use of computer-calculated EOP times may incur errors, especially for low stresses where strains are small. If the test specimen is reloaded too quickly at early stages of the test, the remaining data may not be useable and the quality of the test may be compromised.

3-2.6.2 Constant Rate of Strain Consolidation Test (ASTM D4186).

The constant rate of strain (CRS) consolidation test (ASTM D4186 – Standard Test Method for One-Dimensional Consolidation Properties of Saturated Cohesive Soils Using Controlled-Strain Loading) can be used as an alternative to the incremental stress consolidation test. The test specimens for the CRS test are the same size as for the incremental stress tests. One of the main advantages of the CRS test is that the compression curve can be obtained in much less time than the incremental stress test. A schematic of the basic test elements and the data acquired is given in Figure 3-14.

The CRS consolidation test can be conducted on intact soil specimens, and also on compacted and remolded soil specimens. However, it is necessary that the test specimen be saturated prior to compression. As shown in Figure 3-14, the consolidometer for the CRS test is very similar to a triaxial cell. The test specimen is back-pressure saturated in the same manner as a triaxial specimen. The cell pressure applied in the cell serves as back pressure in the process. The test specimen is drained only at the top, and during the loading process, the excess pore water pressures are measured at the bottom. Based on an assumed parabolic distribution of pore water pressure in the test specimen, the average effective stress can be calculated.

The test specimen is loaded at a constant strain rate ($\dot{\varepsilon}$). The strain rate is selected such that the excess pore water pressure measured at the base of the test specimen does not exceed 15% of the applied stress. The rate for unloading the test specimen is much slower than loading, and unload-reload loops may slow down the test considerably.

One advantage of the CRS consolidation test is that the compression curve is defined by many more data points than the incremental stress consolidation test. There are so many data points taken that the results are usually portrayed as a curve instead of discrete data points. This allows an increased resolution of the compression curve in

the vicinity of the preconsolidation pressure, and allows a more accurate determination of its value. The CRS consolidation test also allows the determination of the coefficient of consolidation (c_v) over the entire load range as long as the excess pore pressures are in an acceptable range. This method of determining c_v removes some of the subjectivity involved in determining c_v using time curves with the incremental stress consolidation test.

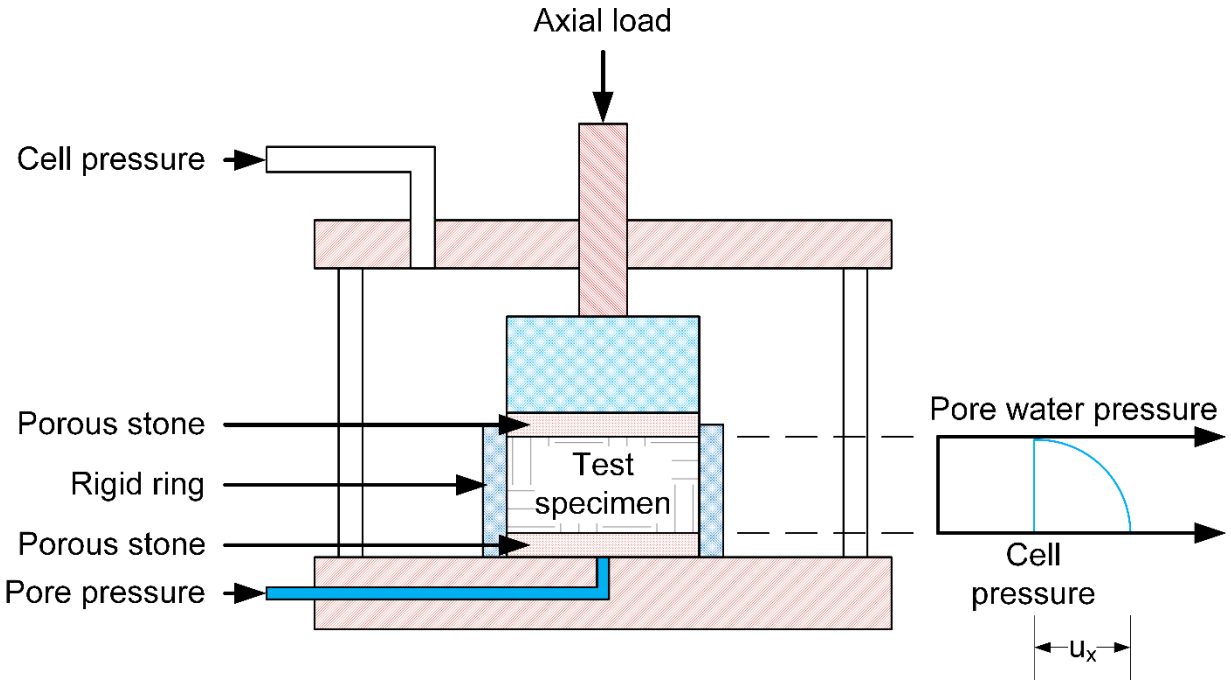

Figure 3-14 Basic Elements of a Constant Rate of Strain Consolidation Test

3-2.6.3 Swell and Collapse Test (ASTM D4546).

When a partially saturated natural soil or a compacted soil is given access to water, the soil can swell at low stresses or collapse at high stresses. ASTM D4546 (Standard Test Methods for One-Dimensional Swell or Collapse of Soils) allows the volume change of the test specimen to be measured as a function of the applied stress. If the soil has no confining stress applied, then *free swell* may occur. Often, free swell is measured under a nominal stress of 20 psf. If the pressure is varied to prevent any swell or volume change from occurring, this pressure is called the *swell pressure* for the soil. ASTM D4546 allows the amount of free swell, swell pressure, and volume change for other stresses to be determined.

The test is very similar to an incremental stress consolidation test, and the same consolidometer is used. Loads can be applied to the test specimen, and after the test specimen has achieved equilibrium under the load, the specimen is inundated. The swell or collapse volume change is measured after the test specimen achieves a new equilibrium. Shown in Figure 3-15 is an example curve that gives the volume change of the soil as a function of the stress at inundation.

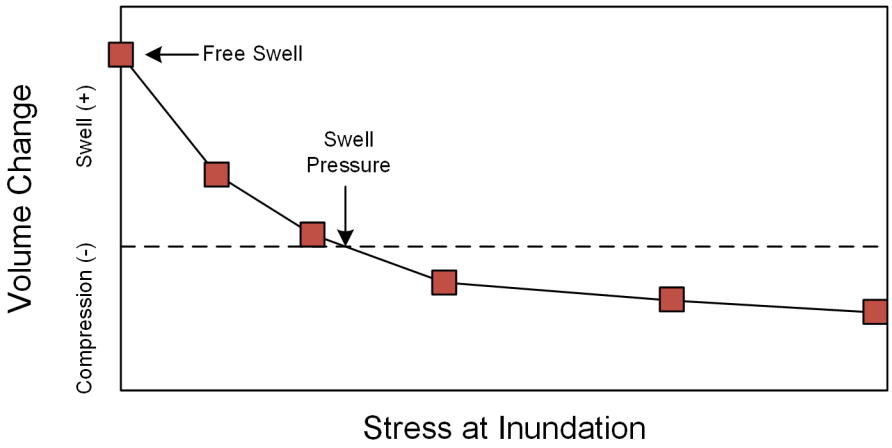

Figure 3-15 Volume Change of Soil as a Function of Stress at Inundation

3-2.6.4 Expansion Index Test (ASTM D4829).

The expansion index test (ASTM D4829 – Standard Test Method for Expansion Index of Soils) determines the swell potential of a soil, but it is less rigorous than D4546. It does not provide engineering design values to calculate volume change, but provides a simple index to assess the swelling potential of soil. This test is conducted on compacted soils. The main use of the expansion index test is to assess if a compacted fill might pose problems if structures are constructed on top of it. The compaction mold is approximately half the height of the 4-inch diameter (1/30 ft^3) compaction mold used for ASTM D698 and the same compaction hammer as used for D698 is used. The goal is to compact the test specimen using a D698 effort at a degree of saturation of 50%. A vertical stress of 1 psi is applied, and the specimen is allowed to equilibrate for 10 minutes. The specimen is then inundated and allowed to swell for 24 hours or until the swell has essentially ceased. The *Expansion Index* (EI) is equal to the percent swell multiplied by 10. The expansion potential is assessed using the criteria shown in Table 3-7.

Table 3-7 Potential Expansion for EI Values

Expansion Index, EI	Potential Expansion
0 – 20	Very Low
21 – 50	Low
51 – 90	Medium
91 – 130	High
>130	Very High

3-2.7 Hydraulic Conductivity (Permeability) Tests.

Test to measure the permeability or hydraulic conductivity of soils have been used since the 1930s. In general, permeability tests have been more widely used for fine-grained soils as opposed to coarse-grained soils. There are many correlations available for the

permeability of coarse-grained soils, but few reliable correlations exist for fine-grained soils. Currently, there are two ASTM standardized tests for hydraulic conductivity. However, hydraulic conductivity can be calculated from incremental stress and constant rate of strain consolidation tests.

3-2.7.1 Compaction Mold Test (ASTM D5856).

The compaction mold test (ASTM D5856 – Standard Test Method for Measurement of Hydraulic Conductivity of Porous Material using a Rigid-Wall Compaction-Mold Permeameter) is intended to be used on compacted soils having a hydraulic conductivity less than 10^{-3} cm/sec.

This test has a major deficiency in that the test specimen cannot be saturated, therefore the measured hydraulic conductivity may be too low. There also is a problem that leakage can occur between the compacted test specimen and the wall of the compaction mold. This test is best suited as a quality control test for compacted clay liners for landfills and reservoirs.

3-2.7.2 Flexible Wall Test (ASTM D5084).

The flexible wall test (ASTM D5084 – Standard Test Methods for Measurement of Hydraulic Conductivity of Saturated Porous Materials Using a Flexible Wall Permeameter) is the most common permeability test. The apparatus used is also called a *triaxial permeameter* because it is essentially a triaxial cell without the loading rod. The sample is enclosed in a flexible membrane, therefore the problem of side-wall leakage experienced in D5856 is not a problem. The membrane conforms to irregularities in the sides of the test specimen. ASTM D5084 also allows for test specimens to be back-pressure saturated in the same manner as CU and CD triaxial test specimens. The flexible wall permeability test also allows control of the effective consolidation stress. This is not possible with the compaction mold test.

This method is recommended only for soils having a hydraulic conductivity less than 10^{-4} cm/sec, so it is best suited to fine-grained soils or soils with a significant percentage of fines. Intact, remolded, and compacted test specimens can be used for this test. The test takes considerable skill to properly conduct, and there are six different methods to promote flow though the test specimen. The test measures vertical hydraulic conductivity, but intact samples can be trimmed at different orientations to measure anisotropy of hydraulic conductivity.

3-2.7.3 Hydraulic Conductivity from Consolidation Tests.

One of the purposes of conducting a consolidation test is to determine the coefficient of consolidation (c_v). For incremental stress consolidation tests, c_v is calculated from the time curves using one of several different methods. For the CRS consolidation test, c_v

can be calculated at every point where the excess pore water pressure, average stress, and strain are known.

The hydraulic conductivity of a soil is related to the value of c_v by the equation below:

$$k = c_v \cdot m_v \cdot \gamma_w \quad \textbf{(3-5)}$$

where:
k = hydraulic conductivity or permeability,
c_v = coefficient of consolidation,
m_v = coefficient of volumetric compressibility, and
γ_w = unit weight of water.

The coefficient of volumetric compressibility can be determined by plotting the strain (y-axis) versus the arithmetic effective stress (x-axis) and determining the slope of the plot corresponding to the stress where c_v is calculated. Consolidation tests are rarely conducted just to determine the value of permeability, but if these data are available for a project where additional values of permeability are useful, little effort is required to calculate the permeability.

It is also possible to determine the permeability from the consolidation phase of CU and CD triaxial tests. This normally requires that the test specimen only be drained at the ends (no filter paper drainage strips) and it may be necessary to consolidate the specimen in stages leading up to the final consolidation stress.

3-3 LABORATORY TESTS ON ROCK.

ASTM also addresses laboratory tests on rock specimens, but there are much fewer tests for rocks than for soils. Most of the common tests on rock focus on the strength in compression and tension. Table 3-8 lists the common rock tests that have ASTM standards available.

Table 3-8 Laboratory Rock Strength Tests with ASTM Standards

ASTM #	Description	Parameters	Comments
D3967	Splitting Tensile Strength of Intact Rock Core Specimens	σ_t	
D5607	Laboratory Direct Shear Strength Tests of Rock Specimens Under Constant Normal Force	c-ϕ, c'-ϕ'	Mainly interpreted as total stress strength parameters.
D5731	Determination of the Point Load Strength Index of Rock and Application to Rock Strength Classifications	I_s, $I_{s(50)}$	Strength index often corrected for specimen diameter of 50 mm.
D7012	Compressive Strength and Elastic Moduli of Intact Rock Core Specimens under Varying States of Stress and Temperatures	σ_u	

3-3.1 Unconfined Compression Test (ASTM D7012).

ASTM D7012 (Standard Test Methods for Compressive Strength and Elastic Moduli of Intact Rock Core Specimens under Varying States of Stress and Temperatures) encompasses more than just unconfined compression tests. There are four different methods of testing outlined in the standard, and two address the unconfined compressive strength. The other two address triaxial compression of rock, which is used less frequently than for soil.

The basic form of the unconfined compression test (Method C) does not measure axial strain during loading, and provides only the unconfined compressive strength. The resulting strength can be used for design or as an index property for the rock. The test is normally conducted on rock cores that are 1.85 inches in diameter, and they are trimmed to be at least 3.7 inches in height. This specimen diameter corresponds to an NQ core barrel, but larger rock cores can be used as well. The specimen can be loaded at a constant rate of load or a constant rate of strain which are chosen to cause failure in 2 minutes to 15 minutes. Unconfined compression tests of rock are normally conducted on many test specimens since there can be wide variations in the compressive strength due to the effects of planes of weakness (joints, fractures, and faults) and other inhomogeneities is rock. The main result of the unconfined compression test in the uniaxial compressive strength (σ_u).

3-3.2 Split Cylinder Test (ASTM D3967).

The *split cylinder test* (ASTM D3967 – Standard Test Method for Splitting Tensile Strength of Intact Rock Core Specimens) is used as an alternative to the direct tensile test. The test specimen is loaded diametrically via hardened steel end platens. The test specimen thickness can range between 0.2 to 0.75 times the specimen diameter. The test specimen is loaded at a rate sufficient to obtain failure in 1 to 10 minutes. The main result of this test is the *splitting tensile strength* (σ_t). Although the tensile strength resulting from the split cylinder test should be essentially equal to that measured from direct tension tests, it is customary to preface the former with “splitting.” Owing to the variability in the test results, split cylinder tests are often run on numerous test specimens.

3-3.3 Rock Direct Shear Test (ASTM D5607).

Rock direct shear tests (ASTM D5607 - Standard Test Method for Performing Laboratory Direct Shear Strength Tests of Rock Specimens Under Constant Normal Force) can be conducted on intact rock specimens, as well as on joints and discontinuities. Unlike the direct shear test conducted on soils, the rock direct shear test is normally considered to be an undrained test. The basic elements of this test are the same as for the soil direct shear tests. Rock direct shear tests are often conducted for a range of normal stresses to determine the strength envelope for the material. One

major difference is that the test specimen is often encapsulated in a super strength gypsum cement to fix its position in the shear box. An example of the test fixture is shown in Figure 3-16.

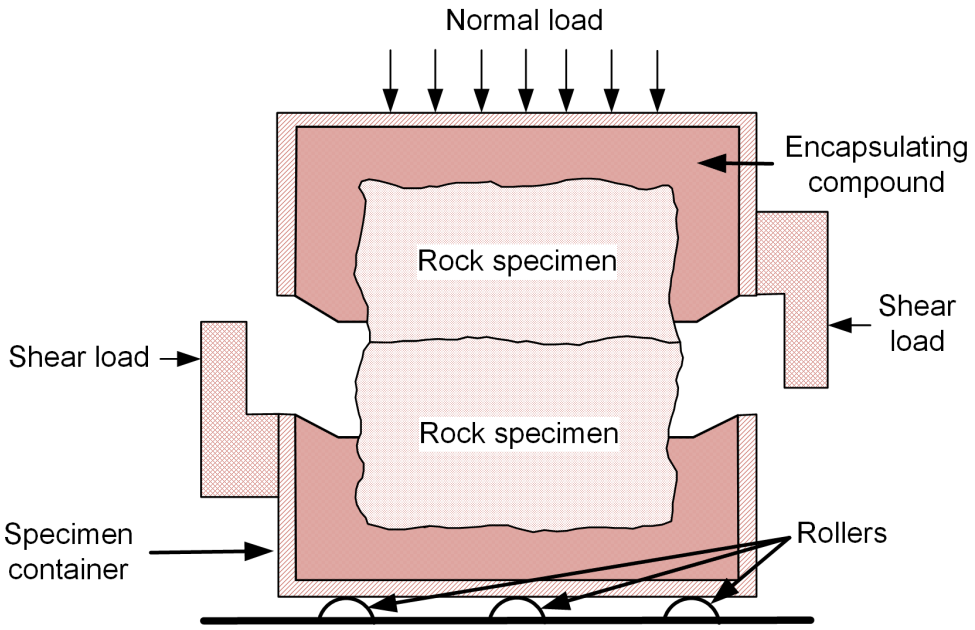

Figure 3-16 Specimen Container for Rock Direct Shear Test (after ASTM D5607)

Figure 3-17 Rock Direct Shear Apparatus for High Normal and Shear Loads

Rock direct shear tests are more complicated than the soil counterpart because of the great variety of loads and displacements the apparatus is required to measure. For large normal stresses, it can take 50,000 lbs. to fail an intact rock direct shear test specimen, and failure may occur at very small (<0.01 inch) displacements. For rock joints at low normal stresses, the failure load might be less than 100 lbs., and the displacement at failure may be greater than 0.1 inch. Shown in Figure 3-17 is a rock direct shear apparatus for high loads and normal stresses.

3-3.4 Point Load Test (ASTM D5731).

The point load test (ASTM D5731 – Standard Test Methods for Determination of the Point Load Strength Index of Rock and Application of Rock Strength Classifications) provides an index value of the rock strength. This test can be performed on rock cores or irregular pieces of rock having diameters in the range of 1 inch to 3 inches. A photograph of the point load apparatus is shown in Figure 3-18. The diameter of the test specimen is considered to be the thickness of the test specimen from loading platen contact points. The load platens are truncated cones, with the point being a semicircular arc of 0.2-inch radius.

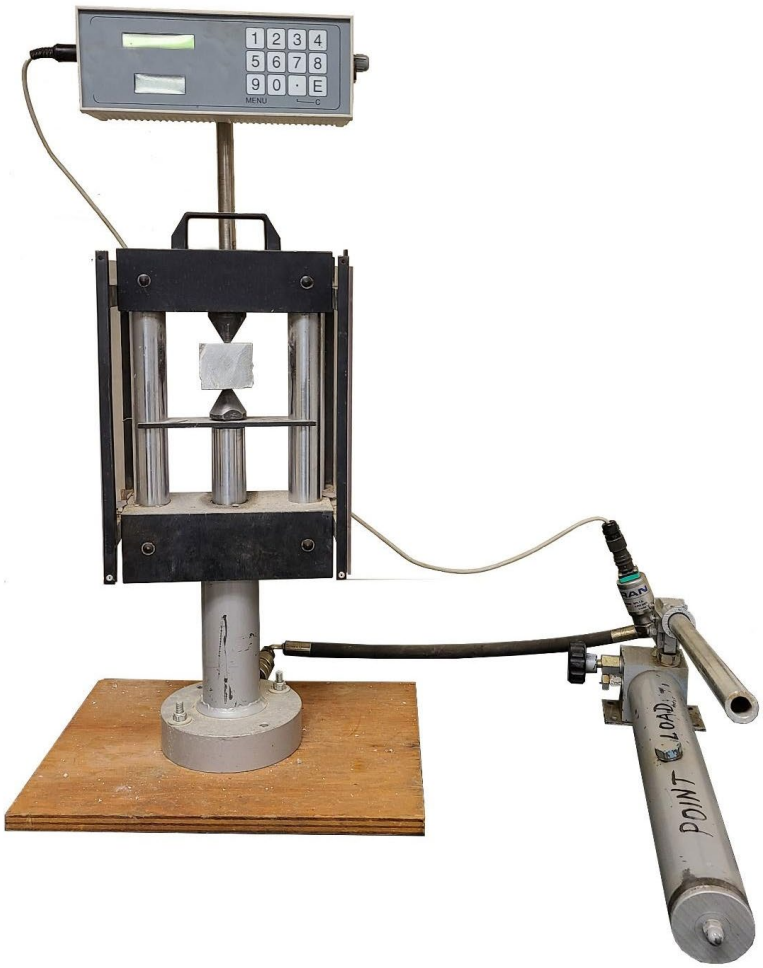

Figure 3-18 Point Load Apparatus for Rock Index Testing

The point load test provides an *uncorrected point load strength index* (I_s). This value can be corrected to reflect differences in test specimen sizes, and is often normalized to an equivalent core diameter of 2 inches (50 mm). This corrected value is called the *size corrected point load strength index* ($I_{s(50)}$). The results of the point load test are used for rock classification and can be correlated to the uniaxial compressive strength, but the values are not considered to have sufficient reliability for design.

3-4 OTHER SOIL AND ROCK TESTS.

This section of the manual has addressed the tests that are the most common in geotechnical engineering practice in the U.S., but there are hundreds of other ASTM standardized tests. There are groups of tests that address partially saturated soils, soil-cement mixtures, peats and organic soils, geosynthetics, and many other materials used in engineering projects.

3-5 SUGGESTED READING.

Topic	Reference
General Laboratory Testing	Head, K. H. 2008. *Manual of Soil Laboratory Testing*, Vol. 1., 3rd Ed., Whittles, 416 pp.
	Head, K. H. and R. J. Epps 2011. *Manual of Soil Laboratory Testing Vol. II, Permeability Shear Strength, and Compressibility Tests*, 3rd Ed., Whittles, 512 pp.
	Head, K. H. and R. J. Epps 2014, *Manual of Soil Laboratory Testing Vol. III, Effective Stress Tests*, 3rd Ed., Whittles, 448 pp.
	Lambe, T. W. and R. V. Whitman 1969. *Soil Mechanics*, John Wiley and Sons, Inc. 553 pp.
Shear Strength	*Laboratory Shear Testing of Soils*, ASTM STP 361, American Society for Testing and Materials, 505 pp., 1964.
	Laboratory Shear Strength of Soils, ASTM STP 740, R. N. Young and F. C. Townsend, Eds., 717 pp, 1981.
	Research Conference on Shear Testing of Cohesive Soils, ASCE, University of Colorado, Boulder, CO, 1164 pp, 1960.
	Saada, A. S. and Townsend, F. C. 1981. "State of the Art: Laboratory Strength Testing of Soils," *Laboratory Shear Strength of Soils*, ASTM STP 740, R. N. Yong and F. C. Townsend, Eds., ASTM, pp. 7-77.
Triaxial Testing	*Advanced Triaxial Testing of Soil and Rock*, ASTM SPT 977, Robert T. Donague, Ronald C. Chaney, and Marshal L. Silver, Eds., American Society for Testing and Materials, Philadelphia, 896 pp, 1988.
	Bishop, A. W. and D. J. Henkel (1957), *Measurement of Soil Properties in the Triaxial Test*, Edward Arnold, Ltd., London, 190 pp.
	Lade, P. 2016. *Triaxial Testing of Soils*, John Wiley & Sons, Ltd., 500 pp.

3-6 NOTATION.

Symbol	Description
c	Total stress cohesion
C_c	Compression index
C_r	Recompression index
c_v	Coefficient of consolidation
c'	Effective stress cohesion
D	Diameter
D_r	Relative density
e	Void ratio
e_{max}	Maximum index void ratio

Symbol	Description
e_{min}	Minimum index void ratio
G_s	Specific gravity
H	Height
I_s	Uncorrected point load strength index
$I_{s(50)}$	Size corrected point load strength index
k	Hydraulic conductivity or permeability
K_0	At-rest earth pressure coefficient
L	Length
m_v	Coefficient of volumetric compressibility
n	Porosity
P_p	Maximum past pressure
RC	Relative compaction
S	Degree of saturation
S_t	Sensitivity
s_u	Undrained shear strength for a ϕ = 0 envelope for saturated soils
t	Thickness
V	Total volume
V_a	Volume of air
V_s	Volume of solids
V_v	Volume of voids
V_w	Volume of water
w	Water content
w_{opt}	Optimum water content
W_s	Weight of solids
W_t	Total weight of sample
W_w	Weight of water
γ_b	Buoyant unit weight or submerged unit weight

Symbol	Description
γ_d	Dry unit weight
$\gamma_{d\text{-}max}$	Maximum dry density from the compaction curve for a particular effort or maximum index dry density (corresponding to e_{min})
$\gamma_{d\text{-}min}$	Minimum index dry density (corresponding to e_{max})
γ_t	Total or wet unit weight
γ_{sat}	Saturated unit weight
γ_w	Unit weight of water
$\Delta\sigma$	Change in applied stress
$\dot{\varepsilon}$	Strain rate
σ_0	Initial total stress
σ_3	Confining pressure
σ'_p	Preconsolidation pressure
σ'_v	Vertical effective consolidation stress
τ_{cyc}	Applied peak cyclic shear stress
ϕ	Total stress friction angle
ϕ'	Effective stress friction angle

CHAPTER 4 DISTRIBUTION OF STRESSES

4-1 INTRODUCTION.

4-1.1 Scope.

This chapter describes the analysis of stress conditions within the ground, including stress at a point, changes in stress caused by the application of soil and structural loads, and empirical methods for estimating loads on buried pipes, conduits, shafts, and tunnels. The calculation of stresses and changes in stress using numerical methods, such as the finite element method, is also discussed.

4-1.2 State of Stress.

The state of stress within the ground can be analyzed assuming that either elastic or plastic conditions prevail. Elastic solutions are most appropriate for cases in which the shear stresses throughout the soil mass are significantly below the shear strength of the soil and shear failure is not likely. If the shear stress in the soil is less than about one-third of the ultimate shear strength, the stresses within the soil mass will be roughly equal to values calculated from elastic theory (Davis and Selvadurai 1996). The stress conditions calculated using the most of the methods in this chapter assume that elastic conditions prevail.

Plastic solutions assume full mobilization of the soil's shear strength within a soil mass or along a specified failure surface. Plastic equilibrium is used for problems, such as slope stability (Chapter 7), foundation bearing capacity, and lateral earth pressures, where shear strength may be fully mobilized.

4-2 STRESS CONDITIONS AT A POINT.

4-2.1 Stress Conditions in Soil.

Soil consists of a compilation of discrete particles, water, and air in varying proportions. Similarly, rock may contain a combination of the mineral components and any void space that may be filled with water or air. These discrete systems are idealized in stress analysis by assuming the soil acts as continuous solid mass without holes or gaps. In this continuum manner, stress is simply conceived as force per unit area and the contact forces at the soil particle level are not considered.

Stress in soil is the result of forces from the self-weight of the overlying and surrounding soil plus any external loading, such as structures or ponded water. For a given plane, it can be particularly useful to consider stress in terms of its normal and shear components. The normal stress can be defined as the sum of the forces acting perpendicular to a plane divided by the area of that plane. Similarly shear stress in a particular direction is ratio of the force acting tangent to a plane divided by its area.

The total normal stress on any plane within the ground is based on the sum of all forces acting on the plane in question. The total stress may be divided into two parts: the effective normal stress and the pore pressure.

4-2.1.1 Total Vertical Stress.

The total vertical stress (or overburden stress) is the normal stress acting on a horizontal plane at some depth within the soil. The total vertical stress, σ_v, at a particular depth is calculated by multiplying the thickness (z_i) of all overlying materials by the total unit weight ($\gamma_{t,i}$) of each material:

$$\sigma_v = \sum_{i=1}^{n} z_i \gamma_{t,i} \quad \textbf{(4-1)}$$

It is imperative to include the weight of water resting on the ground surface (i.e., ponded water) in calculations of total vertical stress. Ponded water can be considered by adding a layer to the total stress calculations with thickness equal to the water depth and unit weight equal to the unit weight of water.

The calculation of total vertical stress is illustrated in Figure 4-1.

4-2.1.2 Pore Water Pressure.

The energy present in ponded water or groundwater is often expressed in terms of the total hydraulic head, which has pressure, elevation, and velocity components. The velocity component is typically ignored in most geotechnical applications. The pore water pressure (u) can be found from the pressure head (h_p) as

$$u = h_p \gamma_w \quad \textbf{(4-2)}$$

where:
γ_w = the unit weight of water (62.4 pcf or 9.81 kN/m^3).

When water is static (not flowing), the total head is constant throughout the system, and elevation head converts directly to pressure head. This is referred to as a *hydrostatic* condition, and the pressure head is simply equal to the distance below the groundwater table or phreatic surface.

Flowing water loses energy as it flows through the soil and the total head decreases in the direction of flow. For flowing water conditions, a flow net or some other type of seepage analysis must be performed. Pore water pressure at any point can be determined by first calculating the total head and the elevation head at any point in the ground. The pressure head for flowing water is found by subtracting the elevation head from the total head. Water pressures act in all directions equally because the water

does not sustain shear stress. For this reason, orientation of the pore water pressure is not important. In some older publications, pore water pressure is also called *neutral stress.*

Vertical Stress and Pore Pressure Examples

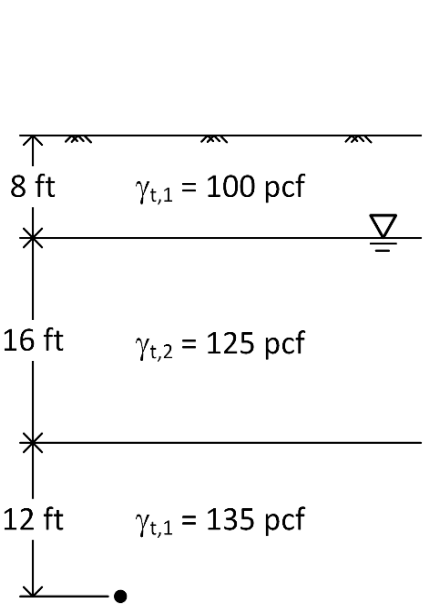

Scenario 1

Layer 1: z_1 = 8 ft, $\gamma_{t,1}$ = 100 pcf
Layer 2: z_2 = 16 ft, $\gamma_{t,2}$ = 125 pcf
Layer 3: z_3 = 12 ft, $\gamma_{t,3}$ = 135 pcf

Total vertical stress

$\sigma_v = z_1\gamma_{t,1} + z_2\gamma_{t,2} + z_3\gamma_{t,3}$
= (8 ft)(100 pcf)+(16 ft)(125 pcf)
+ (12 ft)(135 pcf)
= 4420 psf

Pore pressure

h_p = 16 ft +12 ft = 28 ft
u = (28 ft)(62.4 pcf) = 1747 psf

Effective vertical stress

$\sigma'_v = \sigma_v - u$ = 4420 psf – 1747 psf
= 2673 psf

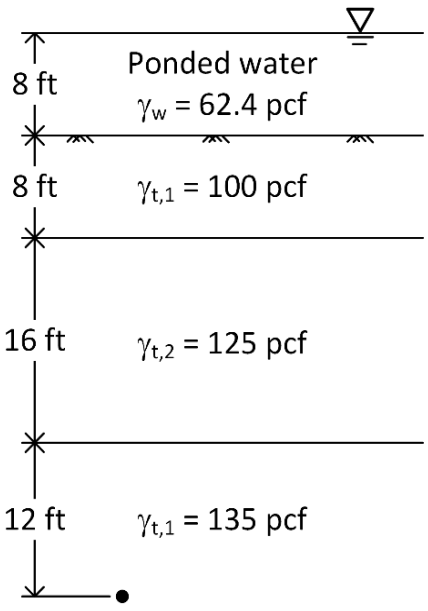

Scenario 2

Water: z_w = 8 ft, γ_w = 62.4 pcf
Layer 1: z_1 = 8 ft, $\gamma_{t,1}$ = 100 pcf
Layer 2: z_2 = 16 ft, $\gamma_{t,2}$ = 125 pcf
Layer 3: z_3 = 12 ft, $\gamma_{t,3}$ = 135 pcf

Total vertical stress

$\sigma_v = z_w g_w + z_1\gamma_{t,1} + z_2\gamma_{t,2} + z_3\gamma_{t,3}$
= (8 ft)(62.4 pcf)+ 4420 psf
= 4919 psf

Pore pressure

h_p = (8 + 8 + 16 +12 ft) = 44 ft
u = (44 ft)(62.4 pcf) = 2746 psf

Effective vertical stress

$\sigma'_v = \sigma_v - u$ = 4919 psf – 2746 psf
= 2173 psf

Figure 4-1 Calculation of Vertical Stresses for Hydrostatic Conditions

4-2.1.3 Effective Vertical Stress.

The effective vertical stress (σ'_v) is found by subtracting the pore water pressure at any point from the total vertical stress at the same point

$$\sigma'_v = \sigma_v - u \quad \textbf{(4-3).}$$

4-2.1.4 Horizontal Stress.

Horizontal stress in a soil mass is influenced by the effective vertical stress, the geologic stress history, and lateral confinement conditions. Horizontal stress cannot be calculated directly from the soil profile and is typically calculated as a proportion of the effective vertical stress:

$$\sigma'_h = K \cdot \sigma'_v \quad \textbf{(4-4).}$$

The lateral earth pressure coefficient (K) depends on stress history and lateral confinement conditions. Common types, applications, and sources of lateral earth pressure coefficients are summarized in Table 4-1.

The total horizontal stress can be found by adding the pore water pressure at any point onto the effective horizontal stress

$$\sigma_h = \sigma'_h + u \quad \textbf{(4-5).}$$

Table 4-1 Lateral Earth Pressure Coefficients

Lateral earth pressure coefficient	Example applications	Method to obtain
At-rest, K_0	Level, natural ground Unyielding retaining wall	Estimate based on ϕ' and OCR Measure with field tests
Active, K_A	Near crest of slopes Behind yielding retaining walls	Calculate with analytical methods (see DM 7.2) Estimate based on experience
Passive, K_P	Near toe of slopes In front of retaining wall toe	

4-2.1.5 Applied Loads.

Many civil engineering applications must consider the effects of external (non-soil) loads applied at the surface or at some depth within the soil mass. The influence of existing loads must be included in total stress calculations. New loads cause changes in total

stress within the soil. These load changes will cause changes in the pore water pressures as discussed in more detail in Chapter 5. The duration of the changes in pore water pressure will depend on the permeability and compressibility of the soil.

Analytical methods for calculating changes in stress are provided in Section 4-3, including methods for point loads, line loads, and uniformly loaded areas. In Section 4-6, numerical methods for calculating changes in stress are summarized.

Changes in total stress caused by applied loads should be within the soil mass to at least the critical depth. The critical depth is the depth over which soil compression caused by the changes in stress contributes to significant surface settlement. The critical depth in fine-grained soils corresponds to the depth at which the change in stress is less than 10% of the existing vertical effective stress. In coarse-grained soils, the critical depth occurs when the change in stress is less than 20% of the existing vertical effective stress.

Interactions between the applied load and the soil foundation must be considered, especially for changes in stress very close to the load. The flexibility of the structure that applies a distributed load to the soil affects the distribution of the change in stress. A completely flexible load, such as a soil fill, will apply a uniform stress to the soil because the load can deform in proportion to the soil. The elastic solutions presented in Section 4-3 assume that the load is completely flexible.

A foundation that is completely rigid with respect to the soil must undergo a uniform deformation. When a rigid foundation deforms uniformly into an elastic solid (i.e., undrained conditions for clay), the load must shift to the edges of the foundation, resulting in a pressure distribution that increases toward the edge (see Figure 4-2). In contrast, a rigid foundation on sand will cause yielding near the edges, resulting a pressure distribution that decreases toward the edge.

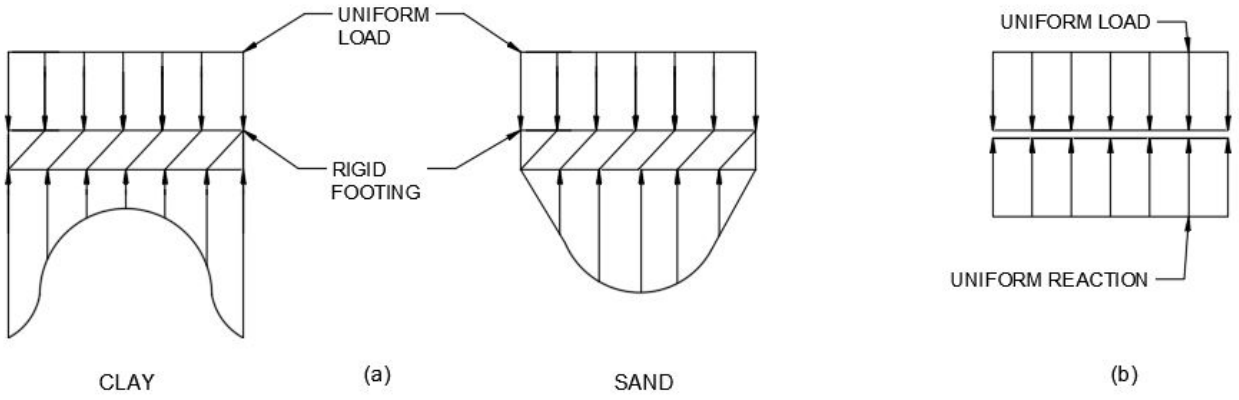

Figure 4-2 Variation in Contact Pressure – a) Rigid Foundation and b) Completely Flexible Foundation

4-2.2 Mohr Circle of Stress.

The normal and shear stress on a plane at any point within the ground depends on the orientation of that plane with respect to the orientation of the stress system. At any point, the will be three mutually perpendicular planes that have no shear stress, which are referred to as the principal planes. The normal stresses that act on these planes are defined as the principal stresses. The major principal stress (σ_1) has the largest magnitude. The minor principal stress (σ_3) has the smallest magnitude. The intermediate principal stress (σ_2) falls between σ_1 and σ_3. For two-dimensional problems, σ_2 is either assumed equal to σ_3 or ignored. For level ground conditions, the principal stresses are often assumed to be aligned with the horizontal and vertical directions with the horizontal normal stress being equal in all directions. The sign convention used herein assigns positive values to compressive stress, shear stress that causes counterclockwise rotation, and counterclockwise angles.

A Mohr circle of stress can easily be plotted from σ_1 and σ_3, or the normal and shear stresses on any two perpendicular planes. More information on the use of the Mohr circle can be found in Parry (2004). From the Mohr circle for a point, the normal and shear stress conditions on any plane can be determined by rotating an angle 2α about the center of the circle, where α is the angle between the major principal plane and the plane of interest. Figure 4-3 illustrates the Mohr circle and mathematical relationships between common stresses.

4-3 ELASTIC SOLUTIONS FOR STRESSES DUE TO APPLIED LOADS.

4-3.1 Use and Applicability.

The elastic solutions presented in this section are useful for simple analyses of changes in stress, especially consolidation settlement. These methods are also useful for understanding the principles of stress distribution and for checking more complicated numerical analyses.

4-3.2 Semi-Infinite Elastic Conditions.

4-3.2.1 Assumptions.

The Boussinesq and related solutions assume the soil is a homogeneous, elastic material in which continuity is maintained and static equilibrium is satisfied. The applied load is completely flexible and is applied at the surface of the material. For embankment loading, the load is strictly vertical and no shear stress is applied to the foundation by the embankment. As discussed in Section 4-2.1.5, the stress distribution below a rigid foundation is not uniform and may not conform to the assumptions of the Boussinesq solutions.

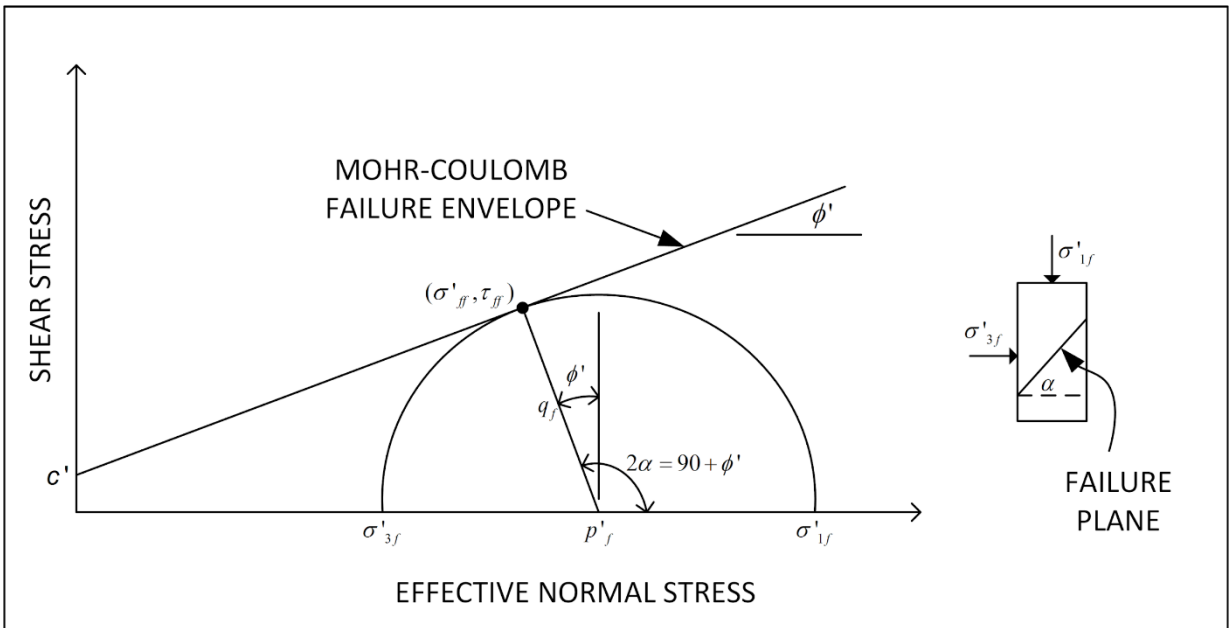

MOHR CIRCLE PROPERTIES

CENTER: $p'_f = \frac{\sigma'_{1f} + \sigma'_{3f}}{2}$ RADIUS: $q_f = \frac{\sigma'_{1f} - \sigma'_{3f}}{2}$ FRICTION ANGLE: $\phi' = \sin^{-1}\left(\frac{q_f - c'/\cos\phi'}{p'_f}\right)$

FAILURE ENVELOPE RELATIONSHIPS

$\sigma'_{ff} = p'_f - q_f \sin\phi'$	$\frac{\sigma'_{3f}}{\sigma'_{1f}} = \left(\frac{\sigma'_{ff} - c'\cos\phi'}{\sigma'_{ff} + c'\cos\phi'}\right)\left(\frac{1-\sin\phi'}{1+\sin\phi'}\right) = \tan^2\left(45 - \frac{\phi'}{2}\right) - 2c'\tan\left(45 - \frac{\phi'}{2}\right)$
$\tau_{ff} = c' + \sigma'_{ff}\tan\phi' = q_f\cos\phi'$	$\frac{\sigma'_{1f}}{\sigma'_{3f}} = \left(\frac{\sigma'_{ff} + c'\cos\phi'}{\sigma'_{ff} - c'\cos\phi'}\right)\left(\frac{1+\sin\phi'}{1-\sin\phi'}\right) = \tan^2\left(45 + \frac{\phi'}{2}\right) + 2c'\tan\left(45 + \frac{\phi'}{2}\right)$

Figure 4-3 Mohr Circle Relationships

Loads with a length to width ratio (L/B) of at least five are commonly assumed to result in *plane strain* conditions, at least near the middle of the length. Under plane strain, deformation only occurs perpendicular to the long axis of the load and the changes in stress do not depend on the elastic properties of the material.

The Boussinesq solutions are not typically applicable to the calculation of shear stress for conditions where shear stress is becoming critical. In this case, the soil is approaching a state of plastic equilibrium and the assumption of elasticity no longer applies. In such cases, stability analysis methods, such as those in Chapter 7 and in DM 7.2, should be used.

4-3.2.2 Stress Distribution Formulas.

Formulas for homogeneous, semi-infinite, isotropic foundations are summarized in Table 4-2. These formulas can be used for hand calculations for simple computations and to check the results of more complex numerical analyses. Such formulas can also

easily be programmed into a spreadsheet solution. Additional formulas for other geometric and loading conditions are summarized in Poulos and Davis (1974).

Horizontal and shear stresses caused by applied loads can also be determined from elastic solutions. In many cases, these calculations require a value of Poisson's ratio (ν) for the soil. Many of the common figures assume ν = 0.5 making it important to verify the value of ν that was used. One application of horizontal stress calculations is for the loading of unyielding walls as discussed in DM 7.2. For conditions where elastic solutions are suitable, the calculation of shear stress is typically not required.

Table 4-2 Equations for the Calculation of Change in Vertical Stress Below Various Loading Conditions

Loading Condition	Stress Diagram	Equation
Point Load	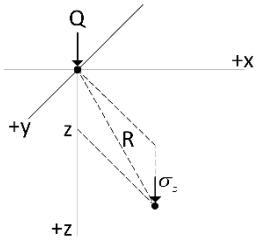	$\sigma_z = \frac{3 \cdot Q \cdot z^3}{2\pi \cdot R^5}$ $R = \sqrt{x^2 + y^2 + z^2}$
Uniform Line Load of Infinite Length	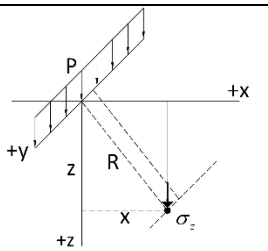	$\sigma_z = \frac{2 \cdot P}{\pi} \cdot \frac{z^3}{R^4}$ $R = \sqrt{x^2 + z^2}$
Uniform Strip Load (Figure 4-4)	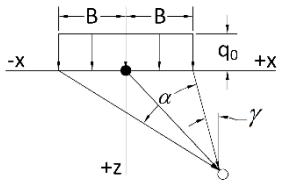	$\sigma_z = \frac{q_0}{\pi}\left[\alpha + \sin\alpha \cdot \cos(\alpha + 2 \cdot \gamma)\right]$ Note: α and γ are in radians
Uniformly Loaded Rectangular Area (Figure 4-5)	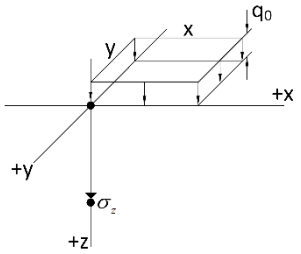	$\sigma_z = \frac{q_0}{2\pi} \cdot \left[\tan^{-1}\left(\frac{y \cdot x}{z \cdot R_3}\right) + \frac{x \cdot y \cdot z}{R_3} \cdot \left(\frac{1}{R_1^2} + \frac{1}{R_2^2}\right)\right]$ $R_1 = \sqrt{y^2 + z^2}$ $R_2 = \sqrt{x^2 + z^2}$ $R_3 = \sqrt{x^2 + y^2 + z^2}$

Table 4 2 (cont.) Equations for the Calculation of Change in Vertical Stress Below Various Loading Conditions

Loading Condition	Stress Diagram	Equation
Uniformly Loaded Circular Area (Figure 4-6)	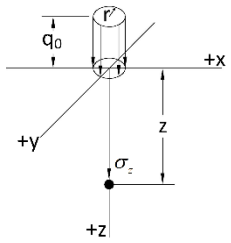	$\sigma_z = q_0\left[1-\frac{1}{\left(1+(r/z)^2\right)^{3/2}}\right]$
Triangular Load	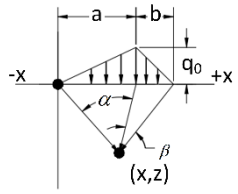	$\sigma_z = \frac{q_0}{\pi}\left[\frac{x\cdot\alpha}{a}+\left(\frac{a+b-x}{b}\right)\cdot\beta\right]$ Note: α and β are in radians
Slope Load	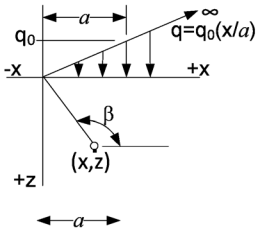	$\sigma_z = \frac{q_0}{\pi\cdot a}(x\cdot\beta+z)$ Note: β is in radians
Terrace Load	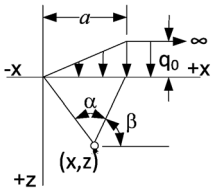	$\sigma_z = \frac{q_0}{\pi\cdot a}(a\cdot\beta+x\cdot\alpha)$ Note: α and β are in radians
Semi-infinite Uniform Load	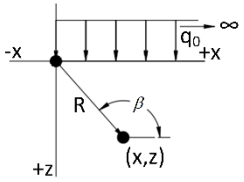	$\sigma_z = \frac{q_0}{\pi}\left[\beta+\frac{xz}{R^2}\right]$

4-3.2.3 Chart Solutions for Vertical Stress beneath Regular Loads.

Figure 4-4 to Figure 4-7 provide chart solutions for regularly shaped loads and Boussinesq theory. These charts are all based on the assumption of $\nu = 0.5$, where required, to determine the change in vertical stress. Example calculations are provided in Figure 4-9. Additional guidance on the calculation of changes in stress under elastic conditions can be found in Poulos and Davis (1974).

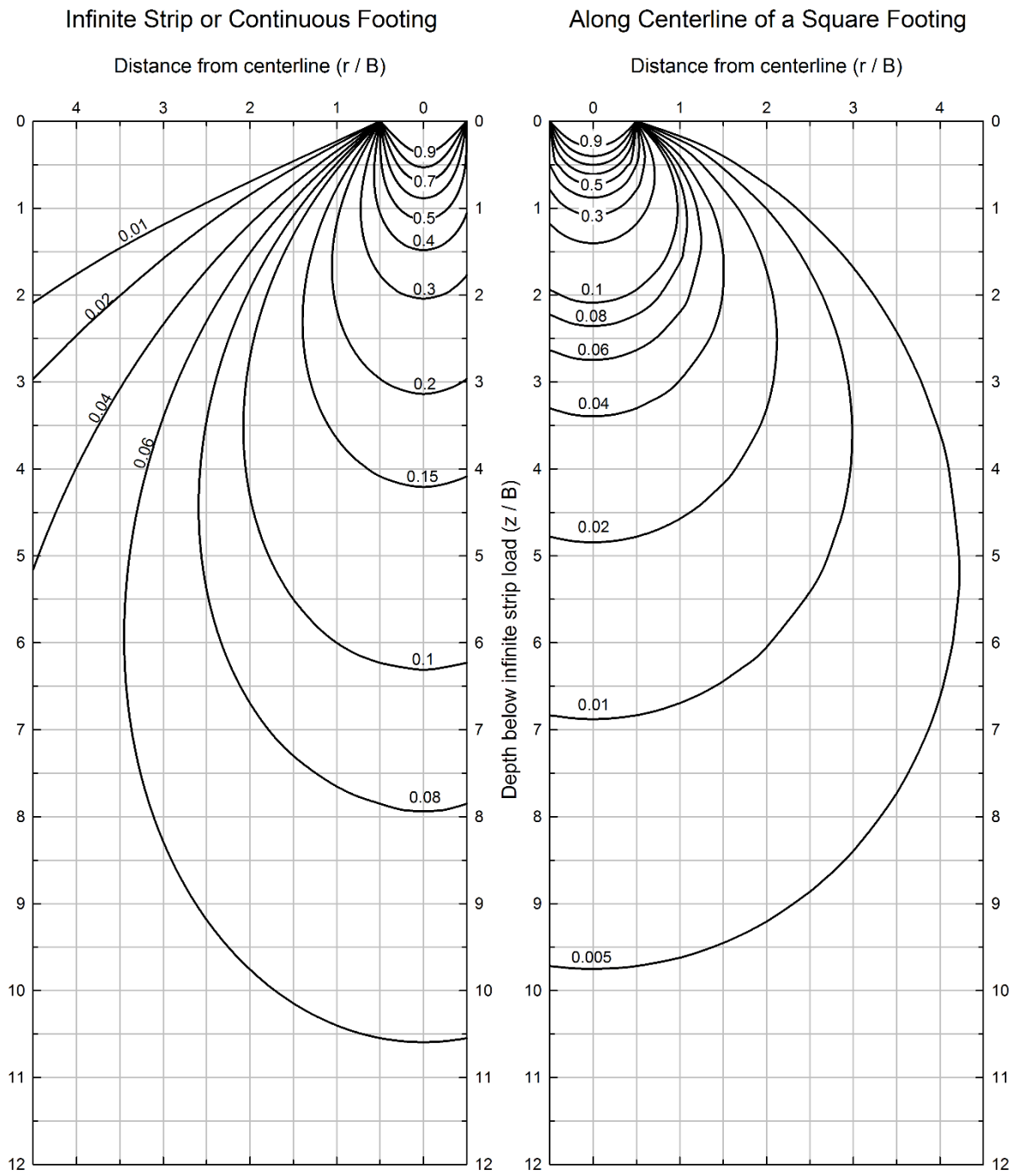

Variables: B = foundation width, r = horizontal distance from centerline of foundation, and z = depth below the applied load.
Numbers shown adjacent to contour lines are values of the influence factor, I.
For an applied foundation stress equal to q_0, the change in vertical stress is $\Delta\sigma_v = q_0 I$
Based on Boussinesq theory presented in Poulos and Davis (1972).

Figure 4-4 Vertical Stress Contours from Strip and Square Loaded Areas – Boussinesq

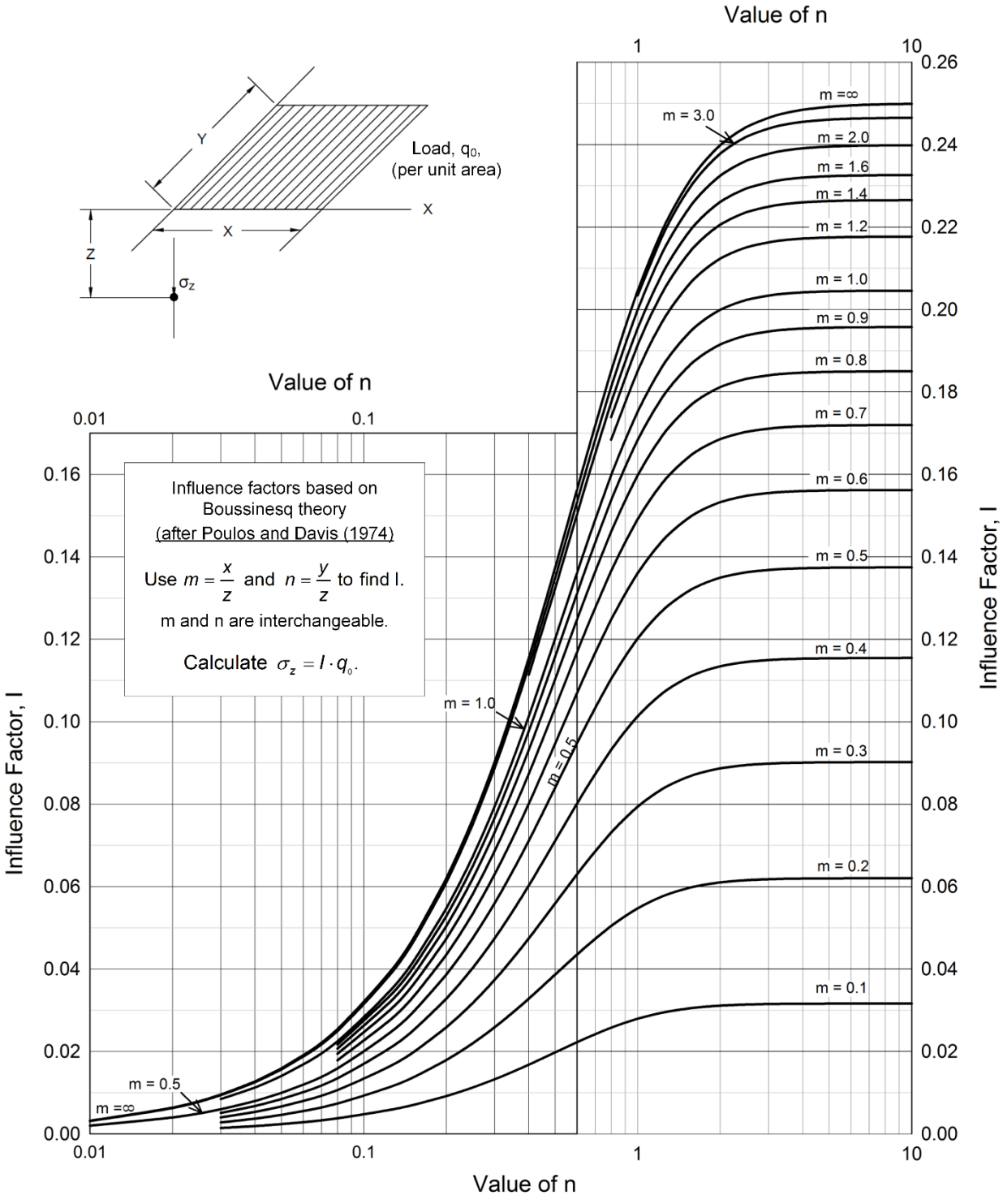

Influence Value for Vertical Stress Beneath a Corner of a Uniformly Loaded Rectangular Area

Figure 4-5 Influence Factors for a Rectangular Loaded Area – Boussinesq

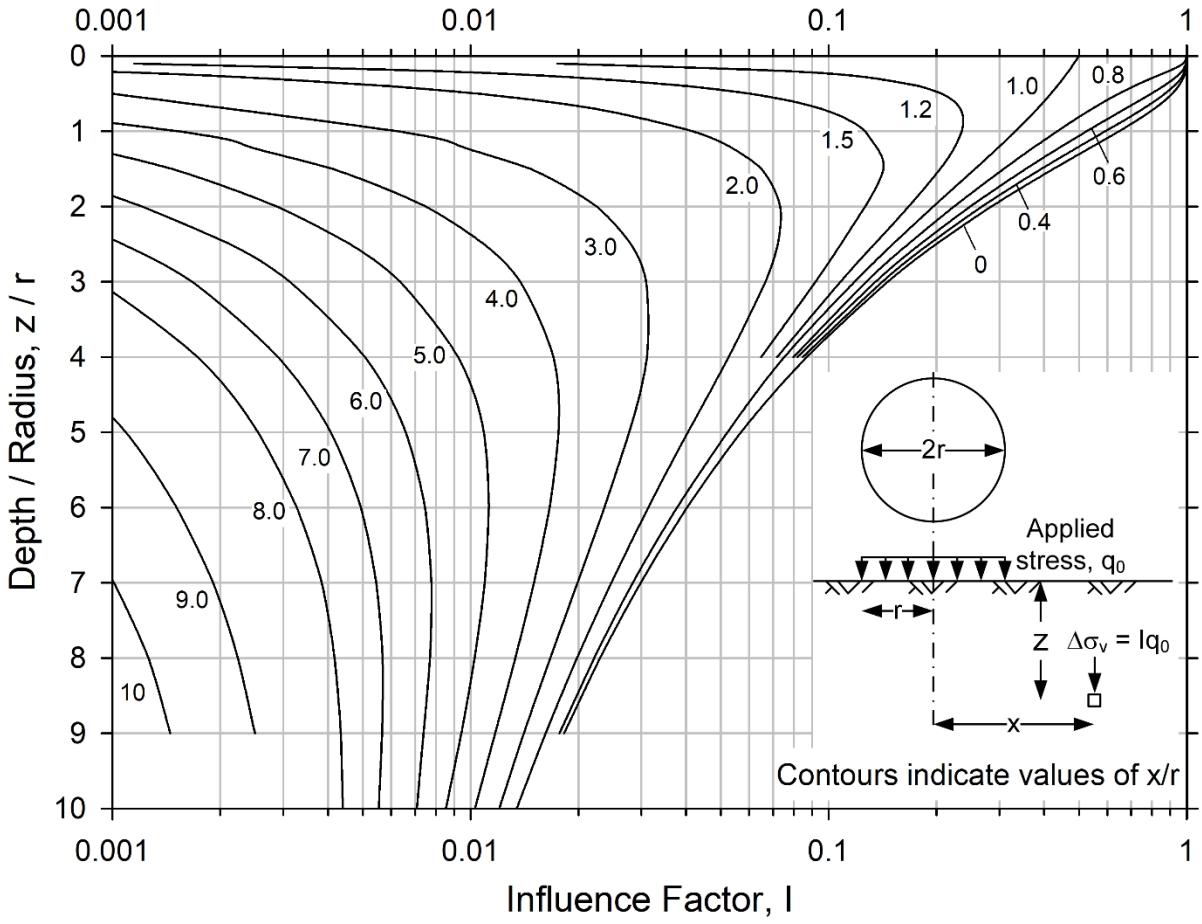

Figure 4-6 Influence Factors for a Circular Loaded Area – Boussinesq (after Ahlvin and Ulery 1962, Poulos and Davis 1974)

In the past, changes in stress caused by irregularly shaped loaded areas were calculated using chart solutions such as those proposed by Newmark (1942) and Jimenez Salas (1948). However, for complex loading conditions, numerical analysis has become the most common means to evaluate changes in stress.

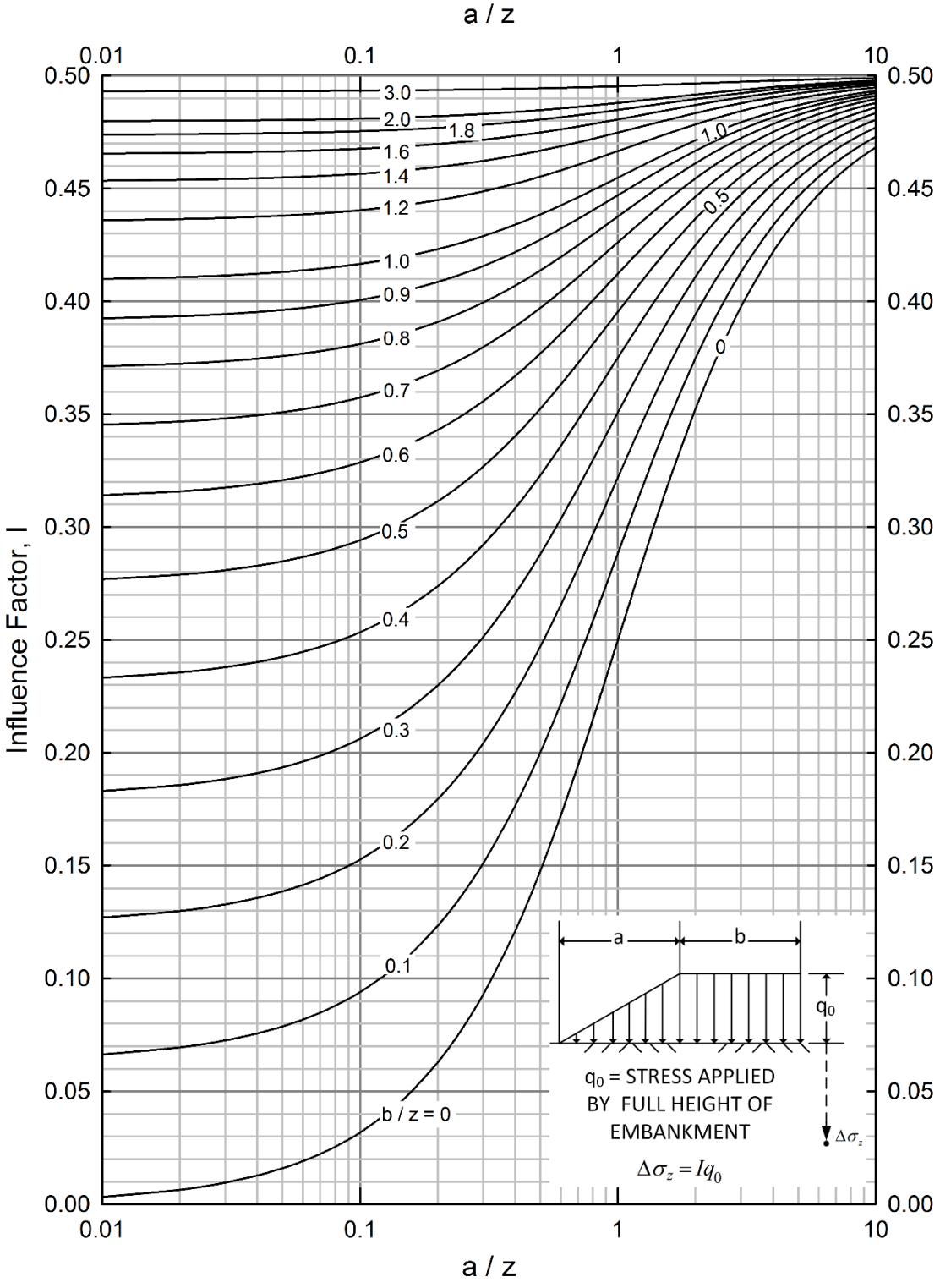

Figure 4-7 Influence Factors for Embankment Loading – Boussinesq (after Poulos and Davis 1974)

4-3.2.4 Superposition.

The assumption of linear elasticity inherent in the Boussinesq solutions allows for *superposition* of stresses that result from applied loads. This means that the change in stress from one load can be added or subtracted from those caused by other loads, provided the same point is being considered in all cases. This principle is especially useful for determining the change in stress below and outside of loaded areas as illustrated in Figure 4-8.

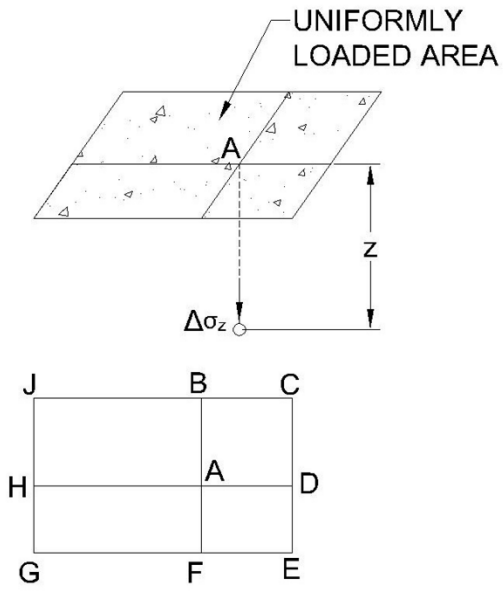

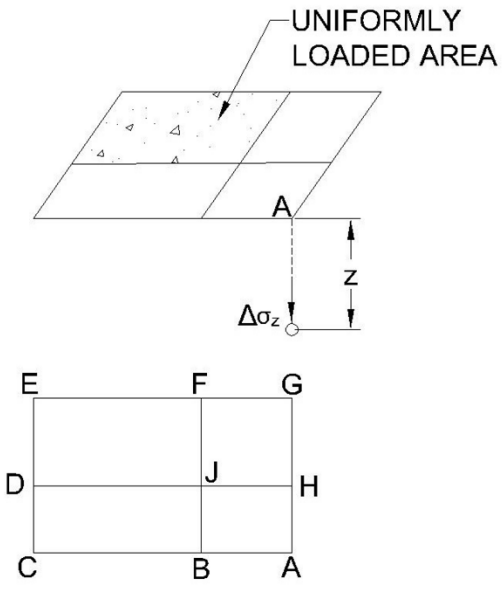

INFLUENCE FACTOR	RECTANGLE
I_1	ABCD
I_2	ABJH
I_3	AFGH
I_4	ADEF
$I_A = I_1 + I_2 + I_3 + I_4$	

(a) Point below middle of rectangular area

INFLUENCE FACTOR	RECTANGLE
I_5	ACEG
I_6	ABFG
I_7	ACDH
I_8	ABJH
$I_A = I_5 - I_6 - I_7 + I_8$	

(b) Point outside of rectangular area

Figure 4-8 Use of Superposition to Determine Change in Vertical Stress

RECTANGULAR MAT FOUNDATION

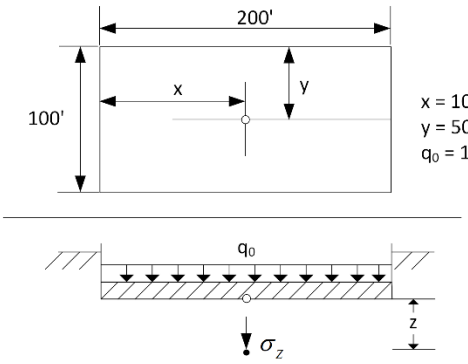

UNIT AREA LOAD (INCL. MAT) = 2 TSF, UNIT LOAD EXCAVATED = 0.8 TSF, NET AREA LOAD = 1.2 TSF. DETERMINE PROFILE OF APPLIED STRESS BENEATH CENTER OF MAT

REFER TO FIGURE 4-5 FOR INFLUENCE VALUE I FOR VERTICAL STRESS UNDER CORNER OF UNIFORMLY LOADED RECTANGULAR AREA TO FIND I FOR 1 OF 4 ADJOINING RECTANGULAR AREAS.

z (FT)	m	n	I 1 RECT.	4I 4 RECT.	$\sigma_z = 4Iq_0$ (TSF)
5	20	10	0.250	1.000	1.199
10	10	5	0.249	0.997	1.196
20	5	2.50	0.244	0.976	1.171
30	3.33	1.67	0.233	0.932	1.118
40	2.50	1.25	0.218	0.870	1.044
60	1.67	0.83	0.182	0.727	0.873
80	1.25	0.63	0.148	0.593	0.711
100	1.00	0.50	0.120	0.481	0.577

SEPARATE COLUMN FOOTINGS

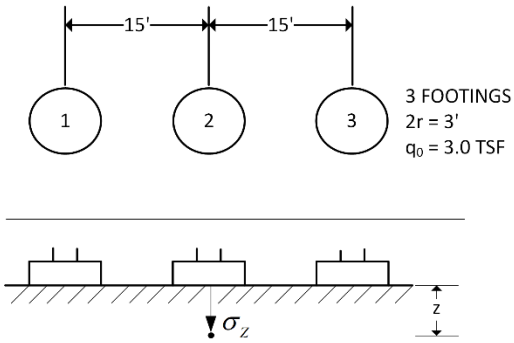

DETERMINE PROFILE OF APPLIED STRESS σ_Z BELOW CENTER OF MIDDLE CIRCULAR FOOTING (#2).

REFER TO FIGURE 4-6 (VERTICAL STRESS UNDER CIRCULAR LOADED AREA) TO DETERMINE INFLUENCE VALUE, I, FOR EACH FOUNDATION.

z (FT)	$\frac{z}{r}$	I_1 $x/r = 10$	I_2 $x/r = 0$	I_3 $x/r = 10$	$\sum I$	$\sigma_z = \Sigma Iq_0$ (TSF)
2	1.33	0.000	0.646	0.000	0.646	1.939
4	2.67	0.000	0.200	0.000	0.200	0.600
6	4.00	0.001	0.087	0.001	0.088	0.265
10	6.67	0.002	0.035	0.002	0.039	0.117
15	10.00	0.003	0.015	0.003	0.021	0.062
20	13.33	0.003	0.009	0.003	0.015	0.045
25	16.67	0.003	0.007	0.003	0.013	0.039

EMBANKMENT LOAD

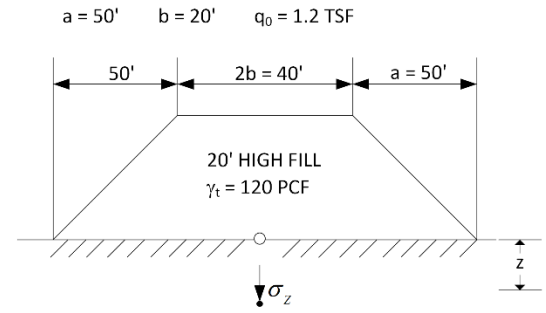

DETERMINE PROFILE OF APPLIED STRESS σ_Z BENEATH CENTER LINE OF EMBANKMENT OF INFINITE LENGTH. MAX STRESS, q_0 = (20 FT)(120 PCF) = 2400 PSF = 1.2 TSF

REFER TO FIGURE 4-7 FOR INFLUENCE VALUE I FOR VERTICAL STRESS UNDER EMBANKMENT LOAD OF INFINITE LENGTH. INFLUENCE FACTOR FROM THE CHART IS FOR 1/2 OF EMBANKMENT WIDTH.

z (FT)	$\frac{a}{z}$	$\frac{b}{z}$	I	2I	$\sigma_z = 2Ip$ (TSF)
5	10	4	0.499	0.999	1.199
10	5	2	0.496	0.992	1.190
20	2.5	1.0	0.476	0.952	1.142
30	1.67	0.67	0.445	0.889	1.067
40	1.25	0.50	0.410	0.819	0.983
60	0.83	0.33	0.343	0.686	0.824
80	0.63	0.25	0.289	0.578	0.694
100	0.50	0.20	0.247	0.494	0.593

Figure 4-9 Stress Distribution Examples

4-3.2.5 St. Venant's Principle.

St. Venant's principle is another useful concept for the calculation of change in stress due to applied loads. According to this principle, the change in stress caused by two statically equivalent loads becomes equal as the distance from the load becomes sufficiently large. Practically, this means that a square or circular load can be replaced with a point load, or a strip load can be considered a line load. It is commonly assumed that St. Venant's principle can be applied to the calculation of change in vertical stress, $\Delta\sigma_z$, for depths greater than three times the width of the applied load.

4-3.3 Layered or Anisotropic Foundations.

While the Boussinesq solutions offer a relatively simple means to calculate changes in stress, soil is not a homogeneous, isotropic, and semi-infinite medium. For example, different layers typically have different values of elastic modulus. Soil layers are often more rigid horizontally than vertically. These deviations from the assumptions of Boussinesq have led to the development of other methods for the calculation of changes in stress, most notably the Westergaard type of analysis.

4-3.3.1 Westergaard Analysis.

Westergaard analysis assumes that the soil below the load is reinforced by closely spaced horizontal layers that prevent horizontal displacement. This reinforcement effect causes the changes in stress predicted by Westergaard to be less than those calculated by the Boussinesq assumptions. The Westergaard type of analysis is most appropriate for soil profiles that have alternating layers of stiff and soft soils, such as soft clay with intermittent horizontal layers of sand. Figure 4-10 provides influence factors for points below the corner of a rectangular loaded area, assuming Westergaard theory.

4-3.3.2 Layered Foundations.

Soil profiles may have layers of significant thickness and very different elastic properties. The changes vertical stress induced in these cases differs significantly from that predicted by Boussinesq assumptions. Analytical and chart-based solutions have been suggested to account for such differences using rigidity factors (e.g., Mehta and Veletsos 1959). For these conditions, numerical analysis is the preferred method to determine changes in stress or as a means of comparison to simpler solutions.

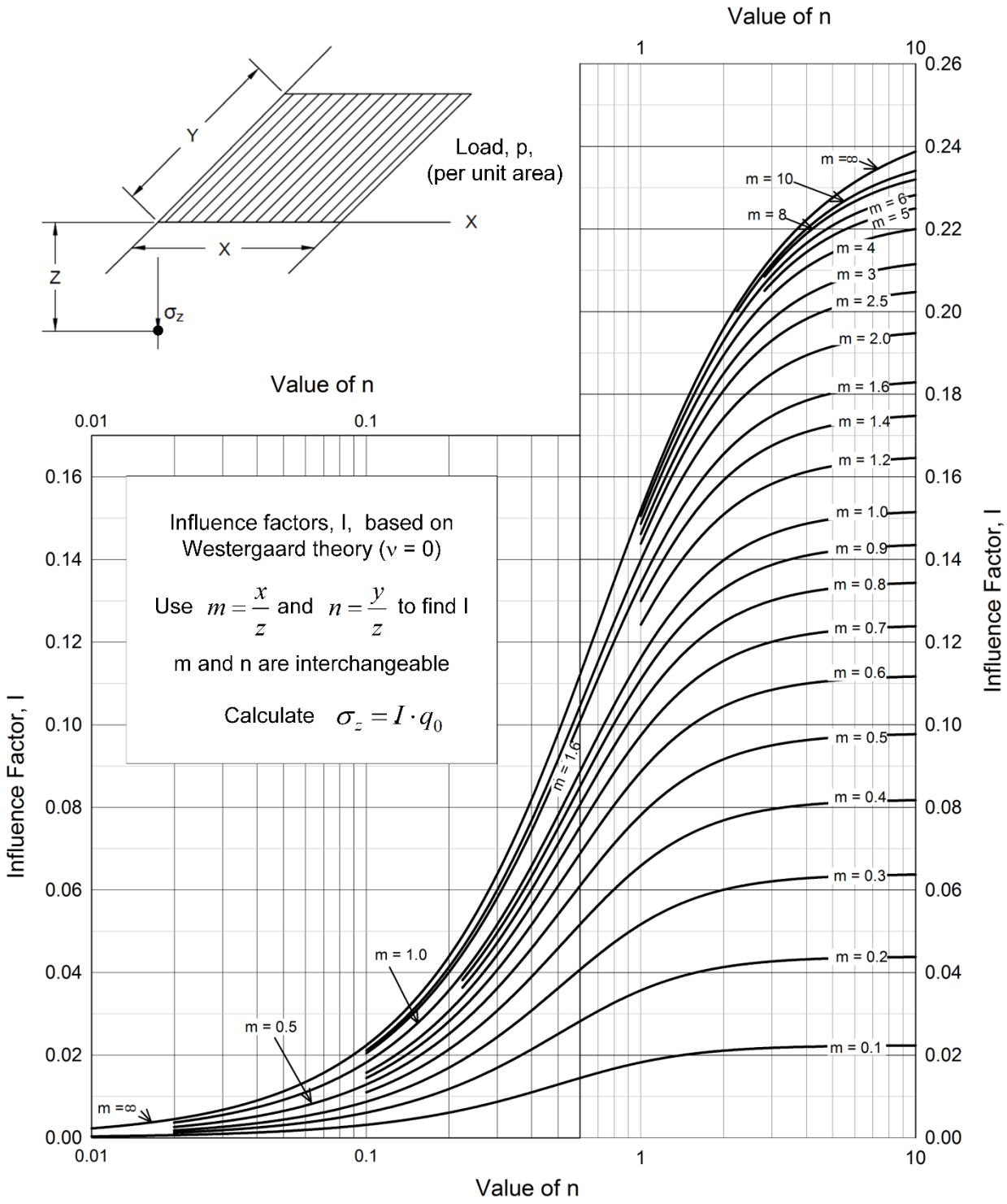

Figure 4-10 Influence Factors for a Rectangular Loaded Area – Westergaard

4-4 SHALLOW PIPES AND CONDUITS.

4-4.1 General.

The stresses on shallow pipes and conduits due to applied loads is one important application of concepts presented in this chapter. The factors influencing these stresses include the relative rigidity of the pipe to the soil, the depth of cover, the type of loading, the maximum width (span) of the structure, the method of construction, and the shape of the pipe.

This section presents simple empirical procedures based on observations. More detailed analysis can be conducted numerically or by consulting Moser (1990) or American Lifelines Alliance (2001).

4-4.2 Vertical Loads on Rigid Pipe.

Rigid pipes are those made of precast concrete, cast-in-place concrete, or cast iron.

4-4.2.1 Dead Load.

Estimates of the load caused by vertical stress on a rigid pipe can be made using the approach suggested by Marston and Anderson (1913) and subsequent work by Spangler (1948). The load per length of pipe (W_d) in a trench can be calculated as:

$$W_d = C_d \gamma_t B_d^2 \quad \textbf{(4-6)}$$

where:
C_d = a load coefficient,
γ_t = the total unit weight of the soil, and
B_d = the width of the trench.

The value of C_d can be calculated as:

$$C_d = \frac{1 - e^{-K\mu'\left(H/B_d\right)}}{2K\mu'} \quad \textbf{(4-7)}$$

where:
H = the depth of the trench above the top of the pipe,
K = a lateral earth pressure coefficient, and
μ' = the coefficient of friction for the trench fill.

Recommended values of γ_t, K, and μ' for use with this equation are provided in Table 4-3 as summarized by Moser (1990).

Table 4-3 Recommended Values for Trench Load Coefficient (after Moser 1990)

Soil type	Unit weight, γ (pcf)	Lateral earth pressure coefficient, K	Coefficient of friction, μ'	$K \times \mu'$
Partially compacted moist topsoil	90	0.33	0.5	0.17
Saturated top soil	110	0.37	0.4	0.15
Partially compacted moist clay	100	0.33	0.4	0.13
Saturated clay	120	0.37	0.3	0.11
Dry sand	100	0.33	0.5	0.17
Saturated sand	120	0.33	0.5	0.17

4-4.2.2 Live Load.

The primary live loads considered in the design of buried pipes are those from vehicles, including trucks, railroad, and airplanes. The stress at the top of the pipe is typically calculated using Boussinesq theory multiplied by an impact factors that account for dynamic effects. The equations presented in Table 4-2 can be used to estimate the vertical stress transferred to the top of the pipe from surface loading. Appropriate live load impact factors are summarized in Table 4-4.

Live load pressures (including an impact factor of 1.5) are summarized in Table 4-5. The values in this table indicate that the changes in stress become negligible below depths of 8 feet, 30 feet, and 24 feet for standard truck, railroad, and airport loads, respectively.

Table 4-4 Impact Factors for Live Loading of Buried Pipe (from American Lifelines Alliance 2001)

Depth of cover above pipe (ft)	Highway	Railway	Runway	Taxiways and aprons
0 to 1	1.50	1.75	1.00	1.50
1 to 2	1.35	1.50	1.00	1.35
2 to 3	1.15	1.50	1.00	1.35
Over 3	1.00	1.35	1.00	1.15

4-4.3 Vertical Loads on Flexible Pipe.

Flexible pipes include corrugated metal, plastic, and thin-wall smooth steel pipes. These pipes deform when loaded and develop horizontal restraining pressures on the sides that may be approximately equal to the vertical pressure if the backfill is well-compacted. The vertical pressure on the top of the pipe depends on the surrounding soil. In highly compressible soil, the vertical pressure may exceed the overburden pressure. In contrast, arching in coarse-grained soils may significantly reduce the overburden pressure.

Table 4-5 Live Load Pressures from Various Vehicle Loading (after American Lifelines Alliance 2001)

Depth of cover above pipe (ft)	Live load transferred to pipe (psi)		
	Truck Load (AASHTO HS-20)	Railway Load (Cooper E-80)	Airport (180 kip gear assembly)
1	12.5	Not recommended	
2	5.56	26.39	13.14
3	4.17	23.61	12.28
4	2.78	18.4	11.27
5	1.74	16.67	10.09
6	1.39	15.63	8.79
7	1.22	12.15	7.85
8	0.69	11.11	6.93
10	NA	7.64	6.09
12		5.56	4.76
14		4.17	3.06
16		3.47	2.29
18		2.78	1.91
20		2.08	1.53
22		1.91	1.14
24		1.74	1.05
26		1.39	NA
28		1.04	
30		0.69	

4-4.3.1 Dead Load.

For very flexible pipe with outside diameter (B_c) the Marston load theory predicts a load (W_c) of:

$$W_c = C_d \cdot \gamma_t \cdot B_c \cdot D \quad \textbf{(4-8)}$$

where:
C_d = the load coefficient for rigid pipe (see Equation 4-7),
γ_t = the total unit weight of the trench backfill, and
D = the outer diameter of the pipe (Moser 1990).

This method assumes that the pipe stiffness and soil stiffness are equal, which may lead to unconservative values of W_c.

The prism load is a more conservative approach for determining the dead load on a buried flexible pipe. The prism load (W_p) is simply the total weight of the soil above the pipe and is equal to:

$$W_p = \gamma_t \cdot H \cdot D \quad \textbf{(4-9)}$$

where:
γ_t = the backfill total unit weight,
H = the depth of soil cover, and
D = the outer diameter of the pipe.

4-4.3.2 Live Load.

The Boussinesq approach described in Section 4-4.2.2 should also be used to calculate live loads on flexible pipes.

4-4.4 Long Span Metal Culverts.

The previously discussed methods do not apply to the calculation of stresses and design of long span metal culverts. The use of finite element analysis software specifically formulated for culverts, such as CANDE, is likely required. For additional guidance see Duncan (1979).

For the design of long span metal culverts, the engineer must distinguish between shallow and deep cover conditions (Duncan 1979). Shallow cover conditions apply to cases where the cover is less than one-fourth of the culvert span. Culverts with shallow cover must be designed for flexural stresses caused by live loads. The factor safety is calculated by comparing the predicted axial stresses and moment loading to the culvert capacity.

In contrast, deep cover conditions occur when the cover is greater than one-fourth of the span. Deep cover culverts only require design for ring compression, such that the seams don't collapse under the design loads. Design axial ring loads are higher than those calculated solely based on ring compression theory. This occurs because the culvert is much stiffer in ring compression than the surrounding soil and a negative arching condition occurs.

4-5 DEEP UNDERGROUND OPENINGS.

4-5.1 General Factors.

Prior to excavation of a tunnel, the rock or soil is typically at a state of equilibrium under the stresses imposed by overburden and external loads. Excavation disturbs that equilibrium condition and requires load to transfer to surrounding rock, soil, or tunnel support system. The soil and rock will always exhibit an immediate response to the

changes in stress caused by the excavation. Often a time-dependent response also occurs, especially in saturated compressible soils. A good discussion of the development of equilibrium conditions during and after tunneling in soft ground, as well as tunneling and support methods, is provided in FHWA (2009).

Changes in stress are typically accompanied by displacement of the rock, soil, or support structure. Similar to retaining walls, some movement is desirable to create a suitable balance between the load carried by the structure and the load distributed to the soil. Due to the effects of this soil-structure interaction, the type of support system and tunneling method used will significantly affect the deformations experienced during and after tunneling, and therefore the loading imposed on tunnel support.

The stresses acting on an underground opening will also depend on the depth of the opening below the ground surface and the characteristics of the surrounding soil or rock. One common distinction between the terms deep and shallow compares the depth of cover to the diameter of the opening. Openings for which this ratio is less than 2 should be considered shallow and arching of the soil or rock should be ignored. Deep openings have a cover to diameter ratio greater than 3 and benefit from the effects of arching.

For deep underground openings, deformation toward the opening allows the release of stress and the development of arching in the surrounding soil or rock. For this reason, the stresses are heavily dependent on the amount of deformation allowed during construction and the degree of restraint provided by the lining.

Numerical methods, such as finite element analysis, can be used to calculate stresses and deformations of underground openings. These methods can be quite accurate and account for significant complexity provided the soil and rock are characterized properly and the construction sequence is adequately modeled. The methods presented in this section are useful for simple calculations and to check the results of more complex numerical models.

4-5.2 Openings in Rock.

Rock can be separated into two groups for the purposes of determining stresses: (1) sound, non-swelling rock that can sustain considerable tensile stress and (2) fractured, blocky, seamy, squeezing, or swelling rock. For more detailed explanations of rock properties, see Chapter 1. The behavior of these two groups is distinguished primarily by the ability of the rock to resist tensile stress and/or significant deformation.

4-5.2.1 Sound Rock.

Elastic analysis can be used to determine stresses surrounding tunnels or openings in intact, isotropic rock (e.g., crystalline igneous, homogeneous sandstone and limestone). Analytical methods are summarized in rock mechanics texts such as Goodman (1989).

For these materials, stresses in rock surrounding spheroidal cavities are lower than those for tunnels with the same cross-section. Elastic analysis can be used to determine the best arrangement of openings and pillars, such that supports are provided at locations of stress concentration.

4-5.2.2 Broken and Fractured Rock.

Pressure on tunnels in chemically or mechanically altered rock must be analyzed by approximate rules based on experience, such as those presented in Table 4-6. The rock conditions used in Table 4-6 are compared to other common rock quality indices in Table 4-7.

4-5.2.3 Squeezing and Swelling Rock.

Rocks in categories 7 to 9 of Table 4-6 and Table 4-7 are the result of clay deposits that have been heavily preloaded during their geologic history. The transition from very dense soil to soft rock is not well-defined. In some cases, very dense clays that have not fully lithified may be included in this category.

Rock properties are closely tied to the properties of the minerals from which it is comprised. The rocks in this category contain significant amounts of clay minerals with properties ranging from the non-swelling kaolinite group to the highly swelling montmorillonite group. Soil and rock that has a high fraction of clay minerals will tend to expand, absorb water, and lose shear strength while undergoing stress relief. Thus, rocks with significant amounts of clay minerals will tend to swell as a result of the stress relief around an underground opening. Swelling leads to a loss of shear strength and a tendency of the tunnel walls to squeeze into the opening.

4-5.3 Loads on Underground Openings in Rock.

4-5.3.1 Vertical Rock Load.

A common starting point for the estimation of vertical roof pressure is found in Table 4-6. It should be noted that the values presented in this table were largely based on observations by Terzaghi (1946) for tunnel widths in the range of 16 to 32 feet (5 to 10 meters) prior to the advent of “modern” tunneling methods. Table 4-6 provides an approximate means of calculating the vertical pressure or rock load that must be supported by roof lining. The height of rock (H_p) that must be supported is a function of the tunnel width (B) for high quality rock and also the tunnel height (H_t) for lower quality

rock. The total vertical pressure can be found by multiplying H_p by the total unit weight of the rock.

Table 4-6 Approximate Overburden Rock Load Carried by Roof Support

Rock Condition	Rock Load H_p (same units as B)	Remarks
1. Hard and intact	0	Sometimes spalling or popping occurs.
2. Hard stratified or schistose	0 to $0.5 \cdot B$	Light pressures.
3. Massive, moderately jointed	0 to $0.25 \cdot B$	Load may change erratically from point to point.
4. Moderately blocky and seamy	$0.25 \cdot B$ to $0.35 \cdot (B+H_t)$	No side pressure.
5. Very blocky and seamy	0.35 to $1.10 \cdot (B+H_t)$	Little or no side pressure.
6. Completely crushed, chemically intact	$1.10 \cdot (B+H_t)$	Considerable side pressure. Softening effect of seepage towards bottom of tunnel.
7. Squeezing rock, moderate depth	(1.10 to 2.10) $\cdot (B+H_t)$	Heavy side pressure.
8. Squeezing rock, great depth	(2.10 to 4.50) $\cdot (B+H_t)$	Heavy side pressure.
9. Swelling rock	Up to 250 ft, not related to value of $(B+H_t)$	Very heavy pressure.

Notes:

1. After Proctor and White (1977) based on observations by Terzaghi (1946).
2. Rock loads apply to tunnels at depth greater than $1.5 \cdot (B + H_t)$.
3. The roof of the tunnel is assumed to be located below the water table. If the tunnel is located permanently above the water table, the values given for Conditions 4 to 6 can be reduced by fifty percent.
4. Some very dense clays which have not yet acquired properties of shale rock may behave as squeezing or swelling rock.

5. Where sandstone or limestone contain horizontal layers of immature shale, roof pressures will correspond to rock condition “very block and seamy.”

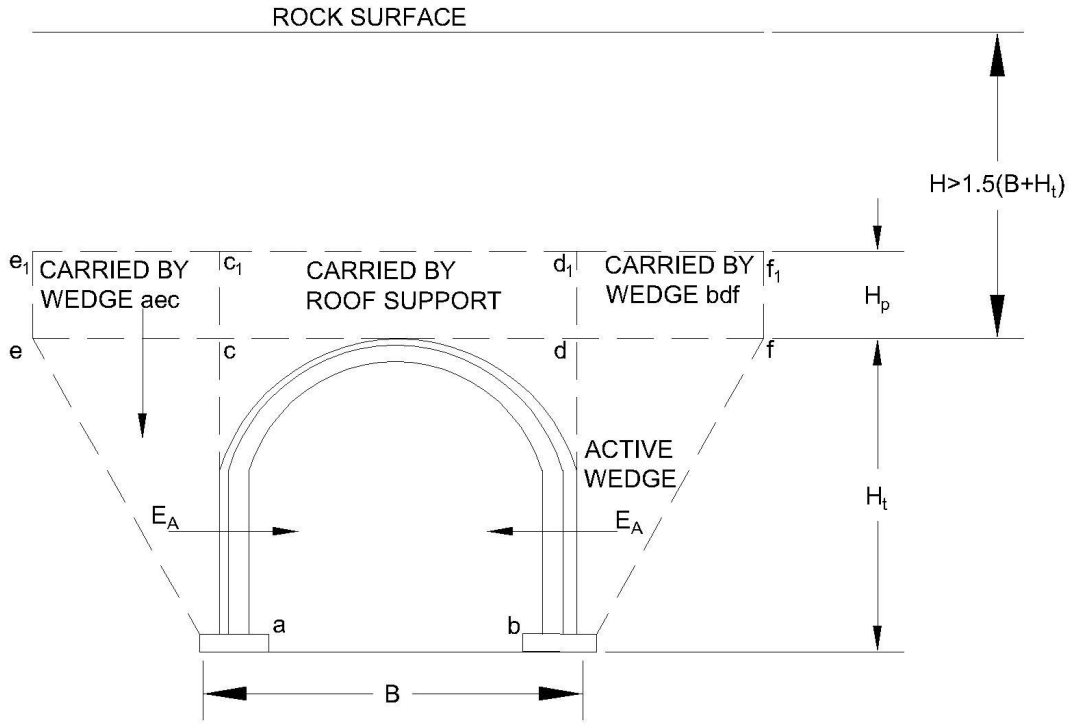

Table 4-7 Approximate Relationship Between Rock Quality Indices (after Deere et al. 1970, Barton et al. 1974, Bieniawski 1990, Hemphill 2012)

Rock Condition	RQD	Rock Tunneling Quality Index, Q^A	Rock Mass Rating, RMR^B
1. Hard and intact	95 to 100	≥ 200	> 80
2. Hard stratified or schistose	90 to 99	25 to 50	65 to 75
3. Massive, moderately jointed	85 to 95	10 to 20	60 to 65
4. Moderately blocky and seamy	75 to 85	2 to 6	50 to 60
5. Very blocky and seamy	30 to 75	0.4 to 1	40 to 50
6. Completely crushed but chemically intact	0 to 30	0.04 to 0.08	20 to 25
7. Squeezing rock, moderate depth	NA	0.01 to 0.03	10 to 20
8. Squeezing rock, great depth	NA	0.001 to 0.004	< 5
9. Swelling rock	NA	0.001 to 0.003	0

[A] After Barton et al. (1974)
[B] After Bieniawski (1990)

4-5.3.2 Horizontal Pressures.

Horizontal pressures acting on a tunnel can be approximated using an active wedge type analysis, such as Coulomb, with the diagram shown at the bottom of Table 4-6. The vertical forces included in these calculations are the weight of the active wedge and the weight of the rock for a height (H_p) above the wedge. Shear strength parameters can be assumed or selected using guidance in Chapter 3. The critical inclination of the active wedge may be determined by either the shear strength of the rock or by the rock structure. The possibility of movement along a weak bedding plane or stratum should be considered.

4-5.3.3 Other Methods for Tunnel Support Pressures.

Alternate empirical methods for estimating tunnel support pressures are available. The two most common are the rock tunneling quality index, Q, presented in Barton et al. (1974) and the rock mass rating system (e.g., Bieniawski 1976). These systems are described in more detail in Chapter 1. The roof pressure and support requirements for tunnels can be estimated from the value of Q and some of the joint properties. While not solely intended for tunneling applications, the RMR can be related to stand-up time, unsupported active span length, and roof pressure. See Bieniawski (1990) for additional comparison of methods for estimating tunnel support requirements.

4-5.4 Openings in Soft Ground (Soil).

4-5.4.1 Ground Behavior.

Selection of an appropriate method for tunnel construction in *soft ground* (i.e., soil tunneling) depends upon the response of the soil during and after excavation. This response is often referred to in terms of *stand-up time*, which is the amount of time the soil will support itself prior to the installation of tunnel supports. The stand-up time depends on the type of soil, the position of groundwater, and the size of the opening. Terzaghi's (1950) *Tunnelman's Ground Classification* provides a commonly used means of describing various types of ground response. The types of ground behavior for tunneling are summarized in Table 4-8.

Table 4-8 Types of Ground Behavior

Type of Ground	Applicable Soil Types	Support / Ground Behavior	Comments
Firm	Loess above water; hard clay; marl; lightly stressed cemented sand and gravel	No initial support required. Construction final lining before movement occurs.	None perceptible
Raveling (slow to fast)	Sand with clay binder (slow above water table, fast below); stiff fissured clays	Chunks or flakes of soil fall as a result of loosening, overstress, or brittle fracture. Time to start of raveling may be a few minutes (fast) or more (slow)	Stand-up time decreases with size of opening. Raveling ground can become running ground if the water table rises.
Running	Clean, dry coarse-grained soils unable to stand at an angle greater than angle of repose.	Support should be prior to excavation. Removal of side supports results in inflow of material.	Stand-up time is zero. In moist soils, suction may allow soil to stand briefly before running. This is referred to as “cohesive-running.”
Flowing	Silt, sand, and gravel without clayey fines below water table; disturbed highly sensitive clay	Without support, material flows into opening from all sides like a viscous fluid. If unchecked, may completely fill the tunnel.	Material acts like a thick liquid.
Squeezing	Very soft to medium stiff clay at shallow depths; stiff to hard clay at great depth; soil with low frictional strength	Soil moves into tunnel gradually without indication of rupture or change in water content.	Stand-up time adequate. Behavior results from plastic flow caused by overstress. Rate of advance is related to the degree of overstress.
Swelling	High OCR clays with swelling minerals and PI greater than about 30.	Soil absorbs water over time, increases in volume, and expands toward the tunnel. Pressure on support members may increase with time.	Advances into opening occur due to an increase in volume allowed by stress relief.

In addition to the descriptions provided in Table 4-8, the behavior of fine-grained soils and silty sands above the water table can be evaluated using Table 4-9. The undrained stability factor (N_{crit}) is used to assess the ground behavior as suggested by Peck (1969). This factor is defined as:

$$N_{crit} = \frac{\sigma'_v - \sigma_t}{s_u} \quad \textbf{(4-10)}$$

where:
σ'_v = effective overburden pressure at the tunnel centerline,
σ_t = interior applied pressure from compressed air or breasting, and
s_u = undrained shear strength.

Table 4-9 Ground Behavior for Clayey Fine-Grained Soils and Silty Sand (after FHWA 2009)

Soil Type	Stability Factor, N_{crit}	Ground Behavior
Clayey Fine-Grained	1	Stable
	2 to 3	Small amount of creep
	4 to 5	Creeping, usually slow enough to permit tunneling
	6	May experience general shear failure. Clay likely to invade tail space too quickly to handle.
Silty Sand above Water Table	0.25 to 0.33	Firm
	0.33 to 0.5	Slow raveling
	0.5 to 1	Raveling

For coarse-grained soils, the ground behavior depends on the grain-size distribution, relative density, and the amount of clayey fines (binder) as indicated in Table 4-10. Uniform, loose materials (C_u < 3 and N < 10) with round grains run more freely than well-graded, dense materials (C_u > 6 and N > 30) with angular particles. Soils with properties between those listed in Table 4-10 will tend to exhibit intermediate ground behavior. Very high flowrates should be expected in tunnels below the water table through soils with relatively large particles, such as gravel and medium to coarse sand.

Table 4-10 Ground Behavior for Coarse-Grained Soils (after FHWA 2009)

Soil Description	Relative Density (SPT blow count)	Typical Ground Behavior	
		Above Water Table	Below Water Table
Very fine clean sand	Loose (N < 10)	Cohesive running	Flowing
	Dense (N > 30)	Fast raveling	Flowing
Fine sand with clay binder	Loose (N < 10)	Rapid raveling	Flowing
	Dense (N > 30)	Firm or slowly raveling	Slowly raveling
Sand or sandy gravel with clay binder	Loose (N < 10)	Rapid raveling	Rapid raveling or flowing
	Dense (N > 30)	Firm	Firm or slow raveling
Sandy gravel and medium to coarse sand	Any	Running	Flowing

4-5.4.2 Soft Ground Support Loads.

Support pressures on tunnels in soft ground are governed by many factors, including the unit weight of the overlying material, the groundwater level, soil properties, the amount deformation allowed during excavation, the interaction between soil and the supports, the opening shape, and the length of time between excavation and lining installation. Other factors should also be considered include the presence of other nearby openings, superimposed loads from neighboring structures, and the possibility of changes in groundwater conditions.

Figure 4-11 illustrates the loading mechanism surrounding soft ground tunnels. In coarse-grained soils, arching occurs above the tunnel. Arching transfers some of the overburden load to the surrounding ground so that only a portion of the total load above the tunnel is applied to the tunnel. In clay soils, undrained conditions tend to control. In this case, the undrained shear strength can be considered to provide support of a portion of the load above the tunnel.

A simplified approach to the selection of tunnel support loads is provided in Table 4-11 (FHWA 2009). More detailed guidance for the selection of tunnel support loads is summarized in Table 4-12. These tables are used by first determining the ground behavior type using Table 4-8 to Table 4-10.

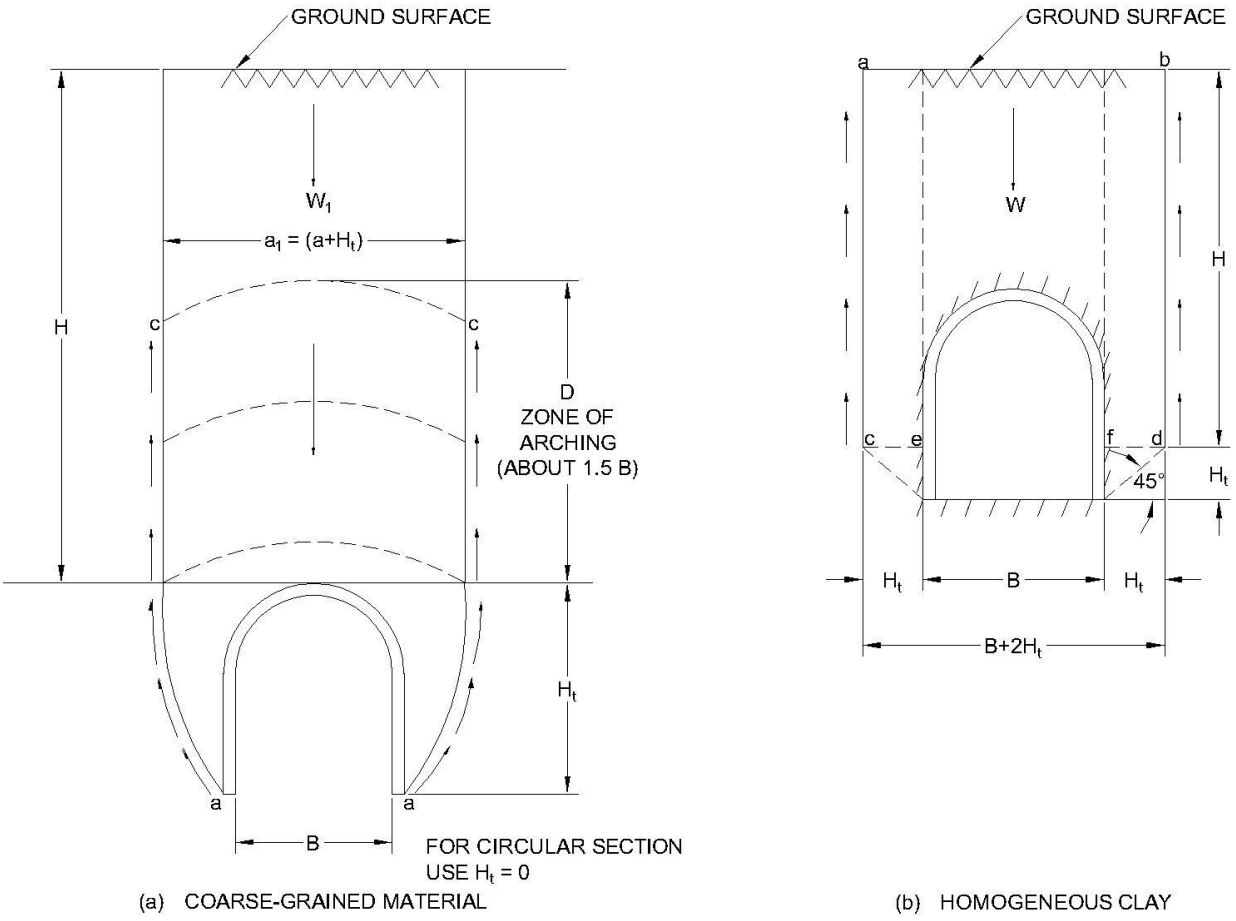

Figure 4-11 Loading Mechanisms for Soft Ground Tunneling

4-5.4.3 Loss of Ground.

As underground excavation is made, the surrounding ground starts to move toward the opening. These displacements occur as the soil around the opening expands due to stress release in addition to soil lost to the tunnel from raveling, runs, flows, etc. The resulting loss of ground causes settlement of the ground surface. The loss of ground associated with stress reduction can be predicted reasonably well, but the ground loss due to raveling, runs, flows, etc. requires a detailed knowledge of the subsurface conditions to avoid unacceptable amounts of settlement. A summary of methods to predict surface settlement resulting from lost ground can be found in FHWA (2009).

Table 4-11 Simplified Tunnel Support Loads based on Ground Behavior (FHWA 2009)

Ground Behavior	Design Load Thickness, H_p	
	Circular Tunnel[A]	Horseshoe Tunnel[A]
Running ground	$\min\begin{Bmatrix} H \\ B \end{Bmatrix}$	$\min\begin{Bmatrix} H \\ 2B \end{Bmatrix}$, See Note B
Flowing ground in air free	$\min\begin{Bmatrix} H \\ 2B \end{Bmatrix}$	$\min\begin{Bmatrix} H \\ 4B \end{Bmatrix}$, See Note C
Raveling ground above water table	$\min\begin{Bmatrix} H \\ B \end{Bmatrix}$	$\min\begin{Bmatrix} H \\ 2B \end{Bmatrix}$, See Notes B and C
Raveling ground below water table	$\min\begin{Bmatrix} H \\ 2B \end{Bmatrix}$	$\min\begin{Bmatrix} H \\ 4B \end{Bmatrix}$, See Note C
Squeezing ground	Depth to tunnel springline	
Swelling ground	Same as raveling ground	

[A] B is the tunnel width
[B] Floor is required in a horseshoe tunnel if compressed air is used, otherwise ignore compressed air.
[C] Stiff floor required in horseshoe tunnel

4-5.5 Pressure on Vertical Shafts.

In contrast to the methods presented in Section 4-3, the stress calculations for vertical shafts represent either active or passive earth pressure. These limiting earth pressure conditions correspond to a plastic rather than elastic state of stress within the soil.

4-5.5.1 Shafts in Coarse-Grained Soil.

During excavation of a vertical cylindrical shaft in coarse-grained soil, the horizontal pressures around the shaft approach active earth pressure values. If outward-directed forces from a structure (e.g., buried silo) move the structure walls into the soil, the earth pressures will approach passive conditions. Earth pressures are discussed in more detail in DM 7.2.

Active earth pressures for cylindrical shafts have been determined using analytical, limit equilibrium, slip line, numerical, and experimental methods. The active earth pressure coefficient depends on the shaft dimensions and the soil strength. For shallow shafts (i.e., depth ≤ two diameters), theoretical solutions tend to be applicable while the effects of horizontal arching become significant at greater depths (Tobar and Meguid 2010). Horizontal arching is taken into account in some solutions by the coefficient λ, which is the ratio of the circumferential stress to the vertical stress. The value of λ is equal to 1

in analytical solutions, such as Terzaghi (1943) but may be as low as K_0. Cheng et al.'s (2007) solution is plotted in Figure 4-12 for λ = 1 and $\lambda = K_0$.

Active pressures must be modified if rigid bracing at the top of the shaft prevents development of an active state. For restrained vertical shafts, horizontal pressures may be as large as the at-rest pressure on a long wall with plane strain conditions.

Table 4-12 Soft Ground Tunnel Support Loads for $H > 1.5 \cdot (B+H_t)$

Type of Ground	Tunnel Conditions	Design Load, H_p
Running	Above water	Loose: $0.5 \cdot (B+H_t)$ Medium: $0.4 \cdot (B+H_t)$ Dense: $0.3 \cdot (B+H_t)$
Running	Compressed air	Disregard air pressure; H_p, equal to that for running ground, above water table with equal density
Flowing	Free air	$\min \begin{cases} H \\ 2(B+H_t) \end{cases}$
Raveling	Above water	Multiply H_p for running ground by $\frac{T-t}{T}$
	Below water, free air	Multiply H_p for running ground by $\frac{T-t}{T}$
	Below water, compressed air	Using H_p for running ground: $2 \cdot \left(\frac{T-t}{T}\right) H_p - \frac{p_c}{\gamma_t}$
Squeezing[A]	Homogenous clay	$H - \frac{p_c}{\gamma_t} - \frac{Hs_u}{\gamma_t(B+2H_t)}$
	Soft roof, stiff sides	$H - \frac{p_c}{\gamma_t} - \frac{Hs_u}{\gamma_t B}$
	Stiff roof, soft sides	$H - \frac{p_c}{\gamma_t} - \frac{Hs_u}{\gamma_t(B+6H_t)}$
Swelling[B]	Intact clay	Very small
	Fissured clay	Use H_p for raveling ground with same standup time
Variables:	p_c = tunnel air pressure, s_u = undrained shear strength, γ_t = total unit weight of soil t = stand up time, T = elapsed time between excavation and completion of permanent structure H = vertical distance between ground surface and tunnel roof, H_p = design load in terms of depth (multiply by γ_t to determine design pressure), H_t = height of the tunnel, and B = width of the tunnel	

[A] After complete blowout, p_c = 0

[B] Permanent roof support should be completed within a few days after excavation

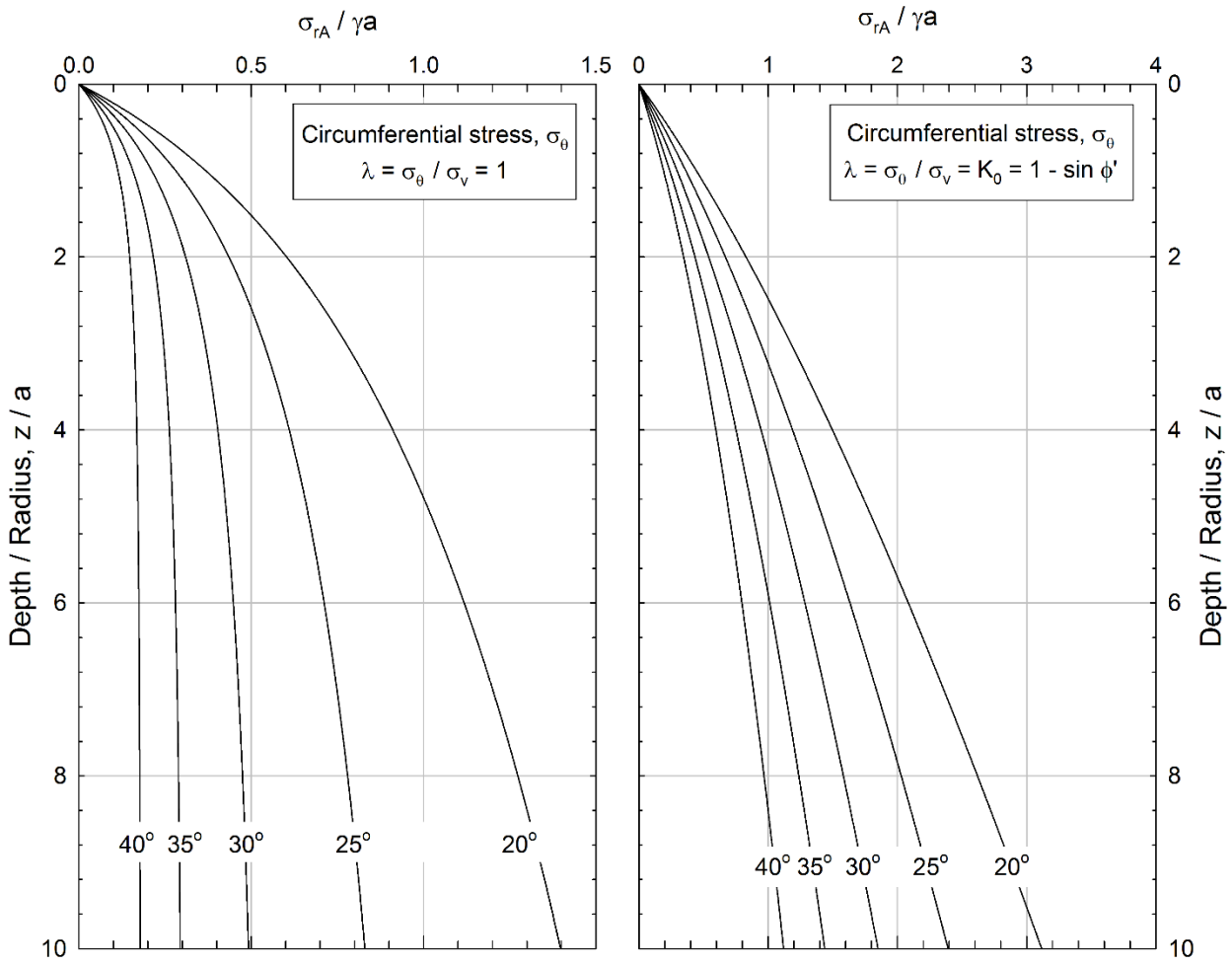

Figure 4-12 Radial Stress at the Sides of a Vertical Shaft in Sand (based on Cheng et al. 2007)

4-5.5.2 Shafts in Clay.

No support is needed from the ground surface to a depth of z_{crit} for shafts in clay. The critical depth (z_{crit}) is:

$$z_{crit} = \frac{2s_u}{\gamma_t} \quad \textbf{(4-11)}$$

where:
s_u = the undrained shear strength of the soil and
γ_t = the total unit weight of the soil.

At greater depths, the ultimate horizontal pressure (σ_h) on a shaft lining in soft clay can be estimated as:

$$\sigma_h = \gamma' \cdot z - s_u \quad \textbf{(4-12)}$$

where:
γ' = effective unit weight of the soil,
z = depth below the ground surface, and
s_u = undrained shear strength of the soil.

This pressure will likely occur after several months of unsupported excavation. The stability factors for fine-grained soils in Table 4-9 can be used as guidelines for the behavior of vertical shafts in clay.

In stiff, intact or fissured clays, the initial horizontal stress on vertical shaft walls will be small. Over time the pressure may increase to a value several times larger than the effective vertical stress (and ultimately to the swelling pressure if the shaft lining is sufficiently rigid). Local experience is important to provide useful information for soil pressures on vertical shafts in stiff clays.

4-6 NUMERICAL SOLUTIONS FOR STRESSES IN SOIL.

The analytical and chart-based solutions presented in this chapter are an excellent starting point for evaluation of stresses within a soil mass. However, their applicability is limited by the constraints and assumptions of each. These methods also struggle to effectively model complex subsurface profiles and loading conditions.

Computer programs and numerical solutions are an important part of geotechnical engineering practice. This section provides a brief overview of the application of numerical methods to the evaluation of stresses.

4-6.1 Numerical Analysis Types.

Some computer programs (e.g., Settle3D, CONSOL, SETOFF) are available that directly rely upon elastic solutions, such as those presented in this chapter, to calculate changes in stress. These programs are specifically formulated for the solution of consolidation settlement problems discussed in the next chapter. The benefit provided by these programs is the automated calculation of changes in stress and the ability to consider time-dependent changes. However, the solutions depend on the same assumptions as the elastic solutions on which they are based.

Many continuum-based numerical analysis techniques are available. The most common of these in geotechnical engineering are the finite element and finite difference methods, with the former being somewhat more popular for stress analysis problems. These approaches divide the soil or rock into elements or grid points. The relationships

between the external and gravitational forces acting on the elements (or grid) and the corresponding displacements are defined using constitutive (stress-strain) laws and failure criteria.

The following sections provide a condensed overview focused on the calculation of stresses using the finite element method. The use of finite element analysis (FEA) to determine stresses is relatively straight-forward. Calculation of accurate deformations requires significantly more expertise and experience. For a practical introduction to the use of FEA in geotechnical engineering see Bradley and VandenBerge (2015). A more in-depth perspective can be found in the books by Potts and Zdravkovic (1999, 2001).

4-6.2 Linear Elastic Stress Analysis.

The simplest FE analyses use linear elastic constitutive theory, which relates changes in stress linearly to strains (or displacements). For a linear elastic analysis, the only required material parameters are the elastic modulus, E, and Poisson's ratio, ν (or any other two elastic constants such as shear modulus or bulk modulus). For problems with only one material type (and one value of E), the calculated stresses will be independent of the value of E selected. However, when more than one material type is present, the relative values of E assigned to each material in the analysis can impact the calculated stresses because of arching and similar phenomena.

4-6.3 Nonlinear Elastic Stress Analysis.

The stress-strain behavior of geological materials is truly linear over only a small range of strains. A properly selected nonlinear constitutive model will provide a more accurate prediction of behavior but will require additional input parameters and expertise. VandenBerge et al. (2014) found that major principal effective stresses calculated for embankments with linear elastic analysis were typically within 10% of the values calculated using more rigorous and time-consuming nonlinear procedures.

One of the earliest and most common nonlinear constitutive theories for soil is the hyperbolic model proposed by Duncan and Chang (1970) and described in more detail in Duncan et al. (1980). This model can also consider stress dependent variations in Poisson's ratio (or bulk modulus). It can be used with either effective stress (drained) or total stress (undrained) problems, provided the model parameters are determined using the appropriate type of test.

The Duncan-Chang model is based on the following observations;

- The principal stress difference ($\sigma_1 - \sigma_3$) tends to vary in a hyperbolic manner with strain,
- The initial modulus (E_i) increases with increased confining stress in a manner that can be described by a power function,

- The ultimate value of ($\sigma_1 - \sigma_3$) predicted by the hyperbola tends to be greater than the value measured by the test,
- The bulk modulus (B_t) of soil increases with increased confining stress in a manner that can be described by a power function.

Soil tends to respond in a stiffer, approximately linear manner with modulus (E_{ur}) when unloaded and reloaded after some amount of shearing. The required parameters are summarized and illustrated in Table 4-13 and Figure 4-13.

Table 4-13 Summary of Model Parameters for Duncan-Chang Model

Duncan-Chang Parameter	Meaning / Use	Equation
K	Controls rate of increase of E_i with σ'_3	$E_i = KP_a\left(\frac{\sigma'_3}{P_a}\right)^n$
n	Controls nonlinearity of E_i relationship	
R_f	Reduces ($\sigma_1 - \sigma_3$) from its ultimate hyperbolic value to match maximum value measured by testing	$R_f = \frac{(\sigma_1-\sigma_3)_{max}}{(\sigma_1-\sigma_3)_{ult}}$
K_b	Controls rate of increase in B_t with σ'_3	$B_t = K_b P_a\left(\frac{\sigma'_3}{P_a}\right)^m$
m	Controls nonlinearity of B_t relationship	
K_{ur}	Controls rate of increase of E_{ur} with σ'_3	$E_{ur} = K_{ur} P_a\left(\frac{\sigma'_3}{P_a}\right)^n$

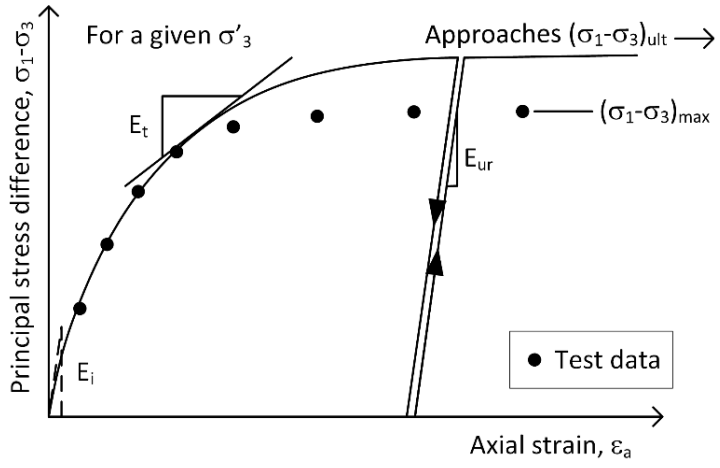

Calculate E_t using c' and ϕ'

$$E_t = E_i\left[1 - \frac{R_f(1-\sin\phi')(\sigma_1-\sigma_3)}{2c'\cos\phi' + 2\sigma'_3\sin\phi'}\right]^2$$

Figure 4-13 Parameters Used in Duncan-Chang Model

4-6.4 Numerical Modeling Best Practice.

Both linear and nonlinear finite element analysis can be used to make accurate predictions of stresses. The following guidelines have been found to yield the most consistent and uniform stress predictions (VandenBerge et al. 2014).

- Use isoparametric elements (i.e., 8-noded rectangles or 6-node triangles).
- Use a uniform mesh with elements of approximately the same shape, especially within any zones of interest.
- Use elements with an appropriate aspect ratio, preferably longest to shortest dimension, less than or equal to five.
- Keep the element size as small as practical with respect to the overall dimensions. A maximum element height of approximately 1 to 2% of the height of the problem domain is preferred.
- Remember to include the boundary water pressures from any impounded water present in the model.

4-6.4.1 Initial or Geostatic Stresses.

The initial stress state in a FE model is dependent on the process used to "turn on" gravity and stress within the model. Vertical stresses are governed mostly by gravity loading. As the mesh deforms in response to gravity, horizontal stresses will develop and tend toward at rest (K_0) conditions for a level, laterally-constrained mesh. For a linear elastic model, the value of K_0 will be equal to $\nu/(1-\nu)$. Calculation of initial horizontal stresses in this manner will yield correct results, and K_0 will be less than 1.0, which is always the case for primary loading. The calculation of initial horizontal stresses in this way will lead to initial deformation of the model and the layer thicknesses may no longer match the *in situ* conditions. These displacements are a numerical artifact and should be zeroed or removed prior to examining the effects of new loading conditions. Overconsolidated conditions with K_0 greater than 1.0 can be modelled by loading and then unloading the model, following the process by which K_0 > 1.0 conditions occur in nature.

In many cases, the details of the initial stress process are program specific. The engineer using FEA should become familiar with the various options available so that appropriate methods are applied.

4-6.4.2 Staged Construction or Stress History.

Finite element analysis allows the sequence of loading and construction staging to be modeled numerically. To a lesser extent, geologic stress history can also be modeled. Within the model, this occurs by adding and subtracting elements (or their weight) in steps. Staged models are especially important for nonlinear analysis because the properties of the material change with stress level.

For example, a staged approach is required to predict stresses and displacements around open excavations and tunnels. The initial ground conditions should be modeled after which the effects of removing soil or rock can be considered.

For cases where only stress distributions are required, such staging is unnecessary in linear elastic analysis. The use of a staged model is required, even for linear elasticity, to predict correct patterns displacement.

4-6.5 Evaluation of Stress Due to Applied Loads.

Changes in stress due to applied loads can be evaluated using a staged FE model. The first stage(s) of the model are used to create the desired initial state of stress that best represents the *in situ* conditions. At this point, the new loading can be added to the model in various forms, including distributed loads, point loads, and new soil layers. The predicted changes in stress can then be evaluated by comparing the predicted stress at convenient points within the model between subsequent stages. Where possible, the changes in stress predicted by FE models should be checked with analytical solutions such as those presented earlier in this chapter.

Engineers should be aware of the limitations of their numerical analyses. For example, two-dimensional FEA are useful for predicting changes in stress below long foundations, embankments, and large area fills because such problems can be analyzed in a plane strain manner. However, a three-dimensional program would be required to predict changes in stress below more complex conditions, such as a rectangular foundation.

4-6.6 Evaluation of Stress within Embankments and Slopes.

The calculation of stresses is more complex for slopes and embankments compared with relatively level ground. First, no closed-form analytical solution is available for comparison because the soil in a slope is not laterally restrained. The lack of lateral restraint also means that K_0 conditions will not be present, especially close to the face of a slope.

Stresses near natural slopes are best evaluated by starting with level ground in the FE model and progressively removing (excavating) elements to form the slope. Multiple stages of analysis may be required to establish the initial conditions. The removal of elements mimics the process by which the slope was formed in nature.

Likewise, stresses in an embankment can be modeled by adding layers of elements in stages. The fill zone can be “built” within the FE model in thin layers, mimicking the actual construction process. Deformations caused by the initial application of gravity loading should preferably be removed. However subsequent deformations of each

layer of fill under the weight of the overlying material are realistic. This approach allows the true pattern of displacements within the embankment to be examined.

4-7 SUGGESTED READING.

Topic	Reference
Stress and Mohr Circles	Parry, R. H. 2004. *Mohr circles, stress paths and geotechnics*, CRC Press, 2004.
Elastic Solutions	Poulos, H. G. and Davis, E. H. 1974. *Elastic Solutions for Soil and Rock Mechanics*, John Wiley & Sons Inc.
Stress on Pipes	Moser, A. P. 1990. *Buried Pipe Design*, McGraw-Hill Inc., (third edition also available by Moser and Folkman).
Underground Openings	FHWA. 2009. *Technical Manual for Design and Construction of Road Tunnels – Civil Elements, FHWA-NHI-09-010*, Federal Highway Administration.
Numerical Stress Analysis	Bradley, N. and VandenBerge, D. R. 2015. *Beginner's Guide for Geotechnical Finite Element Analyses*, CGPR Report No. 82, Center for Geotechnical Practice and Research, Virginia Tech.
	Potts, D. M. and Zdravkovic, L. 2001. *Finite Element Analysis in Geotechnical Engineering: Theory and Application*, ICE Publishing.

4-8 NOTATION.

Symbol	Description
B	Width of a foundation, loaded area, or tunnel
B_c	Diameter of a flexible pipe
B_d	Width of trench in pipe loading calculations
B_t	Bulk modulus of soil
C_d	Load coefficient in pipe loading calculations
C_u	Coefficient of uniformity (from grain-size distribution)
D	Outer diameter of pipe
E	Elastic modulus
E_A	Active earth pressure force
E_i	Initial tangent modulus
E_{ur}	Unload-reload modulus for Duncan-Chang model
h_p	Pressure head

Symbol	Description
H	Depth of soil cover or vertical distance between ground surface and tunnel roof
H_p	Design load thickness in terms of depth
H_t	Tunnel height
I	Influence factor for change in stress calculations
K_a	Active earth pressure coefficient
K_b	Bulk modulus parameter for Duncan-Chang model
K_0	At-rest earth pressure coefficient
K_p	Passive earth pressure coefficient
K_{ur}	Unload-reload modulus parameter Duncan-Chang model
N	Standard Penetration Test blow count
N_{crit}	Undrained stability factor
p_c	Tunnel air pressure
p'_f	Center of Mohr circle at failure (MIT stress path space)
P_a	Atmospheric pressure
u	Pore water pressure
q_f	Radius of Mohr circle at failure
q_0	Applied pressure or load
Q	Rock tunneling quality index
r	Horizontal distance from centerline of a foundation
R_f	Reduction factor for Duncan-Chang model
RMR	Rock mass rating
RQD	Rock quality designation
s_u	Undrained shear strength
t	Stand up time for tunneling in raveling soils
T	Elapsed time between excavation and completion of permanent structure
W_c	Flexible pipe load
W_d	Rigid pipe load

Symbol	Description
W_p	Prism load on pipe
z	Depth below an applied load
z_{crit}	Critical depth for unsupported shafts in clay soils
Z_i	Soil layer thickness
α	Angle between the major principal plane and the plane of interest
$\Delta\sigma_z$	Change in vertical stress
ϕ'	Effective stress friction angle
γ'	Effective unit weight
γ_t	Total unit weight
g_w	Unit weight of water
λ	Ratio of the circumferential stress to the vertical stress
μ'	Coefficient of friction for trench backfill
ν	Poisson's ratio
σ_1	Major principal stress
σ_2	Intermediate principal stress
σ_3	Minor principal stress
σ_h	Total horizontal stress
σ'_h	Effective horizontal stress
σ_t	Interior tunnel pressure from compressed air or breasting
σ_v	Total vertical stress
σ'_v	Effective vertical stress

This Page Intentionally Left Blank

CHAPTER 5 ANALYSIS OF SETTLEMENT AND VOLUME EXPANSION

5-1 INTRODUCTION.

5-1.1 Scope.

This chapter explains the practical aspects of the process of volume change in soil. Many of the cases relate to the compression of soil layers due to changed conditions, such as placement of an engineered fill, foundation loading, or lowering of the groundwater table. Compression of soil results in *settlement*, which is vertical displacement of the ground surface or a structure supported by the ground. Both immediate and long-term settlement will be considered, along with tolerable settlement criteria, the rate of settlement, and methods to reduce or accelerate settlement. Swelling soils can also change volume by expansion, which is often referred to as *heave*.

Guidance on special cases, such as collapsing soils, is provided in DM 7.2 (UFC 3-220-20). Chapter 2 of this document provides guidance on methods for monitoring settlement.

5-1.2 Occurrence of Settlement.

Settlement is the result of three primary mechanisms: (1) immediate *distortion* that occurs in response to the application of a new load, (2) *consolidation,* which is compression of the soil skeleton in response to changes in effective stress, and (3) *secondary compression*, which is rearrangement of the soil structure under constant effective stress. All three mechanisms will be explained in more detail in later sections of this chapter.

In saturated fine-grained soils, the settlement associated with the three mechanisms can be distinguished and separated for the practical purpose of estimating settlement magnitude. This separation is possible because these soils have low hydraulic conductivity and relatively high compressibility, which causes consolidation to occur over a measurable period of time. The processes and magnitudes of settlement typically associated with fine-grained soils are summarized in Table 5-1.

Coarse-grained soils are much less compressible than fine-grained soils and have higher hydraulic conductivity. Because of these characteristics, consolidation occurs very quickly and can be difficult to separate from immediate deformation. Much of the compression of coarse-grained soil is related to particle rearrangement under changed stress. Vibrations from earthquakes, blasting, or machinery can also cause settlement of coarse-grained soil. Submergence and soaking of coarse-grained soils, particularly fill materials, can lead to settlement as discussed in Section 5-9.

5-1.3 Occurrence of Heave.

Heave or swell occurs primarily due to the reduction of total vertical stress or the reduction of matric suction, which both lower the effective stress on the soil and therefore allow an increase in the void ratio. The reduction of total stress occurs as the result of excavation or erosion of soil, as well as the removal of man-made loading. The matric suction in a soil depends on the soil type and the past and present atmospheric conditions. Especially important is the degree of saturation of the soil. The factors affecting the degree of saturation include climate history, topography, vegetation, and groundwater level. The amount of swelling that occurs as a result of either mechanism depends on the size and type of minerals that comprise the soil. Clay minerals with very small particles and high specific surface area, such as montmorillonite and vermiculite, are most susceptible to swelling. Heave can also occur as a result of the formation of ice lenses in frozen soil. Volumetric expansion from chemical reactions, such as pyrite, can also cause heave.

5-1.4 Applicability.

The methods to analyze settlement that are presented in this chapter apply to conditions where shear stresses are well below the shear strength. In addition, these analyses of consolidation magnitude and rate as well as secondary compression assume that the soil is saturated.

Table 5-1 Settlement Calculation Methods for Different Soil Types (after Coduto et al. 2011, Salgado 2008)

Soil Type	Time Frame	Process	Relative Magnitude	Method of Calculation
Coarse-Grained	Short-Term	Distortion	Negligible to small	Semi-empirical immediate or “elastic” settlement
		Consolidation	Small to moderate	
	Long-Term	Secondary Compression	Negligible to small	Semi-empirical methods
	Other	Vibration, submergence	Small to moderate	Specialized methods
Fine-Grained	Short-Term	Distortion	Negligible to small	Semi-empirical immediate or “elastic” settlement
	Long-Term	Consolidation	Moderate to large	Primary consolidation calculations
		Secondary Compression	Small to large	Secondary consolidation calculations

5-2 MECHANICS OF CONSOLIDATION.

5-2.1 Consolidation Process.

Consolidation of soil is caused by changes in effective stress. For this reason, it is necessary to consider the process by which effective stresses change within a soil mass. Saturated soil consists of two relatively incompressible components, the mineral particles and water. In comparison, the overall soil structure is compressible because the particles can rearrange to encompass more or less void space. The compressible soil structure must strain or deform in order to support a change in stress.

When a soil mass experiences an abrupt change in the applied total normal stress, the soil must respond in one of two ways: (1) the compressible soil structure strains instantaneously, or (2) a pressure change occurs in the incompressible water within the soil voids. The first option is not possible because strain of the soil structure requires a change in the void ratio of the soil. The void ratio of a saturated soil can only change if the amount of water in the soil changes, and time is required for water to leave or enter the soil voids. Instead, the instantaneous soil response follows the second option, and a change in the pore water pressure occurs. This temporarily altered pressure is often referred to as *excess pore water pressure*, u_x. For saturated, one-dimensional conditions, the magnitude of u_x will be roughly equal to the change in total vertical stress, $\Delta\sigma_z$. Because $\Delta\sigma_z$ is balanced by u_x, the instantaneous change in effective stress is negligible, and there is no instantaneous settlement as a result of consolidation.

The excess pore water pressure in the soil creates a hydraulic gradient between the conditions within the soil and those at its boundaries. The gradient causes water to flow out of or into the soil, as time progresses following the application of $\Delta\sigma_z$. When $\Delta\sigma_z$ is positive, the soil volume decreases as the water flows out and the excess pore water pressures decrease. After a relatively long period of time, the excess pore water pressure dissipates completely (i.e., $u_x = 0$), all of the change in total vertical stress is transferred to the soil structure, and the consolidation settlement is complete. The time required to reach this state can range from seconds or minutes for thin layers of coarse-grained soils to years for thick layers of fine-grained soil.

Estimates of the magnitude of consolidation require (1) knowledge of the initial vertical stress state, (2) prediction of the change in total stress caused by new loading, (3) an understanding of the stress history of the soils impacted by the changes, and (4) knowledge of the compressibility characteristics of those soils.

Estimates of the rate of consolidation settlement require knowledge of (1) the hydraulic boundary conditions, (2) the thickness, (3) the compressibility, and (4) the hydraulic conductivity of the compressible soil layers.

5-2.2 Initial Vertical Stress State.

Consolidation analysis focuses on volume change caused by changes in vertical stress. The initial geostatic vertical total stress (σ_{z0}), pore water pressure (u_0), and vertical effective stress (σ'_{z0}) should be calculated using methods discussed in Chapter 4. Figure 5-1(a) illustrates initial vertical stress conditions for hydrostatic water conditions.

Artesian water conditions are associated with confined aquifers in which higher pore water pressure is present in a more permeable soil layer below a confining stratum. Artesian conditions affect the calculation of pore water pressure within the compressible layer as well as the calculated vertical effective stress. As illustrated in Figure 5-1(b), the hydrostatic pore water pressure is labeled u_0 while the artesian pressure at any depth is Δu. The artesian pressure must also be subtracted from the total vertical stress in order to obtain the correct initial effective stress.

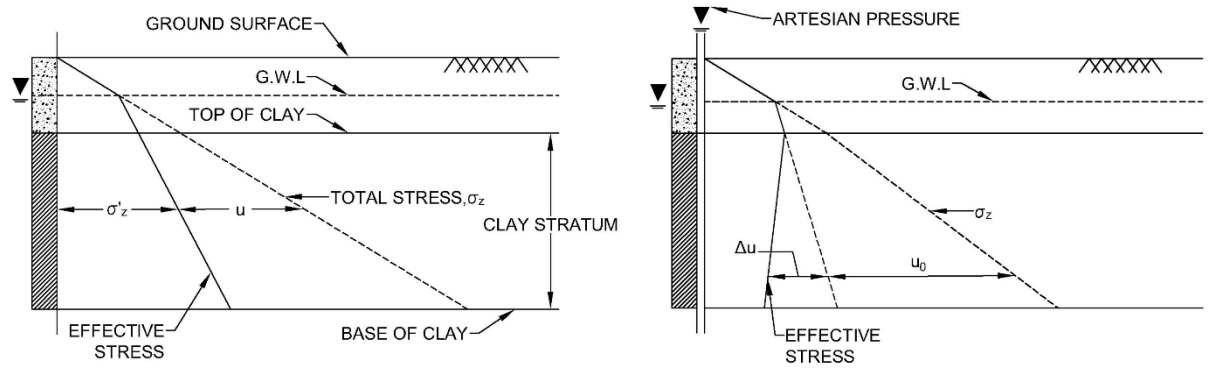

(a) Hydrostatic conditions (b) Artesian conditions

Figure 5-1 Initial Vertical Stresses for a) Hydrostatic and b) Artesian Pore Water Pressure Conditions

5-2.3 Stress History.

The *stress history* of a soil refers to the past stress states that the soil has experienced. It will affect the structure and behavior of the soil under new loading. This is especially true for fine-grained soils. Of particular importance is the highest vertical effective stress to which the soil has been consolidated, which is known as the *preconsolidation stress* or *maximum past* pressure, σ'_p. A method for determining the preconsolidation stress is shown in Figure 3-12.

For some soil deposits, the existing vertical effective stress is the highest vertical effective stress the soil has ever experienced and σ'_p is equal to σ'_{z0}. This type of soil deposit is referred to as *normally consolidated* and sometimes abbreviated “NC.”

More commonly, soil deposits have been preloaded or preconsolidated at some point in the past, and σ'_{z0} is less than σ'_p. This type of soil is referred to as *overconsolidated* and sometimes abbreviated "OC." The *overconsolidation ratio* (OCR) is a helpful measure of soil behavior and is found as:

$$OCR = \frac{\sigma'_p}{\sigma'_{z0}} \quad \textbf{(5-1)}$$

where:
σ'_p = preconsolidation stress and
σ'_{z0} = current vertical effective stress.

In situ vertical stress profiles for steady state conditions are summarized in Figure 5-2. In Figure 5-2(a), the clay layer is normally consolidated because the preconsolidation stress is equal to the effective vertical stress. The clay in Figure 5-2(b) is slightly overconsolidated as a result of a higher groundwater level compared to (a), which reduces the current vertical effective stress. Similarly, overconsolidation as a result of excavation (or erosion) and previous loading are depicted in Figure 5-2(c) and (d).

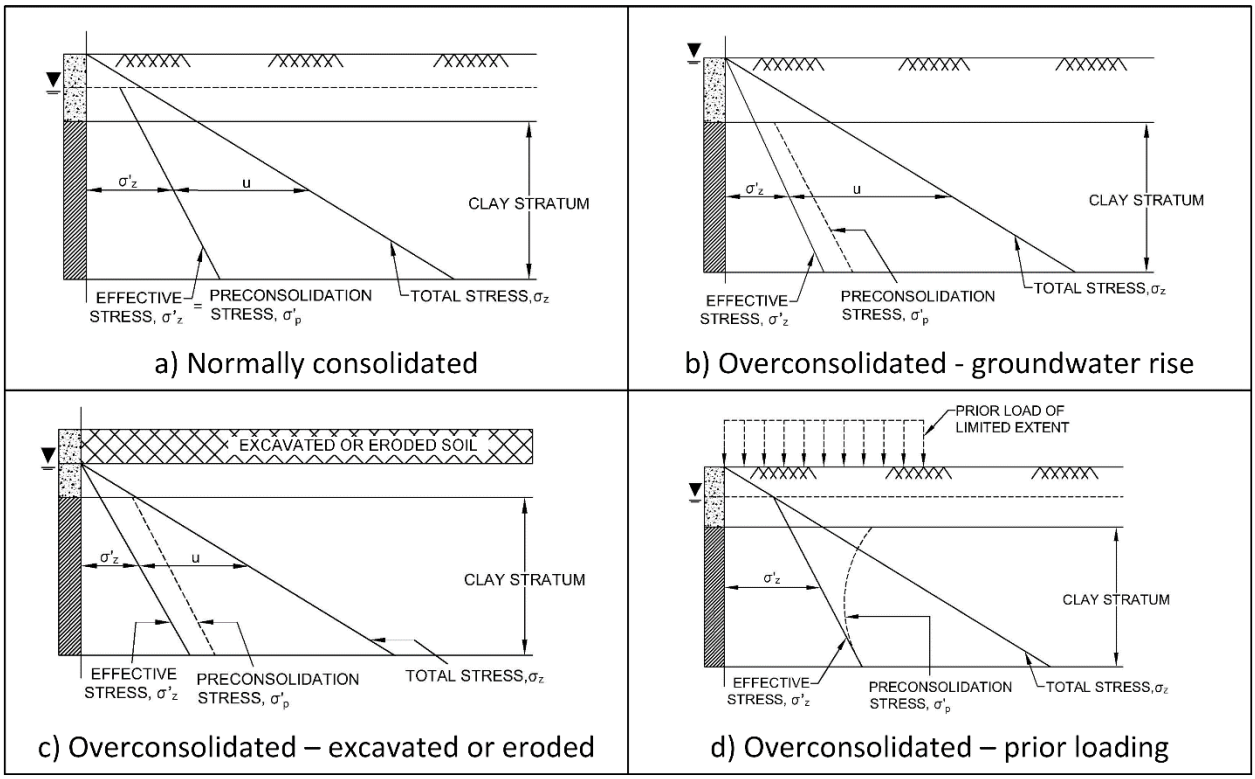

Figure 5-2 Vertical Stress History Examples

In some cases, a soil layer may be encountered that has not yet finished consolidating as a result of a prior change in effective stress. This state is referred to as *underconsolidated*. In this case, the pore water pressures in the soil have not yet

reached equilibrium following a change in stress and are higher than the hydrostatic values. Two examples are provided in Figure 5-3. In the first example, the groundwater level has been lowered in the sand layers. The decrease in pore pressure (and corresponding consolidation) of the low permeability clay layer will be time-dependent. The second example is partial consolidation under a prior applied stress. In either case, the initial pore pressure variation with depth within the clay layer must be measured or estimated in order to calculate the variation of initial vertical effective stress within the soil.

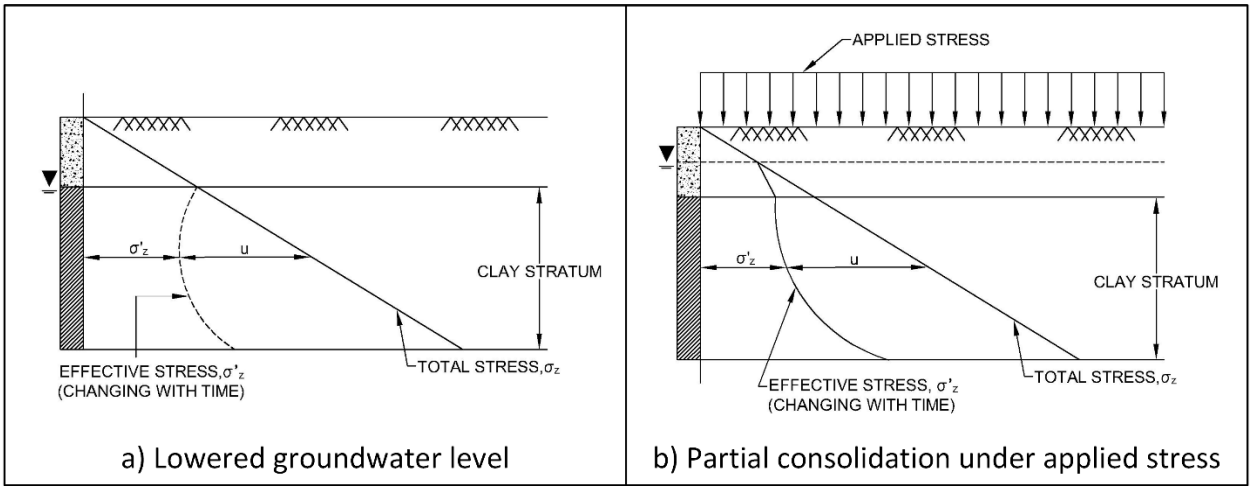

Figure 5-3 Vertical Stress Profile Cases – Transient

5-2.4 Evaluation of Existing Conditions.

For purposes of settlement calculations, the existing conditions at the start of construction or the application of a new load must be evaluated. At a minimum, this evaluation should include the following steps:

- Review the available site and geologic data. In particular, determine potential sources of overconsolidation (e.g., glaciation, erosion, human activity, groundwater fluctuations) and estimate the likely magnitude of preconsolidation and/or OCR.
- Determine the variation of the preconsolidation stress with depth from laboratory consolidation tests (see Chapter 3). Measurements of undrained shear strength can also be used along with correlations to provide additional estimates of preconsolidation stress. For example, undrained strength (s_u) is often related to the *in situ* vertical stress and the OCR by:

$$s_u \approx USR_{NC} \cdot \sigma'_{z0} \cdot OCR^m \quad \textbf{(5-2)}$$

where:
USR_{NC} = the soil's normally consolidated undrained strength ratio, and
m = an empirical coefficient (See Section 8-3).

Equation 5-2 can be rearranged to obtain:

$$\sigma'_p \approx \sigma'_{z0}\left(\frac{s_u}{USR_{NC}\cdot\sigma'_{z0}}\right)^{1/m} \quad \textbf{(5-3)}$$

- Compare estimates of preconsolidation stress to current vertical effective stress. A helpful tool for this purpose is a plot showing the subsurface profile, the laboratory test data, and the variation of effective vertical stress with depth, such as that shown in Figure 5-4.

- If underconsolidation is expected or indicated, measurements of pore water pressure with depth are required to identify the extent of the underconsolidation.

Likely Sources of Overconsolidation

- Erosion of surficial soil (estimated magnitude = 10 ft x 125 pcf = 1250 psf)
- Groundwater fluctuation

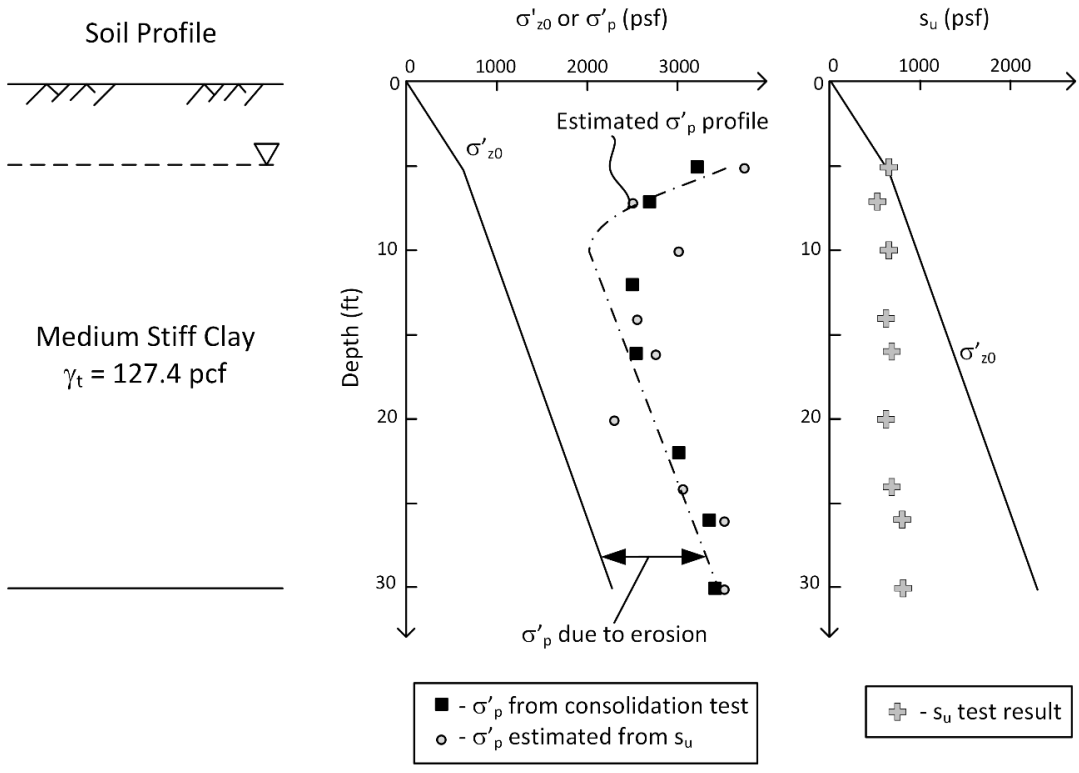

Estimation of Preconsolidation Stress from Undrained Strength

At z = 10 ft, s_u = 600 psf and σ'_{z0} = 962 psf. Assume USR_{NC} = 0.25 and m = 0.8

$$\sigma'_p \approx (962\,psf)\left(\frac{600\,psf}{0.25(962\,psf)}\right)^{1/0.8} \approx 3000\,psf$$

Figure 5-4 Example Evaluation of Existing Conditions

5-2.5 Change in Vertical Stress.

The methods presented in Chapter 4 should be used to evaluate the change in vertical stress at the required depths within the compressible soil layer. Surcharge loads of wide lateral extent will result in constant value of $\Delta\sigma_z$. Most other loading conditions will result in $\Delta\sigma_z$ that varies with both depth and lateral location below the applied load. It is the responsibility of the engineer to determine the critical locations at which settlement will be evaluated.

5-3 SETTLEMENT CALCULATIONS.

5-3.1 Basic Formulation.

At the most basic level, settlement at the ground surface is equal to the change in thickness of the soil underlying a load. The change in thickness (ΔH) divided by the initial thickness (H) is equal to the vertical strain (engineering strain). Thus, settlement (s) is the sum of the vertical strain (ε_z) caused by $\Delta\sigma_z$ for each compressible soil layer multiplied by the initial thickness of each layer, or:

$$s = \Delta H = \sum_{i=1}^{n} \varepsilon_{z,i} H_i \qquad \textbf{(5-4)}$$

where:
H_i = thickness of each layer in same units as s.

Most settlement calculations can be split into a component related to the vertical strain and a component related to the initial layer thickness. This concept can be used understand the calculation procedures at a deeper level.

Many of the settlement prediction methods in this chapter use foundation geometry to define influence factors or to select the appropriate procedure. The shortest dimension of the foundation or loaded area will be designated as B while the longest dimension is L. The applied stress at the base of the foundation is indicated by q_0.

5-3.2 Soil Layers in Settlement Calculations.

Calculations of distortion settlement of fine-grained soils and total settlement of coarse-grained soils often treat the soil as one layer. In this case, the effect of the variation in strain with depth below the load is built into the calculation procedure and influence factors. This approach is illustrated by Figure 5-5(a).

In contrast, consolidation settlement of fine-grained soils is typically calculated by dividing the soil into multiple layers. The vertical strain is determined for each soil layer,

which allows the effects of load geometry and changing soil conditions to be considered explicitly. Figure 5-5(b) shows a layer of compressible soil divided into many thin layers of equal thickness. This method is flexible and theoretically sound but requires a large number of calculations that may be tedious if not automated. Figure 5-5(c) illustrates an approach in which the layer thickness increases with depth. This method recognizes that conditions change most quickly near the load. Regardless of the method used to define soil layers, soil properties within a given layer should be constant. Actual layer boundaries in the subsurface profile must supersede the layer division suggestions in Figure 5-5.

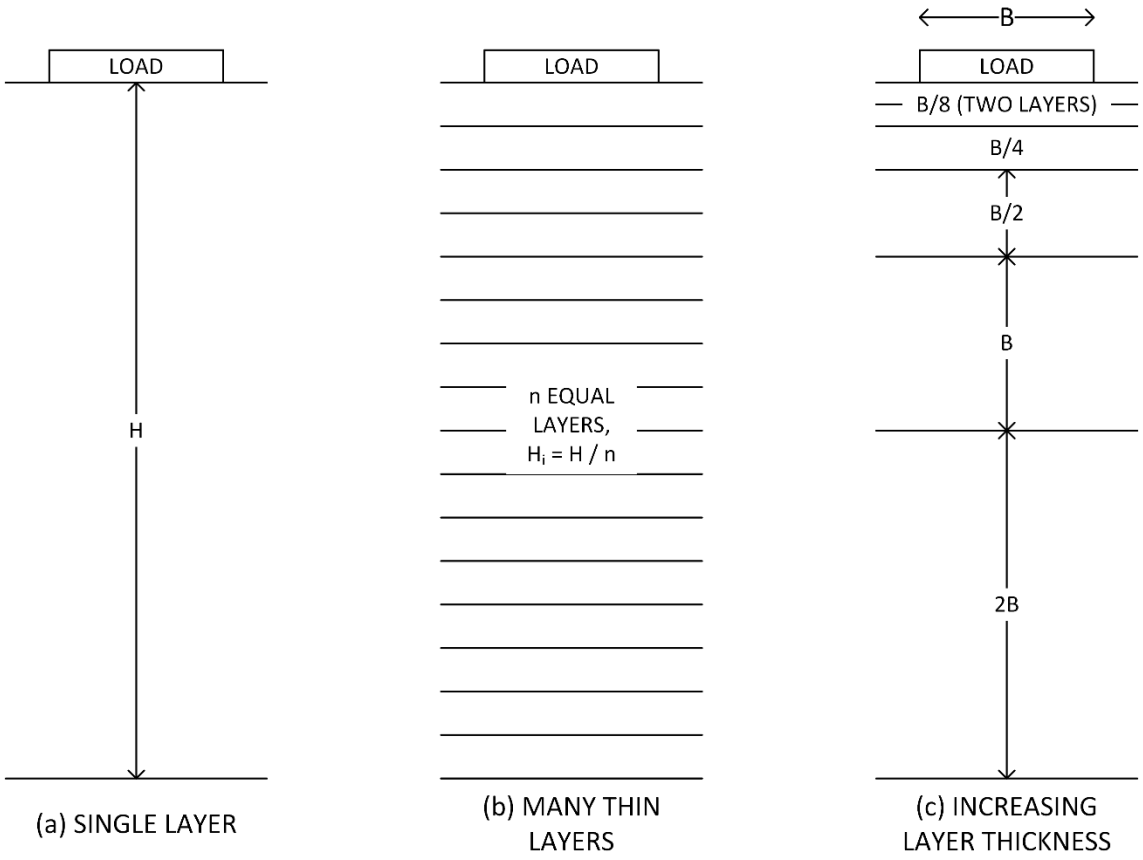

Figure 5-5 Three Possible Methods to Define Layers for Homogeneous Conditions

5-4 SETTLEMENT OF COARSE-GRAINED SOILS.

As indicated in Table 5-1, distortion and consolidation settlement occur in coarse-grained soils in a relatively short time span. If considered, secondary compression of these soils is typically estimated as a proportion of the calculated short-term settlement. For this reason, it is common practice to combine the components of settlement for coarse-grained soils. A variety of calculation methods are available. The soil properties

for most of the methods are based on the results of field tests, such as CPT or SPT, due to the variability and difficulty of sampling coarse-grained soils.

5-4.1 Short Term Settlement of Coarse-Grained Soil.

5-4.1.1 Elastic Method.

If the soil supporting a load is idealized as an elastic medium with a modulus equal to E_s and Poisson's ratio of ν, the resulting settlement (s) is:

$$s = \frac{q_0}{E_s}\left(B\mu_0\mu_1\right) \quad \textbf{(5-5)}$$

where:
q_0 = stress applied by load,
B = width of the applied load,
μ_0 = influence factor associated with embedment of the load, and
μ_1 = influence factor associated with the problem geometry and Poisson's ratio.

Some sources report Equation 5-5 with a ($1-\nu^2$) term. This term is often combined with the influence factors directly. When using charts and tables for μ_1, the engineer must check carefully to determine whether or not the ($1-\nu^2$) term has been included and what value of ν has been assumed, if appropriate.

The influence factors, μ_1 and μ_0, can be found using Figure 5-6 for the ratios of L/B, H/B, and D/B represented by the problem geometry. Note that H/B ratios can theoretically be very high, when a significant depth of soil is present below a loaded area. However, based on the concept of critical depth (see Section 4-2.1.5), the zone that contributes to settlement typically has a thickness of $4B$ to $5B$ below the loaded area. The use of H/B ratios greater than 4 to 5 may overestimate settlement.

The settlement predicted by Equation 5-5 will be directly related to the value of E_s, which is a difficult parameter to measure or obtain. General guidance for the selection of E_s for coarse-grained soils is provided in Table 5-2. Most of the correlations summarized in this table are based on the results of Standard Penetration Test (SPT) blow counts. An average SPT value (N') is used to predict settlement in coarse-grained soils. In most cases, N' is equal the average N_{60} value from the bottom of the loaded area to a depth of B below the load. In dense, saturated silty sands, the value of N'_{SM} is calculated as:

$$N'_{SM} = 15 + 0.5\left(N' - 15\right) \quad \textbf{(5-6)}$$

where:
N' = average N_{60} value.

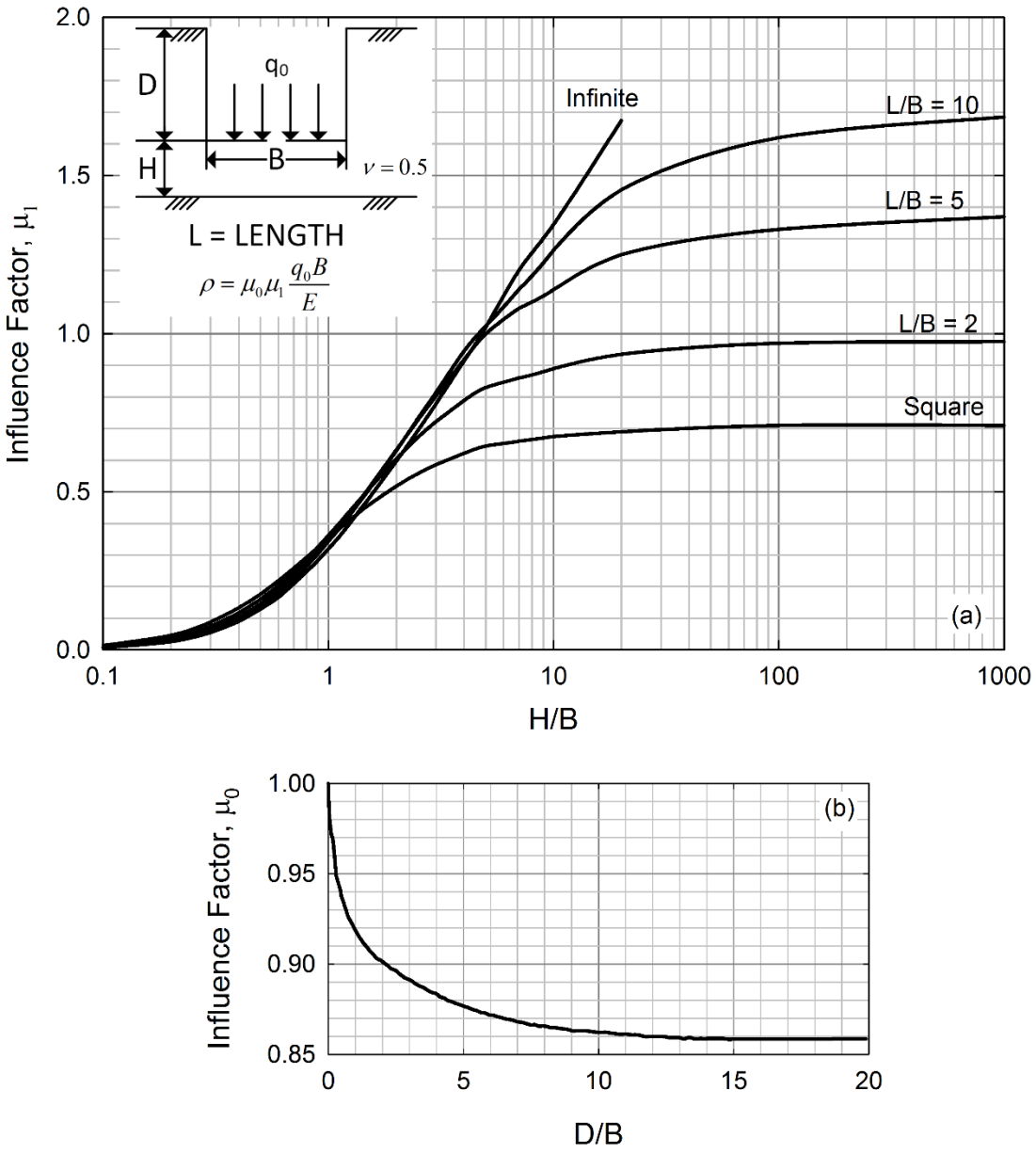

Figure 5-6 Elastic Influence Factors for $\nu = 0.5$ for (a) μ_I (after Giroud 1972) and (b) μ_0 (after Burland 1970)

Table 5-2 Approximate Modulus Values for Coarse-Grained Soil (after Bowles 1996, Duncan and Mokwa 2001)

Soil Conditions		Normally Consolidated	Preloaded or Compacted
Loose Sand	D_r = 40%	200 to 400 ksf	400 to 800 ksf
Medium Dense Sand	D_r = 60%	300 to 500 ksf	500 to 1000 ksf
Dense Sand	D_r = 80%	400 to 600 ksf	600 to 1200 ksf
Dry or Moist Sand		Lower: $E_s = 11.5\ (N'+7.5)$ Upper: $E_s = 15\ (N'+30)$	$E_s = 20\ (N'+42)$
Clayey, Silty, or Saturated Sand		Lower: $E_s = 5.6\ (N'+9)$ Upper: $E_s = 7.7\ (N'+15)$	Not available

Note: Correlations provide values of E_s in ksf units.

5-4.1.2 Schmertmann Method.

The Schmertmann Method is a common approach for the calculation of settlement for coarse-grained soils. This method uses typical patterns of vertical strain below a rigid foundation along with estimates of modulus based on either CPT or SPT. The variation of the strain influence factor (I_z) with depth is based on observations from model scale tests as well as numerical simulations. As shown in Figure 5-7, I_z increases with depth below the loaded area up to a peak value (I_{zp}) and then decreases to zero at a depth of $2B$ for square footings and $4B$ for continuous footings. The magnitude of I_{zp} is a function of the applied load and the effective vertical stress (σ'_{zp}) at the depth of the peak influence factor.

The compressibility of the coarse-grained soil is incorporated through layer moduli estimated from CPT or SPT results. The soil profile immediately below the foundation is divided into layers with relatively constant cone tip bearing resistance, q_c (or SPT blow count). Schmertmann et al. (1978) recommend that CPT q_c values should be multiplied by 2.5 to obtain E_s for axisymmetric ($L=B$) conditions. Similarly, CPT q_c values should be multiplied by 3.5 to obtain E_s for plane strain ($L/B > 10$) conditions.

Schmertmann (1970) provided multipliers to estimate q_c from SPT blow count, N. Robertson and Cabal (2014) found a similar correlation between CPT and SPT. Table 5-3 combines the SPT-CPT correlation with the $q_c - E_s$ correlation to provide approximate correlation between N_{60} and E_s. The general values in Table 5-3 can be replaced by regional correlations that follow the principles provided in Schmertmann (1970) and Robertson et al. (1983).

Table 5-3 Estimates of E_s based on SPT N_{60} values.

Soil Type	Approximate E_s Value (ksf)	
	Axisymmetric ($L = B$)	Plane Strain ($L/B > 10$)
Silt, sandy silt, slightly cohesive silt-sand mixtures	$10 \cdot N_{60}$	$14 \cdot N_{60}$
Clean fine to medium sand, and slightly silty sand	$17.5 \cdot N_{60}$	$24.5 \cdot N_{60}$
Coarse sand and sand with little gravel	$25 \cdot N_{60}$	$35 \cdot N_{60}$
Sandy gravel	$30 \cdot N_{60}$	$42 \cdot N_{60}$

The settlement (s) is then calculated for n layers as:

$$s = C_1 C_2 \left(q_0 - \sigma'_{z0}\right) \sum_{i=1}^{n} \left(\frac{I_{z,i}}{E_{s,i}} \right) \cdot z_i \qquad \textbf{(5-7)}$$

where:
C_1 = coefficient to correct for the effects of embedment,
C_1 = coefficient to correct for the effects of time,
q_0 = applied foundation pressure,
σ'_{z0} = the existing vertical effective stress at the bottom foundation,
$I_{z,i}$ = the average strain influence factor for the layer,
$E_{s,i}$ = the layer modulus, and
z_i = the layer thickness.

The correction for foundation embedment is found from:

$$C_1 = 1 - 0.5 \left(\frac{\sigma'_{z0}}{q_0 - \sigma'_{z0}} \right) \geq 0.5 \qquad \textbf{(5-8)}$$

The correction for time (t) in years after initial loading is:

$$C_2 = 1 + 0.2 \log \left(\frac{t}{0.1\,\text{yr}} \right) \qquad \textbf{(5-9).}$$

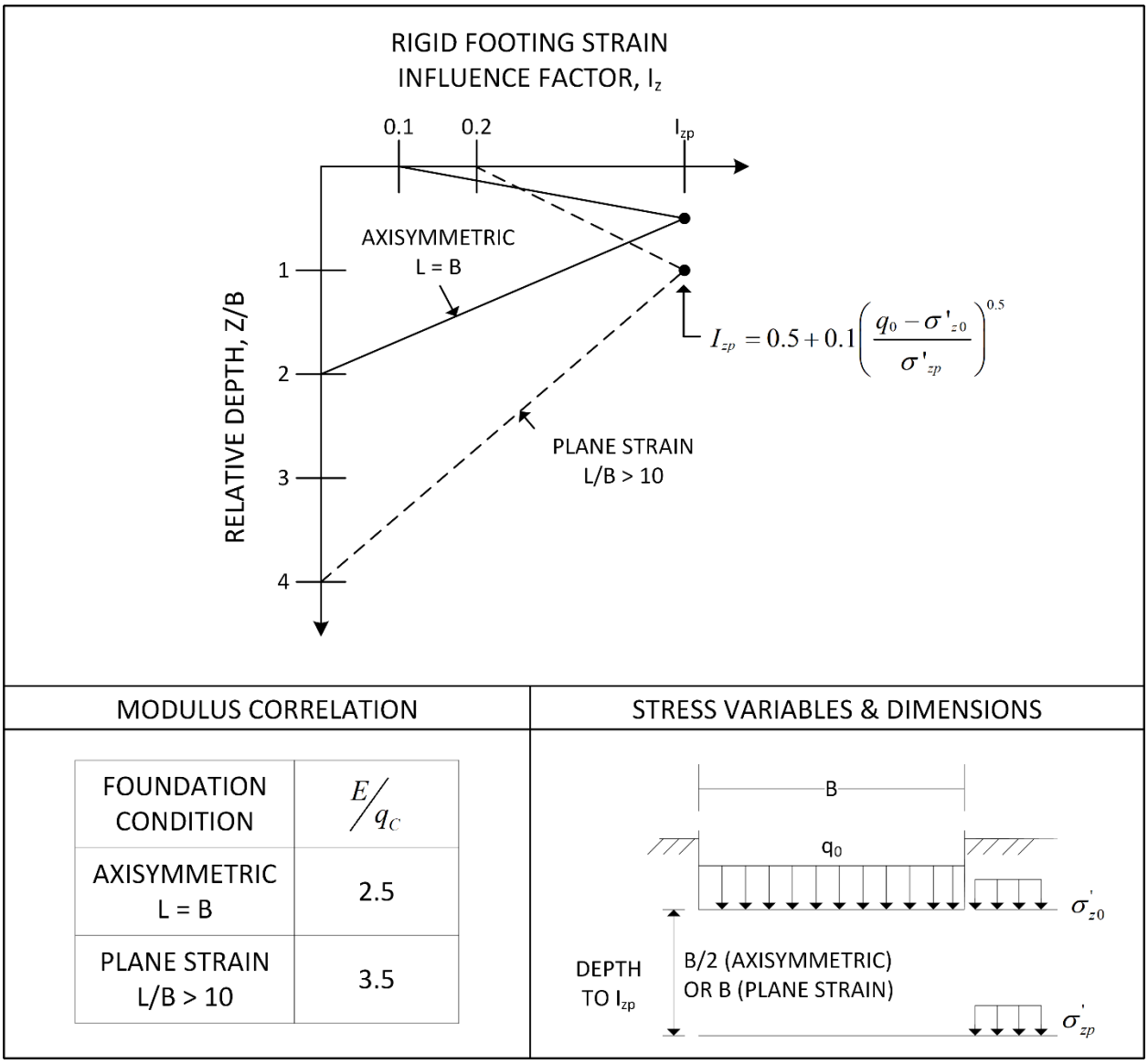

Figure 5-7 Influence Diagram and Modulus Correlation for Schmertmann CPT Method (Schmertmann 1970, Schmertmann et al. 1978)

5-4.1.3 Empirical Methods.

The difficulty of obtaining representative measures of compressibility or modulus for coarse-grained soils has led to the development of many different empirical methods. These methods are based on measurements and observations of load-settlement behavior from plate load tests as well as actual foundations. The underlying basis of these methods remains the elastic theory presented in Equation 5-5 but the soil modulus and influence factors are replaced with empirical correlations to SPT blow count and foundation dimensions. Three of the more popular relationships are provided in Table 5-4.

Table 5-4 Empirical Equations for Settlement of Coarse-Grained Soils

Method	Equation	Comments
Terzaghi and Peck (1967)	$s = \frac{6q_0}{N'}\left(\frac{B}{B+1}\right)^2$	s in inches B in ft q_0 in ksf A range of constants have been used.
Meyerhof (1965), Duncan and Buchiagnani (1987)	$s = \frac{2.5q_0}{(N'-1.5)C_B}$ $C_B = \begin{cases} 1.0 \text{ for } B < 4\,\text{ft} \\ \text{Interpolate for 4 to 12 ft} \\ 0.8 \text{ for } B \geq 12\,\text{ft} \end{cases}$	s in inches q_0 in ksf
Burland and Burbridge (1985), Terzaghi et al. (1996)[A]	$s = B^{0.75}\left(\frac{1.31}{N'^{1.4}}\right)q_0 C_s$ $C_s = \left[\frac{1.25(L/B)}{(L/B)+0.25}\right]^2$, $C_s \rightarrow 1.56$ for strip load	s in inches B in ft L in ft q_0 in ksf

A Settlement for load applied at the ground surface to normally consolidated sand. See the provided references for methods to correct for the effects of embedment and overconsolidation.

5-4.1.4 Accuracy and Reliability.

Tan and Duncan (1991) provide a helpful perspective for assessing the usefulness of the various settlement methods for coarse-grained soils. They evaluated the accuracy and "reliability"[11] of 12 SPT-based methods and the Schmertmann CPT Method using more than 90 case histories. The most accurate methods will make a reliably conservative estimate of settlement (i.e., greater than or equal to the actual value) only about half of the time. Likewise, more reliable methods, such as Terzaghi and Peck (1967), tend to greatly over-predict settlement, which is well-documented. Figure 5-8 can be used to select an appropriate method for determining settlement for each project based on considerations of accuracy and reliability. In cases where more accuracy is required, one of the methods that plots to the lower left may be used. Where it is critical not to exceed the calculated settlement, a method with higher reliability can be used.

[11] In this context, reliability was defined as the percentage of cases where the measured settlement was less than the predicted settlement. Reliability is not used in a formal probabilistic sense in this case.

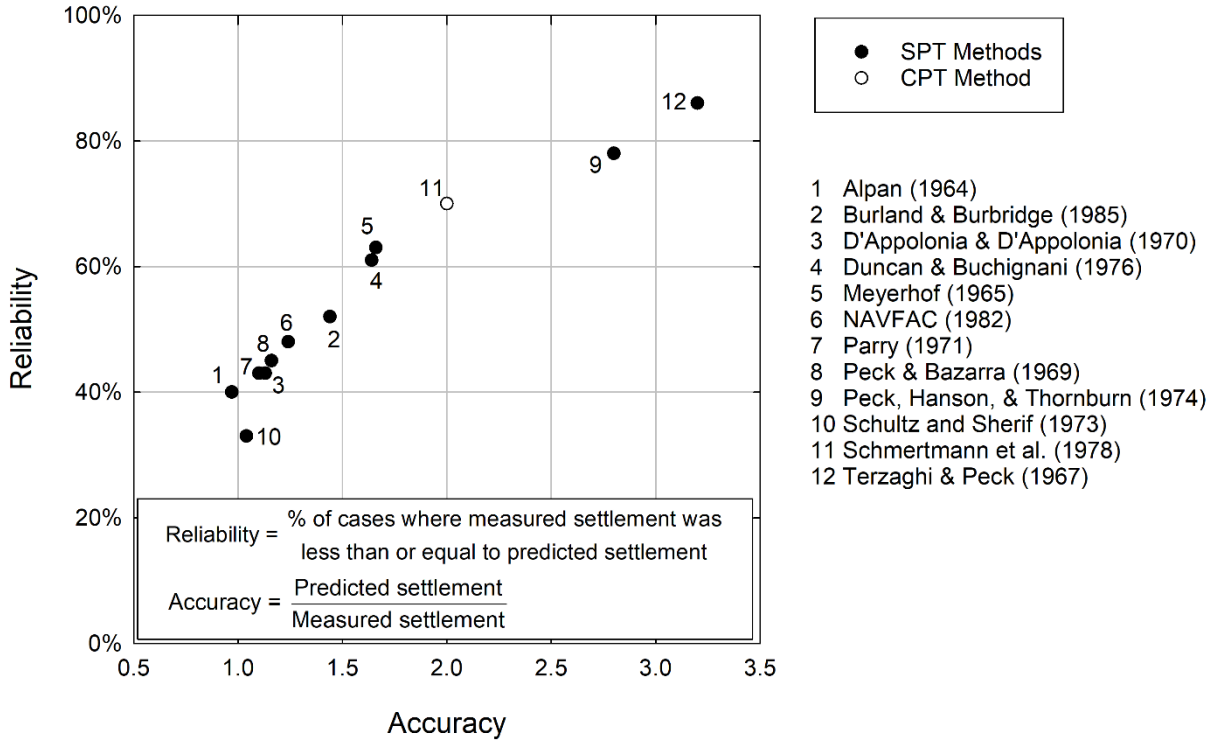

Figure 5-8 Comparison of Settlement Calculation Methods for Coarse-Grained Soils based on SPT Blow Count (after Tan and Duncan 1991)

5-4.2 Long-Term Settlement of Coarse-Grained Soil.

Creep or secondary compression of coarse-grained soil is sometimes considered by multiplying the calculated short-term settlement by a time-dependent influence factor. One suggested relationship is the creep factor (C_2) included in the Schmertmann Method. This factor can also be applied to the results of other coarse-grained settlement methods. Terzaghi et al. (1996) suggest a similar approach to calculate a creep factor (C_t) which is related to the magnitude of the applied stress. The resulting values of C_t for their approach are summarized in Figure 5-9 where the applied stress (q_0) is normalized by atmospheric pressure, P_a. For larger loads, this method predicts lower values of C_t because creep movements are a smaller proportion of the overall expected settlement. The creep factors for both methods have the same mathematical form. The total settlement at time (t) is found by multiplying the short-term settlement by the value of C_t.

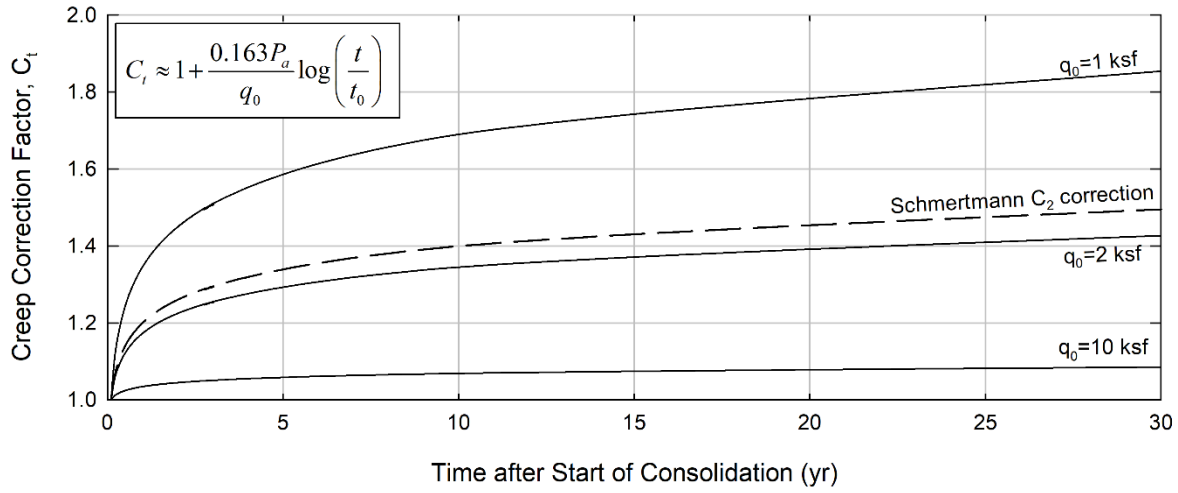

Figure 5-9 Creep Factors for Settlement of Coarse-Grained Soils (t_0 = 0.1 year and q_0 in same units as P_a) (after Schmertmann 1970, Terzaghi et al. 1996)

5-5 SETTLEMENT OF FINE-GRAINED SOILS.

5-5.1 Immediate Settlement of Fine-Grained Soils.

Immediate settlement of fine-grained soil is the result of one of two mechanisms: (1) “elastic” compression and volume change of the unsaturated soil or (2) distortion of saturated soil without volume change. Immediate settlement may be a significant proportion of settlement for unsaturated or heavily overconsolidated clay.

Similar to coarse-grained soil, immediate settlement of fine-grained soil can also be calculated using Equation 5-5 and the influence factors provided in Figure 5-6. For saturated clay, a Poisson’s ratio of 0.5, which is the value assumed in the construction of the figure. In most cases, the undrained modulus (E_u) should be used. Values of E_u can be measured in laboratory or field tests, such as the pressuremeter. Caution should be used as laboratory tests may underestimate the magnitude of E_u. Similarly, field tests typically load the soil horizontally rather than vertically, which may lead to erroneous results. Empirical correlations, such as those in Figure 5-10, can be used for comparison or in place of test values when appropriate. OCR can be estimated from empirical correlations or measured using one-dimensional consolidation tests as described in Chapter 3.

If the factor of safety against bearing capacity failure is less than about 3 (see DM 7.2), then the immediate settlement should be modified to account for partial yield of the soil. D’Appolonia et al. (1971) can be used to determine the appropriate adjustment for this condition.

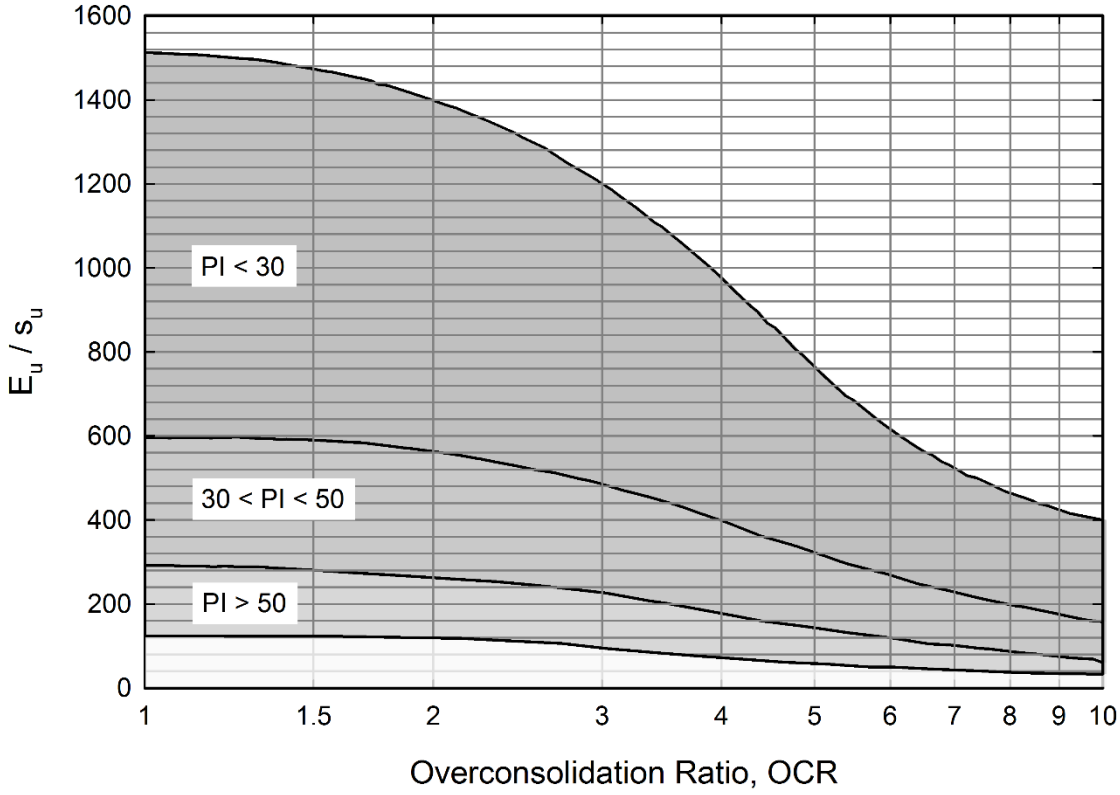

Figure 5-10 Correlation of Normalized Undrained Modulus and Overconsolidation Ratio (after Duncan and Buchignani 1987)

5-5.2 Primary Consolidation Settlement of Fine-Grained Soils.

Primary consolidation occurs as water flows from saturated soil and the excess pore water pressures caused by loading are able to dissipate. The magnitude of primary consolidation settlement can be predicted with reasonable accuracy when the soil's preconsolidation stress can be determined reliably and when the change in total stress can be accurately predicted. Settlement calculations involving recompression of overconsolidated soils tend to have the largest percent error. The amount of error for overconsolidated soils is related heavily to the quality of the samples used for consolidation tests, which affects the accuracy of the predicted recompression index and preconsolidation stress.

5-5.2.1 Use of Consolidation Test Results.

One-dimensional consolidation tests are used to predict swell, recompression, and virgin compression of soils. Specific details about the testing process are described in further detail in Section 3-2.6. The results of consolidation tests are typically plotted in terms of void ratio vs. vertical effective stress or vertical strain vs. vertical effective

stress.[12] In either case, vertical effective stress (σ'_z) will be plotted on a logarithmic scale.

Ideally, the soil behaves in the manner depicted in Figure 5-11 with log-linear segments describing the volume change or vertical strain that occurs as the vertical effective stress changes. The initial condition corresponds to initial vertical effective stress (σ'_{z0}) and either the initial void ratio (e_0) or to zero initial vertical strain, $\varepsilon_z = 0$. From the initial condition, the loading of overconsolidated soil results in relatively elastic recompression until the preconsolidation stress is reached. Any increase in σ'_z that extends beyond σ'_p results in plastic deformation or virgin compression. The slopes of these two lines are defined by the *recompression index* (C_r) and the *compression index* (C_c). A normally consolidated soil ($\sigma'_{z0} = \sigma'_p$) will experience virgin compression due to any increase in σ'_z.

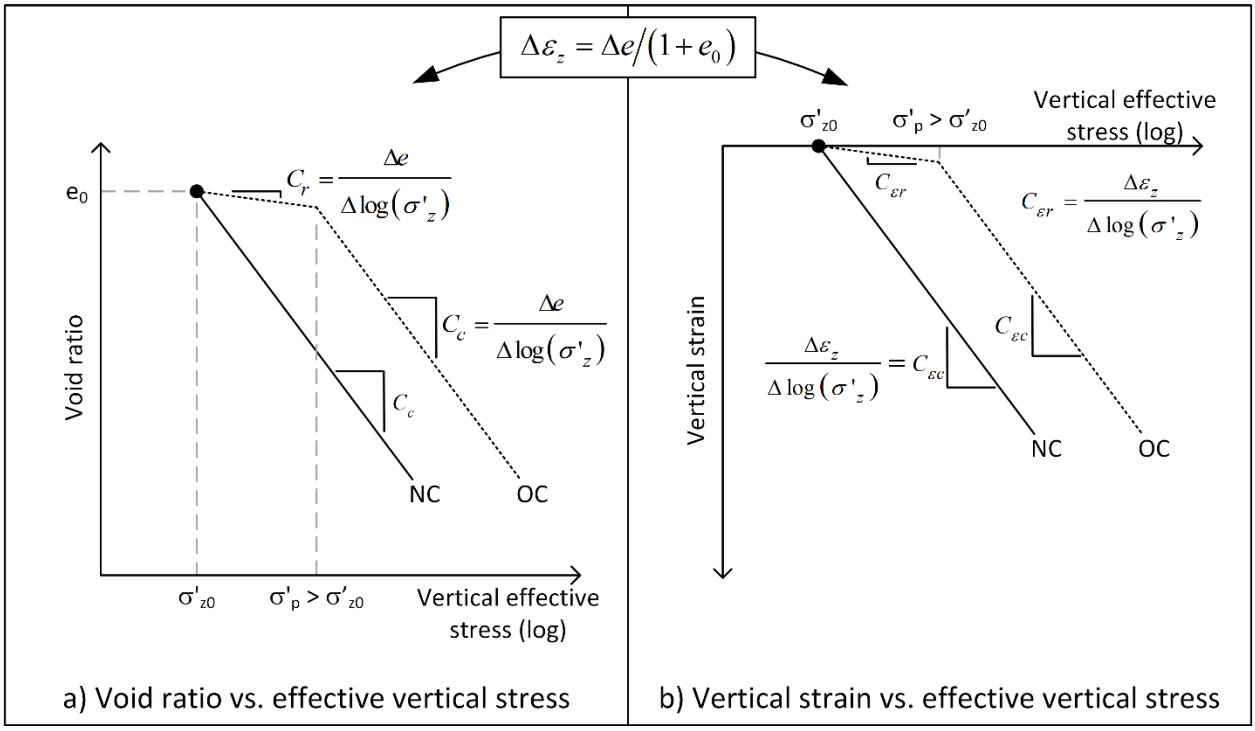

Figure 5-11 Consolidation Behavior based on (a) Void Ratio and (b) Vertical Strain

Interpretation of consolidation tests in terms of vertical strain is often a more practical approach. This method emphasizes that prediction of strain is the intent of the

[12] In old soil mechanics references, the water content was often used in lieu of void ratio. For saturated soils, the water content is equal to the void ratio divided by the specific gravity.

calculations and will be used in much of the discussion in this chapter. The *modified recompression index* ($C_{\varepsilon r}$) and the *modified compression index* ($C_{\varepsilon c}$) are defined as:

$$C_{\varepsilon r} = \frac{C_r}{1+e_0} \quad \textbf{(5-10)}$$

and

$$C_{\varepsilon c} = \frac{C_c}{1+e_0} \quad \textbf{(5-11)}$$

where:
C_r = recompression index,
C_c = compression index, and
e_0 = initial void ratio.

Methods for determining C_r, C_c, and σ'_p from laboratory tests are illustrated in Figure 3-12. Many useful correlations have been developed between C_c and soil index properties. Table 5-5 provides a list of some of these correlations. Azzouz et al. (1976) found that correlations to e_0 produced the most accurate prediction of C_c. Nine of the correlations are compared in Figure 5-12. Additional correlations can be found in Chapter 8.

The recompression index is typically 5 to 10% of the magnitude of C_c. Typical values for C_r fall in the range of 0.015 to 0.035 with nearly all results between 0.005 and 0.05 (Leonards 1976).

Table 5-5 Correlations for Compression Indices

Basis	Correlation	Applicable soil type	Source
LL	$C_c = 0.009 \cdot (LL - 10)$	Inorganic soils with sensitivity less than 4	Terzaghi and Peck (1967)
	$C_c = 0.007 \cdot (LL - 7)$	Remolded clays	Skempton (1944)
	$C_c = 0.006 \cdot (LL - 9)$	Predominantly lean to fat clay	Azzouz et al. (1976)
e_0	$C_c = 1.15 \cdot (e_0 - 0.35)$	All clays	Nishida (1956)
	$C_c = 0.3 \cdot (e_0 - 0.27)$	Inorganic soil; silt; silty clay; some clay	Hough (1957)
	$C_c = 0.75 \cdot (e_0 - 0.5)$	Very low plasticity soils	Sowers (1970)
	$C_{ec} = 0.15 \cdot e_0 + 0.017$	All clays	Elnaggar and Krizek (1971)
	$C_c = 0.4 \cdot (e_0 - 0.25)$	Predominantly lean to fat clay	Azzouz et al. (1976)
w_n	$C_c = 0.01 \cdot w_n$	Chicago clays	Osterberg (1972) (in Azzouz et al. 1976)
	$C_c = 0.0115 \cdot w_n$	Organic soils, peat	Moran et al. (1958)
	$C_{ec} = (0.1 + 0.006 \cdot (w_n - 25))$	Varved clays	Prior NAVFAC DM 7.1
	$C_c = 17.6 \times 10^{-5} \cdot w_n^2 + 5.93 \times 10^{-3} \cdot w_n - 0.135$	Chicago clays	Peck and Reed (1954)
	$C_c = 0.01 \cdot w_n - 0.05$	Predominantly lean to fat clay	Azzouz et al. (1976)

Note: Liquid limit (LL) and natural water content (w_n) are in percent.

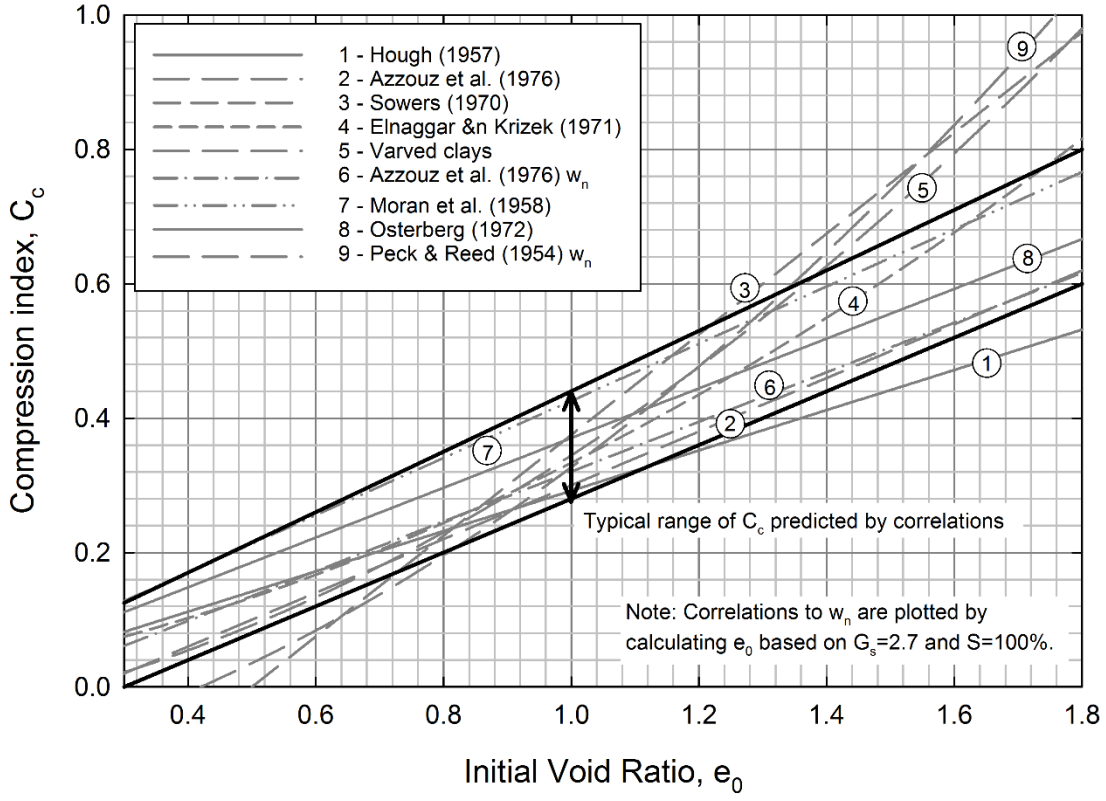

Figure 5-12 Common Compression Index Correlations

5-5.2.2 Magnitude of Primary Consolidation.

Primary consolidation settlement (s_c) should be determined for each compressible layer. Thick layers should be divided into a series of sublayers (e.g., Figure 5-5b and c). For each layer, the appropriate equation for s_c must be selected based on whether the soil is normally or overconsolidated and the relative magnitude of the change in vertical stress.

For normally consolidated soil ($\sigma'_{z0} \approx \sigma'_p$), calculate s_c as:

$$s_c = \left(C_{\varepsilon c} \log \left(\frac{\sigma'_{z0} + \Delta\sigma_z}{\sigma'_{z0}} \right) \right) H \quad \textbf{(5-12)}$$

where:
$C_{\varepsilon c}$ = modified compression index,
σ'_{z0} = initial vertical stress at the midpoint of the soil layer or sublayer,
$\Delta\sigma_z$ = change in vertical stress at layer midpoint, and
H = initial thickness of the soil layer or sublayer.

For overconsolidated soil layers in which the final stress is less than or equal to the preconsolidation stress ($\sigma'_{z0} + \Delta\sigma_z \leq \sigma'_p$), calculate s_c as:

$$s_c = \left(C_{\varepsilon r} \log \left(\frac{\sigma'_{z0} + \Delta\sigma_z}{\sigma'_{z0}} \right) \right) H \quad \textbf{(5-13)}$$

where:
$C_{\varepsilon r}$ = modified recompression index.

For overconsolidated soil layers in which the final stress is greater than the preconsolidation stress $\sigma'_{z0} + \Delta\sigma_z > \sigma'_p$), calculate s_c as:

$$s_c = \left(C_{\varepsilon r} \log \left(\frac{\sigma'_p}{\sigma'_{z0}} \right) + C_{\varepsilon c} \log \left(\frac{\sigma'_{z0} + \Delta\sigma_z}{\sigma'_p} \right) \right) H \quad \textbf{(5-14)}$$

where:
σ'_p = preconsolidation stress.

Equations 5-12 to 5-14 all follow a consistent pattern in which the compression or recompression index is multiplied by the logarithm of the change in stress to obtain the vertical strain. The strain is then multiplied by the layer thickness to obtain the change in thickness or expected settlement of the layer. In each of these equations, $C_{\varepsilon c}$ and $C_{\varepsilon r}$ can be replaced with C_c and C_r along with the initial void ratio, if desired, using Equations 5-10 and 5-11. Example calculations are shown in Figure 5-13.

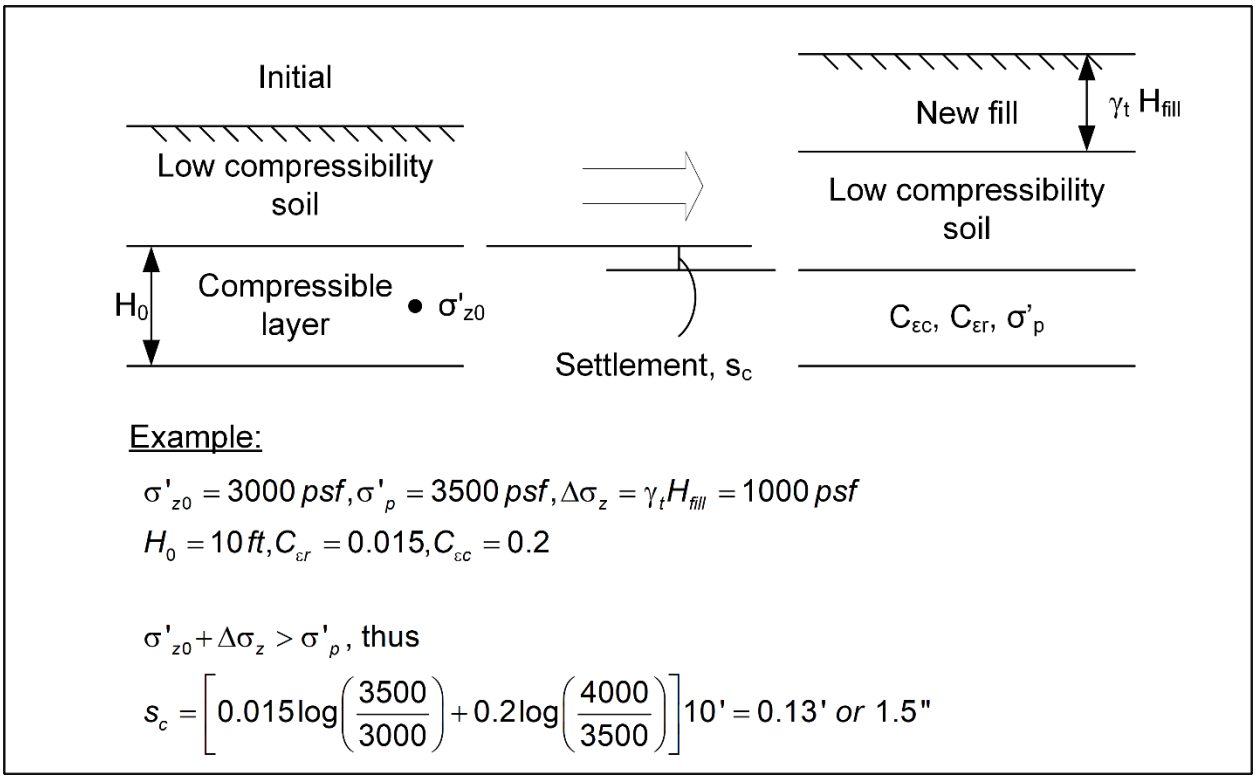

Figure 5-13 Primary Consolidation Example

5-5.2.3 Typical Construction Process.

An example of the primary consolidation caused by changes in stress associated with typical construction processes is illustrated in Figure 5-14. In this example, the clay is overconsolidated by past loading. The construction process involves lowering the groundwater level, excavating for a basement level, and applying the structural load. Some aspects of construction will cause increases in effective stress and settlement. Other phases, such as excavation and groundwater rise, will result in swelling. As noted, the amount of settlement or swell experienced during the first phases of construction will depend on the rate of construction as well as the rate at which pore water pressures dissipate in the clay layer.

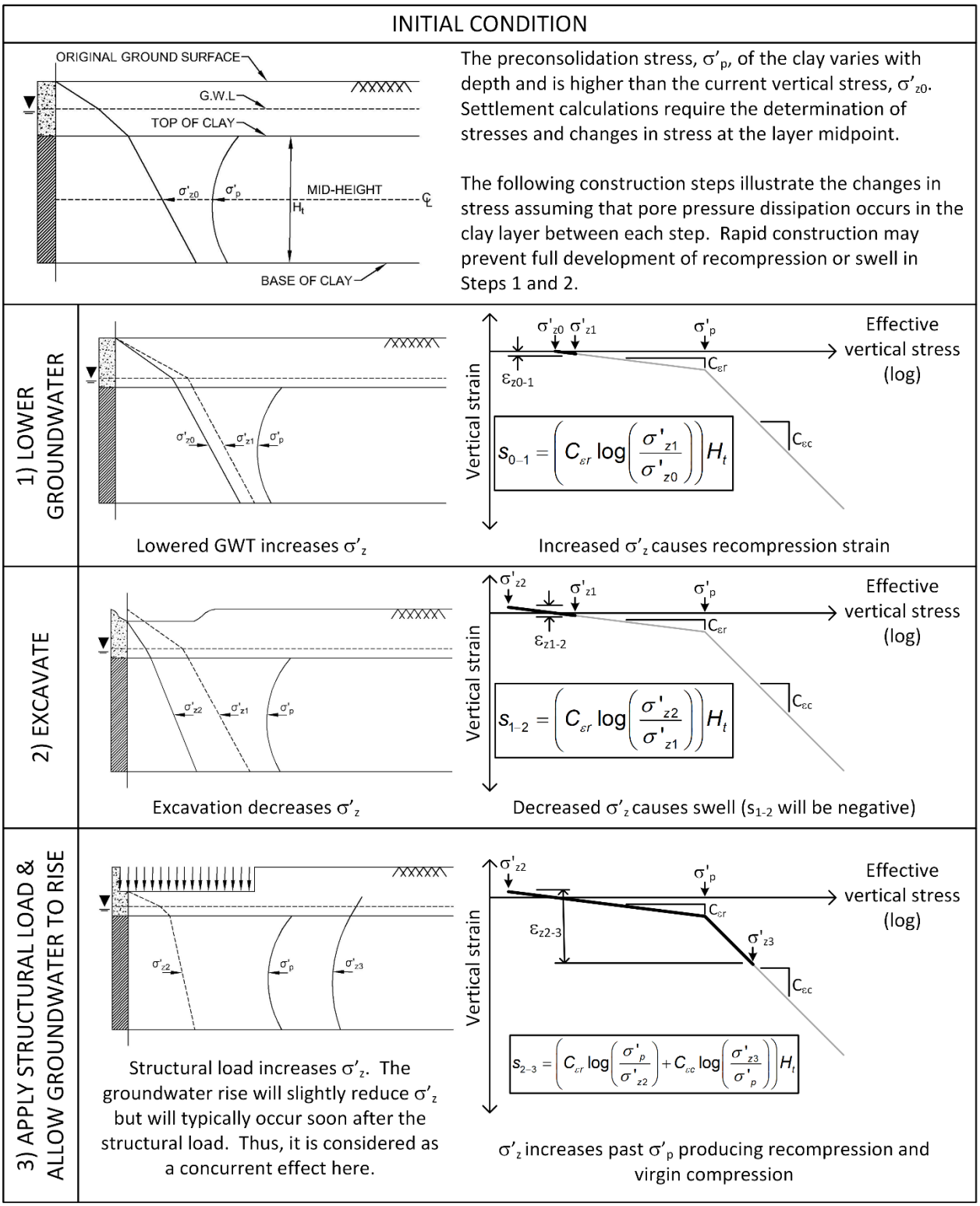

Figure 5-14 Vertical Movements during a Typical Construction Process

5-5.2.4 Corrections to the Magnitude of Consolidation Settlements.

Settlement of overconsolidated clay layers may be overestimated using Equations 5-13 and 5-14 for loads of limited lateral extent. For cases where the width of the load is less than four times the thickness of the clay layer, conditions deviate significantly from one-dimensional consolidation. Leonards (1976) recommended that the corrected primary consolidation settlement can be found by multiplying the calculated value (Equation 5-13 or 5-14) by a correction factor, α. Values of α can be found using Figure 5-15.

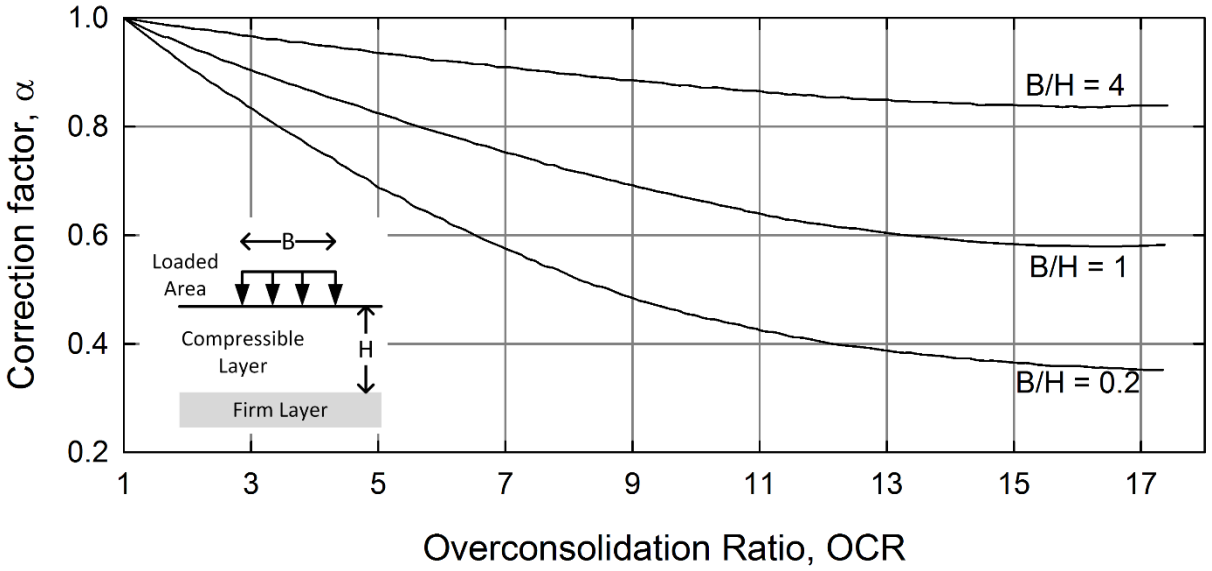

Figure 5-15 Correction Factor for Overconsolidated Clays and Loads of Limited Lateral Extent (after Leonards 1976)

5-5.3 Time Rate of Primary Consolidation.

The time rate of primary consolidation is considered for situations where predicted settlement exceeds tolerable values. In these cases, treatment of the foundation soil, such as acceleration of consolidation or placement of a surcharge to increase in preconsolidation stress, may be considered. Knowledge of the settlement rate or consolidation completed at a particular time is important for planning remedial measures for structures damaged by settlement.

Time rate calculations can be performed with greater accuracy and flexibility using numerical methods, such as the finite difference method. Various computer programs are available for this purpose. The analytical methods presented in this section are useful for understanding time rate of settlement concepts and checking the results of numerical methods.

The time rate of consolidation is typically assessed starting with one-dimensional theory applied to vertical drainage. The average *degree of consolidation* ($\bar{U}_z$) is the average

percentage of the excess pore pressure that has dissipated at a particular time (t) following the addition of a load. The amount of settlement experienced at the ground surface is typically assumed to be proportional to $\bar{U}_z$. The value of $\bar{U}_z$ can be related to a time factor (T) for a given set of conditions. The time factor for vertical drainage (T_v) is calculated as:

$$T_v = \frac{c_v t}{H_{dr}^2} \quad \textbf{(5-15)}$$

where:
c_v = coefficient of consolidation for the soil layer in the vertical direction,
t = time after application of load, and
H_{dr} = drainage path length.

The relationship between T_v and $\bar{U}_z$ is provided in Figure 5-16.

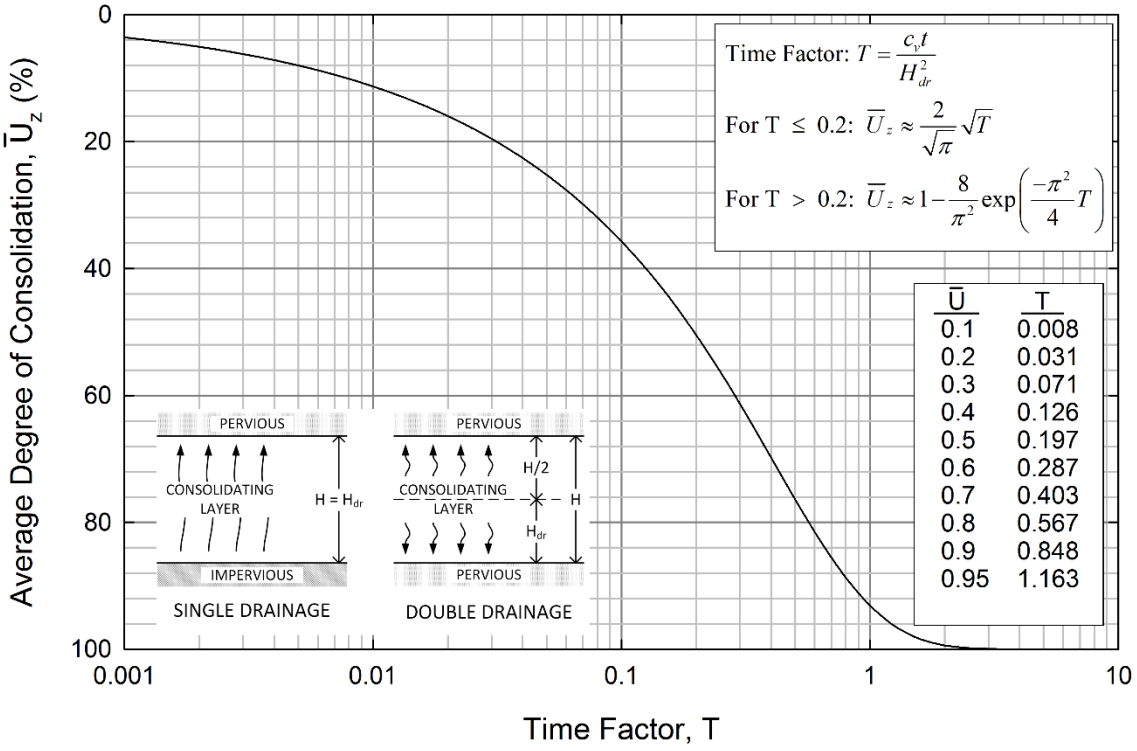

Figure 5-16 Degree of Consolidation for Instantaneous Uniform Loading and One-Dimensional Flow

Two conditions are typically considered for vertical drainage. Single (or one-way) drainage refers to conditions where water can flow one direction to leave the consolidating soil layer as shown in the inset to Figure 5-16. Double (or two-way)

drainage occurs when pervious layers lie above and below the consolidating layer, and H_{dr} is half of the layer thickness (H) in this case.

The *degree of compression* (U_z) is the amount of pore water pressure that has been dissipated at a particular depth within the soil layer. The degree of compression will vary with time and depth within the consolidating layer as illustrated in Figure 5-17. It can be used to estimate the remaining excess pore pressures at any depth and time following application of a change in vertical stress. The upper half of this figure can be used for single drainage conditions.

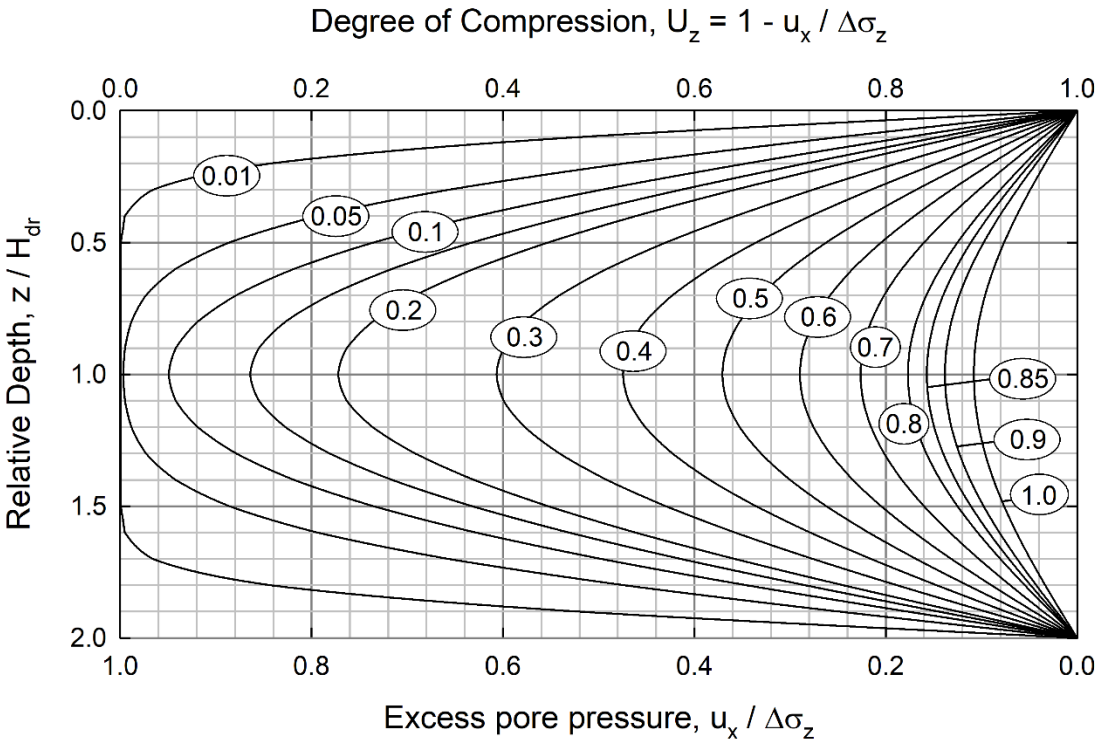

Figure 5-17 Degree of Compression and Excess Pore Pressure (Contours Indicate the Time Factor)

5-5.3.1 Effect of Initial Excess Pore Pressure Distribution.

The rate of consolidation can be affected by the initial distribution of excess pore water pressure, especially for single drainage conditions. The degrees of consolidation and compression predicted in Figure 5-16 and Figure 5-17 are appropriate for a uniform distribution of initial excess pore pressure, which is a reasonable assumption for relatively wide loads, regardless of the type of drainage.

Other scenarios, such as foundation loading and consolidation of hydraulic fill, can result in a distribution of initial excess pore pressure that is not constant with depth.

Figure 5-16 is also appropriate for double drainage when the distribution of initial u_x varies linearly. Solutions for single drainage and linearly varying distributions of initial u_x can be found in Terzaghi et al. (1996). However, for these more complex loading conditions, numerical solutions are preferred.

5-5.3.2 Accuracy of Time Rate Predictions.

The time rate of primary consolidation observed in field measurements is often faster than that predicted by the methods described in this section. This discrepancy is the result of a number of effects.

The theoretical conditions of one-dimensional consolidation and vertical drainage rarely mimic the *in situ* conditions. In most cases, loading and subsequent drainage is actually two or three-dimensional, which tends to increase the time rate of consolidation. As the width of the loaded area becomes small with respect to the thickness of the compressible layer, consolidation proceeds much more quickly. Figure 5-18 allows the time required to reach a degree of consolidation of either 50% or 90% to be corrected for two- and three-dimensional effects. The results are plotted for soil profiles with an impermeable layer below the compressible soil and for those with an underlying permeable layer. See Davis and Poulos (1972) for further details on these effects. Numerical methods can be used to account for some of these differences; however, many of the common programs used for consolidation calculations only consider one-dimensional flow.

Many clay soils contain thin seams of sand and silt, which have significantly higher permeability. These seams provide internal drainage boundaries, greatly reducing the maximum vertical drainage path length. For example, the presence of a single additional drainage layer can increase the time rate of settlement by a factor of four. In addition, soil deposits tend to have a higher horizontal hydraulic conductivity, which coupled with three-dimensional effects can increase the settlement rate. Figure 5-19 provides a simple means to account for effect of anisotropy in the coefficient of consolidation on the time required to reach 50% consolidation.

Finally, disturbance of soil samples tends to decrease the coefficient of consolidation measured in laboratory tests. Even high-quality samples and tests have some degree of disturbance, leading to lower c_v and slower time rate of settlement predictions.

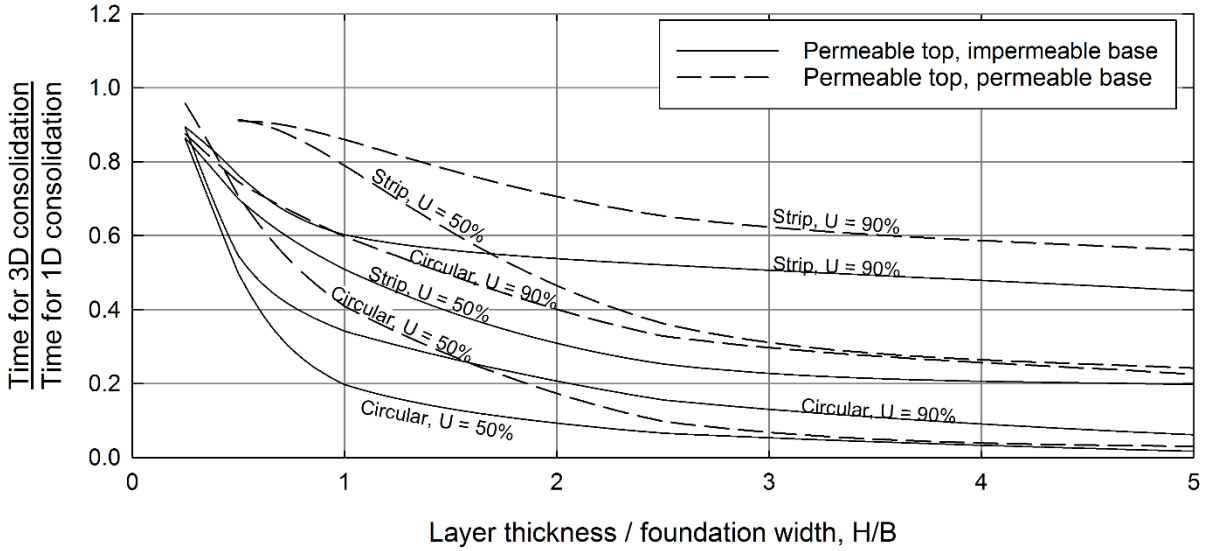

Figure 5-18 Effect of Load Geometry on Time Rate of Consolidation (after Davis and Poulos 1972)

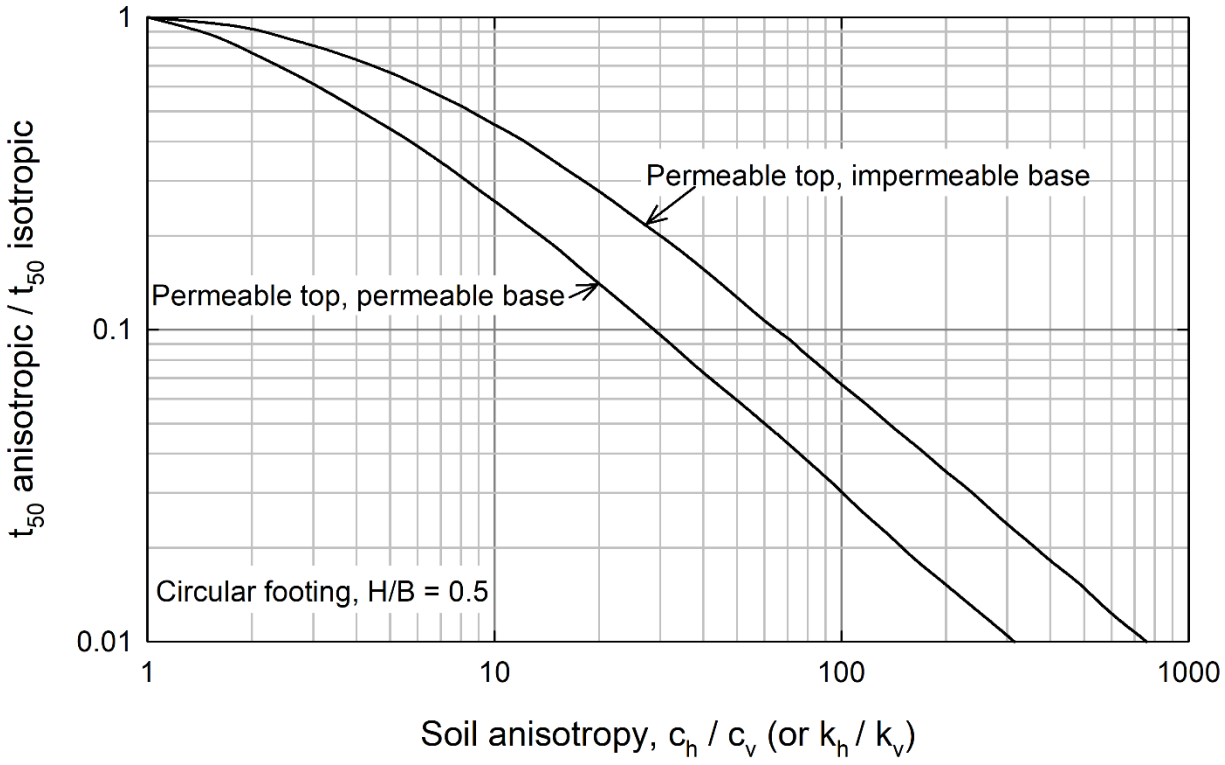

Figure 5-19 Effect of Anisotropy on Time Rate of Consolidation (after Davis and Poulos 1972)

5-5.3.3 Gradual Load Application.

The length of the construction period or the amount of time required to apply the load can also affect the time rate of primary consolidation. Gradual load application modifies the relationship between the degree of consolidation and the time factor. Figure 5-20 provides a method to account for gradual loading.

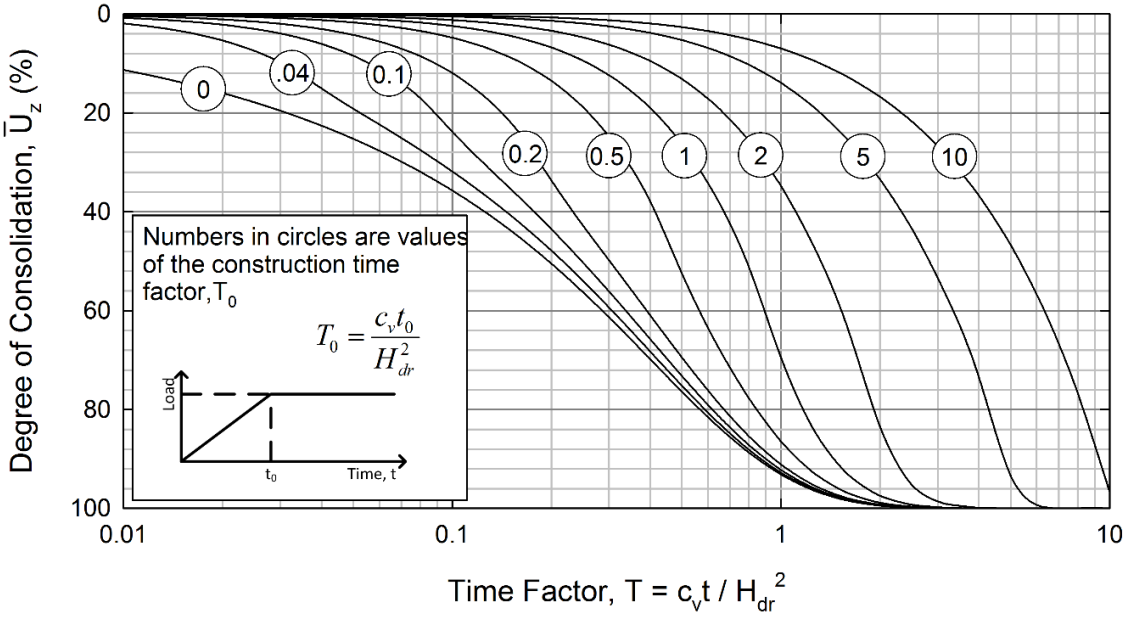

Figure 5-20 Degree of Consolidation for Gradual Load Application for Vertical Drainage (after Olson 1977)

5-5.3.4 Coefficient of Consolidation.

The coefficient of consolidation can be estimated based on index properties (see Chapter 8), calculated from volume change vs. time measurements in laboratory tests, or inferred from field measurements of pore pressure dissipation.

5-5.3.4.1 Laboratory Measurement of Coefficient of Consolidation.

The vertical coefficient of consolidation, c_v, is often found from data obtained using incrementally loaded one-dimensional consolidation tests on vertically oriented specimens. The coefficient of consolidation in other directions can be determined by trimming and mounting specimens in other orientations in the testing equipment. Regardless of the specimen orientation, the data is normally assessed using either the Casagrande or the Taylor method, which are described in Figure 5-21. Volume change measured during the consolidation phase of shear strength tests can also be used with these procedures. Other methods exist for determining c_v from incrementally loaded consolidation tests, and a single equation can be used to determine c_v from constant rate of strain consolidation tests.

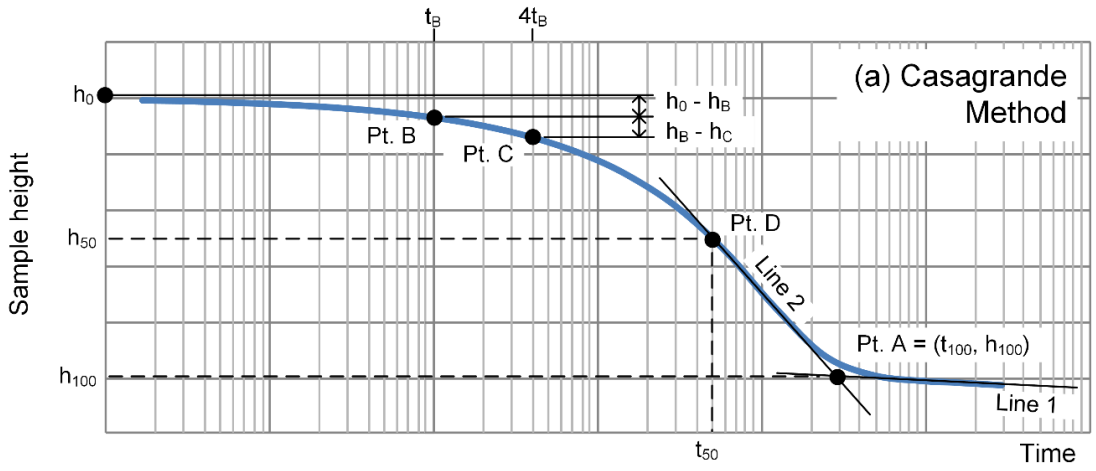

Instructions:

-Plot height (or void ratio) v. time (log) data
-Plot Line 1 through final linear portion of data
-Plot Line 2 through middle steepest portion of data
-Pt. A is the intersection of Lines 1 and 2 with coordinates, t_{100} and h_{100}.
-Pick two points, B and C, at low time such that $t_c = 4t_b$.
-Find the initial increment height, $h_0 = 2h_B - h_C$ (initial portion of the time curve is parabolic).
-Calculate $h_{50} = (h_0 - h_{100}) / 2$.
-Plot Pt. D on time curve at h_{50}. Read t_{50} from the plot.
-Calculate the coefficient of consolidation, c_v.

$$c_v = 0.197 h_{dr}^2 / t_{50}$$

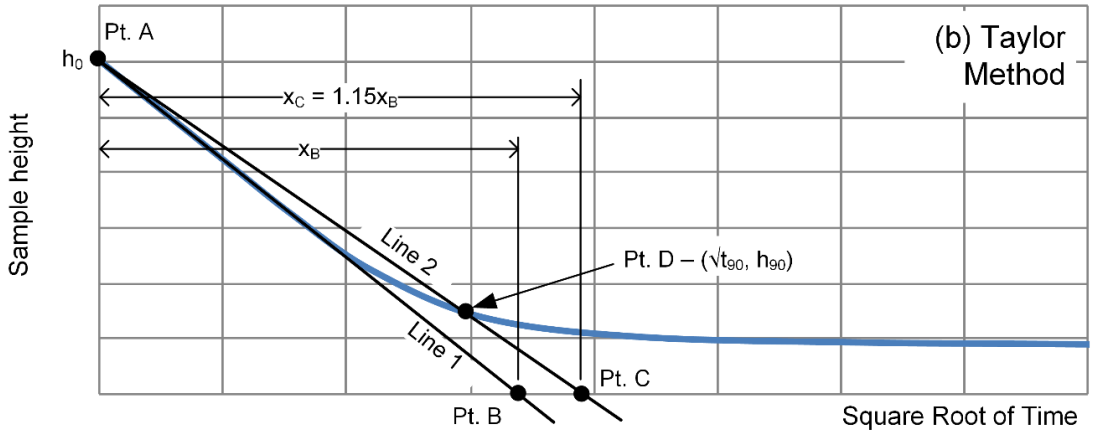

Instructions:

-Plot height (or void ratio) v. √time from data
-Plot Line 1 initial linear portion of data to find the intersection point with the y-axis at Pt. A.
-Pt. B is the intersection point with the √time axis.
-Scale x_B from the plot and multiply by 1.15 to find x_C.
-Connect Pts. A and C with Line 2.
-Plot Pt. D ($\sqrt{t_{90}}$, h_{90}) where Line 2 crosses the data.
-Calculate the coefficient of consolidation, c_v.

$$c_v = 0.848 h_{dr}^2 / t_{90}$$

-If desired, h_{100} is equal to:

$$h_{100} = h_0 - \frac{h_0 - h_{90}}{0.9}$$

Figure 5-21 Determination of Coefficient of Consolidation from Laboratory Data (Note: the y-axis can also be plotted as volume or void ratio)

5-5.3.4.2 Use of Field Measurements.

Field observations of excess pore pressure dissipation with time can be used to measure the *in situ* coefficient of consolidation. At any given time after loading, the ratio of excess pore pressure to change in vertical stress ($u_x/\Delta\sigma_v$) can be measured and plotted at the appropriate normalized depth on Figure 5-17. The corresponding time factor can be estimated from the contours, and c_v can be calculated using Equation 5-15.

An example of both laboratory and field determination of c_v is provided in Figure 5-22.

5-5.3.5 Time Rate of Consolidation for Layered Profiles.

The consolidating soil may contain layers with varying values of c_v. In this situation, the behavior of a layered system can be approximated by conversion to an equivalent single layer system using the following procedure:

1. Select any layer (i) with properties $c_{v,i}$ and H_i.
2. Transform the thickness of every other layer with properties $c_{v,n}$ and H_n to an equivalent layer with the soil properties of layer i as follows:

$$H'_n = H_n \sqrt{\frac{c_{v,i}}{c_{v,n}}} \quad \textbf{(5-16)}$$

3. Calculate the total thickness (H'_t) of the transformed system as:

$$H'_t = \sum H'_n \quad \textbf{(5-17)}$$

4. Treat the system as a single layer of thickness (H'_t) with coefficient of consolidation ($c_{v,i}$),
5. Use the appropriate method, such as Figure 5-16, to determine the percent consolidation at various times.

The complexity introduced by multi-layer problems is well-suited to the use of numerical analysis for the calculation of time rate of settlement. An example of multi-layer time rate of consolidation calculation is provided in Figure 5-23.

(a) Example Conditions

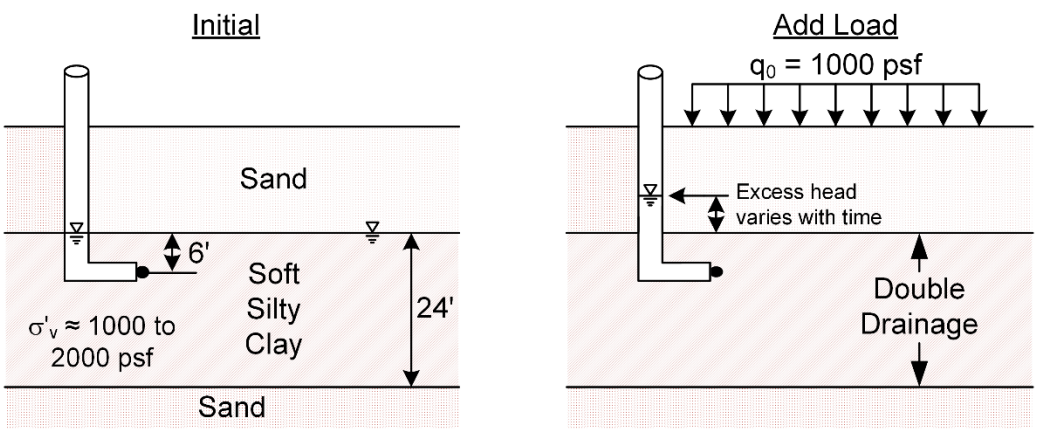

(b) Lab Measurements — From load increment of σ'_v from 1000 to 2000 psf in 1D consolidation test

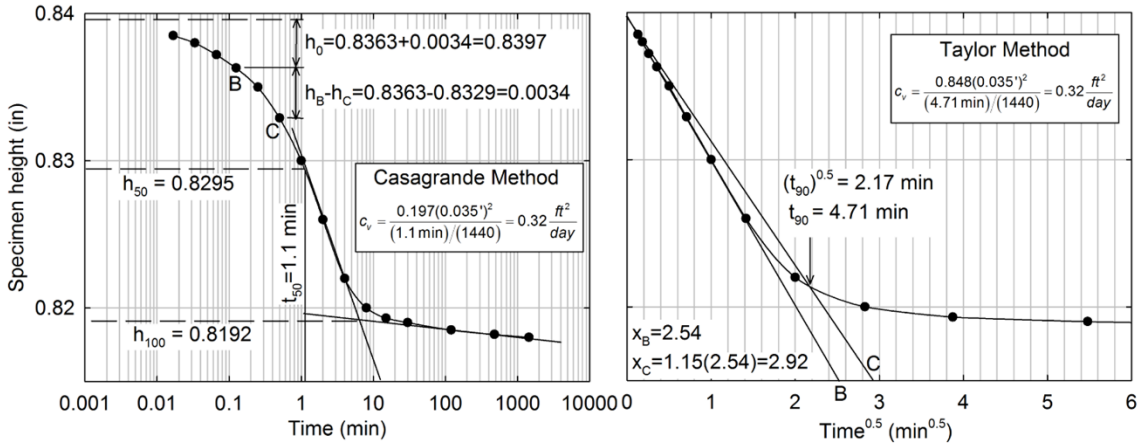

(c) Field Measurements

Piezometer Location: $H_{dr} = \frac{24'}{2} = 12'$ $\frac{z}{H_{dr}} = 0.5$ $U_z = 1 - \frac{u_x}{q_0}$

Time (days)	Excess Head in Piezometer (ft)	Excess u (psf)	U_z	T
30	12'	749	0.25	0.09
100	8'	499	0.5	0.26

$$c_v = \frac{\Delta T}{\Delta t} H_{dr}^{\,2} = \frac{(0.26 - 0.09)}{(100\,days - 30\,days)}(12')^2 = 0.35\,ft^2/day$$

Figure 5-22 Determination of c_v from Lab and Field Data

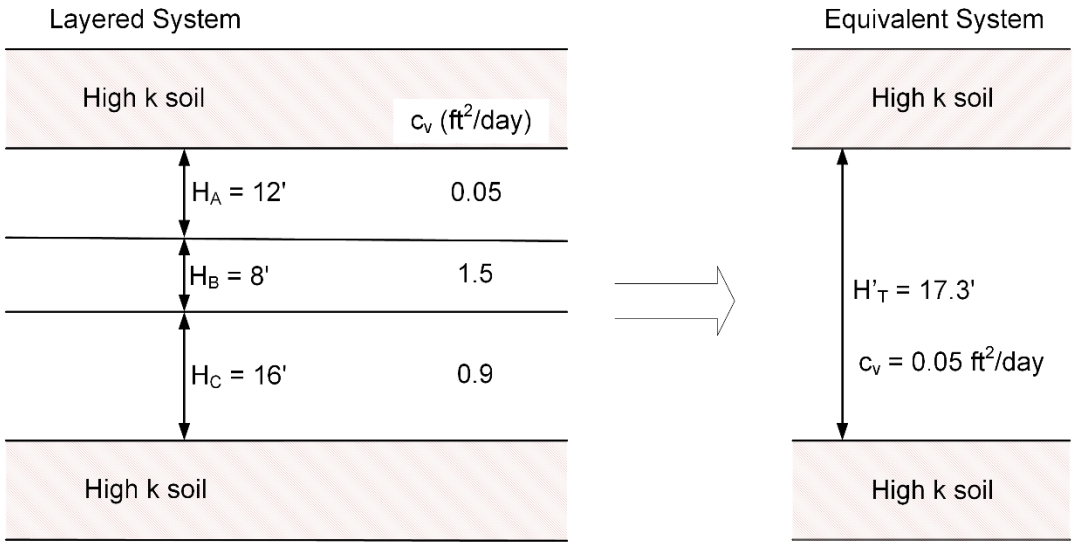

Transform layer B : $H'_B = H_B\left(\frac{c_{vA}}{c_{vB}}\right)^{1/2} = 8'\left(\frac{0.05}{1.5}\right)^{1/2} = 1.5'$

Transform layer C : $H'_C = H_C\left(\frac{c_{vA}}{c_{vC}}\right)^{1/2} = 16'\left(\frac{0.05}{0.9}\right)^{1/2} = 3.8'$

Total : $H'_T = H'_A + H'_B + H'_C = 12' + 1.5' + 3.8' = 17.3'$

Assuming double drainage, the percent consolidation could be found for one year as:

$$T_{1YR} = \frac{c_v t}{H_{dr}^2} = \frac{(0.05\,\text{ft}^2/\text{day})(365\,\text{days})}{(17.3'/2)^2} = 0.24$$

From Fig. 5-15, $\bar{U}_z$ = 56%

Figure 5-23 Multi-layer Consolidation Example

5-5.4 Secondary Compression of Fine-Grained Soils.

Secondary compression settlement (s_s) occurs as soil particles rearrange and the soil structure creeps under constant vertical effective stress. For practical purposes, secondary compression can be assumed to occur after the end of primary consolidation and to follow a relatively linear trend with respect to time on a log scale such that:

$$s_s = \left(\frac{C_\alpha}{1+e_0} \log\left(\frac{t}{t_p} \right) \right) H_0 = \left(C_{\varepsilon\alpha} \log\left(\frac{t}{t_p} \right) \right) H_0 \quad \textbf{(5-18)}$$

where:
C_α = secondary compression index,
$C_{\varepsilon\alpha}$ = modified secondary compression index,
e_0 = initial void ratio,
t = time after loading,
t_p = time required to finish primary consolidation, and
H_0 = initial layer thickness.

Values of C_α or $C_{\varepsilon\alpha}$ can be obtained from the results of a one-dimensional consolidation test that is allowed to creep for a significant length of time past the end of primary consolidation. The magnitude of C_α is stress dependent for a particular soil and should be determined at an effective stress similar to that expected *in situ*. For a variety of clays, silts, and organic soils, Mesri (1973) showed that $C_{\varepsilon\alpha}$ is approximately related to the natural water content, w_n, (in percent) by:

$$C_{\varepsilon\alpha} \approx 10^{-4} w_n \quad \textbf{(5-5-19)}$$

The secondary compression index is closely linked to the compression index, C_c. For this reason, an excellent method for estimating C_α is the use of the C_α / C_c ratio. Typical values of this ratio are found in Table 5-6. Recognizing that C_c is also stress-dependent, these ratios should be used with the slope of the laboratory virgin compression curve at the effective stress of interest (Mesri and Godlewski 1977, Mesri and Castro 1987) rather than the field corrected value typically used in consolidation calculations. An example of secondary compression settlement calculations is provided in Figure 5-24.

Table 5-6 Typical Values of C_α / C_c (after Terzaghi et al. 1996)

Soil Type	C_α / C_c
Granular soils including rockfill	0.02 ± 0.01
Shale and mudstone	0.03 ± 0.01
Inorganic clays and silts	0.04 ± 0.01
Organic clays and silts	0.05 ± 0.01
Peat and muskeg	0.06 ± 0.01

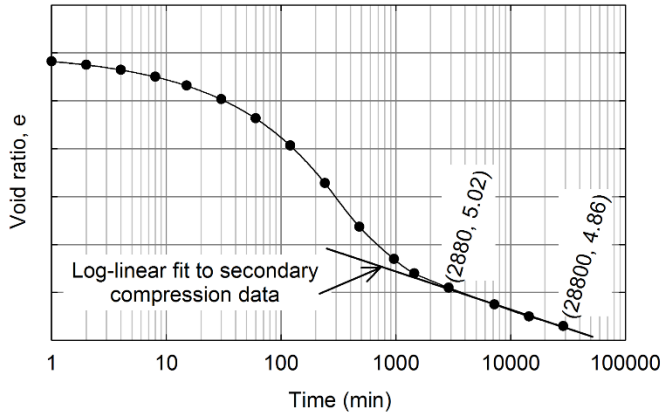

Example

- Organic clay: H_0=10'
- $w_n \approx 250\%$
- $e_0 \approx 6$
- $C_c = 3$ @ in-situ stress

Based on Lab Data

$$C_\alpha = \frac{\Delta e}{\log(\Delta\sigma)} = \frac{(5.02-4.86)}{\log\left(28800/2880\right)} = 0.16$$

$$C_{\varepsilon\alpha} = C_\alpha/(1+e_0) = 0.16/(1+6) = 0.023$$

Based on Table 5-6

$$C_\alpha/C_c = 0.05$$

$$C_\alpha = (0.05)(3) = 0.15$$

$$C_{\varepsilon\alpha} = C_\alpha/(1+e_0) = 0.15/(1+6) = 0.021$$

Based on Eqn. 5-19

$$C_{\varepsilon\alpha} \approx 10^{-4} w_n = 10^{-4}(250)$$

$$C_{\varepsilon\alpha} \approx 0.025$$

Based on the three methods $C_{\varepsilon\alpha} \approx 0.023$ and t_p = 1 year, the secondary compression settlement expected after 50 years, s_s, is approximately:

$$s_s = C_{\varepsilon\alpha} \log\left(\frac{t}{t_p}\right) H_0 = 0.023 \cdot \log\left(\frac{50\text{ yr}}{1\text{ yr}}\right)(10\text{ ft}) \approx 0.4\text{ ft} \approx 5\text{ in.}$$

Figure 5-24 Calculation of Secondary Compression

In many cases, one-dimensional consolidation tests are presented using the void ratio or vertical strain corresponding to the end of 24-hour load increments. Some amount of secondary compression will have occurred during this time period and is thus included in the laboratory consolidation curve. The engineer should be aware that consolidation settlements calculated with such data will account for some degree of secondary compression.

If secondary compression is expected to be important in the analysis, consolidation test results should be plotted based on the void ratio or vertical strain at the end of primary (EOP) consolidation for each load increment. Primary consolidation settlement calculated using the EOP consolidation curve can be added directly to estimates of secondary compression settlement.

5-5.5 Organic Soils and Peat.

Settlement of organic soils and peat can be calculated using the procedures for inorganic fine-grained soils. Primary consolidation tends to occur more rapidly in these

soils due to their relatively high hydraulic conductivity. Large secondary compression is typically measured and contributes a significant portion of the total settlement.

5-6 DIFFERENTIAL AND TOLERABLE SETTLEMENT.

5-6.1 Differential Settlement.

For important structures, settlement should be calculated for a number of points across the footprint of the structure in order to establish the expected settlement pattern. Figure 5-25 illustrates various types of settlement profiles.

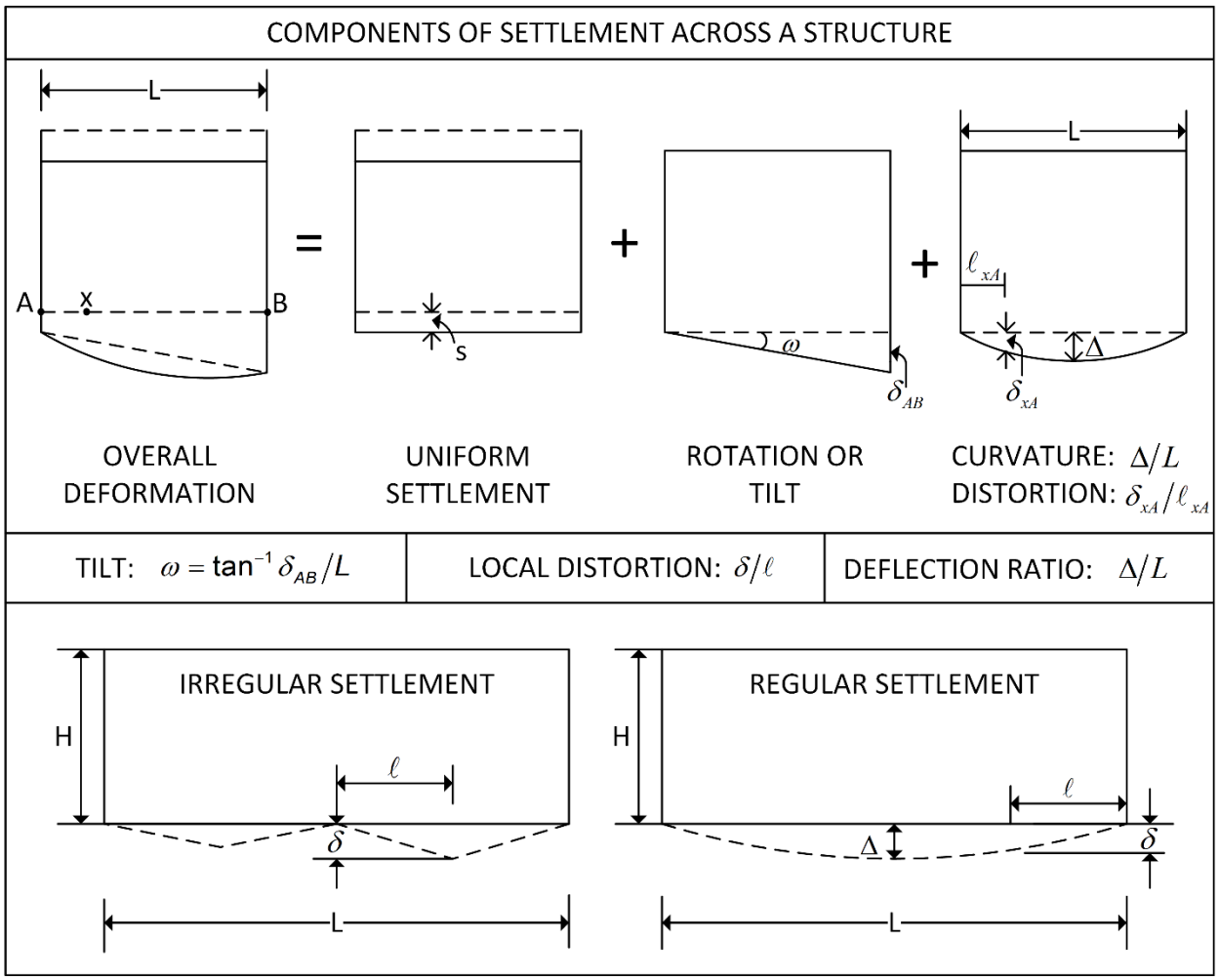

Figure 5-25 Components of Settlement
(after Duncan and Buchignani 1987, Ricceri and Soranzo 1985)

Differences in settlement across a structure can be considered in multiple ways. The simplest is to consider the maximum difference in predicted settlement across the structure, which is often referred to as the *differential settlement,* δ_{max}. However, it is often necessary and more informative to consider the effects of the size and flexibility of the structure when evaluating the impact of differential settlement. In some cases, a

structure will tilt over an angle (ω) which causes difference in settlement between various points but does not necessarily cause structural distress.

Differential settlement that results in non-uniform deflection or non-uniform tilt causes bending and tensile strain in the structure. Differential movement that causes a concave upward shape is referred to as *sagging* while a concave downward shape is called *hogging*. This type of movement can be quantified by either the angular distortion or the deflection ratio. *Angular distortion* (δ / l) is the slope of the expected settlement profile or the ratio of the settlement between two points to the distance (l) separating the points. The *deflection ratio* (Δ / L) is the maximum expected deviation from uniform settlement divided by the overall length of the structure and is an approximate measure of the curvature caused by settlement. These two measures have been shown to provide the best indication of structural distress.

Natural variation in soil deposits causes settlement calculations to be highly uncertain. For this reason, it may be sufficient to use approximate relationships to estimate differential based on magnitude of total settlement. For example, Terzaghi et al. (1996) suggest that the differential settlement for footings on sand will likely be 75% or less of the predicted total settlement. For clays, the differential settlement can sometimes approach the magnitude of the total settlement.

5-6.2 Tolerable Settlement.

5-6.2.1 Criteria.

Most of the guidance regarding acceptable settlement is based on experience with measured settlement of real structures and observations of the associated damage. Wahls (1981) summarizes four important points regarding settlement: (1) settlement must be expected, (2) some form of differential settlement is the most important to consider for structural distress, (3) structural design can reduce the level of differential movement, and (4) many structures can tolerate large settlements and remain safe.

Table 5-7 provides guidance for the selection of tolerable angular distortion for various types of structures. In some cases, the limits that are provided that include a margin of safety to reduce or prevent cracking or damage. Most of these guidelines ignore the size and stiffness of the structure, which control the magnitude of the strains in the structure.

Table 5-7 Angular Distortion Limits for Various Structures (after Skempton and MacDonald 1956, Polshin and Tokar 1957, Duncan and Buchignani 1987, and Day 1990)

Type of Structure / Condition	*L/H*	Tolerable *d / l*	
		Decimal	Ratio
Small slab-on-grade structures – damage to structure	---	0.01	1/100

Steel frame with flexible siding	---	0.008	1/125
Circular steel tanks on flexible base with fixed top	---		
Considerable cracking – brick and panel	---	0.0067	1/150
Structural damage begins	---		
Safe limit – flexible brick walls (includes safety factor)	> 4		
Tilting of high buildings becomes visible	---	0.004	1/250
Slab-on-grade structures – drywall cracking	---	0.0033	1/300
Overhead cranes			
Steel or reinforced concrete frame with insensitive finish such as dry wall, glass or moveable panels	---	0.002 to 0.003	1/500 to 1/333
Circular steel tanks on flexible base with floating top	---		
Tall slender structures, such as stacks, silos, and water tanks with rigid mat foundations	---	0.002	1/500
Safe limit –cracking of buildings (includes safety factor)	---		
Steel or reinforced concrete frame with brick, block, plaster, or stucco finish	≥ 5 ≤ 3	0.002 0.001	1/500 1/1000
Frames with diagonal bracing	---	0.00167	1/600
Machinery sensitive to settlement	---	0.0013	1/750
Load-bearing brick, tile, or concrete block walls	≥ 5 ≤ 3	0.0008 0.0004	1/1250 1/2500

Wroth and Burland (1974) proposed a deflection ratio criterion that allow the properties of the structure to be explicitly considered in terms of the controlling type of strain, the length to height ratio of the structure, and the structure's relative stiffness, E/G. Figure 5-26 plots these criteria for three different types of bending, assuming the critical strain for structural distress (ε_{crit}) is 0.075%. Other values of E/G and ε_{crit} can be considered using the equations provided on the figure.

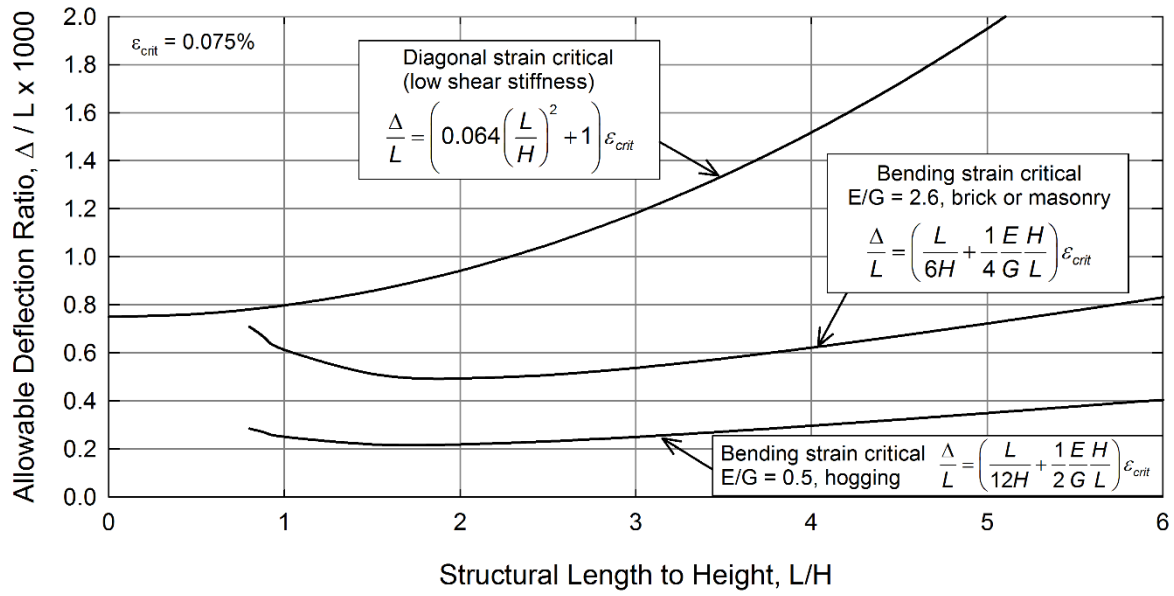

Figure 5-26 Allowable Deflection Ratios Related to Structural Proportions (after Burland and Wroth 1974, Wahls 1981)

5-6.2.2 Reduction of Differential Settlement.

The reduction of total settlement (Section 5-7) is also the primary means of reducing differential movement. Settlement that occurs early in the construction process doesn't generally contribute to structural distress. The sequence and rate at which the load is applied can be compared to the expected rate of consolidation to estimate the total and differential settlement that will be experienced by different parts of the structure. If the consolidation rate is relatively fast, building finishes and other sensitive components may be installed after much of the total settlement has occurred and thus will experience less differential settlement than the superstructure. Estimates of this type of effect are heavily dependent on the rate of construction and consolidation and must be considered on a project-specific basis.

Some buildings, such as light steel frame structures, are very flexible and can tolerate large settlements. In this case, limitation of damage to utilities and machinery housed in the facility may control design.

5-6.3 Differential Settlement of Mat Foundations.

Settlement calculations for mat or raft foundations are often made based on changes in stress calculated assuming uniform loading. The rigidity of the foundation structure will affect the accuracy of this assumption and the distribution of settlement. The flexibility of the foundation and the soil structure interaction can be difficult to assess. Predictions of differential settlement are often less accurate than those for total or average settlement for these reasons, especially for mat foundations.

Mat behavior can be estimated using a mat stiffness factor (K_m) which compares the foundation to the stiffness of the underlying soil. As indicated in Table 5-8, mats with low stiffness ratios can be considered completely flexible. Flexible mats will apply a relatively uniform pressure distribution, and the center, edges, and corners will settle differentially. Mats with high values of K_m will act in a rigid manner and will tend to settle uniformly. Influence factors for intermediate stiffness are provided by Brown (1969) and Frazer and Wardle (1976).

Table 5-8 Relative Mat Stiffness and Behavior (after Brown 1969, Frazer and Wardle 1976)

Foundation Shape	Mat Stiffness Factor, K_m	Mat Behavior		
		Flexible	Intermediate	Rigid
Circular	$K_m = 8\frac{E_m(1-\nu_s)^2}{E_s}\frac{t_m^3}{B^3}$	$K_m \le 0.08$	$0.08 \le K_m \le 5$	$5 \le K_m$
Rectangular	$K_m = \frac{4}{3}\frac{E_m(1-\nu_s)^2}{E_s(1-\nu_m)^2}\frac{t_m^3}{B^3}$	$K_m \le 0.05$	$0.05 \le K_m \le 10$	$10 \le K_m$
Variables:	E_m = modulus of elasticity of mat, ν_m = Poisson's ratio of mat E_s = modulus of elasticity of soil, ν_s = Poisson's ratio of soil t_m = thickness of mat, B = diameter or width of mat (least dimension)			

5-7 METHODS OF CONTROLLING SETTLEMENT.

Methods for reducing or accelerating settlement are summarized in Table 5-9. Further details for some of the basic methods are discussed in the following sections. For a more in-depth summary of ground modification techniques that can be used to remove settlement potential, reduce excess settlement, or accelerate settlement, see FHWA's *Ground Modification Vol. 1 and 2* (2017).

5-7.1 Removal or Displacement of Compressible Soils.

Excavation and replacement is a simple method of reducing or eliminating settlement for cases were the compressible stratum is shallow and relatively thin. This method is particularly useful for sites where extensive earthwork is already required.

Surficial soils with low shear strength and high compressibility, such as organic soils, should be removed and replaced with engineered fill. The suitability of deeper soils to support the planned fill or structure will depend on the shear strength and compressibility of the underlying soils as judged by an appropriate subsurface exploration. A common example of removal and replacement is the removal of topsoil which occurs prior to the placement of most fills.

In some cases, partial excavation of very soft foundation soils can be accompanied by displacement caused by the weight of the new fill. The boundary between the new fill and the displaced soil should be kept as vertical as possible. This method is most applicable to the displacement of peat and muck deposits and has been used successfully for soft soils up to 65 feet deep. Jetting and blasting methods can be used in the fill and foundation to facilitate displacement of the soft soil. Caution should be used with partial displacement in fibrous organic soils, as these materials tend to resist displacement, which can result in trapped pockets and differential settlement.

Table 5-9 Methods to Reduce, Accelerate, or Prevent Excess Settlement (after FHWA 2017)

Primary Purpose	Method / Technology	Description / Comments
Reduce amount of soft soil	Removal and replacement	Full or partial removal of compressible soil reduces or eliminates settlement potential. Displacement methods may include jetting or various types of blasting.
	Partial displacement	
Reinforce soft soil	Column-supported embankments	Compressible soil is bypassed by much stiffer, reinforcing elements, typically columns. The columns transfer most of the load from the fill or structure through the soft soil to deeper and stiffer materials. A reinforced load transfer platform is often required at the ground surface. In some cases, the reinforcing elements also improve the surrounding soil.
	Reinforced load transfer platforms	
	Non-compressible columns	
	Stone columns	
	Rammed aggregate piers	
Improve soft soil	Deep mixing methods	Compaction and/or chemical modification of soft soil can reduce its compressibility and reduce settlement potential. Compaction methods are typically more effective on coarse-grained materials.
	Vibro-compaction	
	Dynamic compaction	
Accelerate consolidation of soft soil	Surcharge	Increased gradients cause the consolidation process to proceed more quickly. Final settlements can be equal to or greater than the settlement caused by the design load. Often used along with vertical drains.
	Pumping or vacuum	
	Electro-osmosis	
	Prefabricated vertical drains (PVDs)	Vertical drainage elements are used to shorten the drainage path. This allows pore pressures to dissipate and consolidation to occur more quickly.
	Aggregate columns or sand drains	
Reduce applied load to soft soil	Balanced / compensated foundation	Reduction of the applied stress will reduce the magnitude of the consolidation settlement. This can be accomplished by permanent excavation or the use of lightweight construction materials.
	Lightweight granular fill	
	Geofoam or foamed concrete	

5-7.2 Balancing Load by Excavation.

The *balanced load approach* (a.k.a. *compensated foundation* or *floating foundation*) can sometimes be used to support heavy structures over compressible strata. In this approach, the weight of the structure is balanced, completely or partially, by soil that is permanently excavated from the building footprint. The construction of a permanent basement level is required to create stress relief. This method works particularly well for situations where a stronger surface layer overlies a compressible stratum.

Excavation for the structure results in vertical stress relief and some amount of swelling or heave. If the weight of the structure is equal to or less than the weight of the excavated material, the total settlement experienced by the structure will be the result of recompression of the compressible strata. The magnitude of swelling and subsequent recompression will depend on construction and site factors, such as the amount of time between excavation and loading, the construction sequence, and the subsurface drainage conditions.

Dewatering may be required to facilitate the construction of a balanced foundation. If the groundwater is significantly lowered, the amount of heave and subsequent recompression will be reduced because of negative excess pore pressures in the soil.

Settlement for balanced foundations can be predicted using the methods in Sections 5-3 to 5-5. The net vertical stress ($q_{0\text{-}net}$) is found by subtracting the vertical stress reduction ($\sigma_{z\text{-}red}$) from the building load, q_0. The final groundwater conditions affect the value of $\sigma_{z\text{-}red}$. For cases where the groundwater is not lowered or is allowed to return to its initial condition following construction, $\sigma_{z\text{-}red}$ is equal to the total vertical stress at the foundation level prior to construction. If the groundwater is lowered permanently below the foundation level, $\sigma_{z\text{-}red}$ is equal to the effective vertical stress at the foundation level prior to construction.

5-7.3 Preconsolidation by Surcharge.

A surcharge causes some or all of the consolidation to occur prior to construction. This method works well for fill beneath paved areas, for large floor loadings, and for structures with relatively light column loads. For heavier structures, improvement by surcharging may not be sufficient to provide adequate bearing resistance. In this case, a portion of the surficial layer of the compressible soil may need to be replaced with a more rigid compacted fill or reinforced fill.

A portion of the predicted consolidation and secondary compression can be removed by surcharging as illustrated in Figure 5-27. The calculations in this figure assume that the time rate of consolidation is the same under both the surcharge load and the final load. This should be approximately true provided the coefficient of consolidation is not significantly different under the two loading conditions. In order to eliminate the

settlement due to primary consolidation under the final load, the degree of consolidation required under the surcharge ($\overline{U}_{f+s}$) is:

$$\overline{U}_{f+s} = \frac{\log\left[1+\frac{q_f}{\sigma'_{z0}}\right]}{\log\left[1+\frac{q_f}{\sigma'_{z0}}\left(1+\frac{q_s}{q_f}\right)\right]} \quad \textbf{(5-20)}$$

where:
q_f = final applied load,
q_s = additional surcharge load, and
σ'_{z0} = initial vertical effective stress at midpoint of the consolidating layer.

If some amount of secondary compression must also be removed by surcharging, the required degree of consolidation becomes:

$$\overline{U}_{f+s} = \frac{\left[\log\left(1+\frac{q_f}{\sigma'_{z0}}\right)+\frac{C_\alpha}{C_c}\log\left(\frac{t}{t_p}\right)\right]}{\log\left[1+\frac{q_f}{\sigma'_{z0}}\left(1+\frac{q_s}{q_f}\right)\right]} \quad \textbf{(5-21)}$$

where:
q_f = final applied load,
q_s = additional surcharge load,
σ'_{z0} = initial vertical effective stress at midpoint of the consolidating layer,
C_α / C_c = ratio of secondary to primary compression indices,
t_p = time required for primary consolidation, and
t = time after loading for which secondary compression is considered.

An example of the calculations for the surcharge approach is provided in Figure 5-28. The major limitations of the surcharge method are time and cost. The time required for consolidation to occur may not fit within the construction schedule. Use of vertical drains as described in the following section can alleviate this difficulty. In soft soils, shear failure can be induced at the edge of the surcharge. This should be considered using slope stability methods (Chapter 7) or bearing capacity theory (DM 7.2).

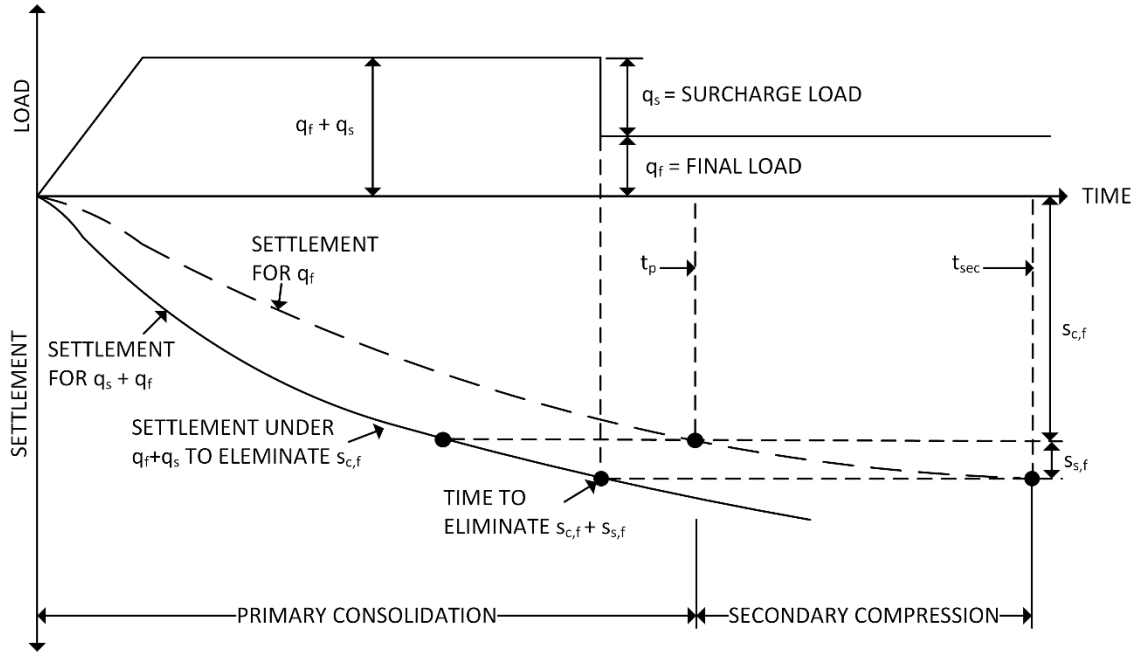

BY SELECTING AN APPROPRIATE SURCHARGE LOAD & DURATION OF SURCHARGE LOADING, ALL OR PART OF THE SETTLEMENT UNDER FINAL LOADING CAN BE ELIMINATED

σ'_{z0} = EXISTING OVERBURDEN PRESSURE
s_{cf} = SETTLEMENT DUE TO PRIMARY CONSOLIDATION UNDER q_f
s_{sf} = SETTLEMENT DUE TO SECONDARY CONSOLIDATION UNDER q_f
$s_{c,f+s}$ = SETTLEMENT DUE TO PARTIAL PRIMARY CONSOLIDATION UNDER $q_f + q_s$

$\overline{U}_{f+s} = \frac{s_{c,f}}{s_{c,f+s}}$ or $\frac{s_{c,f} + s_{s,f}}{s_{c,f+s}}$ = DEGREE OF CONSOLIDATION UNDER $q_f + q_s$ REQUIRED TO ELIMINATE PRIMARY CONSOLIDATION OR PRIMARY + SECONDARY UNDER q_f

t_p = TIME REQUIRED FOR COMPLETION OF PRIMARY CONSOLIDATION UNDER q_f OR $q_f + q_s$.
t_{sec} = TIME TO COMPLETE SPECIFIC AMOUNT OF SECONDARY COMPRESSION

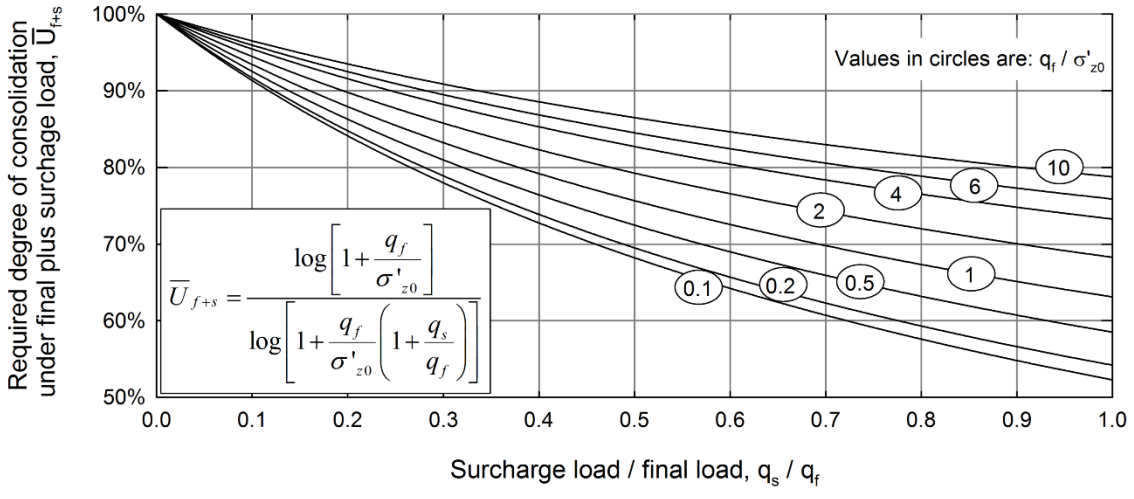

Figure 5-27 Surcharge Load and Consolidation Required to Eliminate Settlement under Final Load

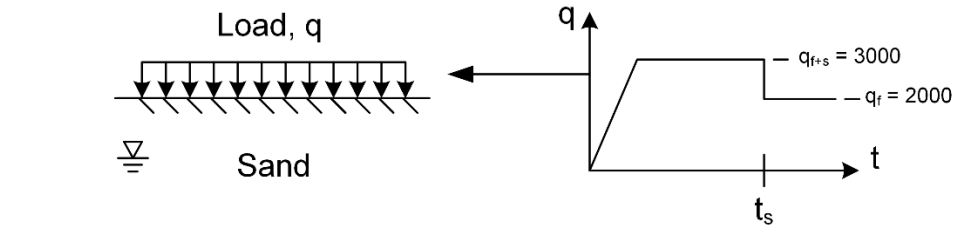

- Average σ_{z0} = 4000 psf
- Expected settlement under final load, s_f = 2.5"

How long must surcharge be applied to remove 100% of s_f?

$$\frac{q_f}{\sigma'_{z0}} = \frac{2000\,psf}{4000\,psf} = 0.5 \qquad \frac{q_s}{q_f} = \frac{1000\,psf}{2000\,psf} = 0.5$$

From Fig 5-27: $$\overline{U}_{f+s} = \frac{\log\left[1+\frac{q_f}{\sigma'_{zo}}\right]}{\log\left[1+\frac{q_f}{\sigma'_{zo}}\left[1+\frac{q_s}{q_f}\right]\right]} = \frac{\log[1+0.5]}{\log[1+0.5[1+0.5]]} = 72\%$$

The time factor can be found using Fig 5-15, and the amount of time the surcharge must remain in place is:

$$T = -\frac{4}{\pi^2}\ln\left[\frac{\pi^2}{8}(1-\overline{U}_{f+s})\right] = 0.44 \qquad \text{Time, } t_s = \frac{T\,H_{dr}{}^2}{c_v} = \frac{0.44(20\,ft)^2}{1\,ft^2/day} = 176\,\text{days}$$

Figure 5-28 Surcharge Loading Example

5-7.4 Vertical Drains.

Vertical drains are constructed or inserted vertically through compressible soil layers. The drains intercept horizontal water flow. The water is then transmitted to a drainage layer at the surface and/or to underlying coarse-grained soil, depending on the drainage conditions. The drains are typically installed in triangular or square patterns as shown in Figure 5-29 with spacing ranging from 3 to 6.5 feet. Drains typically shorten the maximum drainage path to 8 feet or less. While vertical drains were constructed mostly of sand prior to the 1980s, current practice is to use drains comprised of a plastic core encased in geotextile fabric, typically referred to as *prefabricated vertical drains* (*PVD*). For detailed information on PVD materials and drain construction practices, see FHWA (2017).

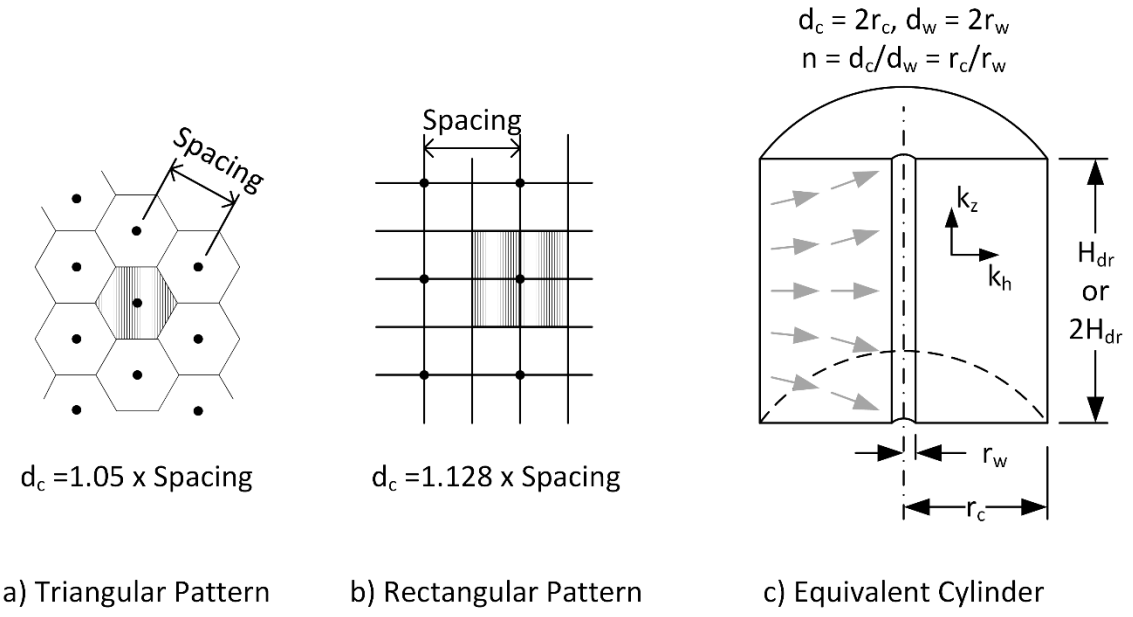

Figure 5-29 Vertical Drains – (a) Triangular Pattern, (b) Rectangular Pattern, and (c) Equivalent Cylinder for Theoretical Solutions

In addition to shortening the drainage path, vertical drains take advantage of the higher hydraulic conductivity and coefficient of consolidation often found in horizontal direction in many soils. While the vertical coefficient of consolidation can be measured in laboratory tests or estimated based on index tests (see Chapters 3 and 8), the horizontal coefficient of consolidation (c_h) is rarely measured directly. More often, c_h is assumed to be about 1.5 to 4 times higher than c_v, depending on the amount of horizontal layering present. Higher ratios of c_h to c_v are encountered when layers of silt and sand are present. Asaoka (1978) presents a method for determining c_h from field measurements on a test fill.

Many analytical and numerical methods have been proposed for radial drainage theory, most based on Barron (1948). The differences in the methods tend to have less effect on predictions of consolidation rate than the uncertainty and variability in c_h. Using the calculation method presented by FHWA (2017), the time factor (T_r) for a desired degree of radial consolidation ($\bar{U}_r$) is found by:

$$T_r = \frac{1}{8}\left(F_n + F_s + F_r\right)\ln\left(\frac{1}{1-\bar{U}_r}\right) \quad \textbf{(5-22)}$$

where:
F_n = factor related to drain spacing,
F_s = factor related to soil disturbance (smear), and
F_r = factor related to well resistance in the drain.

If smear and well resistance are ignored, F_s and F_r are set equal to zero.

Figure 5-29 illustrates the relationship between the drain configuration and the *effective drainage diameter*, d_c. The drain spacing is often expressed in terms of the ratio (n) between the drainage diameter and the diameter of the well, d_w. The drainage factor (F_n) is equal to:

$$F_n = \frac{n^2}{n^2-1}\ln(n) - \frac{3n^2-1}{4n^2} \approx \ln(n) - 0.75 \quad \textbf{(5-23)}$$

where:
n = ratio of d_c to d_w.

The error in the approximation is less than 10% for n greater than 4 and less than 1% for n greater than 12.

Most PVDs have a rectangular cross section while the solutions to radial consolidation problem assume a circular drain. Hansbo (1979) found that the equivalent drain diameter can be approximated as:

$$d_w = \frac{2(a+b)}{\pi} \quad \textbf{(5-24)}$$

where:
a and b = PVD dimensions.

Values of d_w for modern PVDs range from 1.5 to 5.5 inches. A diameter of 2 inches is commonly used, which results in n values in the range of 20 to 50 for typical drain spacing.

Given the uncertainties with the measurement or estimation of soil properties, the effects of soil disturbance or smear around the drains and drain resistance are often ignored (FHWA 2017). Smear tends to be important mostly for drains in high plasticity clays or sensitive soils, or where c_h has been directly and accurately measured. In order to account for smear, the soil disturbance factor (F_s) can be calculated as

$$F_s \approx \frac{k_h}{k_s}\ln(s) \quad \textbf{(5-25)}$$

where:
k_h = hydraulic conductivity of the soil layer,
k_s = hydraulic conductivity of the disturbed zone, and
s = ratio of the diameter of the disturbed zone to the diameter of the drain.

Resistance to water flow within the drain can also decrease the effectiveness of vertical drains. If desired, this effect can be estimated by:

$$F_r = \pi z\left(2L_m - z\right)\frac{k_h}{q_w} \quad \textbf{(5-26)}$$

where:
z = depth along the drain,
L_m = maximum distance water must flow through the drain, and
q_w = discharge capacity of the drain.

5-7.4.1 Combination of Vertical and Horizontal Drainage Effects.

Prediction of the degree of consolidation from vertical drainage can be combined with the effects of horizontal drainage to vertical drains using the method proposed by Carrillo (1942). The combined degree of consolidation ($\overline{U}_c$) in percent is:

$$\overline{U}_c = 100 - \frac{\left(100 - \overline{U}_r\right)\left(100 - \overline{U}_z\right)}{100} \quad \textbf{(5-27)}$$

where:
$\overline{U}_r$ = degree of consolidation for radial drainage, and
$\overline{U}_z$ = degree of consolidation for vertical drainage.

5-7.4.2 Vertical Drain Design.

Vertical drain design involves the selection of the appropriate drain type, drain spacing, and construction procedures based on the time available for consolidation, design degree of consolidation for that time period, and soil properties. The appropriate time factor for radial drainage (T_r) can be determined from Equation 5-22 or from Figure 5-30 or Figure 5-31. Figure 5-30 plots the relationship between $\overline{U}_r$ and T_r for a range of drain spacing for three smear conditions. Figure 5-31 provides solutions for gradual loading and radial drainage. From T_r and the time available for consolidation (t) the required effective drain diameter (d_c) can be calculated as:

$$d_c = \sqrt{\frac{c_h t}{T_r}} \quad \textbf{(5-5-28)}$$

where:
c_h = coefficient of consolidation in the horizontal direction.

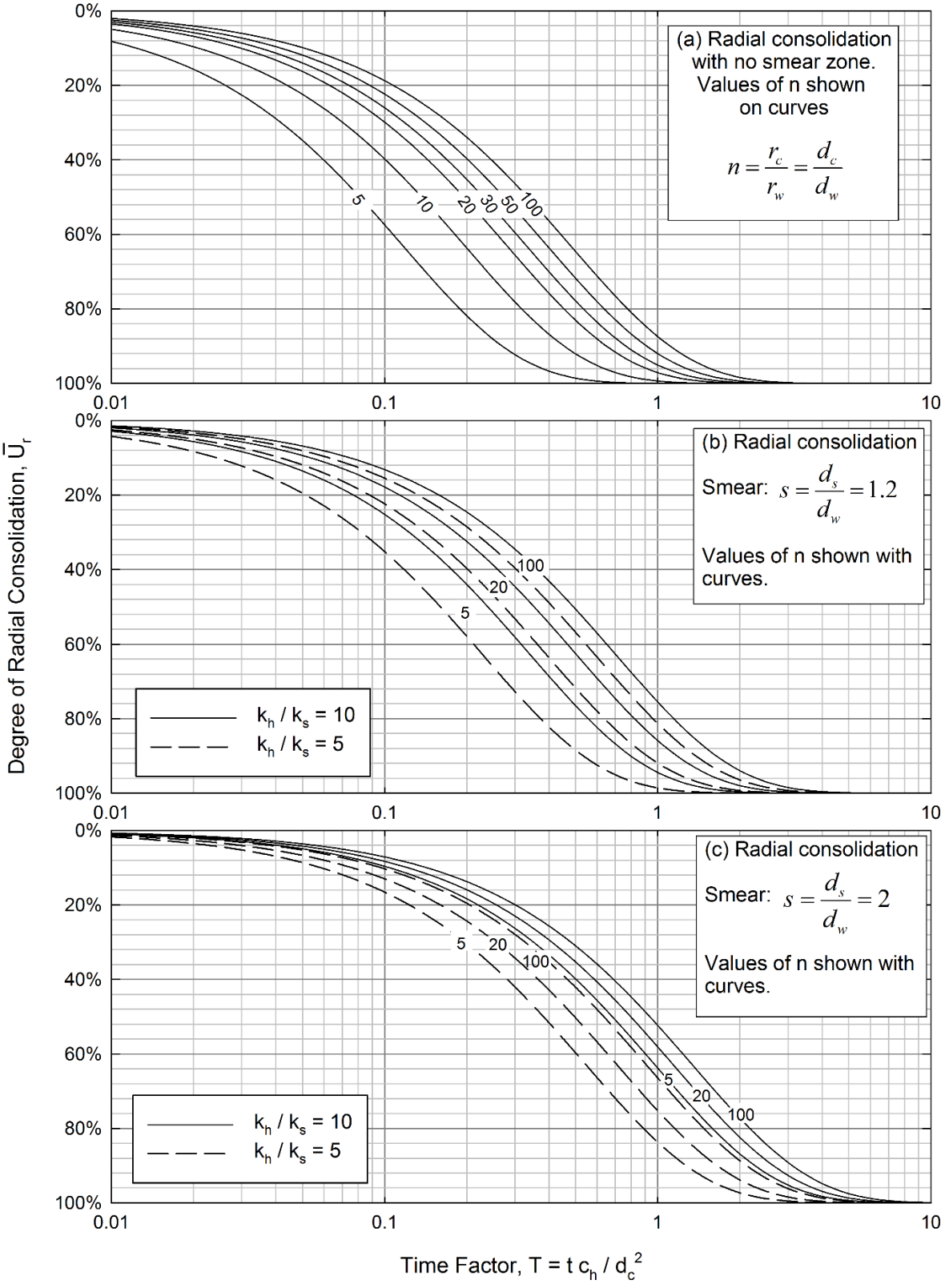

Figure 5-30 Degree of Radial Consolidation

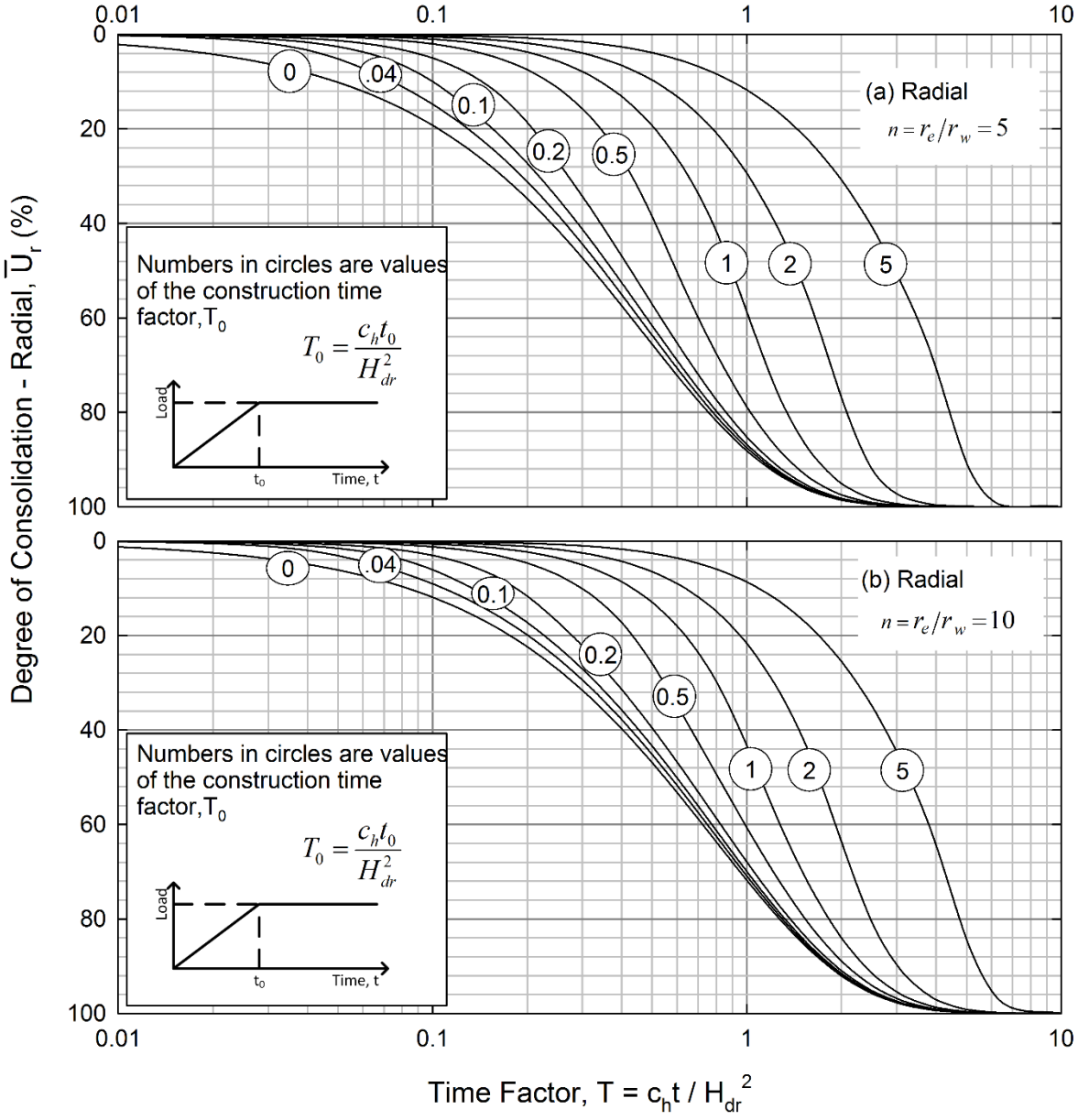

Figure 5-31 Radial Consolidation with Gradual Loading (after Olson 1977)

An alternative approach is provided in the design chart in Figure 5-32. This chart allows the spacing to be selected directly based on the other properties and variables. Other drain design considerations include stability against foundation failure and provision of adequate flow in the surface drainage blanket. An example of vertical drain design is provided in Figure 5-33.

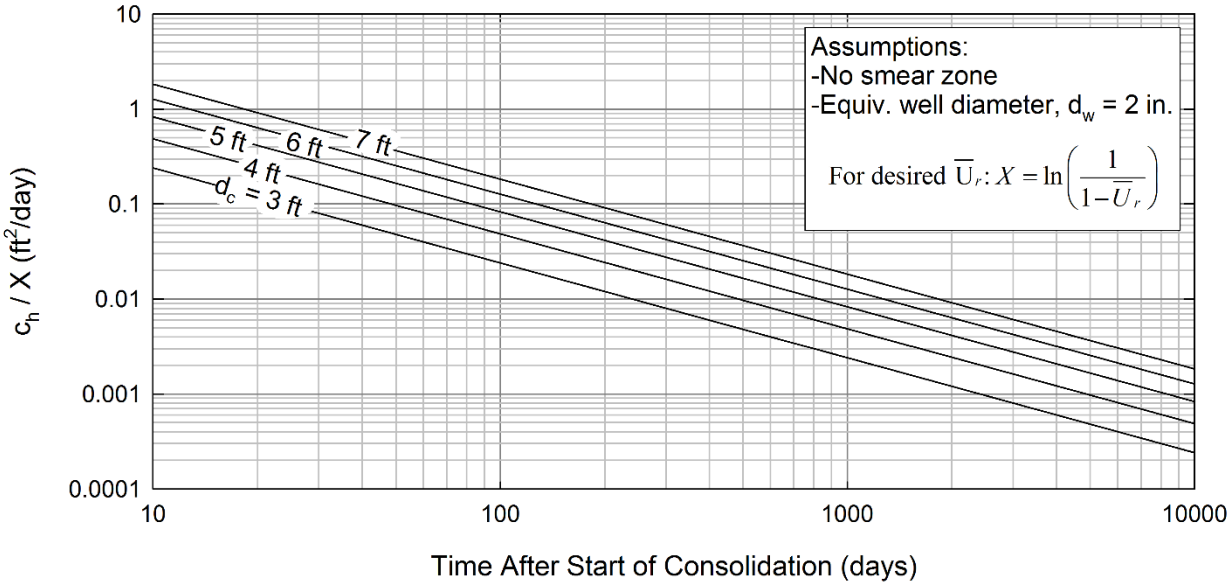

Figure 5-32 Design Chart for Radial Drainage

5-7.4.3 Vertical Drains with Surcharge.

In some cases, a surcharge is used along with vertical drains to accelerate the rate of settlement and reach the final settlement more quickly. Surcharges are especially important for soil conditions in which a large amount of secondary compression is likely to occur. The method presented in Figure 5-27 can also be used with vertical drains.

5-7.4.4 Construction Control Requirements.

Extensive discussion of specifications, quality assurance, site preparation, and installation procedures for vertical drains can be found in FHWA (2017). Field instrumentation should be installed to monitor performance of the drains, progress of consolidation, and horizontal deformations. The type of instrumentation required depends on the application. For cases where instability is not likely, such as a low height fill of large lateral extent, the primary purpose of instrumentation is to monitor progress of consolidation. Settlement plates are sufficient for this purpose. On the other hand, stability and pore pressure dissipation is a concern for the construction of large embankments over soft soil. Piezometers should be used to monitor the dissipation of excess pore pressure during consolidation. Inclinometers should be installed to monitor horizontal deformations in the foundation soil.

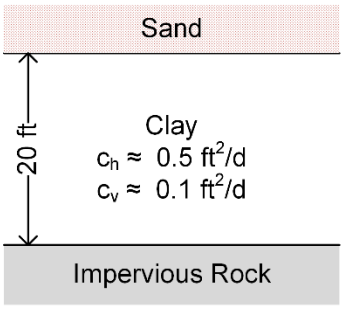

Proposed Vertical Drain Design

-Triangular pattern with spacing of 6 ft
-Equiv. well diameter, d_w = 2 in. = 0.167 ft
-Ignore smear and well effects

A) Determine the time required to reach 90% degree of consolidation based on radial drainage alone.

Equivalent diameter, d_c = 1.05 x spacing = 1.05 (6 ft) = 6.3 ft

$n = d_c / d_w$ = 6.3 ft / 0.167 ft = 38

$F_n \approx \ln(n) - 0.75 = \ln(38) - 0.75 = 2.88$, assume $F_s = 0$ and $F_r = 0$

From Eqn. 5-22: $T_r = (1/8) F_n \ln (1 / (1 - U_r)) = 0.125 (2.88) \ln(10) = 0.83$

(Also matches value obtained for n = 38 and U_r = 90% on Fig. 5-25a)

Time required:

$$t = \frac{T_r \cdot d_c^2}{c_h} = \frac{0.83(6.3\,ft)^2}{0.5\,ft^2/day} = 66\,days$$

B) Determine the combined degree of consolidation including vertical drainage after 66 days.

Vertical time factor:

$$T_v = \frac{t \cdot c_v}{H_{dr}^2} = \frac{(66\,days)(0.1\,ft^2/day)}{(20\,ft)^2} = 0.017$$

From Fig. 5-15:

$$\overline{U}_z = 0.14$$

Combined $\bar{U}_c$:

$$\overline{U}_c = 100\% - \frac{(1-\overline{U}_r)(1-\overline{U}_z)}{100\%} = 100\% - \frac{(1-90\%)(1-14\%)}{100\%} = 91\%$$

Figure 5-33 Radial Consolidation Example

5-8 VOLUME EXPANSION.

5-8.1 Mechanics of Volume Expansion.

Positive volume change or volume expansion of soil is controlled by a variety of factors. For fine-grained soils, these factors include physical particle interactions, chemical interactions, mineralogy, soil fabric or structure, stress history, temperature, and pore water chemistry.

Unloading or reduction in effective stress is the most important physical process that causes swelling in non-frozen soils. This unloading can be the result of a decrease in the total stress, such as that caused by an excavation, or as the result of increased positive pore water pressure from a raised groundwater level.

Various theories have attempted to explain the chemical processes associated with swelling, including osmotic pressure theory and water adsorption theory (Mitchell 1993). These theories predict the *swell pressure*, which is the pressure exerted by the swelling soil on an unyielding boundary. While such theories have a limited degree of accuracy and are not typically useful for practical application, they provide insight into general trends in soil behavior. The osmotic pressure concept shows that pore water with low electrolyte concentration leads to higher swell pressures. Similarly, according to water adsorption theory, the specific surface area of the clay particles is the most important factor for determining the amount of water required for hydration. For this reason, clay minerals with very thin particles with high surface area, such as montmorillonite, smectite, and vermiculite, are the most susceptible to swelling. The liquid limit and clay fraction are indicators of the amount of these swelling clay minerals present in a soil (Terzaghi et al. 1996).

Soil and rock that has been consolidated to a relatively low void ratio is the most susceptible to swelling. Low void ratios are the result of either high normal stresses or high levels of matric suction (ψ) under unsaturated conditions. The deformation experienced during consolidation stores energy in the soil particles. In addition, the water content in these soils may be lower than that required to fully hydrate the clay particles. If either the normal stress or the suction is lowered, the clay will tend to swell to release the stored energy and to hydrate the clay minerals. Some clay minerals, such as kaolinite, exhibit swelling mostly at the low void ratio associated with heavy overconsolidation. Clays containing more active minerals, such as sodium montmorillonite, experience similar amounts of swell regardless of void ratio because the swelling behavior is dominated by hydration.

Clay shales and shales containing pyrite (iron sulfide) or anhydrite (calcium sulphate) are also susceptible to swelling when exposed to water and/or air. The oxidation and hydration of pyrite and anhydrite can cause a volumetric expansion of ten times the original volume.

Soils can also experience volume expansion caused by freezing and the formation of ice lenses within the soil. Silts, silty sands, and fine sands are particularly susceptible to frost-related swell. These soils have moderate hydraulic conductivity which allows water to flow easily and a small enough void space to permit a significant level of capillary rise. For design of foundations in frost-susceptible soils, see ASCE (2001).

5-8.2 Effects of Volume Expansion.

Below an excavation, the total vertical stress is reduced, which initially causes a reduction in pore water pressure. As the pore water pressures return to equilibrium, the effective stress on the soil reduces and the soil swells. In most cases, excavation is followed by the construction of a building and the application of a pressure (q_0) that meets or exceeds the reduction in total stress. In this case, the heave caused by stress reduction will be cancelled out by reloading. Movements during these stages of construction are typically difficult to predict.

Negligible heave is observed for excavations in coarse-grained soils above the water table. Soft clays will experience immediate distortion-related swell that can be predicted using the method in Section 5-5.1. However, the required elastic modulus can be very difficult to predict. Over time, clay soils will experience an increase in water content and swell as a result of the change in effective stress.

In arid climates, changes in water content tend to vary depending on the location below a structure. The soil below the middle of the structure interacts less with the environment, and the water content in this zone tends to increase with time. This results in swell below the middle of the structure. Around the edges, the soil experiences more fluctuation in water content and can shrink, leading to perimeter settlement. The combination of these two mechanisms can result in the hogging shape of differential movement described earlier.

5-8.3 Estimates of Heave or Swell Pressure.

Many methods have been proposed to estimate one-dimensional heave (vertical movement) or swell pressure. Some of these methods are empirical, based mostly on index properties of the soil. Other methods use theory and oedometer testing to predict swelling caused by both changes in total stress and changes in suction.

Most methods predict a swell percentage or vertical strain of the soil, which must be multiplied by the thickness of soil that experiences swell. The thickness of soil that swells as a result of a change in total stress, such as an excavation, is related to the size of the excavation. This depth of influence can be estimated using the methods presented in Chapter 4. The thickness of soil that swells due to changes in suction is related to the depth of the groundwater table and the depth of seasonal water content fluctuations, which is commonly in the range of 3 to 15 feet depending on climate.

In some cases, it is helpful to consider the swell pressure that an expansive soil or rock can develop against an unyielding support or structure under a certain set of initial conditions. ASTM D4546 provides three different methods to measure the swell pressure in a one-dimensional consolidation apparatus. The swell pressure mobilized *in situ* is often less than that measured in the laboratory (Terzaghi et al. 1996).

5-8.3.1 Empirical Relationships.

Some of the available empirical correlations related to swelling are summarized in Table 5-10. These methods are mostly based on the Atterberg limits, clay fraction, and initial soil state as described by unit weight and water content. A few of the correlations require the soil's specific gravity or initial matric suction.

Table 5-10 Empirical Correlations to 1D Heave and Swell Pressure and Required Input Parameters (after Rao et al. 2011, Vanapalli and Lu 2012)

Empirical Method for Prediction of:	Source	Atterberg Limits	Grain-Size Distribution	Initial State (γ, w)	Specific Gravity	Initial Suction
1D Heave	Seed et al. (1962)	X	X			
	Van der Merwe (1964)	X	X			
	Ranganatham and Satyanarayan (1965)	X	X			
	Vijayvergiya and Ghazzally (1973)	X		X		
	McCormack and Wilding (1975)		X	X		
	O'Neil and Ghazzally (1977)	X		X		
	Johnson and Snethen (1978)	X		X		
	Weston (1980)	X		X		
	Bandyopadhyay (1981)	X	X			
	Chen (1975)	X				
	Cokca (2002)	X	X			X
	TXDOT (2014)	X	X	X		
Swell Pressure	Komornik and David (1969)	X		X		
	Nayak and Christensen (1971)	X	X	X		
	Schneider and Poor (1974)	X		X		
	McCormack and Wilding (1975)		X	X		
	Johnson (1978)	X				
	Nayak (1979)	X				
	Erzin and Erol (2004)	X		X		
	Sridharan and Gurtug (2004)			X	X	
	Thakur and Singh (2005)					X
	Erzin and Erol (2007)	X		X		X

Correlations, such as those listed in Table 5-10, are useful because of their simplicity and the ready availability of input information. However, the correlations are based on limited data sets and are most appropriate for application in similar soils. In addition, correlations that are only based on Atterberg limits and clay fraction will not be able to account for differences caused by initial soil conditions. None of the correlations presented in Table 5-10 is able to account for the contribution of change in stress to heave or the effects of total normal stress on swelling.

5-8.3.2 Stress-Strain-Suction Relationships.

More rigorous predictions of one-dimensional swelling consider the vertical strain that results both from changes in total stress and from changes in suction. These methods require measurement of the soil's stress-strain relationship, often at different levels of controlled suction. Suction-controlled oedometer tests and coefficient of linear extensibility tests are two means to obtain this data.

A variety of methods have been developed to predict the swelling strain caused by changes in total stress and changes in suction (or water content). Terzaghi et al. (1996) describes how the swelling process can be described in a manner analogous to consolidation. Vanapalli and Lu (2012) summarize many different methods to account for the stress-strain-suction relationship in the calculation of vertical strain based on the results of one-dimensional swell pressure measurements, suction-controlled oedometer tests, and coefficient of linear extensibility tests. Some of the methods also require measurement of matric suction as a function of water content. Terzaghi et al. (1996) also emphasizes that the deterioration of the clay structure during swelling often leads to a significant amount of time-dependent secondary swelling.

While theoretically sound, predictions of swell based on stress-strain-suction relationships are usually impractical. The amount of swell predicted by these methods is heavily dependent on soil moisture conditions at the start of construction, which cannot be accurately predicted during the design phase. In addition, the advanced soil testing required to use these methods is typically unavailable.

5-8.4 Design in Expansive Soils.

In many cases, heave and swell pressure estimates are used mostly to make decisions regarding remedial treatment of expansive soils and rock because of the uncertainties inherent in these estimates. Design of structures and pavements focuses on efforts to eliminate or reduce the effects of shrink-swell behavior of expansive soils and rock that are deemed to be problematic. Table 5-11 summarizes common approaches to foundation design in expansive soil and rock.

Table 5-11 Foundation Design Approaches in Expansive Soil (after Bowles 1996)

Approach	Comments
Alter the soil	Possible admixtures include lime, cement, or kiln dust. The admixtures reduce the hydration demands of the clay minerals and also increase bonding that resists swelling. Limited to depths for which it is practical to mix and recompact the soil.
Wet compaction	Compaction on the “wet” side of the line of optimums results in degree of saturation greater than 80 to 85%. High initial saturation reduces the potential for swelling but will increase shrinkage potential in areas exposed to the atmosphere. Wet compaction results in lower dry unit weight that may have lower shear strength and stability.
Control direction of swelling	Construct void zones within the foundation system, such as waffle slabs. If the soil has a tendency to swell, it will first swell into the voids prior to affecting the structure.
Eliminate changes in water content	Environmentally driven changes in water content cause most problematic swelling. Swelling can be bypassed by extending the structure below the zone of active water content change. If the structure cannot be constructed at this depth, the excavation can be filled with soils that are not susceptible to swelling and have low hydraulic conductivity.
Use a capillary break	In cases where the source of water is migration from deeper soils, a capillary break of coarse-grained material or geomembrane may be useful.
Use a sealing compound	Asphaltic sealing compounds can be used on expansive shale to reduce or prevent water from reaching the rock.
Design against swelling	The foundations can be extended below the active zone depth and designed with sufficient uplift capacity to resist the forces applied to the structure by swelling soil. Drilled piers with a bond break along the side of the shaft in the active zone are one common approach using this method.
Balance swell pressure	For some structures, the structural loads can be concentrated to increase the bearing pressure to levels that meet or exceed the swell pressure. This approach is not practical for most low-rise buildings because the structural loads are too light. In addition, the bearing pressure required to resist swell may exceed the allowable bearing capacity of the soil.

5-8.5 Construction Practices in Expansive Soils.

Good construction and maintenance practices in expansive soils and rock are primarily related to limiting exposure to the atmosphere and changes in water content. For swelling caused mostly by a temporary reduction in vertical stress, swelling can be reduced by collecting and removing surface water, pumping down groundwater, and placing a concrete mudmat immediately after excavation. Inert shale should be protected from wetting both during construction and long-term through the elimination of underdrainage, use of impervious backfill, and placement of appropriate surface drainage features. Excavations in shale should not be completed to final grade until foundation concrete is ready for placement. Some level of temporary and permanent protection can be provided through asphaltic coatings.

Some structures extend below future surface water or the groundwater table. In this case, access to water is impossible to avoid. The methods described in Table 5-11 can be used to reduce or restrict swelling. Where rock is shallow, rock bolts can be used with appropriately reinforced slabs and foundations to resist swelling.

For buildings in semi-arid and arid climates, changes in suction within the soil are the major cause of shrinking and swelling. Efforts should be made to collect surface and rain water near structures to prevent wetting of the soils during wet periods. During dry periods, evaporation and transpiration remove water from soil and increase suction leading to shrinkage. These effects can be limited through the use of pavement and avoiding placement of vegetation around structures.

Engineered fill constructed from high plasticity clays will tend to shrink and swell in response to the climate. In addition to deformation, this volume change results in a time-dependent reduction in shear strength that must be accounted for in slope design. If possible, high plasticity clays should not be used for the portions of embankments exposed to fluctuation in water content. Swelling of high plasticity clay fill can be avoided by compaction at high water content (i.e., wet of the line of optimums). Fill compacted wet will have lower dry unit weight, lower shear strength, and higher compressibility. High plasticity clay can be placed wet for structural fill below lightly loaded buildings provided the lower bearing capacity is considered. Consistent relative compaction is important to avoid differential settlement. Admixtures, such as cement or lime, can also be mixed with high plasticity clay fill during construction to reduce swelling potential.

5-9 HYDROCOMPRESSION.

Hydrocompression refers to the volume change of compacted soil when wetted following construction. This phenomenon is especially problematic in deep fills constructed from sandy clays and clayey sands (Brandon et al. 1990). Significant settlement can occur in the regions of deep fill while net swelling may result in areas of

relatively shallow fill depth. Damage to structures by hydrocompression tends to be worst over locations where the fill depth is changing rapidly and strains are extensional at the surface. The damaging effects of hydrocompression can be reduced by increasing the relative compaction of the fill and/or increasing the compaction water content.

The magnitude of hydrocompression can be predicted using the procedure described in Brandon et al. (1990). Specimens of the fill material can be compacted and loaded incrementally in one-dimensional consolidation to a range of total vertical stresses corresponding to those present in the planned or existing fill. After the intended total vertical stress is applied, the specimen is inundated with water and the volumetric strain caused by wetting is measured. In this manner, the relationship between volumetric strain caused by wetting and confining stress can be estimated. The expected hydrocompression can be found by dividing the fill depth into thin sublayers (see Figure 5-5c) and determining the change in thickness from the corresponding strain.

5-10 SUGGESTED READING.

Topic	Reference
Settlement Calculations	Duncan, J. M. and Buchiagnani, A. L. (1987). *Engineering Manual for Settlement Studies,* CGPR #2, Center for Geotechnical Practice and Research, Virginia Tech, 94 pp.
Vertical Drains	Federal Highway Administration (FHWA) (2017). *Ground Modification Methods Reference Manual – Volume I*, FHWA-NHI-16-027, Geotechnical Engineering Circular 13, Washington D.C.
Volume Expansion	Vanapalli, S. K. and Lu, L. (2012). "A state-of-the-art review of 1-D heave prediction methods for expansive soils." *International Journal of Geotechnical Engineering*, 6, 15-41.

5-11 NOTATION.

Symbol	Description
B	Shortest dimension of foundation or loaded area
C_1	Schmertmann coefficient to correct for the effects of embedment
C_2	Schmertmann coefficient to correct for the effects of time (creep)
C_c	Compression index
$C_{\varepsilon c}$	Modified compression index
c_h	Coefficient of consolidation in horizontal direction
C_r	Recompression index

Symbol	Description
$C_{\varepsilon r}$	Modified recompression index
C_t	Creep factor for coarse-grained settlement methods
c_v	Coefficient of consolidation in vertical direction
C_α	Secondary compression index
$C_{\varepsilon\alpha}$	Modified secondary compression index
d_c	Effective drainage diameter
d_w	Equivalent diameter of well or PVD
e_0	Initial void ratio
E_m	Modulus of elasticity of mat
E_s	Modulus of elasticity of soil
E_u	Undrained modulus
E/G	Relative stiffness for structures
F_n	Radial drainage factor related to drain spacing
F_r	Radial drainage factor related to well resistance
F_s	Radial drainage factor related to soil disturbance (smear)
H	Initial thickness in settlement calculations
H_{dr}	Drainage path length
H_i	Thickness of each soil layer (may be listed without subscript)
H'_t	Total thickness of transformed soil system
I_z	Schmertmann strain influence factor
I_{zp}	Schmertmann peak influence factor
k_h	Hydraulic conductivity in horizontal direction
K_m	Mat stiffness factor
k_s	Hydraulic conductivity of the disturbed zone
k_v	Hydraulic conductivity in vertical direction
l	Distance between two points along a structure
L	Longest dimension of a foundation or loaded area
LL	Liquid limit
L_m	maximum distance water must flow through a vertical drain
m	Empirical exponent used to relate undrained shear strength to OCR

Symbol	Description
N_{60}	Standard Penetration Test corrected blow count
n	Vertical drain spacing ratio
N	Standard Penetration Test blow count
N'	Average Standard Penetration Test value
N'_{SM}	Standard Penetration Test blow count for saturated silty sands
OCR	Overconsolidation ratio
P_a	Atmospheric pressure
q_c	Cone tip bearing resistance
q_0	Applied stress at the base of the foundation or structure
$q_{0\text{-}net}$	Net vertical stress applied by the structure
q_f	Applied stress following removal of surcharge
q_s	Surcharge load
q_w	Discharge capacity of the drain
s	Ratio of the disturbed zone diameter to the diameter of the drain
s	Settlement
s_c	Primary consolidation settlement
s_s	Secondary compression settlement
s_u	Undrained shear strength
t	Time after start of consolidation
T	Time factor
t_m	thickness of mat
t_p	Time required to finish primary consolidation
T_r	Time factor for radial consolidation
T_v	Time factor for vertical drainage
u_0	Initial pore water pressure
$\bar{U}_c$	Combined degree of consolidation
$\bar{U}_{f+s}$	Degree of consolidation following surcharge application
$\bar{U}_r$	Degree of radial consolidation
USR_{NC}	Undrained strength ratio for normally consolidated conditions
u_x	Excess pore water pressure

Symbol	Description
U_z	Degree of compression
$\bar{U}_z$	Average degree of consolidation
w_n	Natural water content
z	Depth along vertical drain
z_i	Layer thickness for settlement calculations
α	Settlement correction factor
γ_w	unit weight of water
δ / l	Angular distortion
δ_{max}	Differential settlement
ΔH	Change in layer thickness
Δ/L	Deflection ratio
$\Delta\sigma_z$	Change in total vertical stress
ε_{crit}	Critical strain for structural distress
εz	Vertical strain
μ_0	Influence factor associated with embedment of the load
μ_1	Influence factor associated with problem geometry and Poisson's ratio
ν	Poisson's ratio
ν_m	Poisson's ratio of mat
ν_s	Poisson's ratio of soil
σ'_p	Preconsolidation stress
σ'_z	Vertical effective stress
σ'_{z0}	Initial or *in situ* vertical effective stress
σ'_{zp}	Initial vertical effective stress at depth of Schmertmann peak influence factor
$\sigma_{z\text{-}red}$	Vertical stress reduction
ψ	Matric suction
ω	Tilt angle due to differential settlement

CHAPTER 6 SEEPAGE AND DRAINAGE

6-1 INTRODUCTION.

6-1.1 Scope.

This chapter discusses methods for analyzing seepage in soils and bedrock and provides design guidance for drainage elements in structures and foundations. The chapter provides a summary of available methods for analyzing the seepage regime, descriptions and analysis methods for internal erosion mechanisms, and discussion of seepage and internal erosion mitigation methods.

6-1.2 Background.

Seepage is the flow of water through interstitial voids of soil or rock. Seepage is driven by differential potential energy of water (i.e., *hydraulic head*) acting across the soil or rock mass, resulting in the flow of water from higher to lower potential energy.

Seepage is a common phenomenon in geotechnical engineering applications and can occur as natural groundwater flow, seepage through dams and levees or their foundations, or flow into excavations extending below the groundwater surface. While the movement of water occurs in unsaturated soils above the groundwater table, this chapter deals only with seepage that occurs under saturated conditions.

Undesirable consequences of seepage can include internal erosion, excessive water loss or accumulation, and excessive pore water pressures. Under the right conditions, seepage can result in erosion of soil or rock, or internal erosion. Several different mechanisms of internal erosion have been identified that can occur by one of several mechanisms. In cases where seepage quantities are large, problems can occur, including: excessive water loss from reservoirs, flooding of excavations, and unstable ground due to excess moisture. Seepage may also result in excess water pressures under structures leading to instability and uplift forces.

This chapter also discusses a number of strategies and methods for mitigating the undesirable effects of seepage discussed in the previous paragraph. Each method utilizes one or a combination of three basic strategies: 1) blocking or lengthening the seepage pathway, 2) draining the excess water pressures in a controlled manner, and 3) filtering the seepage to block the transportation of soil particles.

6-2 SEEPAGE ANALYSES.

6-2.1 Hydraulic Head.

Hydraulic head is a measure of the energy of the water acting on or within geologic media, expressed in terms of length units and referenced to a consistent datum. The

total hydraulic head (h_t) at any given point is composed of three components: the pressure head (h_p), the elevation head (h_z), and the velocity head (h_v). In geologic media, the velocity head is typically negligible and the total head is expressed as:

$$h_t = h_p + h_z = \frac{u}{\gamma_w} + z \qquad \textbf{(6-1)}$$

where:
u = the water pressure at the point of interest,
γ_w = the unit weight of water, and
z = the elevation of the point of interest above the elevation datum.

The total hydraulic head (h_t) at a point is the height above the elevation datum that water would rise in a piezometer if the tip of that piezometer were located at the point of interest as illustrated in Figure 6-1a. The total hydraulic head will vary within a flow regime unless conditions are completely static (i.e., no flow is occurring).

As an example, consider the pressurized tank in Figure 6-1b. Piezometers have been set at two points in the side of the tank and the water rises in the piezometer above the elevation of the tank due to the pressure in the tank. The pressure head (h_p) is the height that the water rises above the point of interest and the elevation head (h_z) is the height of the point of interest above the datum that has been set below the tank. The total head (h_t) is the combined heights of h_p and h_z and is the total height that the water rises above the set datum. Since there is no flow within the tank, h_t is constant throughout the tank although h_p and h_z vary with elevation.

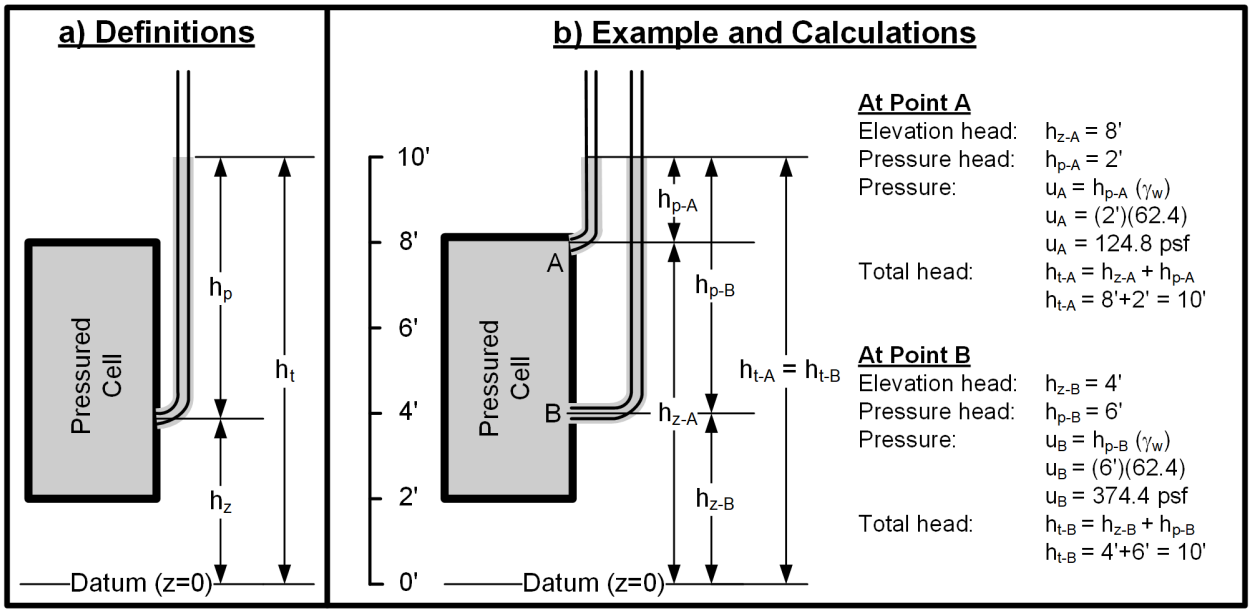

Figure 6-1 Example of the Components of Hydraulic Head

6-2.2 Darcy's Law and One-Dimensional Flow.

The principles of seepage mechanics and analysis of the seepage regime are best illustrated by considering the example of one-dimensional flow illustrated schematically in Figure 6-2. A soil-filled conduit with a cross section of area (A) and a length (L) is attached to water reservoirs with different total heads. The difference in water height in piezometers at each end of the conduit indicates the differential total head (h_L) or head loss across the soil. This head also represents the amount of energy that must be dissipated as the water flows through the soil. The differential head creates a *hydraulic gradient* (i), which is defined as:

$$i = \frac{h_L}{L} \qquad \textbf{(6-2)}$$

where:
i = the hydraulic gradient,
h_L = the differential total head (or head loss), and
L = the length over which h_L occurs.

The hydraulic gradient forces the water to flow through the soil at a *volumetric flow rate* (q) that is sufficient to create the head loss associated with h_L. The volumetric flow rate is defined as the flow volume that passes through the soil per unit of time.

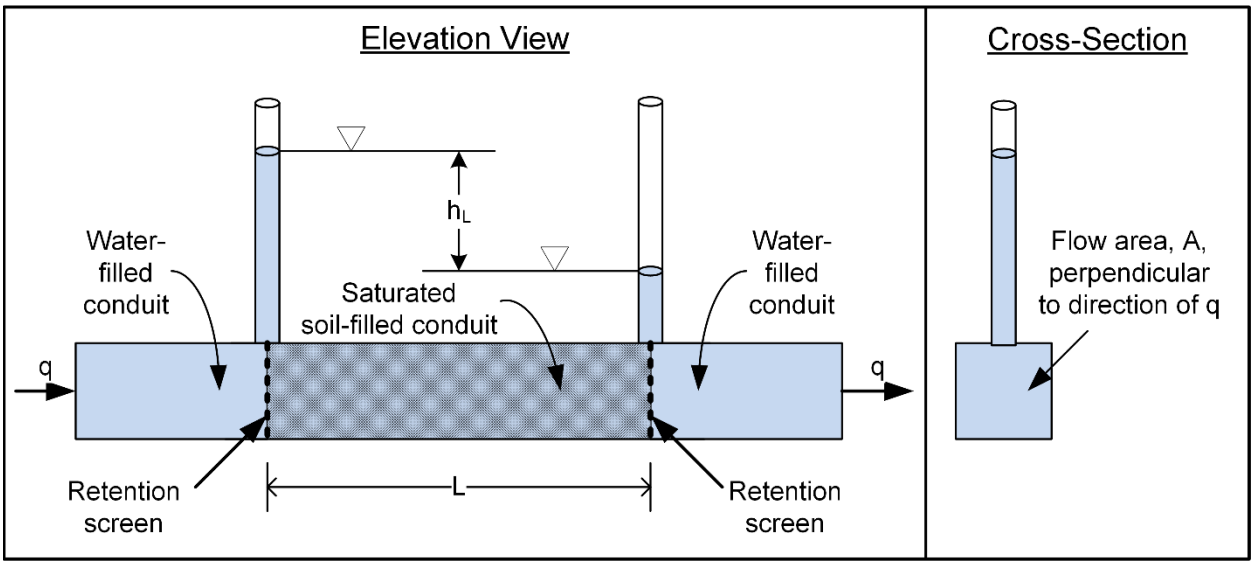

Figure 6-2 One-Dimensional Flow through Soil

One-dimensional flow is governed by Darcy's Law:

$$q = kiA \quad \textbf{(6-3)}$$

where:
q = the volumetric flow rate through the soil,
k = the hydraulic conductivity of the soil,
i = the hydraulic gradient across the flow region, and
A= the cross sectional area of the flow region perpendicular to the flow direction.

If the flow region has a constant height and an extended width (perpendicular to the page), the flow area (A) can be defined by the height of the flow region times a unit width. In this case, the flow rate per unit length of the model is:

$$q = kiy \quad \textbf{(6-4)}$$

where:
q = the flow rate per unit length of the model,
k = the hydraulic conductivity of the soil,
i = the hydraulic gradient across the flow region, and
y = the height of the flow region.

The *discharge velocity* (v_d) can be calculated by dividing the volumetric flow rate by the cross-sectional area:

$$v_d = \frac{q}{A} = ki \quad \textbf{(6-5)}$$

It should be noted that v_d is not a true particle velocity but rather the velocity based on the total area of the flow region. Since the water only flows through the pore space of a soil or rock, a water particle actually flows faster through than v_d. The *seepage velocity* (v_s) which measures how fast a water particle moves as a result of the hydraulic gradient, is calculated as:

$$v_s = \frac{v_d}{n} = v_d \frac{1+e}{e} \quad \textbf{(6-6)}$$

where:
n = the porosity of the soil and
e = void ratio.

Darcy's law is valid for conditions where the seepage flow is laminar, which includes most cases of seepage through soils. High velocity flows through coarse, open-graded gravels may fall in the transition between laminar and turbulent flow. Turbulent flow

results in more resistance to seepage and thus a lower volumetric flow rate than predicted by Darcy's law.

6-2.3 Two-Dimensional Seepage.

Analysis of seepage in a two-dimensional regime requires expansion of Darcy's law. The governing equation for steady state, two-dimensional flow is the LaPlace equation:

$$\frac{\partial^2 h}{\partial x^2} + \frac{\partial^2 h}{\partial y^2} = 0 \qquad \textbf{(6-7)}$$

where:
h = total hydraulic head and
x and y = coordinate directions.

The LaPlace equation is derived by applying the conservation of mass principle to an element of soil, thereby using equilibrium to spatially link changes in total head within the flow region. The first term in Equation (6-7) represents the change in hydraulic gradient in the x direction through an element of soil while the second term represents the change in gradient in the y direction in the same element. Derivation and further discussion of the LaPlace equation can be found in books on groundwater, such as Bear (1979) or Freeze and Cherry (1979).

Solutions to the LaPlace equation can be performed through (1) graphical solutions such as flow nets, (2) closed-form equations such as the method of fragments or the U.S. Army Corps of Engineers blanket theory equations (USACE 2000), or (3) numerical solutions such as finite element analyses.

6-2.4 Flow Nets.

Flow nets are a relatively quick graphical solution tool for analyzing two-dimensional flow regimes using few resources; namely a pencil, paper, and a good eraser. The act of drawing of a flow net also helps the engineer to visualize and understand the behavior of seepage flows. The understanding gained by drawing a flow net is often deeper than that gained by numerical analyses.

A flow net for seepage in an isotropic soil layer beneath an impermeable dam is presented in Figure 6-3. The flow region is divided into *flow elements*, most of which resemble squares or are as close to square as possible. The long-short dashed lines represent *equipotential lines* or contours of constant total head within the soil. Note that the level upstream ground surface is an equipotential line since the reservoir level applies a constant total head along this boundary. The level downstream ground surface is also an equipotential line since the pressure is constant on the surface (equal to zero pressure head) and the elevation is constant (constant elevation head). If the

downstream exit face were sloped and not submerged, the total head would not be constant and it would not be an equipotential line. The short dashed lines are *flow lines,* which represent average paths that water particles will follow while flowing through the soil. The bottom impervious boundary and the bottom of the impervious structure are also flow lines.

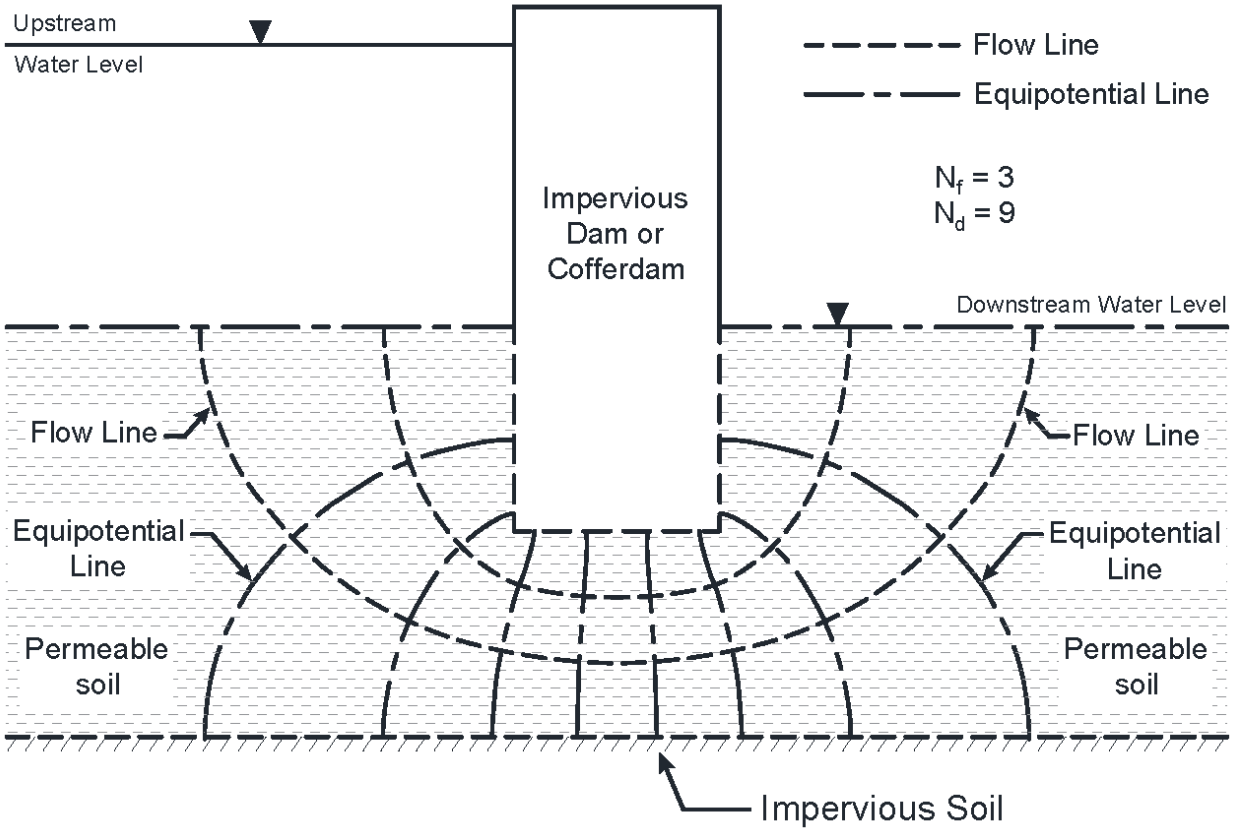

Figure 6-3 Flow Net for Seepage Through an Isotropic Soil Layer Beneath an Impermeable Dam

6-2.4.1 Drawing Flow Nets.

Flow nets for seepage through soil with isotropic permeability must comply with the following rules in order to be correct:

a. Flow lines and equipotential lines should intersect at right angles.
b. The flow elements formed between the flow lines and equipotential should resemble curvilinear squares. A circle can be inscribed in a curvilinear square and touch all four boundaries of the flow element. More guidance on the shape of admissible flow elements can be found in USACE (1986).
c. An impermeable boundary will act as a flow line. Common examples are the top of an underlying layer and the bottom of an impermeable dam or levee.

d. Submerged inflow or outflow boundaries through which seepage passes are equipotential lines with head equal to the water level elevation.
e. Where the flow is unconfined (such as through an embankment) the top flow line will be the phreatic surface. Points on this line will have pressure equal to zero and, consequently, the total head is equal to the elevation of the line (see Equation 6-1).
f. Along a phreatic surface for unconfined flow, equipotential lines will intercept the phreatic surface at equal vertical intervals.

Flow nets constructed according to the above rules will have the following characteristics:

a. Each flow channel, bounded by two adjacent flow lines, will convey the same amount of flow as the other flow channels in the flow net.
b. Each total head drop, bounded by two adjacent equipotential lines, represents the same decrease in total head as the other head drops in the flow net.
c. The flow elements can be subdivided into regions representing partial head drops and partial flow channels.

Flow nets can be drawn for flow through non-homogenous soil profiles and soil with anisotropic hydraulic conductivity. In stratified soil profiles, the flow will be dominated by the permeable layers. If the ratio of a layer's hydraulic conductivity compared to that of the most permeable layer exceeds 10 to 100, the layer can be considered impermeable. If this ratio is less than 10, the flow will be through both layers. However, the flow lines and equipotential lines will be deflected at the interface as illustrated in Figure 6-4.

Flow through soil with anisotropic permeability can be transformed into an equivalent isotropic region using the transformation factor (a):

$$a = \sqrt{\frac{k_{\max}}{k_{\min}}} \qquad \textbf{(6-8)}$$

where:
a = isotropic transformation factor,
k_{max} = the maximum hydraulic conductivity in anisotropic soil, and
k_{min} = the minimum hydraulic conductivity in anisotropic soil.

The dimensions of the flow region are transformed by dividing all of the dimensions of parallel to the direction of k_{max} by a. A flow net is drawn for the transformed system following the rules for isotropic hydraulic conductivity. For example, if k is largest in the horizontal direction, then all of the x-coordinates will be divided by a in the transformed system. If needed, the flow region and flow net can be transformed back to "real space" by multiplying the dimensions parallel to the direction of k_{max} by a.

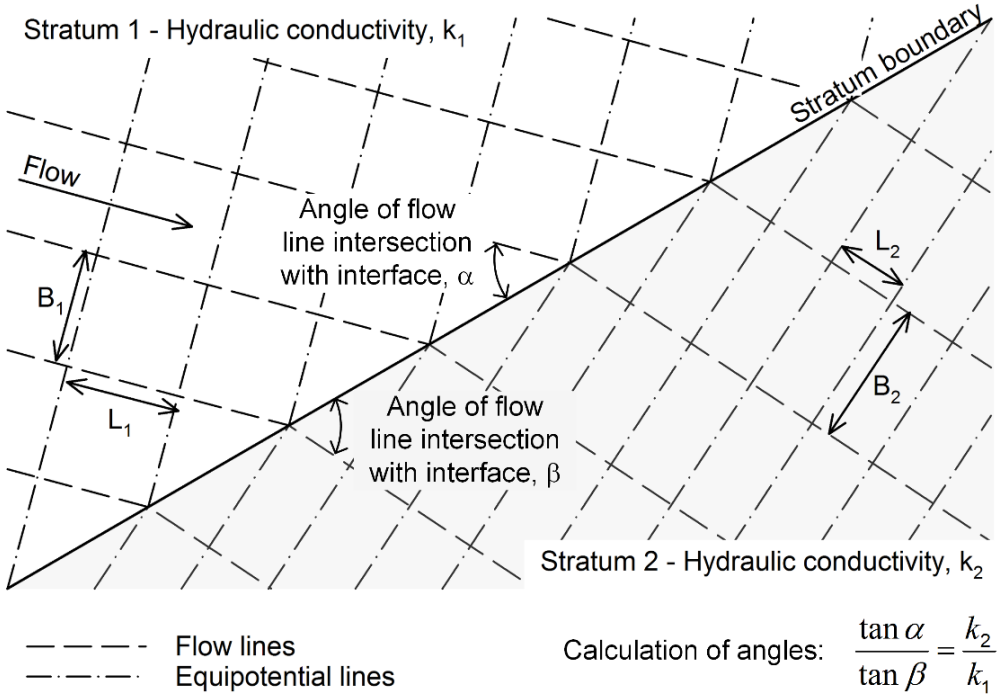

Note: If flow elements in Region 1 are squares (B_1=L_1), then $B_2/L_2 = k_1/k_2$.

Figure 6-4 Deflection of Flow at a Boundary with Changed Permeability

6-2.4.2 Interpreting Flow Nets.

Once drawn, flow nets can be used to calculate a number of properties including: seepage quantities, pore pressures, uplift forces, and hydraulic gradients. The volumetric flow rate through a flow net section can be calculated as:

$$q = k \cdot h_L \cdot \left(\frac{N_f}{N_d} \right) \cdot W \qquad \textbf{(6-9)}$$

where:
h_L = the total differential head or head loss across the flow net,
k = the isotropic hydraulic conductivity (use $\sqrt{(k_{max} \cdot k_{min})}$ for transformed flow nets),
N_f = the number of flow channels in the flow net,
N_d = the total number of equipotential (head) drops in the flow net, and
W = the width of the system perpendicular to the page, often taken as a unit width.

The ratio N_f / N_d from the flow net is sometimes referred to as the *shape factor* (SF). The shape factor incorporates the influence of geometry into the calculation of flow. Two flow nets with a different number of flow lines but the same value of SF will predict the same flow rates, total heads, and pore pressures.

The flow net divides the total head loss across the system into N_d equal head drops. The head loss associated with each head drop is:

$$\Delta h_L = \frac{h_L}{N_d} \quad \textbf{(6-10)}$$

where:
Δh_L = the total differential head or head loss across one head drop,
h_L = the total differential head or head loss across the flow net, and
N_d = the total number of head drops in the flow net.

The total head at any point within the flow net can be calculated by reference to the known total head at either the upstream or downstream boundary. The change in head from the boundary for any point is equal to the number of head drops from the boundary multiplied by Δh_L. By knowing the total head and elevation at a point of interest, the pore water pressure at any point can be calculated from the flow net as:

$$u = h_p \gamma_w = \left(h_t - h_z \right) \gamma_w \quad \textbf{(6-11)}$$

where:
h_p = the pressure head at the point in question,
h_t = the total head at the point in question,
h_z = the elevation head at the point in question, and
γ_w = the unit weight of water.

The hydraulic gradient can be calculated between any two points in the flow region by dividing the change in total head that occurs between two points by the distance over which the head loss occurs. When calculating gradients, it may be useful to subdivide flow net sections for more precision.

Figure 6-5 presents an example flow net with example calculations for discharge, uplift pressure, and hydraulic gradient.

6-2.5 Closed-Form Equations.

The *method of fragments* and *blanket theory* are two closed-form solutions for calculation of seepage flow below water retaining structures. The method of fragments (Pavlovsky 1956, Harr 1977) subdivides the flow region into fragments of standard geometry. Based on the geometry, the SF for each fragment is determined along with the overall SF for the problem. The overall flow rate and pore pressures at particular points can be determined from the results. The blanket theory equations are based on the method of fragments and are particularly useful for seepage analyses of levees. These equations are specifically derived for a levee foundation condition consisting of a

low-permeability “blanket” layer overlying a high-permeability “foundation” layer. The potential for soil heave occurring on the landside of the river can be readily assessed.

Both methods can be implemented in a spreadsheet application. For further information on the method of fragments and blanket theory equations, see Holtz et al. (2011) and Appendix B of USACE (1986), respectively.

Other common solutions have been developed for: (1) flow, heave potential, and exit gradients into excavations, (2) relief well design, and (3) dewatering well design. These specific solutions are presented in the later sections of this chapter.

Example

Using the flow net in Figure 6-3, calculate the flowrate per foot of structure and the pore pressure at the middle of the base. Assume the following:

-Head loss from upstream to downstream: h_L = 36 ft
-Hydraulic conductivity of permeable soil: k = 1×10^{-3} cm/s = 2.8 ft/day
-Thickness of permeable soil: 40 ft
-Depth of embedment of the structure: 20 ft

Flowrate, q, per foot of structure (i.e., W=1)

$$q = kh_L\left(\frac{N_f}{N_d}\right)W = \left(2.8\frac{ft}{day}\right)(36\,ft)\left(\frac{3}{9}\right)(1ft) = 34\frac{ft^3}{day}$$

Pore pressure at base of structure

There are 4.5 equipotential drops from the upstream to the middle of the structure. Each drop represents a head loss of:

$$\Delta h_L = \frac{h_L}{N_d} = \frac{36\,ft}{9} = 4\frac{ft}{drop}$$

Setting the datum at the base of the permeable soil, the total head at this point is:

$$h_{t,base} = h_{t,up} - (\text{Number of drops})\Delta h_L = 76\,ft - (4.5\,drops)(4\,ft/drop) = 58\,ft$$

The elevation head at the base of the structure is 20 ft, which means the pressure head is:

$$h_{p,base} = h_{t,base} - h_{z,base} = 58\,ft - 20\,ft = 38\,ft$$

The pore pressure is then calculated as:

$$u_{base} = h_{p,base}\gamma_w = (38\,ft)(62.4\,pcf) = 2371\,psf$$

Figure 6-5 Flow Net Example Calculations

6-2.6 Numerical Seepage Analysis.

Numerical analysis, such as finite element or finite difference, is the appropriate tool for most seepage analysis problems. These methods are user-friendly and allow easy input of soil properties and complex geometric configurations, while providing rich graphical output. Numerical analyses also can be extended to three-dimensions and

used to model unsaturated soils and transient flow conditions. However, those topics are beyond the scope of this chapter. The graphical and analytical methods discussed in Sections 6-2.4 and 6-2.5 provide an important means of validating numerical seepage models.

Finite element analysis (FEA) is the most common numerical approach used for seepage analysis, and this section is written from the perspective of FEA. Other numerical approaches, such as finite difference, will also provide suitable results but may use slightly different terminology.

6-2.6.1 General Concepts of Finite Element Seepage Analysis.

In finite element analysis, the flow region is divided into areas or volumes (referred to as elements) within which the flow of water can be easily defined. Elements are formed by connecting points in space (referred to as nodes) with lines. Two-dimensional elements are often three-node triangles or four-node quadrilaterals. Within each element the flow is defined with a system of equations that relate the hydraulic head at each node with the hydraulic gradient and flow within the element. These equations are described in an element matrix by linking the values of the common nodes. The equations (matrices) for each of the elements are assembled into a global matrix that represents a set of equations that define the flow through the entire system. For each node there is one equation and one unknown value for each node.

In the simplest form of element, the direction and magnitude of the hydraulic gradient throughout the element are constant. This results in the hydraulic head varying linearly along the element boundaries and within the elements themselves. In more advanced element types, the head varies according to a polynomial equation. Before solving the problem, the one unknown for each node is either (1) the total head at the node or (2) the total flow into and out of the system associated with the node. In general, nodes within the body of the problem and along no-flow boundaries have unknown head and total flow of zero (i.e., flow in equals flow out). At boundaries where flow enters the system, the flow is unknown but the head is generally specified.

6-2.6.2 Boundary Conditions.

Boundary conditions describe the head, pressure, and flow conditions at the boundaries of the model. Table 6-1 describes the most common boundary conditions used in basic finite element models. Table 6-2 illustrates the application of boundary conditions to finite element models.

6-2.6.3 Interpreting Output.

The primary mathematical result of a finite element analysis are values of total hydraulic head and nodal flow for each node in the finite element mesh. By post-processing the total head and flow results from the FEA, the hydraulic gradient, hydraulic velocity, volumetric flow rate, pressure head, and uplift force along a boundary segment can be obtained. Most of the commercially available finite element seepage analysis software

have post processors that will calculate these values through interpolation algorithms. Several of these interpretations are discussed below.

Table 6-1 Common Finite Element Analysis Boundary Conditions

Boundary Condition		General Description	Specific Description	Common Usage
Specify head	Constant Head	Flow allowed to enter or exit the system along the boundary. Nodal heads are known. Nodal flow is calculated during the analysis.	Total head held at a constant value along the boundary	Submerged boundaries (total head = water surface elevation) Horizontal seepage exits (total head = ground surface elevation) Sides of numerical models
	Constant Pressure		The pressure head held at a constant value along the boundary.	Seepage exits (pressure head = 0) Internal drains (pressure head = 0)
Specify flow	No-Flow (impermeable boundary)	Total nodal flow is specified. May be specified as zero for no-flow boundaries Nodal heads are unknown. Nodal heads are calculated during the analysis.	Flow is not allowed across the boundary.	Boundaries with impermeable soil, rock, or structures Sides of numerical models
	Nodal Flow		The inflow or outflow rate from the system is specified for a node (often an internal node).	Injection or extraction well
	Infiltration		Inflow along an external boundary is specified.	Rainwater or other infiltration along a surface
Unknown or Variable		The boundary is set to be either a no-flow or constant pressure boundary, depending on the results of the analysis.		Seepage exit areas where the phreatic surface is unknown, such as the downstream slope of a dam or levee

6-2.6.3.1 Pore Water Pressure.

The pore water pressure is calculated from the total head and the elevation using Equation 6-11. Generally, commercial software will calculate the hydraulic pressure for each node and provide a contour map of the pressure throughout the flow region.

6-2.6.3.2 Uplift Force.

Uplift force due to hydraulic pressure on a structure or mass of soil is calculated by integrating the hydraulic pressures along a specified set of the boundary segments in the model. A simple estimate of the uplift force can be calculated by plotting the pore water pressure contours and assigning a representative area along the boundary segment to each contour interval. The total uplift force can be calculated by summing product of the interval length and the representative pressure for each interval.

Table 6-2 Examples of Boundary Condition Usage

Schematic of Seepage Regime	Model and Boundary Conditions
Impermeable Dam	
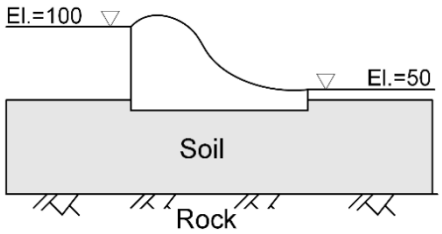	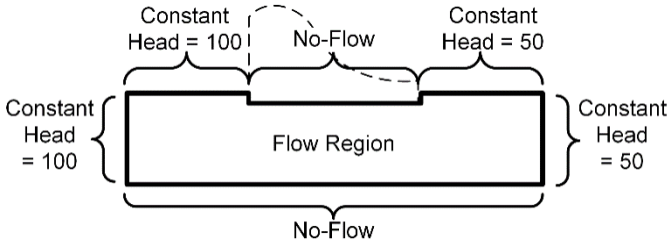
Coffer Dam	
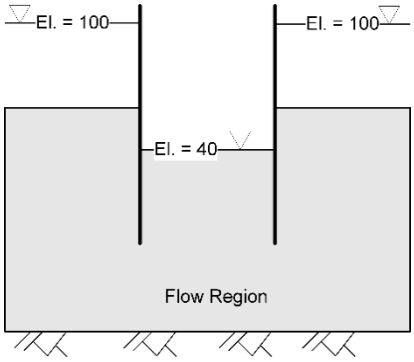	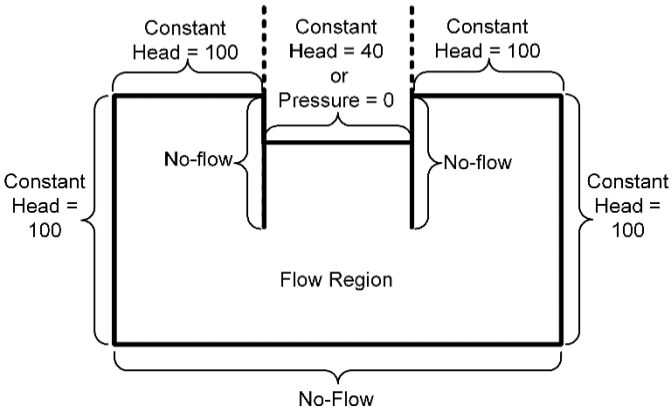
Permeable Dam or Levee	
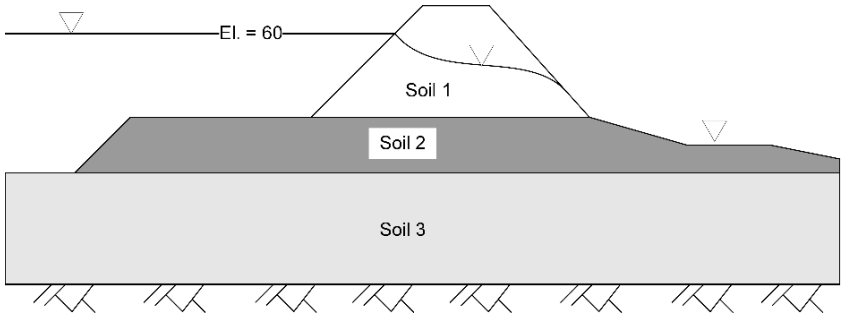	
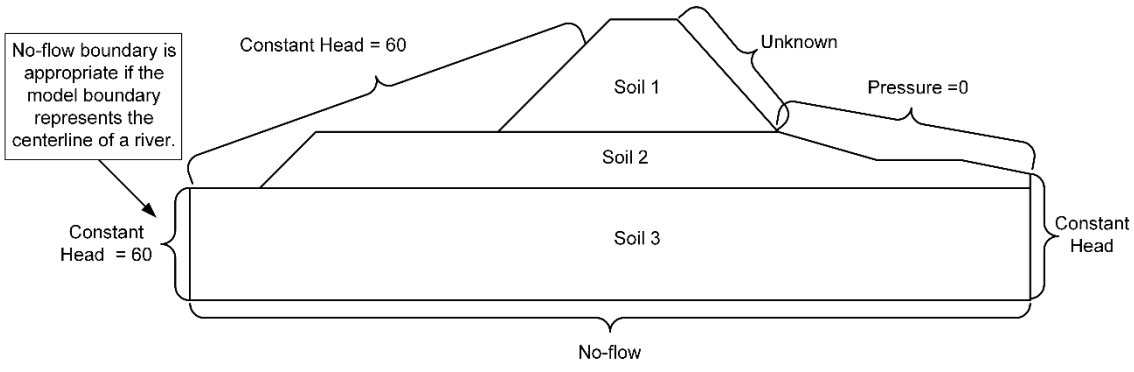	

6-2.6.3.3 Hydraulic Gradients.

Hydraulic gradients are calculated for each element based on the hydraulic heads at the element nodes. Strictly speaking for simple elements, the hydraulic gradient in a given direction should be constant within each element. However, commercial software will often interpolate contours of hydraulic gradient based on the calculated head at each node. For higher order elements, the hydraulic gradient in a given direction may vary within the element. In these cases, the calculated gradients may be interpreted by plotting its variation within the flow region.

As a note of caution, the calculated hydraulic gradient will vary depending on the size of the element used near sharp corners in the flow region (often termed singularities). In this case, the calculated hydraulic gradients will increase as the element size decreases. As the element dimension approaches zero, the calculated hydraulic gradient may approach infinity. At these locations, the hydraulic gradients should be calculated over a distance consistent with the mechanisms of concern and known ground conditions. For example, the hydraulic gradient at the toe of a levee resting on a blanket layer of low k soil should be calculated across the thickness of the blanket.

6-2.6.3.4 Discharge Velocity.

Discharge velocity is calculated from the hydraulic gradient and the hydraulic conductivity assigned to the element using Equation 6-5.

6-2.6.3.5 Seepage Flow Volume.

Seepage volumes are calculated for elements using Darcy's law (Equation 6-3). For flow across a model boundary, the flow rate through each element is calculated, using the vector component of hydraulic gradient perpendicular to the boundary, the hydraulic conductivity assigned to the element, and the area of the element boundary along the model boundary. The flow rate across a portion of an FEA model can be assessed by calculating the flow across a line using a similar methodology applied to the area associated with the elements intersected by the line.

6-3 HYDRAULIC CONDUCTIVITY (COEFFICIENT OF PERMEABILTY).

One of the most varied soil properties in geotechnical engineering is *hydraulic conductivity*, which can be defined as the discharge velocity of water through a unit area under a unit hydraulic gradient. Common hydraulic conductivity values can range from less 10^{-8} cm/sec for high plasticity clay to in excess of 1 cm/sec for open graded gravels; a range of over 8 orders of magnitude. Small changes in soil gradation, especially changes in the fines content, can result in significant variation in hydraulic conductivity.

Terminology regarding hydraulic conductivity is varied across the profession. The term *coefficient of permeability* is used as a synonym for hydraulic conductivity in literature. The practicing geotechnical community commonly uses the term "permeability" interchangeably with hydraulic conductivity. However, this is technically incorrect as

permeability is a property of the porous media alone and does not consider the viscosity of the permeant fluid. Hydraulic conductivity is the preferred term, but both hydraulic conductivity and permeability are used in this manual.

Hydraulic conductivity is most often required for *in situ* soil conditions. Hydraulic conductivity can be assessed for these conditions by several strategies: 1) laboratory testing, 2) field testing, and 3) empirical correlations including equations, charts, and tables. Each of these are discussed in the following subsections.

6-3.1 Laboratory Testing.

Laboratory tests can be performed on intact samples or reconstituted samples. Details of laboratory testing procedures are presented in Section 3-2.7. While laboratory tests can measure the hydraulic conductivity of a wide range of soils, the limitations of laboratory testing must be acknowledged. First, laboratory tests use a small sample of soil or rock and usually test the vertical permeability because the samples are obtained from boreholes. As a result, laboratory test results may not be representative of the large-scale properties of a soil deposit if the layering and structure of the deposit is not considered. Natural soils usually exhibit anisotropy with the horizontal permeability being larger than the vertical. Thus, laboratory tests are likely to result in lower values than are appropriate for many types of analyses. Finally, intact samples of coarse-grained soils cannot be obtained using normal sampling procedures. Laboratory tests on reconstituted specimens of these materials are likely no more reliable than correlations. With the above in mind, laboratory permeability testing is most appropriately reserved for reconstituted samples for applications such as fill materials, cutoff wall backfills, pond liners, and filter materials.

6-3.2 Field Testing.

Two classes of field hydraulic conductivity testing are borehole tests and field pumping tests. Details of field testing procedures are presented in Chapter 2. Borehole tests are effective in measuring the permeability of the soil in the general area of the borehole. To measure permeability characteristics over a broader area, a pumping test can be performed.

6-3.3 Empirical Relationships for Hydraulic Conductivity.

Numerous empirical and semi-empirical relationships have been developed for correlating hydraulic conductivity with other soil properties (predominantly grain size and gradation). The simplest of these relationships relate soil type to typical values of ranges of k. Figure 6-6 correlates k with soil classification types for various unit systems.

The United States Bureau of Reclamation (USBR 2014) has determined typical values for the horizontal hydraulic conductivity of natural soil and rock deposits based on field testing as indicated in Table 6-3 and the vertical hydraulic conductivity of embankment fill materials based on laboratory testing as summarized in Table 6-4.

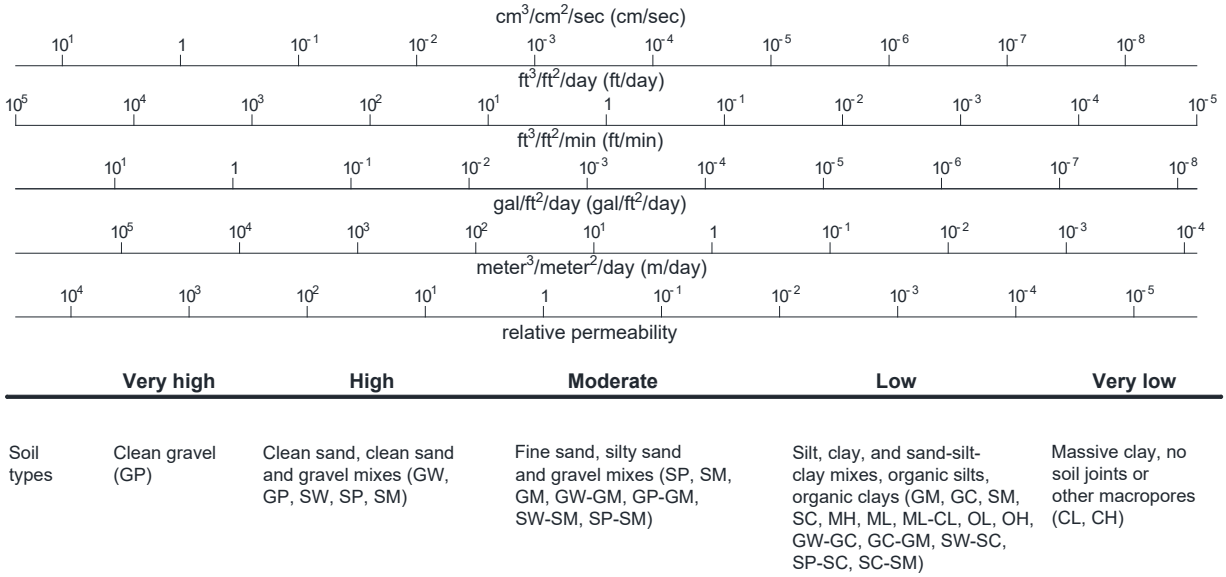

Figure 6-6 Variation of Hydraulic Conductivity with Soil Type for Various Unit Systems (after Freeze and Cherry 1979)

Table 6-3 Typical Ranges of Horizontal Hydraulic Conductivity for Natural Soil and Unfractured Rock Deposits (after USBR 2014)

Soil Type	k_h (cm/sec)
Gravel, open-work	> 2
Gravel (GP)	$2x10^{-1}$ to 2.
Gravel (GW)	$1x10^{-2}$ to 1
Sand, coarse (SP)	$1x10^{-2}$ to $5x10^{-1}$
Sand, medium (SP)	$1x10^{-3}$ to $1x10^{-1}$
Sand, fine (SP)	$5x10^{-4}$ to $5x10^{-2}$
Sand (SW)	$1x10^{-4}$ to $5x10^{-2}$
Sand, silty (SM)	$1x10^{-4}$ to $1x10^{-2}$
Sand, clayey (SC)	$1x10^{-6}$ to $1x10^{-3}$
Silt (ML)	$1x10^{-6}$ to $1x10^{-3}$
Clay (CL)	< $3x10^{-6}$

Rock Type	k_h (cm/sec)
Sandstone, medium	$1x10^{-4}$ to $2x10^{-1}$
Sandstone, silty	< $5x10^{-3}$
Limestone	< $1.5x10^{-2}$
Granite, weathered	$2x10^{-4}$ to $1x10^{-5}$
Schist	< $2x10^{-3}$
Tuff	< $1x10^{-3}$
Gabbro, weathered	$5x10^{-5}$ to $5x10^{-4}$
Basalt	< $5x10^{-5}$
Dolomite	< $5x10^{-6}$
Gneiss	< $2x10^{-6}$

Note: Materials with no indicated lower bound can range from practically impervious to the upper limit indicated in the table.

Table 6-4 Typical Range of Vertical Hydraulic Conductivity for Compacted Soil in Embankments (after USBR 2014)

Embankment Core Materials	
Unified Soil Classification	**k_v (cm/sec)**
GM-SM	< $1x10^{-5}$

Embankment Shell Materials	
Unified Soil Classification	**k_v (cm/sec)**
GP	$2x10^{-3}$ to 1.0

GM or GC	< $1x10^{-5}$
SP-SM	< $1x10^{-5}$
SM	< $1x10^{-5}$
SM-SC	< $3x10^{-6}$
SC	< $3x10^{-6}$
ML	< $1x10^{-5}$
ML-CL	< $1x10^{-6}$
CL	< $1x10^{-6}$
MH	< $1x10^{-7}$

GW	$1x10^{-3}$ to $1x10^{-1}$
GP-SP	$1x10^{-3}$ to $5x10^{-1}$
GW-SW	$5x10^{-4}$ to $5x10^{-3}$
GM	$1x10^{-5}$ to $5x10^{-4}$
SP (medium to coarse)	$1x10^{-2}$ to $2x10^{-2}$
SP (fine to medium)	$5x10^{-3}$ to $1x10^{-2}$
SP (very fine to fine)	$5x10^{-4}$ to $5x10^{-3}$
SW	$3x10^{-4}$ to $5x10^{-3}$
SP-SM	$1x10^{-5}$ to $1x10^{-3}$
SM	$1x10^{-5}$ to $5x10^{-4}$

Note: Materials with no indicated lower bound can range from practically impervious to the upper limit indicated in the table.

The size of the pore spaces is one of the most important factors controlling the hydraulic conductivity of a soil, especially for coarse-grained materials. The *effective diameter* or *effective grain size* (D_α) is the grain size that has the primary influence on the average pore size of the soil. In terms of the effects on hydraulic conductivity, the α refers to a particular percent passing on the grain-size distribution and typically has been assigned a value of 5, 10, 15, or 20. In other words, the effects of pore size on hydraulic conductivity has been found to correlate best with particle diameters corresponding to the 5 to 20% passing size. Correlations that relate hydraulic conductivity to an effective grain size or grain-size distribution can be expressed as (Kenney et al. 1984):

$$k = \beta_\alpha D_\alpha^x \qquad \textbf{(6-12)}$$

where:
k = hydraulic conductivity,
B_α = empirical or semi-empirical coefficient,
D_α = effective grain size,
α = percent passing corresponding to effective grain size, and
x = exponent - theoretically equal to 2 and empirically slightly above 2.

Most of the published correlations for the hydraulic conductivity of coarse-grained soils can be expressed in terms of Equation 6-12. These correlations are summarized in Table 6-5. Some of the relationships also account for the effect of void ratio on k.

Table 6-5 Estimating Hydraulic Conductivity based on Effective Grain Size

Source	Reported Application	α	β_α (cm/sec/mm^2)	x
Kenney et al. (1984)	Sand and fine gravel, C_u = 1 to 12	5	1	2
Hazen (1892, 1911)	Loose sands with D_{10} between 0.01 and 0.3 cm	10	Varies by source from 0.01 to 10 Often taken to equal to 1	2

Slichter (1905) and (McCook 2010)	Sands with D_{10} between 0.01 and 0.5 cm	10	$0.0147 \exp\left(\frac{9.3071e}{1+e}\right)$	2
Chapuis (2004)	Sand	10	$2.4622\left(\frac{e^3}{1+e}\right)^{0.7825}$	1.565
Carrier (2003)	Sand, assuming uniform spheres	10	$5.52\left(\frac{e^3}{1+e}\right)$	2
Sherard et al. (1984)	Sand and gravel with low fines content	15	Average = 0.35, range = 0.2 to 0.6	2
Notes: k is estimated in cm/sec, C_u = coefficient of uniformity = D_{60} / D_{10}, e = void ratio				

The Kozeny-Carman equation (Carrier 2003) can be used to account for the effect of the entire grain-size distribution and the particle shape:

$$k = 1.99 \times 10^2 \frac{cm}{s \cdot mm^2} \left[\frac{100\%}{\sum \frac{f_i}{D_{li}^{0.404} \times D_{si}^{0.596}}} \right]^2 \left(\frac{1}{S^2} \right) \left(\frac{e^3}{1+e} \right) \quad \textbf{(6-13)}$$

where:
k = hydraulic conductivity (cm/sec),
f_i = fraction of particles (by mass) between two adjacent sieve sizes,
D_{li} = the particle size of the coarser sieve (mm),
D_{si} = the particle size of the finer sieve (mm),
S = surface area factor ranging from 6 for spheres to 8.5 for angular particles, and
e = void ratio.

For a given soil, the ratio of hydraulic conductivities under two different void ratios can be considered by (Kozeny 1927):

$$\frac{k_1}{k_2} = \frac{1+e_2}{1+e_1} \frac{e_1^3}{e_2^3} \quad \textbf{(6-14)}$$

where:
k_1 = hydraulic conductivity for void ratio, e_1, and
k_2 = hydraulic conductivity for void ratio, e_2.

For fine-grained soils, the hydraulic conductivity would be expected to decrease as liquid limit, plasticity index, or fines content increase. Figure 6-7 shows that hydraulic conductivity decreases as the fine content (percent passing the No. 200 sieve) increases. For a given fines content, the range of k_v is 2.5 to 3 orders of magnitude with sandy and silty soils having higher k_v than clayey soils.

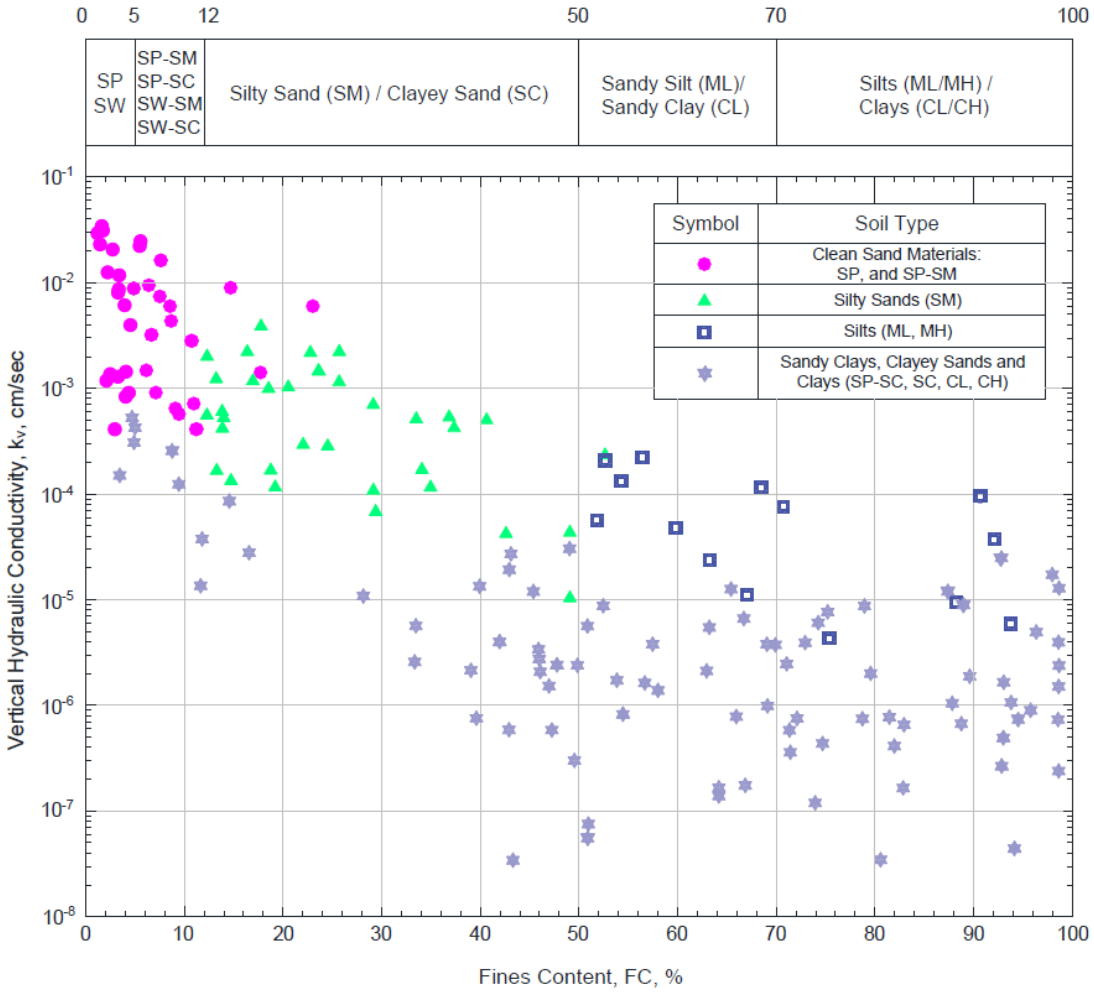

Figure 6-7 Variation of Hydraulic Conductivity with Fines Content (after California Department of Water Resources 2013)

6-3.4 Anisotropy.

More often than not soils exhibit anisotropy with respect to hydraulic conductivity. In natural soils this is usually a consequence of depositional layering of the soil and results in horizontal hydraulic conductivity greater than in the vertical direction. However, in some cases, often related to the formation and filling of vertical cracks, the vertical hydraulic conductivity can be greater than the horizontal. In engineered fills, anisotropy can form as a consequence of soil variation between lifts, differential compaction between the top and bottom of lifts, and planes that form between lifts. Table 6-6 and Table 6-7 present typical values for anisotropy in natural soil deposits and compacted fill.

Anisotropy can greatly affect the seepage behavior in a soil deposit and can have a significant effect on the calculated pressures, flows, and hydraulic gradients in the seepage regime.

Table 6-6 Typical Values of Anisotropy in Natural Soils (after USBR 2014)

Formation	k_h / k_v		Ratio depends on:
	Lower	Upper	
Stratified Deposits	10	1000	Range of k for laminations
Intact Soil or Rock	1	3	Particle shape and orientation
Fractured Bedrock	0.1	10	Arrangement and orientation of apertures and joints
Loess	0.02	2	Orientation of fissures and cracks that form during consolidation and desiccation

Table 6-7 Typical Values of Anisotropy in Engineered Fill (after USBR 2014)

Fill Zone or Method	k_h / k_v	
	Lower	Upper
Core Zone, USBR Compaction Procedures	4	9
Core Zone, Standard Compaction Procedures	9	36
Hydraulic Fill	64	225
Embankment Shell, USBR Compaction Procedures	4	9
Embankment Drains, USBR Compaction Procedures	1	4
Note: USBR compaction procedures are based on Standard Proctor (ASTM D698). Requirements for compaction water content and relative compaction and/or relative density vary based on grain-size distribution and embankment height.		

6-4 INTERNAL EROSION.

About half of dam failures and accidents can be attributed to internal erosion through the foundation and/or through the embankment or along a penetration through the embankment (e.g., Foster et al. 2000). *Internal erosion* is a generic term that describes erosion of particles caused by water seeping through a body of soil or rock. The water may be seeping through the interstitial voids of a soil or rock mass, or may be flowing along pathways of preferential flow (cracks or other defects).

Terminology describing the various mechanisms of internal erosion has evolved in recent years as understanding of the mechanisms of erosion have developed. Nomenclature for these mechanisms has been and continues to be inconsistent in practice and in the literature due to this rapid evolution of understanding and nomenclature. For example, the terms “piping” and “seepage-related erosion” have been used as generic terms for internal erosion, and the term “internal erosion” has been used to denote a specific internal erosion mechanism.

In 2014, the International Commission on Large Dams (ICOLD) adopted a system of nomenclature describing the various mechanisms of internal erosion. The ICOLD nomenclature is summarized in the following sections along with additions to the nomenclature where necessary.

6-4.1 Heave.

Effective stress heave (a.k.a., quick condition) is the uplift of a mass of coarse-grained soil due to a high hydraulic gradient acting on soil particles at an unprotected exit. Seepage forces developed through viscous drag tend to lift the soil mass, resulting in uplift or a quick condition, as illustrated in Figure 6-8a.

Coarse-grained soils with high vertical hydraulic exit gradients are susceptible to effective stress heave. These gradients may occur at the base of deep excavations into sand and at the toe of hydraulic structures founded on sand.

Total stress heave (a.k.a., blowout) is the uplift of a mass of low-permeability soil due to high hydraulic pressure in an underlying aquifer as shown in Figure 6-8b. When the pressure beneath a layer with low hydraulic conductivity exceeds the total weight of the layer, uplift occurs and often results in cracking of the upper layer. Total stress heave occurs in fine-grained soils with underlying aquifers, such as deep excavations into clay and fine-grained blankets.

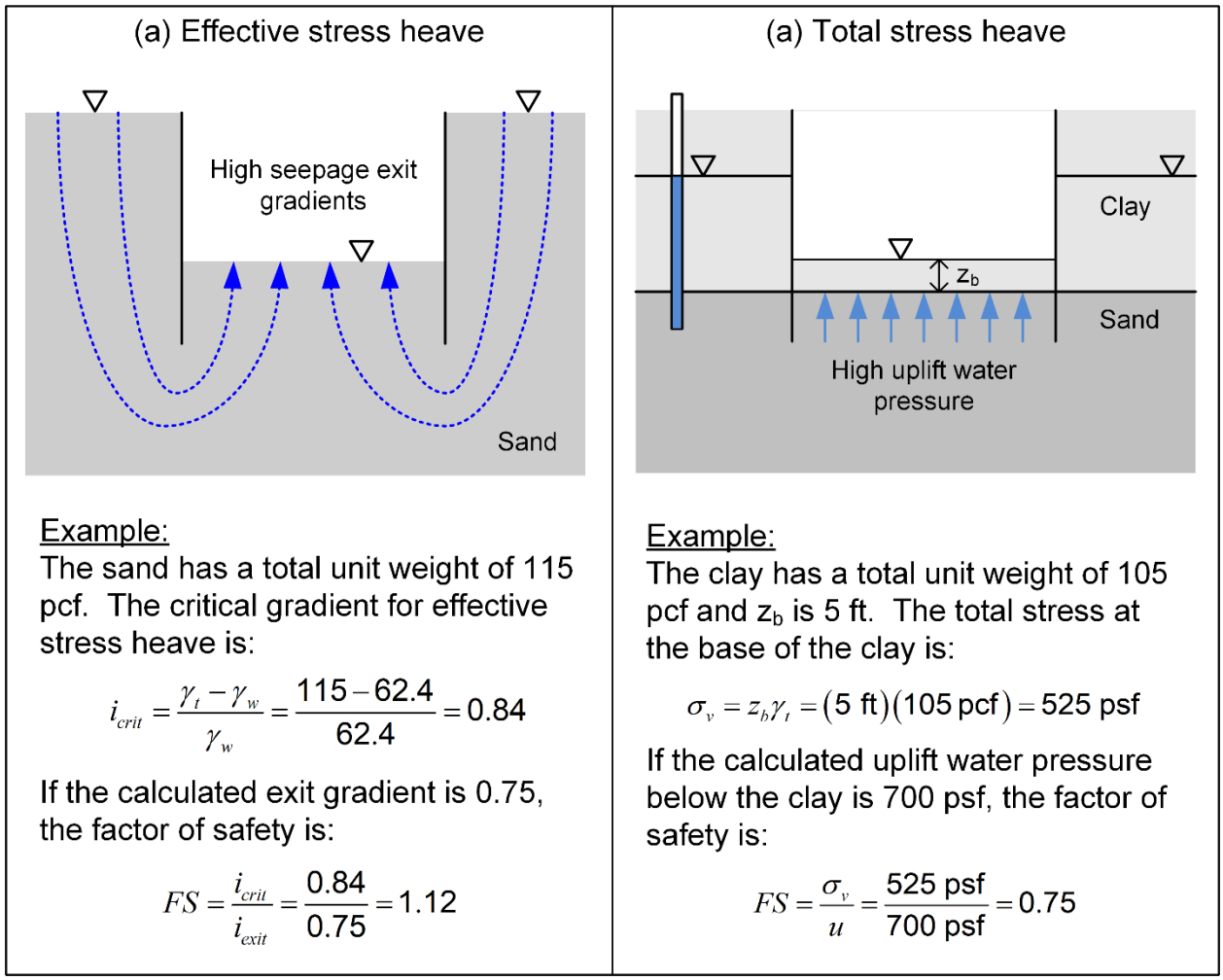

Figure 6-8 Heave – (a) Effective Stress and (b) Total Stress

6-4.2 Erosion and Stoping.

Backward erosion piping (a.k.a., classical piping) is the successive removal of soil particles at an unprotected exit resulting in the formation of an open pathway or *pipe* that progresses toward the source of the seepage. A stable roof prevents collapse of the pipe and allows its progression, as illustrated in Figure 6-9a. The toes of dams and levees are especially susceptible to backward erosion piping, along with unprotected exits, such the ground surface, internal voids or pathways, or defects in a conduit or outlet.

General backward erosion (a.k.a., progressive sloughing or internal migration) is the successive removal of soil particles at an unprotected exit resulting in progressive sloughing of a slope. This type of erosion initiates similar to backward erosion piping, but the lack of a “roof” prevents the progression of a pipe (Figure 6-9b). Slopes and embankments consisting of coarse-grained soils with high seepage flows are susceptible to general backward erosion.

Stoping (a.k.a., sinkhole) is the near-vertical progression of a void caused by successive collapse into a cavity as shown in Figure 6-9c. The cavity is often the result of another internal erosion mechanism. Stopes often manifest as sinkholes at the ground surface and occur in embankments with moderate to low cohesive strength.

Concentrated leak erosion (a.k.a., scour) is erosion that occurs along a concentrated flow path and is caused by shear forces imposed by the flowing water (Figure 6-9d). Concentrated leaks may be cracks within the soil or rock, gaps between soil and a conduit or structure, or other pathways of low flow-resistance capable of carrying eroded soil particles. Conditions that are susceptible to concentrated leak erosion include cohesive embankments, outlet pipes and structures in embankments, and dam and levee fill placed along steep rock abutments.

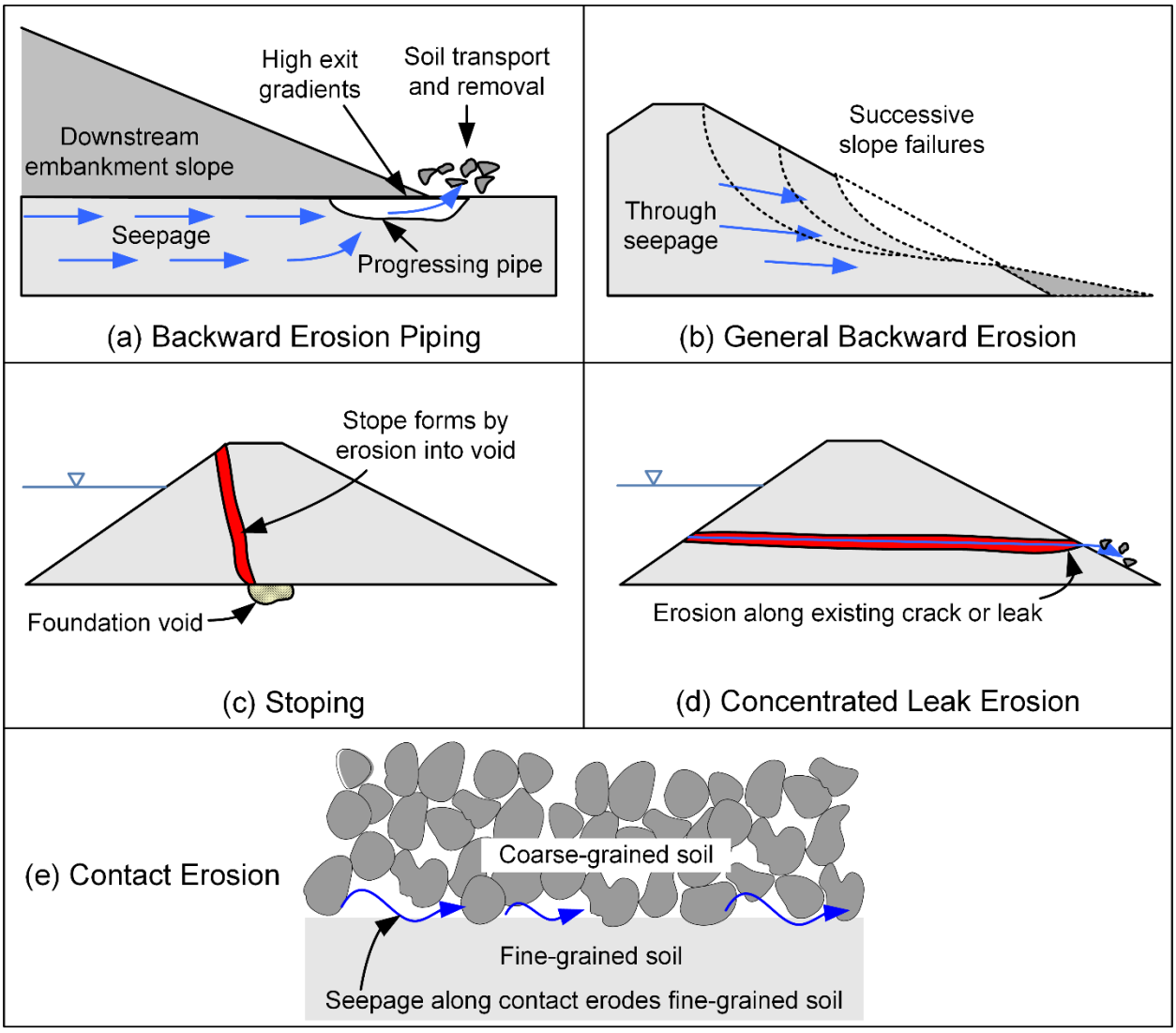

Figure 6-9 Erosion and Stoping Mechanisms

Contact erosion (a.k.a., scour) is erosion that occurs along a contact between a highly permeable material and an erodible soil. Contact erosion is caused by shear forces imposed by high seepage velocities in the highly permeable material as illustrated in Figure 6-9e. The contacts between erodible soil and open-graded gravel or open joints in bedrock are locations susceptible to this type of erosion.

6-4.3 Internal Instability.

Soils can be internally unstable such that fine-grained particles erode from within a framework or "skeleton" of coarse-grained particles as illustrated in Figure 6-10. The process is called *suffusion* if the coarse-grained particles are in contact with each other before erosion. Thus, no volume change results from suffusion. The process is called *suffosion* if the coarse-grained particles are not in contact with each other before erosion. Suffosion results in volume change or collapse. Well-graded, gap-graded, and glacial till soils can be susceptible to either suffusion or suffusion.

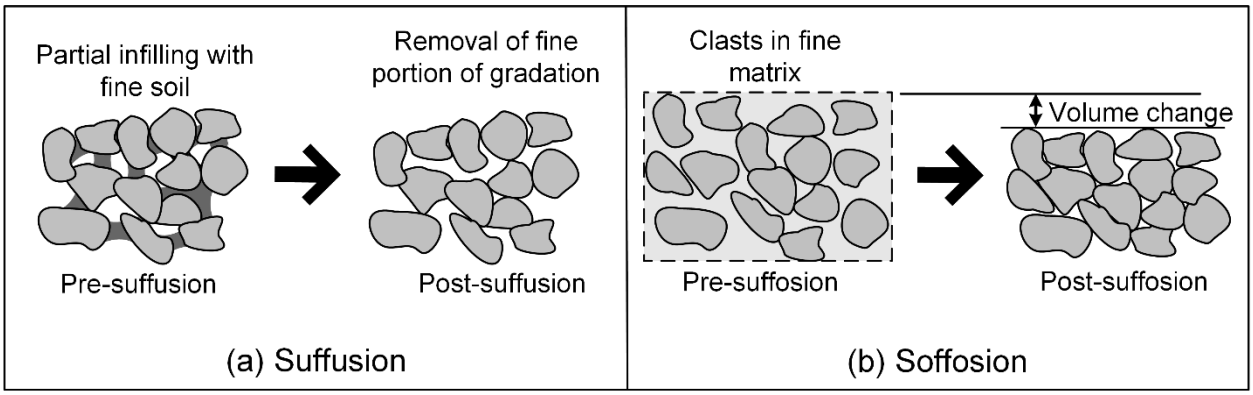

Figure 6-10 Internal Instability – (a) Suffusion and (b) Suffosion

6-5 SEEPAGE AND INTERNAL EROSION MITIGATION METHODS.

6-5.1 Problems and General Strategies.

Seepage occurs through all earthen dam and levee embankments and their foundations, into excavations below the water table, and below other structures subjected to differential water pressure conditions. In many cases, the quantity of seepage is such that it poses no adverse consequences or risk to the structure. However, if seepage is excessive or the pressures and forces associated with the seepage are too great, mitigation of the seepage issues may be required. Problems associated with seepage can be classified into three categories:

a. Excess volumetric flow rate of seepage
Undesirable consequences of excess flow include the loss of valuable water from

a reservoir, flooded or soft ground in excavations, and wet ground conditions below a dam or levee that prevent activities or usage of the land.

b. High pore water pressures
High pore water pressures can result in unacceptable uplift forces beneath or within dams and levees that lead to instability with respect to sliding or overturning. Excessive water pressure forces can also act on buildings, retaining walls, and other appurtenant structures.

c. Internal erosion potential
Some seepage conditions may create a condition where internal erosion is likely through one of the mechanisms described in Section 6-4. Internal erosion problems are often tied to high pore water pressures. Assessment of internal erosion potential should be paired with an evaluation of the severity of seepage. Table 6-8 provides a means to evaluate seepage severity and assess if further investigation is required. This approach recognizes that the flow rate must be sufficiently high for problematic internal erosion to occur

Table 6-8 Seepage Severity Categories (after Duncan et al. 2011, USACE 1956)

$q / h_L / W$ (cfs per foot of head per foot of levee)	Severity of Seepage	Seepage Remediation Needed
> 2.2×10^{-4}	Heavy	Yes
1.1×10^{-4} to 2.2×10^{-4}	Medium	Possible
2.2×10^{-5} to 1.1×10^{-4}	Light	Marginal
<2.2×10^{-5}	Negligible	Not Needed
Notes: q = estimated volumetric flow rate, h_L = head loss across the structure, W= width 1 cfs/ft of head/ft. of levee = 44,883 gpm/ft of head/100 ft. of levee		

If one or more of the problems described above must be mitigated, the mitigation typically employs one of three general strategies:

a. Seepage barriers
This strategy consists of constructing an element that either directly blocks the seepage pathway or lengthens the seepage pathway. Blocking seepage can result in increased hydraulic pressures and hydraulic gradients in some locations within an embankment or foundation. When methods to block seepage are used, the engineer must assess whether the resulting pressures and gradients will be detrimental to structural stability and the internal erosion potential.
b. Providing controlled drainage
In locations where high pore water pressures result in either high hydraulic

gradients or uplift forces, the pressures can be reduced by providing a controlled drainage system. The control in such a system involves assuring that the water can be drained without causing internal erosion or resulting in excessive water losses. Controlled drainage typically increases the volumetric flow rate.

c. Providing Filtration
In locations where there is potential for internal erosion, the progression of erosion can be halted by providing adequate filtration of the eroding soil particles. The most reliable and long-lasting filters are constructed using sands and gravels graded to specifications that provide both soil particle retention and adequate seepage flow capacity.

Specific methods for seepage and internal erosion mitigation options are provided in the following sections.

6-5.2 Seepage Barriers.

Seepage barriers include a range of options for (1) blocking flow through a high-permeability layer of soil or rock or (2) extending the seepage pathway to reduce seepage volume and hydraulic gradients.

6-5.2.1 Vertical Barriers.

Vertical barriers or seepage cutoff walls are zones with low hydraulic conductivity that are constructed (1) through permeable dam and levee embankments, (2) through dam and levee foundations with permeable layers, (3) surrounding excavations below the ground water table, or (4) blocking aquifers to prevent the spread of groundwater contamination. Vertical barriers are generally classified based on the excavation or construction method and the backfill type.

The various construction methods, their application, characteristics, and requirements are summarized in Table 6-9. Continuous slurry trenches are generally backfilled using one of three material types: Soil-Bentonite (SB) backfill, Cement-Bentonite (CB) backfill, and Soil-Cement-Bentonite (SCB) backfill. Element slurry walls are generally backfilled with concrete or plastic concrete using the Tremie method that fills the element from the bottom up while displacing the slurry. The characteristics of vertical barrier backfill materials are presented in Table 6-10.

Table 6-9 Construction Methods for Vertical Seepage Barriers (Cutoff Walls)

Construction Method/Type	Description and Applicability	Characteristics and Requirements
Steel Sheet Piles	Interlocking steel sheets are typically driven into the ground with a vibratory hammer with rapid installation in mixed soils with limited amounts of gravel and cobbles. Interlocking of steel sheets becomes difficult with increased driving depth, increased soil density, and increased gravel and cobbles.	Leakage occurs only through interlocks, making performance reliant on maintaining interlock integrity. Predrilling in soil with gravel and cobble improves chances of interlock integrity. Seepage resistance tends to increase with age due to clogging and oxidation along the interlocks. Corrosion may be a concern for structural integrity.
Vinyl Sheet Piles	Interlocking vinyl sheets are pushed into very soft ground or installed in excavated trenches. Depth is limited by excavation stability (see slurry walls).	Leakage occurs only through interlocks, making performance reliant on interlock integrity. Corrosion is not a concern although chemical stability in harsh environments should be assessed.
Continuous Slurry Trench Wall	Wall constructed in a continuous trench that is excavated with a long-reach excavator and/or clamshell. Trench is stabilized with slurry consisting of either a mixture of bentonite and water or a polymeric slurry. Wall material can vary from SB and SCB backfill to self-hardening CB slurry (see Table 6-10).	Continuous construction avoids construction joints but is susceptible to “windows” in the wall due to partial trench wall collapse or sand settling from slurry. Walls are generally ductile but of low strength and high erodibility. Backfill compressibility can result in vertical and lateral consolidation leading to distress to overlying and adjacent structures. Stability of long excavations can be a concern. Generally limited to soil and soft rock.
Element Slurry Wall	Continuous wall constructed by sequentially overlapping vertical elements. Slurry-supported rectangular elements are excavated using a hydraulic clamshell in soils and soft rock and using a hydrocutter in moderate to hard rock. Circular elements can overlap to form a secant wall. Backfill is usually concrete or plastic concrete placed from the bottom up using the tremmie method.	The length of elements is determined by considering trench and embankment stability, backfill procedures, and other construction considerations. Care should be taken to ensure good connection with construction joints. Excavation stability is less of a concern because of the limited duration of excavation. Elements can be excavated into most soils and rock using a variety of excavation equipment.
Vertical Membrane	Insertion of a geotextile membrane into an excavated trench forms a very low hydraulic conductivity barrier. Membranes are often placed in slurry trench excavations. Interlocking elements are glued or welded to edges of membrane sheets to form interlocks with adjacent sheets.	Membrane creates a very low hydraulic conductivity continuous seepage barrier. Membranes are often used in environmental applications where very small leakage volumes are critical.

Table 6-9 Construction Methods for Vertical Seepage Barriers (Cutoff Walls)

Construction Method/Type	Description and Applicability	Characteristics and Requirements
Deep Mixing Method	*In situ* soils are mixed in-place with a slurry consisting primarily of bentonite, cement, and water to produce a soil-cement material that has reduced permeability and increased strength. The soil mixing can be performed using the multi-axis mixing or vertically-mixing cutter soil mixing techniques. Multi-axis mixing uses overlapping soil augers that are drilled into the ground as the slurry is pumped through the tips of the augers.	Sets of three or more augers are drilled at one time and overlapped with adjacent sets to provide continuity of the wall. This method often results in layering in the wall as the augers encounter different soil types with depth. Cutter soil mixing uses a continuous cutter (resembling a very large chain saw) to mix the entire column of soils simultaneously in a vertical column. This method results in more uniform wall properties with depth. Strength and permeability of the "soil-cement" can be adjusted by the components and dosing of the slurry. Deep mixing is limited to soil and very soft rock.
Jet Grout Walls	Jet grout columns are constructed with a probe that uses high-pressure jets to simultaneously erode soil and fill the column with a grout mixture. Soil-cement is formed as varying amounts of eroded soil are mixed with water and grout. The procedure can be performed with single-, double-, and triple-fluid methods. The single-fluid method injects the cement grout out of a single nozzle that simultaneously erodes the soil and provides the grout. The double-fluid method uses a double nozzle that shoots a stream of grout through a shroud of air, increasing the range of the grout jet so that a larger diameter column can be produced. The triple-fluid method uses a jet of water shrouded in air to cut the column followed by a jet of grout to fill the column.	Because the column is formed by jets, walls can be constructed that seal against irregular rock or concrete surfaces that are otherwise difficult with rigid excavation. Equipment is adaptable for construction in limited-space and low-overhead conditions. Due to very high pressures, the risk of hydrofracturing embankments is high, limiting the applicability in dams and levees. The jet grout method is typically more expensive than other methods, thus limiting its use to limited access and special needs projects.

Table 6-10 Backfill Material Description and Characteristics for Vertical Seepage Barriers (Cutoff Walls)

Backfill Type	Description and Applicability	Characteristics and Requirements
Soil-Bentonite (SB) Backfill	SB backfill consists of a mixture of the excavated soils and bentonite and is used primarily for continuous slurry trenches. The SB mixture is often created by adding the trench slurry to the trench spoils on the ground adjacent to the trench. The mixing is often done using a bulldozer or a soil-mixing machine.	SB backfill is a low-strength, high-ductility, and low-hydraulic conductivity material. While the material is highly compressible, friction on the sidewalls may reduce vertical stress on the backfill, causing it to remain in an underconsolidated state in the trench. The SB may be susceptible to vertical and horizontal consolidation and hydraulic fracture.
Cement-Bentonite (CB) Backfill	CB backfill is a self-hardening slurry that is used to support continuous slurry trenches and then hardens into a consistency similar to stiff clay. The slurry is mixed in a batch plant and may contain additives to increase strength or retard setup.	CB is less prone to consolidation than SB. The strength of CB can be adjusted but generally has the consistency of very stiff to hard clay.
Soil-Cement-Bentonite (SCB) Backfill	SCB backfill is often blended and placed similar to SB backfill but with the addition of cement to give strength to the backfill for a more robust element within the embankment. Primarily used as backfill for continuous slurry trenches.	SCB is less prone to consolidation than SB. The strength of SCB can be adjusted. It should be noted that some SCB walls have been found to have discontinuities or windows near the bottom of the wall. These windows are thought to be the result of premature setting of the backfill that breaks into blocks due to the slumping that occurs during normal placement.
Soil Cement	Soil cement is a term often used to describe the product of deep soil mixing. In the wet method, a slurry consisting primarily of bentonite, cement, and water is blended with the *in situ* soil (see deep mix method in Table 6-9). The less common dry method injects cement and bentonite powders directly into the soil for mixing.	The strength and permeability of soil cement will vary depending on the amount of cement and bentonite in the slurry and the type of soil it is mixed with. Gravelly or clean coarse-grained soils will tend to have higher strength and higher permeability than sands and silts that are mixed with the same amount of an identical slurry.
Plastic Concrete	Plastic concrete is conventional concrete with bentonite added to increase ductility with the intent of making the wall more compliant with the surrounding soils, decreasing cracking of the wall and surrounding soils.	The bentonite results in reduced strength and erosion resistance of the concrete. Thus, a balance of robustness and compliance should be considered when choosing between conventional and plastic concrete.
Conventional Concrete	Conventional concrete adds a robust element to an excavation or dam/levee embankment that is high-strength, stiff, and highly erosion resistant.	The rigidity of the wall may cause stress concentrations in other elements of the embankment, resulting in cracking of the wall or surrounding soil.

6-5.2.2 Required Penetration for Cutoff Walls in Supported Excavations.

To prevent instability of the base of supported excavations due to heave (i.e., quick condition or blowout), the vertical cutoffs must extend deep enough to reduce hydraulic gradients or uplift pressures to acceptable levels. The first option to consider for embedment is to extend the cutoff to a low-permeability layer having considerable thickness. However, this is not always feasible.

In uniform pervious sands, critical hydraulic gradients may develop at the base of the excavation. The required wall penetration to provide a factor of safety against effective stress heave (quick condition) and piping in homogenous, isotropic sands can be calculated using Figure 6-11. For homogenous, anisotropic sands, the penetration depth can be reduced by the transformation factor, a (see Section 6-2.4.1 Equation 6-8). For clean sand, exit gradients greater than about 0.5 to 0.75 will cause unstable conditions for men and equipment operating on the subgrade. To avoid instability, provide sheeting penetration for a safety factor of 1.5 to 2 against effective stress heave as calculated in Figure 6-8.

In layered sands, variation in permeability results in a change of seepage conditions from that assumed in Figure 6-11. Figure 6-12 presents guidance for situations with layered sands. In layered soils with layers of very fine sand, silty or clayey sand, or silt and clay, the risk of bottom heave (total stress heave) must be considered. Figure 6-13 presents guidance for avoiding bottom heave in excavations. Alternatively, the conditions can be assessed using flow nets or finite element analyses, and Figure 6-11 through Figure 6-13 can be used to confirm the results.

The relationships presented in Figure 6-11 through Figure 6-13 were developed based on the results of laboratory modeling performed by Marsland (1953). The results were reported for loose and dense sands. Loose sands were placed “with a water jet” while the dense sands were placed “with an electrically vibrated” hammer. No relative densities were reported although porosities of 42 percent and 37 to 38 percent were reported for the loose and dense sands, respectively.

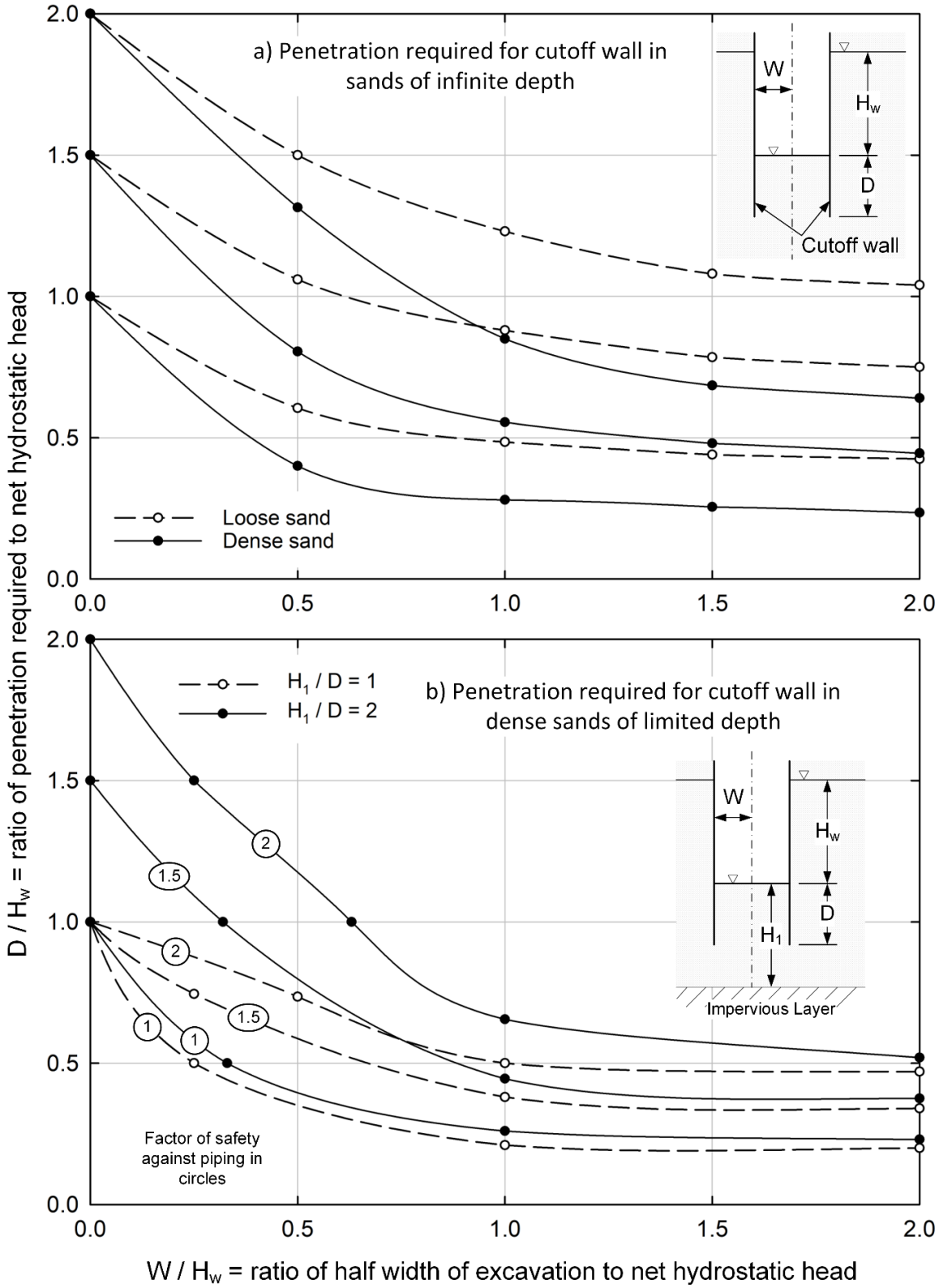

Figure 6-11 Required Depth of Penetration of Cutoff Wall-Supported Excavations in Homogenous Isotropic Sand (after Marsland 1953)

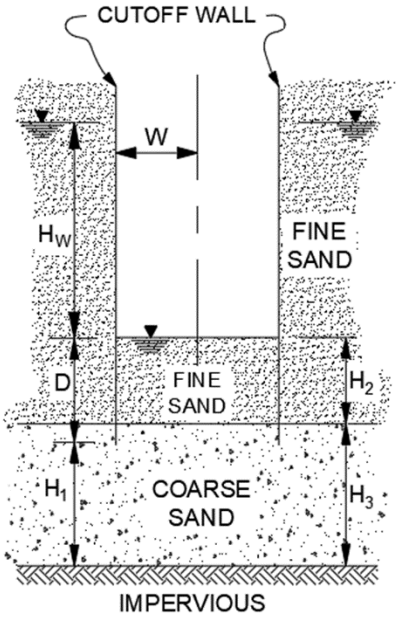

Coarse Sand Underlying Fine Sand

The presence of the coarse sand layer makes flow in the fine sand nearly vertical and generally increases hydraulic gradients in the fine sand layer when compared with the homogenous case.

If the top of the coarse sand layer is at a depth greater than the excavation width below the depth of the cutoff, the safety factors for the homogenous case apply.

If the top of the coarse sand layer is at a depth less than the excavation width below the depth of the cutoff, the uplift pressures will be greater than for the homogenous case. If the permeability of the coarse layer is more than 10 times the permeability of the fine layer, the failure head (H_w in Figure 6-9) will equal the thickness of the fine layer, H_2.

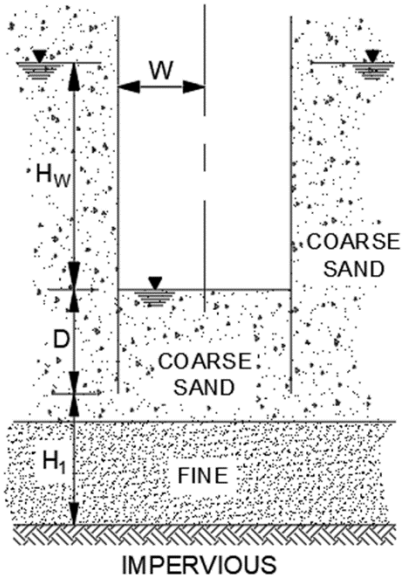

Fine Sand Underlying Coarse Sand

The presence of the fine sand constricts the flow beneath the cutoff wall and generally decreases hydraulic gradients at the base of the excavation when compared with the homogenous case.

If the top of the fine sand layer is below the depth of the cutoff, the safety factors are intermediate between those for the homogenous case (calculated using Figure 6-9) for an impermeable boundary located between the top and bottom the fine layer.

If the top of the fine sand layer is at a depth less than the depth of the cutoff, the factors of safey for the homogenous case (calculated using Figure 6-9) will be somewhat conservative.

Figure 6-12 Corrections to Required Depth of Penetration of Cutoff Wall-Supported Excavations for Stratified Sand (after Marsland 1953)

Fine-Grained Layer Within Homogenous Sand Stratum

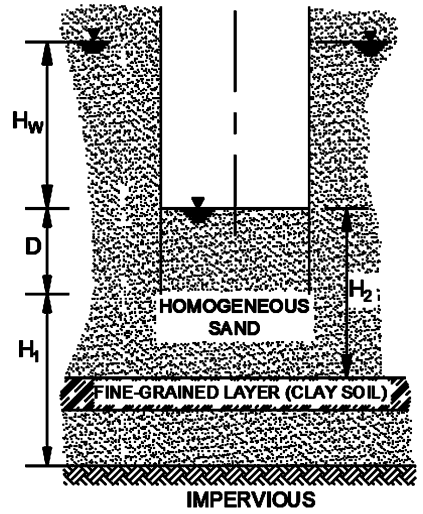

If the top of the fine layer is at a depth greater than the excavation width below the depth of the cutoff wall, the safety factors for the homogenous case (in Figure 6-13) apply, assuming the impervious base is at the top of the fine layer.

If the top of the fine-grained layer is at a depth less than the excavation width below the depth of the cutoff, pressure relief is required so that the differential head (H_w) does not exceed the height of soil above the fine layer (H_2).

If the fine-grained layer lies above the final base of the excavation, the final condition is safer than the homogenous case. However, dangerous conditions may arise during excavation above the base of the fine layer and pressure relief may be required as outlined above.

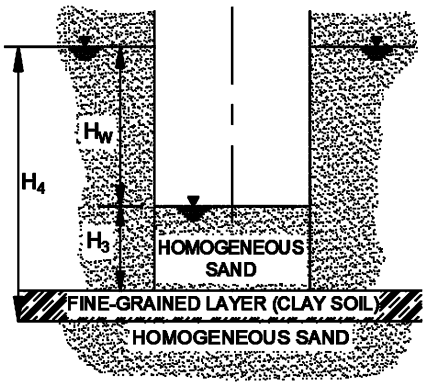

To avoid bottom heave, the weight of the soil above the base of the fine layer ($\gamma_t \cdot H_3$) should be greater than the water pressure acting at the base of the fine-grained layer ($\gamma_w \cdot H_4$),

where:

γ_t = the total unit weight of the soil

γ_w = unit weight of water

Figure 6-13 Corrections to Required Depth of Penetration of Cutoff Wall-Supported Excavations in Sand Containing Fine-Grained Layers (after Marsland 1953)

6-5.2.3 Seepage Blankets and Berms.

Upstream seepage blankets are constructed upstream of a dam or levee to increase the seepage pathway as depicted in Figure 6-14a. Upstream blankets are constructed of compacted fill with low hydraulic conductivity or a geomembrane protected with a coarse-grained soil cover. The increased seepage pathway will tend to decrease the amount of seepage, decrease uplift pressures below the dam or levee, and decrease

exit gradients. The primary design concern of seepage blankets is providing a uniform foundation for the blanket. Differential settlement of the blanket under reservoir loading can result in tearing or cracking of the blanket and concentrated leakage, decreasing the effectiveness of the blanket.

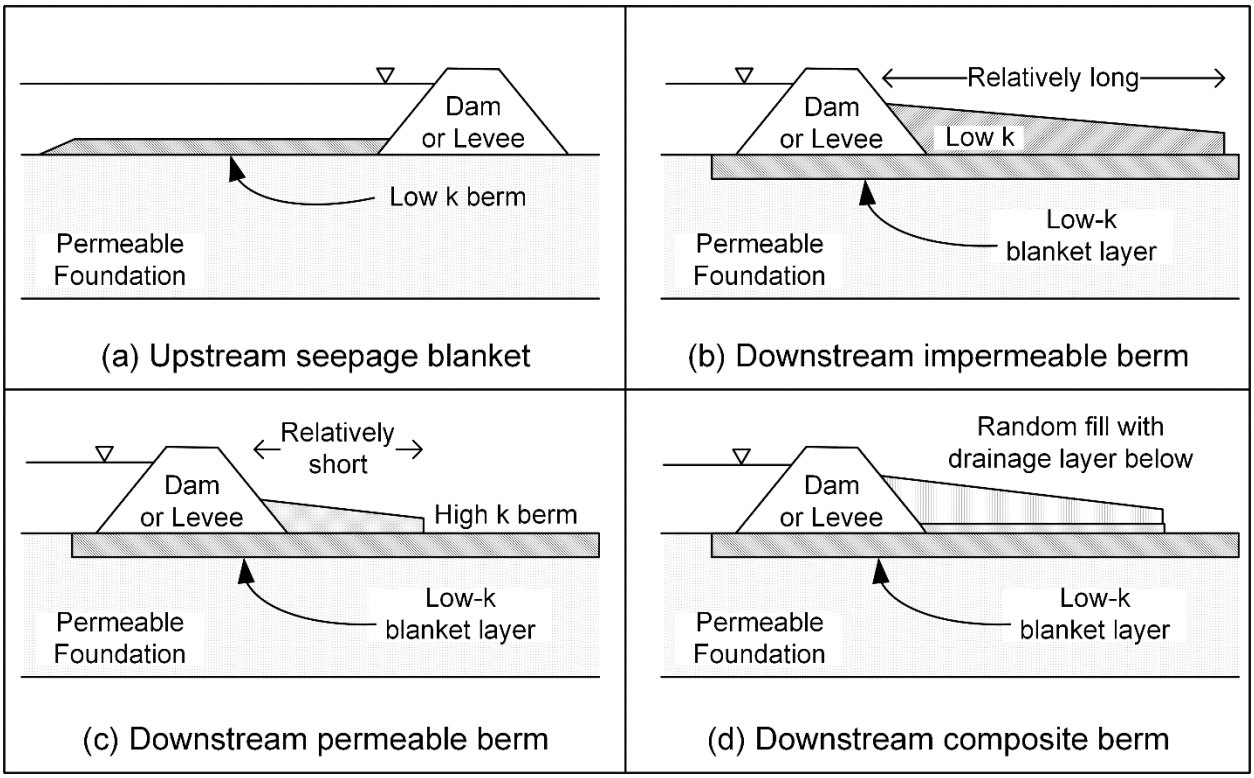

Figure 6-14 Seepage Blankets and Berms

Downstream seepage berms are designed to prevent excessive hydraulic pressures on the downstream side of a small dam or levee. Often these pressures are the result of a low hydraulic conductivity soil layer (blanket layer) that blocks the exit of seepage water. Seepage berms are usually constructed using one of three designs: (1) an impermeable berm, (2) a permeable berm, or (3) a composite berm.

The concept of an impermeable berm used to resist uplift pressures on a low-permeability blanket layer is presented in Figure 6-14b. The berm is constructed of generally low-permeability soils and is designed to increase the weight of the blanket layer thereby resisting total-stress heave. For blanket layers that allow some seepage, the impermeable berm will increase the resistance to seepage flow through the blanket layer, resulting in higher pressures below the levee and downstream toe. This also requires the berm to extend long distances from the levee in order to produce low uplift pressures beyond the berm.

A permeable seepage berm is illustrated in Figure 6-14c. The permeable berm is constructed of permeable materials (generally sand) that increase the total weight on

the blanket without significantly increasing seepage resistance. Where the blanket layer is sufficiently permeable allow seepage on the landside, permeable berms can be much shorter than impermeable berms. A disadvantage of this berm type is that appropriate high-permeability soils can be very expensive in some locales.

A composite seepage berm consists of an upper layer of undifferentiated fill underlain by a drain and filter layer (see Figure 6-14d). Thus, the berm acts similar to the permeable berm but is less expensive because less of the filter material is required. The drainage layer must be designed with adequate flow capacity to prevent the buildup of water pressure in the layer. In some cases, pipes have been included in the drainage layer to increase flow capacity. However, such pipes increase the amount of maintenance needed for the berm.

6-5.2.4 Other Types of Seepage Barriers.

6-5.2.4.1 Cutoff Trench.

Cutoff trenches are constructed in the foundations of dams and levees as part of the original construction. The cutoffs are generally a broad trench with sloped sidewalls that is backfilled with low hydraulic conductivity material. The trench extends partially or fully through permeable soil and rock layers in the foundation. In addition to the seepage control offered, cutoff trenches provide an opportunity to visually inspect the subsurface conditions beneath the dam or levee. Care should be taken to ensure that the downstream side of the berm is properly filtered (see Section 6-5.3) to prevent internal erosion into permeable foundation soil or rock.

6-5.2.4.2 Foundation Grouting.

Foundation grouting is performed by pumping stabilized cement grout into boreholes to fill joints and voids in bedrock and reduce the effective hydraulic conductivity of the formation. Foundation grouting can be performed prior to dam construction or after construction as a remedial measure. Grout is pumped into discrete depth intervals of the boring by sealing off an interval using inflatable bladders called packers. Grout lines consisting of evenly spaced boreholes are typically aligned parallel to the axis of the dam although other configurations may be applicable for special circumstances. In many cases, multiple grout lines (grout curtains) are installed along the dam axis with the boreholes inclined in opposite directions to increase the chances of encountering all of the joints and voids in the rock.

6-5.2.4.3 Liners.

Leakage from ponds and reservoirs can be reduced by installing a liner in the base of the pond or reservoir. Such liners can consist of compacted clay, synthetic geomembrane liners, or native soils supplemented with bentonite or other materials to reduce hydraulic conductivity. Similar to upstream blankets, the foundation for the liner

must be sufficiently uniform to prevent differential settlements under the reservoir loading, which could tear or crack the liner.

6-5.3 Filters and Drains.

Drainage systems provide relief of hydraulic pressures in foundations, intercept paths of concentrated seepage, and control the release of the drained water to prevent internal erosion. Properly designed drainage elements will have adequate flow capacity to reduce the pressures for which they are designed while being filter compatible with the surrounding soils to prevent internal erosion through the drainage elements.

Filters and drains are essential components for the drainage systems of a dam, levee, excavation or other geotechnical construction. A *filter* prevents the migration of the base soil into another soil layer or zone, into a drain, or out of the system through surface flow. The *base soil* is the material from which the seepage flow is exiting. A *drain* removes collected water from the collection point to a suitable discharge location. Drains can consist solely of coarse-grained soil that allows rapid seepage through its interstitial voids or can include drainage pipes that collect water from the surrounding coarse-grained drain material.

6-5.3.1 Mineral Filter Criteria.

In order to satisfy its purpose, the filter must (1) have a gradation fine enough to prevent the migration of the base soil into the filter, (2) have high enough hydraulic conductivity to not restrict flow from the base soil, and (3) have the ability to collapse so that cracks in the base soil are not propagated through the filter. Mineral filters consist of sand and gravel that are specifically graded to meet these criteria. Design procedures for mineral filters are have been developed by most U.S. agencies involved in dam design. These criteria have been summarized by FEMA (2011). A brief summary of the design procedure is provided in this section.

In the design procedure, the soil being filtered is the base soil and characteristics of the base soil gradation will be followed by a B (e.g. the grain size of which 85 percent of the base soil is passing will be denoted: $D_{85}B$). Similarly, the filter gradation will be followed by an F (e.g. $D_{15}F$). Examples of the grain sizes associated with filter design are provided in Figure 6-15.

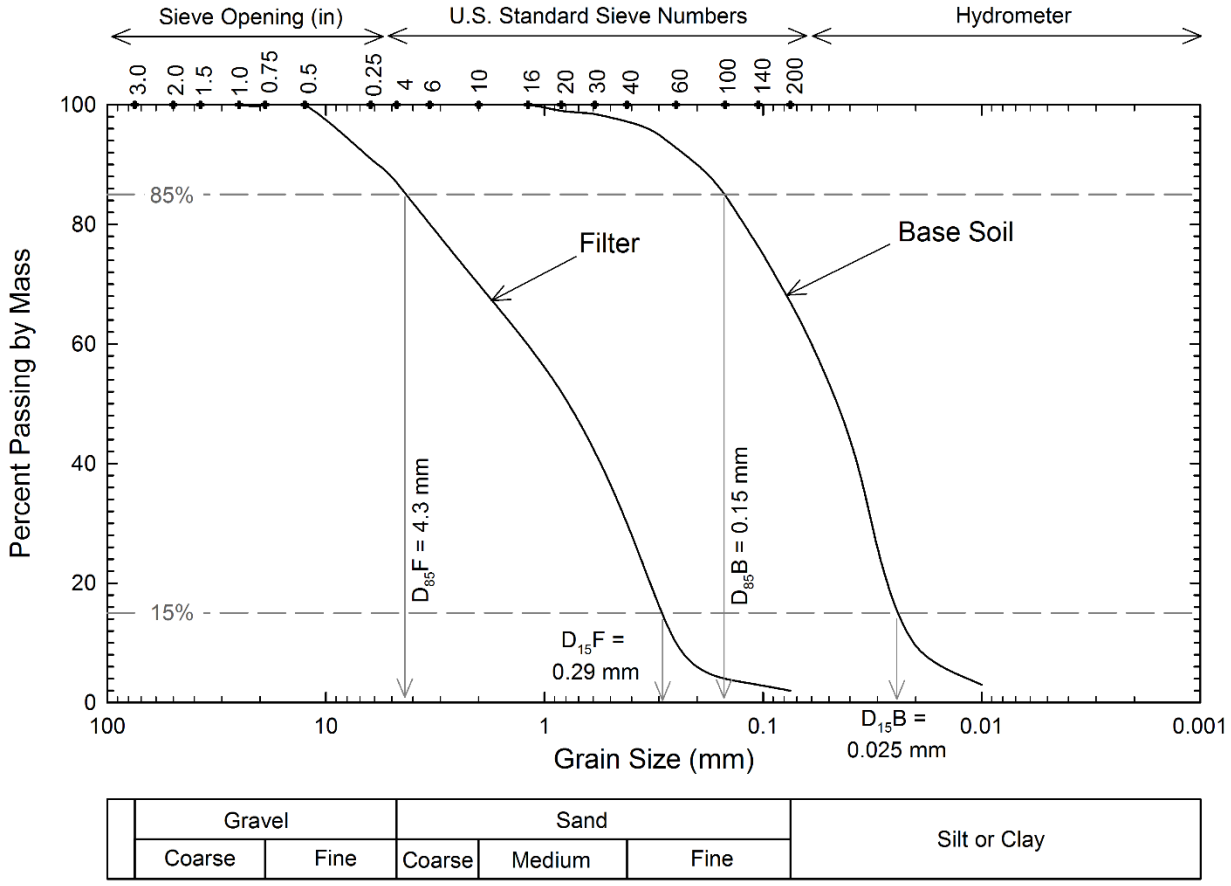

Figure 6-15 Example Base Soil and Filter Gradations

Based on FEMA (2011), filter design is completed using the following steps:

Step 1. Plot the grain-size distributions for the base soil and assess whether the base soils contain dispersive soils (e.g., soils that disaggregate when in contact with water). ASTM D6572 and D4647 can be used to identify dispersive soils.

Step 2. Assess if the base soil has particles larger than the No. 4 sieve or is gap graded. Gap graded soil may be susceptible to internal instability. Special consideration should be given to a gap graded soil to insure the fine portion of the base soil is protected from erosion.

Step 3. If the base soil contains particles larger than the No. 4 sieve, regrade the grain-size distribution to include only the portion of the distribution finer than the No. 4 sieve. FEMA (2011) provides details on the regrading procedure.

Step 4. Determine the base soil category using Table 6-11.

Table 6-11 Base Soil Categories for Mineral Filter Design (after FEMA 2011)

Base Soil Category	Percent Finer Than No. 200 Sieve (0.075-mm) (after re-grading where applicable)	Base Soil Description
1	> 85	Fine silt and clays
2	40 –85	Sands, silts, clays, and silty sands
3	15 –39	Silty and clayey sands and gravels
4	< 15	Sands and gravels

Step 5. Determine the filter criteria for base soil retention by calculating the maximum $D_{15}F$ based on the criteria in Table 6-12. The retention criteria are based on the principle that the larger particles in the base soil (represented by $D_{85}B$) must be retained by the voids in the filter (controlled by $D_{15}F$). By providing a maximum $D_{15}F$, the criteria ensure that the filter voids are sufficiently small. If the base soil has a range of grain-size distributions, the smallest value of $D_{85}B$ should be used for the retention criteria.

Table 6-12 Restraint Criteria for Mineral Filter Design (after FEMA 2011)

Base Soil Category	Filtering Criteria–Maximum $D_{15}F$	
	Non-Dispersive Soil	Dispersive Soil
1	$\text{Max } D_{15}F \le 9 \cdot D_{85}B$ $\text{Max } D_{15}F \ge 0.2\,\text{mm}$	$\text{Max } D_{15}F \le 6.5 \cdot D_{85}B$ $\text{Max } D_{15}F \ge 0.2\,\text{mm}$
2	$\text{Max } D_{15}F \le 0.7\,\text{mm}$	$\text{Max } D_{15}F \le 0.5\,\text{mm}$
3	$\text{Max } D_{15}F \le \left[\frac{40-A}{25}\right][B-C]+C$ where: A = % passing No. 200 sieve, $B = 4 \times D_{85}B \ge 0.7$ mm, and C = 0.7 mm	$\text{Max } D_{15}F \le \left[\frac{40-A}{25}\right][B-C]+C$ where: A = % passing No. 200 sieve, $B = 4 \times D_{85}B \ge 0.5$ mm, and C = 0.5 mm
4	$\text{Max } D_{15}F \le 4 \cdot D_{85}B$	$\text{Max } D_{15}F \le 4 \cdot D_{85}B$

Note: $D_{85}B$ and percent passing No. 200 sieve are determined after regrading.

Step 6. Determine the flow criteria for the filter by calculating the minimum $D_{15}F$ based on the criteria in Table 6-13. The permeability criteria are based on the principle that the filter's hydraulic conductivity is strongly related to $D_{15}F$. By providing a minimum $D_{15}F$, the filter will have sufficient flow capacity in comparison to the base soil. If the base soil has a range of grain-size distributions, the largest value of $D_{15}B$ should be used for the permeability criteria. Plot the minimum and maximum $D_{15}F$ on a gradation

plot and adjust the minimum $D_{15}F$ to ensure that the ratio between the minimum and maximum $D_{15}F$ is not greater than 5 (i.e., $Min\ D_{15}F$ / $Max\ D_{15}F$).

Table 6-13 Flow Criteria for Mineral Filter Design (after FEMA 2011)

US Agency	Filter Permeability Criteria
USBR	$Min(D_{15}F) \geq 5 \cdot D_{15}B$
USACE	$Min(D_{15}F) \geq (3 \text{ to } 5) \cdot D_{15}B$
NRCS	$Min(D_{15}F) \geq (4 \text{ to } 5) \cdot D_{15}B$
All	$Min(D_{15}F) \geq 0.1$ mm

Note: $D_{15}B$ is determined prior to regrading.

Step 7. Filters should also have a coefficient of uniformity ($C_u = D_{60}F / D_{10}F$) is between 2 and 6.

Step 8. Limit the amount of oversized material and fines in the filter. Most agencies require that the maximum particle size of the filter ($D_{100}F$) be less than 2 inches (51 mm) although the USACE allows particles up to 3 inches (76 mm). The minimum particle size associated with 5% passing for the filter (D_5F) is the No. 200 sieve or 0.075 mm. Any fines present in the filter soil should be non-plastic (i.e., PI = 0).

Step 9. Limit segregation potential of the filter by determining the maximum $D_{90}F$ from Table 6-14. Segregation occurs more easily if a wide range of particle sizes is present.

Table 6-14 Segregation Criteria for Mineral Filter Design (after FEMA 2011)

Minimum $D_{10}F$ (mm)	Maximum $D_{90}F$ (mm)
< 0.5	20
0.5 – 1.0	25
1.0 – 2.0	30
2.0 – 5.0	40
5.0 – 10	50
10 – 50	60

Step 10. Plot the criteria for minimum D_5F, minimum and maximum $D_{15}F$, maximum $D_{90}F$, and maximum $D_{100}F$ on a gradation plot to create an acceptable gradation band for the filter. Compare candidate filters with the criteria and gradation band.

Design for Drainpipe Perforations. If the filter is to contain a drainage pipe, the filter soil around the pipe is referred to as the envelope material. The smallest value of $D_{50}E$ (E stands for envelope) allowed by the gradation should be larger than the size of the maximum pipe perforation.

An example of a filter design for a Type 4 base soil is presented in Figure 6-16.

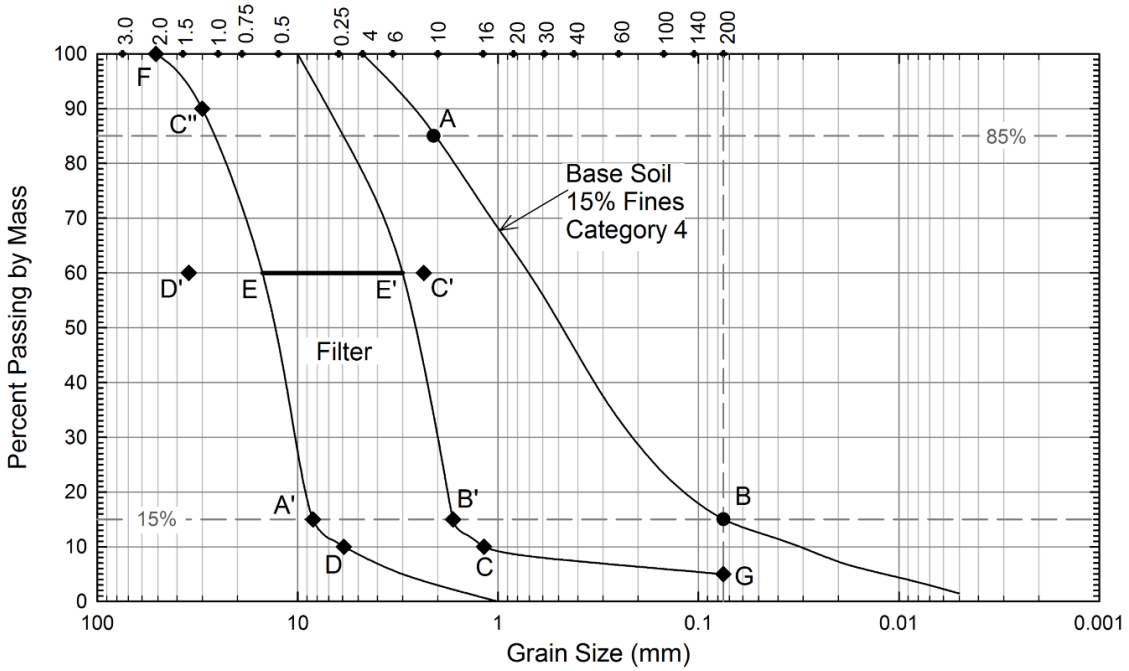

Steps 1-3: Plot the grain size distribution(s) for the base soil. If necessary, regrade the grain size distribution to include only the portion of the distribution finer than the No. 4 sieve.

Step 4: Determine the base soil category using Table 6-12. The example soil falls in Category 4.

Step 5: $D_{85}B$ = 2.1 mm for the base soil (Pt. A). To satisfy the criteria for base soil restraint or retention, the maximum $D_{15}F$ should be ≤ 4 × $D_{85}B$ of base soil, or 8.4 mm (Pt. A').

Step 6: $D_{15}B$ = 0.075 mm for the base soil (Pt. B). To satisfy the flow criteria the minimum $D_{15}F$ should at least 5×$D_{15}B$, or 0.375 mm. The minimum $D_{15}F$ should also be at 1/5 of the maximum $D_{15}B$, or 1.7 mm. The larger of these two values is plotted as Pt. B'.

Step 7: Select a range of $D_{60}F$ values to keep C_u between 2 and 6.
(a) Find the minimum $D_{10}F$ size and plot as point *C*: $D_C \approx D_{B'} \times 0.7 = 1.7 \times 0.7 = 1.18$ mm
(b) Find the minimum $D_{60}F$ size for C_u= 2 (point C'): $D_{C'} = D_C \times 2 = 1.18 \times 2 = 2.36$ mm
(c) Find the maximum $D_{10}F$ size and plot as point *D*: $D_D \approx D_{A'} \times 0.7 = 8.4 \times 0.7 = 5.9$ mm
(d) Find the maximum $D_{60}F$ size for C_u=6 (point *D'*): $D_{D'} \approx D_{A'} \times 6 = 5.9 \times 6 = 35.4$ mm
(e) Select a "sliding bar" defined by points E and E' where: D' > E > *E'* > *C'* and E = E' × 5, This bar can be adjusted back and forth between points *D'* and *C'*.

Step 8: The maximum $D_{100}F$ size is 51 mm (2 in.) shown as point F. The minimum D_5F size is 0.075mm (No.200 sieve), shown as point G.

Step 9: In order to prevent possible segregation during construction, select the maximum $D_{90}F$ size. The minimum $D_{10}F$ size is 1.18 mm (Pt. C), the maximum $D_{90}F$ size is 30 mm (Pt. C'').

Step 10: Compare the grain size distributions of candidate filters to the range delineated by curves D-A'-E-C''-F and G-C-B'-E'.

Figure 6-16 Example Filter Design

6-5.3.2 Geotextile Filter Criteria.

In some cases, geotextiles can be used for soil filtration and drainage in lieu of mineral filters and gravel drains. In general, the FEMA (2011) guidelines do not recommend the use of geotextiles in critical areas of dams. The term *geotextiles* refers to a wide variety of synthetic, fabric-like products that vary depending on the types of fibers used in the manufacturing and how these fibers are interconnected. The most common forms include woven, nonwoven, and knitted fabrics. Woven geotextiles are manufactured by weaving two perpendicular sets of synthetic fibers to form a fabric. Nonwoven geotextiles have a random orientation often resembling a felt fabric and are manufactured by either needle punching, spun bonding, or resin bonding. Knitted geotextiles consist of interlocking series of loops of fiber yarns that form a fabric.

A common drainage and filtration application for geotextile filter fabrics is a subsurface drain such as presented in Figure 6-17. In this application the drainage is provided by the poorly-graded gravel drainage rock and the slotted outlet pipe. The role of the geotextile is to prevent migration of the surrounding soils into the drainage rock and pipe. In this way, the geotextile prevents erosion of the surrounding soil and/or clogging of the drain. Other applications include drains within retaining wall backfill and drainage blankets below embankments.

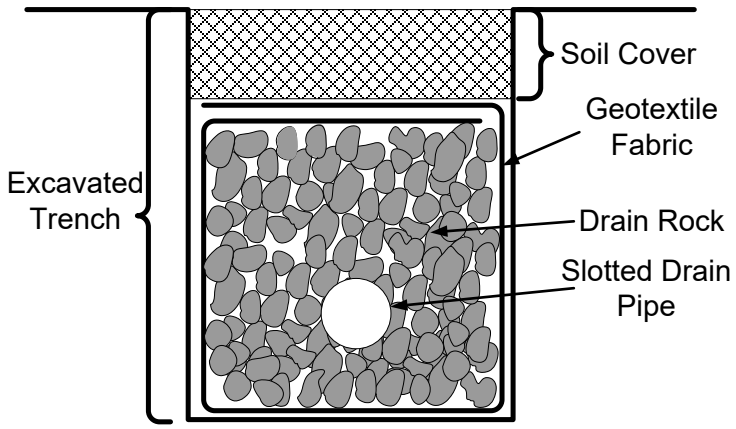

Figure 6-17 Subsurface Drain Constructed of Filter Fabric, Drainage Rock, and a Slotted Pipe

For the geotextile fabric in Figure 6-17 or other applications to perform adequately, the geotextile should be designed to have the ability to: (1) retain particles of the base soil to prevent migration through the fabric, (2) allow the passage of water without significant buildup of water pressure, and (3) resist clogging due to accumulation of fine soil particles, chemical precipitates, and biological precipitates.

Criteria for retention of soil particles was proposed by Giroud (2010) based on $D_{20}B$ and the soil's *linear coefficient of uniformity* (C'_u). As shown in Figure 6-18, a log-linear approximation is used to represent the base soil's gradation curve. The linear particle

size (D'_x) is the obtained the log-linear approximation. The values of D'_{100} and D'_0 are defined by the ends of a straight line drawn through the middle part of the gradation plot (i.e., through D_{10} and D_{60}).

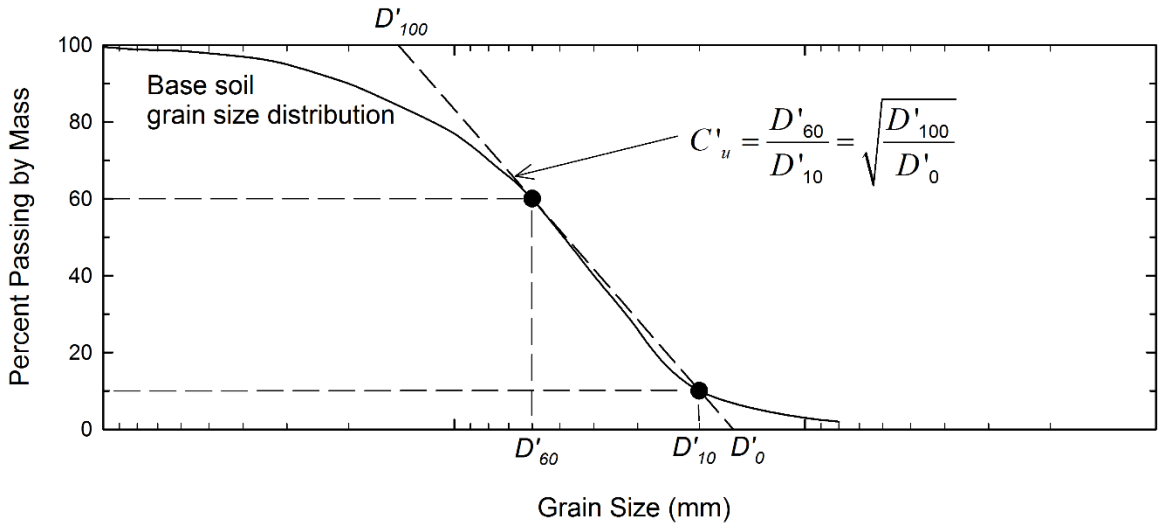

Figure 6-18 Linear Coefficient of Uniformity (after Giroud 2010)

Geotextiles are designed for retention based on the *geotextile opening size* (O_{95}), which indicates the size at which 95 percent of openings are smaller. According to Luettich (1992), geotextile retention criteria for soils with less than 10% fines can be selected using the base soil gradation and Table 6-15.

For soils with more than 10% fines and PI greater than 5, the geotextile should have O_{95} less than 0.21 mm, provided the soil is non-dispersive. For dispersive soils with more than 20% clay sized particles, a filter of 75 to 100 mm of sand should be placed between the base soil and the geotextile, and the geotextile should be designed to retain the filter sand. Retention of non-plastic soils with more than 10% fines can be designed using Table 6-15.

Geotextile filters also must have a much higher hydraulic conductivity than the base soil. A filter cake of trapped particles often forms on the face of a geotextile. These particles must not reduce the hydraulic conductivity of the geotextile to the point that it restricts seepage flow out of the base soil. However, clogging is difficult to quantify. Some clogging will occur when the geotextile is put into service. The geotextile must remain sufficiently open so that accumulation of particles and chemical and biological precipitates will not reduce the hydraulic conductivity to the point where the filter cake/geotextile system becomes less permeable than the base soil. The USBR (2014) recommends the following considerations be taken to assess clogging potential:

- Use the largest opening size that satisfies the retention criterion.

- Do not use geotextile filters in environments where precipitates are likely to form. Avoid high alkalinity groundwater, which can form calcium, sodium, or magnesium precipitates. Also avoid acidic seepage, which can form iron and aluminum hydroxide precipitates.
- Avoid use of geotextiles with internally unstable (C_u > 20) or dispersive soils.
- Avoid organic-rich environments such as agricultural runoff, landfill leachates, and sites known to form iron bacteria.
- Make sure that the geotextile filter makes intimate contact with the soil.
- Do not place geotextile filters against cohesive soils containing voids.

Table 6-15 Geotextile Opening Size Criteria for Soils with Less than 10% Fines (after Luettich et al. 1992)

Base Soil Description					Geotextile Retention Criteria
Primary Category Description	**Secondary Characteristic**	**Gradation Description**		**Relative Density (D_r)**	
Less than 10% fines and less than 90% gravel	Stable Soil *($1 < C_c < 3$)*	Obtain C_u from straight line drawn through D_{60} and D_{30}	Widely Graded ($C'_u > 3$)	Loose D_r < 35%	$O_{95} < \frac{9}{C'_u} D'_{50} B$
				Medium dense 35% < D_r < 65%	$O_{95} < \frac{13.5}{C'_u} D'_{50} B$
				Dense 65% < D_r	$O_{95} < \frac{18}{C'_u} D'_{50} B$
	Unstable Soil *($C_c < 1$, $3 < C_c$)*	Obtain C_u from straight line drawn through D_{30} and D_{10}	Uniformly Graded ($C'_u < 3$)	Loose D_r < 35%	$O_{95} < C'_u D'_{50} B$
				Medium dense 35% < D_r < 65%	$O_{95} < 1.5 \cdot C'_u D'_{50} B$
				Dense 65% < D_r	$O_{95} < 2 \cdot C'_u D'_{50} B$

The permeability requirement for a geotextile can be stated as:

$$FS_g = \frac{k_g}{k_s} = \frac{\psi_g \cdot t_g}{k_s} \quad \textbf{(6-16)}$$

where:
FS_g = factor of safety for geotextile permeability,
k_g = hydraulic conductivity of the geotextile across the plane of the fabric,
k_s = hydraulic conductivity of the base soil,
ψ_g = permittivity of the geotextile, provided by manufacturers or from testing (ASTM D4491), and
t_g = geotextile thickness.

Giroud (2010) suggests that an FS_g of 10 to 20 is appropriate to maintain adequate filter permeability. Others (e.g., Loudiere et al. 1983, Christopher and Fischer 1991) recommend that the FS_g value be between 10 and 100.

Over the past several decades geotextile filter fabrics have been developed to provide filtration between base soil and coarse-grained drain materials. While these fabrics are inexpensive compared to mineral filters, they are considered by many to be far less reliable than mineral filters due to their propensity to clog and the potential to be damaged during construction. For this reason, all major dam owning and regulating agencies in the U.S. (U.S. Army Corps of Engineers, U.S. Bureau of Reclamation, FEMA, and FERC) do not allow the use of filter fabrics within critical areas of dam embankments or in high-hazard structures.

6-5.3.3 Surface and Subsurface Drainage.

Pavements and other surface treatments can be destabilized by water ponded at the ground surface or shallow phreatic surfaces. Near-surface groundwater may be collected by intercepting drains prior or collected in the pavement base material as it exits the subgrade. Accumulation of surface water in wide flat areas, due to rainfall or other surface sources, can be mitigated using trench drains connected to deeper drainage systems.

6-5.3.3.1 Intercepting Drains.

Intercepting drains (a.k.a., stability trenches or stability drains) can be used in locations where water seeping from a hillside has a detrimental effect on slope stability or the performance of roadways. These drains consist of shallow trenches with collector pipes surrounded by drainage material, placed to intercept seepage moving horizontally in an upper pervious stratum as illustrated in Figure 6-19. The trench backfill can consist of a filter material compatible with the surrounding soil as shown in Figure 6-20 or a drainage aggregate wrapped in filter fabric (Figure 6-17). The type of trench backfill and filtering mechanism used will depend on the criticality of the drain. Drain designs should aim to be as simple and constructible as possible while still providing suitable filtering.

The effect of intercepting drains on seepage patterns can be evaluated using flow nets or modeled by finite element analyses. Such analyses should also assess the volumetric flow rate into the drains so that the drain pipes and outlets can be properly designed.

6-5.3.3.2 Surface Blanket Drains.

Surface blanket drains are used to intercept ground water beneath pavements and structures to mitigate the buildup of water pressure or destabilization of subgrades. In many cases, the aggregate base layer of pavements may be assessed for its

effectiveness as a blanket drain. Design of surface blanket drains should consist of: (1) assessment of the flow rate of drainage into the blanket to calculate the needed spacing for outlets and (2) assessment of the tolerable uplift pressure in the blanket to prevent damage to the overlying pavement, embankment, or structure.

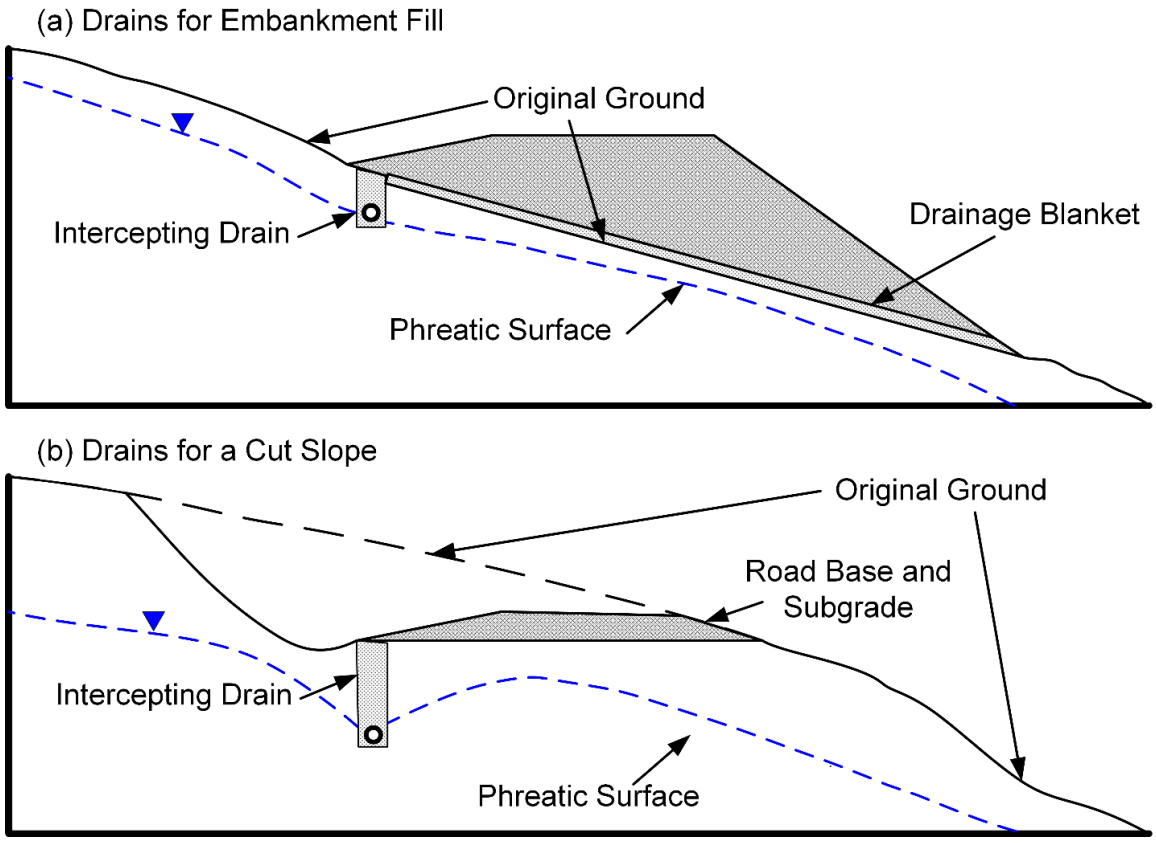

Figure 6-19 Use of Subsurface Interceptor Drains and Blanket Drains for Roadway Drainage

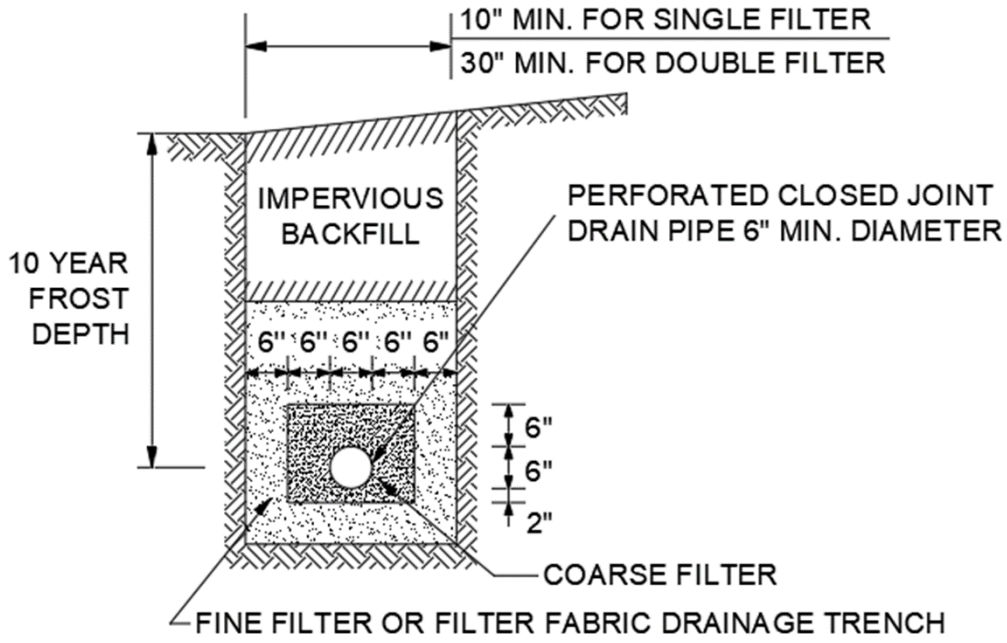

Figure 6-20 Subsurface Drain with a Two-Stage Filter and a Slotted Pipe

The thickness of aggregate base course needed to provide effective drainage can be calculated using Figure 6-21. For a range of slopes, the degree of drainage is related to the porosity and hydraulic conductivity of the aggregate base, the thickness of the base layer, the subgrade slope, the drain spacing, and the time allowed for drainage. Figure 6-21 can be used to select drain spacing or evaluate suitability of base material. *Effective porosity* (also called *specific yield*) is the quantity of water per unit volume that is not retained in the soil by capillarity during discharge (Barber 1959). It ranges from 25 percent for a uniform material, such as medium to coarse sand, to 15 percent for a well-graded sand-gravel mixture.

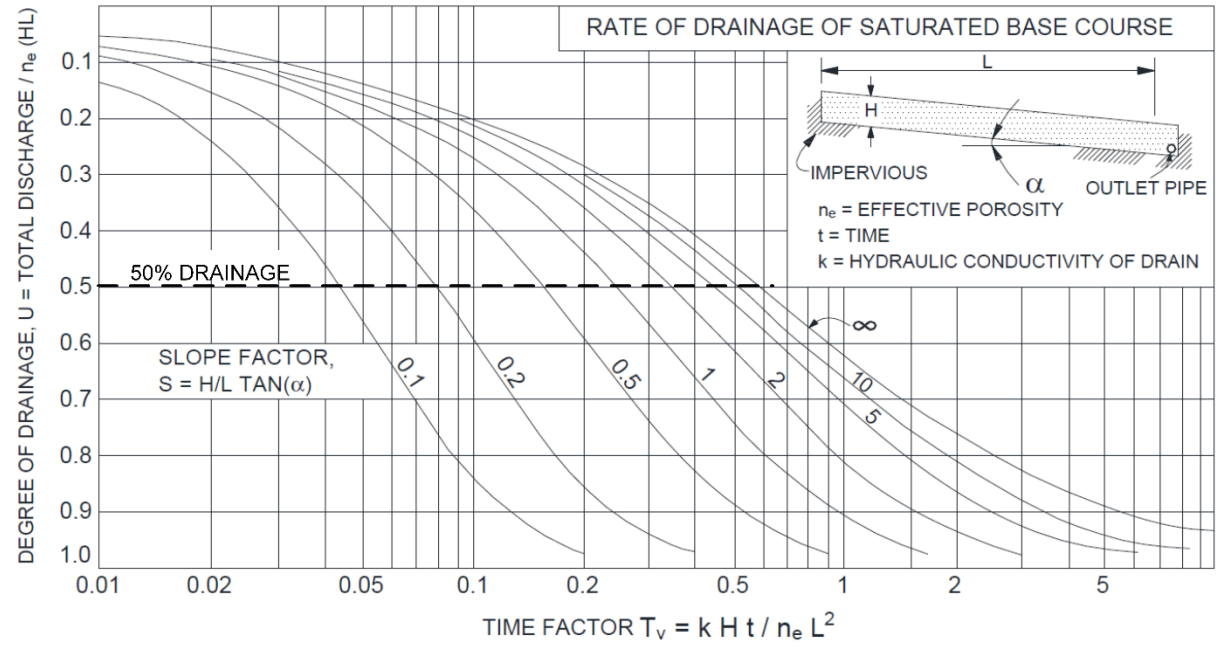

Required Drain Spacing and Discharge Estimate

1. Select the desired maximum time for 50% drainage (t_{50}) and the slope factor (S).
2. Enter the graph horizontally at the U = 0.5 line and read the time factor (T_V) corresponding to S.
3. Solve the time factor equation for L to determine the required drain spacing:

$$L = \sqrt{\frac{kHt_{50}}{n_e T_V}}$$

4. Estimate the flowrate at time = t_{50}:

$$q = kH\frac{H + L\tan\alpha}{2L}$$

Figure 6-21 Drainage of an Aggregate Base Course (after Barber 1959)

6-5.3.3.3 Drainage of Ponded Areas.

During times of heavy rainfall or runoff from adjacent areas, vertical drainage trenches can be used to mitigate ponding water in level areas or enclosed basins. The flow rate of seepage into parallel trenches can be estimated using Figure 6-23 for an underlying zone that is either completely pervious or completely impervious in comparison to the surface layer. The trench spacing ($2\times S$) can be designed such that the calculated flow rate into the trenches meets or exceeds the required surface infiltration for an area of $1\times 2\times S$. The trench must also be designed to sustain the required flow rate and may include collector pipes. If sufficient drainage capacity cannot be provided using trenches, surface drainage facilities are required to prevent ponding.

6-5.3.1 Retaining Wall Drainage.

Water imposes additional destabilizing forces on retaining and basement walls that can lead structural distress or collapse. Drainage systems should be designed to prevent the buildup of water behind walls. Figure 6-22 presents several alternatives for providing retaining wall drainage.

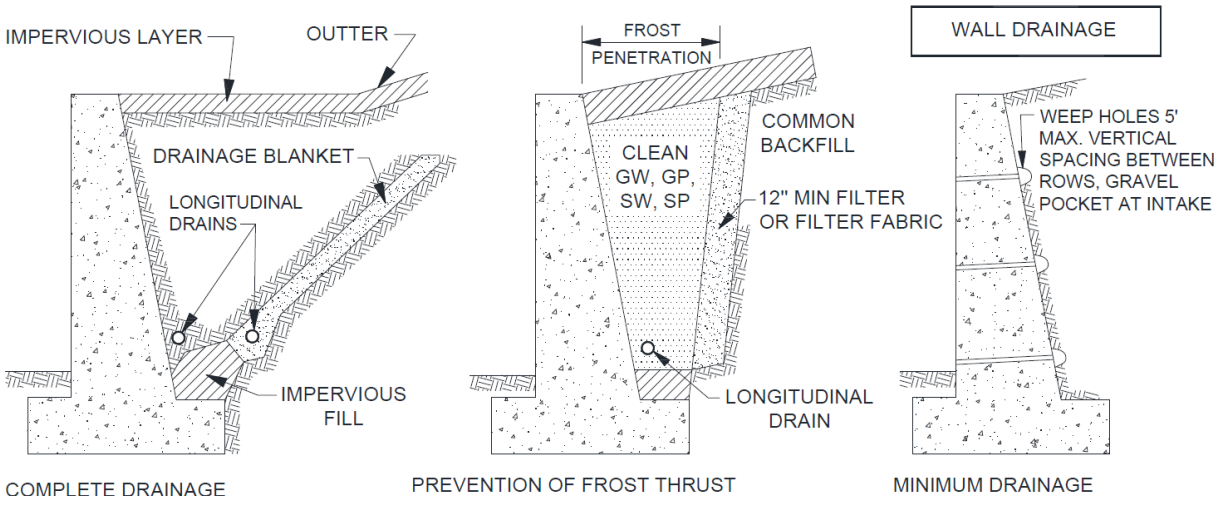

Figure 6-22 Retaining Wall Drainage Alternatives

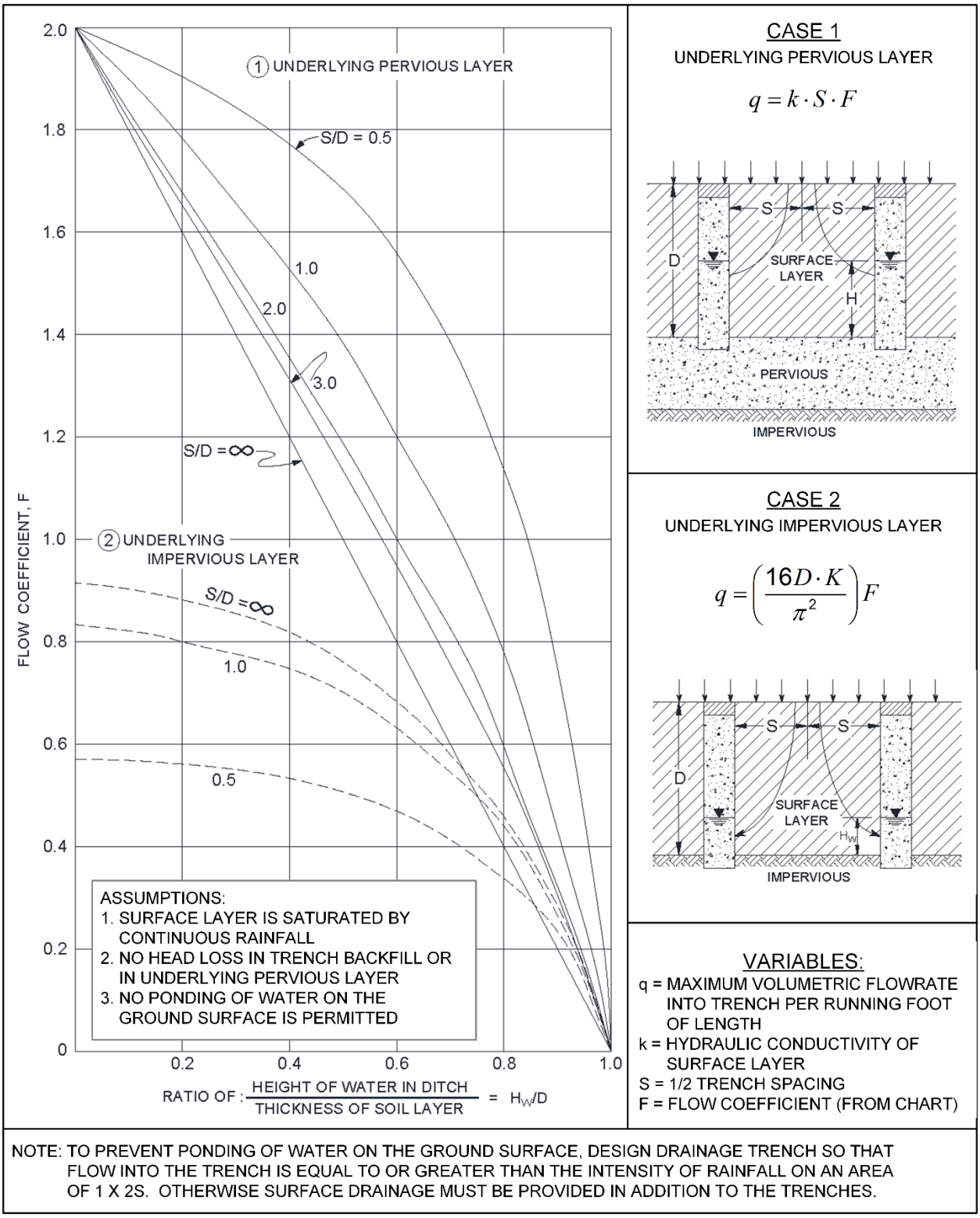

Figure 6-23 Seepage into Drainage Trenches Used for Draining Ponded Areas (after Kirkham 1950 and 1960)

6-5.3.2 Filters and Drains for Embankments.

Drains and filters are constructed within dams, levees, and other embankments or slopes to drain excess pressures and intercept pathways for internal erosion. The following paragraphs discuss the different types of embankment drains and their applications. In general, embankment drains act to lower the phreatic surface and piezometric pressures in an embankment or slope, resulting in increased slope stability and decreased internal erosion potential. All drain systems should be designed to filter the base soil and provide adequate drainage capacity for the designed purpose.

Embankment subdrains are located below embankment fills to intercept seepage from native soil and bedrock and reduce seepage into the embankment as illustrated in Figure 6-24. Subdrains consist of filter soil or drainage aggregate wrapped in filter fabric. The drains often contain a slotted or perforated collection or outlet pipe.

The other major types of embankment drains are used for intercepting and controlling seepage through or below water retaining structures.

Toe drains consist of a filter and drain located at or near the toe of a dam to collect exiting seepage through the embankment (Figure 6-25a). Toe drains are common in small homogenous dams and levee embankments as well as below the toe of small zoned earth dams. Toe drains do not effectively intercept cracks or defects in dam or levee embankments or shells.

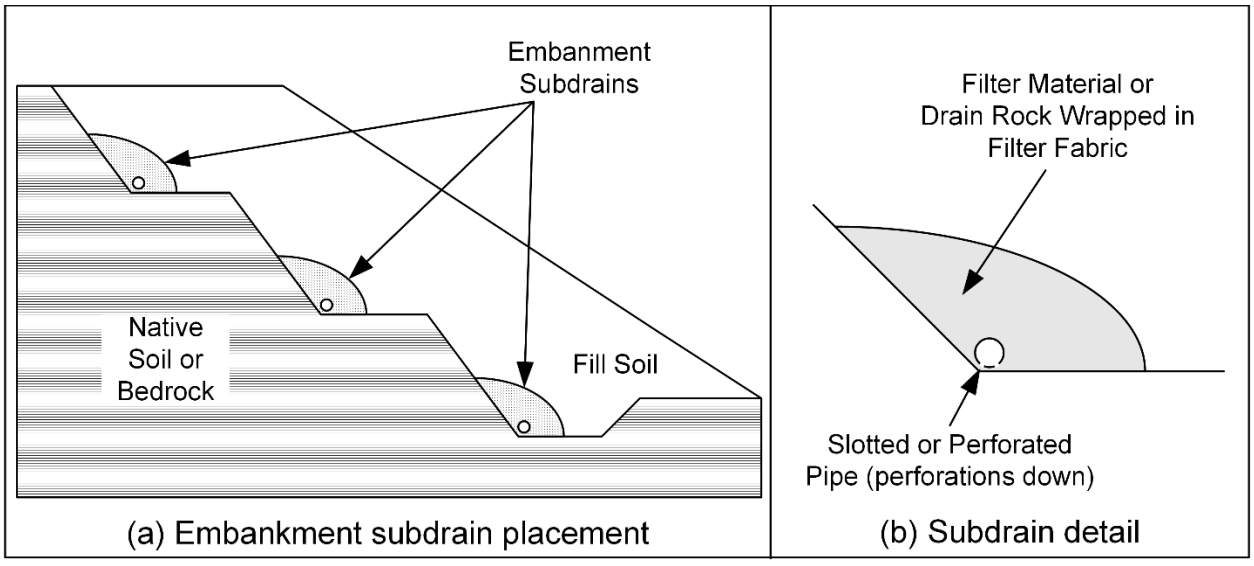

Figure 6-24 Embankment Fill Subdrains

Blanket drains are located at the downstream base of a dam or levee and are designed to collect seepage exiting the embankment (Figure 6-25b). Blanket drains are common

in small to moderate sized dam and levee embankments. They are not an effective means of intercepting cracks or defects in dam or levee embankments or shells.

Chimney drains are usually located near the centerline of a dam or levee and are designed collect seepage through the embankment (Figure 6-25c). Chimney drains are a standard component of all modern, large embankment dams. Chimney drains are designed to intercept cracks, defects, or permeable layers in dam or levee embankments or cores. They typically are connected to a blanket drain below the downstream or landside portion of the embankment.

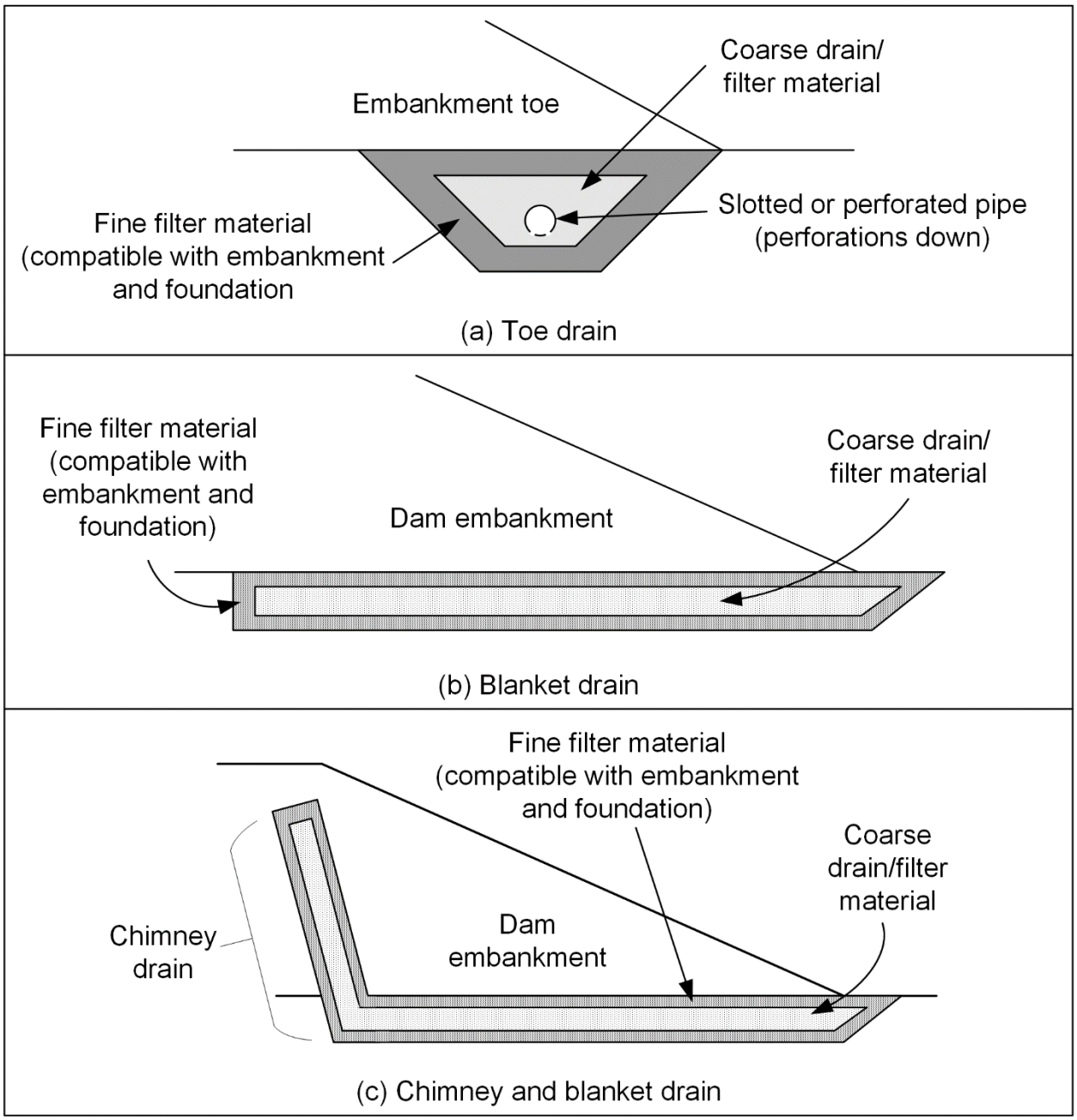

Figure 6-25 Toe, Blanket, and Chimney Drains

An *outlet filter collar* is a zone of filter material located along an outlet or other penetration through an embankment as shown in Figure 6-26. The outlet filter collar prevents concentrated leak erosion along the penetration. These filters are generally not connected to a drain.

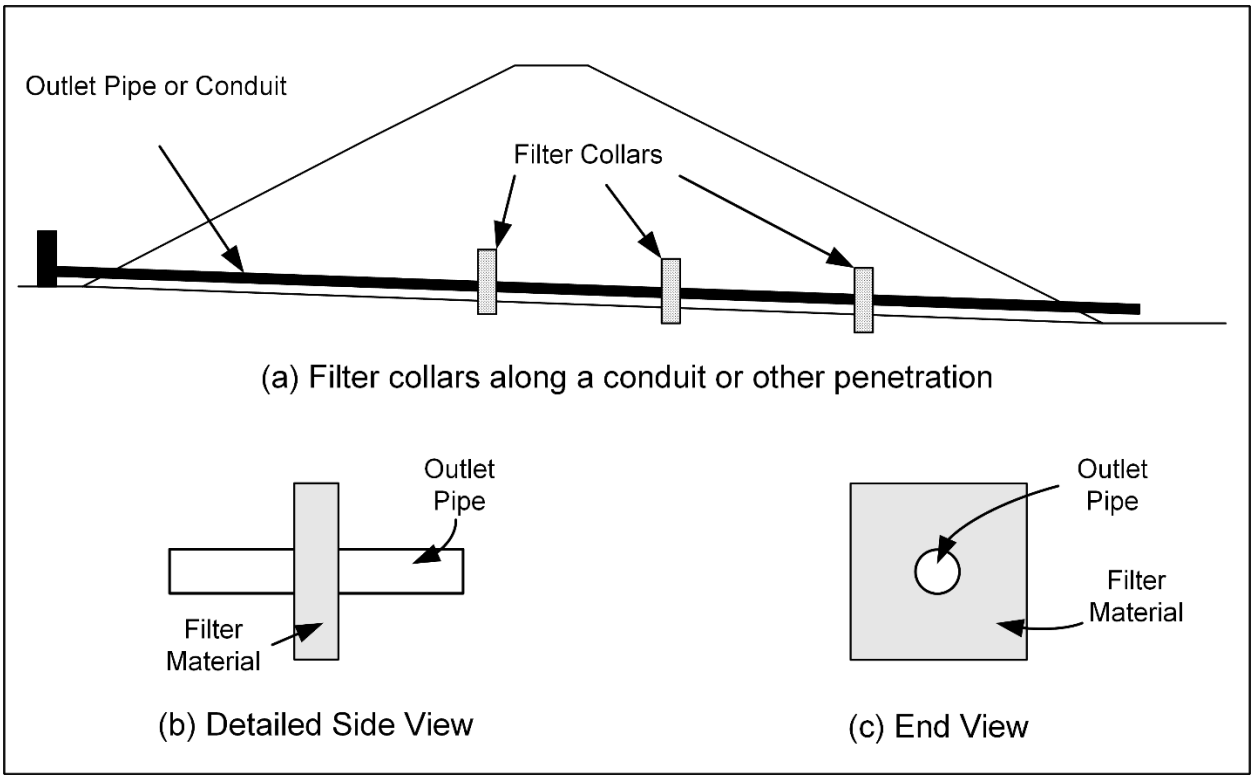

Figure 6-26 Outlet Filter Collars

6-5.3.3 Foundation Drainage.

Under certain conditions, excessive water pressure is present in the soil or rock below or adjacent to a dam or levee. High water pressures can lead to risk of heave, internal erosion, or instability of slopes or structures. These conditions often occur when a low hydraulic conductivity layer prevents drainage from an underlying layer with higher k. Drainage methods for mitigating such pressures include relief trenches and wells.

6-5.3.3.1 Relief Trenches.

A *relief trench* penetrates the upper layer and allows high pressures in the deeper pervious layer to dissipate by upward seepage as shown in Figure 6-27. The relief trench is filled with an appropriate filter material. The width of the trench should be sufficient to reduce the upward pressures beneath the low hydraulic conductivity layer while limiting upward hydraulic gradients in the relief trench to 0.4. Commonly, relief trench design is performed using two-dimensional finite element analysis.

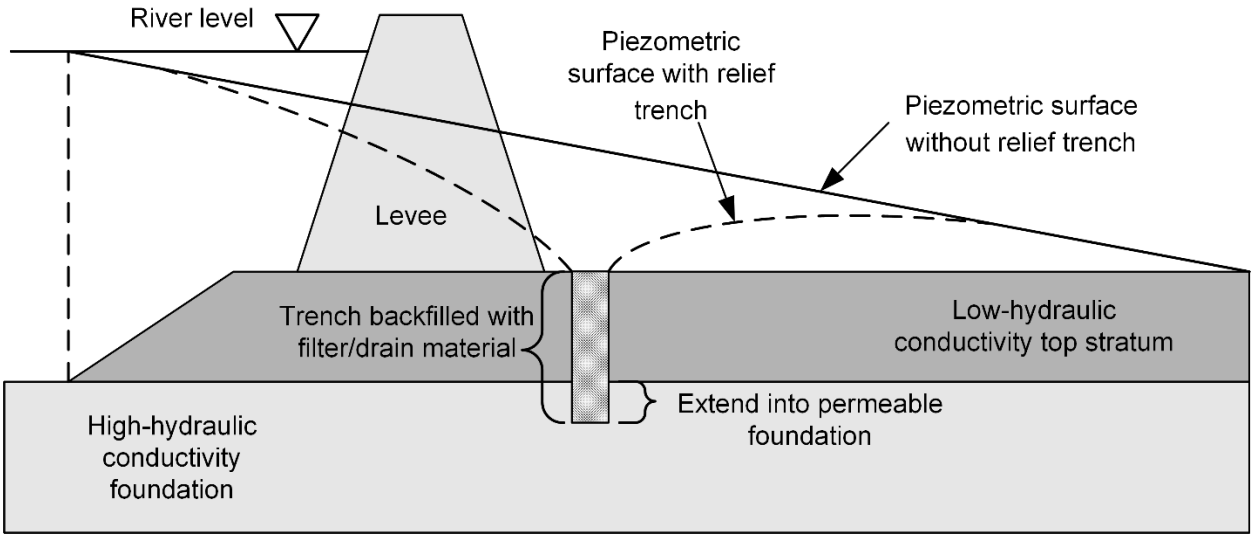

Figure 6-27 Relief Trench Used to Relieve Pressure from Beneath a Blanket Layer with Low Hydraulic Conductivity (not to scale)

Relief trenches reduce the drainage path and increase the flow rate below a hydraulic structure. Seepage at the ground surface must be managed when relief trenches are used. A typical seepage water management system includes collection trenches leading to a sump where the water can be pumped away.

6-5.3.3.2 Relief Wells.

A *relief well* is a large diameter well that extends into a layer of high hydraulic conductivity. Rows of relief wells are installed in areas of excess foundation pressure, often along the downstream side of a levee or dam. Similar to trenches, relief wells reduce water pressure by providing a vertical seepage pathway and reducing the length of the flow path as indicated in Figure 6-28.

Relief wells are constructed in large diameter shafts, often 0.5 to 1.0 meters in diameter, cased with a 15 to 30 cm diameter casing. Details of a typical relief well installation are presented in Figure 6-29. The portion of the relief well that extends into the pervious foundation soil is cased with slotted or screened casing and packed with a filter material designed to filter the surrounding base soil. Most modern casings consist of PVC solid pipes with either slotted PVC or stainless steel screens. However, some wood-stave screen wells are still in operation. The upper portion of the well consists of a solid casing with an annular space sealed with concrete and bentonite to prevent flow and erosion of the upper blanket material.

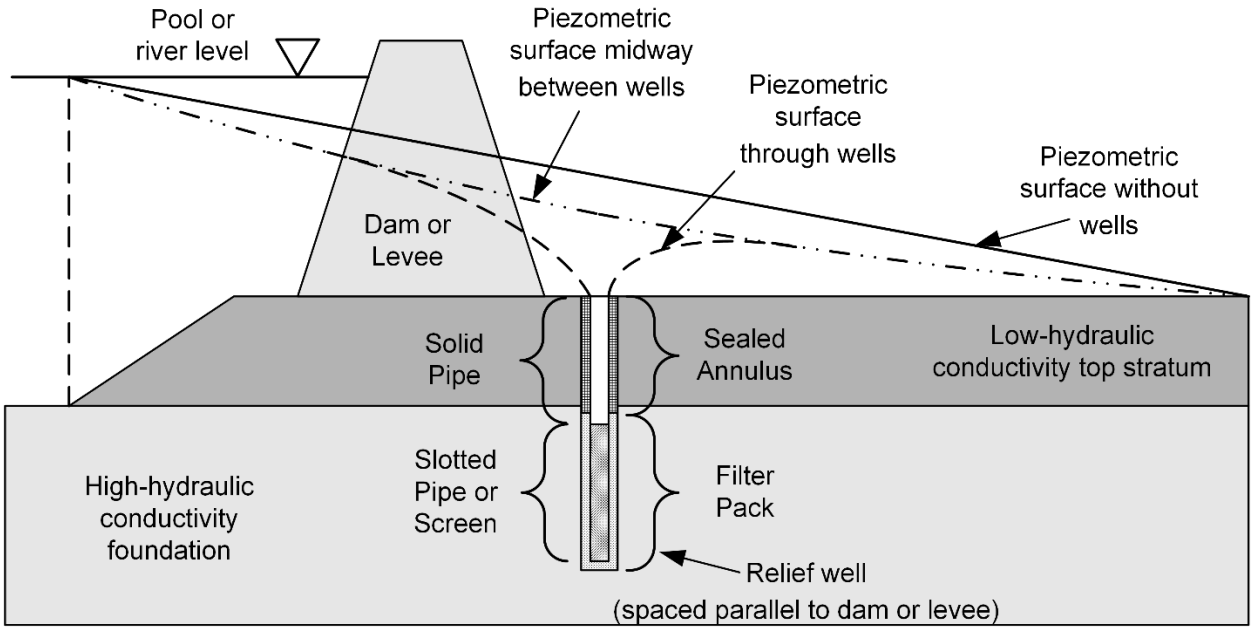

Figure 6-28 Relief Well Used to Relieve Pressure from Beneath a Blanket Layer with Low Hydraulic Conductivity (not to scale)

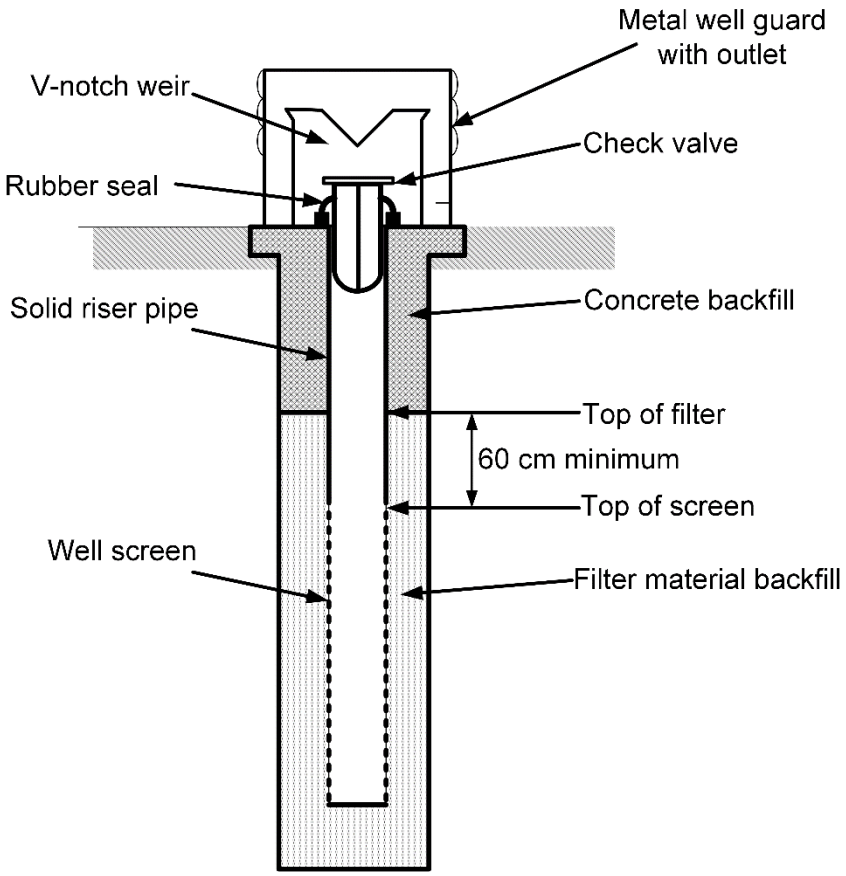

Figure 6-29 Typical Relief Well Construction

The design of relief wells is a three-dimensional problem and can be visualized in terms of the lowering of the piezometric surface that occurs at the wells. The piezometric surface is lowered the most at the well locations as shown in Figure 6-30. Along the line of the wells, the piezometric surface is typically highest at the midpoint between any two wells. Figure 6-30 can be used to estimate the relief well discharge in terms of the well spacing, the well radius, geometric variables, and an extra length factor that empirically accounts for well resistance. The appropriate extra length factor can be determined for wells that penetrate 25, 50, and 100 percent of the pervious foundation layer thickness using the lower diagrams. Alternatively, relief wells can be designed using three-dimensional finite element analyses.

Relief wells require a periodic program of well cleaning and maintenance to prevent clogging of the well screen and filter. Relief well flows should be documented throughout their life span and flows compared with river or reservoir levels to monitor any changes that may be occurring in well efficiency.

6-6 DEWATERING.

Sometimes it is necessary to lower the groundwater level to allow for subsurface construction or to prevent flooding of existing facilities. Dewatering options include: (1) a collection system at the base of the excavation leading to a sump, (2) a well point system, and (3) deep extraction wells. The selection of a dewatering system depends on the expected inflows into the excavation, the potential for heave (see Section 6-4.1), and the required depth of groundwater lowering. There are engineering firms and consultants that specialize in dewatering.

6-6.1 Collection and Sump.

When the volume of inflow into an excavation is low (i.e., excavation into low hydraulic conductivity soils) and the potential for heave is not a concern, a collection and sump system may be sufficient. The collection system may consist of a series of trenches on the bottom of the excavation or a system of relief trenches (see Section 6-5.3.3.1) at the base of the excavation. In some temporary cases, a layer of poorly-graded gravel can be placed over the bottom of the excavation that allows water to flow toward the sump. The collection system leads to a sump with a pump to remove the inflow. Sump pumps can be either electric or gasoline-powered (i.e., “trash” pumps).

6-6.2 Wellpoint Systems.

Wellpoints are 1-1/2- or 2-inch diameter pipes that are connected to a suction system to remove the groundwater. The lower section of each wellpoint is slotted or perforated and screened to prevent removal of the surrounding soil into the pipe. The pipes are pushed or jetted in place, or installed in predrilled holes. The wellpoints are each connected to a header leading to suction pumps.

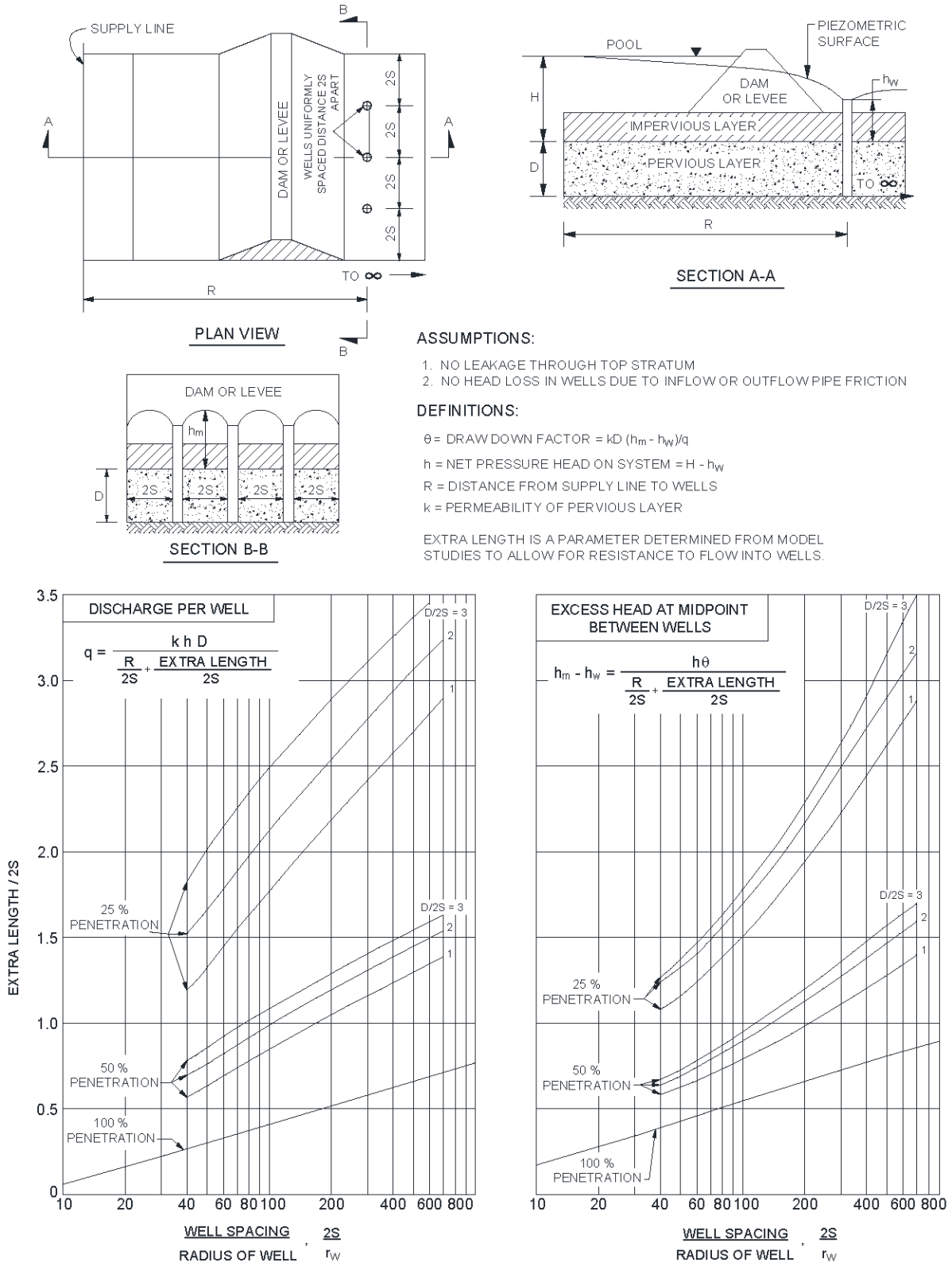

Figure 6-30 Calculation of Relief Well Discharge and Spacing (after USACE 1952)

Wellpoints are generally effective when the soil has D_{10} greater than 0.05 mm or if the soil has a structure, such as varves or laminations, for conducting groundwater horizontally. The maximum differential pressure that can be developed in wellpoints is limited by atmospheric pressure. Thus, the drawdown of the groundwater level using wellpoints is ordinarily limited to 15 to 18 feet below the center of the suction header. If a greater amount of drawdown is required, wellpoints can be installed in successive tiers or stages as excavation proceeds as illustrated in Figure 6-31.

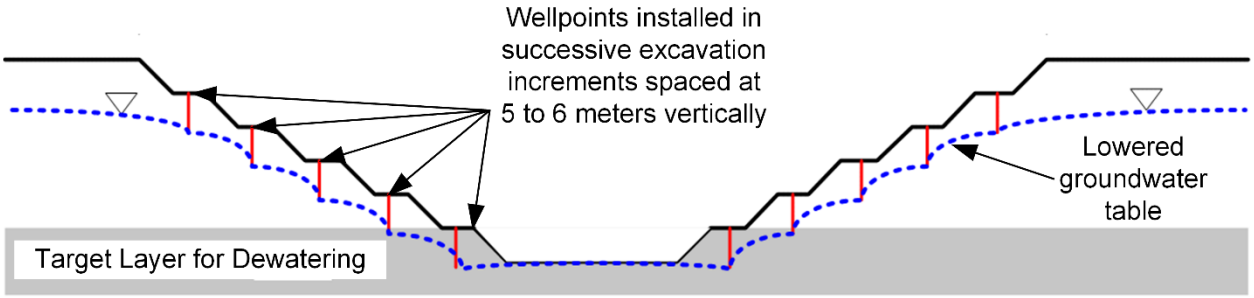

Figure 6-31 Staged Installation of Wellpoints to Lower the Groundwater Table for a Deep Excavation

The discharge capacity for each wellpoint is generally 15 to 30 gpm (3 to 6 m^3/hour). Wellpoint spacing is typically between 3 and 10 feet (1 and 3 m). Closer spacing should be used for soils with lower hydraulic conductivity. In such soils, the effectiveness of wellpoints can be increased by predrilling the locations and backfilling with sand around the wellpoint.

Due to the close spacing of wellpoints, a two-dimensional analysis is generally sufficient. The drawdown and flow into the line of wellpoints can be analyzed either with a flow net or two-dimensional finite element analysis. For soil with high k (clean fine sand or coarser), the quantity of water to be removed controls wellpoint layout. For silty soils, the flow rate is relatively small, and the number and spacing of wellpoints will be influenced by the time available to accomplish dewatering.

6-6.3 Extraction Wells.

Extraction wells consist of a bored hole containing a well casing with a screened section in the aquifer, a filter pack, and a pipe column. A turbine-type pump with a motor at the surface can be used, or a submersible pump may be placed within the well casing. Extraction wells are used if (a) the dewatering system must be kept outside the excavation area, (b) large quantities of water must be pumped for a long period of time, (c) pumping must commence before excavation to obtain the necessary time for drawdown, or (d) pressures must be lowered in a confined aquifer that is below a low-

permeability layer underlying an excavation. Extraction wells may be used for soils with classifications ranging from gravel to silty fine sand, and for water bearing rocks.

Bored shallow wells with suction pumps can be used to replace wellpoints where pumping is required for several months or in silty soils where correct filtering is critical. Ejector or eductor pumps may be utilized within wellpoints for lifts up to about 60 feet. The ejector pump has a nozzle arrangement at the bottom of two small diameter riser pipes which remove water by the Venturi principle. They are used in lieu of a multistage wellpoint system and if the large pumping capacity provided by extraction wells is not required. Their primary application is for sands, but with proper control they can also be used in silty sands and sandy silts.

Figure 6-32 presents equations for analysis of drawdown and pumping quantities for single wells or a group of wells in a circular pattern. The *radius of influence* (R) is often defined as the radius beyond which the well has no influence. R is a function of the discharge (q) and thus changes depending on the rate of pumping. The equations presented allow the calculation of R from data in a single observation well. Once R is known, drawdown at other locations can be calculated.

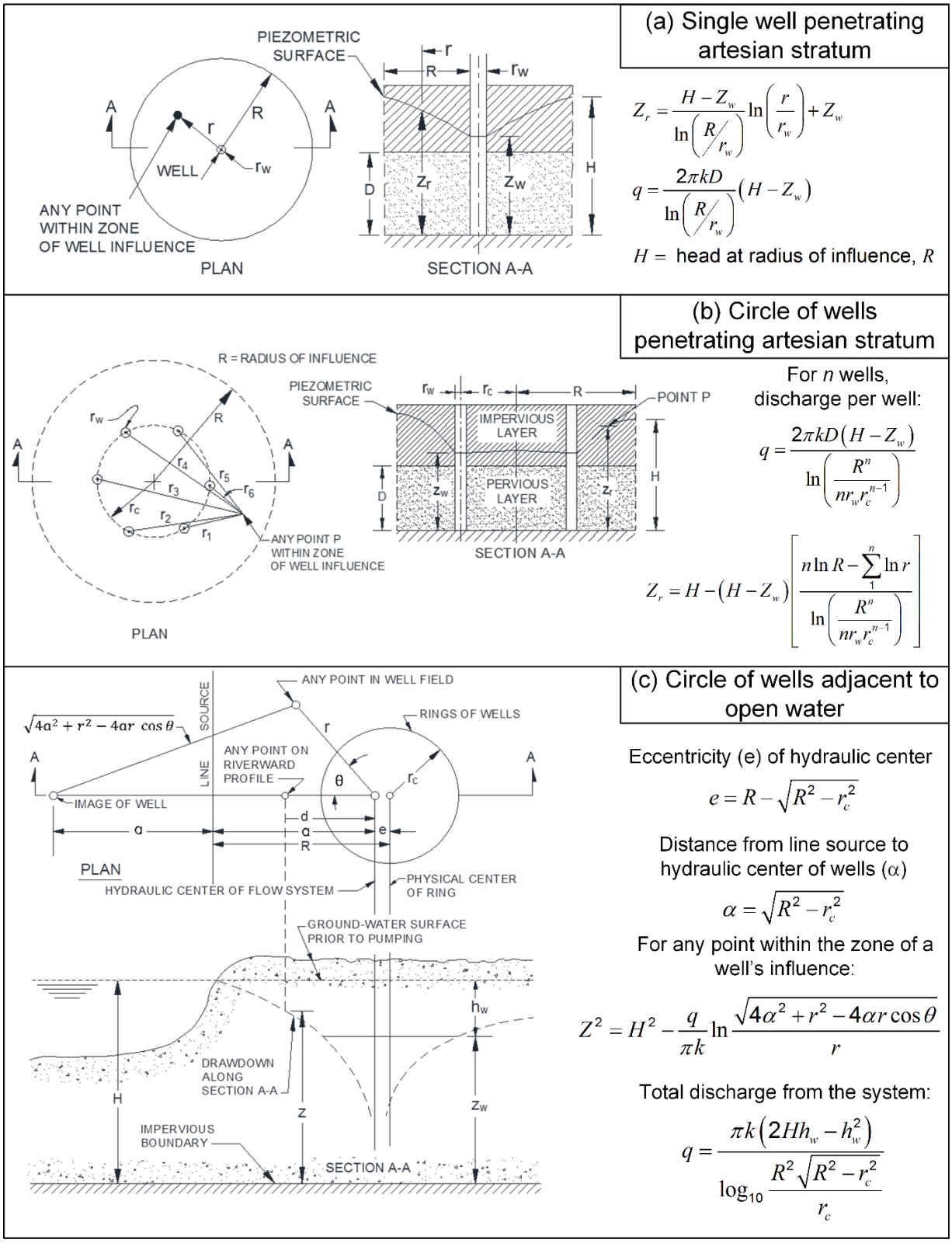

Figure 6-32 Drawdown and Pumping Quantities for Single Extraction Wells and Groups of Extraction Wells (after USACE 1952)

6-7 SUGGESTED READING.

Topic	Reference
Groundwater Flow	Cedergren, H. R. 1977. *Seepage, Drainage, and Flow Nets,* John Wiley and Sons, Inc., New York.
	Freeze, R. A. and Cherry, J.A.1979. *Groundwater* Prentice-Hall, Englewood Cliffs, NJ.
Filter Design	Federal Emergency Management Agency (FEMA), 2011. *Filters for Embankment Dams, Best Practices for Design and Construction*.
Numerical Seepage Analysis	Bradley, N. and VandenBerge, D. R. 2015. *Beginner's Guide for Geotechnical Finite Element Analyses*, Center for Geotechnical Practice and Research, Virginia Tech.
	Potts, D. M. and Zdravkovic, L. 2001. *Finite Element Analysis in Geotechnical Engineering: Theory and Application* ICE Publishing.

6-8 NOTATION.

Symbol	Description
a	Isotropic transformation factor for flow nets
A	Cross sectional area of the flow region perpendicular to the flow direction
C'_u	Linear coefficient of uniformity (geotextile design)
D_{li}	Particle size of the coarser sieve (Kozeny-Carman equation)
D_{si}	Particle size of the finer sieve (cm)
D_α	Effective grain size - α is the percent of soil particles smaller than the stated size, values of 5, 10, 15, and 20 are commonly used for α
D_x	Particle size for which X% of the soil is finer
D'_x	Particle size for which X% of the soil is finer for linearized particle distribution (geotextile design)
D_xB	Particle size for which X% of the soil is finer for a base soil
D_xF	Particle size for which X% of the soil is finer for a filter material
e	Void ratio of the soil
f_i	Fraction of particles between two adjacent sieve sizes (Kozeny-Carman equation)
FS_g	Factor of safety for geotextile permeability
h_L	Head loss across flow region
h_p	Pressure head
h_t	Total hydraulic head

Symbol	Description
h_v	Velocity head
h_z	Elevation head
i	Hydraulic gradient
k	Hydraulic conductivity of soil (various subscripts)
k_g	Hydraulic conductivity of geotextile across plane of fabric
L	Length of flow path
n	Porosity of the soil
N_d	Number of equipotential (head) drops in the flow net
N_f	Number of flow channels in the flow net
O_{95}	Geotextile apparent opening size
q	Volumetric flow rate
R	Radius of influence in well design
S	Surface area factor for grain shape (Kozeny-Carman equation)
t_g	Geotextile thickness
u	Water pressure at the point of interest
v_d	Discharge velocity
v_s	Seepage velocity
x	Exponent on effective grain size for hydraulic conductivity correlations
Y	Height of the flow region
Z	Elevation of a point of interest above the elevation datum
β_α	Empirical or semi-empirical coefficient relating k to D_α
γ_w	Unit weight of water
Δh_l	Total head loss for one equipotential drop on a flow net
ψ_g	Geotextile permittivity, provided by manufacturers or from testing (ASTM D4491)

This Page Intentionally Left Blank

CHAPTER 7 SLOPE STABILITY

7-1 INTRODUCTION.

Slope stability analysis is a common category of analyses in geotechnical engineering practice. The analysis contains elements of statics, rock or soil mechanics, and numerical methods. The techniques used range from simple chart solutions to complicated numerical computer solutions. Regardless of the solution method employed, the most important element in slope stability analysis is the shear strength of the soil or rock.

Although rock slope stability and soil slope stability rely on the same basic mechanics, the modes of failure can be very different. In this chapter, rock slope stability will be discussed in a separate stand-alone section.

7-2 TYPES OF SLOPES AND MODES OF FAILURE.

There are many different categories of slopes. *Natural slopes* are those that are ungraded and the slope geometry is controlled by nature. Figure 7-1 shows some general cross-sections and failure conditions for natural slopes. If the slope is steepened by grading or excavation, it is called a *cut*, a *cut slope* or an *excavated slope*. Dam abutments can be natural slopes or cut slopes.

Embankments constructed of compacted soil form another category of slopes. These embankments can be *highway embankments*, *dams* and *levees*, *fill slopes*, *Mechanically Stabilized Earth* (*MSE*) *slopes*, and others. Figure 7-2 shows cross-sections through example embankment slopes and details about the failure conditions.

Principal modes of failure in soil or rock are (i) rotation on a curved slip surface approximated by a circular arc, (ii) translation on a planar surface whose length is large compared to depth below ground, and (iii) displacement of a wedge-shaped mass along one or more planes of weakness. Other modes of failure include toppling of rock slopes, falls, block slides, lateral spreading, earth and mud flow in clayey and silty soils, and debris flows in coarse-grained soils. Figure 7-1 and 7-2 show examples of potential slope failure problems in both natural and man-made slopes.

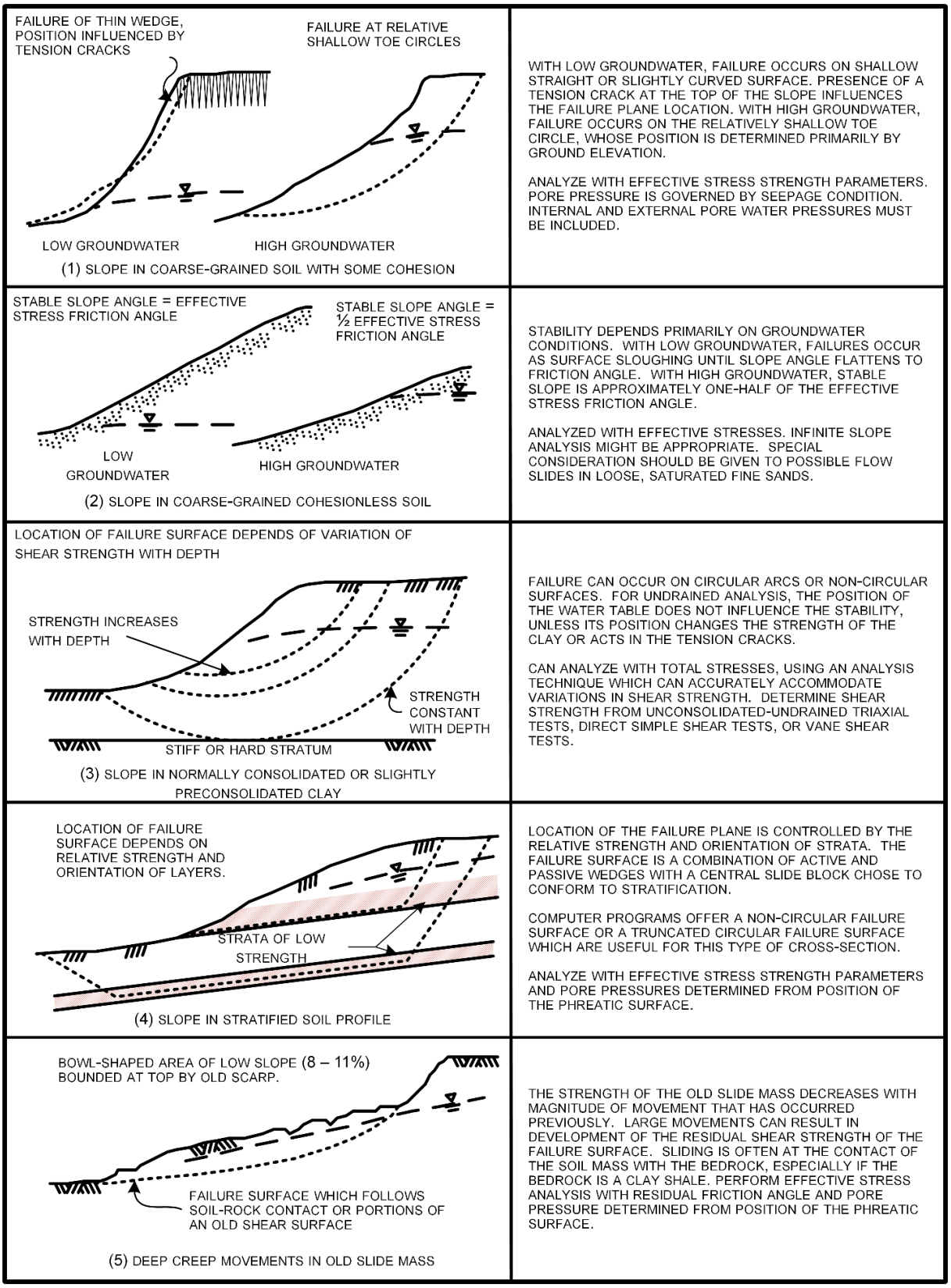

Figure 7-1 Failure Conditions for Cross-sections through Natural Slopes

LOCATION OF FAILURE SURFACE DEPENDS ON MATERIAL STRENGTHS AND GEOMETRY

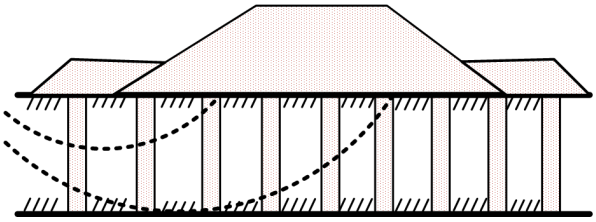

(1) FAILURE FOR FILL ON SOFT COHESIVE FOUNDATION WITH DRAINS

MINIMUM STABILITY USUALLY OCCURS DURING PLACING OF FILL. IF THE RATE OF CONSTRUCTION IS CONTROLLED, CAN ALLOW FOR GAIN IN STRENGTH WITH CONSOLIDATION FROM DRAINAGE. UNDRAINED ANALYSES CAN BE PERFORMED USING STRENGTHS OBTAINED FROM UU TRIAXIAL TESTS, DSS TESTS, OR VANE SHEAR TESTS. IN ORDER TO INVESTIGATE THE INCREASE IN STRENGTH WITH CONSOLIDATION, CAN USE DSS TESTS.

EFFECTIVE STRESS ANALYSIS CAN BE PERFORMED USING DRAINED STRENGTH PARAMETERS OBTAINED FROM CU TRIAXIAL TESTS OR DIRECT SHEAR TESTS ALONG WITH THE PORE PRESSURES CALCULATED FORM CONSOLIDATION THEORY.

FAILURE SURFACE MAY BE ROTATION ON A CIRCULAR ARC OR TRANSLATION WITH ACTIVE AND PASSIVE WEDGES.

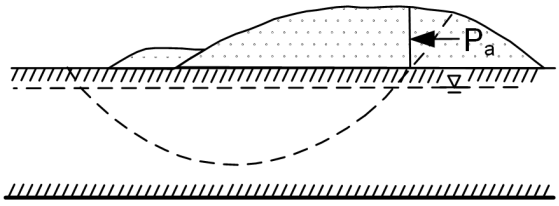

(2) FAILURE OF STIFF COMPACTED FILL ON SOFT CLAY FOUNDATION.

USUALLY, MINIMUM FACTOR OF SAFETY OBTAINED AT END OF CONSTRUCTION. FAILURE MAY BE IN THE FORM OF ROTATION OR TRANSLATION, AND BOTH SHOULD BE CONSIDERED.

FOR RAPID CONSTRUCTION, IGNORE CONSOLIDATION IN THE CLAY LAYER AND USE UNDRAINED STRENGTH OBTAINED FROM UU TRIAXIAL TESTS, DSS TESTS, OR VANE SHEAR TESTS, AND PERFORM AN UNDRAINED ANALYSIS.

ANALYZE LONG-TERM STABILITY USING EFFECTIVE STRESS STRENGTH PARAMETERS FOR CU TRIAXIAL TESTS OR DIRECT SHEAR TESTS. USE PORE PRESSURES FROM STATIC PHREATIC SURFACE.

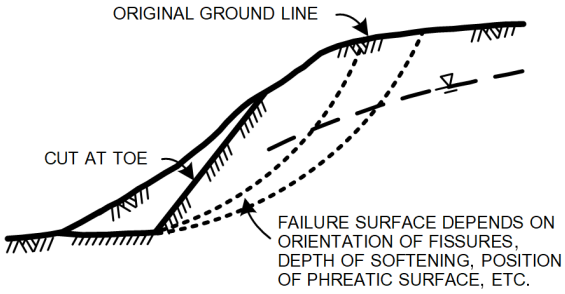

(3) FAILURE SURFACE FOLLOWING CUT IN STIFF FISSURED CLAY

CUTS IN STIFF FISSURED CLAYS MAY RESULT IN FAILURES MANY YEARS AFTER THE CUT IS MADE. RELEASE OF HORIZONTAL STRESSES BY EXCAVATION CAUSES EXPANSION OF THE CLAY AND OPENING OF FISSURES, ALLOWING SOFTENING AND REDUCTION OF STRENGTH.

PERFORM AN EFFECTIVE STRESS ANALYSIS USING THE FULLY SOFTENED SHEAR STRENGTH ENVELOPE AND PORE PRESSURES CALCULATED FROM THE POSITION OF THE PHREATIC SURFACE.

Figure 7-2 Failure Conditions in Embankment Foundations and Cut Slopes

7-3 DEFINITION OF FACTOR OF SAFETY.

The stability of slopes is characterized by the *factor of safety*, F. Although there have been various methods of defining the factor of safety found in the engineering literature, the most common is shown below:

$$F = \frac{s}{\tau} \quad \textbf{(7-1)}$$

where:
s = shear strength,
τ = shear stress required for equilibrium.

If the factor of safety is equal to unity, the slope is in a condition of barely stable equilibrium, right at the point of failure. As the factor of safety increases above unity, the stability of the slope increases. Slopes having a factor of safety less than one are considered unstable.

The value of s used in the calculation of factor of safety depends on the strength model used to characterize the soil, which is often associated with the drainage conditions assumed as well as the soil type. Table 7-1 shows different strength models that can be used in the analyses for different soil types and drainage conditions.

The shear stress required for equilibrium (τ) is calculated by statics along with assumptions regarding the conditions for equilibrium and other factors. The number of unknowns exceeds the number of equilibrium equations in most forms of slope stability analysis, so assumptions must be made. A major difference in the various methods used to perform slope stability analyses is the conditions of equilibrium that are satisfied.

7-4 METHODS OF ANALYSIS OF SOIL SLOPES.

Slope stability analysis in geotechnical engineering practice has evolved over the past 100 years. Initial methods of assessing the stability of slopes involved mapping areas of instability and determining slope angles from surveys to create *landslide hazard maps*. These types of maps are still produced and can be useful in screening potential stability issues with natural slopes and examining regional landslide risk. Beginning in the 1920s, assessment procedures were developed that provided a more quantitative basis for determining the stability of slopes.

Three numerical procedures are used, with varying degrees of popularity, to assess the stability of slopes: (1) limit equilibrium analysis, (2) finite element and finite difference analysis, and (3) plasticity analysis.

Table 7-1 Strength Models for Different Soil Types and Drainage Conditions

Soil type	Drainage conditions	s, strength	Comments
Coarse-grained soils	Drained	$s = \sigma'_{ff} \cdot tan(\phi')$	Drained conditions are often assumed for coarse-grained soils, such as sands and gravels under static loading conditions. Non-linear envelopes can be used as well.
Coarse-grained soils	Undrained	$s = s_{su}$	Used for dynamic loading and certain conditions of static loading. Can be used for clays and silts as well for dynamic or cyclic loading. For normal undrained analysis, the effective stress strength parameters should be used for coarse-grained soils.
Overconsolidated fine-grained soils	Drained	$s = c' + \sigma'_{ff} \cdot tan(\phi')$	A non-linear envelope can be used for this case as well. Some engineers do not like to use effective stress cohesion for any soil.
Normally consolidated fine-grained soils	Drained	$s = \sigma'_{ff} \cdot tan(\phi')$	The effective stress friction angle should correspond to the soil in a normally consolidated state. This is equal to the fully softened friction angle.
Fine-grained soils (saturated)	Undrained	$s = s_u$	The undrained shear strength can be determined using a variety of laboratory or *in situ* tests. The magnitude of s_u can vary with depth.
Fine-grained soils (partially saturated)	Undrained	$s = c + \sigma_{ff} \cdot tan(\phi)$	This strength model is used for partially saturated soils like compacted clays. The shear strength parameters should be measured using Unconsolidated Undrained triaxial tests. Only use a linear envelope for the range of stress where it appears to be appropriate.

Note: σ'_{ff} = effective stress on failure plane, ϕ' = effective stress friction angle, c' = effective cohesion, σ_{ff} = total normal stress on failure plane, ϕ = total stress friction angle, c = total stress cohesion, s_{su} = undrained steady state shear strength, and s_u = undrained shear strength

7-4.1 Limit Equilibrium Analysis.

Limit Equilibrium Analysis is the most popular method of analysis to quantify the stability of soil slopes. The procedure involves dividing the sliding mass into one or more *free bodies*, and determining the forces acting on the free bodies using equations for force and/or moment equilibrium. The shear stress required for a condition of barely-stable equilibrium (τ) is determined for each free body from the analysis of the system of free bodies. These shear stresses are used with Equation 7-1 to calculate the factor of safety of the slope.

Figure 7-3 shows the division of slopes into one, three, and multiple free bodies for analysis using the limit equilibrium method. For these analyses, the failure surface can be linear, circular, or a combination of linear and arc segments. For most limit equilibrium analyses, assumptions must be made so that the equilibrium equations can be satisfied. In many cases, iteration must be performed to obtain a solution, and it takes a computer program to efficiently apply the analysis method.

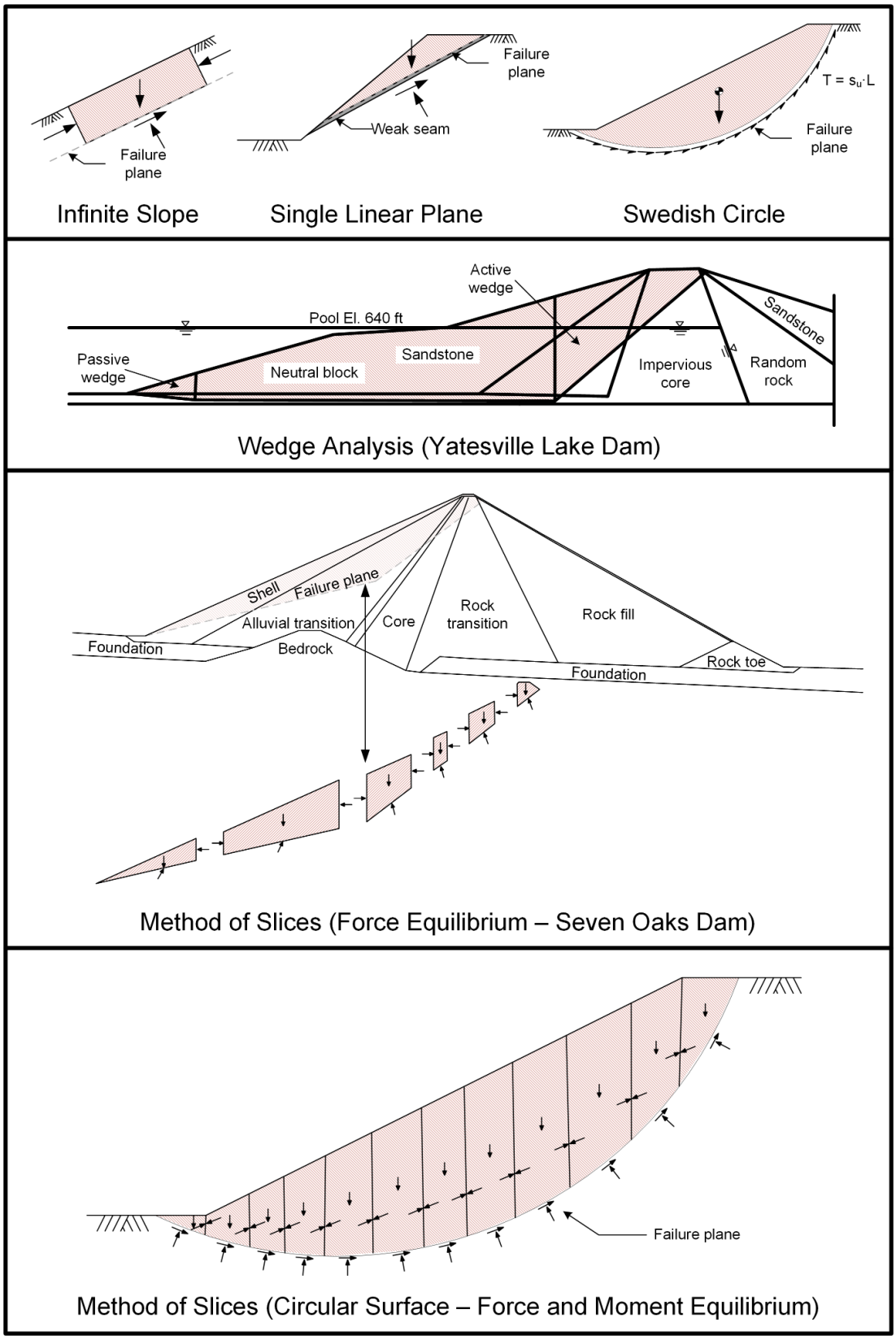

Figure 7-3 Examples of Limit Equilibrium Analysis

In general, the most common methods used in practice assume that the failure surface is circular or a surface comprised of many line segments. The methods that solve for all conditions of equilibrium (force and moment) provide the most accurate answers. These include Spencer's Method (Spencer 1967) and the Morgenstern and Price Method (Morgenstern and Price 1963). Most of the commercially available computer programs can perform these two methods.

In some cases, the potential critical failure surface may be easily identified by a feature such as a thin weak seam. In most other cases, it is necessary to search for the critical failure surface. The common slope stability programs have very robust search routines for circular and noncircular failure surfaces.

Figure 7-4 shows the formulas and calculations for a slope stability analysis using Bishop's Simplified Method. In this method, the soil mass is divided into vertical slices. The free body diagram for a slice is shown on the figure. This method uses circular failure surfaces, and the side forces are assumed to be horizontal. Moment equilibrium is satisfied, but only equations for vertical force equilibrium are used. Horizontal force equilibrium is not satisfied.

7-4.2 Finite Element Analysis of Slopes.

Use of finite element analysis to analyze slope stability is becoming more popular in geotechnical practice. A thorough assessment of the use of the finite element method is presented by Griffiths and Lane (1999). The finite difference method is an alternative to the finite element method, and both of these assess the slope in a similar fashion. Instead of calculating a factor of safety as defined by Equation 7-1, the finite element and finite difference solutions use a *strength reduction factor* (SRF). The SRF is a factor by which the cohesion (c) and the tangent of the friction angle (ϕ) are reduced to a point where the solution no longer converges. At the critical SRF, the displacements increase rapidly and the equations for equilibrium can no longer be solved.

The finite element method has a few advantages over the more common limit equilibrium method. The failure surface does not have to be identified prior to the analysis. The FE method actively seeks out the critical failure surface automatically as part of the analysis procedure. In addition, the equations for equilibrium are satisfied.

7-4.3 Limit Analysis.

Limit analysis is based on the upper and lower bound theorems for the theory of plasticity. The process involves section of a potential failure surface, and analyzing the failure mass based on a kinematically admissible velocity field and a statically admissible stress field. The use of limit analysis for slope stability calculations has been around for over 40 years, but it has found limited use in geotechnical engineering practice. Commercially available programs that use limit analysis have recently become available, and the popularity may increase.

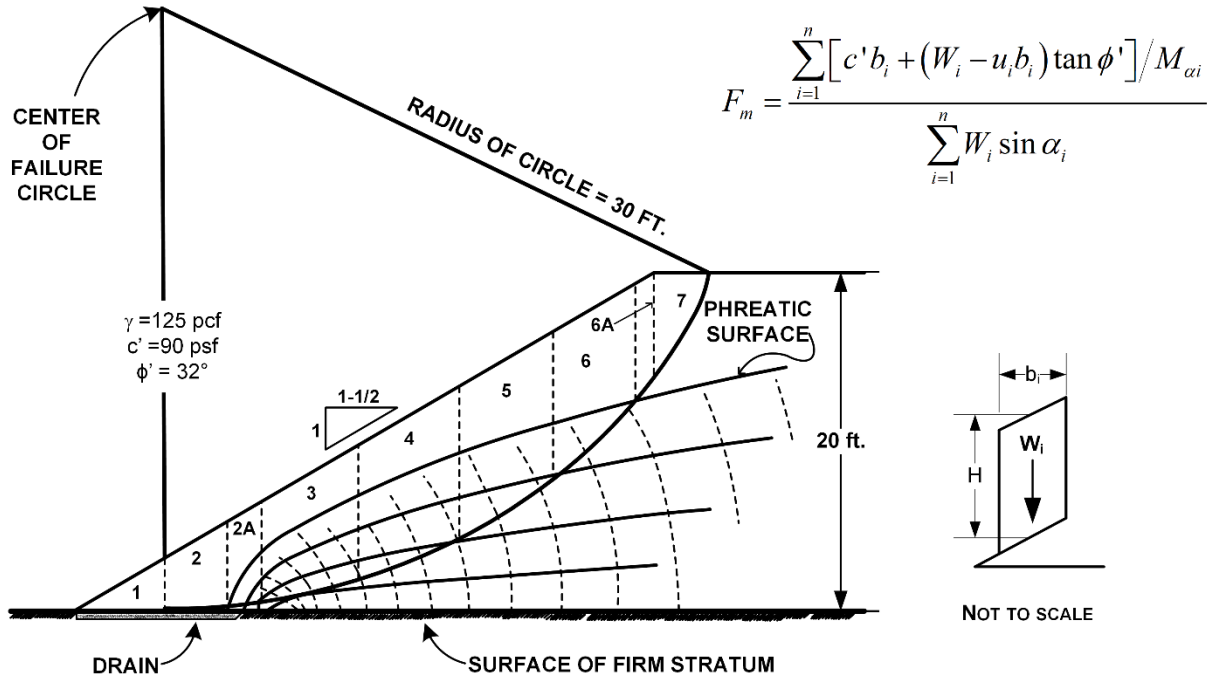

Considering the equilibrium of forces in the vertical direction, but neglecting the shearing forces between slices, the factor of safety for moment equilibrium can be calculated as indicated above. This equation can be solved by iteration using a spreadsheet. Values of $M_{\alpha i}$ can be obtained from the chart below.

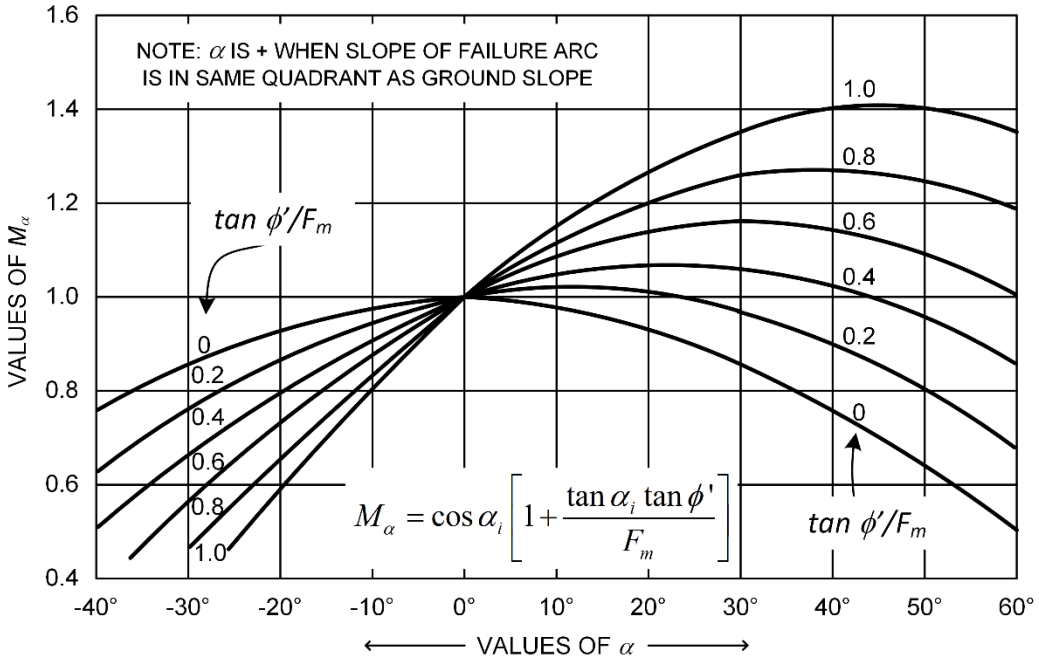

Figure 7-4 Example Slope Stability Analysis using Bishop's Simplified Method for an Effective Stress Analysis

Example Calculations

Find F_m for the trial slip circle shown. Strength properties are c'= 90 psf, ϕ'= 32°, and γ_t = 125 pcf. Slope is 1.5H:1V. Flow conditions are shown.

Procedure (Numbers in parentheses correspond to column in example):

1. Divide cross section into vertical slices. (1)
2. Calculate the weight of each slice (W_i) using total unit weights, where is the width of the slice and H_i is the average height of the slice. (2) (3) (4)
3. Calculate $W_i \sin\alpha_i$ for each slice where α_i is equal to the angle between the tangent to the failure surface and the horizontal. (5) (6)
4. Multiply the effective stress cohesion (c') times the width of each slice () (7)
5. Multiply the average pore water pressure along the failure surface of each slice by the width of each slice. (8).
6. Calculate $(W_i - u_i b_i)\tan(\phi')$ for each slice (9).
7. Add $c'b_i$ to (9) for each slice. (10)
8. Select two factors of safety (F_m) and find $M_{\alpha i}$ for each slice using the graph or equation on the previous page (11).
9. Divide column (10) by $M_{\alpha i}$ for each slice and sum the resultants (12).
10. Divide $\sum_{i=1}^{n}[c'b_i + (W_i - u_i b_i)\tan(\phi')]/M_{\alpha i}$ by $\sum_{i=1}^{n} W_i \sin(\alpha_i)$ to calculate F_m.
11. Compare calculated F_m to assumed F_m in Step 8. Reiterate Steps 8, 9, and 10 until assumed F_m of Step 8 equals calculated F_m of Step 10.
12. Repeat above analysis for different failure surfaces to obtain the surface with the smallest factor of safety.

Slice (1)	b_i ft (2)	H_i ft (3)	W_i kips (4)	$\sin\alpha_i$ (5)	$W_i \sin\alpha$ kips (6)	$c'b_i$ kips (7)	$u_i b_i$ kips (8)	(4-8) $\tan\phi'$ kips (9)	(7+9) kips (10)	$M_{\alpha i}$		10÷11	
										F_m =1.25	F_m =1.35	F_m =1.25	F_m =1.35
										(11)		(12)	
1	4.5	1.6	0.9	0.03	0.0	0.40	0.00	0.55	0.95	0.97	0.97	1.00	1.00
2	3.2	4.2	1.7	0.05	0.1	0.29	0.00	1.05	1.35	1.02	1.05	1.30	1.30
2A	1.8	5.8	1.3	0.14	0.2	0.16	0.05	0.80	0.95	1.06	1.05	0.90	0.90
3	5.0	7.4	4.6	0.25	1.2	0.45	1.05	2.25	2.70	1.09	1.08	2.50	2.50
4	5.0	9.0	5.6	0.42	2.3	0.45	1.45	2.55	3.00	1.12	1.10	2.70	2.75
5	5.0	9.3	5.8	0.58	3.4	0.45	1.25	2.70	3.15	1.10	1.08	2.85	2.90
6	4.4	8.4	4.6	0.74	3.4	0.40	0.50	2.65	3.05	1.05	1.02	2.90	2.95
6A	0.6	6.7	0.5	0.82	0.4	0.05	0.00	0.30	0.35	0.98	0.95	0.35	0.40
7	3.2	3.8	1.5	0.87	1.3	0.29	0.00	0.95	1.25	0.93	0.92	1.30	1.35
					12.3							15.80	16.05

For an assumed F_m = 1.25, calculated F_m = 15.8/12.3 = 1.29
For an assumed F_m = 1.35, calculated F_m = 16.05/12.3 = 1.31

A trial assuming F_m= 1.3 would yield F_m= 1.3

Figure 7-4 (cont.) Example Slope Stability Analysis using Bishop's Simplified Method for an Effective Stress Analysis

7-5 WATER PRESSURE EFFECTS.

Water pressures have a profound effect on the stability of slopes. As an example, many failures that occur in natural and constructed slopes occur during periods of heavy precipitation. There are two categories of water pressures in slope stability analysis: (1) *internal water pressures* and (2) *external water pressures*. Examples of these are shown in Figure 7-5.

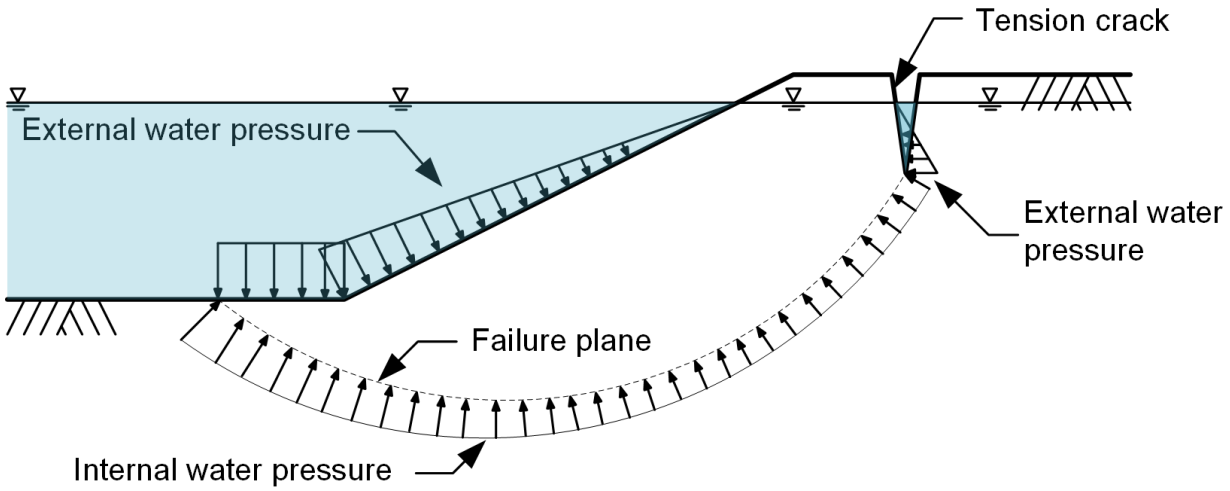

Figure 7-5 Examples of Internal and External Water Pressures in Slope Stability Analyses

Internal water pressures are the same as pore water pressures. These are the static or dynamic water pressures that act on the failure plane within the soil mass. Internal water pressures must be included in slope stability analyses where the soil is characterized by effective stress or drained shear strength parameters (c' and ϕ'). Internal water pressures are not included in the analysis where the soil is characterized by total stress or undrained shear strength parameters (s_u or c and ϕ).

External water pressures are the pressures applied to the free body where standing water is in contact with the soil mass at locations other than the failure surface. Examples of external water pressures are the pressures applied by the reservoir on the upstream slope of a dam or water-filled tension cracks. External water pressures are included in both effective stress and total stress slope stability analyses.

7-5.1 Incorporating Water Pressures in Computer Analyses.

It is important that the engineer fully understand the way that water pressures are specified in computer programs that they use, and how to verify that the correct water pressures are being used. The nomenclature for inputting water pressures is not consistent between the many different programs available for slope stability analysis.

The *water table* or *groundwater table* is normally defined as a line that connects points where the pore water pressure (u) is equal to zero. Water table is often used synonymously with *phreatic surface*. The *piezometric surface* is a surface connecting the height or elevation that water would rise in a series of standpipe piezometers. For hydrostatic conditions with a horizontal water table, the water table, phreatic surface, and piezometric surface are the same. For hydrodynamic cases where water is flowing, the piezometric surface can be at a higher elevation than the water table (upward flow of water) or at a lower elevation than the water table (downward flow of water). An example of this is shown in Figure 7-6. At Point A, the vertical distance to the phreatic surface is indicated on the drawing. However, the pore water pressure is controlled by the distance to the piezometric line, which is also shown on the figure.

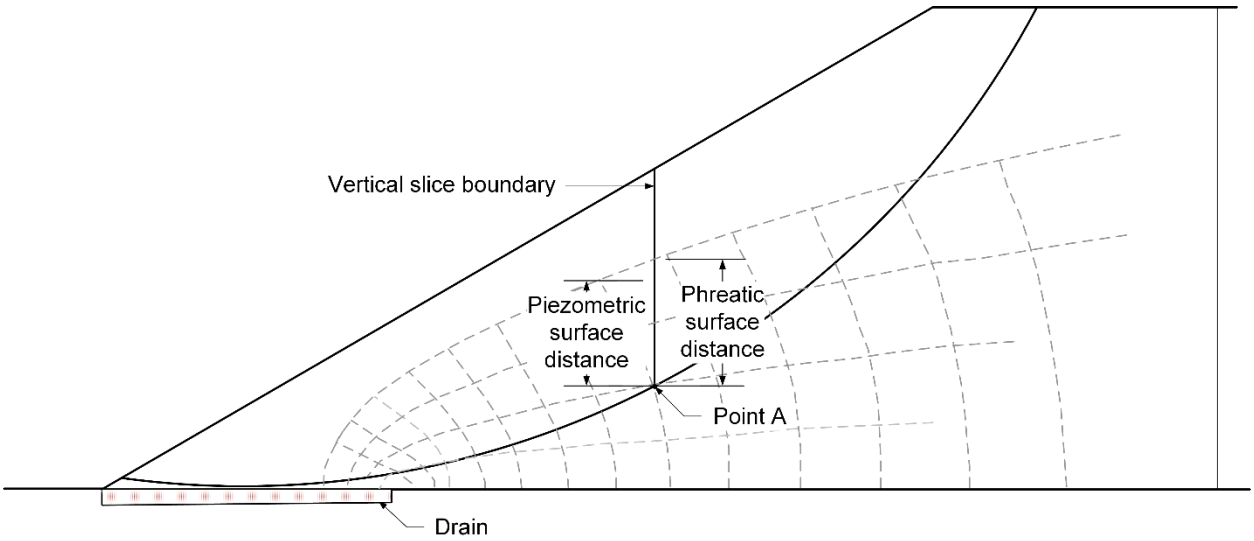

Figure 7-6 Approximate Flow Net for Seepage into a Drain Showing the Difference between the Piezometric Surface and the Phreatic Surface

Internal water pressures can be accommodated in slope stability software in one or more of the following methods:

(1) Water table or phreatic surface – can be corrected to approximate the piezometric surface based on the slope of the surface above the specific point,
(2) Piezometric surface,
(3) Finite element seepage analysis,
(4) Point-by-point entry in x-y coordinates with subsequent interpolation between points, and
(5) Pore pressure coefficient, r_u.

Of these different methods, the finite element seepage analysis is probably the best. It allows a large density of pore water pressure points to be calculated and interpolation between these points is sufficiently accurate with most interpolation methods. Use of

the pore pressure coefficient is perhaps the least accurate of the methods listed and is normally only used to verify results from historic analyses.

External water pressures can be automatically applied by most programs by the use of the water table or phreatic surface. As an alternative, external water pressures can be applied by the use of triangular and rectangular distributed loads. A third method is to assign the water properties of a soil material, having the unit weight of water but no shear strength. External water pressures in tension cracks are normally handled automatically by the computer program, but triangular distributed loads can also be used to model water-filled tension cracks.

7-5.2 Seepage Forces.

The flow of water through a slope can serve to destabilize slopes. As indicated in Figure 7-1, the flow of water parallel to the surface of a slope can reduce the factor of safety to about half of the factor of safety without flowing water. As water flows through a soil, a seepage force (S) is imparted to the soil from the viscous resistance to the flow of water. The seepage force can be calculated from:

$$S = i \cdot \gamma_w \quad \textbf{(7-2)}$$

where:
i = hydraulic gradient, and
γ_w = unit weight of water.

The seepage force equation provides a force per volume for the volume where the hydraulic gradient or head loss occurs. For slope stability analyses, the effect of flowing water can be handled by (1) calculating the seepage forces for each slice or free-body and (2) using the buoyant unit weight of the soil below the phreatic surface. Unfortunately, using this method requires that the calculations be largely done by hand. The computer programs that are commercially available do not perform these calculations automatically. The alternative method, which is accommodated by current computer programs, correctly calculates the factor of safety of slopes where flow is occurring by using total unit weights of soils below the water table along with boundary water pressures as discussed above. This method is currently used in geotechnical engineering practice.

7-6 STRENGTH MODELS AND ANALYSIS CASES.

Slope stability analysis cases are often categorized as undrained (or total stress) or drained (effective stress) analyses. These are often called short-term and long-term analyses because their respective use is related to the amount of time required for the soil to consolidate under the changed loading. For this reason, both effective stress and undrained (total stress) strength parameters can be assigned to the different soils in a cross section depending on their drainage condition during the duration of loading.

The general analysis cases are listed below with guidance on strength models to be employed with each.

7-6.1 End of Construction (Short Term).

End of construction or *post-construction* analyses are performed to examine the stability after construction is completed and prior to any dissipation of pore water pressures in fine-grained soils. An example of a valid end of construction analysis is construction of a compacted clay embankment over saturated fine-grained soils. A cross section of this is shown in Figure 7-7a. For this case, the compacted clay embankment would be partially saturated, and the strength would be represented as a c-ϕ soil, with the strength parameters determined from UU triaxial tests. The *in situ* fine-grained soils would be essentially saturated, and the strength would be characterized as $\phi = 0$, $s_u = c$. The shear strength of the *in situ* soils could be measured by UU triaxial tests, DSS tests, laboratory miniature vane shear tests, field vane shear tests, and under some conditions, cone penetration tests.

7-6.2 Cut Slope in Clay.

The cross section of a cut slope in a stiff clay is shown in Figure 7-7b. The critical time in the performance of the cut slope occurs long after the cut is made, when the phreatic surface has reached a steady-state condition. For this type of scenario, effective stress or drained shear strengths should be used for the clay. If the clay has a relatively low plasticity (LL < 40 and PI < 20), it would be appropriate to use the peak drained strength parameters (c' and ϕ') determined from CU triaxial tests or CD direct shear tests. The use of a non-linear effective stress envelope for the clay would also be appropriate (Duncan et al. 2014). If the clay has a high plasticity, contains fissures, and/or is heavily overconsolidated, then the fully softened shear strength should be used to account for changes in shear strength that will likely occur over time. The fully softened shear strength can be measured using remolded test specimens in a direct shear apparatus. Again, the use of a non-linear envelope would be appropriate.

7-6.3 Steady State Seepage in Dams.

One of the stability analyses required for earth and rockfill dams is the evaluation of the factor of safety for the condition of steady state seepage (Figure 7-7c). This case assumes that the reservoir has been at a relatively constant elevation for long enough that a steady-state seepage pattern has developed. The pore water pressures in the dam and foundation can be calculated using finite element analysis. The pore pressures above the phreatic surface are normally assumed to be equal to zero. Effective stress strength parameters (c' and ϕ') are used in the dam and foundation soils. The effect stress strength parameters for the dam materials can be measured with CD direct shear, CD triaxial, or CU triaxial tests on compacted test specimens. In the example, the strength parameters for the silty sand can be determined using *in situ* tests.

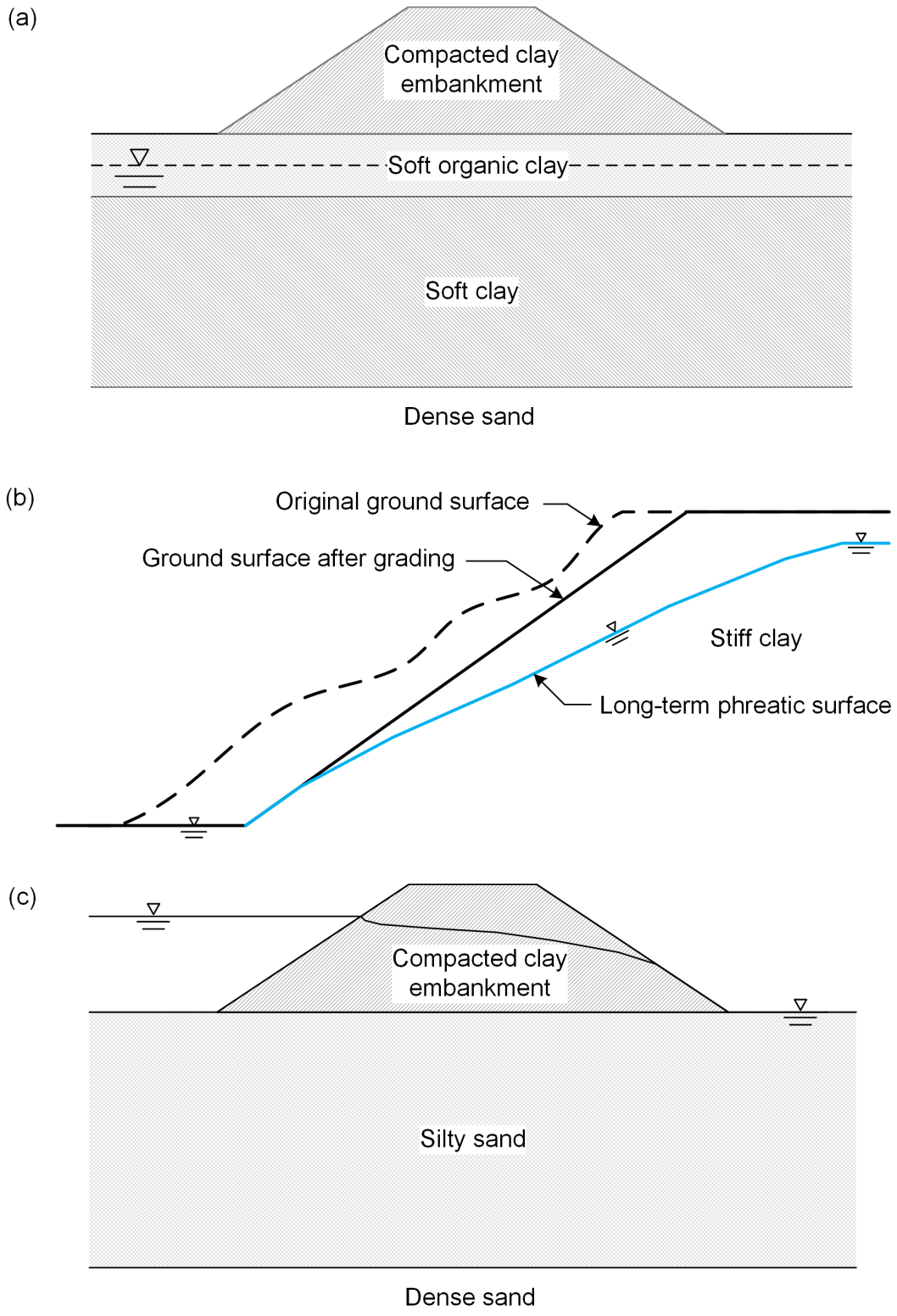

Figure 7-7 Analysis Cases for (a) End of Construction for Embankment on Clay, (b) Cut Slope in Clay, and (c) Levee or Dam in a Condition of Steady State Seepage

7-6.4 Stabilizing Berm for Failed Slope.

Berms are often used to stabilize failed slopes. For example, Figure 7-8 is a cross section of a slope that failed in a fat clay. A stability berm has been constructed at the toe of the slope to increase the factor of safety. It is presumed that the failure surface is known based on inclinometer readings or borings. If sufficient displacement has occurred on the failure surface, then the appropriate shear strength to use is the residual shear strength. The residual friction angle (ϕ'_r) or a nonlinear residual effective stress envelope is best determined by ring shear tests conducted on remolded test specimens of the fat clay. This should be an effective stress analysis with the appropriate phreatic surface used in the analysis.

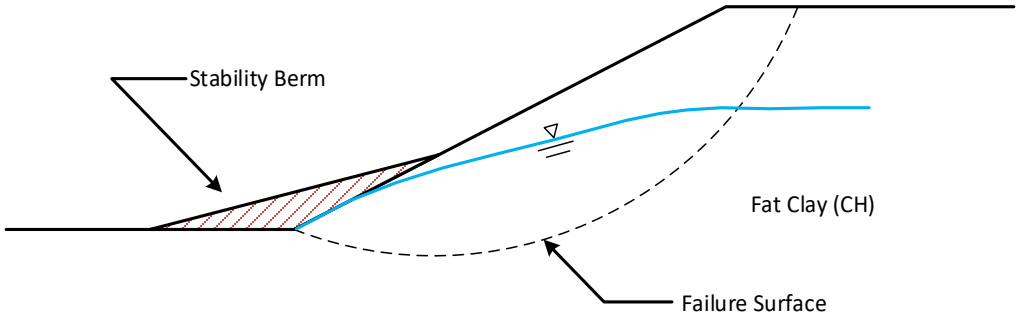

Figure 7-8 Stabilizing Berm Used to Increase the Factor of Safety of a Failed Slope

7-6.5 Other Analysis Cases.

Many other analysis cases are analyzed in geotechnical engineering practice that can be significantly more complex than the simple examples provided. For earth and rockfill dams, a critical case for the upstream slope is *rapid drawdown*. This occurs when the steady state seepage condition is changed by lowering the reservoir. If the reservoir is lowered rapidly (meaning days or weeks), the upstream slope no longer has the stabilizing support of the external water pressure. The shear strengths in the dam are based on the effective stresses prior to drawdown, and the lowering of the reservoir can cause an undrained failure. This is normally performed as a three-stage analysis, and it uses a strength model that is more complex than those used in the other cases described above (Duncan et al. 2014). These types of require considerable technical ability and they should be performed by engineers who have experience with rapid drawdown analysis. Effective stress rapid drawdown methods, such as those based on uncoupled transient seepage analyses, should be avoided.

The stability of slopes is also analyzed for cases of earthquake loading. These analyses can range from simple pseudostatic methods, where a horizontal force is applied to the free body of the limit equilibrium analysis, to very complex numerical analyses. Earthquake analyses are another category that require considerable

judgment and experience to obtain meaningful results and should be conducted by engineers skilled in this branch of geotechnical engineering.

7-6.6 Back-Analysis of Slopes.

Failed slopes offer a unique opportunity to develop a model of the shear strengths and ground water conditions at the time of failure. This type of model can be very useful in designing slope stabilization or in analyzing nearby slopes. When performing a forward analysis, the most important unknown is the factor of safety for a specific failure surface. When conducting a back-analysis of a slope, the factor of safety is known ($F = 1$), so a different unknown can be calculated. Normally, the shear strength of a soil layer is the desired property to be determined from back-analysis. If the back-analysis is performed on a slope that failed in an undrained condition, then the average undrained shear strength of a soil layer can be determined from the analysis. If the back-analysis is performed on a slope that failed in a drained condition, then only one of the effective stress strength parameters (c' or ϕ') can be determined. Often, the effective stress cohesion is assumed to be equal to zero, and the friction angle is calculated.

It is important that the other parameters used in a forward analysis be known with confidence for back-analysis. These include the slope geometry, soil stratigraphy, shear strength parameters for layers where strengths are not back-calculated, unit weights, etc. For back-analysis of drained failures, it is important that the pore pressure conditions *at the time of failure* be known. The location of the failure surface should also be known to obtain the most accurate results. Often, the failure surface location may be known from the results of inclinometer readings. In other cases, the location of the failure plane can be determined by careful drilling and sampling. If only the head scarp and toe exit of the failure plane is known, then the failure surface can be determined from the computer program's search routine by only searching for surfaces which go through those two points. If the position of the failure surface is not known, it is important to search for the critical surface and not to assume the location. If the location of the failure surface is assumed, then the resulting shear strength back-calculated will be too low.

7-6.7 Evaluation of Slope Stability Results.

Limit equilibrium slope stability calculations involve thousands of calculations. Since the adoption of computer programs to perform these calculations, project specifications often required that hand calculations be used to verify the results of the computer analyses. While this was possible when simpler methods of slope stability were used, such as Bishop's Simplified Method and the Ordinary Method of Slices, this requirement became impractical for more complex methods, like's Spencer's Method and Morgenstern and Price's Method. The time required to perform the calculations by hand for one failure surface for a cross section containing many slices and an advanced shear strength model has become excessive. In recognition of this, Wright (2013) suggested that new project specifications should require that two different slope stability computer programs should be used to verify analyses. After the minimum factor of safety for the critical failure surface is determined using one program, a different

program should be used to analyze the same failure surface using the same method. If the analyses are correct, the factors of safety calculated should be within about 1% of each other.

It is important for the engineer to be able to examine the forces acting on each slice. In particular, the forces at the boundary between slices should be in compression, and the normal force at the base of the slice should be in compression. Many computer programs allow the *line of thrust* to be plotted on the cross section. The line of thrust is a line that is plotted at the point of application of each of the side forces. Ideally, the line of thrust should be located within the soil mass defined by the slices. If portions of the line of thrust plot outside of the free body being analyzed, it often indicates tensile forces between slices or tensile forces at the base of slices. The addition of tension cracks to the cross section can be used to prevent tensile forces between slices, and these can be readily accommodated in commercial computer programs. Further information regarding the utility of the line of thrust can be found in Whitman and Bailey (1967).

The search routines for common commercial slope stability computer programs analyze thousands to tens of thousands of failure surfaces. The stability methods that solve for all conditions of equilibrium have iterative solutions, and the solutions do not always converge. There can be various reasons why the solutions do not converge, including geometry issues with invalid failure surfaces, problems with interpolation of advanced strength models, numerical issues with the solution procedure, etc. Critical failure surfaces can be missed as a result of non-convergence. The engineer should be able to identify when convergence issues are present. The location of this information varies depending on the program that is used, and is sometimes difficult to find. Prior to performing any analyses for record, the engineer should find this information and assess the validity of their results.

7-6.8 Slope Stability Charts.

Chart solutions for slope stability analyses have been available since the 1930s. Prior to the introduction of computers into geotechnical engineering practice, slope stability charts allowed an approximate solution to be quickly obtained. The charts are also useful in estimating the critical failure circle, showing the mode of failure (toe circle vs. deep circle), and other valuable information.

Charts have been developed for many different categories of slope stability analysis, including drained analyses, undrained analyses, rapid drawdown analyses, infinite slope analyses, surcharge loading at the crest, tension cracks, and other specialty cases. A comprehensive set of chart solutions can be found in Duncan et al. (2014). An example of a chart for infinite slope analysis is shown in Figure 7-9. Infinite slope analysis is useful for explaining sloughing failures for slopes having an effective stress cohesion equal to zero, and to examine the effects of seepage on the factor of safety of slopes.

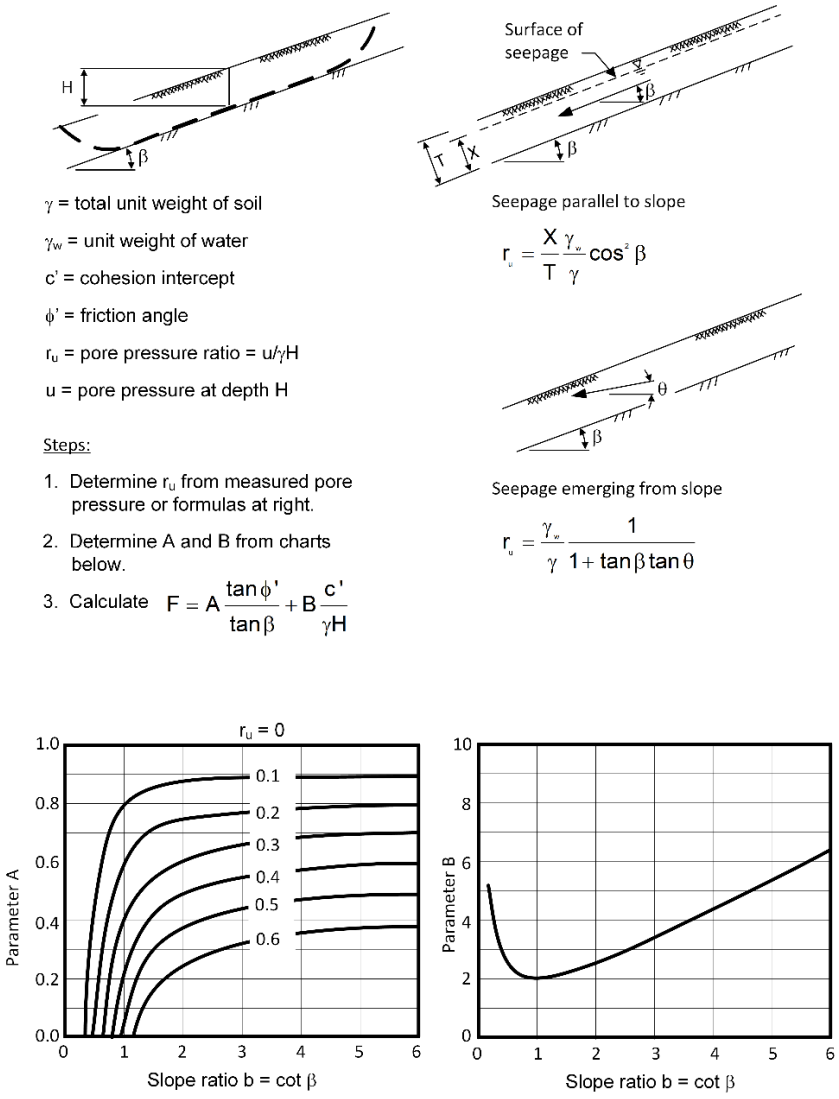

Figure 7-9 Chart Solution for Infinite Slope Analysis (after Duncan et al. 2014)

Charts have historically been used to obtain a quick solution to slope stability problems. Even with the advent of computer-based slope stability analyses, chart solutions still provided an approximate factor of safety in less time than required to run a computer analysis. However, the modern computer programs allow slope stability problems to be defined and solved very quickly, and the speed advantage of chart solutions has been diminished. Chart solutions are best suited for slope stability problems that have simple soil profiles and straightforward strength interpretations. As the soil profiles and strength interpretations become more complex, the accuracy of chart solutions decreases. Even so, chart solutions still offer a viable complementary analysis method to computer solutions.

7-7 SLOPE STABILIZATION.

It is often necessary to increase the factor of safety of existing slopes or to repair slopes that are moving or have failed. Figure 7-10 shows different methods of stabilizing slopes.

Scheme	Applicable Methods	Comments
1. Changing Geometry - Excavation 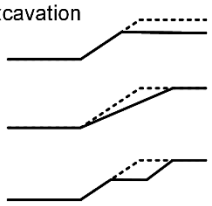	1. Reduce slope height by excavation at the top of slope. 2. Flatten the slope. 3. Excavate a bench in the top of the slope.	1. Area has to be accessible to construction equipment. Disposal site needed for excavated soil. Drainage sometimes incorporated into this method.
2. Toe Berm Fill 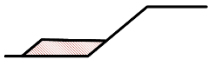	1. Compared earth or rock berm placed at the toe. Drainage may be required behind berm.	1. Sufficient width and thickness of berm required so failure will not occur below or through berm. Borrow soils required.
3. Retaining Structure 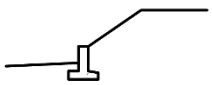 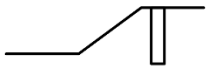 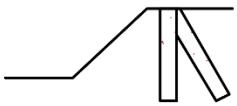 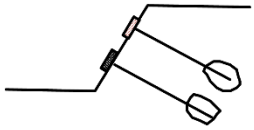 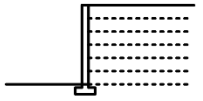	1. Retaining structure – Crib, Cantilever, or MSE. 2. Drilled, cast-in-place vertical piles founded well below the slide plane. Generally, 18 to 30 inches in diameter at 4 to 8 foot spacing. Larger diameter piles at closer spacing may be required in some cases to mitigate failures of cuts in highly fissured clays. 3. Drilled, cast-in-place vertical piles tied back with battered piles or a deadman. Piles founded well below the slide plane. Generally, 12 to 30 inches in diameter at 4 to 8 foot spacing. Larger diameter piles at closer spacing may be required in some cases to mitigate failures of cuts in highly fissured clays. 4. Earth and rock anchors and rock bolts with anchor plates. 5. MSE Wall	1. Usually expensive. Cantilever walls may have to be tied back. 2. Spacing should be such that soil can arch between piles. Grade beam can be used to tie piles together. Very large diameter piles (6+ feet) have been used for deep slides. 3. Space close enough so soil will arch between piles. Piles can be tied together with grade beam. 4. Can be used for high slopes in restricted areas. Conservative design should be used, especially for permanent support. Use may be essential for slopes in rocks where joints dip toward excavation and daylight in the slope. 5. Various types of geosynthetics and wall facings are available.
4. Other Methods	See DM 7.2.	

Figure 7-10 Methods of Stabilizing Slopes

7-8 REQUIRED FACTOR OF SAFETY FOR SOIL SLOPES.

There are many different sources that specify the minimum factor of safety. Often, the design values are determined by municipal or government organizations. For earth dams, the U.S. Army Corps of Engineers' EM 1110-2-1902 (2003) recommends the values listed in Table 7-2. Other organizations dealing with earth dams, such as the U.S. Bureau of Reclamation (USBR), have specified their own values. The values recommended by USBR are given in Table 7-3.

Table 7-2 Factors of Safety for New Earth and Rockfill Dams (USACE 2003)

Analysis Condition	Required F_{min}	Slope
End of Construction	1.3	Upstream and downstream
Steady state seepage (Long term)	1.5	Downstream
Maximum pool level	1.4	Downstream
Rapid drawdown	1.1 to 1.3	Upstream

Table 7-3 Factor of Safety for Dams using Spencer's Method for Dams (USBR 2011)

Loading Condition	Shear Strength Parameters	Pore Pressure Characteristics	Minimum factor of safety
End of construction	Effective	Generation of excess pore pressures in embankment and foundation materials with laboratory determination of pore pressure and monitoring during construction.	1.3
		Generation of excess pore pressures in embankment and foundation materials and no field monitoring during construction and no laboratory determination	1.4
		Generation of excess pore pressures in embankment only with or without field monitoring during construction and no laboratory determination	1.3
	Undrained Strength		1.3
Steady-state seepage	Effective	Steady-state seepage under active conservation pool	1.5
Operational conditions	Effective or undrained	Steady-state seepage under maximum reservoir level (during a probably maximum flood)	1.2
	Effective or undrained	Rapid drawdown from normal water surface to inactive water surface	1.3
		Rapid drawdown from maximum water surface to active water surface (following a probable maximum flood)	1.2
Other	Effective or undrained	Drawdown at maximum outlet capacity (inoperable internal drainage; unusual drawdown)	1.2
	Effective or undrained	Construction modifications (applies only to temporary excavation slopes and the resulting overall stability during construction).	1.3

The required minimum factor of safety is dependent on many different factors, including: (1) type of structure, (2) type of analysis, (3) consequences of failure, (4) uncertainty involved with design parameters, (5) frequency of specific loading event, and many others. An important concept in arriving at a minimum factor of safety involves the degree of uncertainty associated with the design parameters. Sometimes, the minimum factor of safety depends on if the analysis has "well-defined conditions" or "poorly-defined conditions." Engineering judgment is required to classify a particular site or project into one of these two categories. In some cases, the designation of "well-defined conditions" can only be applied for sites that have already been built upon.

In general, well-defined conditions means that the site exploration and field or laboratory testing program was thorough enough for the engineer to have confidence in the soil stratigraphy and shear strength interpretation. A poorly-defined condition can occur when the borings are spread far apart, few laboratory tests have been conducted, and/or the soil stratigraphy is highly variable. An example of this is the geotechnical guidelines for a large Washington DC suburb. The requirements for factors of safety for two different soil formations are given as follows[13]:

> "For long-term stability, a minimum Factor of Safety (FS) of 1.25 is required when supported with sufficient field and laboratory characterization of the slope's soils. Otherwise, a minimum FS of 1.5 is required. In case of Critical slope or structure, a minimum FS of 1.5 is required unless a laboratory measured residual strength test is obtained and used in the analysis. In this case, a minimum FS of 1.25 is required when supported with sufficient field and laboratory characterization of the soils."
>
> "For long-term stability of the soil formations other than Potomac Formation clay if slope stability analysis is deemed necessary by the engineer or if it is required by the County, a minimum Factor of Safety (FS) of 1.25 is only acceptable when the slope is not critical and the analysis is supported with sufficient site-specific *in situ* or laboratory strength tests of the encountered soils. Otherwise, a minimum factor of safety of 1.5 must be used in the analysis."

7-9 MECHANICALLY STABILIZED EARTH SLOPES.

Mechanically stabilized earth (MSE) is a term that refers to soil retention structures that include both retaining walls and earth slopes. This section discusses the application of MSE technology to slopes. The design of MSE retaining walls is discussed in DM 7.2.

[13] This example is intentionally left uncited to maintain anonymity of the source.

Design and analysis of MSE slopes is a specialty area in geotechnical engineering. There are engineering consultants who specialize in MSE walls and slopes. In this manual, the rudiments of design and analysis are presented in order that outside designs can be evaluated and not for the purpose of completing a full MSE design.

7-9.1 Applications of MSE.

Reinforced earth slopes are fill structures in which discrete layers of geosynthetic or steel elements are installed during construction at specified locations. A typical cross section of an MSE slope is shown in Figure 7-11.

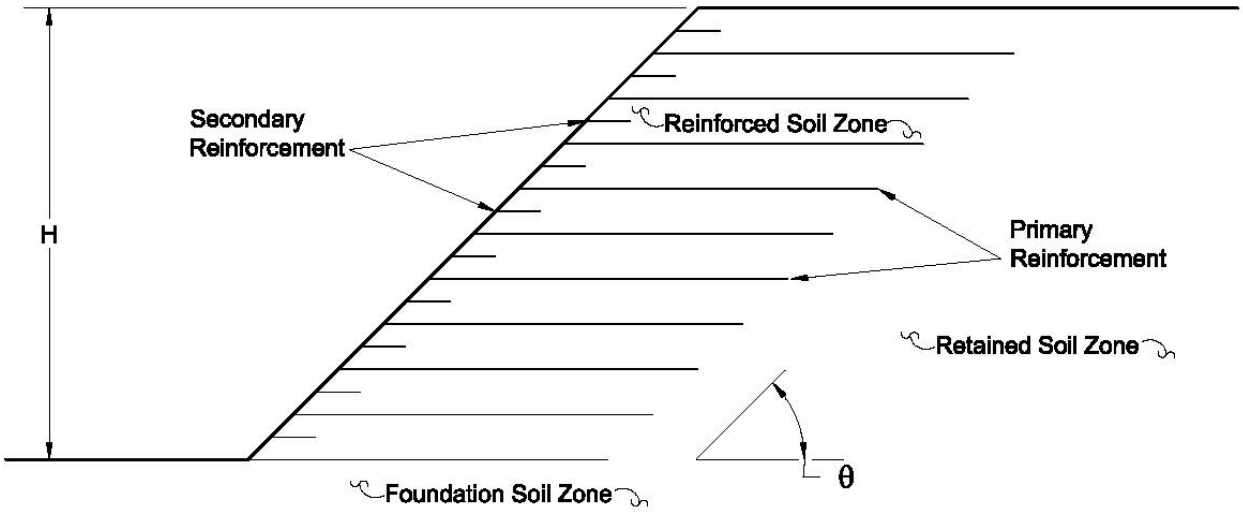

Figure 7-11 Typical Cross-Section of an MSE Slope

The *reinforced soil zone* is that portion of the slope in which layers reinforcement are installed. The *retained soil zone* and *foundation soil zone* are located behind and below the reinforced soil zone, respectively. The layers of primary reinforcement shown in Figure 7-11 resist the development of failure planes through the reinforced soil zone. The layers of secondary reinforcement prevent surficial failure at the slope face.

The primary limitations on the use of MSE slopes relate to constructability and utilities. Constructability is not typically an issue if the slope is part of a larger fill area but may be a concern when an existing hillside must be excavated to build the slope. Utilities can be significant factors in the poor performance of MSE structures, particularly if the utility is *wet* such as a storm sewer or water main. The malfunction of wet utilities may contribute to about one-third of the failures of MSE retaining walls (Valentine 2013).

The distinction between an MSE retaining wall and an MSE slope has been defined by the Federal Highway Administration (FHWA) based on the face angle, θ (FHWA 2009b). If $\theta < 70°$, then the structure is a slope. If $\theta \geq 70°$ or greater, then the structure is a wall. The distinction between an MSE retaining wall and slope has important implications for

land use efficiency as illustrated in Figure 7-12. However, the increased land use efficiency of MSE walls and slopes is accompanied by complications related to facing requirements and structural deformations, as well as increased cost.

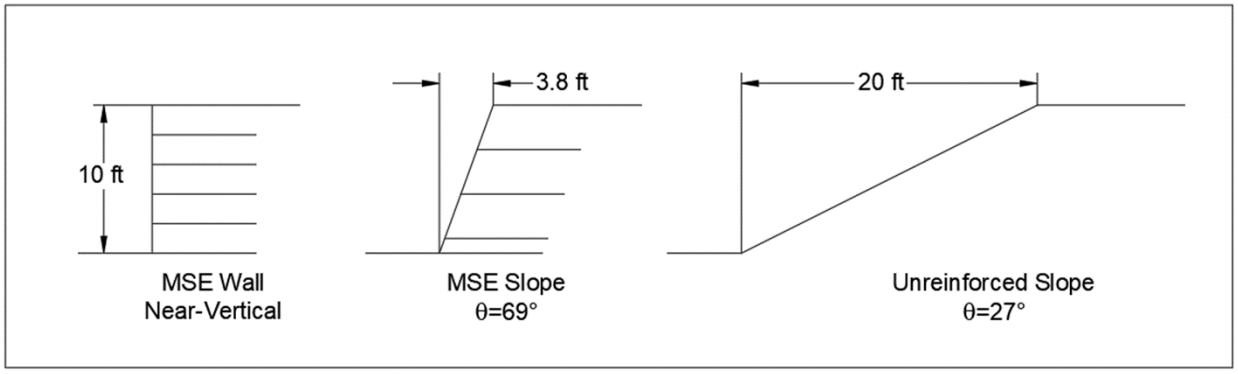

Figure 7-12 Difference in Usable Land for Walls and Slopes

7-9.2 Reinforced Slope Materials.

The soil that is installed in the reinforced zone of an MSE slope is an important structural component of the slope. The properties that are required of reinforced soil should be based on the geometry of the slope and the structures that may depend on the slope for support. FHWA's recommendations for the properties of fill soil in the reinforced zone of MSE slopes permit up to 50% fines that have a $PI \leq 20$ (FHWA 2009b). The fill properties shown in Table 7-4 are recommended for relatively tall or steep slopes; however, the recommendations are only applicable to slopes with a height less than 70 feet.

Table 7-4 Recommendations for Reinforced Fill Soil in MSE Slopes Based on Geometry

Slope Geometry	Recommended Properties for Reinforced Fill		
Slope < 1.2H:1V ($\theta < 40°$) and $H < 70$ ft	Gradation ASTM D6913	Sieve Size	Percent Passing
		4 in	100
		No. 4	20-100
		No. 40	0-60
		No. 200	0-50
	Plasticity Index ASTM D4318	$PI \leq 20$	
1.2H:1V ≤ Slope < 0.36H:1V ($40° \leq \theta \leq 70°$) and $H < 70$ ft	Gradation ASTM D6913	U. S. Standard Sieve	Percent Passing
		4 in	100
		No. 4	20-100
		No. 40	0-60
		No. 200	0-35
	Plasticity Index ASTM D4318	$PI \leq 10$	

Other important components of MSE walls and slopes include internal and external drains, filters, separators and erosion control. The use of geosynthetics for these applications is summarized in Table 7-5.

Table 7-5 Summary of Applications and Materials for Reinforced Soil Slopes

Application	Component	Material	Purpose	Comments
Reinforcement	Primary and Secondary Reinforcement	Polyester (PET) and Polypropylene (PP) Geotextile; PET, PP and High-Density Polyethylene (HDPE) Geogrid	Provide tensile strength and confinement to fill soil.	PET and HDPE are usually used for primary reinforcement. PET, HDPE and PP can be used for secondary reinforcement.
Facing	Soft Armor Face ($\theta < 40°$)	Rolled Erosion Control Product (RECP)	Prevent erosion caused by surface water runoff	Consult manufacturers for recommendations of RECP specifications based on θ and service period.
	Hard Armor Face ($\theta \geq 40°$)	Welded Wire Fabric (WWF)		Typically, galvanized WWF 4x4-W4.0xW4.0 should be used. Hardware cloth required behind WWF to prevent spilling of retained gravel fill.
		Nonwoven PP Geotextile	Separation and filtration	Separate gravel fill at slope face from finer reinforced soil.
		Gravel	Fill soil immediately behind WWF	GP or GW with 1.0 in minimum particle size.
Internal Drainage	Blanket Drain	Gravel	Drainage medium	Typically, ASTM C33 No. 57 or No. 67 stone.
		Nonwoven PP Geotextile	Separation and filtration	Install above and below drainage gravel to separate from adjacent finer grain soil.
	Chimney Drain	Gravel	Drainage medium	Typically, ASTM C33 No. 57 or No. 67 stone. Can be replaced by drainage composite.
		Drainage Composite	Drainage medium	Use drainage composite with geonet core to replace drainage gravel. Space drainage composite to typically provide 33% to 75% coverage.
External Drainage	Drainage Swale	RECP in form of Turf Reinforcement Mat (TRM)	Divert and control surface water runoff	Line swale with TRM. Consult manufacturer for specifications. Locate swale 5 ft. to 10 ft. behind slope crest. Size swale based on hydraulic analyses. Use bench with swale at mid-slope for H over 25 to 30 ft.

7-9.3 Geosynthetic Reinforcement Strength.

Geosynthetics that are used in soil reinforcement applications are typically designed to exhibit their maximum tensile strength in one direction. In this respect, such geosynthetics are said to be *uniaxial* and the design strength direction usually corresponds to the material's MD or *roll-direction*. Geosynthetics that exhibit significant tensile strength in both the MD and cross machine direction (XMD) are said to be *biaxial*.

The tensile strength of a geosynthetic that is used for the design of an MSE slope is based on a *minimum average roll value* ($MARV$) that is reported by the manufacturer. In the United States, the industry practice is to reduce the average value by two standard deviations and to define the result as the minimum average roll value ($MARV$). Reduction factors are then applied to the strength $MARV$ to account for potential degradation of strength as a result of creep, environmental conditions and installation damage.

7-9.3.1 Long-Term Design Strength.

The assessment of a geosynthetic's long-term tensile strength (T_{al}) for use in the design of an MSE slope follows current FHWA procedures (FHWA 2009b):

$$T_{al} = \frac{T_{ULT}}{RF_{CR} \times RF_{D} \times RF_{ID}} \quad \textbf{(7-3)}$$

where:
T_{ULT} = ultimate tensile strength of the geosynthetic based on the MARV,
RF_{CR} = reduction factor applied to account for creep under sustained tensile loading,
RF_{D} = reduction factor applied to account for the degradation due to environment, and
RF_{ID} = reduction factor applied to account for damage during installation.

The reduction factors are discussed briefly in the following sections. Details regarding the determination of RF_{CR}, RF_{D}, and RF_{ID} for a geosynthetic can be found at Appendix B of FHWA (2009b).

7-9.3.2 Reduction Factor for Creep (RF_{CR}).

The tendency of a geosynthetic to elongate under sustained tensile loading is called *creep* and it is a property of materials that are manufactured using PET, HDPE, PP and other polymers. If the magnitude of the load is sufficiently great and if it is maintained for a sufficient period of time, the creep can induce rupture or result in such elongation that the material's performance is compromised.

In the United States, the standard of practice to determine a *reduction factor for creep* (RF_{CR}) that is based on the sustained load that will induce creep rupture at the end of the design service period. For permanent MSE slopes the design service period should be no less than 75 years. A longer service period may be appropriate for structures that support critical infrastructure.

7-9.3.3 Reduction Factor for Durability (RF_D).

Geosynthetics may degrade depending on their base polymer and if they are exposed to certain environmental conditions. Polyester geosynthetics may degrade as a result of hydrolysis. Geosynthetics manufactured with HDPE and PP are subject to degradation by their reaction with oxygen, particularly in the presence of elevated temperatures. Oxidation can also be initiated by exposure to UV light (i.e., UV-oxidation). The resistance of these polymers to oxidation can be significantly increased by the addition of antioxidants during the manufacturing process. Polyester is also susceptible UV-oxidation but to a lesser degree than HDPE and PP (FHWA 2009a). Protection of PET yarns is typically provided in the form of coatings. In the case of all geosynthetics, the protective roll wraps should not be removed until the material is installed to minimize UV light exposure.

The FHWA recommends a default *reduction factor for durability* (RF_D) of 1.3 for PET, HDPE, and PP geosynthetics provided certain criteria are satisfied. Also, a lower RF_D may be used if it is indicated by product specific testing. Further details are given in FHWA (2009b).

7-9.3.4 Reduction Factor for Installation Damage (RF_{ID}).

The standard of practice in the United States is for the manufacturers of geosynthetic reinforcement to assess the potential for installation damage through the performance of full-scale tests. Such testing programs typically evaluate the damage induced by compaction of coarse gravel, sandy gravel and silty or clayey sand.

The geosynthetic manufacturer should be consulted to obtain its recommendation for the *reduction factor for installation damage* (RF_{ID}). The manufacturer should also be consulted for its recommendations regarding measures to reduce installation damage. Typical measures include the following:

- Tracked vehicles should not traffic directly on panels of geosynthetic reinforcement. There should be no less than 8 inches of fill soil between the tracks and the geosynthetic. Sharp turns by tracked vehicles on fill soil should be avoided.
- Rubber tire vehicles may operate directly on the geosynthetic reinforcement at speeds less than 10 miles per hour. Sudden braking and turning should be avoided.

- Fill soil should not be dumped directly onto geosynthetic reinforcement. Rather, it should be dumped onto fill soil that has already been spread and then bladed onto the geosynthetic by a dozer.

7-9.4 Soil-Geosynthetic Interaction.

The determination of geosynthetic reinforcement length in the design of an MSE slope is based in part on the resistance of the reinforcement to pullout from between layers of confining soil. In FHWA (2009b) the FHWA defines a geosynthetic's resistance to pullout as:

$$P_r = F^* \cdot \alpha \cdot \sigma'_v \cdot L_e \cdot C \quad \textbf{(7-4)}$$

where:
P_r = geosynthetic reinforcement's resistance to pullout,
F* = pullout resistance factor,
α = scale correction factor to account for nonlinear stress reduction,
σ'_v = effective vertical stress at the soil-reinforcement interface,
L_e = length of reinforcement embedded behind the trial failure surface, and
C = number of surfaces on which pullout resistance is mobilized (i.e., 2 for geosynthetics).

The critical failure surface used to calculate L_e should be that surface that exhibits the minimum F deemed acceptable. Also, L_e should be no less than 3 feet to assure adequate pullout resistance.

Some manufacturers of geosynthetic reinforcement have characterized soil-geosynthetic interaction in terms of a *coefficient of interaction* (C_i) based on pullout tests with C_i defined as:

$$C_i = \frac{\tan\delta}{\tan\phi'} \quad \textbf{(7-5)}$$

where:
ϕ' = the effective stress internal angle of friction, and
δ = the effective soil-geosynthetic interface friction angle.

The values of F* and C_i are related by:

$$F^* = C_i \tan(\phi') \quad \textbf{(7-6)}$$

7-9.5 Analysis and Design of Reinforced Slopes.

The most technically challenging aspect of the design of an MSE slope is deciding the required strength, length and vertical spacing of the layers of reinforcement. The critical failure surface for a slope with layers of horizontally-oriented geosynthetic reinforcement is frequently a combination of circular and linear segments, particularly if the critical failure surface is entirely outside of the reinforced soil zone (i.e., a global failure surface rather than a compound failure surface).

Most of the software packages that are used for soil slopes can also be used for MSE slopes. There are some software packages specifically written for MSE slopes, and these are listed in Appendix B. Spencer's Method (Spencer 1967) and the Morgenstern and Price Method (Morgenstern and Price 1963) both lend themselves to the analyses of noncircular failure surfaces, solve for all conditions of equilibrium (i.e., moment and force), and provide the most accurate solutions. Either of these two methods is preferred for the analysis of MSE slopes.

One of the most important considerations in the modeling of an MSE slope in a limit equilibrium slope stability computer program is the definition of F given in Equation 7-1. However, the presence of geosynthetic reinforcement requires that its strength be applied to the right side of the equation in the numerator or the denominator (Duncan et al. 2014). Two options are available as summarized in Table 7-6. The method used by slope stability software can be determined using the simple approach suggested by Duncan et al. (2014).

Table 7-6 Methods of Incorporating Geosynthetic Reinforcement Strength in Factor of Safety Equation

Method of Including Reinforcement Strength	Factor of Safety Equation
Method A (Active)	$F = \frac{\text{shear strength}}{\text{shear stress required for equilibrum} - \text{reinforcement resistance}}$
Method B (Passive)	$F = \frac{\text{soil strength+reinforcement resistance}}{\text{shear stress required for equilibrium}}$

If Method A is used to define F, then the strength of the geosynthetic used to calculate F is T_d. To account for potential uncertainties in the geosynthetic T_d should be divided by a factor of safety for geosynthetic strength (F_R) of at least 1.3. If Method B is used, then T_d will be reduced by F and the application of F_R is not necessary.

The reinforcement force orientation assumed by limit equilibrium analysis can vary from one that is parallel to the reinforcement to one that is tangent to the slip surface. Setting the orientation parallel to the reinforcement in a slope stability computer program is

common practice and tends to result in a lower F compared to setting the orientation tangent to the slip surface.

A detailed discussion of the procedure to determine the reinforcement requirements of MSE slopes is provided by the FHWA (2009), particularly for the case in which Bishop's simplified method is used. The FHWA manual also considers the mechanics of internal sliding failure and locally soft foundation soil at the slope toe. The steps provided in Table 7-7 are intended to help an engineer to construct a computer model for in MSE slope design.

Table 7-7 Steps for Designing an MSE Slope

Step	Procedure
1	Draw a scaled cross section of the slope that reflects the existing and proposed grades as well as external water conditions, and permanent and temporary loads. Use high quality site plans to locate these features as accurately as possible.
2	Use the available geotechnical information to determine and draw the boundaries of soil and rock strata as well as groundwater.
3	Use the results of Steps 1 and 2 it to construct the cross section in a computer program model.
4	Assign physical, strength and hydraulic properties to the sections of the model as indicated by the available geotechnical information.
5	Select either Spencer's method or the Morgenstern and Price method to analyses failure surfaces.
6	Select one to three values of geosynthetic reinforcement strength (T_{al}) based on manufacturer information, or assume typical values.
7	Determine whether the computer program used Method A or B to defined F. If the program provides an option, select Method A and then reduce the geogrid strength by $F_R = 1.3$ or more.
8	Set the reinforcement force orientation parallel to the reinforcement.
9	Assign the F^* or C_i parameter based on recommendations by the manufacturer of the geosynthetic reinforcement. If recommendations are not available or if they are not supported by test data, assume that $C_i = 0.67$. This will be conservative for the soil parameters shown in Table 7-4.
10	If the computer program provides an option, select 100% reinforcement coverage as opposed to partial coverage.
11	Assign layers of geosynthetic reinforcement to the cross section. Vertical spacing of 3 ft. is a good initial starting point. In general, the vertical spacing of reinforcement should not exceed 3 ft.
12	Set the length (L) of each layer of reinforcement to about $0.7 \cdot H$. The required L will increase if there is a slope below (i.e., a toe slope) or behind (i.e., a crest slope) the MSE structure.
13	Perform preliminary analysis by setting the search limits to evaluate only those surfaces which exit through the face of the slope. Evaluate both circular and noncircular failure surfaces. If the resulting F is too low, then change the layers in the vicinity of the bottom of the failure surface to types with higher strengths.
14	After designing for failure surfaces that exit through the slope face, change the search limits to evaluate compound and global surfaces that pass below the toe of the structure.
15	If a compound failure surface is indicated that has an unacceptably low F, then increase the strength of the lower reinforcement layers or decrease their vertical spacing. If a global failure surface is indicated that has an unacceptably low F, then increase the length of the reinforcement layers.

Using the process in Table 7-7, the modifications required to obtain a satisfactory F that is balanced with geosynthetic efficiency is an iterative process in which geosynthetic

strengths and lengths are adjusted. Once the optimum design is determined, the parameters that may have significant uncertainty should be considered. For example, if rock is thought to be present below the toe of the MSE slope, changing the elevation of the top of rock by a few feet in the computer model can have a profound effect that makes the difference between a stable slope and slope failure. Similarly, there is frequently significant uncertainty regarding the location of groundwater and soil shear strength. The effect of these uncertainties should be investigated through parametric analyses coupled with engineering judgment.

The designer is cautioned to avoid making the design over-complicated. Small savings in material obtained from optimized lengths or spacings are often offset by potential for error in construction or an increased difficulty in constructability.

7-9.6 Required Factor of Safety for MSE Slopes.

An MSE slope should be designed to a target F that is based on considerations of the uncertainties regarding site conditions, material properties and the consequences of slope failure. In general, the standard of practice is to provide a F in the range of 1.3 to 1.5. If the site conditions and material properties are understood well and if the consequences of failure are relatively low, then a minimum F of 1.3 may be appropriate. However, if site conditions are subject to unforeseeable changes and if soil types, strengths and locations are poorly understood, then F of 1.5 or higher may be necessary. Similarly, if the proper performance of the MSE slope is required for the operation of important structures, then F of 1.5 or higher may be indicated. For MSE slopes designed in accordance with FHWA guidance, a minimum factor of safety of 1.5 is required.

7-10 ROCK SLOPE STABILITY.

The stability of rock slopes may become a concern during the excavation for the construction of roads, buildings and infrastructure components. Often a stability issue cannot be identified until the excavation is underway and information that is needed to assess the potential for various modes of failure becomes available. Analyses of rock slope stability may need to be performed expeditiously to avoid project delays. The potential for delays can be exacerbated by a need to design stabilization measures. In other cases, rock slope instability does not occur until well after the initial excavation and rock weathering has taken its toll.

This section provides an overview of some of the aspects of rock slopes and a more in-depth discussion of others. The fundamental mechanics of rock slope failure are covered by a discussion of sliding blocks, plane failure, wedge failure, and toppling failure. Stabilization measures for rock slopes and mitigation of rock falls are also addressed. More in-depth discussion can be found in FWHA (1998), Hoek and Bray (1981), and Rowland et al. (2007).

7-10.1 Modes of Rock Slope Failure.

Fortunately, the stresses in most rock slopes are much less than the rock strength, and for this reason most rock slopes are relatively stable. The potential for rock slope failure becomes a concern under two general conditions. First, discontinuities in the rock mass propagate and the rock separates as blocks, wedges, columns, or other types of sections. Second, rock that has already separated in the form of cobbles and boulders can translate downslope under the influence of gravity as a rock fall. In both cases, the separated rock may pose a hazard to both property and lives.

There are six typical configuration of rock slopes, some of which may pose risks of instability. Four possible configurations of rock discontinuities are shown in Figure 7-13 while rock slopes with weak and weathered rock are depicted in Figure 7-14.

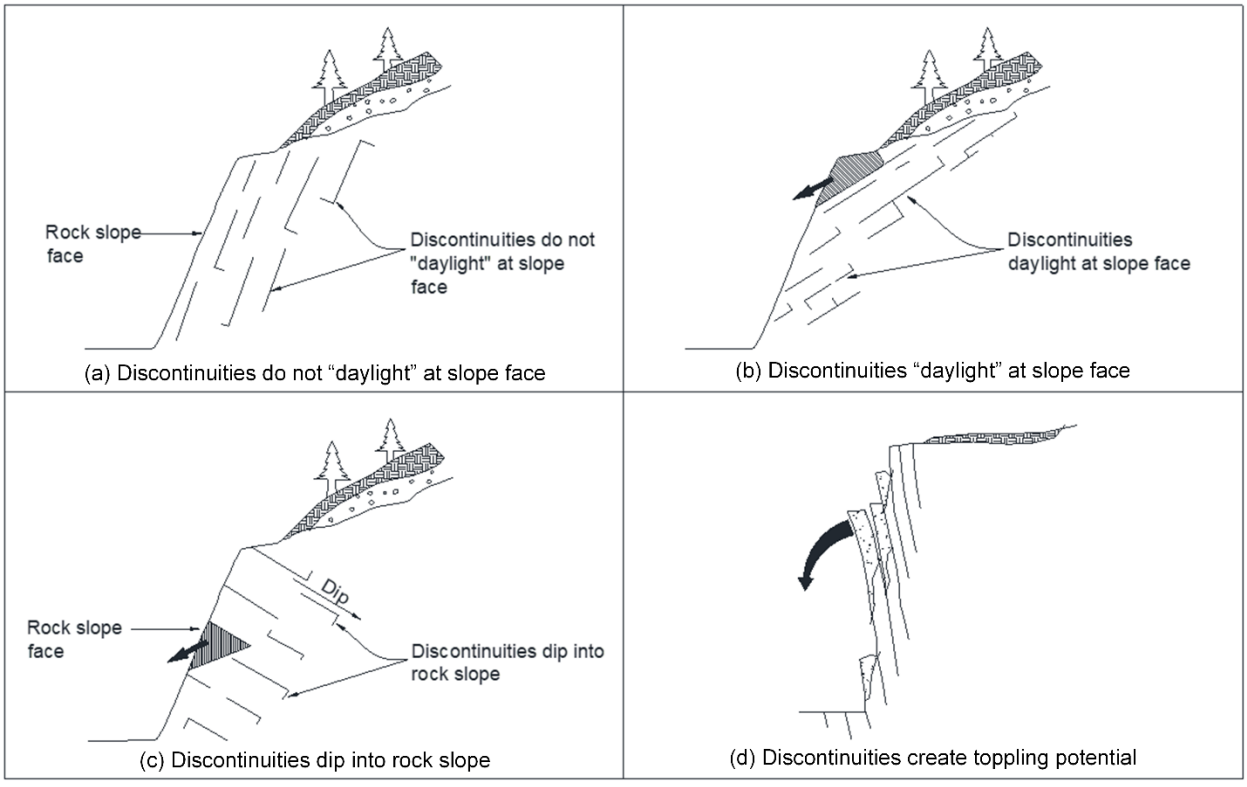

Figure 7-13 Rock Discontinuity Conditions (after FHWA 1998)

The term *discontinuity* refers to faults, joints, bedding planes, or any other surface upon which rock may move. The pattern of discontinuities shown in Figure 7-13a is typical for sedimentary rock, such as limestone, sandstone, and shale, that has been deposited in bedded layers and later uplifted by geologic processes. The orientation of the discontinuities in Figure 7-13a is roughly parallel to the rock slope face, but they do not *daylight* at the slope face. That is, the discontinuities do not extend to and intersect the exposed surface of rock at the slope face. In such a configuration the rock slope face is

expected to remain stable. In contrast, Figure 7-13b shows a rock slope with discontinuities that daylight at the slope face. With such orientation of discontinuities, a potential for rock slope failures exists.

Figure 7-13c shows a rock slope with generally favorable bedding in that the discontinuities *dip* into the rock slope (dip is discussed later in this section) and there is little potential for rock to slide out of the slope face. However, blocks of rock at the slope face may become instable when discontinuities daylight at the slope face. The potential for the development of such conditions are increased if blasting was performed during slope excavation.

A rock slope configuration that illustrates the conditions for the toppling of rock columns is shown in Figure 7-13d. Toppling becomes a risk for rock with relatively thin bedding with steeply dipping discontinuities. The stability of rock columns can degrade relatively quickly if water seeps readily into the discontinuities from surface water runoff and increases the rate of weathering. In regions with frequent freeze-thaw cycles the rate of degradation may accelerate further because the frozen water can cause the rock columns to separate.

Sandstone and shale are often found with near-horizontal bedding. Excavation of such a bedding sequence generally results in a shale layers that weather faster than sandstone. In such conditions layers of sandstone may be undermined and form ledges that are prone to fracturing and failure. Such a condition is illustrated in Figure 7-14a. Weak rock slopes with closely spaced impersistent joints may fail along a circular or noncircular surface much like a soil slope as shown in Figure 7-14b.

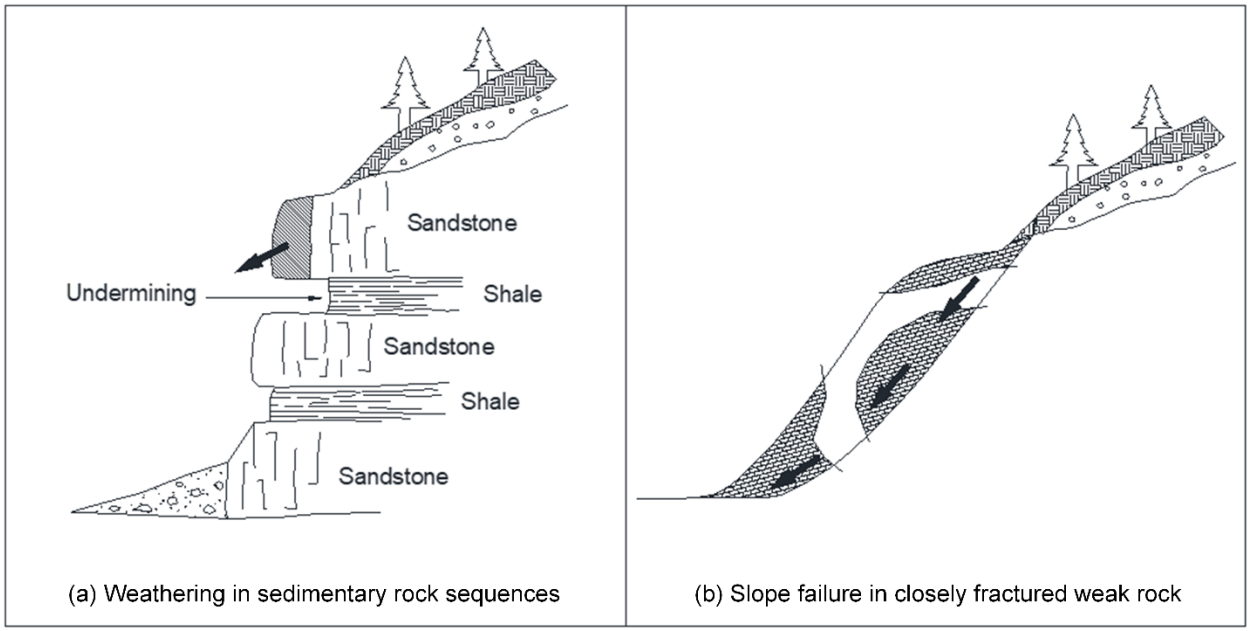

Figure 7-14 Weathering and Weak Rock Conditions (after FHWA 1998)

An assessment of the potential for one of the above modes of failure to develop often requires a geologic investigation, field mapping of discontinuities, stereographic projection of geologic data, and an evaluation of rock strength. Each of these tasks represent significant sections in comprehensive publications on the topic of rock slope engineering.

7-10.2 Mechanics of a Sliding Block.

The mechanics of a sliding block are central to two types of rock slope stability analyses. Considering the rock slope depicted in Figure 7-15, the weight of the block ABC is represented by force W, which acts through the block's centroid. The component of W that acts perpendicular to the sliding plane AC is F_N. The component of W that acts parallel to the sliding plane AC is F_S. The relationship of these three forces is defined by the angle, or *dip*, of the sliding plane (Ψ_P) with respect to the horizontal plane.

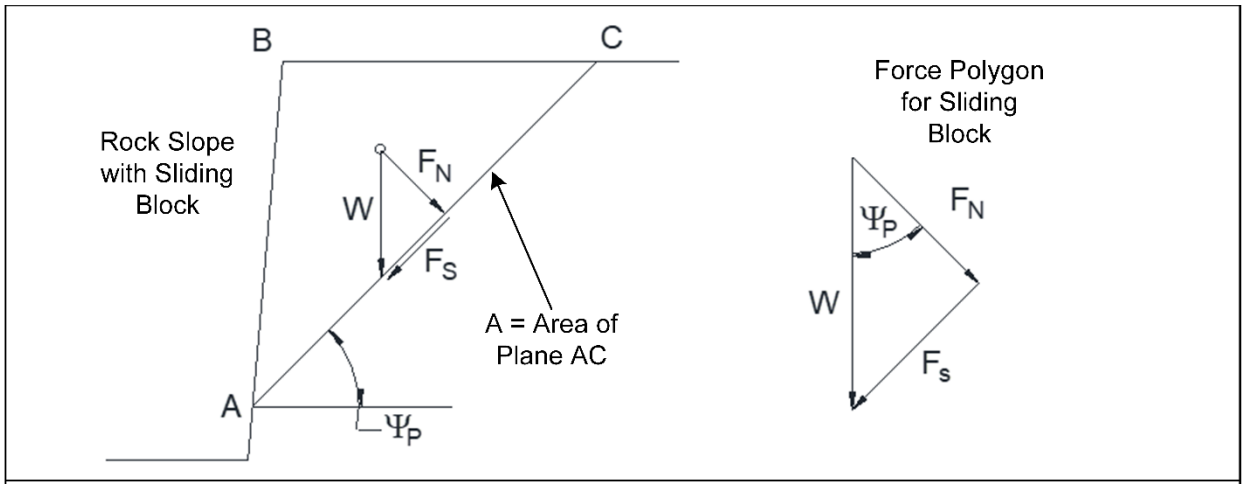

Stability Equations

Block Forces	Stresses on Plane AC	Block Stability
$F_N = W\cos\Psi_P$	$\sigma = \frac{F_N}{A} = \frac{W\cos\Psi_P}{A}$	Shear strength, $s = c' + \sigma'\tan\phi'$
$F_S = W\sin\Psi_P$	$\tau = \frac{F_S}{A} = \frac{W\sin\Psi_P}{A}$	$F = \frac{s}{\tau} = \frac{c'A + W\cos\Psi_P\tan\phi'}{W\sin\Psi_P}$

Notes: This solution assumes no pore pressure on the sliding plane. Pore pressure will reduce the factor of safety. The shear strength (s) can be defined with any failure envelope appropriate for the rock conditions.

Figure 7-15 Rock Slope with Sliding Block

The factor of safety against sliding on plane AC is calculated as shown Figure 7-15. This solution assumes no pore pressure is acting on the sliding plane. Positive pore pressure will reduce the effective normal stress, shear strength, and the factor of safety.

7-10.3 Plane Failure.

The rock slope with a sliding block shown in Figure 7-15 is a simple version of a plane failure. It is not a type of failure that is often encountered because the conditions for its development rarely occur. However, the mechanics of a plane failure also apply to the more frequently encountered wedge failure. For this reason, it is instructive to further consider plane failures.

7-10.3.1 Sloped Surface Orientation Terms.

A discussion of plane failure requires the definition of three terms that are used to describe the orientation of sloped planes such as a slope face or a potential failure surface. The dip (Ψ) of a sloped plane is the inclination of that surface as measured from a horizontal plane, as shown in Figure 7-16. The *dip direction* or *dip azimuth* (α) is the direction of the horizontal trace of the line of dip measured clockwise from north. Often the term *strike* is used to describe the orientation of a sloped plane. It is the direction of a line that is formed by an intersection of the sloped plane with an imaginary horizontal plane. The orientation of the strike of a sloped surface is perpendicular to the dip direction of the sloped surface.

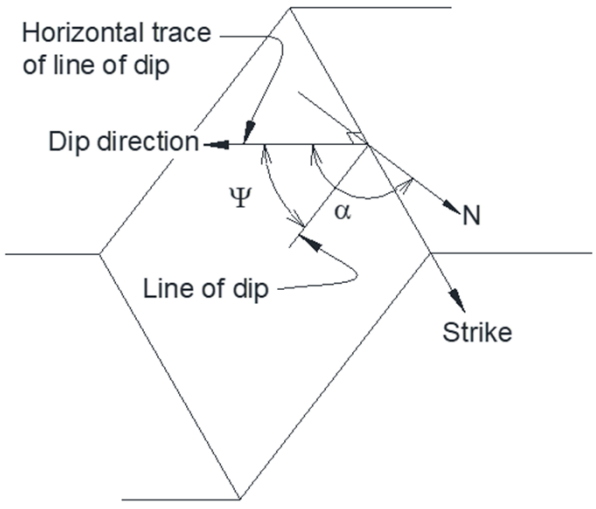

Figure 7-16 Definition of Sloped Surface Orientation Terms

7-10.3.2 General Conditions for Plane Failure.

For sliding to occur on a single plane the four conditions must be satisfied (Hoek and Bray 1981):

1. The plane on which sliding occurs must strike nearly parallel (i.e., within about 20º) to the slope face.
2. The failure plane must daylight in the slope face (i.e., intersect the slope face). Therefore, the dip of the failure plane (Ψ_P) must be less than the dip of the slope face, Ψ_F. That is, $\Psi_P < \Psi_F$.
3. The dip of the failure plane must be greater than the angle of friction at the failure plane. That is, $\phi' < \Psi_F$.
4. Release surfaces that provide negligible resistance to sliding must be present in the rock mass to define the lateral boundaries of the slide.

The relative positions of the planes defined by Ψ_F, Ψ_P, and ϕ' are shown in Figure 7-17a. The release surfaces associated with a sliding plane are shown in Figure 7-17b.

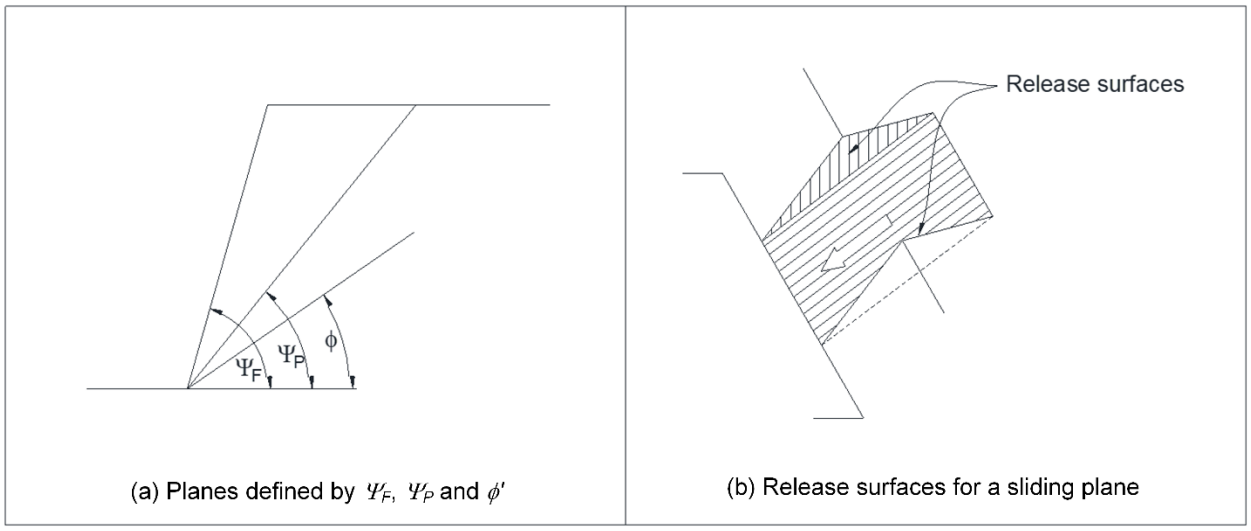

Figure 7-17 Geometry for Plane Failure (after Hoek and Bray 1981)

7-10.4 Plane Failure Analyses.

Rock slopes analyzed for plane failure can also consider the presence of a tension crack, which may contain water. The crack may be located either above or below the slope crest as shown in Figure 7-18. The uplift force applied by water at the failure plane is designated as U. The force applied by water in the tension crack is designated as V. The factor of safety for such conditions can be calculated using the equation presented in Figure 7-18.

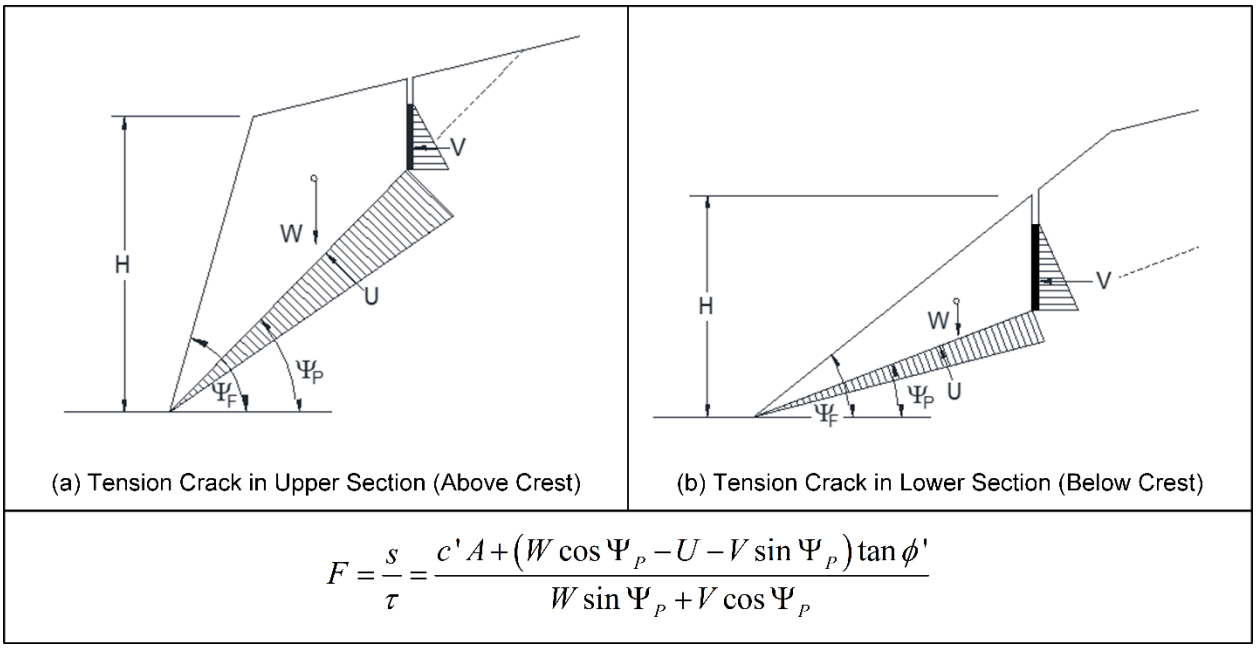

$$F = \frac{s}{\tau} = \frac{c'A + \left(W\cos\Psi_P - U - V\sin\Psi_P\right)\tan\phi'}{W\sin\Psi_P + V\cos\Psi_P}$$

Figure 7-18 Rock Slopes with Tension Cracks (after Hoek and Bray 1981)

Further details regarding the stability analyses of sliding planes are described in the FHWA (1998) and by Hoek and Bray (1981). While such analyses can be practically performed using hand calculations, analytical efficiency can be significantly improved by use of computer programs.

7-10.5 Wedge Failure.

The rock slope with a sliding wedge shown in Figure 7-19 is similar to a sliding plane, but the presence of Plane A and Plane B make it possible to model a geometry that is encountered in the field more frequently.

The convention adopted in the FHWA (1998) and by Hoek and Bray (1981) is that the release surface designated as Plane A is the flatter of the two release surfaces. The steeper release surface is designated as Plane B. These two surfaces intersect along the *line of intersection*.

As with a plane failure, there are certain geometrical requirements for wedge failure to occur. Specifically, $\Psi_{Fi} > \Psi_{Fi} > \phi'$, where Ψ_{Fi} is the inclination of the slope face as measured at right angles to the line of intersection, Ψ_i is the dip of the line of intersection and ϕ' is the average friction angle of Plane A and Plane B. Note that Ψ_{Fi} is not the same as Ψ_F unless the dip direction of the line of intersection is the same as the dip direction of the slope face (Hoek and Bray 1981).

The factor of safety of the wedge in Figure 7-19 may be determined by assuming that sliding is resisted only by friction at the surface of Plane A and Plane B. With this

simplifying assumption, the resisting forces on these planes can be determined by calculation of the normal forces R_A and R_B on each plane, as illustrated in Figure 7-20a. The component forces of the weight of the wedge perpendicular and parallel to the line of intersection are shown in Figure 7-20b.

Hoek and Bray (1981) relate the factor of safety against wedge failure (F_W) to that for a slope with a face that is inclined at Ψ_{Fi} and a failure plane that is inclined at Ψ_i by a wedge factor K. This wedge factor can be graphically determined using a figure provided in both the FHWA (1998) and Hoek and Bray (1981).

The analysis of a wedge failure for which cohesion or water are present is more complicated than for a wedge failure in which only the friction angle at the failure planes is considered. Both the FHWA (1998) and by Hoek and Bray (1981) discuss this analytical process in detail. Such an analysis can also be performed efficiently using the computer programs.

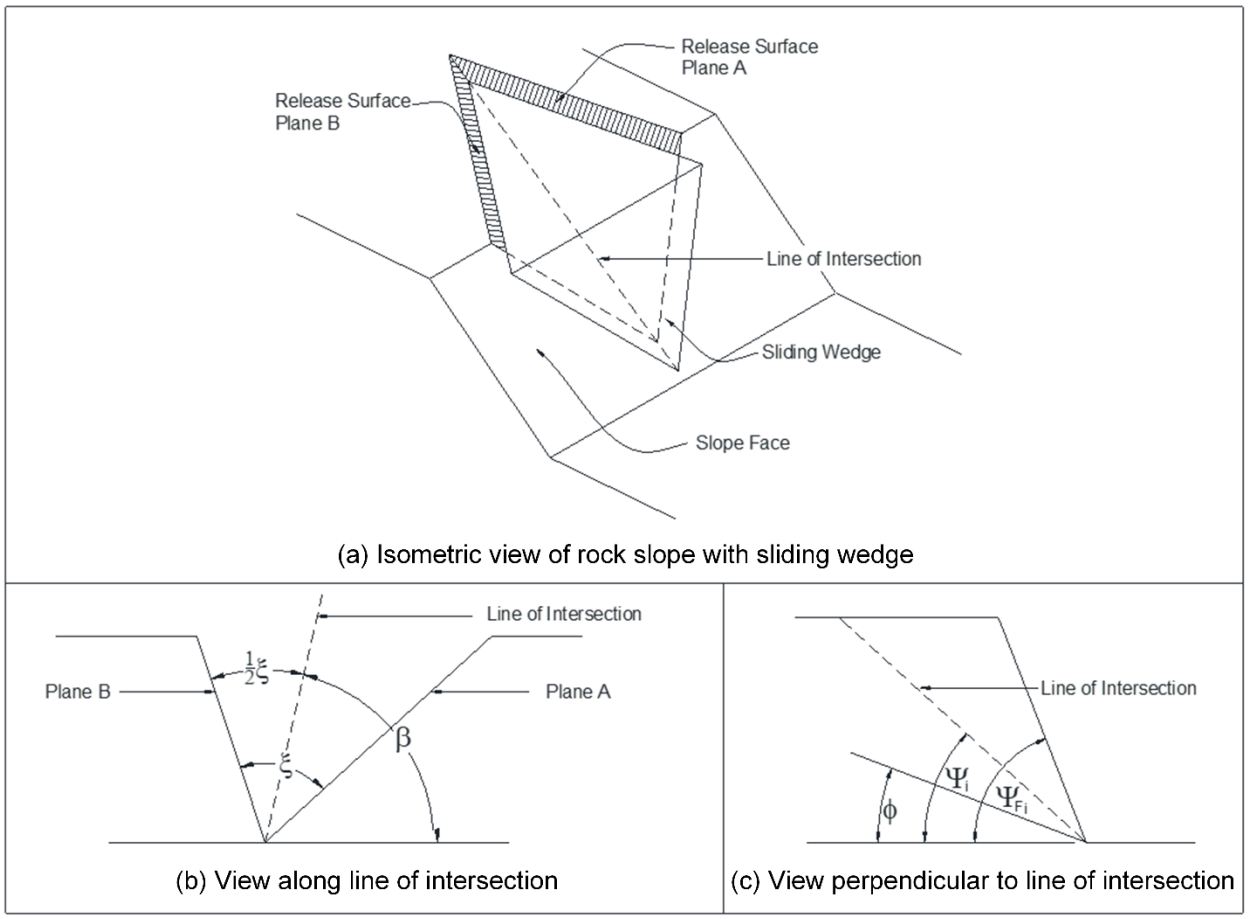

Figure 7-19 Rock Slope with Sliding Wedge (after Hoek and Bray 1981)

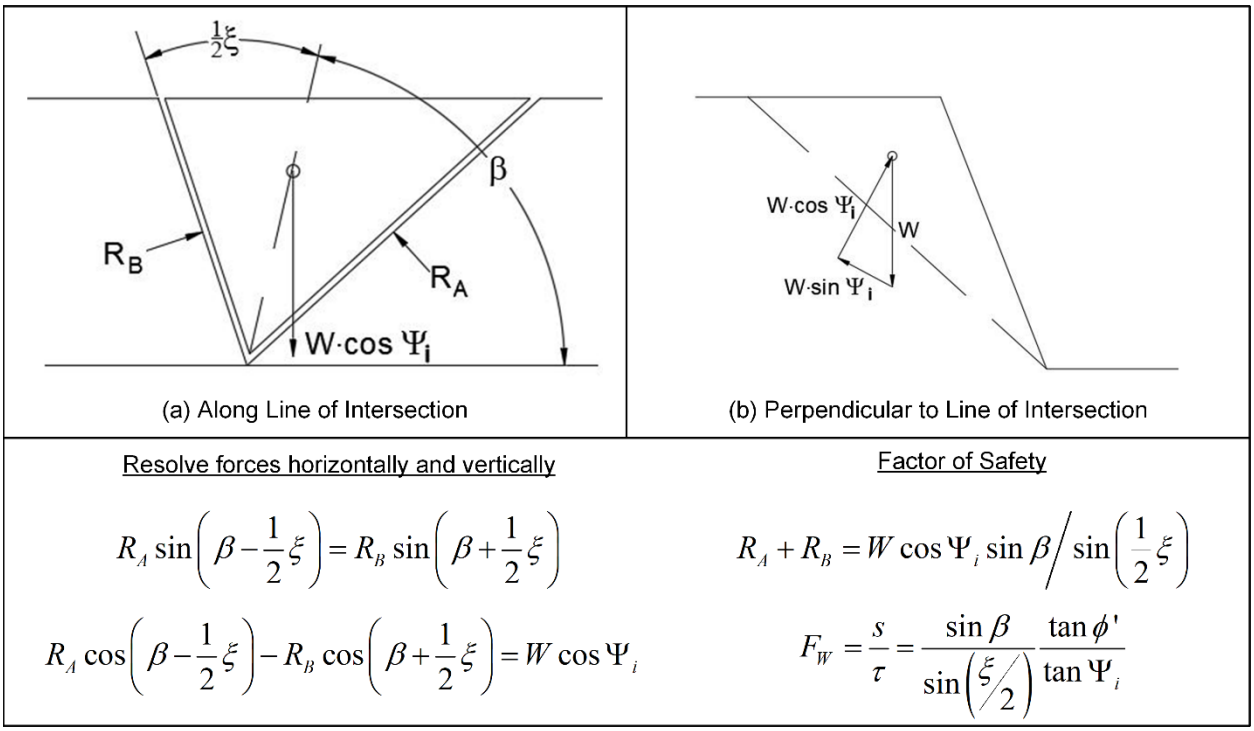

Figure 7-20 View of Wedge Geometry (after Hoek and Bray 1981)

7-10.6 Toppling Failure.

For a column of rock to be subject to toppling failure, the center of gravity of the column must be located on the side of the column at the slope face. In this way, the column is loaded eccentrically. Such loading creates tensile stress on the side of the column away from the slope face, as shown in Figure 7-21. If the tensile capacity of the column is exceeded, failure can ensue.

Analyses of rock toppling can be significantly more complicated than those for plane failure or block failure. A method for hand calculations is described in FHWA (1998) but such a procedure may have limited applicability to actual field conditions.

7-10.7 Circular Failure.

As described in section 7-10.1, if a rock slope consists of weak material with closely spaced, impersistent joints, then the slope may fail along a circular or noncircular surface much as a soil slope. Analyses of these types of failures can be performed using the methods previously discussed for the stability of soil slopes. However, it should be noted that even weak intact rock can exhibit significant cohesive strength. An accurate assessment of the actual cohesive strength may be difficult to make. It is also important to realize that zones of relatively strong rock may exist behind zones of

relatively weak rock. The presence of the strong rock zones may significantly affect the location of the critical failure surface.

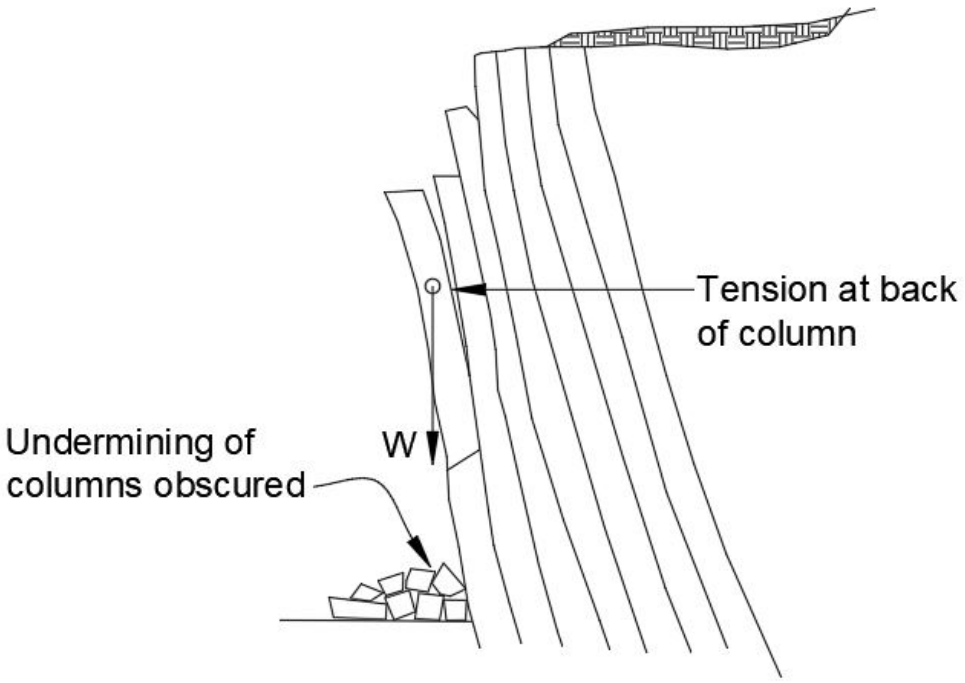

Figure 7-21 Rock Slope Subject to Toppling Failure

7-10.8 Rock Slope Stabilization and Protection.

Several measures can be taken to mitigate the hazards presented by unstable rock slopes. These measures vary from the relatively simple to those which require considerable analytical expertise, construction skill, and expense.

7-10.8.1 Stabilization and Protection Options.

The range of stabilization measures that are typically available include rock reinforcement, rock removal and protective barriers. A range of options is available under each of these categories as shown in Figure 7-22.

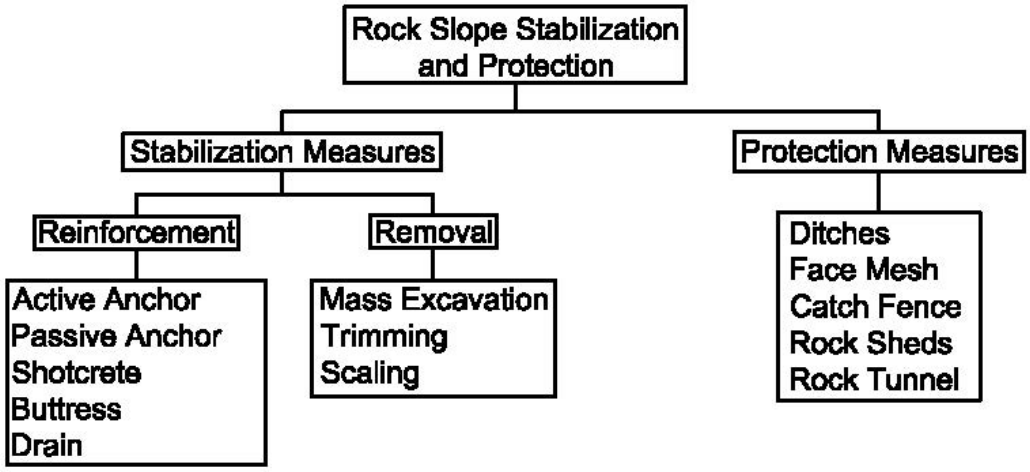

Figure 7-22 Rock Slope Stabilization and Protection Measures (after FHWA 1998)

7-10.8.2 Reinforcement

Anchors have been used for many years to stabilize both soil and rock slopes. In general, anchors can be classified as passive or active. A *passive anchor* that is frequently used for top-down excavation stabilization is the soil nail. For rock slope stabilization it may be referred to as a *rock bolt* or *dowel*. It typically comprises a steel tendon in the form of an all-thread bar that is centered within a drill hole. A cement grout is installed in the drill hole to bond the tendon to the adjacent soil or rock. Grout is usually placed by tremie from the distal end to the anchor head. Typically, such holes are drilled at a declination of about 15° or more below the horizontal plane to prevent spilling of the grout at the excavated face.

The steel bars used for these applications typically exhibit a tensile capacity of at least 75 ksi. Higher capacity bars are readily available. Typical bar diameters correspond to standard reinforcement steel sizes of #8 (i.e., 1.0-inch nominal diameter) to #11 (i.e., 1.41-inch nominal diameter). Resistance to bar corrosion is typically provided by an epoxy coating or galvanization. The grout that surrounds the bar can also provide some protection against corrosion, but the grout is subject to cracking and may not provide complete coverage.

Different types of liquid resins are manufactured for use with rock anchors as an alternative to cement grout. Resin cartridges include a hardener that can be selected to provide a range of hardening times. The cartridges are inserted into the drill hole and then followed by insertion of the steel bar tendon. The tendon is then spun at a prescribed rate to mix the resin and hardening agent and to distribute the mixture to both bar and rock surfaces. Unfortunately, there is some skepticism within the ground anchor contracting industry that resins can be consistently distributed to rock and tendon surfaces and can reliably provide requisite bond capacities. Also, resins do not provide the same level of corrosion protection as does cement grout.

The FHWA has published several manuals on the design of soil nail structures. The current version is *Geotechnical Engineering Circular No. 7* (FHWA 2015). This manual should be consulted in the design of passive anchors for rock stabilization applications.

A passive anchor does not impart a stabilization force to the adjacent rock or soil until the rock or soil tends to displace. At that point the passive anchor provides a resisting force. In contrast, an *active anchor* is stressed as part of its installation process. Such anchors may comprise steel bars like a soil nail. However, if a particularly long anchor or one with high tensile capacity is required, then steel strand tendons may be indicated. The installation of such an active anchor is similar to that of a passive anchor. First, a hole for the anchor is drilled and then the strand is inserted and centered within the hole. Next, the strand is grouted, but only for a certain length of the strand starting from the distal end. A length between the top of the grouted section and the anchor head is left *unbonded*. The reason for the unbonded section is that this portion of the tendon must be left to strain under a design stressing load to provide an active force at the anchor head. This force is transferred to a loading plate or block that is secured against the rock slope face. In this way the active force can be used to stabilize a large rock plane, wedge or unstable columns. This is perhaps the most important distinction between an active anchor and a passive anchor. Unlike a passive anchor, an active anchor does not depend on soil or rock movement to mobilize its strength.

The *bonded* length of the tendon is that portion which is grouted. The length of the bonded section is based on analyses that consider the load in the anchor and the bond strength between the grout and the adjacent soil or rock.

Steel strand tendons are typically available in configurations that provide a working tensile capacity of about 35 to 500 kips. Tendons with considerably higher capacities can be fabricated.

The design of active anchor systems is discussed in the FHWA's *Geotechnical Engineering Circular No. 4* (FHWA 1999). This manual should be consulted in the design of active anchors for rock stabilization applications.

When anchors are designed for the stabilization of rock slopes, some consideration should be given to the potential for conditions that may cause steel corrosion. Such conditions often prevail in areas where coal and acidic runoff are present or where sodic and pyritic soils are found. The FHWA provides the electrochemical parameters in Table 7-8 as limits for the use of steel reinforcement in MSE structures. These limits should be considered when designing the corrosion protection for active and passive anchors.

Table 7-8 Recommended Limits of Electrochemical Properties for Reinforced Fill with Steel Reinforcement (after FHWA 2009b)

Property	Criteria	Test Method
Resistivity	>3000 ohm-cm	AASHTO T-288
pH	>5 and <10	AASHTO T-289
Chlorides	<100 ppm	ASTM D4327
Sulfates	<200 ppm	ASTM D4327

7-10.8.3 Shotcrete.

Shotcrete is essentially concrete that has little to no gravel-size particles (i.e., larger than the No. 4 sieve) that can be sprayed onto vertical and near-vertical surfaces. It is usually applied in layers to build up the total coating to a specified thickness. Both steel welded wire fabric (WWF) and bars may be used within the shotcrete to provide reinforcement.

Shotcrete can be used to stabilize rock slopes that are subject to raveling and dislodgement of gravel, cobble and boulders. It will tend to adhere to such unstable faces but it should be secured with relatively short passive anchors (i.e., soil nails, rock bolts or dowels). Otherwise, the shotcrete may delaminate from the rock slope in a short period of time. The length of the anchors can be 10 feet or less if they are not actually needed for stabilization of rock planes and wedges. If the rock slope surface is mostly unstable then the anchors should be spaced at intervals no greater than about 6 feet.

A common cause for separation of shotcrete from the face of a rock slope is the presence of water behind the shotcrete. Water frequently seeps from rock slopes, and it should be drained using a drainage composite. Drainage is especially important in climates where the water can freeze. Drainage composites can be successfully used behind shotcrete. The composites typically are available in a width of 4 feet. They should be installed with a coverage of 50%. A drainage grate should be installed at the base of each drainage composite strip and daylighted by a weep hole through the shotcrete.

7-10.8.4 Buttress.

Buttresses have been used for more than 1,000 years to stabilize slopes, walls and buildings. In general, a buttress is a gravity structure that provides passive resistance to displacement. For rock slope stabilization a buttress may comprise piled soil or rock, or it may be an engineered reinforced concrete structure or an MSE structure. The engineering analyses of the mass requirements of a buttress are relatively straightforward and similar to those of a gravity retaining wall.

7-10.8.5 Drains.

Drains are often used in conjunction with rock slope reinforcement measures to counter the destabilizing effects of water that is retained behind a slope face. In general, relief drains are drilled using equipment similar to that used for anchors. However, instead of being angle below the horizontal plane relief drains are typically angle 2° or more above the horizontal plane.

An unfortunate reality of relief drains is that they often become clogged by the accumulation of organic material. Removal of the organic obstructions is generally not practical.

7-10.8.6 Rock Removal.

The stability of rock slopes can often be improved by the removal of material. On a large scale, such removal may take the form of *mass excavation* using drilling and blasting measures followed by dozers, track hoes and haul trucks.

On a smaller scale *trimming* may be used to more selectively remove problematic formations such as overhangs (see Figure 7-14), planes, wedges and columns. Trimming may also employ drilling and blasting and may be preferable to mass excavation in terms of cost and also in terms of potential disruption of adjacent transportation or commercial operations.

If the rock slope includes loose cobbles and boulders that may present a rock fall hazard, then *scaling* may be the most appropriate method of rock removal. In a scaling operation, personnel traverse the slope face while secured by ropes and harnesses. They use hand tools to dislodge rock and may even remove soil deposits and vegetation

7-10.8.7 Rock Fall Protection Measures.

Measures to protect against rock falls may include the installation of surface restraints, barriers or ditches. However, the design of any of these measures usually requires an assessment of the risk posed by rock falls.

Rock fall analyses are generally beyond the capabilities of hand calculations, although some graphical aids have been developed for this purpose (FHWA 1998). When the FHWA (1998) was published, the computer-supported analysis of rock falls was at a relatively early stage. The complexity of the problem was such that computer modeling had to be paired with videography and surveying to render solutions with meaningful accuracy.

After a rock fall analysis has been performed and a reasonable estimate of the final location of fallen rocks can be obtained, ditches can be designed to capture errant

cobbles and boulders. Guidelines for the dimensioning of capture ditches are provided in FHWA (1998).

Steel face mesh can be installed over rock slope surfaces to restrain material that might otherwise dislodge. The mesh may be relatively fine twisted wire or it may comprise larger diameter elements depending on strength requirements. If the mesh is placed directly on the slope face, it must be secured by anchors that are installed in a regular pattern. In a separate application, the top of the mesh can be secured to a stable section of rock slope and left suspended to drape in front of the slope at lower elevations. Rocks that dislodge from the slope and would otherwise represent a rock fall hazard are intercepted by the mesh curtain. In such applications, a ditch is usually installed below the mesh to capture fallen material. As with reinforcement anchors, steel mesh is subject to corrosion in aggressive electrochemical environments. Both the mesh and its anchor components should be designed with corrosion protection.

Catch fences have become a common feature along highways that pass through mountainous terrain. In general, they are a practical and cost-effective measure to protect against rock falls. However, an assessment of rock fall trajectories is essential to determine both the proper location, height, and structural capacities of such barriers.

7-10.8.8 Rock Sheds and Tunnels.

Rock sheds are an effective method of protecting vehicular traffic from rock falls, but their use is rarely justified unless the cost of other mitigation measures is especially high. They are typically needed on roadways that have been cut into hillsides. They are designed with a roof that slopes downhill. On the uphill side of the roof, the roof support beams are secured onto benches. On the downhill side of the roof, the roof support beams can be supported by columns.

In locations where it is not practical to construct a rock shed it may be necessary to construct a tunnel. FHWA (1998) describe such an example for a railway in Canada.

7-11 SUGGESTED READING.

Topic	Reference
Stability Analysis - General	Bishop, A. W. and Bjerrum, L. (1960). The relevance of the triaxial test to the solution of stability problems, *Proceedings of the ASCE Research Conference on the Shear Strength of Cohesive Soils*, Boulder, CO.
	Skempton, A. W. (1948). The Φ = 0 analysis of stability and its theoretical basis, *Proceedings of the 2nd International Conference on Soil Mechanics and Foundation Engineering,* Rotterdam, Vol. 1, pp. 72–78.
	Terzaghi, K. Peck, R. B., and Mesri, G. (1996). *Soil Mechanics in Engineering Practice,* 3rd ed., Wiley, Hoboken, NJ, 549 pages.
Limit Equilibrium Methods	Bishop, A. W. (1955). The use of slip circles in the stability analysis of earth slopes, *Geotechnique*, 5(1), 7–17.
	Bromhead, E. N. (1992). *The Stability of Slopes*, 2nd ed., Blackie, New York.
	Janbu, N. (1954a). Application of composite slip surface for stability analysis, *Proceedings of the European Conference on Stability of Earth Slopes,* Stockholm, Vol. 3, pp. 43–49.
	Janbu, N. (1954b). *Stability Analysis of Slopes with Dimensionless Parameters,* Harvard Soil Mechanics Series 46, Harvard University Press, Cambridge MA.
	Janbu, N. (1968). Slope stability computations, *Soil Mechanics and Foundation Engineering Report,* The Technical University of Norway, Trondheim.
Progressive Failure	Bjerrum, L. (1967). Progressive failure in slopes of overconsolidated plastic clay and clay shales, *ASCE, Journal of the Soil Mechanics and Foundation Division*, 93(5), 1–49.
Back Analysis	Chandler, R. J. (1977). Back analysis techniques for slope stabilization works: a case record, *Geotechnique*, 27(4), 479–495.
	Filz, G. M., Brandon, T. L., and Duncan, J. M. (1992). *Back Analysis of Olmsted Landslide Using Anistropic Strengths,* Transportation Research Record 1343, Transportation Research Board, National Research Council, National Academy Press, Washington, DC, pp. 72–78.
Geosynthetic Reinforcement	Koerner, R. M. (1998). *Designing with Geosynthetics,* 4th ed., Prentice Hall, Upper Saddle River, NJ.
Seismic Slope Stability	Makdisi, F. I., and Seed, H. B. (1978). A simplified procedure for estimating dam and embankment earthquake–induced deformations, *ASCE, Journal of the Geotechnical Engineering Division,* 104(7), 849–867.
	Seed, H. B. (1979). Considerations in the earthquake–resistant design of earth and rockfill dams, Nineteenth Rankine Lecture, *Geotechnique*, 29(3), 215–263.
Staged Construction of Slopes	Ladd, C. C. (1991). Stability evaluation during staged construction, *ASCE, Journal of Geotechnical Engineering,* 117, 540–615.
Residual and Fully-Softened Conditions	Skempton, A. W. (1977). Slope stability of cuttings in brown London clay, *Proceedings of the 9th International Conference on Soil Mechanics*, Tokyo, Vol. 3, pp. 261–270.
	Skempton, A. W. (1985). Residual strength of clays in landslides, flooded strata and the laboratory, *Geotechnique*, 35(1), 3–18.

7-12 NOTATION.

Symbol	Description
b_i	Width of the slice
c	Total stress cohesion
C	Number of surfaces on which pullout resistance is mobilized
c'	Effective stress cohesion
F	Factor of safety
F_m	Factor of safety for Bishop's Simplified Method in effective stress example.
F_N	Component of W that acts perpendicular to the rock block sliding plane
F_R	Factor of safety for geosynthetic strength
F_S	Component of W that acts parallel to the rock block sliding plane
F_W	Factor of safety against wedge failure
F^*	Pullout resistance factor
H_i	Average height of the slice
i	Hydraulic gradient
K	Wedge factor
L_e	Length of reinforcement embedded behind the trial failure surface
$MARV$	Minimum average roll value
M_α	Denominator in equation for calculating normal force at the base of a slice used for assessing validity of normal force.
P_r	Geosynthetic reinforcement's resistance to pullout
RF_{CR}	Reduction factor for creep
RF_D	Reduction factor for durability
RF_{ID}	Reduction factor for installation damage
r_u	Pore pressure coefficient
s	Shear strength
S	Seepage force
SRF	Strength reduction factor
s_{su}	Undrained steady state shear strength

Symbol	Description
s_u	Undrained shear strength
T_{al}	Geosynthetic's long-term tensile strength
T_{ULT}	Ultimate tensile strength of the geosynthetic based on the $MARV$
u	Pore water pressure
U	Uplift force applied by water at the failure plane
V	Force applied by water in the tension crack
W	Rock block weight
W_i	Weight of each slice
α	Dip direction or dip azimuth
α	Scale correction factor to account for nonlinear stress reduction
α_i	Angle between the tangent to the failure surface and the horizontal
γ	Unit weight
γ_w	Unit weight of water
δ	Effective soil-geosynthetic interface friction angle
θ	Face angle
σ	Total stress
σ'	Effective stress
σ'_v	Effective vertical stress
τ	Shear stress required for equilibrium
ϕ'	Effective stress friction angle
ϕ	Total stress friction angle
ϕ'_r	Residual friction angle
Ψ	Dip
Ψ_{Fi}	Inclination of the slope face as measured at right angles to the line of intersection in a wedge failure analysis
Ψ_i	Dip of the line of intersection in a wedge failure analysis
Ψ_P	Angle of a sliding block plane with respect to horizontal

CHAPTER 8 CORRELATIONS FOR SOIL AND ROCK

8-1 INTRODUCTION.

Correlations are useful tools for obtaining values of engineering parameters based on index properties or other easily measured soil parameters. Correlations are often used when measured values are not available. The accuracy and applicability of correlations depend on the data source, the statistical approach for determining the correlation, and the causal relationship between the index property and the engineering parameter. For these reasons, engineers should use correlations with caution. It is often prudent to seek out the original source of the correlation to ensure that it is applicable to the engineering problem at hand.

Often, correlations provide an uncertain, empirical prediction of the parameter, which means that there are usually values above and below the proposed trend line. Uncertainty results from both scatter in the measured data and the inability of the chosen mathematical relationship to perfectly predict the observed trends. Because of this uncertainty, correlations are typically most appropriate for preliminary design or as a check that measured values are in general agreement with the behavior of the soils used to develop the correlation. In addition, correlations can provide the basic form of an equation that can be used with experimental data to create site-specific correlations for an individual project or area.

For cases where the required property cannot be measured and correlations are used for final designs, the uncertainty in the parameter should be evaluated by the engineer. Different approaches can be used, including (1) the use of a range of values rather than a single value of a parameter, (2) use of the lowest likely value, (3) application of confidence limits, or (4) explicit consideration of uncertainty in the correlation using formal reliability analysis.

Confidence limits are trend lines that are offset from the mean based on the standard deviation ($S.D.$) of the residuals between the data and the mean. Confidence limit boundaries plotted with mean trends help to illustrate the variability in a data set. Confidence limits or the standard deviation can be used to select appropriately conservative values from correlations. For example, if a correlated parameter is assigned a value that is one standard deviation below the mean, the probability is only 16% that the actual value is lower than the assigned value. This probability reduces to 2% for an assigned value that is two standard deviations below the mean. These probability margins assume that the error in the correlation follows a normal or log-normal distribution and that the selected trend line fits the data well.

The selection of an appropriate confidence limit above or below the mean trend depends on the effect of parameter on the particular analysis. In most cases, it is better to use a confidence below the mean. This will decrease the probability that the

correlated parameter is greater than the actual value, which undesirable in many cases (e.g., shear strength, Young's modulus, etc.). In a few cases, the opposite might be the case (e.g., compression index).

8-2 EFFECTIVE STRESS (DRAINED) SHEAR STRENGTH.

8-2.1 Coarse-Grained Soils.

Most of the correlations presented for coarse-grained soils have been developed for relatively clean sands unless otherwise noted. These correlations should not be used in micaceous sands. The presence of mica tends to reduce some index properties (e.g. the SPT N value) significantly but might not affect the drained friction angle when compared to clean sands (Sabatini et al. 2002). These correlations should not be used for gravelly soils unless specified.

8-2.1.1 Correlations with Soil Type.

Carter and Bentley (2016) summarized typical values for the effective stress friction angles of coarse-grained soils as presented in Table 8-1 and Table 8-2. Table 8-1 presents values for the drained friction angle of different types of coarse-grained soils in loose and dense conditions and Table 8-2 presents the values of effective stress friction angle for coarse-grained soils compacted to the maximum dry density based on ASTM D698.

Table 8-1 Typical Values of the Effective Stress Friction Angle for Coarse-grained Soils (Carter and Bentley 2016)

Soil Description	ϕ' (in degrees)	
	Loose	Dense
Uniform sand, round grains	27	34
Well-graded sand, angular grains	33	45
Sandy gravel	35	50
Silty sand	27-33	30-34
Inorganic silt	27-30	30-35

Table 8-2 Typical Values of the Effective Stress Friction Angle for Compacted Coarse-grained Soils (Carter and Bentley 2016)

Soil Description	USCS	ϕ' (in degrees)
Well-graded sand-gravel mixtures	GW	>38
Poorly-graded sand-gravel mixtures	GP	>37
Silty gravels, poorly-graded gravel-sand-silt	GM	>34
Clayey gravels, poorly-graded gravel-sand-clay	GC	>31
Well-graded clean sand, gravelly sand	SW	38
Poorly-graded clean sand, gravelly sand	SP	37

A correlation for the drained friction angle as a function of relative density, dry unit weight and soil type is presented in Figure 8-1.

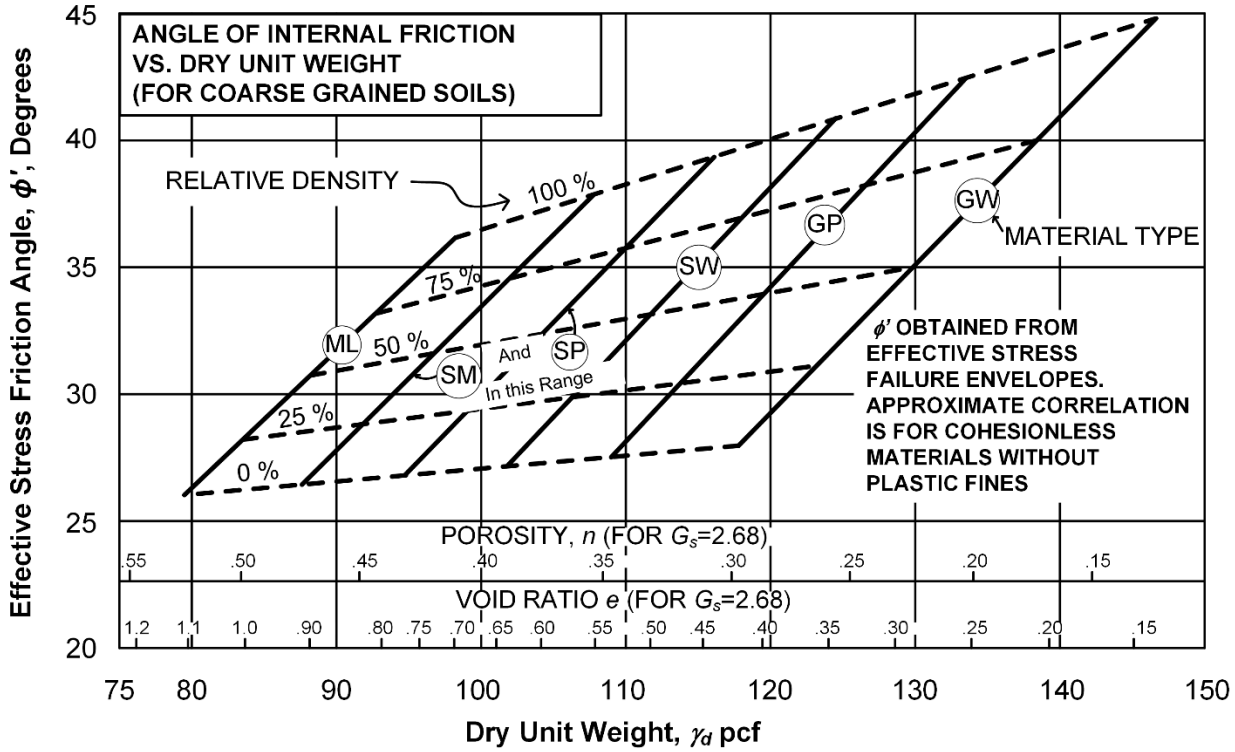

Figure 8-1 Approximate Relationship between the Effective Stress Friction Angle and Dry Unit Weight for Various Relative Densities and Types of Soil

8-2.1.2 Correlations with Standard Penetration Test.

Many relationships have been presented in the literature to estimate drained shear strength parameters of coarse-grained soils using results from the standard penetration test. In older correlations where no energy correction for the SPT N value was used, it was assumed that the reported N values were equal to N_{60}.

Relationships between SPT N values and static cone tip resistance presented by Duncan et al. (1989) summarizing the work presented by Meyerhof (1956) and Mitchell (1981) are shown in Table 8-3 and Table 8-4, respectively.

Table 8-3 Relationship between SPT N Value, Relative Density and Effective Stress Friction Angle (Meyerhof 1956)

State of Packing	Relative Density (%)	N_{60} (blows/ft)	Static Cone Tip Resistance, q_c (tsf)	Effective Stress Friction Angle (degrees)
Very Loose	< 20	< 4	< 20	< 30
Loose	20 - 40	4 - 10	20 - 40	30 - 35
Compact (Medium)	40 - 60	10 - 30	40 - 120	35 - 40
Dense	60 - 80	30 - 50	120 - 200	40 - 45
Very Dense	> 80	> 50	> 200	> 45

The effective stress friction angles presented in Table 8-3 are for clean sands and should be decreased by 5° for clayey sands and increased by 5° for gravelly sands. To use Table 8-3 on saturated very fine or silty sand, the measured SPT N should be corrected using the equation below:

$$N' = \begin{cases} N_{60} & \text{for } N_{60} \le 15 \\ 15 + 0.5\left(N_{60} - 15\right) & \text{for } N_{60} > 15 \end{cases} \quad \textbf{(8-1)}$$

where:
N' = blow count corrected for dynamic pore pressure effects, and
N_{60} = measured blow count corrected for 60% energy.

Table 8-4 Relationship between SPT N Value, Relative Density, and Angle of Internal Resistance (after Mitchell 1981)

State of Packing	Relative Density[1] (%)	Standard Penetration Resistance, $N_{1,60}$ (blows/ft)[2]	Static Cone Resistance, q_c (tsf)	Effective Stress Friction Angle (degrees)	Dry Unit Weight (kN/m^3)
V. Loose	< 15	< 4	< 50	< 30	< 14
Loose	15 - 35	4 - 10	50 - 100	30 - 32	14 - 16
M. Dense	35 - 65	10 - 30	100 - 150	32 - 35	16 - 18
Dense	65 - 85	30 - 50	150 - 200	35 - 38	18 - 20
V. Dense	85 - 100	> 50	> 200	> 38	> 20

[1] Freshly deposited, normally consolidated sand
[2] Corrected to an effective vertical overburden pressure of 1 atm.

Sowers (1979) related the effective stress friction angle to SPT N values for depths less than 5 feet and greater than 20 feet as presented in Figure 8-2. Interpolation can be used for depths between 5 and 20 feet. Shioi and Fukui (1982) also correlated the effective stress friction angle to N_{60} using (also shown in Figure 8-2):

$$\phi' = \sqrt{15 \cdot N_{60}} + 15 \quad \text{(For roads and bridges)} \qquad \textbf{(8-2)}$$

$$\phi' = 0.3 \cdot N_{60} + 27 \quad \text{(For buildings)} \qquad \textbf{(8-3)}$$

where:
N_{60} = SPT N value corrected for 60% energy.

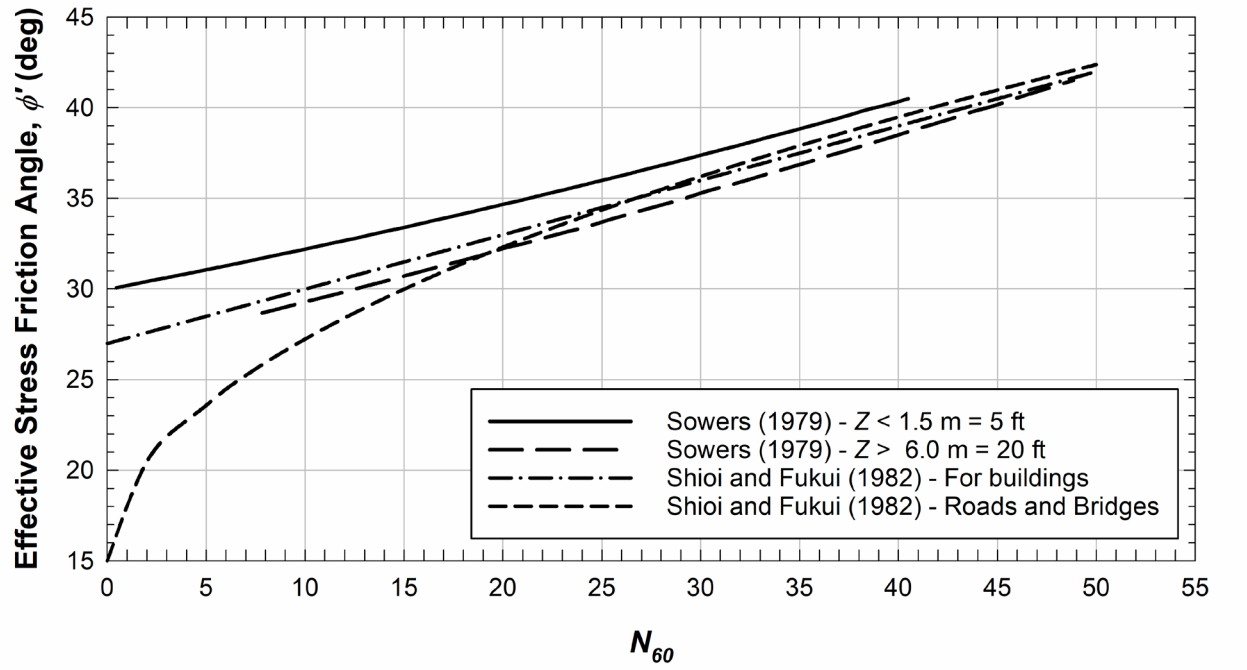

Figure 8-2 Relationship between Effective Stress Friction Angle of Coarse-Grained Soils and SPT N_{60} Value

Parry (1977) and Schmertmann (1975) considered the effects of overburden pressure on the relationship between the effective stress friction angle and SPT N, resulting in the correlations shown in Figure 8-3.

Kulhawy and Mayne (1990) approximated the trends in Figure 8-3(bottom) as:

$$\phi' = \tan^{-1}\left[\frac{N_{60}}{12.2 + 20.3\left(\sigma'_v / P_a\right)}\right]^{0.34} \quad \textbf{(8-4)}$$

where:
ϕ' = effective stress friction angle,
N_{60} = SPT N value corrected for 60% energy,
σ'_v = vertical effective stress, and
P_a = atmospheric pressure.

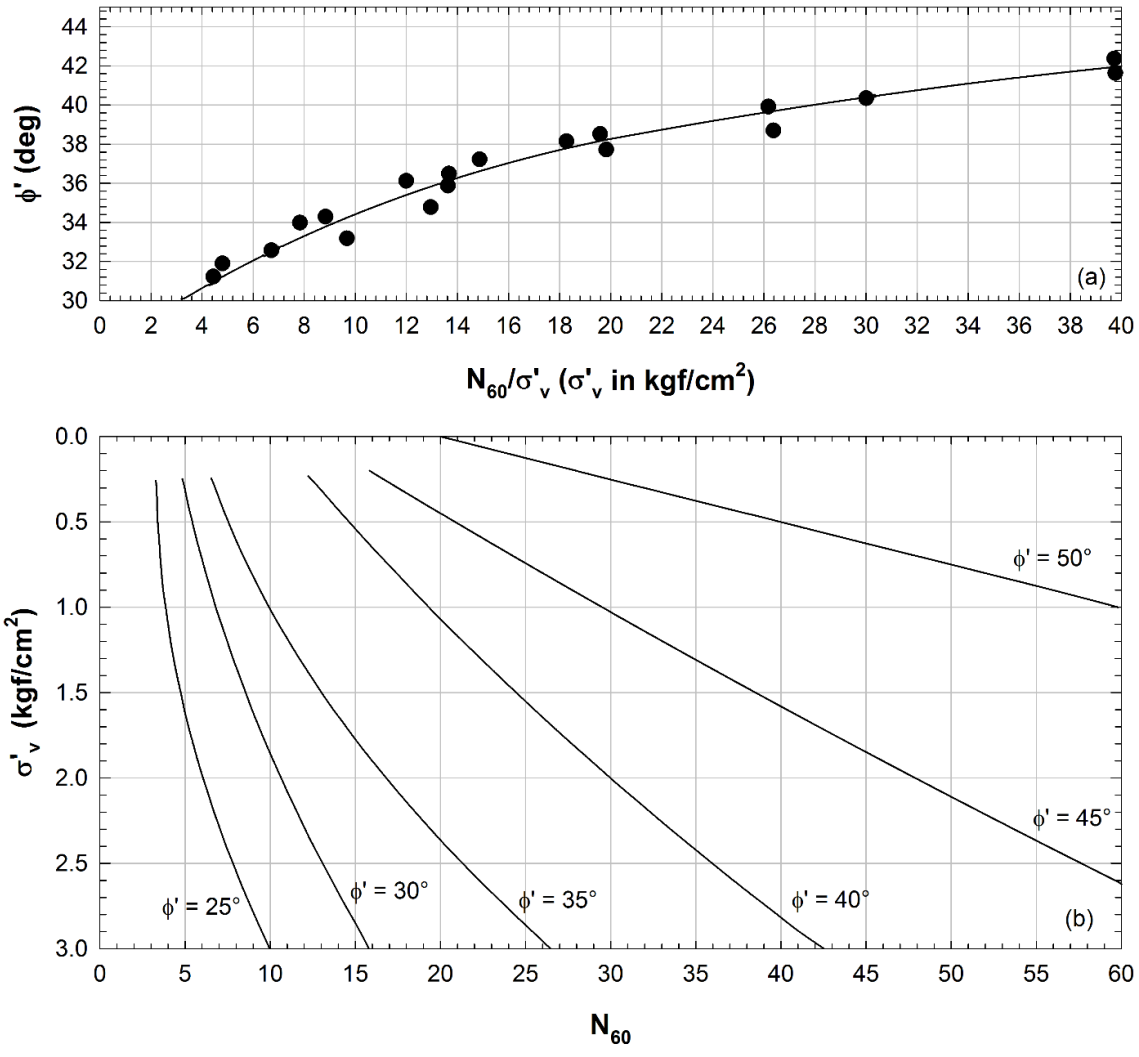

Figure 8-3 Relationship between Peak Effective Stress Friction Angle, Overburden Pressure, and SPT Blow Count for Sands (top) after Parry (1977) and (bottom) after DeMello (1971) and Schmertmann (1975)

Peck et al. (1974) developed the correlation for the effective stress friction angle based on SPT N values shown in Figure 8-4. According to Ameratunga et al. (2016), this correlation is conservative. Wolff (1989) approximated this relationship as:

$$\phi' = 27.1 + 0.3N_{1,60} - 0.00054\left(N_{1,60}\right)^2 \quad \textbf{(8-5)}$$

where:
$N_{1,60}$ = SPT N value corrected for 60% energy and 1 atm overburden pressure.

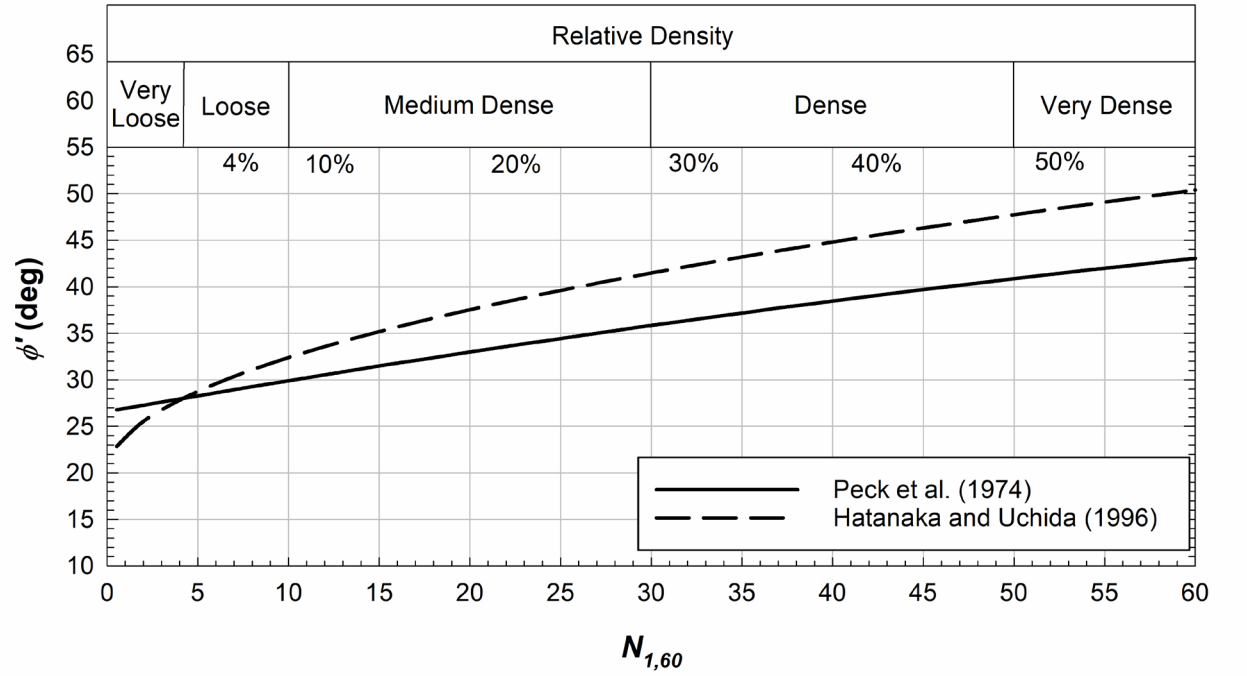

Figure 8-4 Variation of Effective Stress Friction Angle with $N_{1,60}$ (after Peck at al. 1974, and Hatanaka and Uchida 1996)

Hatanaka and Uchida (1996) also correlated the effective stress friction angle of sands to $N_{1,60}$ as shown in Figure 8-4. This equation was developed using the results of triaxial tests from high-quality intact frozen samples of natural sands. Using an SPT hammer with an efficiency of 78%, the relationship was found to be:

$$\phi' = \sqrt{15.4N_{1,60}} + 20 \quad \textbf{(8-6)}$$

8-2.1.3 Correlations with Cone Penetration Test.

Two relationships between CPT results and effective stress friction angle were already presented in Table 8-3 and Table 8-4. Table 8-5 presents a similar relationship developed by Bergdahl et al. (1993), according to Ameratunga et al. (2016).

Table 8-5 Relationship between Relative Density, Cone Tip Resistance, and Effective Stress Friction Angle (after Bergdahl et al. 1993, and Ameratunga et al. 2016)

Relative Density	q_c (tsf)	ϕ' (degrees)
Very loose	0 – 26.1	29 – 32
Loose	26.1 – 52.2	32 – 35
Medium	52.2 – 104.4	35 – 37
Dense	104.4 – 208.8	37 – 40
Very dense	> 208.8	40 – 42

Mayne (2007) used the results of calibration chamber tests to estimate the effective stress friction of coarse-grained soils for CPT results as

$$\phi' = 17.6 + 11 \cdot \log\left(\frac{q_t / P_a}{\sqrt{\sigma'_v / P_a}} \right) \quad \textbf{(8-7)}$$

where:
ϕ' = drained friction angle,
q_t = corrected tip resistance= $q_c + u \cdot (1+a)$,
u = pore pressure measured behind the cone tip, often named the u_2 position,
a = cone net area ratio = ratio of the face area to shoulder area,
σ'_v = effective vertical stress, and
P_a = atmospheric pressure in same units as vertical stress and q_c.

Figure 8-5 correlates the effective stress friction angle with CPT tip resistance as summarized by Meyerhof (1976).

In cases where the tip resistance increases with depth, the method outlined in Figure 8-6 can be used to obtain the bearing capacity factor (N_q). The correlation presented in Figure 8-7 can be used to obtain the effective stress friction angle from N_q.

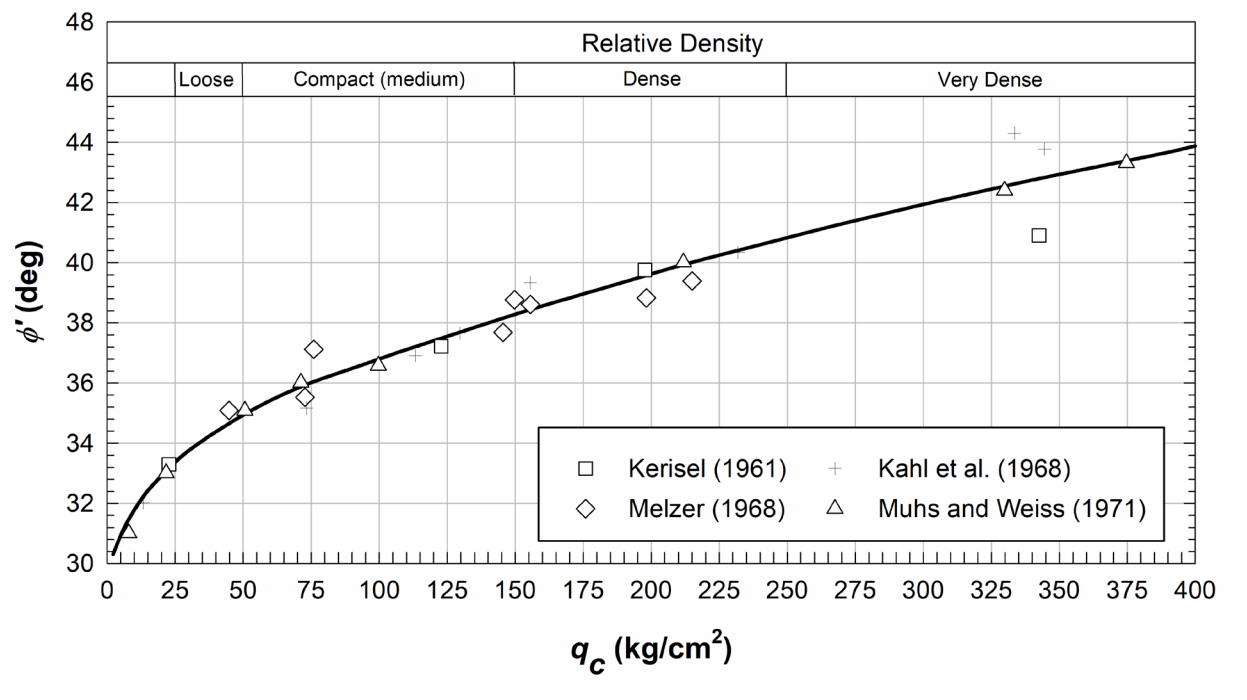

Figure 8-5 Relationship between Effective Stress Friction Angle and Cone Tip Resistance (after Kerisel 1961, Kahl et al. 1968, Melzer 1968, Muhs and Weiss 1971, and Meyerhof 1976)

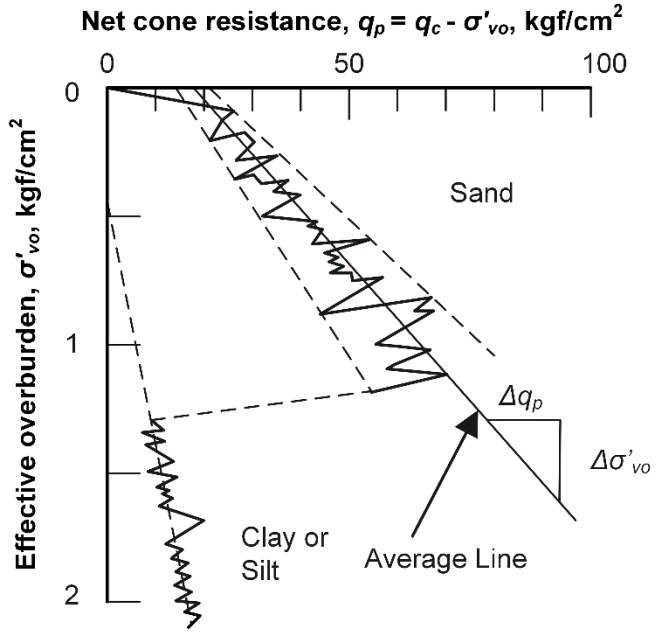

1. Plot the net cone resistance vs. effective overburden stress.
2. Draw an average line to represent the variation of q_p with σ'_{vo} as shown above
3. The slope of the line is N_p:

$$N_p = (\Delta q_p / \Delta \sigma'_{vo})$$

4. Calculate $N_q = N_p + 1$
5. Determine ϕ' using the correlation between N_q and ϕ' shown in Fig.8-7
6. For the example shown above:
   N_p=47, N_q=48, ϕ' = 37°

Figure 8-6 Estimation of ϕ' from a Cone Resistance Profile (after Duncan et al. 1989)

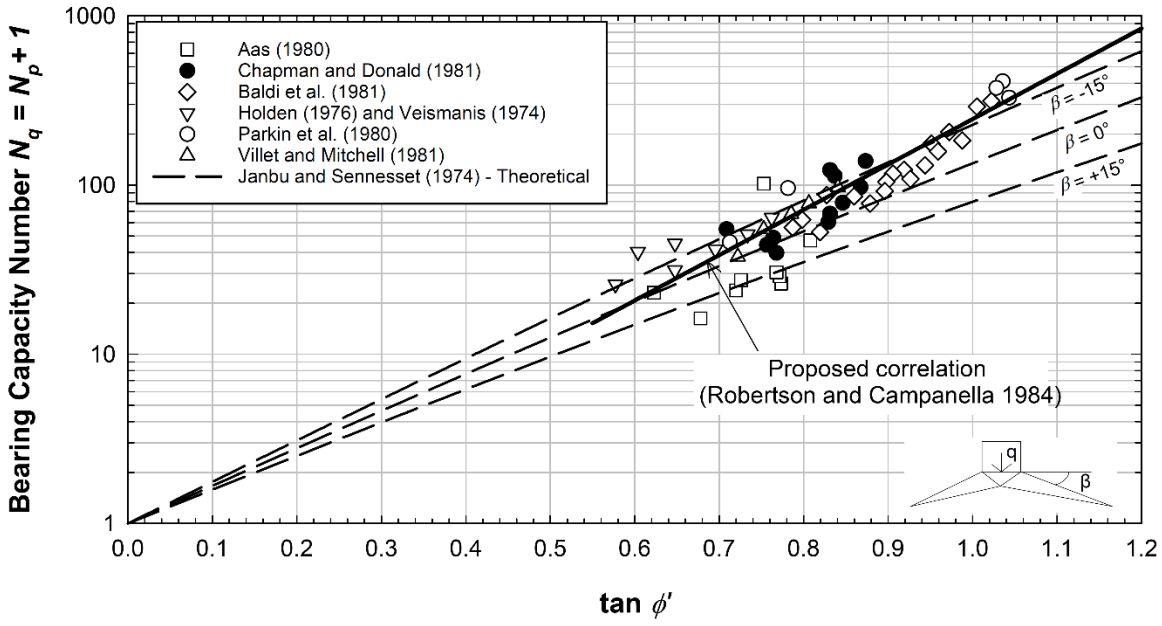

Figure 8-7 Relationship between Bearing Capacity Number N_q and Peak Effective Stress Friction Angle from Large Calibration Tests (after Duncan et al. 1989)

Robertson and Campanella (1983) correlated the effective stress friction angle to the measured CPT tip resistance (electric cone) from tests performed in a calibration chamber. The correlation used drained triaxial tests on uncemented, unaged, moderately compressible quartz sands and considers the effect of overburden pressure as shown in Figure 8-8. The relationship presented in Figure 8-8(a) was approximated by Robertson and Cabal (2014) using the relationship:

$$\tan\phi' = \frac{1}{2.68}\left[\log\left(\frac{q_c}{\sigma'_v}\right) + 0.29\right] \quad \textbf{(8-8)}$$

where:
ϕ' = drained friction angle,
q_c = cone tip resistance, and
σ'_v = effective vertical stress in same units as q_c.

Schmertmann (1975) presented a correlation to determine the effective stress friction angle based on the CPT tip resistance. To use this correlation, the relative density first needs to be determined using Figure 8-9. Using the correlated value of relative density, the effective stress friction angle can be determined from Figure 8-10.

For this purpose, Schmertmann (1978) developed a correction factor (R) such that:

$$R = 1 + 0.75\left(OCR^{\beta} - 1\right) = \frac{q_{c,OC}}{q_{c,NC}} \quad \textbf{(8-9)}$$

where:
OCR = overconsolidation ratio,
β = exponent,
$q_{c,OC}$ = CPT tip resistance in overconsolidated sand, and
$q_{c,NC}$ = CPT tip resistance in normally consolidated sand.

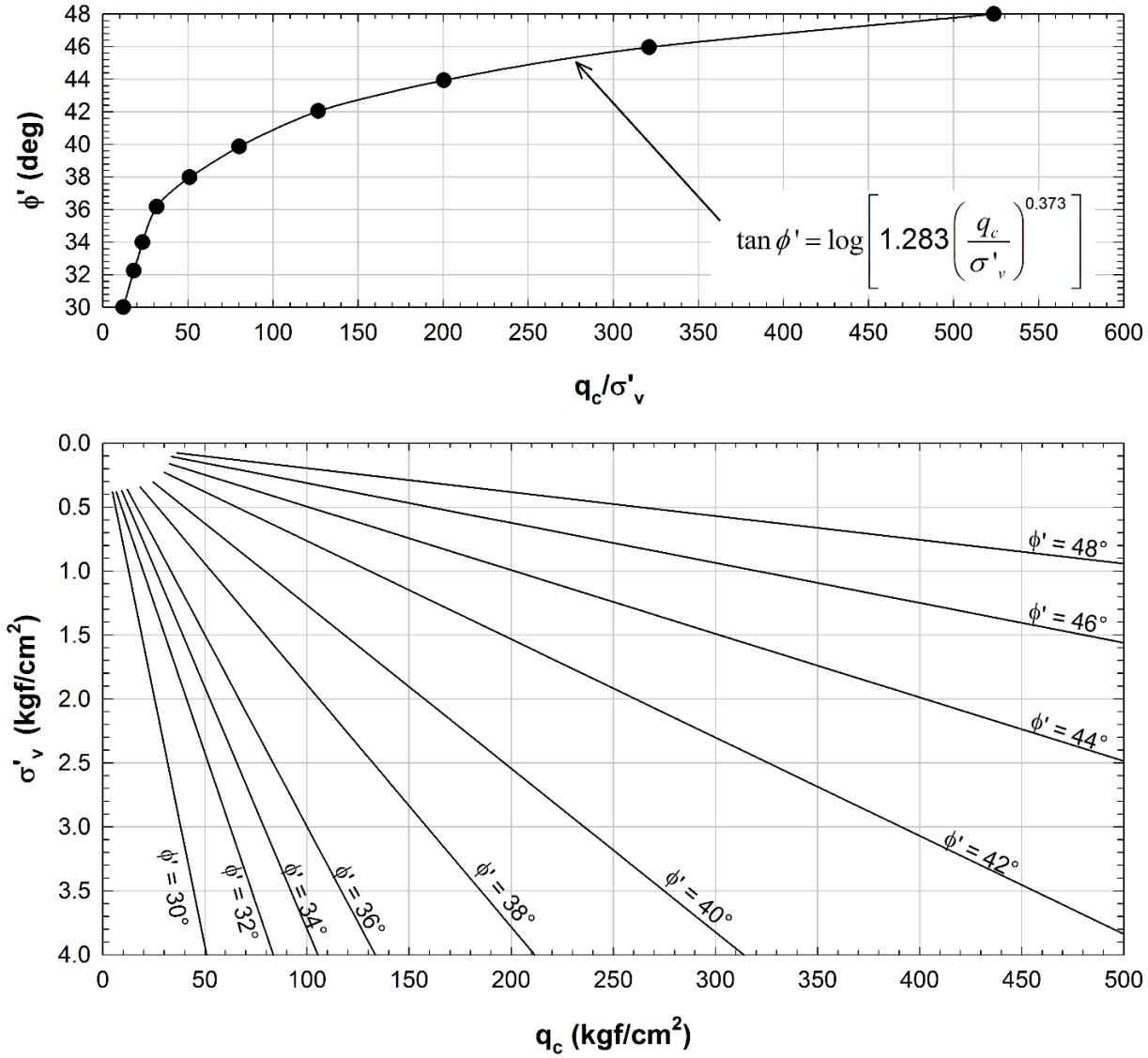

Figure 8-8 Variation of Peak Effective Stress Friction Angle with σ'_v and Cone Resistance for Normally Consolidated, Uncemented, Quartz Sands (after Robertson and Campanella 1983)

For overconsolidated sands, the effect of overconsolidation on the measured tip resistance needs to be considered before using correlations proposed for normally consolidated sands.

An example of using this approach is shown in Figure 8-11. According to Lunne and Christoffersen (1985), β can be assumed as 0.45 for all practical purposes.

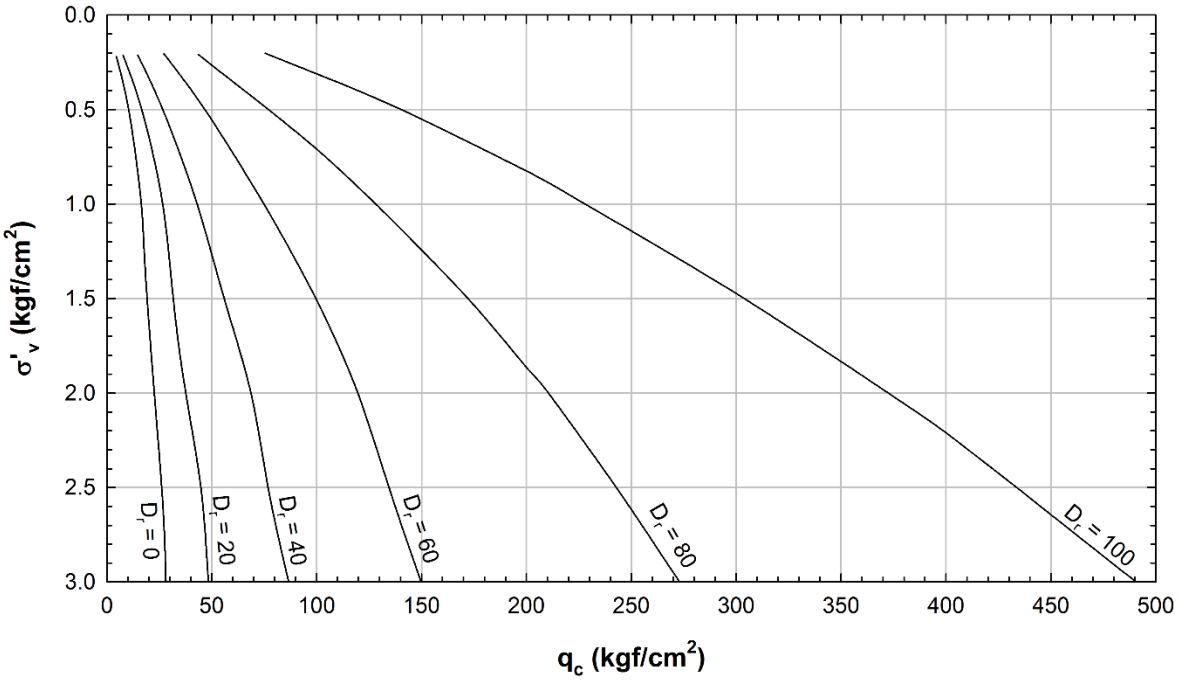

Figure 8-9 Estimation of Relative Density for Normally Consolidated Sands from Cone Penetration Resistance (after Schmertmann 1978)

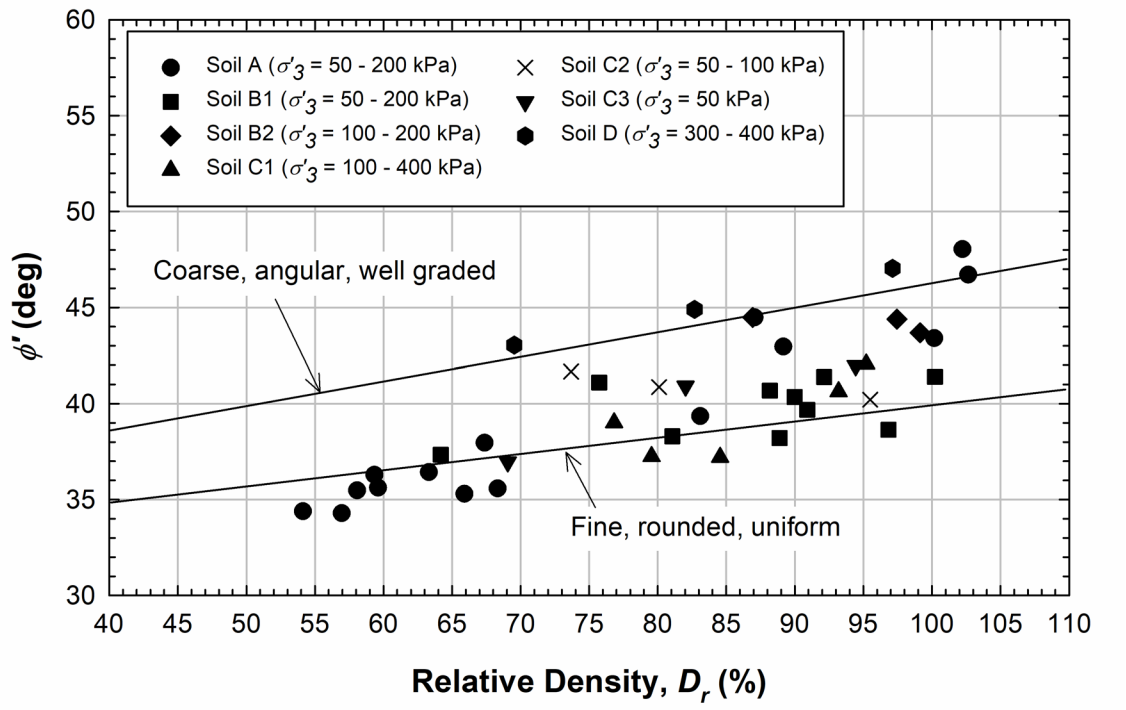

Figure 8-10 Relationship between Friction Angle and Relative Density based on Triaxial Compression Tests on North Sea Sands (after Schmertmann 1975, and Lunne and Kleven 1982)

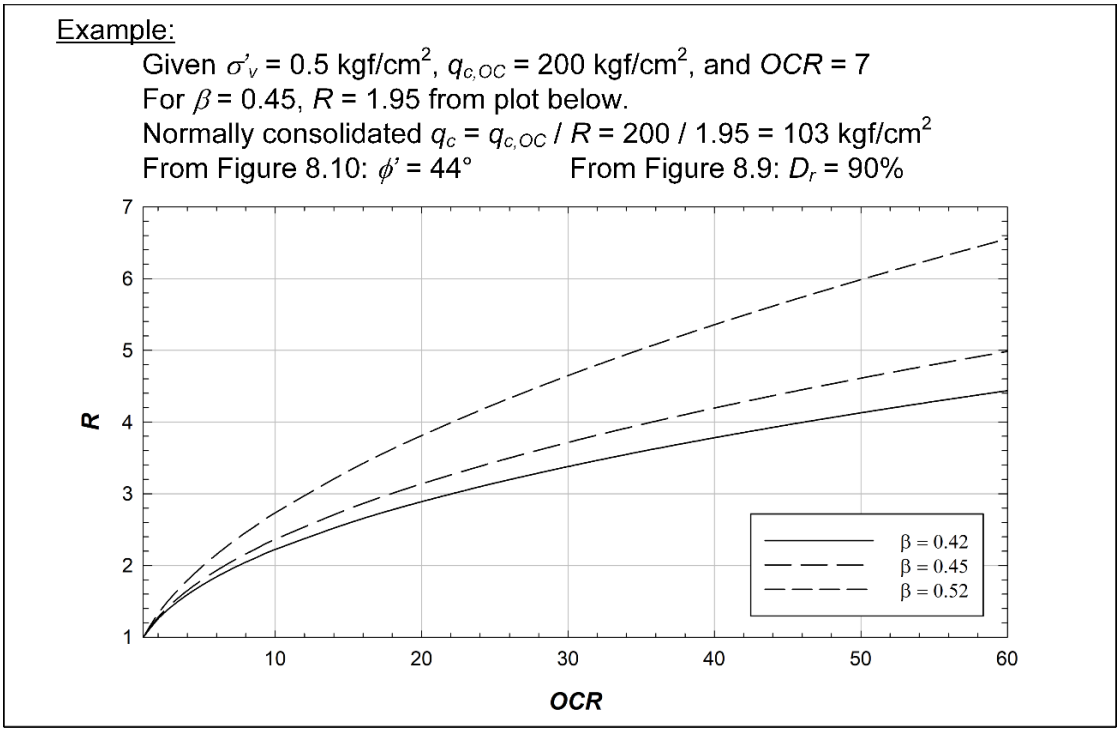

Figure 8-11 Correction for Effects of Overconsolidation on Cone Penetration Tip Resistance in Sand (after Lunne and Christoffersen 1985, and Duncan et al. 1989)

8-2.1.4 Correlations with Dilatometer.

Marchetti (1997) proposed correlations to relate the effective stress friction angle for clean sands to the horizontal stress index (K_D) from the dilatometer test in which:

$$K_D = \frac{p_0 - u_0}{\sigma'_v} \quad \textbf{(8-10)}$$

where:
p_0 = corrected pressure required to initiate movement of the membrane against the soil,
u_0 = hydrostatic pore pressure, and
σ'_v = effective vertical stress.

Ricceri et al. (2002) proposed that the upper bound estimate of effective stress friction angle from dilatometer tests is:

$$\phi' = 31 + \frac{K_D}{0.236 + 0.066 K_D} \quad \textbf{(8-11)}$$

and Marchetti (1997) proposed that the lower bound estimate is:

$$\phi' = 28 + 14.6 \cdot \log K_D - 2.1\left(\log K_D\right)^2 \quad \textbf{(8-12)}$$

where:
ϕ' = effective stress friction angle and
K_D = horizontal stress index.

According to Marchetti, the lower bound solution can underestimate the *in situ* friction angle by 2° to 4°. The upper and lower bound equations are plotted in Figure 8-12.

8-2.2 Fine-Grained Soils.

The effects of overconsolidation on the shear strength preclude the development of accurate correlations for the effective shear parameters of fine-grained soils. However, multiple correlations have been developed for the fully softened (ϕ'_{FS}) and residual (ϕ'_r) friction angles of clays, where the fully softened friction angle is taken to be equal to the normally consolidated peak value.

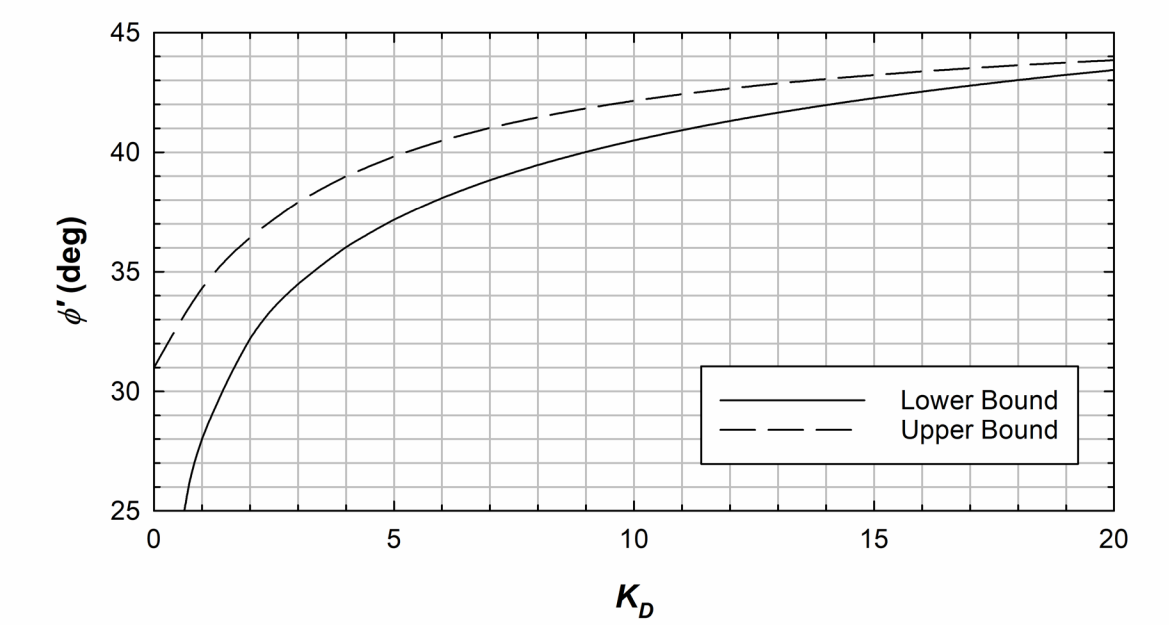

Figure 8-12 Range of Effective Stress Friction Angle for Clean Sands based on the Horizontal Stress Index from the Dilatometer Test (after Marchetti 1997, and Ricceri et al. 2002)

8-2.2.1 Correlations for Fully Softened Shear Strength.

Gibson (1953) presented a relationship for ϕ'_{FS}, which is plotted in Figure 8-13. The standard deviation of the data about the trend is plotted as confidence limits. The mean trend line can be approximated by the equation below according to Carter and Bentley (2016):

$$\phi'_{FS} = 0.0058PI^{1.73} - 0.32PI + 36.2 \quad \textbf{(8-13)}$$

where:
PI = plasticity index.

According to Carter and Bentley (2016) the polynomial fit is in agreement with the original curve to within 1% for the fully softened condition.

A similar correlation was presented by Ladd et al. (1977) based on triaxial tests on intact normally consolidated clays as shown in Figure 8-14. The confidence limits in this figure are plotted at one standard deviation above and below the mean trend.

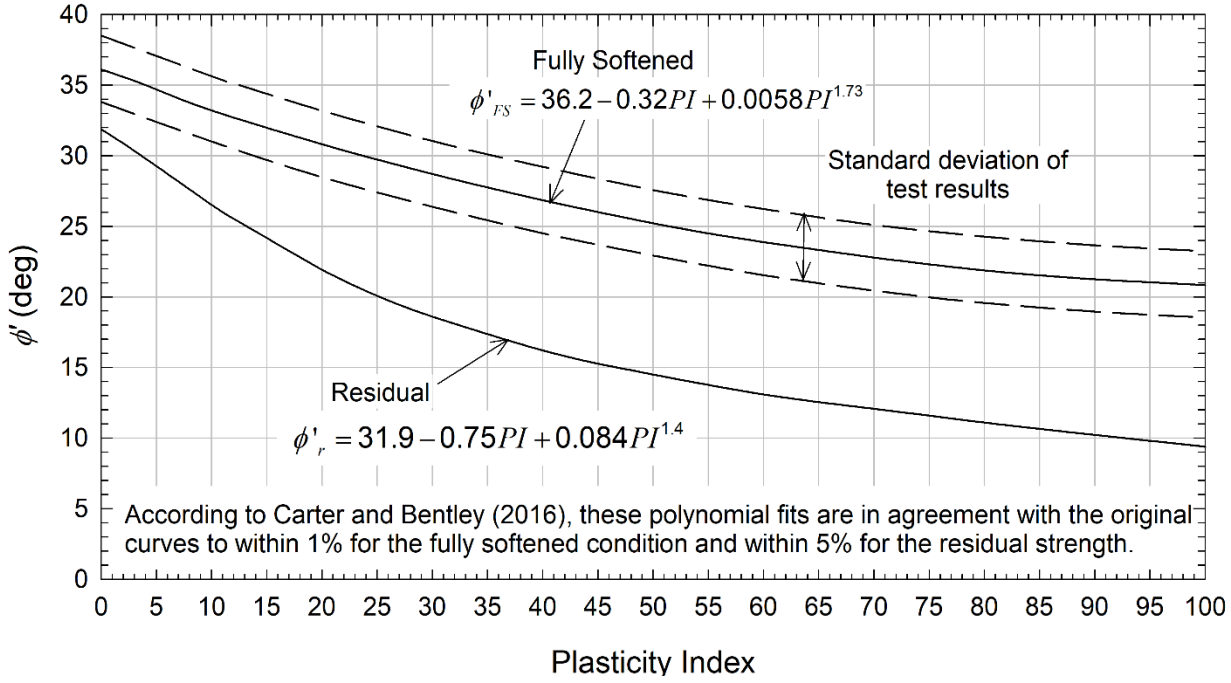

Figure 8-13 Relationship between the Effective Stress Friction Angle of Fine-Grained Soil and Plasticity Index (after Gibson 1953, Carter and Bentley 2016)

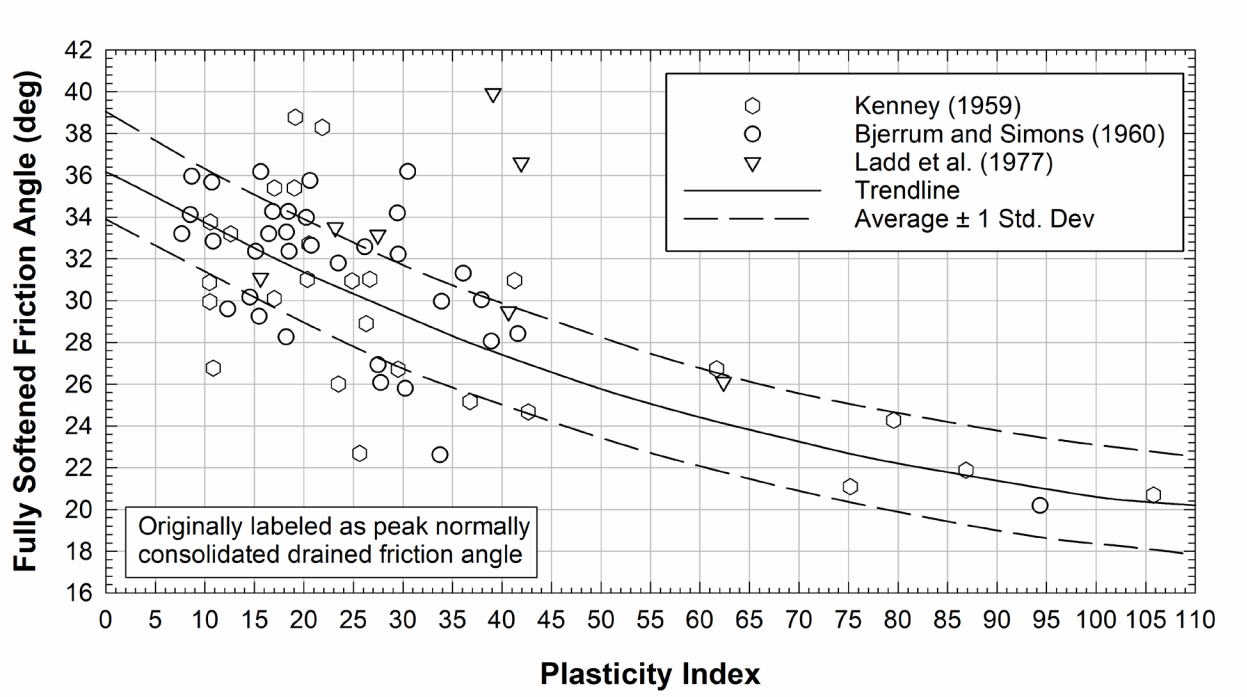

Figure 8-14 Correlation between ϕ'_{FS} and *PI* based on Triaxial Tests on NC Clays (after Kenney 1959, Bjerrum and Simons 1960, Ladd et al. 1977)

A similar relationship between ϕ'_{FS} and PI was proposed by Terzaghi et al. (1996) as shown in Figure 8-15. This relationship was developed from the results of tests on normally consolidated specimens with most of them being remolded.

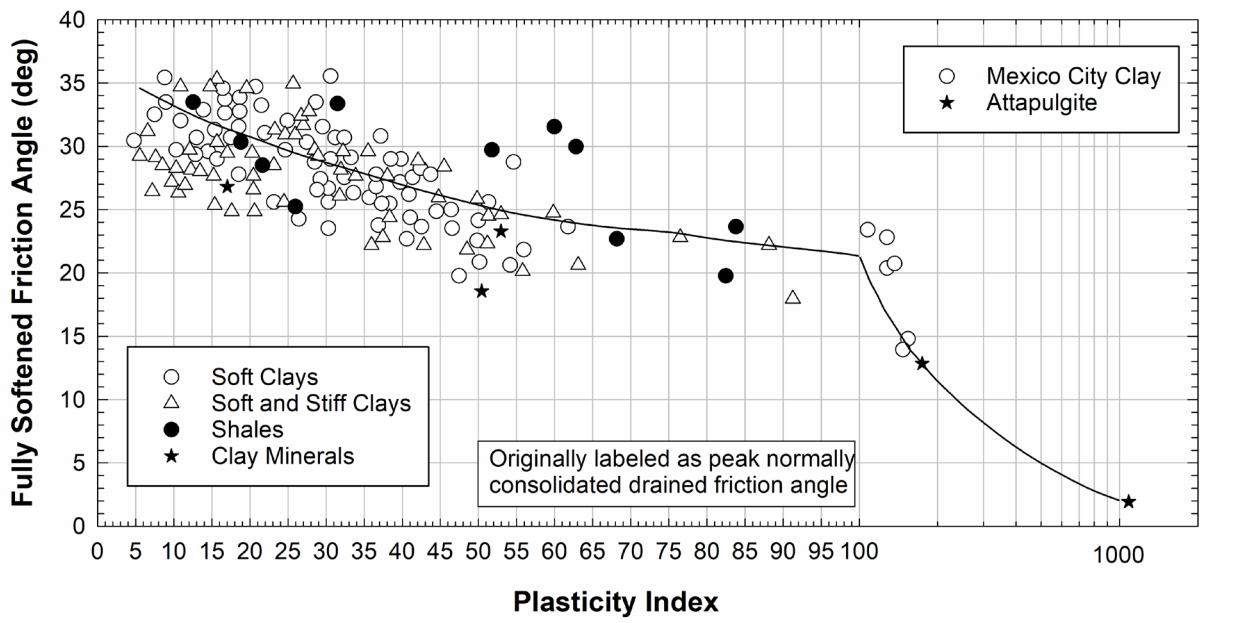

Figure 8-15 Relationship between ϕ'_{FS} and PI (after Terzaghi et al. 1996)

Tiwari and Ajmera (2011) presented the correlations shown in Figure 8-16 and Figure 8-17 for the fully softened friction angle. These correlations were based on direct shear tests performed on 36 artificially created soils. Tiwari and Ajmera (2011) created the artificial soils for this study by mixing different proportions of quartz, kaolinite and montmorillonite.

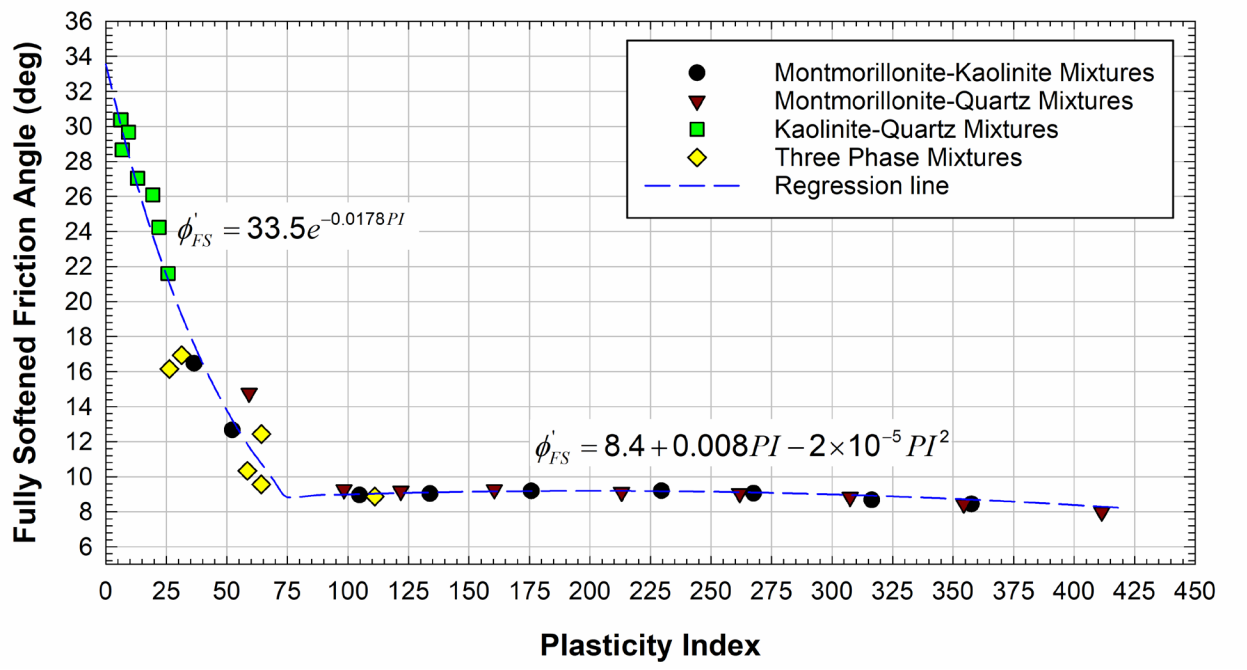

Figure 8-16 Variation of the Fully Softened Friction Angle with Plasticity Index (after Tiwari and Ajmera 2011)

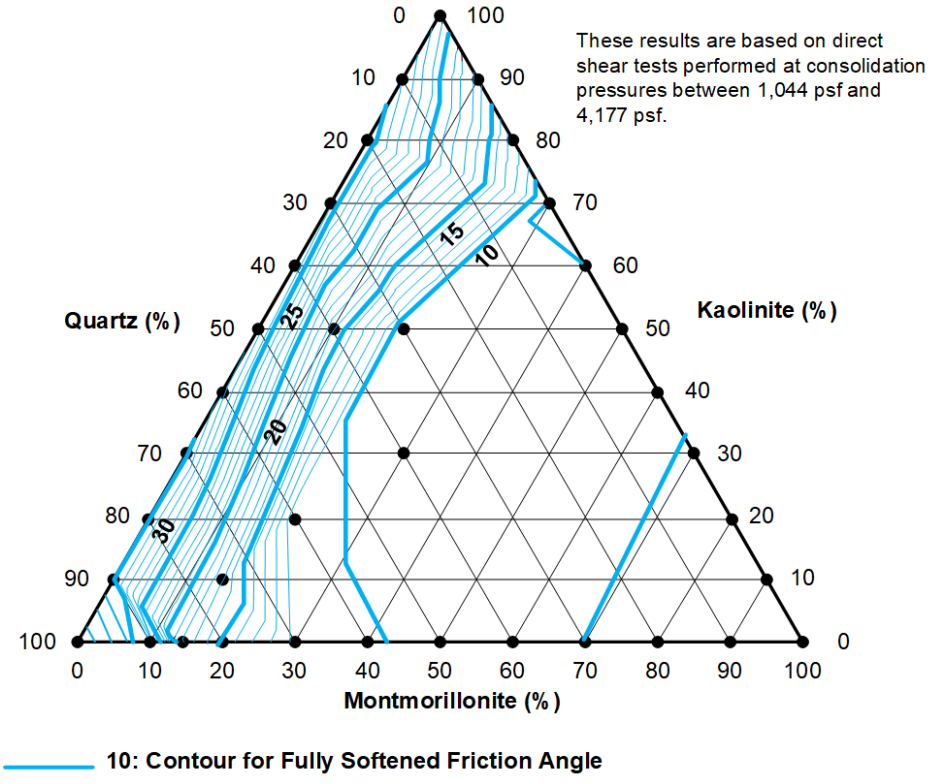

Figure 8-17 Fully Softened Friction Angle based on Mineral Composition (after Tiwari and Ajmera 2011)

The preceding relationships only consider linear failure envelopes (i.e., constant friction angle) while real soils often exhibit a nonlinear failure envelope. Nonlinear failure envelopes have been described by multiple mathematical forms, including normal stress dependent secant friction angle and two-parameter power function with parameters a and b. Shear strength is calculated using a secant friction angle as:

$$s = \sigma'_{ff} \tan \phi'_{\sec} \quad \textbf{(8-14)}$$

where:
s = effective stress shear strength,
σ'_{ff} = effective normal stress on the failure plane, and
ϕ'_{sec} = stress dependent secant friction angle.

The two-parameter power function describes shear strength nonlinearly as:

$$s = aP_a \left(\frac{\sigma'_{ff}}{P_a} \right)^b \quad \textbf{(8-15)}$$

where:
s = effective stress shear strength,
a = empirical coefficient related to the steepness of the power function,
σ'_{ff} = effective normal stress,
P_a = atmospheric pressure in same units as stress, and
b = empirical coefficient related to the curvature of the power function.

Castellanos et al. (2021) presented the correlations for nonlinear fully softened shear strength parameters shown in Figure 8-18 and Figure 8-19. These correlations were developed based on over 400 direct shear tests on 97 soils (Castellanos et al. 2021). The equations and standard deviations provided on the plots allow uncertainty in the correlations to be explicitly considered. Castellanos et al. (2021) also provide statistical measures of the covariance of the correlations for a_{FS} and b_{FS}.

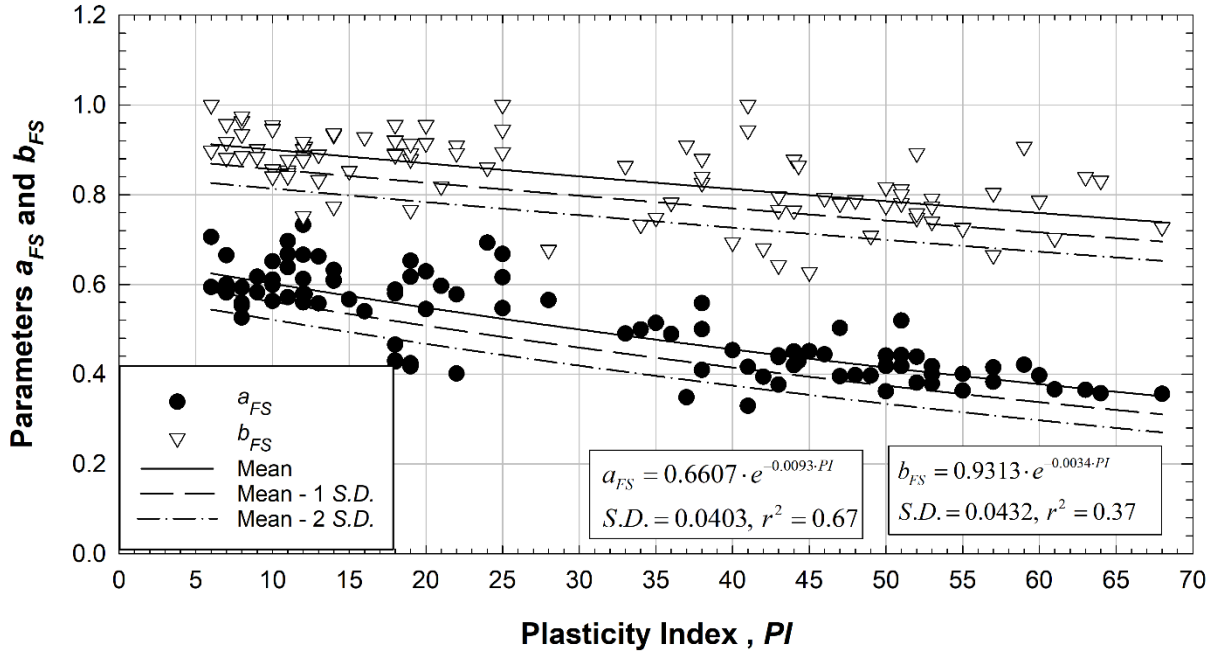

Figure 8-18 Correlation between Power Function Parameters a_{FS} and b_{FS} and Plasticity Index (after Castellanos et al. 2021)

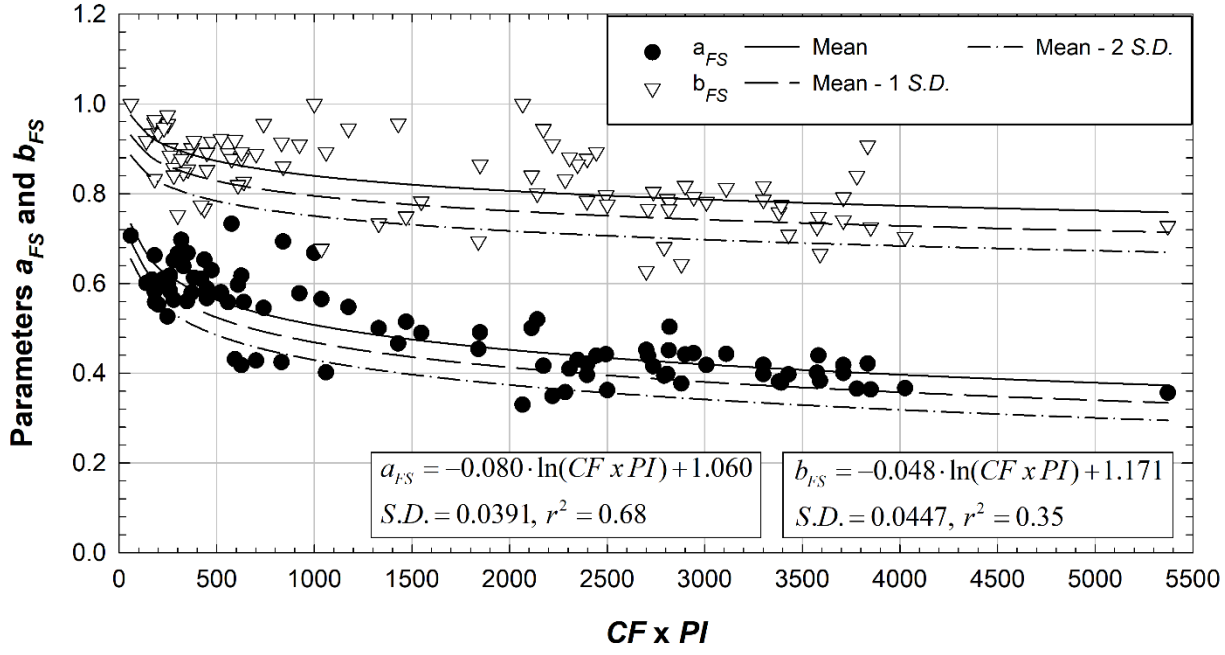

Figure 8-19 Correlation between Power Function Parameters a_{FS} and b_{FS} and $CF \times PI$ (after Castellanos et al. 2021)

8-2.2.2 Correlations for Residual Shear Strength.

Gibson (1953) also presented a relationship for ϕ'_r as plotted in Figure 8-13. The residual friction angle trend line can be approximated by the equation below, according to Carter and Bentley (2016):

$$\phi'_r = 0.084 \cdot PI^{1.4} - 0.75 \cdot PI + 31.9 \quad \textbf{(8-16)}$$

where:
PI = plasticity index.

According to Carter and Bentley (2016) this polynomial fit agrees with the original curves to within 5% for the residual friction angle.

Skempton (1964, 1985) related the residual friction angle to the clay-sized fraction as presented in Figure 8-20. The frictions angles were measured using ring shear tests performed on normally consolidated and overconsolidated samples.

Using published results, Voight (1973) developed the correlation presented in Figure 8-21(top) to estimate the residual strength of clays based on the plasticity index. Voight's correlation was later supported by the residual strength measurements performed by Bovis (1985) whose results can be seen in Figure 8-21(bottom).

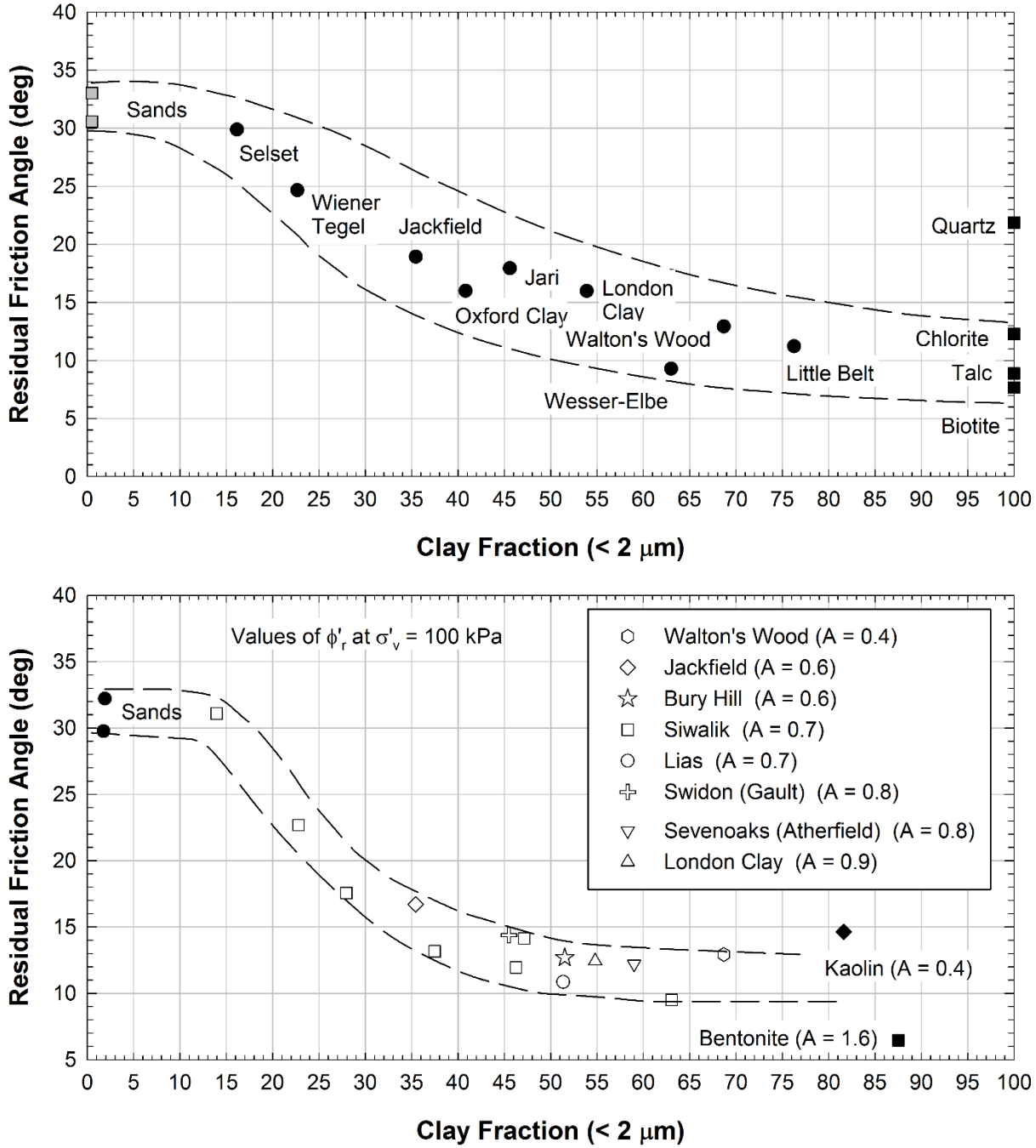

Figure 8-20 Correlation between the Residual Friction Angle and Clay-sized Fraction (after Skempton 1964, 1985)

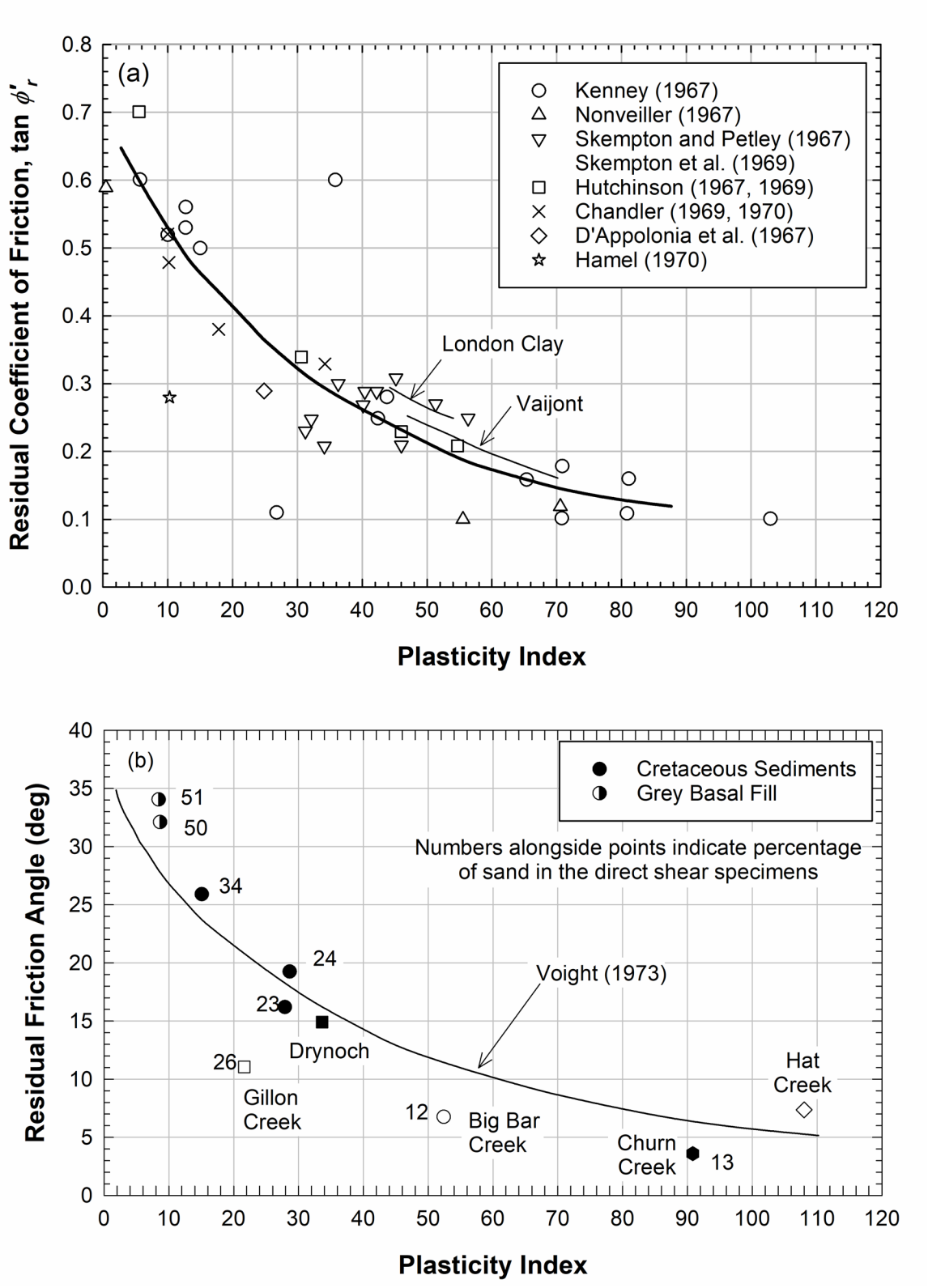

Figure 8-21 Residual Friction Angle vs. Plasticity Index – (top) Data Collected by Voight (1973), and (bottom) Measurements by Bovis (1985)

Stark and Hussain (2013) correlated the residual friction angle of clays to the liquid limit for various ranges of clay sized fraction as shown in Figure 8-22. This correlation needs to be used with care because of the methods that were used to process the soil samples for index property measurements were not consistent. For this correlation, the index properties of clay samples were obtained from specimens sieved through a No. 40 sieve without any other processing. On the other hand, shale samples were ball-milled and sieved through a No. 200 sieve. These differences in the procedures used to process samples for measuring the index properties should be considered when using the correlation.

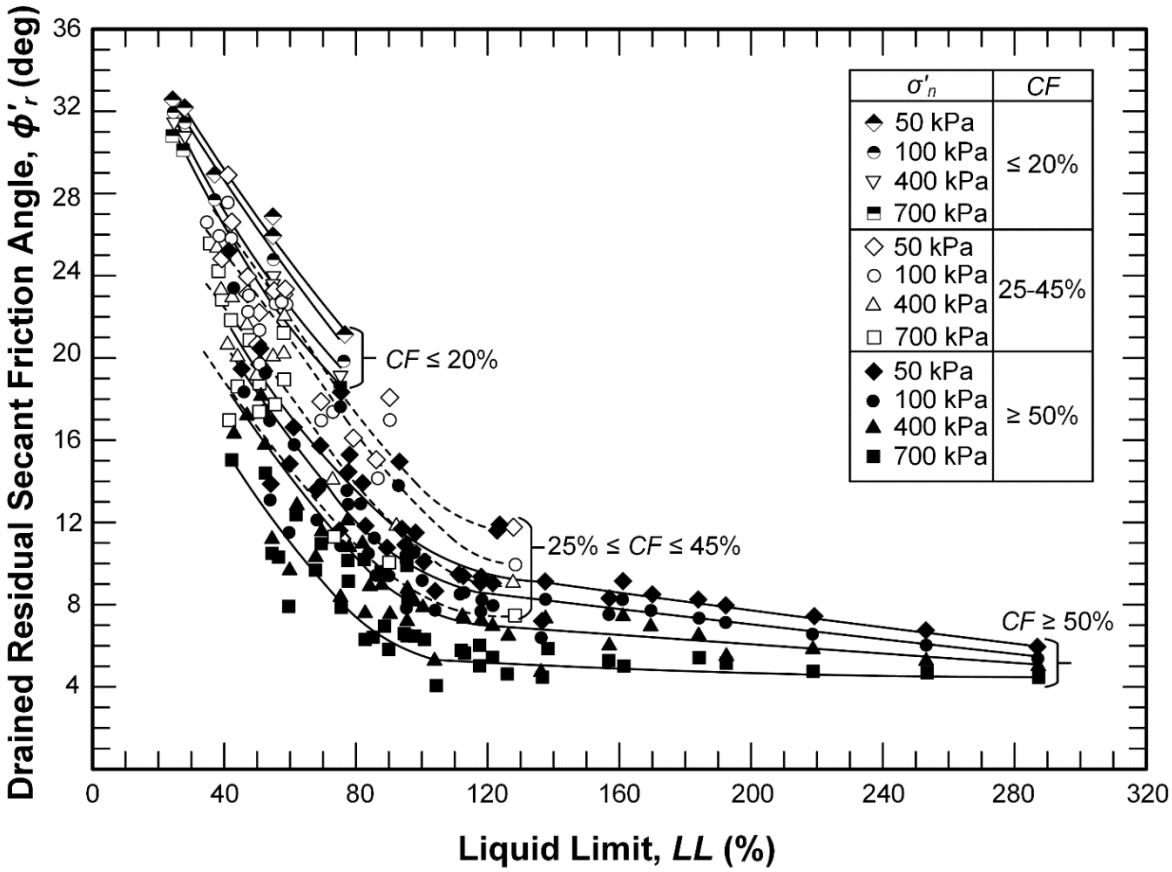

Figure 8-22 Drained Residual Secant Friction Angle as a Function of LL and CF (after Stark and Hussain 2013)

Stark and Hussain (2013) correlation provides stress-dependent residual secant friction angles for four different value of effective normal stress ranging from 50 to 700 kPa. The trends can be calculated as

$$\phi'_r = C_0 + C_1 \cdot LL + C_2 \cdot LL^2 + C_3 \cdot LL^3 \quad \textbf{(8-17)}$$

where:
LL = liquid limit and
C_0, C_1, C_2, and C_3 = empirical coefficients listed in Table 8-6.

Table 8-6 Coefficients for Stark and Hussain (2013) Residual Friction Angle Correlation

CF and *LL* Range	Effective normal stress σ′ (kPa)	Coefficients for Equation 8-17			
		C_0	C_1	C_2	C_3
CF < 20%	50	39.7	-0.29	6.63E-04	0
	100	39.4	-0.298	6.81E-04	0
	400	40.2	-0.375	1.36E-03	0
	700	40.3	-0.412	1.68E-03	0
25% < CF < 45%	50	31.4	-6.79E-03	-3.62E-03	1.86E-05
	100	29.8	-3.63E-04	-3.58E-03	1.85E-05
	400	28.4	-5.62E-02	-2.95E-03	1.72E-05
	700	28.1	-0.2083	-8.18E-04	9.37E-06
CF > 50% and LL < 120	50	33.5	-0.31	3.90E-04	4.40E-06
	100	30.7	-0.2504	-4.21E-04	8.05E-06
	400	29.4	-0.2621	-4.01E-04	8.72E-06
	700	27.7	-0.3233	2.90E-04	7.11E-06
CF > 50% and 120 < LL < 300	50	12.0	-0.0215	0	0
	100	10.9	-0.0183	0	0
	400	8.3	-0.0114	0	0
	700	5.8	-0.0049	0	0

Laboratory testing at Virginia Tech has produced correlations for residual shear strength based on the results of torsional ring shear tests on 102 clays with plasticity indices between 6 and 112, liquid limits between 22 and 143, and clay fractions ranging from 13 to 90%. Figure 8-23 and Figure 8-24 present the relationship between power function parameters (see Equation 8-15), plasticity index, and clay fraction.

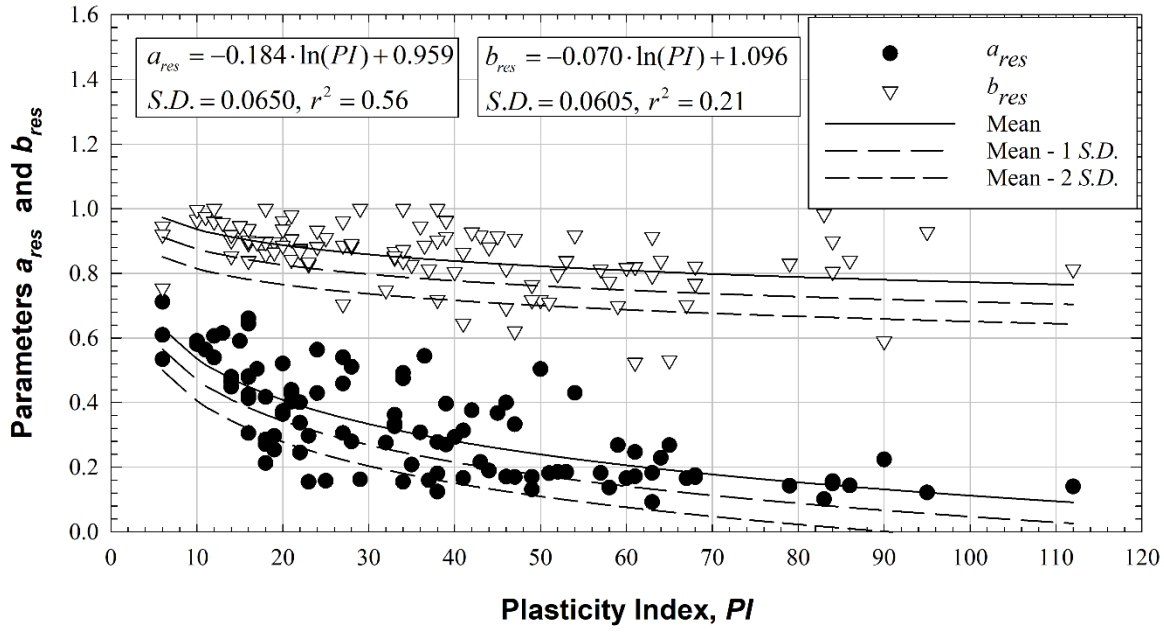

Figure 8-23 Residual Shear Strength Power Function Parameters Related to Plasticity Index (after Castellanos et al. 2021)

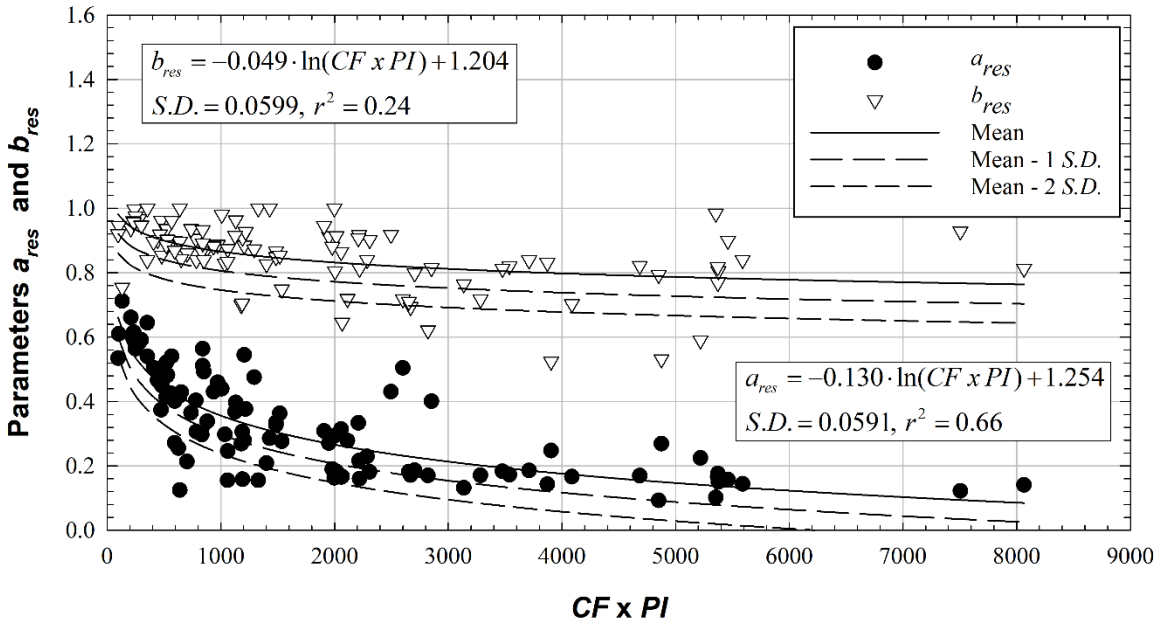

Figure 8-24 Residual Shear Strength Power Function Parameters Related to Plasticity Index and Clay Fraction (after Castellanos et al. 2021)

8-3 UNDRAINED SHEAR STRENGTH.

8-3.1 Correlations with Index Properties.

Skempton and Northey (1952) presented the relationship shown in Figure 8-25 that related the undrained shear strength of normally consolidated clays to the liquidity index. Terzaghi et al. (1996) demonstrated a strong relationship between the undrained shear strength of remolded clays and the liquidity index as shown in Figure 8-26. The results show similar behavior over a wider range of liquidity index to that observed by Skempton and Northey (1952).

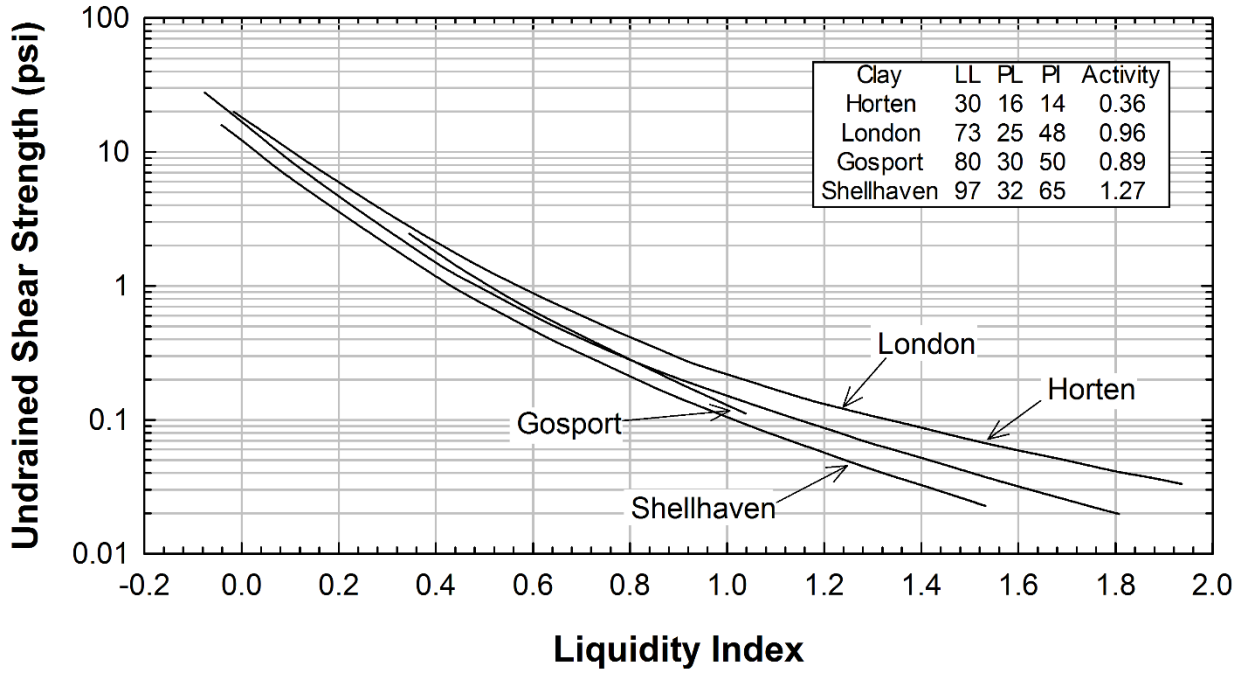

Figure 8-25 Relation between Liquidity Index and Undrained Shear Strength of Remolded Clays (after Skempton and Northey 1952)

Skempton (1957) compiled data from various sources to estimate the undrained shear strength of normally consolidated clay based on plasticity index as:

$$\frac{s_u}{\sigma'_v} = 0.11 + 0.0037PI \qquad \textbf{(8-18)}$$

where:
s_u = undrained shear strength,
σ'_v = vertical effective stress, and
PI = plasticity index (%).

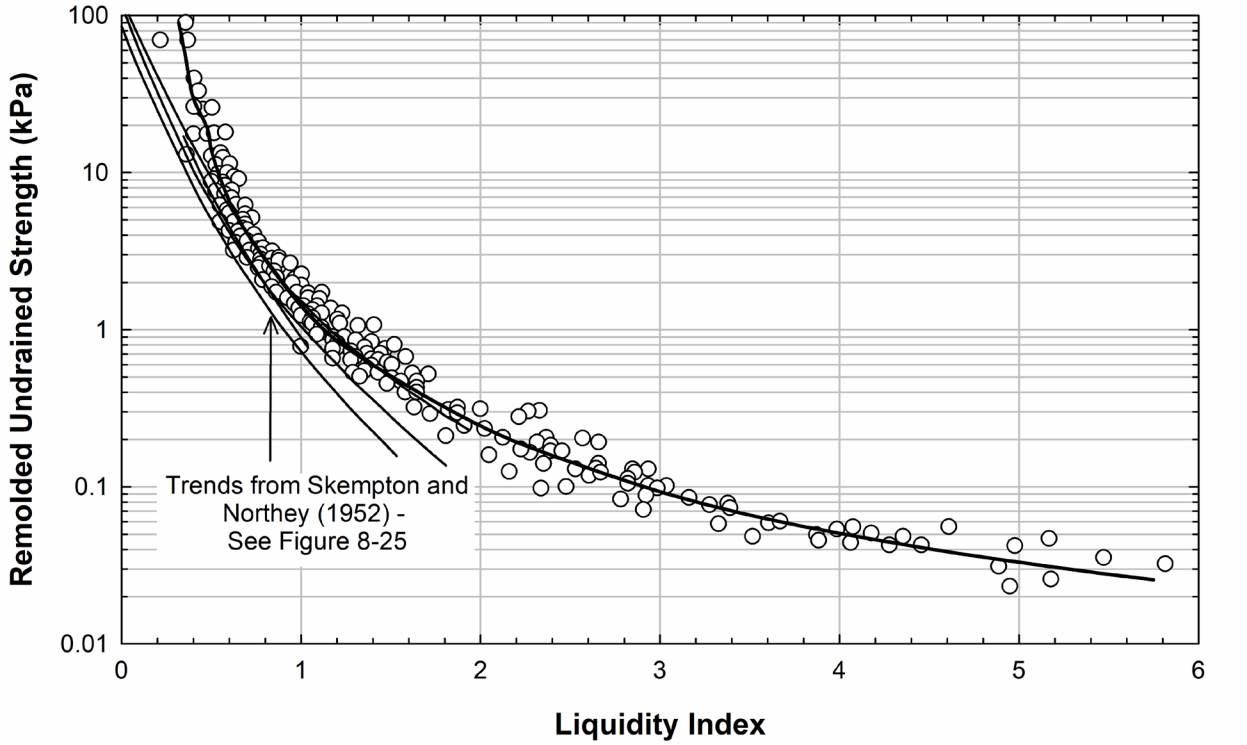

Figure 8-26 Relationship between Remolded Undrained Shear Strength and Liquidity Index (after Terzaghi et al. 1996)

Skempton's (1957) correlation, which is plotted in Figure 8-27, was based primarily on the results of field vane tests. It is unlikely that these shear strengths were corrected as required by ASTM D2573, meaning the values might be too high. The correlation presented by Skempton (1957) was later supported by Robertson and Campanella (1984) using vane shear test results presented by Ladd and Foott (1974).

A similar correlation based on laboratory tests was presented by Ladd and DeGroot (2004) and is shown in Figure 8-28. The correlation presented Ladd and DeGroot (2004) shows the dependency of the undrained shear strength on the laboratory stress path used to obtain the measurement.

Larson (1980) collected the undrained strength ratios and liquid limits of normally consolidated Scandinavian clays from various sources. These data is plotted in Figure 8-29 along with the equation proposed by Hansbo (1957):

$$\left(\frac{s_u}{\sigma'_v}\right)_{NC} = 0.0045LL \qquad \textbf{(8-19)}$$

where:
s_u = undrained shear strength (normally consolidated),
σ'_v = vertical effective stress, and
LL = liquid limit (%).

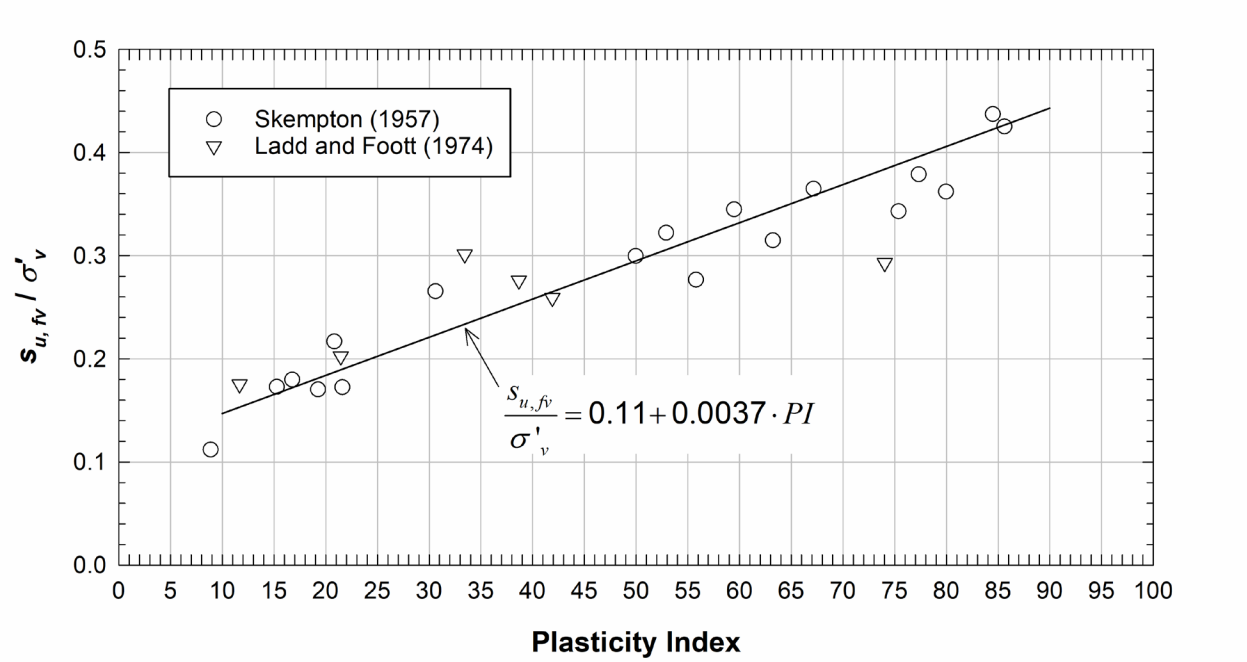

Figure 8-27 Correlation between Undrained Strength Ratio and Plasticity Index – Field Vane (after Robertson and Campanella 1984)

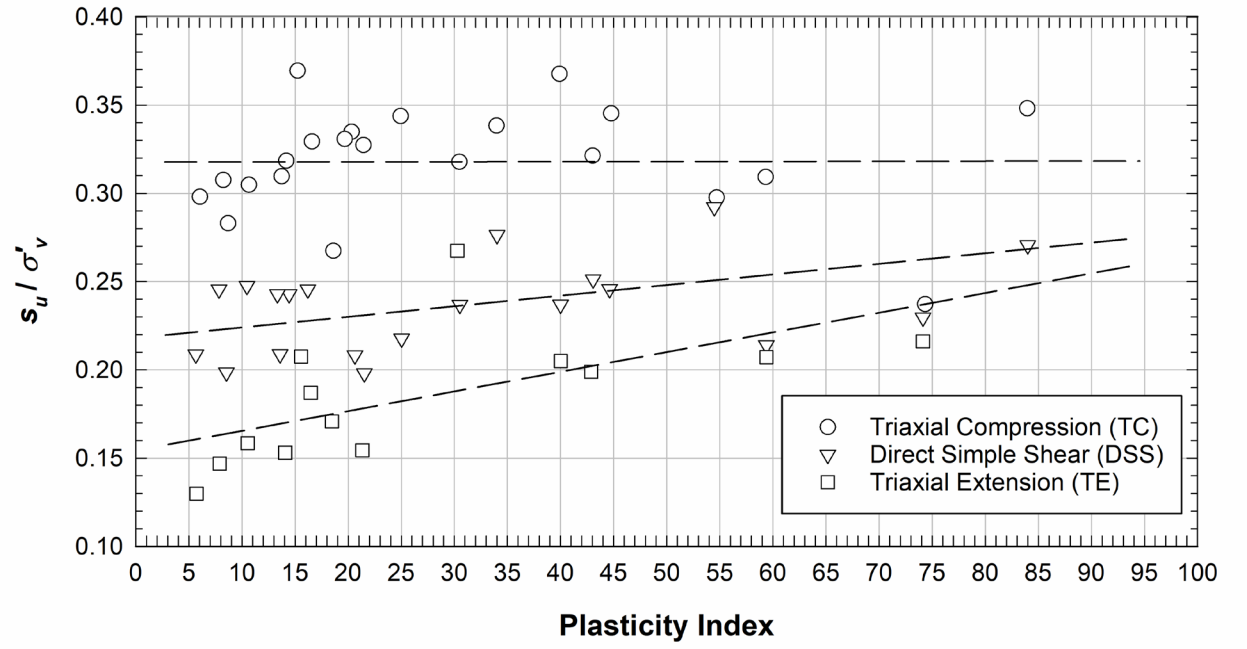

Figure 8-28 Correlation between Undrained Strength Ratio and Plasticity Index – Laboratory Testing (after Ladd and DeGroot 2004)

The data collected by Larson (1980), which is from field vane tests, agrees well with the Equation 8-19. Larson (1980) discusses various methods for correcting undrained strength measured using the vane shear but it is not clear whether or not the data in Figure 8-29 were corrected.

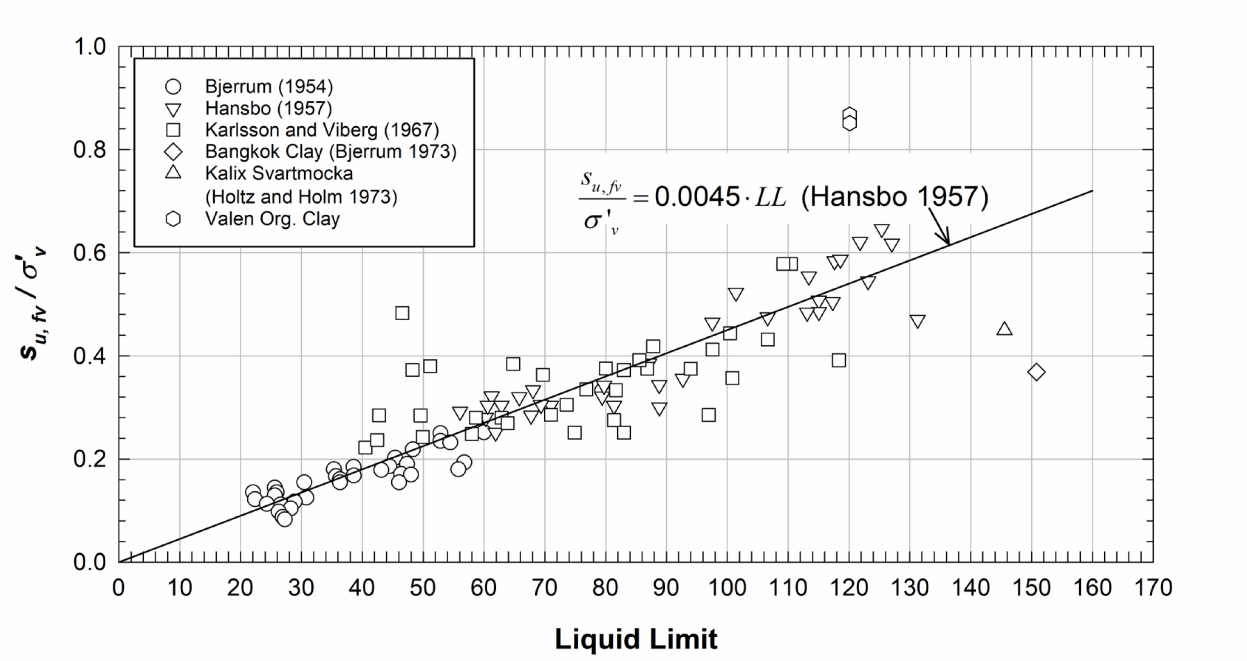

Figure 8-29 Variation of the Undrained Strength Ratio with Liquid Limit (after Larson 1980)

8-3.2 Correlations with Stress History.

Mesri (1975) corrected the results of vane shear tests from the literature with the vane correction factor proposed by Bjerrum (1972) and found that the undrained strength ratio for normally consolidated soil is relatively constant. Similarly, Jamiolkowski et al. (1985) found relatively constant values of normally consolidated undrained strength ratio for clays with PI less than 60. Chandler (1988) and Ladd and DeGroot (2004) also analyzed undrained strength data sets to determine typical values of undrained strength ratio for various types of clay. These trends are summarized in Table 8-7.

Overconsolidation results in an increase in the undrained shear strength. Schmertmann (1978) compared the undrained strength ratio for overconsolidated clays to that for normally consolidated clays as a function of OCR as summarized in Table 8-8 and Figure 8-30.

Table 8-7 Typical Normally Consolidated Undrained Strength Ratios

Source	NC Undrained Strength Ratio	Comments
Mesri (1975)	0.22 ± 0.03	Collection of vane shear test results
Jamiolkowski et al. (1985)	0.23 ± 0.04	Clays with PI less than 60 based on several embankment failures
Chandler (1988)	Range: 0.16 to 0.33 High value: 0.74 Mean (all): 0.28 Mean (discard extreme values): 0.22 ± 0.05	Based on the Mesri (1975) dataset of field vane shear tests on clay
Sabatini et al. (2002)	0.23	Saturated clay
	0.16	Soils with horizontal layering or features
Ladd and DeGroot (2004)	Nominally 0.20 Std. Dev. = 0.015	Sensitive cemented marine clays, Canadian Champlain clays (PI < 30%, LI > 1.5)
	$0.22+0.05\left(\frac{PI}{100}\right)$ Nominally 0.22	Homogeneous CL and CH sedimentary clays of low to moderate sensitivity, no shells or sand lenses layers (PI = 20 to 80%)
	0.16	Northeastern U.S. varved clays, direct simple shear failure mode
	Nominally 0.25 Std. Dev. = 0.05	Sedimentary deposits of silts and organic soils (Atterberg Limits plot below A-line) and clays with shells, excludes peat

Notes: PI = plasticity index, LI = liquid index
Shear strengths presented by Jamiolkowski et al. (1985) and Chandler (1988) were not corrected as required by ASTM D2573 and may be too high.

Table 8-8 Approximate Relation of Undrained Strength Ratio and OCR (after Schmertmann 1978)

OCR	Undrained Strength Ratio
Less than 1	0 – 0.1
1	0.10 – 0.25
1 to 1.5	0.26 – 0.50
3	0.51 – 1.00
6	1.00 – 4.00
Greater than 6	> 4.00

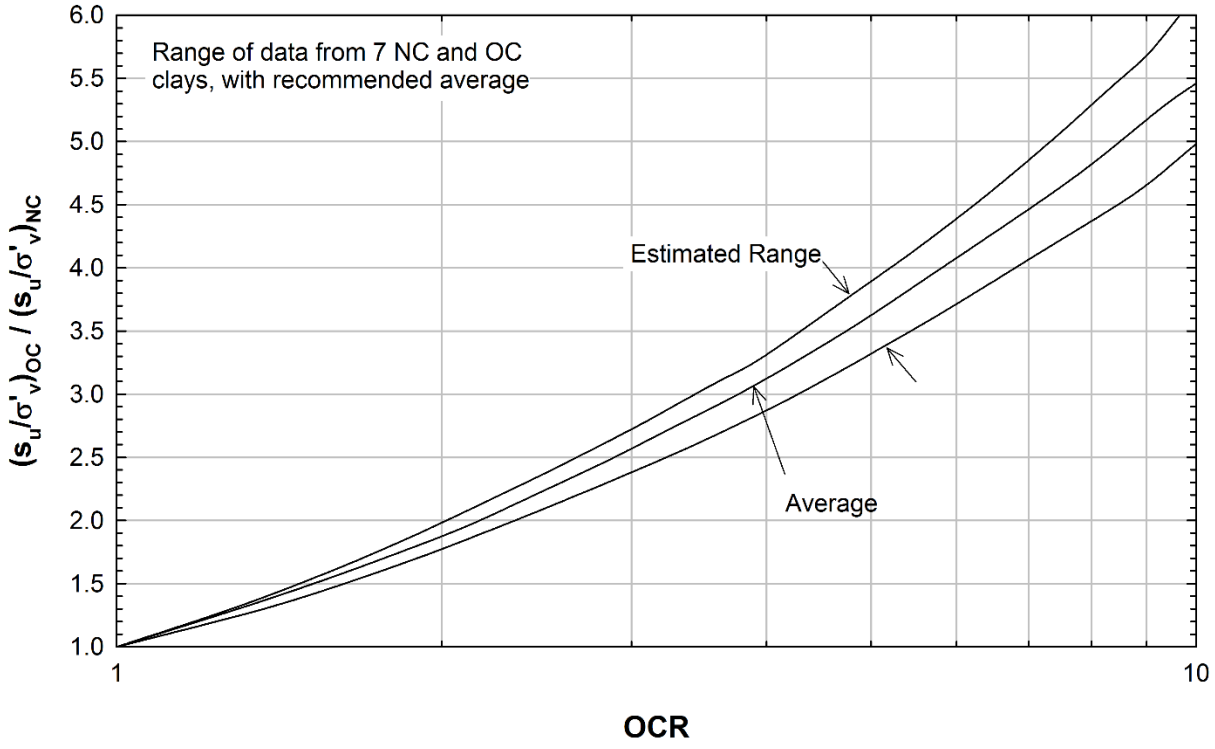

Figure 8-30 Normalized Undrained Strength Ratio vs. OCR (after Schmertmann 1978)

For overconsolidated clays, Jamiolkowski et al. (1985) and Ladd and DeGroot (2004) showed that the effects of stress history on the undrained shear strength ratio can be accounted for by:

$$\left(\frac{s_u}{\sigma'_v}\right)_{OC} = \left(\frac{s_u}{\sigma'_v}\right)_{NC} OCR^m \qquad \textbf{(8-20)}$$

where:
s_u = undrained shear strength (NC = normally consolidated, OC = overconsolidated),
σ'_v = vertical effective stress,
OCR = overconsolidation ratio, and
m = semi-empirical fitting parameter.

The value of m is theoretically related to the recompression and compression indices as shown by Roscoe et al. (1958) and Mitachi and Kitago (1976) for ideal or remolded soils.[14] For real soils, undrained laboratory shear strength tests on soil specimens at different values of OCR can be used to determine m. Ladd et al. (1977) observed that

[14] For this to be true, ideal or remolded soils must be assumed to follow the tenets of critical state soil mechanics. This assumption breaks down for soils exhibiting post-peak strain softening. This idealization also assumes that C_c and C_r are log-linear for all ranges of stresses and for any rebound pressure.

m is approximately 0.8 based on direct simple shear tests. Typical values for m are summarized in Table 8-9.

Table 8-9 Typical Values of m

Source	m	Soil Description
Roscoe et al. (1958), Mitachi and Kitago (1976)	$m \approx 1 - \frac{C_r}{C_c}$	Saturated clay (theoretical)
Jamiolkowski et al. (1985), Chandler (1988)	Range: 0.8 to 1.35 High value: 1.51 Mean (all): 1.03 Mean (discarding extreme values): 0.97	Field vane shear tests on clay
Sabatini et al. (2002)	0.8	Saturated clay
Ladd and DeGroot (2004)	1.00	Sensitive cemented marine clays, Canadian Champlain clays ($PI < 30\%, LI > 1.5$)
	$0.88 \cdot \left(1 - \frac{C_r}{C_c}\right) \pm 0.06$ Nominally 0.8	Homogeneous CL and CH sedimentary clays of low to moderate sensitivity, no shells or sand lenses layers (PI = 20 to 80%)
	0.75	Northeastern U.S. varved clays, direct simple shear failure mode
	$0.88 \cdot \left(1 - \frac{C_r}{C_c}\right) \pm 0.06$ Nominally 0.8	Sedimentary deposits of silts and organic soils with Atterberg Limits below the A-line and clays with shells, excludes peat
Note: C_c = compression index and C_r = recompression index		

For very soft clays with overconsolidation ratios less than 2, Sabatini et al. (2002) found that the undrained shear strength could be estimated as (assumes m equals 1):

$$s_u \approx 0.21\sigma'_p \quad \textbf{(8-21)}$$

where:
s_u = undrained shear strength and
σ'_p = preconsolidation pressure.

The consolidation stress state in triaxial compression tests also influences the undrained shear strength. Based on data from 48 normally consolidated clays, Mayne (1985) found that the ratio was about 0.87 for undrained shear strengths from K_0 consolidated and isotropically consolidated undrained triaxial compression tests.

Kulhawy and Mayne (1990) examined the data and found that the normally consolidated undrained strength ratio for K0-consolidated tests can be related to the isotopically consolidated tests by:

$$\left(\frac{s_u}{\sigma'_v}\right)_{ACU} = 0.15 + 0.49\left(\frac{s_u}{\sigma'_v}\right)_{ICU} \quad \textbf{(8-22)}$$

where:
$(s_u / \sigma'_v)_{ACU}$ = undrained strength ratio in CK_0U triaxial compression, and
$(s_u / \sigma'_v)_{ICU}$ = undrained strength ratio in ICU triaxial compression.

8-3.3 Correlations with Cone Penetration Test.

Undrained shear strength is typically estimated from the cone tip resistance measured in the CPT using methods based on bearing capacity. The three methods are the N_c, N_k, and N_{kt} methods as defined by Lunne et al. (1997). The empirical bearing capacity factors (N_c, N_k, and N_{kt}) should be calibrated on a site- or region-specific basis by relating known values of undrained shear strength measured using the triaxial device (ASTM D2166, ASTM D2850), laboratory miniature vane shear (ASTM D4648), field vane shear (ASTM D2573), or direct simple shear (ASTM D6528) to the predicted values based on Equations 8-23 to 8-25.

The N_c method is the simplest and directly relates the CPT tip resistance to the undrained shear strength as:

$$s_u = \frac{q_c}{N_c} \quad \textbf{(8-23)}$$

where:
q_c = cone tip resistance, and
N_c = empirical bearing capacity factor.

In most cases, the value of N_c is in the range of 17 to 23 for normally consolidated and slightly overconsolidated clays. The N_c method may be less accurate than other methods at depths greater than 15 m because the overburden pressure is not considered.

The N_k method considers the overburden pressure acting at the point of the measurement. Based on this method, the undrained shear strength can be determined from CPT results as:

$$s_u = \frac{q_c - \sigma_v}{N_k} \quad \textbf{(8-24)}$$

where:
q_c = cone tip resistance,
σ_v = total vertical stress, and
N_k = empirical bearing capacity factor.

Data presented by Lunne and Kleven (1982), shows that N_k ranges from about 10 to about 19 with an average of 15. Carter and Bentley (2016) suggest values of 17 or 18 for normally consolidated clays and 20 for overconsolidated clays.

The N_{kt} method is a modification of the N_k method that considers the pore pressure acting at the tip of the cone. The undrained shear strength is calculated as:

$$s_u = \frac{q_t - \sigma_v}{N_{kt}} \quad \textbf{(8-25)}$$

where:
q_c = cone tip resistance,
σ_v = total vertical stress,
N_{kt} = empirical bearing capacity factor,
q_t = corrected tip resistance = $q_c + u \cdot (1+a)$,
u = pore pressure measured behind the cone tip, often called the u_2 position.
a = cone net area ratio = ratio of the face area to shoulder area.

Modern cones have net area ratios above 0.8 and little difference is typically observed in the N_k and N_{kt} methods. Values of N_{kt} are often in the range of 14 to 16.

8-3.4 Correlations with Standard Penetration Test.

Various attempts have been made to correlate the undrained shear strength of clays to SPT N values. Observed ranges of undrained shear strength based on soil consistency and N are summarized in Table 8-10.

Table 8-10 Approximate Undrained Shear Strength for Cohesive Soils Based on SPT N

Soil Consistency	SPT N Value	Undrained Shear Strength (psf)		
		Parcher and Means (1968)	Tschebotarioff (1973)	Terzaghi et al. (1996)
Very soft	< 2	300	-	< 250
Soft	2 – 4	300 – 600	250 – 500	250 – 500
Medium	4 – 8	600 – 1200	500 – 1000	500 – 1000
Stiff	8 – 15	1200 – 2400	1000 – 2000	1000 – 2000
Very stiff	15 – 30	2400	2000 – 4000	2000 – 4000
Hard	> 30	> 4500	> 4000	> 4000

Stroud and Butler (1975) developed a correlation for the undrained shear strength of overconsolidated clays as a function of the SPT N value. As shown in Figure 8-31, the relationship exhibits significant scatter, which reduces the reliability of the correlation. Carter and Bentley (2016) approximated the trendline in Figure 8-31 as:

$$\frac{s_u}{N} = \frac{8910}{PI^3} + 4.36 \quad \textbf{(8-26)}$$

where:
s_u = undrained shear strength (in kPa),
N = SPT-N value, and
PI = plasticity index.

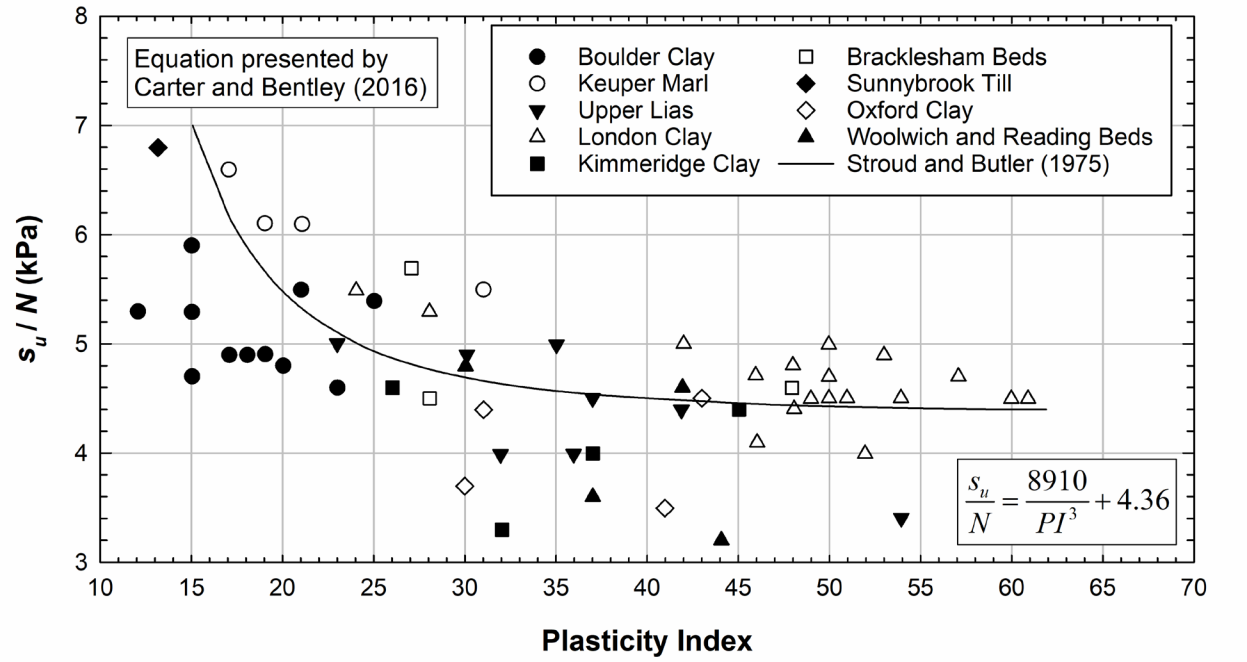

Figure 8-31 Correlation between Undrained Shear Strength, SPT N Value, and Plasticity Index for Overconsolidated Clays (after Stroud and Butler 1975)

Sowers (1979) correlated undrained shear strength to SPT N for different USCS soil classifications as presented in Figure 8-32. Relationships proposed by Hara et al. (1974) and Terzaghi and Peck (1967) are also presented in Figure 8-32. Hara et al.'s correlation is based on undrained shear strengths from triaxial compression tests.

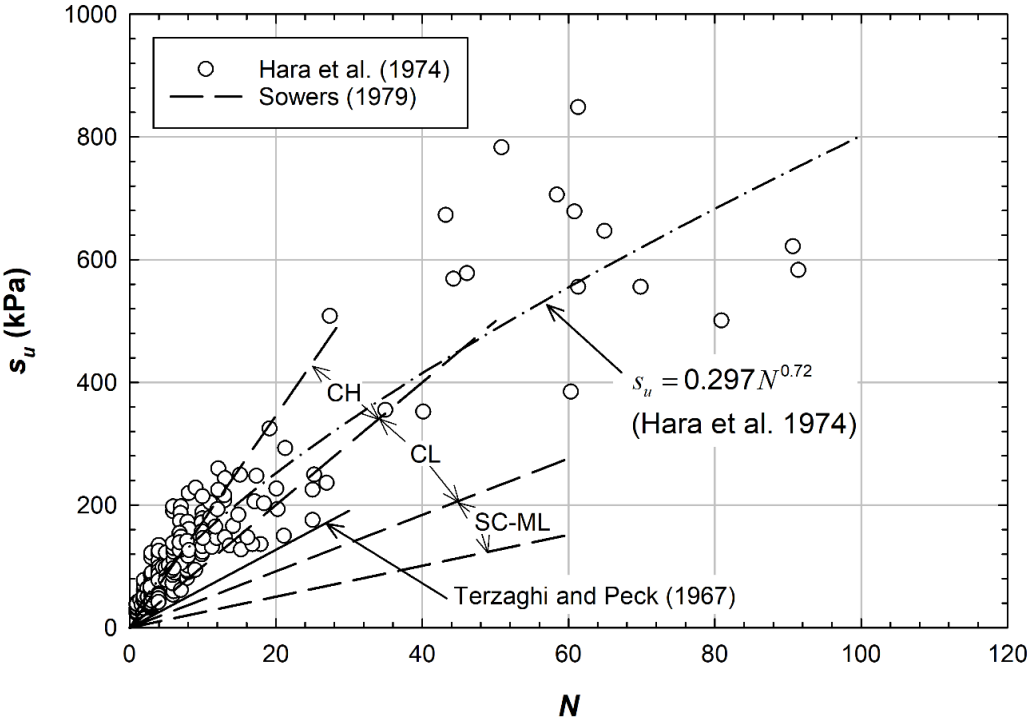

Figure 8-32 Relationship between Undrained Shear Strength and SPT N (after Terzaghi and Peck 1967, Hara et al. 1974, and Sowers 1979)

8-3.5 Correlations with Dilatometer.

The undrained shear strength of overconsolidated clays has been correlated to the horizontal stress index (K_D) and the dilatometer modulus (E_D) as summarized in Table 8-11.

Table 8-11 Undrained Shear Strength Correlations to Dilatometer

Undrained Strength Ratio or Undrained Shear Strength (kPa)	Source
$\left(\frac{s_u}{\sigma'_v}\right)_{OC} = \left(\frac{s_u}{\sigma'_v}\right)_{NC} (0.5K_D)^{1.25} \approx 0.22(0.5K_D)^{1.25}$	Marchetti (1980)
$\left(\frac{s_u}{\sigma'_v}\right)_{OC} = 0.35(0.47K_D)^{1.14}$	Kamei and Iwasaki (1995)
$s_u = 0.018E_D$	Iwasaki and Kamei (1994)

Note:
s_u = undrained shear strength in kPa, σ'_v = vertical effective stress in kPa,
K_D = horizontal stress index from dilatometer, and E_D = dilatometer modulus in kPa.

8-4 CONSOLIDATION PARAMETERS.

8-4.1 Compression and Recompression Indices – Fine-Grained.

The *compression index* (C_c) is the slope of the virgin consolidation line of the e vs. log(σ'_v) plot. The *recompression index* (C_r) is the slope of the recompression line of the e vs. log(σ'_v) plot. These parameters are used to calculate the compression of the clay when subjected to an increase in stress in the normally consolidated and overconsolidated ranges (See Section 5-5.2.1). An alternative of the compression and recompression indices are the *modified compression index* ($C_{\varepsilon c}$) and *modified recompression index*, $C_{\varepsilon r}$ (a.k.a., compression and recompression ratio). The modified compression and recompression indices are equal to the compression and recompression indices divided by ($1+e_0$), respectively. These are the slopes of the compression and recompression curves when vertical strain is used instead of void ratio.

8-4.1.1 Typical Values.

Typical values of the compression index for different clays and silts are summarized in Table 8-12.

Table 8-12 Typical Values for C_c for Undisturbed Clays

Soil	C_c	Reference
Boston Blue Clay, undisturbed (CL)	0.35	Lambe and Whitman (1969)
Chicago clay undisturbed (CH)	0.42	
Cincinnati Clay (CL)	0.17	
Louisiana Clay, undisturbed	0.33	
New Orleans Clay, undisturbed (CH)	0.29	
Siburua clay (CH)	0.21	
Kaolinite	0.21 – 0.26	
Na-Montmorillonite (CH)	2.6	
Normally consolidated medium sensitive clays	0.2 – 0.5	Holtz and Kovacs (1981)
Organic silt and clayey silts (ML-MH)	1.5 – 4.0	
Organic clays (OH)	> 4.0	
Peat (Pt)	10 – 15	
Chicago silty clay (CL)	0.15 – 0.30	
Boston Blue Clay (CL)	0.3 – 0.5	
Vicksburg Buckshot Clay (CH)	0.5 – 0.6	
Swedish medium sensitive clays (CL-CH)	1 – 3	
Canadian Leda clays (CL-CH)	1 – 4	
Mexico City Clay	7 – 10	
San Francisco Bay Mud (CL)	0.4 – 1.2	
Bangkok Clays (CH)	0.4	
Uniform sand, loose (SP)	0.05 – 0.06	USACE (1990)
Uniform sand, dense (SP)	0.02 – 0.03	
Uniform silts (ML)	0.2	

8-4.1.2 Correlations with Index Properties.

Many relationships have been developed to estimate the compression and recompression indices based on parameters, such as water content, liquid limit, and void ratio. Some of these correlations are summarized in Table 8-13 and Table 8-14 and plotted in Figure 8-33 thru Figure 8-38. As can be seen from these plots, the presented correlations estimate values of compression and recompression indices that vary significantly. For the compression index, the correlations using the natural water content tend to be in closer agreement compared to those based on other index properties. Prior to use, the soil type(s) used to develop the correlations and the sensitivity of the project to errors in the prediction of settlement should be considered to determine if the intended application matches.

Leroueil et al. (1983) showed that the sensitivity of the clay also affects the value of the compression index, especially for marine deposits. The results presented in Figure 8-39 show a significant effect of the sensitivity on the compression index.

Lambe and Whitman (1969) presented typical ranges of the modified compression index of clays as a function of the natural water content and these are shown in Figure 8-40.

Table 8-13 Compression Index Correlations

Correlation	Comments	References
$C_c = 0.007(LL - 10)$	Remolded clays.	Skempton (1944)
$C_c = 0.0046(LL - 9)$	Clays from Sao Paulo, Brazil	Cozzolino (1961)
$C_c = LL^{1.673} / 2040$	Hong Kong soft marine clay	Lumb and Holt (1968)
$C_c = 0.0083(LL - 9)$	Remolded clays	Schofield and Wroth (1968)
$C_c = 0.003(LL - 10)$	Cohesive soils of the Rhone Alpes and Valley of the Seine River	Gielly et al. (1969)
$C_c = 0.006(LL - 9)$	Clays for Greece and USA	Azzouz et al. (1976)
$C_c = 0.008(LL - 5)$	Dredging material	Salem and Krizek (1976)
$C_c = 0.00797(LL - 8.16)$	Indiana soils	Lo and Lovell (1982)
$C_c = 0.01(LL - 13)$	All clays	USACE (1990)
$C_c = 0.009(LL - 10)$	Undisturbed clay of sensitivity less than 4. Reliability 30%	Terzaghi et al. (1996)
$C_c = 1.15(e_0 - 0.91)$	All clays (Lower limit)	Nishida (1956)
$C_c = 0.30(e_0 - 0.27)$	Inorganic silty clays	Hough (1957)

Table 8 13 (cont.) Compression Index Correlations

Correlation	Comments	References
$C_c = 0.256 + 0.43(e_0 - 0.84)$	Brazilian motley clays	Cozzolino (1961)
$C_c = 1.21 + 1.055(e_0 - 1.87)$	Brazilian soft silty clays	
$C_c = 0.75(e_0 - 0.50)$	Soils of very low plasticity	Sowers (1970)
$C_c = 0.40(e_0 - 0.25)$	Clays for Greece and USA	Azzouz et al. (1976)
$C_c = 0.22 + 0.29e_0$	Weathered and soft Bangkok clays	Adikari (1977)
$C_c = 0.575e_0 - 0.241$	French clays	Vidalie (1977)
$C_c = 0.5363(e_0 - 0.411)$	Indiana soils	Goldberg et al. (1979)
$C_c = 0.5673(e_0 - 0.4422)$	Wabash Lowland	
$C_c = 0.4941(e_0 - 0.3507)$	Crawford Upland	
$C_c = 0.5621(e_0 - 0.4215)$	Outwash and alluvial deposits	
$C_c = 0.496e_0 - 0.195$	Indiana soils	Lo and Lovell (1982)
$C_c = 0.3745e_0$	Saturated clays	Rendon-Herrero (1983)
$C_c = 0.434(e_0 - 0.336)$	Soils from nine states in the USA	
$C_c = 0.85\left(w_n/100\right)^{3/2}$	Finnish muds and clays	Helenelund (1951)
$C_c = 0.01404w_n - 0.189$	All clays	Nishida (1956)
$C_c = 0.01w_n$	Chicago and Canada clays	Koppula (1981)
$C_c = 0.01(w_n - 5)$	Clays for Greece and USA	Azzouz et al. (1976)
$C_c = 0.008w_n + 0.2$	Weathered and soft Bangkok clays	Adikari (1977)
$C_c = 0.0147w_n - 0.213$	French clays	Vidalie (1977)
$C_c = 0.0133w_n - 0.1621$	Crawford Upland	Goldberg et al. (1979)
$C_c = 0.0126w_n - 0.162$	Indiana soils	Lo and Lovell (1982)
$C_c = 0.01w_n - 0.07549$	Soils from nine states in the USA	Rendon-Herrero (1983)
$C_c = 0.0115w_n$	Organic soils, peats	USACE (1990)
$C_c = 0.012w_n$	All Clays	
$C_c = 0.135PI$	Remolded clays	Wroth and Wood (1978)

$C_c = 0.005PI \cdot G_s$		

Table 8 13 (cont.) Compression Index Correlations

Correlation	Comments	References
$C_c = 0.37(e_0 + 0.003LL - 0.34)$	Clays for Greece and USA	Azzouz et al. (1976)
$C_c = 0.009e_0 + 0.008LL + 0.20$	Weathered and soft Bangkok clays	Adikari (1977)
$C_c = 0.0101(e_0 LL - 0.5765LL + 12.665)$	Crawford Upland	Goldberg et al. (1979)
$C_c = 0.40(e_0 + 0.001w_n - 0.25)$	Clays for Greece and USA	Azzouz et al. (1976)
$C_c = 0.009w_n + 0.002LL - 0.1$		
$C_c = 0.0129(w_n + 0.1015LL - 16.1875)$	Indiana soils	Goldberg et al. (1979)
$C_c = 0.0114(w_n + 0.2491LL - 18.8134)$	Crawford Upland	Goldberg et al. (1979)
$C_c = 0.0082w_n + 0.0043CF - 0.1403$	Cohesive soils in Alberta, Canada	Koppula (1981)
$C_c = 0.37(e_0 + 0.003LL + 0.0004w_n - 0.34)$	Clays for Greece and USA	Azzouz et al. (1976)
$C_c = 0.0153(w_n + 0.1022LL - 0.3104PL - 11.623)$	Indiana soils	Goldberg et al. (1979)
$C_c = 0.5684(e_0 + 0.033LL - 0.0082PL + 0.0329\sigma'_p - 0.4322)$		
$C_c = 0.6076(e_0 + 0.003LL - 0.0095PL + 0.43\sigma'_p - 0.4186)$	Outwash and alluvial deposits	
$C_c = 0.0025CF + 0.1165e_0 + 0.0036w_n + 0.0014PI + 0.0009PL - 0.997$	Cohesive soils in Alberta, Canada	Koppula (1981)
$C_c = 0.5((1 + e_0)/G_s)^{2.4}$	Saturated clay	Al-Khafaji and Andersland (1992)
$C_c = 0.0121 \cdot w_n \cdot G_s$	Saturated sediment fine-grained soil	Rendon-Herrero (1983)
$C_c = 0.185\left[(1 + e_0)^2/G_s - 0.144\right]$	Soils from nine states in USA	
$C_c = 0.489\left[\ln\left(\frac{(1 + e_0)^2}{G_s}\right) + 0.296\right]$		
$C_c = 0.141G_s^{1.2}\left(\frac{1 + e_0}{G_s}\right)^{2.382}$		

Table 8-14 Recompression Index Correlations

Correlation	Comments	References
$C_r = 0.0045LL$	Marine clays of Southeast Asia	Cox (1968)
$C_r = 0.002(LL + 9)$	Clays for Greece and USA	Azzouz et al. (1976)
$C_r = 0.00463LL - 0.013$	Bangkok clays	Balasubramaniam and Brenner (1981)
$C_r = 0.00238LL + 0.0294$	Indiana soils	Lo and Lovell (1982)
$C_r = 0.208e_0 + 0.0083$	Chicago clays	Peck and Reed (1954)
$C_r = 0.156e_0 + 0.0107$	Inorganic and organic clayey and silty soil	Elnaggar and Krizek (1970)
$C_r = 0.14(e_0 + 0.007)$	Clays for Greece and USA	Azzouz et al. (1976)
$C_r = 0.2037(e_0 - 0.2465)$	Indiana soils	Goldberg et al. (1979)
$C_r = 0.221(e_0 - 0.3074)$	Wabash Lowland	
$C_r = 0.152e_0 + 0.0125$	Indiana soils	Lo and Lovell (1982)
$C_r = 0.0043w_{n\ \gamma_m}\delta$	Marine clays of Southeast Asia	Cox (1968)
$C_r = 0.003(w_n + 7)$	Clays for Greece and USA	Azzouz et al. (1976)
$C_r = 0.0039w_n + 0.013$ for $w_n < 100\%$	French clays	Vidalie (1977)
$C_r = 0.403\log(w_n) - 0.478$		
$C_r = 0.0065(w_n - 11.6361)$	Wabash Lowland	Goldberg et al. (1979)
$C_r = 0.00566w_n - 0.037$	Bangkok clays	Balasubramaniam and Brenner (1981)
$C_r = 0.003w_n + 0.0249$	Indiana soils	Lo and Lovell (1982)
$C_r = PI/370$	Remolded clays	Wroth and Wood (1978)
$C_r = 0.126(e_0 + 0.003LL - 0.06)$	Clays for Greece and USA	Azzouz et al. (1976)
$C_r = 0.142(e_0 - 0.0009w_n + 0.006)$		
$C_r = 0.0034(e_0 w_n + 8.3647)$	Wabash Lowland	Goldberg et al. (1979)
$C_r = 0.0033(e_0 w_n + 12.5168)$)	Crawford Upland	
$C_r = 0.003w_n + 0.0006LL + 0.004$	Clays for Greece and USA	Azzouz et al. (1976)
$C_r = 0.135(e_0 + 0.01LL - 0.002w_n - 0.06)$		

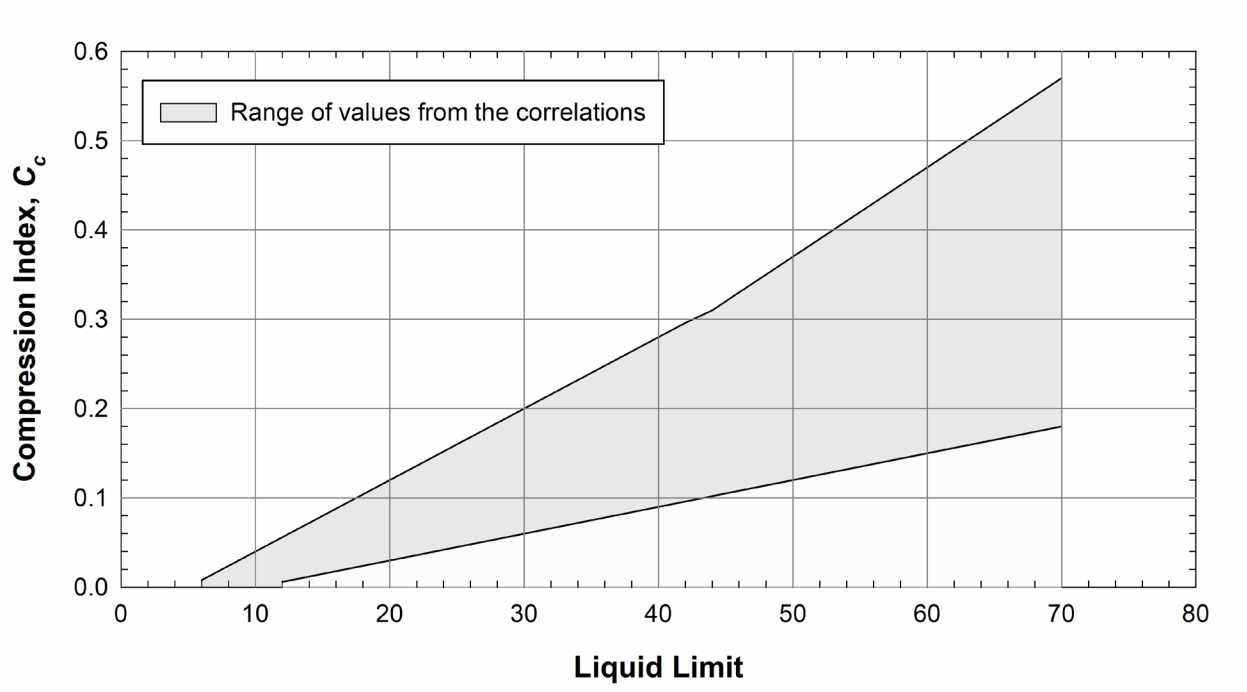

Figure 8-33 Range of Compression Index based on Liquid Limit Predicted by Correlations

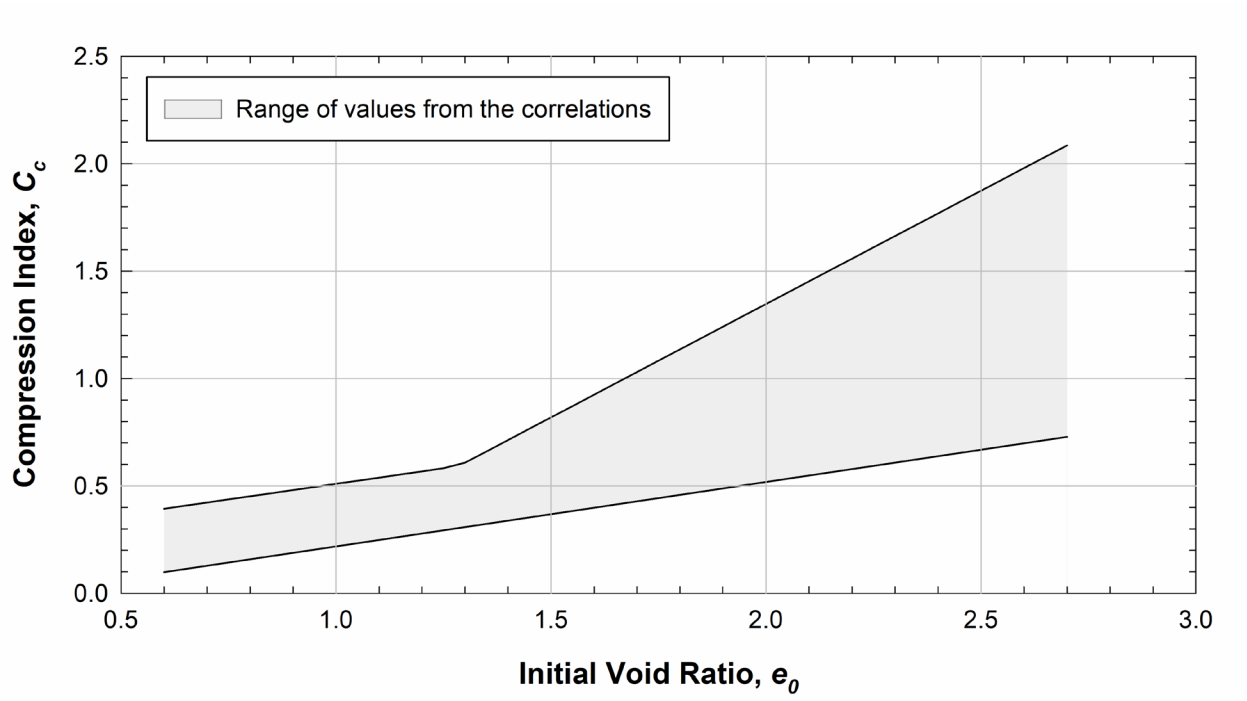

Figure 8-34 Range of Compression Index based on Initial Void Ratio Predicted by Correlations

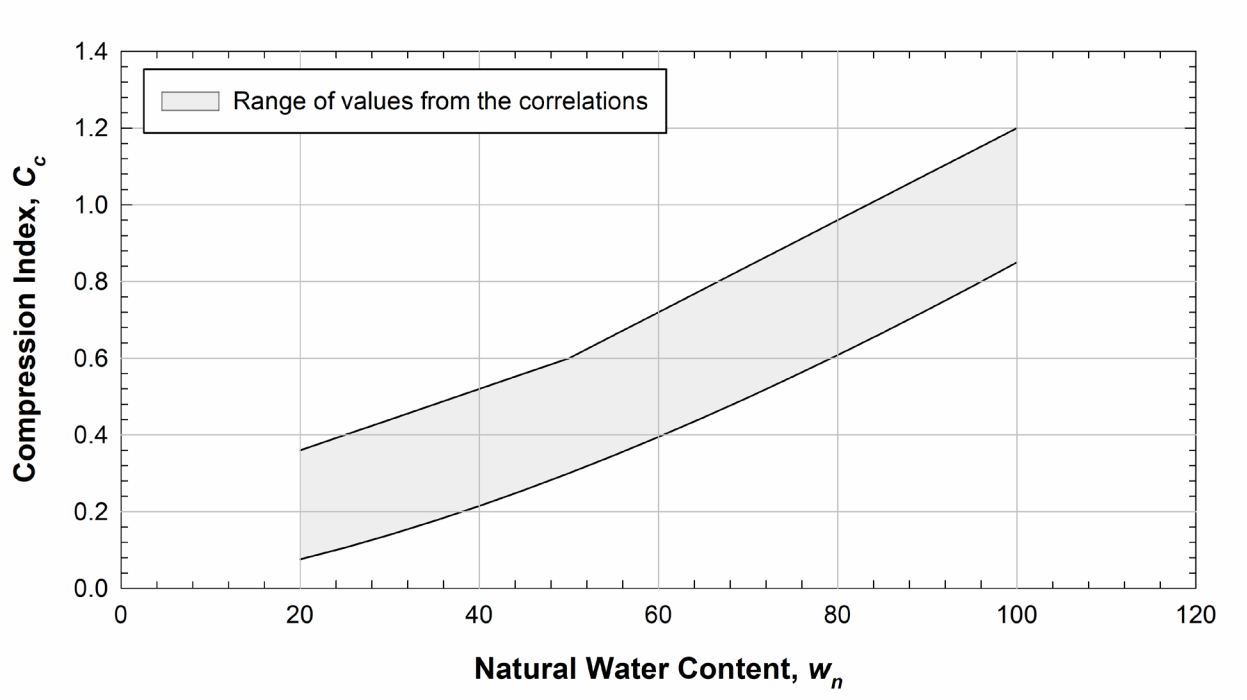

Figure 8-35 Range of Compression Index based on Natural Water Content Predicted by Correlations

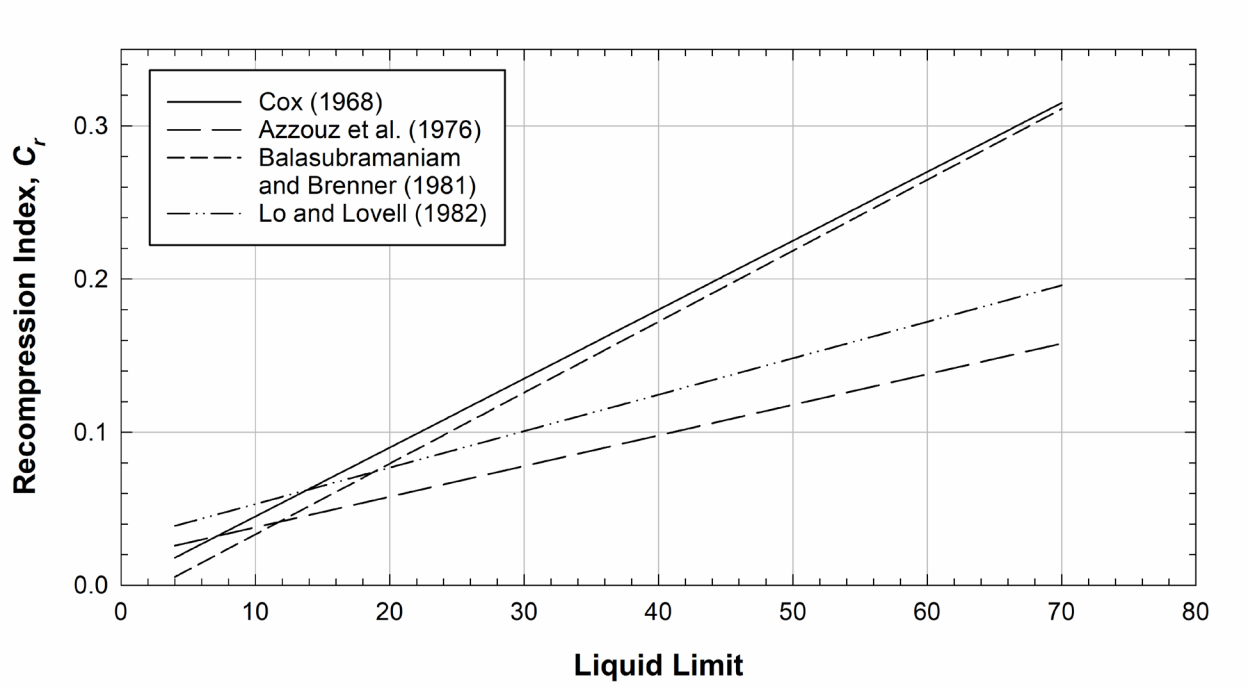

Figure 8-36 Correlations for Recompression Index based on Liquid Limit

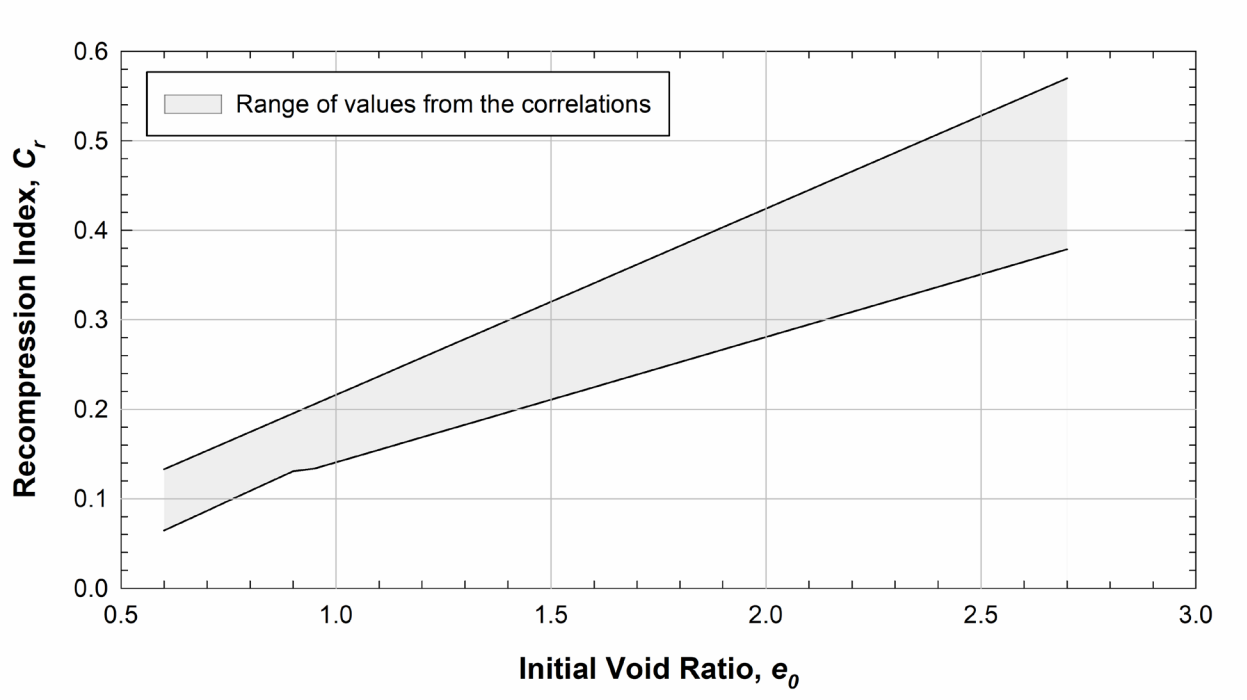

Figure 8-37 Range of Recompression Index based on Initial Void Ratio Predicted by Correlations

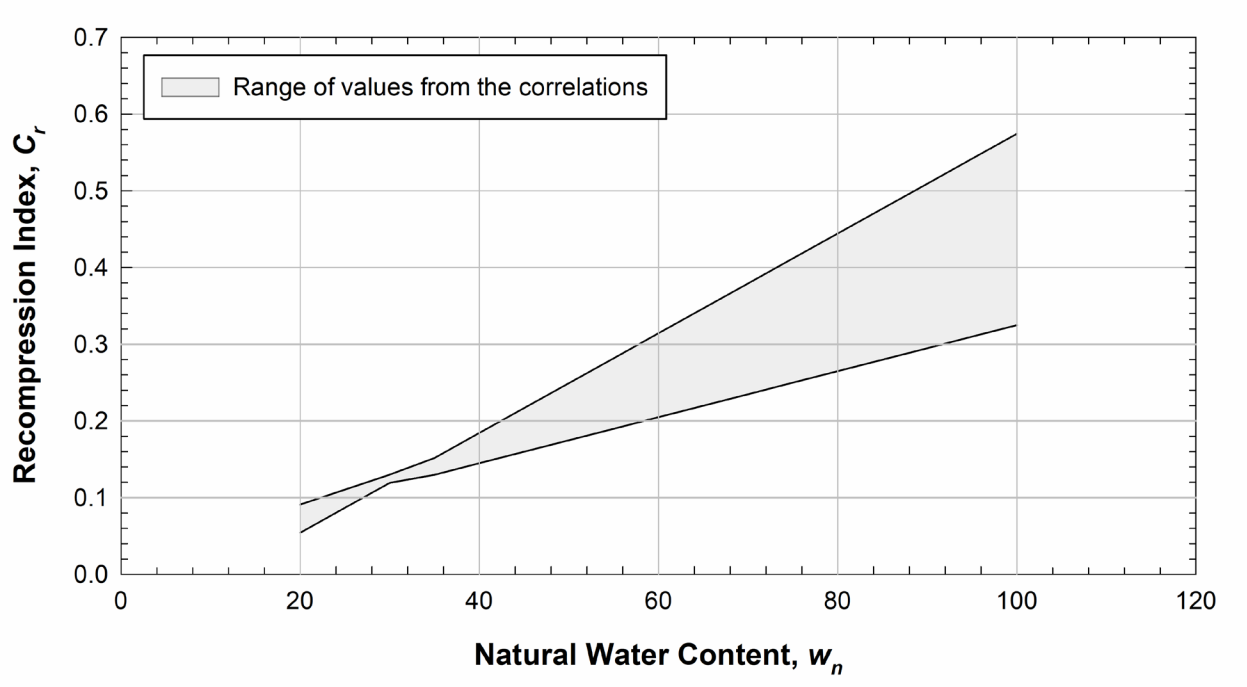

Figure 8-38 Range of Recompression Index based on Natural Water Content Predicted by Correlations

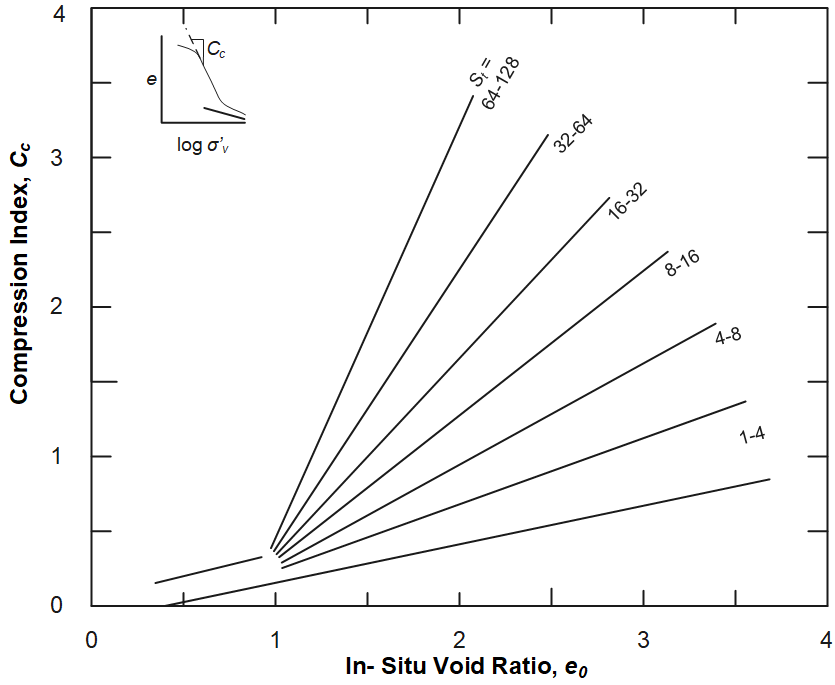

Figure 8-39 Sensitivity (S_t), *In situ* Void Ratio, and Compression Index Relationship (after Leroueil et al. 1983)

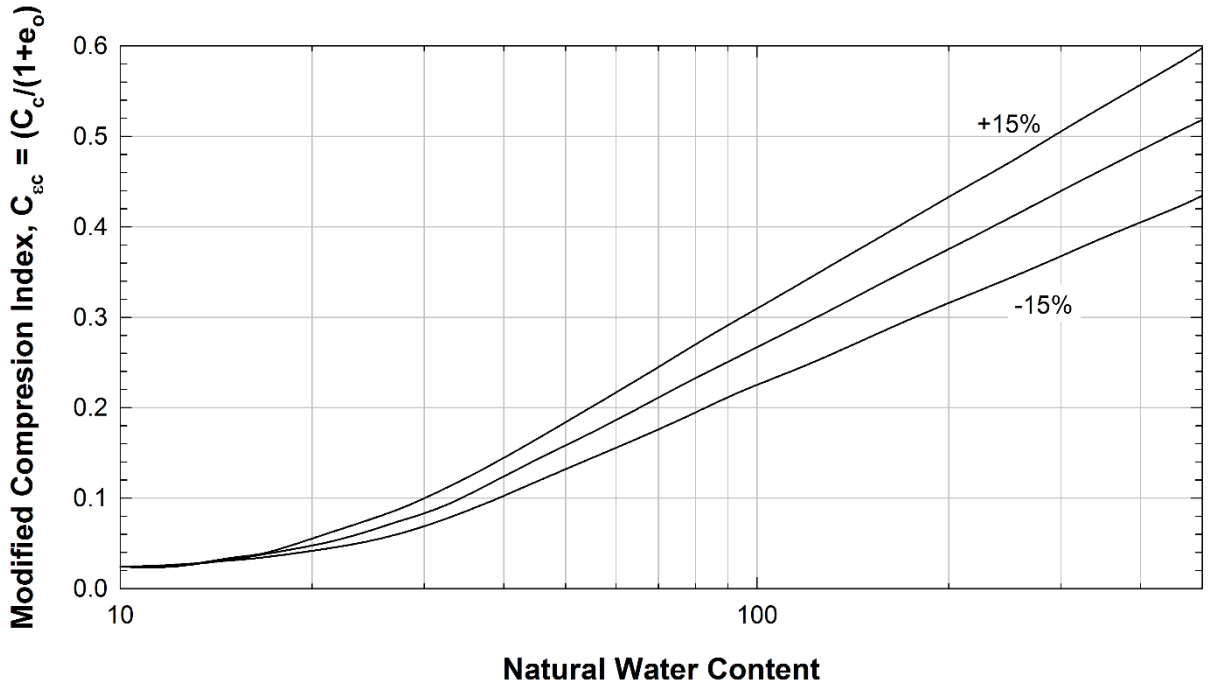

Figure 8-40 Correlation between Modified Compression Index and Water Content (after Lambe and Whitman 1969)

Burland (1990) compiled data from normally consolidated clays, both undisturbed and reconstituted at a liquidity index ranging from 1 to 1.5. Recognizing that vertical

stresses between 100 and 1000 kPa control most consolidation calculations, he defined the normally consolidated void ratios at these stresses as e^*_{100} and e^*_{1000}, respectively. From these void ratios, the intrinsic compression index was defined as:

$$C_c^* = e_{100}^* - e_{1000}^* \quad \textbf{(8-27)}$$

where:
C^*_c = intrinsic compression index,
e^*_{100} = intrinsic void ratio at 100 kPa, and
e^*_{1000} = intrinsic void ratio at 1000 kPa.

By normalizing the current void ratio with respect to $e^*_{100,}$ Burland defined the void index as:

$$I_v = \frac{e - e_{100}^*}{C_c^*} \quad \textbf{(8-28)}$$

where:
I_v = void index,
e = void ratio,
e^*_{100} = intrinsic void ratio at 100 kPa, and
C^*_c = intrinsic compression index.

With the data normalized in this way, he defined the *sedimentation compression line* (SCL) and *intrinsic compression line* (ICL), which describe the typical variation of the *in situ void index* (I_{v0}) with effective stress for a wide range of clays. The SCL represents the typical relationship for the compression of naturally sedimented clays. The ICL represents the typical relationship for the compression of remolded clays. Burland's SCL and ICL are plotted in Figure 8-41.

While the values of e^*_{100} and C^*_c are best determined from laboratory tests, Burland (1990) found that these parameters could be estimated from the void ratio at the liquid limit (e_L) by:

$$e_{100}^* = 0.109 + 0.679e_L - 0.089e_L^2 + 0.016e_L^3 \quad \textbf{(8-29)}$$

and

$$C_c^* = 0.256e_L - 0.04 \quad \textbf{(8-30)}$$

where:
e^*_{100} = intrinsic void ratio at 100 kPa,
e_L = void ratio at water content equal to the liquid limit, and
C^*_c = intrinsic compression index.

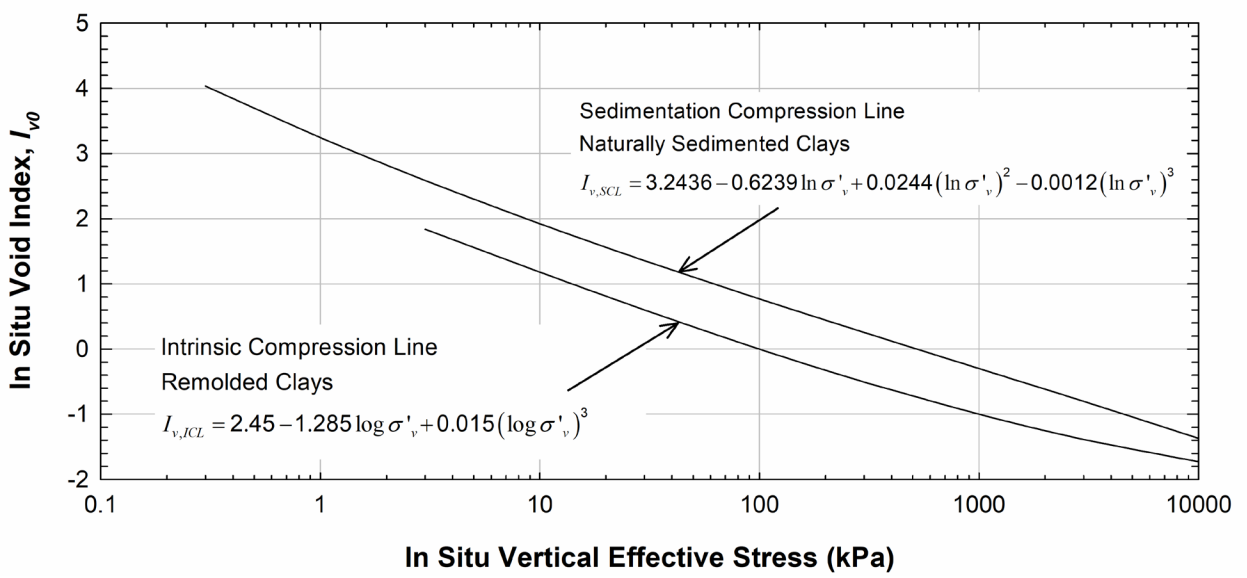

Figure 8-41 Sedimentation and Intrinsic Compression Lines (after Burland 1990)

Using Equations 8-28 through 8-30 and the relationships shown in Figure 8-41, the virgin consolidation line can be approximated solely based on liquid limit for both freshly deposited soils (using ICL) or structured, aged deposits (using SCL). This approach is particularly useful for validation of laboratory consolidation tests. Examples of the ICL and SCL for liquid limits ranging from 25 to 125 are plotted in Figure 8-42.

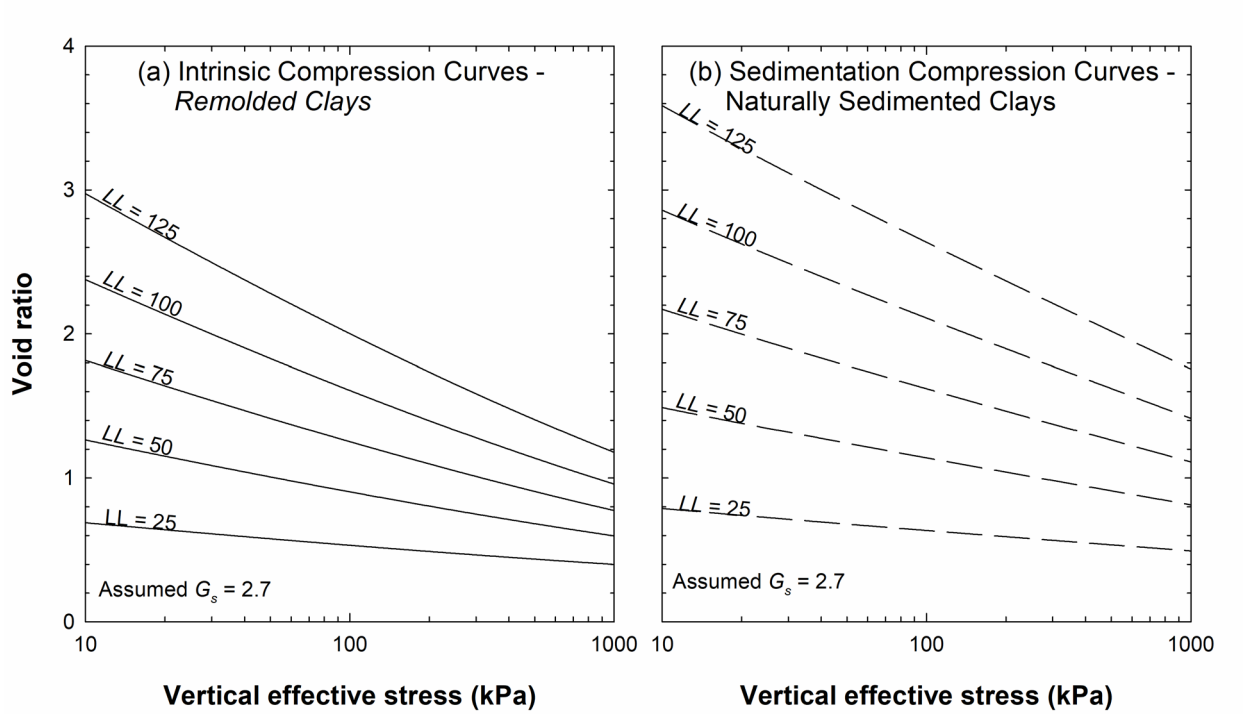

Figure 8-42 Example *NC* Compression Curves based on a) Intrinsic Compression Line and b) Sedimentation Compression Line

8-4.2 Compression and Recompression Indices – Coarse-Grained.

The compressibility of coarse-grained soils is normally significantly smaller than that from fine-grained soils. The compressibility of coarse-grained soils is not typically defined in terms of the compression and recompression indices. Instead the modulus-based methods presented in Chapter 5 are employed. The constrained modulus for coarse-grained soils is usually stress dependent (Kulhawy and Mayne 1990) and may be estimated using correlations in the following section. If required, typical values for the modified compression index of coarse-grained soils are summarized in Table 8-15 and Table 8-16.

Table 8-15 Modified Compression Indices for Saturated, Normally Consolidated Sands (after Burmister 1962, Coduto et al. 2011)

Soil Type	$C_{\varepsilon c} = C_c / (1+e_0)$					
	$D_r = 0\%$	$D_r = 20\%$	$D_r = 40\%$	$D_r = 60\%$	$D_r = 80\%$	$D_r = 100\%$
Medium to coarse sand (SW & SP)	0.010	0.008	0.006	0.005	0.003	0.002
Fine to coarse sand (SW)	0.011	0.009	0.007	0.005	0.003	0.002
Fine to medium sand (SW & SP)	0.013	0.010	0.008	0.006	0.004	0.003
Fine sand (SP)	0.015	0.013	0.010	0.008	0.005	0.003
Fine sand with little fine to coarse silt (SM)	0.017	0.014	0.012	0.009	0.006	0.003

Table 8-16 Compressibility Data for Six Sands (Been et al. 1987)

Sand	e_0	C_c		C_r
		$\sigma'_v / P_a = 1$ to 3	$\sigma'_v / P_a = 20$ to 30	
Monterrey 0	0.854	0.021	0.085	0.006
	0.782	0.018	0.090	0.007
Ticino	0.917	0.025	0.130	0.007
	0.827	0.026	0.085	0.006
Hokksund	0.870	0.024	0.095	0.005
	0.790	0.018	0.056	0.005
Ottawa	0.760	0.025	0.030	0.007
	0.560	0.005	0.100	0.003
Reid-Bedford	0.900	0.013	0.090	0.005
	0.650	0.005	0.019	0.003
Hilton Mines	0.950	0.038	0.210	0.009
	0.732	0.022	0.100	0.006

8-4.3 Constrained Modulus.

The secant drained constrained modulus (M_{ds}) was found to be a function of the vertical effective stress (σ'_v) and a modulus number (m) by Janbu (1963). The constrained modulus for normally consolidated clays, silts, and sands is related in either a linear or nonlinear fashion to vertical effective stress by:

$$M_{ds} = m \cdot \sigma'_v \quad \textbf{(8-31)}$$

or

$$M_{ds} = m \cdot P_a \cdot \left(\frac{\sigma'_v}{P_a} \right)^{0.5} \quad \textbf{(8-32)}$$

where:
M_{ds} = constrained modulus,
m = modulus number,
σ'_v = vertical effective stress, and
P_a = atmospheric pressure (same units as M_{ds} and σ'_v).

Janbu (1963) related the modulus number to the void ratio (or porosity) and the natural water content as shown in Figure 8-43 and Figure 8-44, respectively. In addition, Janbu (1985) presented the relationship for the modulus number of NC silts and sands as a function of the porosity, as presented in Figure 8-45.

8-4.3.1 Correlations with Standard Penetration Test.

Based on results from nine British clays, Stroud (1974) correlated the constrained modulus of clays to the SPT N value as:

$$M_{ds} = f \cdot N \cdot P_a \quad \textbf{(8-33)}$$

where:
M_{ds} = constrained modulus,
f = empirical coefficient related to plasticity index from Figure 8-46,
P_a = atmospheric pressure, and
N = SPT blow count.

According to Kulhawy and Mayne (1990), Stroud's correlation is not very reliable and should be used with caution.

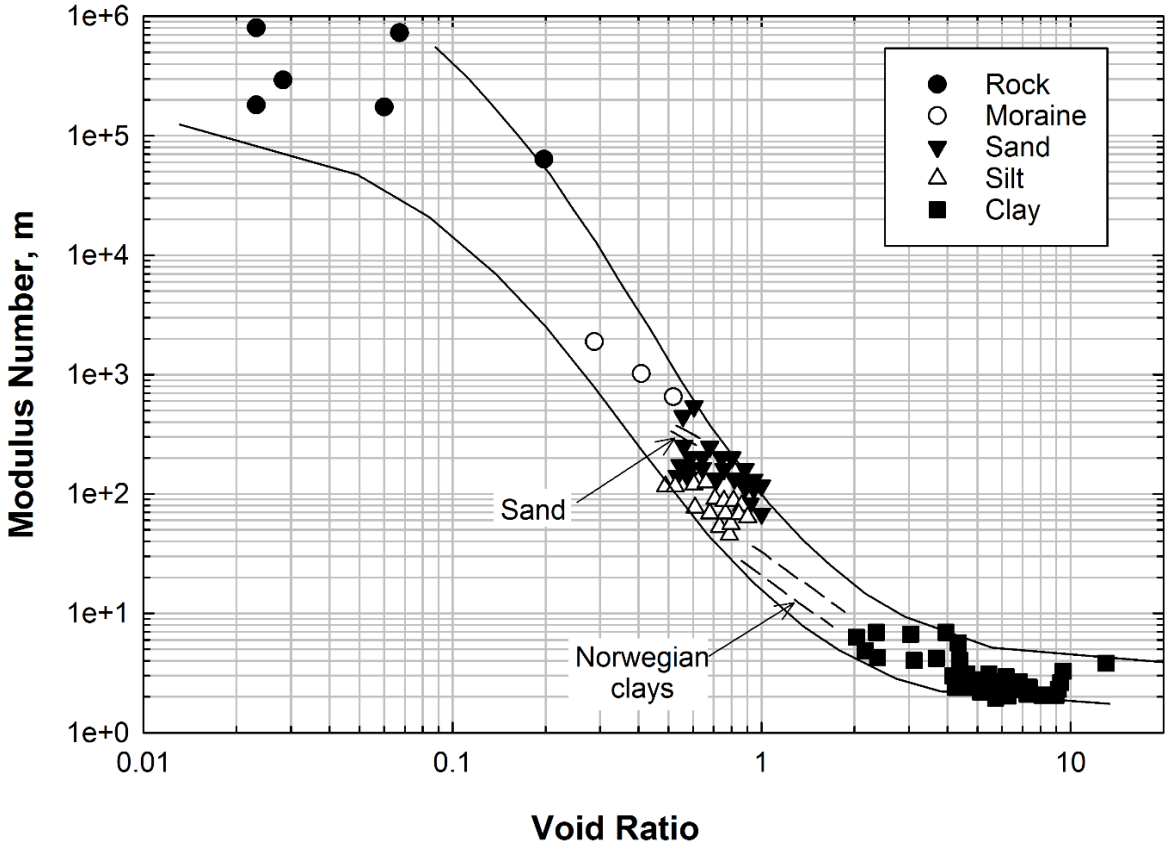

Figure 8-43 Relationship between Modulus Number and Void Ratio for *NC* Soils (after Janbu 1963)

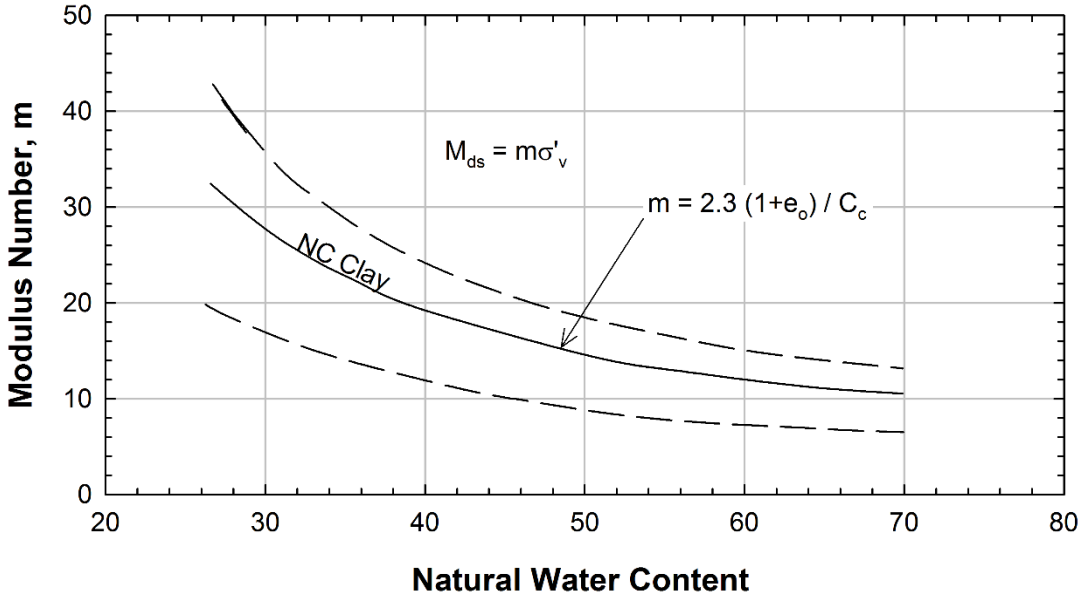

Figure 8-44 Modulus Number for *NC* Clays (after Janbu 1985)

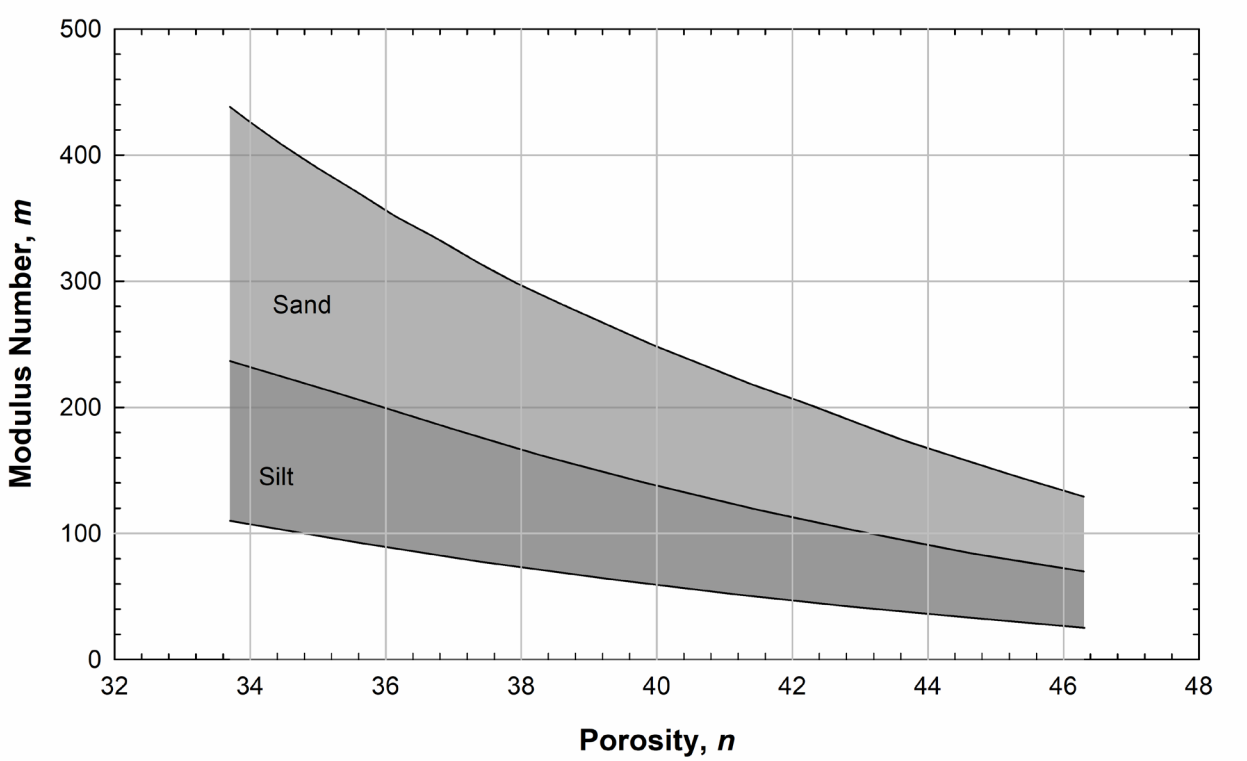

Figure 8-45 Modulus Number for *NC* Silts and Sands (after Janbu 1985)

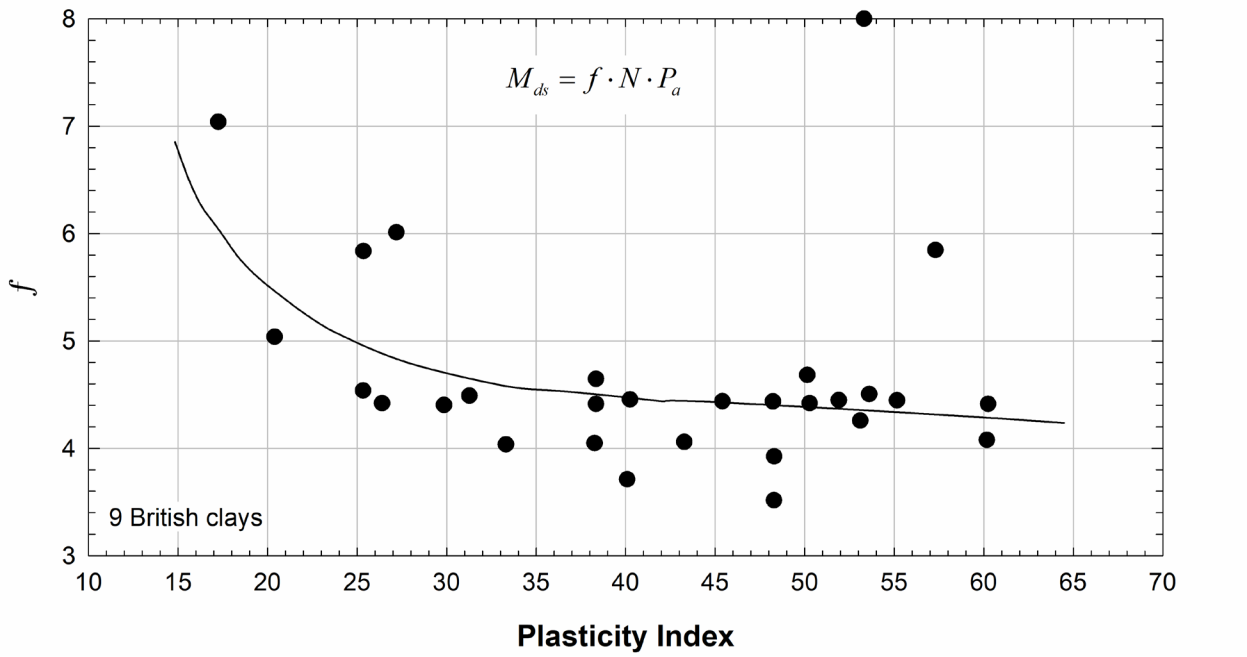

Figure 8-46 Variation of Empirical Coefficient *f* used for Calculating Constrained Modulus with *PI* (after Stroud 1974)

8-4.3.2 Correlations with Cone Penetration Test.

Numerous correlations have been presented to estimate the value of constrained modulus using the results from the cone penetration tests. Most of these correlations use the form of the equation shown below:

$$M_{ds} = \alpha \cdot q_c \quad \textbf{(8-34)}$$

where:
M_{ds} = constrained modulus,
q_c = cone tip resistance, and
α = empirical coefficient.

Mitchell and Gardner (1975) compiled values of α for different soils and showed that α can range from 0.4 to 8. In most cases, α is between 1 and 3. These values were obtained using a variety of cones with different geometries and testing procedures.

Kulhawy and Mayne (1990) presented the correlation shown in Figure 8-47 to obtain the constrained modulus of clays based on CPTu data in the form of tip resistance corrected for pore pressure and overburden stress.

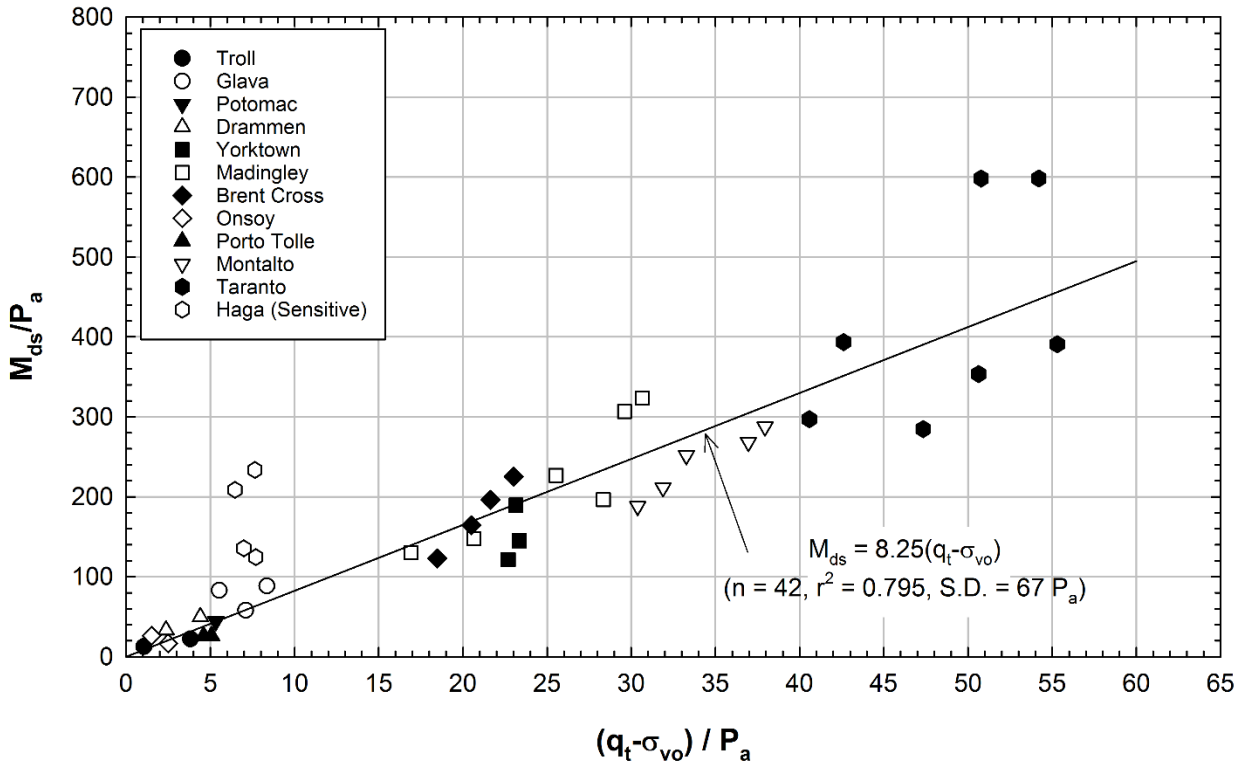

Figure 8-47 Correlation between Normalized Constrained Modulus and Normalized q_t from CPTu for Clays (after Kulhawy and Mayne 1990)

8-4.4 Coefficient of Secondary Compression.

The coefficient of secondary compression defines the settlement as a function of time after primary consolidation is completed. As with the compression ratios, the coefficient of secondary compression can be defined as a function of strain ($C_{\varepsilon\alpha}$) or as a function of the void ratio (C_α). See Section 5-5.4 for more details.

Mesri (1973) summarized the data shown in Figure 8-48 to estimate the coefficient of secondary compression of NC clays using the natural water content. Based on that data, the modified coefficient of secondary compression can be estimated as:

$$C_{\varepsilon\alpha} = 0.0001 \cdot w_n \quad \textbf{(8-35)}$$

where:
$C_{\varepsilon\alpha}$ = secondary compression ratio and
w_n = natural water content.

According to Kulhawy and Mayne (1990), $C_{\varepsilon\alpha}$ ranges from 0.0005 and 0.001 for most overconsolidated clays. The ratio of the coefficient of secondary compression to the compression index ($C_\alpha / C_c = C_{\varepsilon\alpha} / C_{\varepsilon c}$) is more or less constant for a given soil (Mesri and Godlewski 1977). Values of C_α / C_c are summarized in Table 8-17. Another correlation for the coefficient of correlation for silts and clays is presented in Figure 8-49.

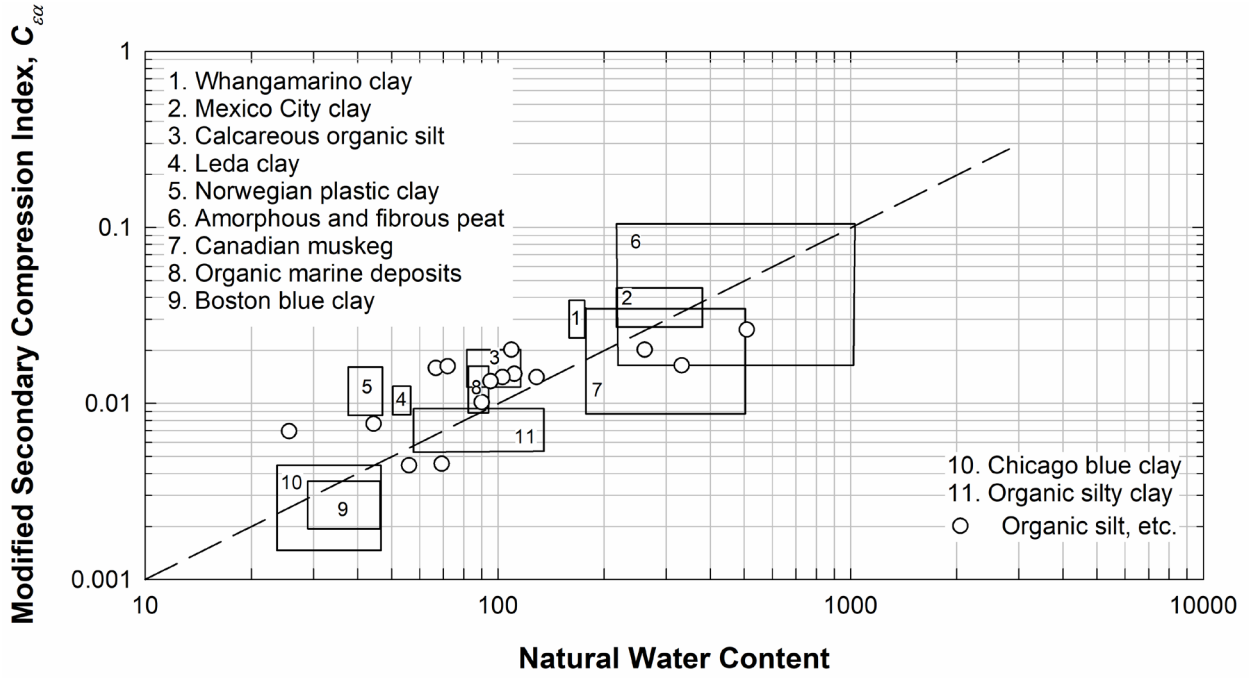

Figure 8-48 Correlation between Modified Secondary Compression Index and Natural Water Content for Normally Consolidated Clays (after Mesri 1973, Holtz and Kovacs 1981)

Table 8-17 Typical Values of C_α / C_c for Natural Soils (after Mesri and Godlewski 1977)

Grouping	Soil Type	C_α / C_c
Inorganic clays and silts	Whangamarino clay	0.03 – 0.04
	Leda clay	0.025 – 0.06
	Soft blue clay	0.026
	Portland sensitive clay	0.025 – 0.055
	San Francisco Bay Mud	0.04 – 0.06
	New Liskeard varved clay	0.03 – 0.06
	Silty clay C	0.032
	Nearshore clays and silts	0.055 – 0.075
	Mexico City clay	0.03 – 0.035
	Hudson River silt	0.03 – 0.06
Organic clays and silts	Norfolk organic silt	0.05
	Calcareous organic silt	0.035 – 0.06
	Post-glacial organic clay	0.05 – 0.07
	Organic clays and silts	0.04 – 0.06
	New Haven organic clay silt	0.04 – 0.075
Peats	Amorphous and fibrous peat	0.035 – 0.083
	Canadian muskeg	0.09 – 0.10
	Peat	0.075 – 0.085
	Peat	0.05 – 0.08
	Fibrous peat	0.06 – 0.085

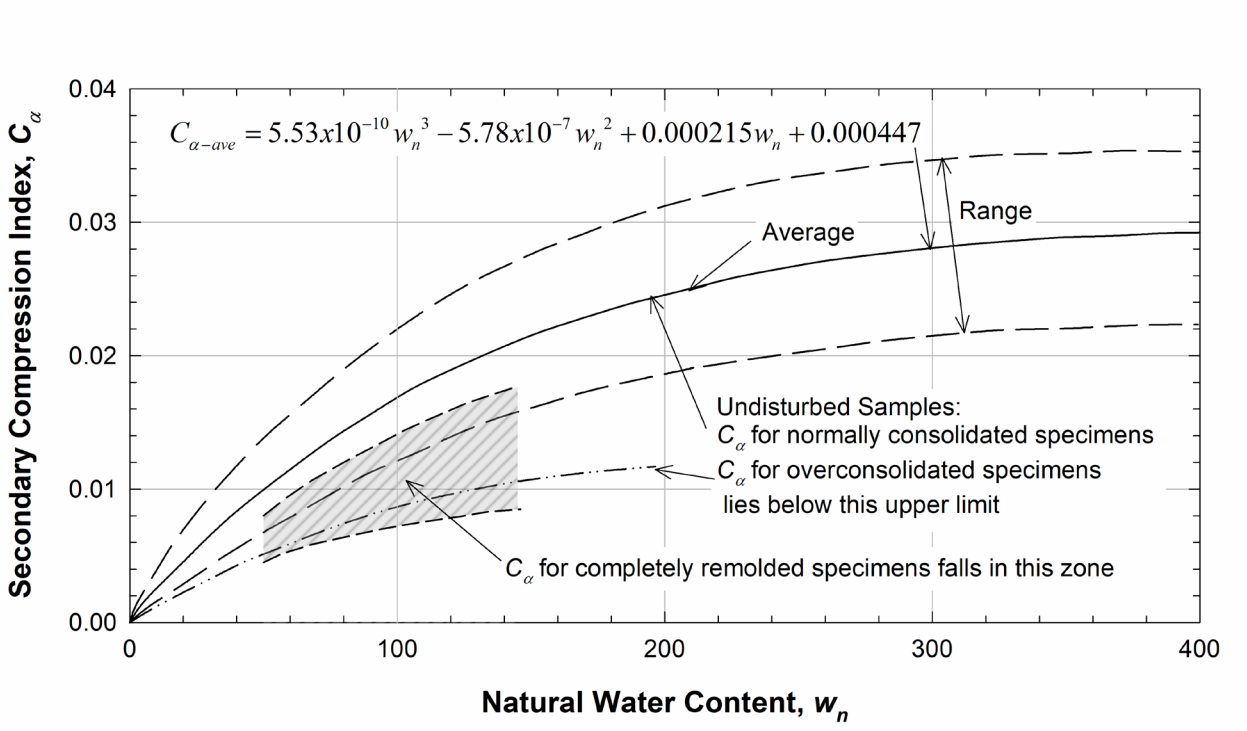

Figure 8-49 Secondary Compression Index for Silts and Clays

8-4.5 Coefficient of Consolidation.

The coefficient of consolidation (c_v) is a difficult parameter to estimate for design use because *in situ* stratigraphy can include sand seams and lenses, varved layers, etc. Small laboratory test specimens may not contain these fabric elements. In addition, the coefficient of consolidation can differ in the vertical and horizontal directions. Laboratory tests normally only measure the coefficient of consolidation in one direction. A first-order approximation for the coefficient of consolidation can be obtained using Figure 8-50.

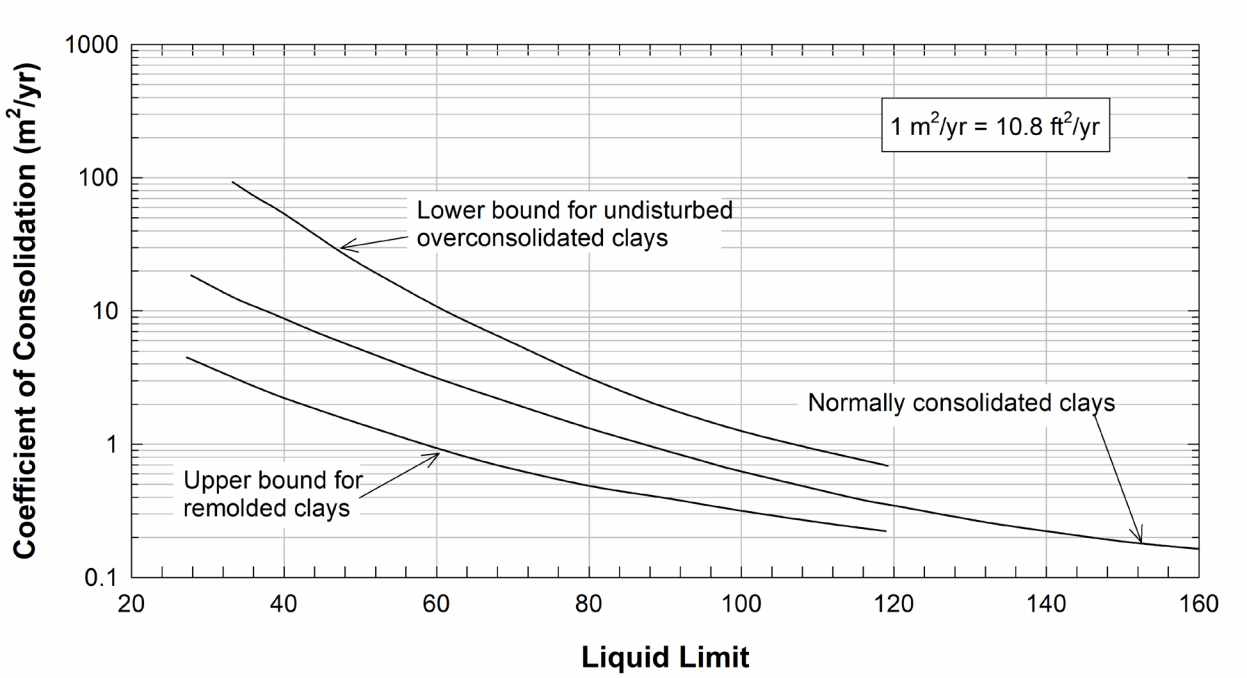

Figure 8-50 Approximate Relationship between Coefficient of Consolidation and Liquid Limit

8-5 ELASTIC PARAMETERS.

8-5.1 Definitions.

Correlations to four elastic parameters will be presented in this section: (1) Young's modulus (E) is the ratio of the change in normal stress in a given direction to the strain in the same direction within the elastic range; (2) bulk modulus (K) is the change in mean stress divided by the corresponding volumetric strain; (3) shear modulus (G) is the ratio of the change shear stress divided by the shear strain caused by that stress; and (4) Poisson's ratio (ν) is the ratio of the lateral strain to the axial strain caused by a change of stress. The relationships between these parameters are summarized in Table 8-18.

Table 8-18 Relationships between Common Elastic Parameters

Parameter	E =	K =	G =	ν =
E & G	---	$\frac{EG}{3(3G-E)}$	---	$\frac{E-2G}{2G}$
E & ν	---	$\frac{E}{3(1-2\nu)}$	$\frac{E}{2(1+\nu)}$	---
E & K	---	---	$\frac{3KE}{9K-E}$	$\frac{3K-E}{6K}$
G & ν	$2G(1+\nu)$	$\frac{2G(1+\nu)}{3(1-2\nu)}$	---	---
G & K	$\frac{9KG}{3K+G}$	---	---	$\frac{3K-2G}{2(3K+G)}$
K & ν	$3K(1-2\nu)$	---	$\frac{3K(1-2\nu)}{2(1+\nu)}$	---

In fine-grained soils, the value of the Young's modulus from field testing is normally derived under undrained conditions (E_u). Assuming a Poisson's ratio for undrained conditions of 0.5, the Young's modulus under drained conditions can be found:

$$E = \frac{2}{3}(1+\nu)\,E_u \qquad \textbf{(8-36)}$$

where:
E = Young's modulus for drained conditions,
ν = Poisson's ratio for drained conditions, and
E_u = Young's modulus for undrained conditions.

The shear modulus represents the response of the soil skeleton and it is independent of drainage conditions (i.e., $G = G_u$) (Kulhawy and Mayne 1990). Assuming a Poisson's ratio for undrained conditions of 0.5, the relationships in Table 8-18 indicate that E_u is three times greater than the shear modulus. According to Kulhawy and Mayne (1990), the undrained Young's modulus of soils is stress path dependent.

8-5.2 Undrained Young's Modulus of Fine-Grained Soils.

8-5.2.1 Typical Values.

Typical values of undrained Young's modulus are summarized in Table 8-19.

8-5.2.2 Correlations with Undrained Shear Strength.

Duncan and Buchignani (1987) proposed a correlation to obtain the ratio of the undrained shear modulus to the undrained shear strength for fine grained soils as a

function of the plasticity index and overconsolidation ratio as shown in Figure 8-51. This correlation is based on results obtained from direct simple shear tests.

Table 8-19 Typical Range of Undrained Young's Modulus for Clays

Clay Consistency	E_u / P_a	
	USACE (1990)	Kulhawy and Mayne (1990)
Very soft	5 – 50	
Soft	50 – 200	15 – 40
Medium	200 – 500	40 - 80
Stiff or silty	500 – 1000	80 – 200
Sandy	250 – 2000	
Clay shale	1000 – 2000	

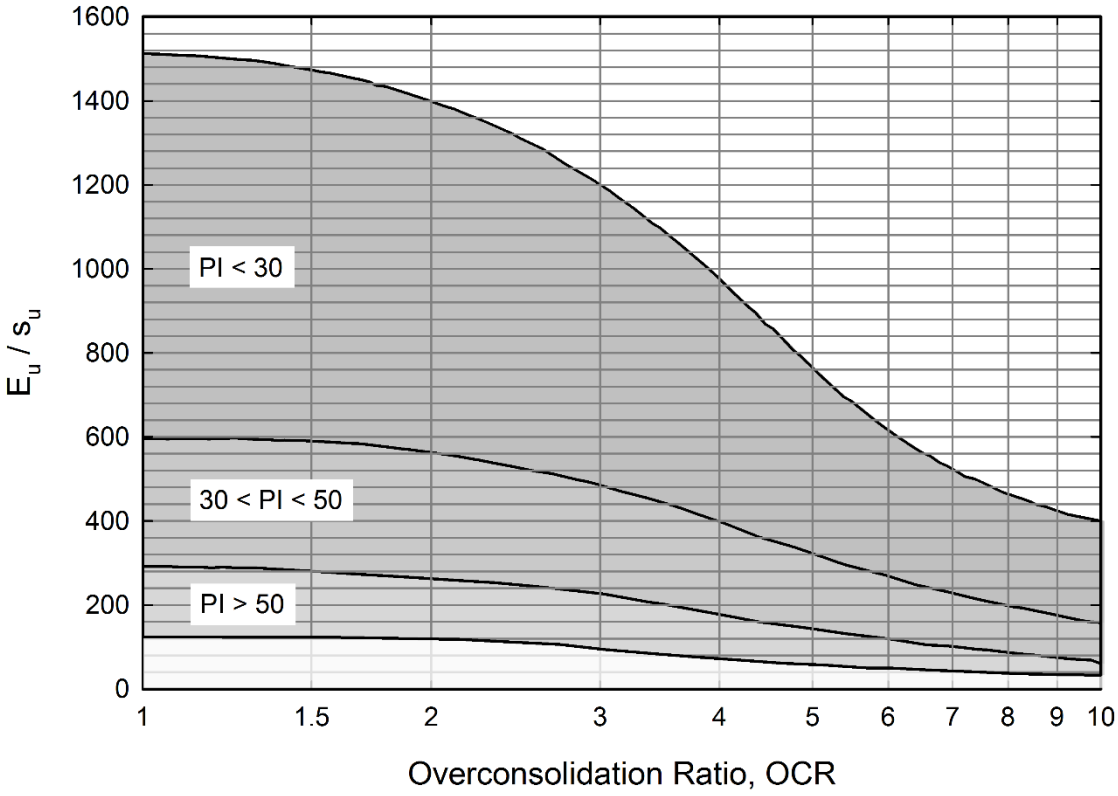

Figure 8-51 Correlation of Undrained Modulus Normalized by Undrained Shear Strength to Overconsolidation Ratio (after Duncan and Buchignani 1987)

8-5.2.3 Correlations with Standard Penetration and Pressuremeter Tests.

The pressuremeter test is used to directly measure a soil modulus in the horizontal direction. According to Kulhawy and Mayne (1990), the horizontal modulus measured in clay using the pressuremeter test is approximately equal to the undrained Young's modulus.

Ohya et al. (1982) presented the relationship for the undrained Young's modulus from the pressuremeter (E_{PMT}) and the SPT N value shown in Figure 8-52. The relationship shown in this figure exhibits a large amount of scatter ($r^2 = 0.39$), and it should be used with caution.

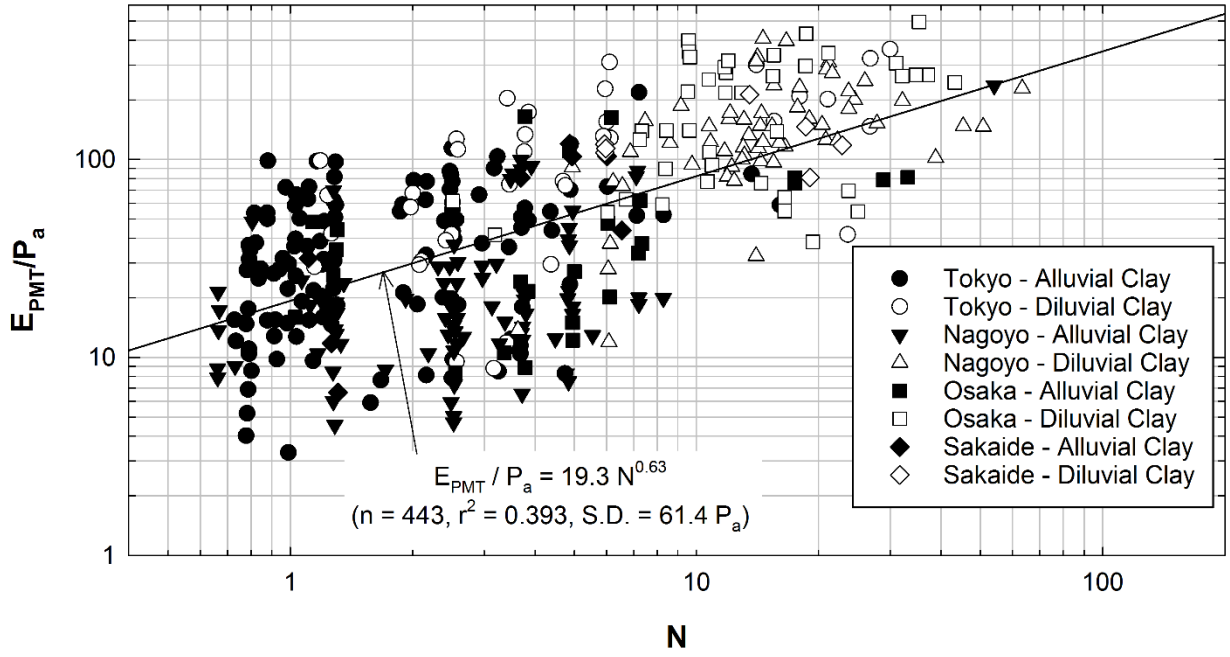

Figure 8-52 Correlation between PMT Modulus for Clays and SPT N (after Ohya et al. 1982)

8-5.2.4 Correlations to Load Tests.

Poulos and Davis (1980) presented the relationship for the undrained Young's modulus calculated from load tests on drilled shafts and driven piles as a function of the undrained shear strength of the clay, as shown in Figure 8-53.

Callanan and Kulhawy (1985) presented the relationship for the undrained Young's modulus of clays back calculated from load tests on drilled shafts and spread foundations presented in Figure 8-54. In the right side of Figure 8-54, σ_{vm} is the mean total vertical stress over the foundation depth.

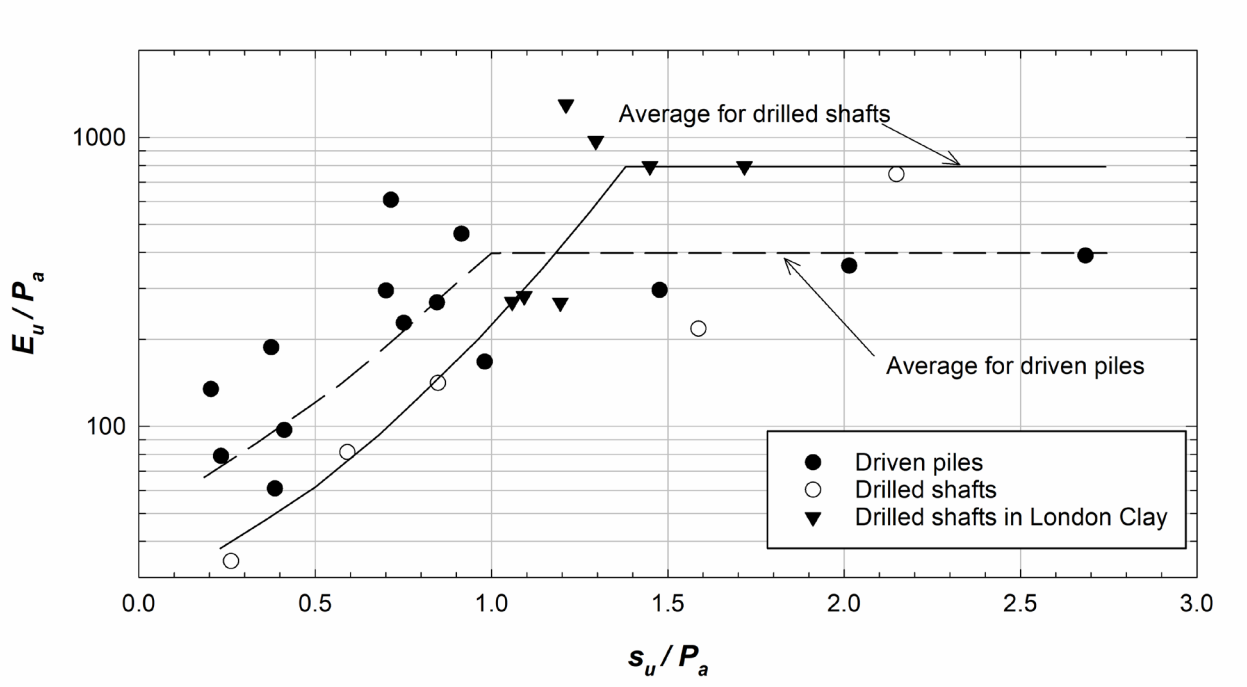

Figure 8-53 Undrained Modulus for Deep Foundations in Compression (after Poulos and Davis 1980)

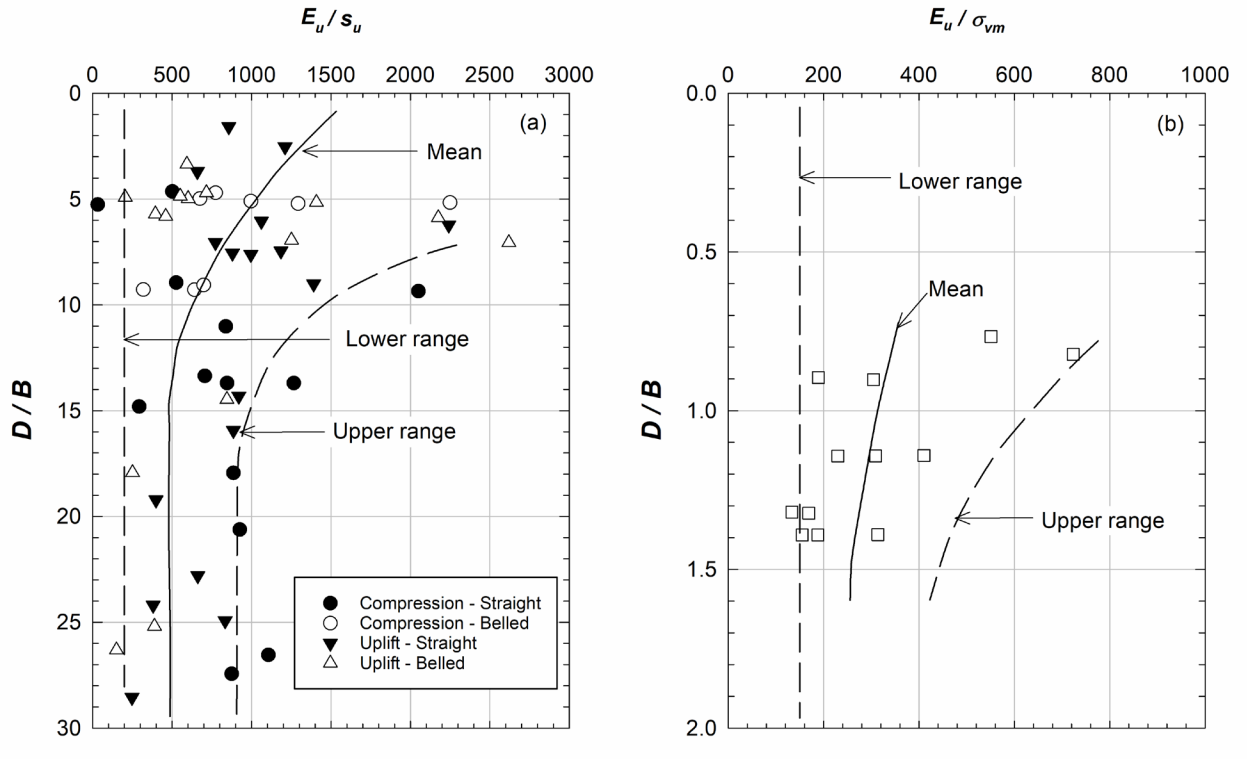

Figure 8-54 Undrained Modulus for (left) Drilled Shafts in Compression and Uplift and (right) Spread Foundations in Uplift (after Callanan and Kulhawy 1985)

8-5.3 Drained Young's Modulus of Coarse-Grained Soils.

Coarse-grained soils only experience undrained conditions for a very short period of time and under special circumstances. For this reason, the Young's modulus is only required for drained conditions in most cases. Typical values of drained Young's modulus (E) based on relative density are summarized in Table 8-20 for coarse-grained soils.

Table 8-20 Typical Ranges of Drained Young's Modulus for Coarse-Grained Soils

Relative Density or Soil Type	Normalized Drained Young's Modulus (E_u / P_a)		
	Poulos (1975)		USACE (1990)
	Typical	Driven Piles	
Loose	100 – 200	275 – 550	100 – 250
Medium	200 – 500	550 – 700	250 – 1000
Dense	500 – 1000	700 – 1100	1000 – 2000
Silty sand	---	---	250 – 2000

8-5.3.1 Correlations with SPT N Values.

Many different correlations have been developed to estimate the drained Young's modulus of coarse-grained soils using SPT N values. Some of these correlations are presented in Table 8-21 and plotted in Figure 8-55.

Table 8-21 Correlations for Drained Young's Modulus of Coarse-Grained Soils using SPT N Values

Equation	Applicable to	Reference
$E/P_a \approx 7.1 \cdot (1-\nu^2) \cdot N$	Sandy soils	After Ferrent (1963)
$E/P_a \approx 4.7(N+15)$	Sands	After Webb (1969)
$E/P_a \approx 3.1(N+5)$	Clayey sands	
$E/P_a \approx C(N+6)$	Silts with sand and gravels with sand with N < 15	Begemann (1974)
$E/P_a \approx 39.5 + C(N-6)$	Silts with sand and gravels with sand with N ≥ 15	
$E/P_a \approx 5N_{60}$	Sands with fines	Kulhawy and Mayne (1990)
$E/P_a \approx 10N_{60}$	NC clean sands	
$E/P_a \approx 15N_{60}$	OC clean sands	

E = drained Young's modulus,
P_a = atmospheric pressure (in same units as E),
N = SPT blow count value (use N_{60} for modern samplers)
ν = Poisson's ratio, and
C = empirical coefficient equal to 3 for silts with sand and 12 for gravel with sand

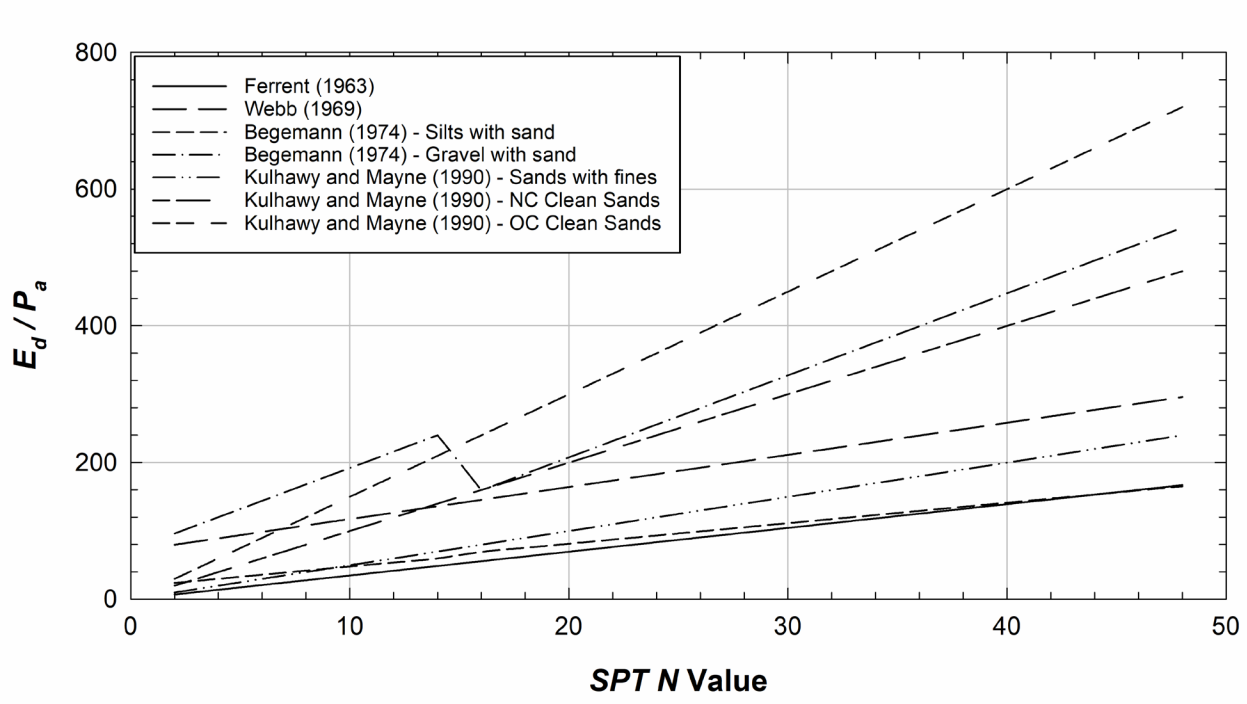

Figure 8-55 Correlations for Drained Young's Modulus of Granular Soils

8-6 CALIFORNIA BEARING RATIO (*CBR*).

The California bearing ratio (*CBR*) is a penetration test developed by the California Department of Transportation to assess the load-bearing capacity of soils used for building roads. This test is described in ASTM D1883. The *CBR* is predominately a laboratory test, but there are methods available to measure *CBR* in the field. *CBR* can be determined for test specimens that have been soaked, or specimens at their compaction water content. Because these correlations apply to specific soil types, the original references should be consulted before using the correlations.

8-6.1 Correlations with Index and Compaction Properties.

Several researchers have presented correlations to estimate the *CBR* using index properties. Correlations to grain size, Atterberg limits, and other index properties are summarized in Table 8-22. Correlations between *CBR* and soil compaction properties are summarized in Table 8-23.

Table 8-22 *CBR* Correlations with Grain Size, Atterberg Limits, and Unit Weight

Equation	Reference / Comment
$CBR = \frac{75}{1 + 0.728\left(FC \times PI\right)}$	NCHRP (2001), $FC \times PI = 0$
$CBR = 28.09 \cdot \left(D_{60}\right)^{0.358}$	NCHRP (2001), $FC \times PI = 0$
$CBR = 95$	NCHRP (2001), $D_{60} \geq 30$ mm
$CBR = 5$	NCHRP (2001), $D_{60} \leq 0.01$ mm
$CBR = 0.24 \cdot GC + 3.1$	Yildirim and Gunaydin (2011)
$CBR = 18.5 - 0.18 \cdot FC$	
$CBR_{unsoaked} = 4.75 - 0.044LL + 0.15PL$	Patel and Desai (2010)
$CBR = 5.18 - 0.028LL - 0.047PL$	
$CBR = 23 + 1.42 \cdot \gamma_d - 0.213 \cdot PI - 0.916 \cdot w - 0.368 \cdot LL$	George et al. (2009)
$CBR = 0.0004 \cdot G_s^{9.7915}$	Yashas et al. (2016)
$CBR = 1.36 \times 10^{-8}\left(\gamma_m\right)^{6.6141}$	
$CBR = 9.27 \times 10^{-10}\left(\gamma_d\right)^{7.4106}$	
$CBR_{soaked} = 1.93\beta - 31$	Al-Hashemi and Bukhary (2016)
FC = fines content = percent passing #200 sieve, SC = sand content = percent retained between #4 and #200 sieve, GC = gravel content = percent retained between 75 mm and #4 sieve, LL = liquid limit, PL = plastic limit, PI = plasticity index, γ_d = dry unit weight (in kN/m^3), γ_m = moist unit weight (in kN/m^3), w = water content (in percent), Gs = specific gravity of solids, and β = angle of repose	

Table 8-23 *CBR* Correlations to Index and Compaction Properties (after Singh et al. 2011)

Equation
$CBR = 33\left(\frac{\gamma_d}{\gamma_{d,\max}}\right) - 5.5\left(\frac{w}{w_{opt}}\right) - 1.15PL - 2.21$
$CBR_{unsoaked} = 24\left(\frac{\gamma_d}{\gamma_{d,\max}}\right) - 67\left(\frac{w}{w_{opt}}\right) - 2PL + 104.7$
PL = plastic limit, γ_d = dry unit weight, $\gamma_{d,max}$ = maximum dry unit weight from Modified Proctor test, w = water content, and w_{opt} = optimum water content from Modified Proctor test. Water contents should be either both in decimal or both in percentage form.

8-6.2 Correlations with Dynamic Cone Penetration.

Many correlations have been developed to estimate CBR from the results of dynamic cone penetration tests. Most of these correlations can take the form

$$CBR = A \cdot DCP^{x} \quad \textbf{(8-37)}$$

where:
CBR = California Bearing Ratio,
A = empirical coefficient,
DCP = dynamic cone penetration index (mm/blow), and
x = empirical exponent.

The values of A and x found by various researchers are summarized in Table 8-24. The range of CBR values expected from these correlations is presented in Figure 8-56.

Table 8-24 *CBR* Correlations with *DCP*

Reference / Comment	A	x
Gabr et al. (2000)	25	-0.55
Feleke and Araya (2016), fine-grained soils	47	-0.90
George et al. (2009)	47	-0.79
White et al. (2018), CL with CBR < 10	59	-2.00
Feleke and Araya (2016), coarse-grained soils	90	-1.17
Feleke and Araya (2016), fine-grained soils	104	-0.91
Feleke and Araya (2016), coarse-grained soils	157	-0.85
George and Kumar (2018)	246	-1.35
White et al. (2018), All soils except CL with CBR < 10	292	-1.12
Smith and Pratt (1983)	363	-1.15
Harrison (1986), clay-like soils with DCP < 10 mm/blow	501	-1.12
Harrison (1986), clay-like soils with DCP > 10 mm/blow	363	-1.16
Kleyn and Van Heerden (1983)	425	-1.27

Nazzal (2003) developed a similar correlation to those in Table 8-24 for soils with DCP values between 6.3 and 67 mm/blow:

$$CBR = \frac{2559}{DCP^{1.84} - 7.35} + 1 \quad \textbf{(8-38)}$$

where:
CBR = California Bearing Ratio, and
DCP = dynamic cone penetration index (mm/blow).

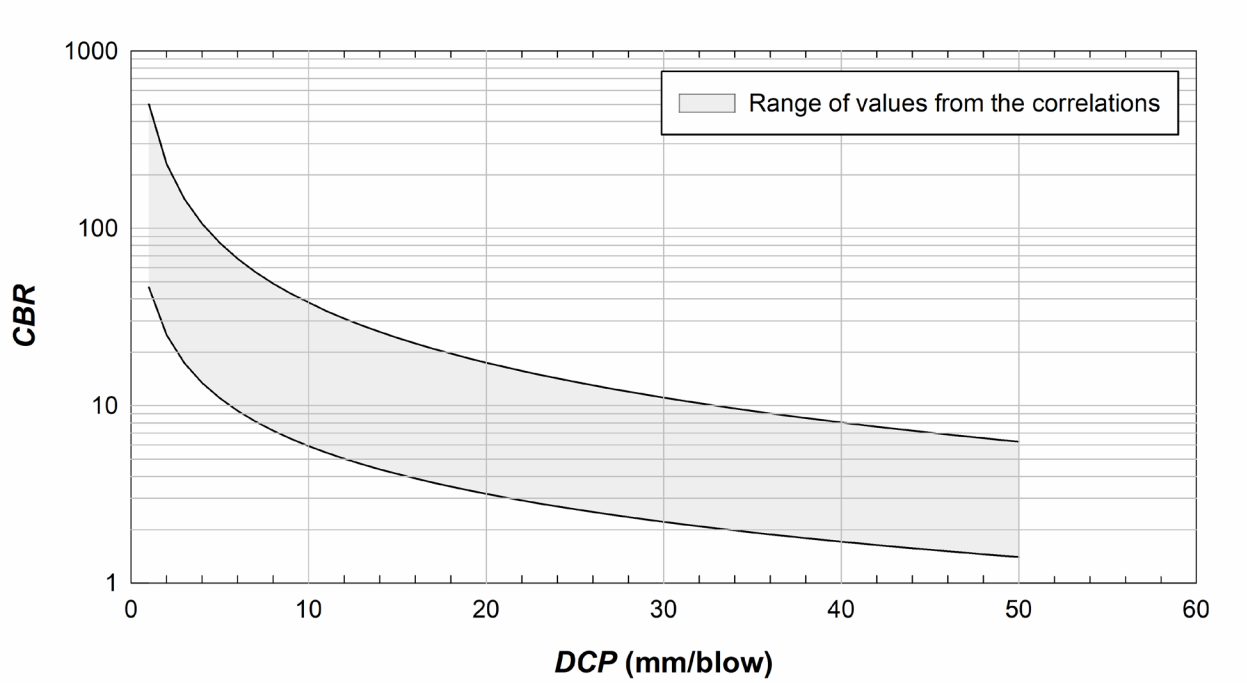

Figure 8-56 Range of CBR based on DCP Predicted by Correlations

8-6.3 Correlations with Standard Penetration Test.

Livneh (1989) found that the CBR could be estimated from the results of the Standard Penetration Test as shown below. The data used to obtain this correlation is presented in Figure 8-57.

$$\log CBR = -5.13 + 6.55\left(\log \frac{300}{N}\right)^{-0.26} \quad \textbf{(8-39)}$$

where:
CBR = California Bearing Ratio, and
N = SPT blow count value (use N_{60} for modern hammers).

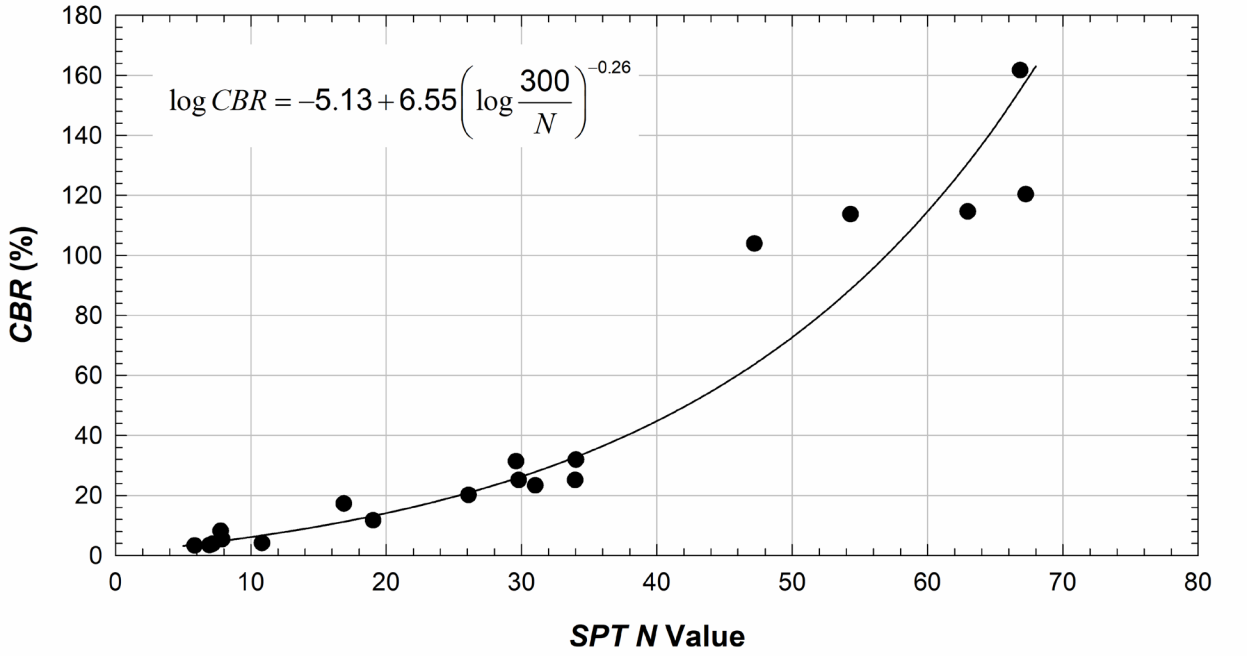

Figure 8-57 Correlation for CBR in Terms of SPT N Value (Livneh 1989)

8-7 HYDRAULIC CONDUCTIVITY.

The hydraulic conductivity (a.k.a., the coefficient of permeability) governs the flow rate and head loss as water flows through a soil mass. The hydraulic conductivity has one of the widest ranges of any engineering parameter as can be seen in Table 8-25. The wide range of possible values and the influence of variable ground conditions on the hydraulic conductivity make this parameter difficult to evaluate with a high degree of accuracy.

8-7.1 Typical Values.

Typical values of hydraulic conductivity based on soil type are presented in Table 8-25. Other typical values based on soil type can be found in Section 6-3.3.

8-7.2 Correlations for Coarse-Grained Soils.

One of the first correlations to estimate the hydraulic conductivity based on grain size was presented by Hazen (1911). This correlation was developed for saturated clean sands with a fines content less than 5% and D_{10} values ranging from 0.1 mm to 3 mm:

$$k = C \cdot (D_{10})^2 \quad \textbf{(8-40)}$$

Where:
k = hydraulic conductivity (cm/s),
C = empirical coefficient, usually taken to be 1 cm/s/mm^2, and
D_{10} = grain size corresponding to 10% passing on the grain-size distribution (mm).

Table 8-25 Typical Ranges of Hydraulic Conductivity based on Soil Type (after Terzaghi et al. 1996)

Soil	Hydraulic Conductivity (m/sec)	Relative Permeability
Gravel	> 10^{-3}	High
Sandy gravel	10^{-3} to 10^{-5}	Medium
Clean sand		
Fine sand		
Sand	10^{-5} to 10^{-7}	Low
Dirty sand		
Silty sand		
Silt	10^{-7} to 10^{-9}	Very low
Silty clay		
Clay	< 10^{-9}	Practically impermeable

Based on data from the middle and lower Mississippi River Valley, the USACE (1993) correlated the *in situ* horizontal permeability of fine to medium, relatively uniform sands (USCS classifications of SP or SW) as shown in Figure 8-58. This correlation was recommended for use only within the geographic area for which it was developed.

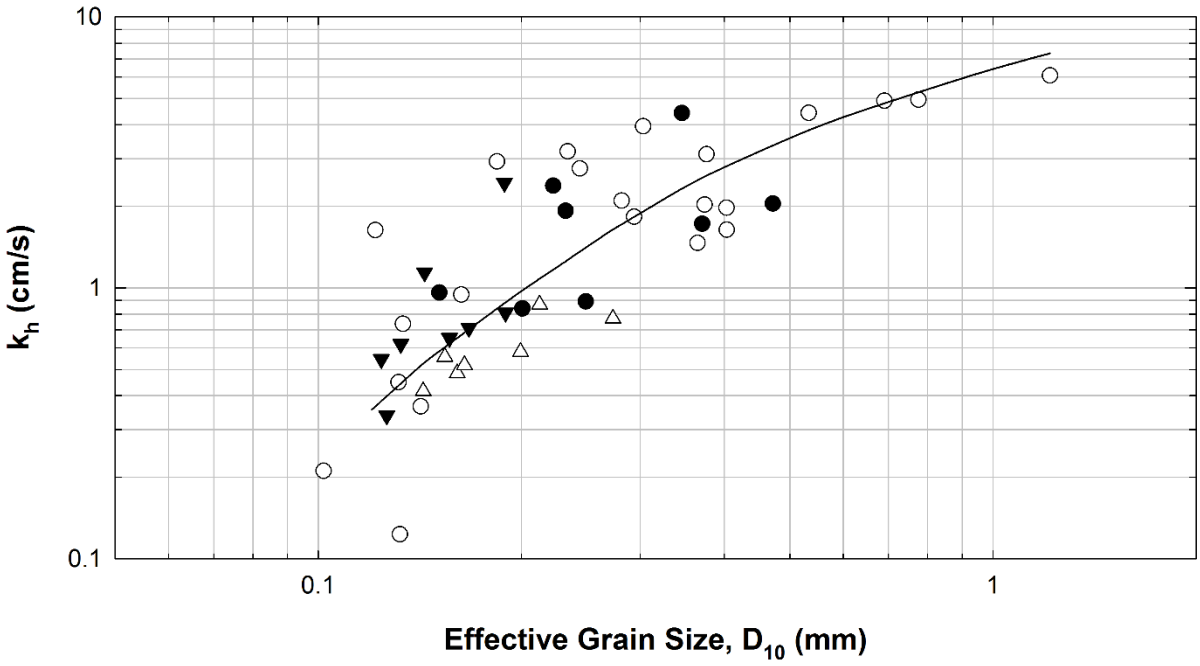

Figure 8-58 Horizontal Hydraulic Conductivity based on D_{10} (after USACE 1993)

As shown in Figure 8-59, Kenney et al. (1984) correlated the hydraulic conductivity of coarse-grained soils to the grain size corresponding to 5% passing on the cumulative grain-size distribution curve (D_5). A similar correlation can be developed between the hydraulic conductivity for clean coarse-grained soils and the D_{10} grain size as shown in Figure 8-60.

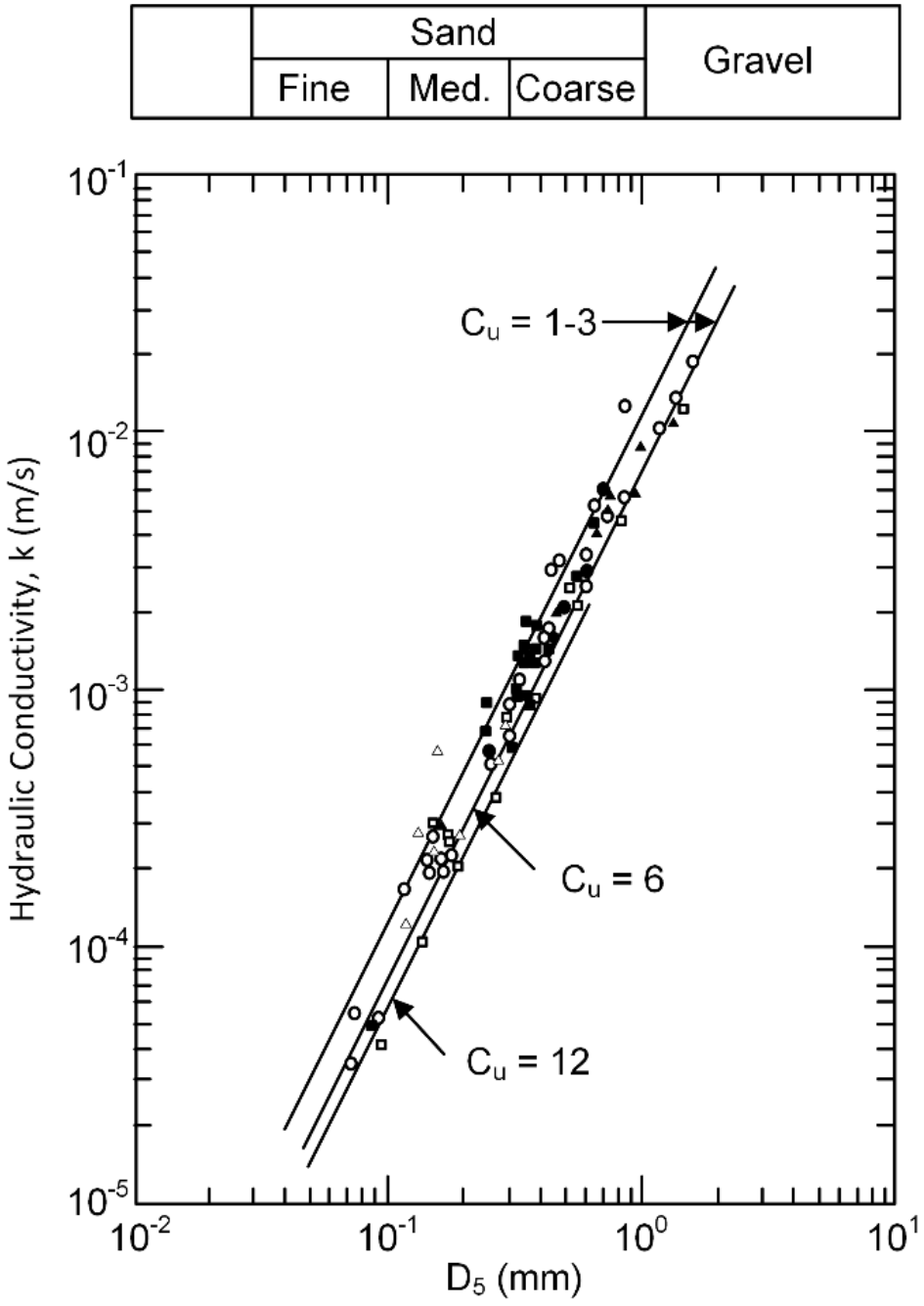

Figure 8-59 Hydraulic Conductivity based on D_5 (after Kenney et al. 1984)

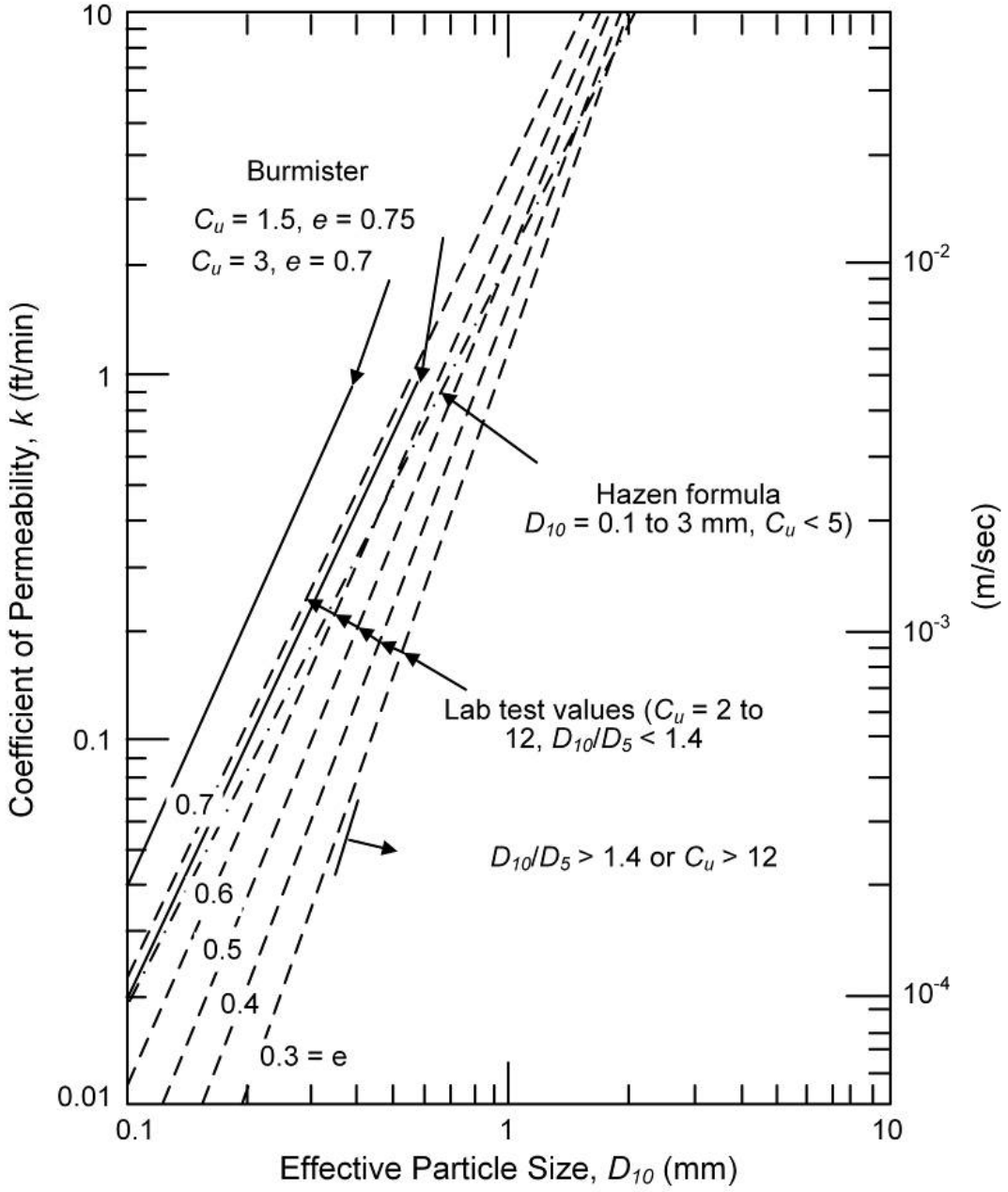

Figure 8-60 Hydraulic Conductivity of Sands and Sand-Gravel Mixtures as a Function of D_5, D_{10}, C_u, and e

Carrier (2003) presented a modified version of the Kozeny-Carman equation (Kozeny 1927; Carman 1938, 1956) to estimate the hydraulic conductivity using the full grain-size distribution of a soil. The modifications introduced by Carrier (2003) to the original equation simplify its use. The hydraulic conductivity can be estimated by:

$$k = 1.99 \times 10^2 \frac{cm}{s \cdot mm^2} \left[\frac{100\%}{\sum \frac{f_i}{D_{li}^{0.404} \times D_{si}^{0.596}}} \right]^2 \left(\frac{1}{S^2} \right) \left(\frac{e^3}{1+e} \right) \quad \textbf{(8-41)}$$

where:
k = hydraulic conductivity (cm/s),
f_i = fraction of particles (by mass) between two adjacent sieve sizes,
D_{li} = the particle size of the coarser sieve (mm),
D_{si} = the particles size of the finer sieve (mm),
S = surface area factor ranging from 6 for spheres to 8.5 for angular particles, and
e = void ratio.

Additional discussion and correlations of k to grain size can be found in Section 6-3.3.

8-7.3 Correlations for Fine-Grained Soils.

Unlike coarse-grained soils, the hydraulic conductivity of fine-grained soils is difficult to estimate from index properties. Hydraulic conductivity correlations for fine-grained soils should be used with caution.

Carrier and Beckman (1984) related the hydraulic conductivity and the Atterberg limits and void ratio of fine-grained soils using:

$$k = 0.0174 \left[\frac{e - 0.027\left(PL - 0.242PI\right)}{PI} \right]^{4.29} \left(\frac{1}{1+e} \right) \quad \textbf{(8-42)}$$

where:
k = hydraulic conductivity in m/s,
e = void ratio,
PL = plastic limit, and
PI= plasticity index.

Benson et al. (1994) measured the hydraulic conductivity on intact test specimens obtained from compacted clay liners from 67 landfills in North America. The results of those tests were found to relate to other measured properties of the clays as:

$$\ln k = -18.35 + \frac{894}{W} - 0.08PI - 2.87\left(\frac{w}{\gamma_w/\gamma_d - 1/G_s}\right) + 0.32\sqrt{GC} + 0.02CF \quad (8\text{-}43)$$

where:
k = hydraulic conductivity in m/s,
CF = clay-sized fraction (percent by mass smaller than 0.002 mm),
GC = gravel content = percent retained between 75 mm and #4 sieve,
W = weight of field compactor (kN),
PI = plasticity index,
w = molding water content,
γ_w = unit weight of the water,
γ_d = dry unit weight, and
G_s = specific gravity of the solids.

Benson and Trast (1995) performed hydraulic conductivity tests on 13 compacted clays used for compacted clay liners around the United States. The test specimens were prepared at different water contents, compacted, and then tested to measure the hydraulic conductivity. The results were correlated by Benson and Trast to k using:

$$\ln k = -15 - 0.087\left(\frac{w}{\gamma_w/\gamma_d - 1/G_s}\right) - 0.054PI + 0.022CF + 0.91E \quad (8\text{-}44)$$

where:
k = hydraulic conductivity (m/s),
w = molding water content,
γ_w = unit weight of the water,
γ_d = dry unit weight,
G_s = specific gravity of the solids.
PI = plasticity index,
CF = clay-sized fraction, and
E = compactive effort index (equal to -1, 0, and 1 for modified, standard, and reduced Proctor compactive effort, respectively).

8-8 SHEAR WAVE VELOCITY.

8-8.1 Correlations with Standard Penetration Test.

Many correlations have been developed to estimate the shear wave velocity (V_s) from SPT N values. Judgment is required regarding the use of uncorrected vs. corrected blow count. Older correlations where likely developed using 60% hammer efficiency as represented by N_{60}. The general form for most of the V_s correlations is:

$$V_s = BN^x z^y \quad \textbf{(8-45)}$$

where:
V_s = shear wave velocity (m/s),
B, x, and y = empirical coefficients,
N = SPT blow count, and
z = depth to the soil layer (m).

Correlations using the form of Equation 8-45 are summarized in Table 8-26. Other correlations are presented in Table 8-27. The range of values expected from these correlations can be seen in Figure 8-61.

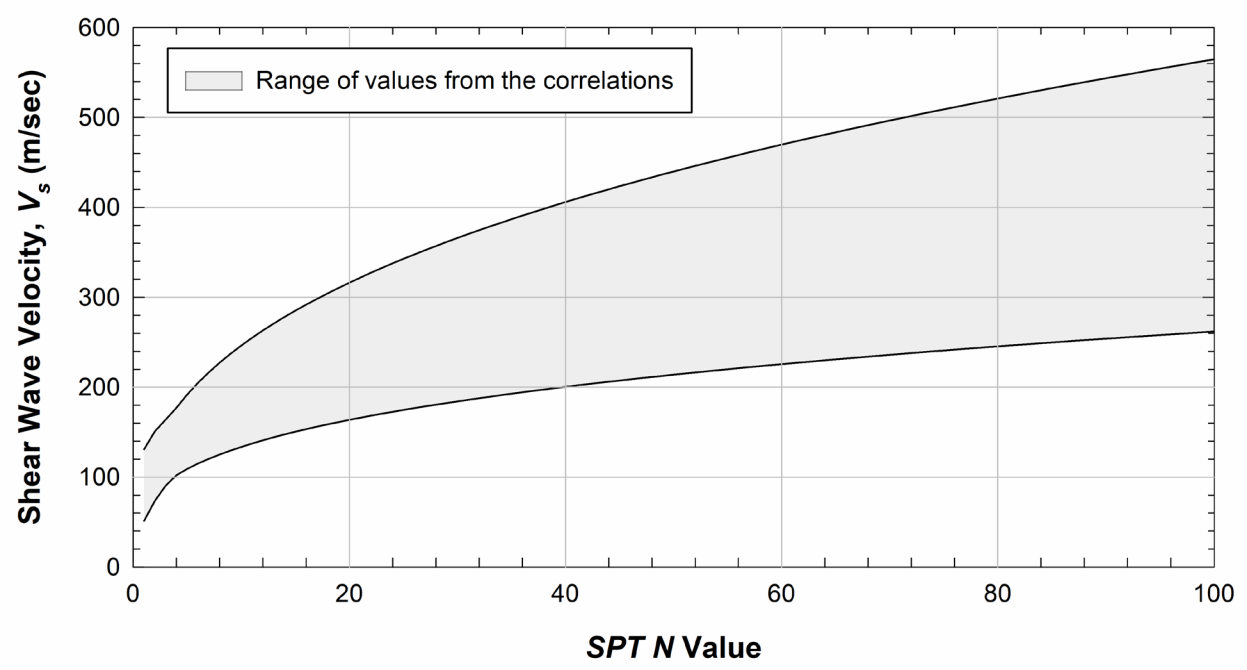

Figure 8-61 Range of Shear Wave Velocities based on SPT N Value Predicted by Correlations

Table 8-26 Shear Wave Velocity Correlated to SPT N Value and Depth

B	x	y	Comments	Reference
131	0.21	0	Sand, use N_{60}	Hasancebi and Ulusay (2007)
108	0.24	0	Use N_{60}	
105	0.26	0	Use N_{60}	
98	0.27	0	Clay	
90	0.31	0		
91	0.32	0	Sands	
101	0.27	0	Sand	Maheswari et al. (2010)
96	0.30	0		
89	0.36	0	Clay	
101	0.29	0		Sykora and Stokoe (1983)
68	0.29	0		Kiku et al. (2001)
80	0.29	0	Clay	Imai (1977)
81	0.33	0	Sand	
91	0.34	0		
84	0.31	0		Ohba and Toriumi (1970)
114	0.31	0	Clay	Lee (1990)
57	0.49	0	Sand	
106	0.32	0	Silt	
97	0.31	0		Imai and Tonouchi (1982)
76	0.33	0		Imai and Yoshimura (1975)
92	0.34	0		Fujiwara (1972)
90	0.34	0		Imai et al. (1975)
85	0.35	0		Ohta and Goto (1978)
108	0.36	0		Athanasopoulos (1995)
59	0.39	0		Dikmen (2009)
81	0.39	0		Ohsaki and Twasaki (1973)
61	0.50	0		Seed and Idriss (1981)
52	0.52	0		Iyisan (1996)
59	0.11	0.43		Akin et al. (2011)
69	0.17	0.20	Clay	Jamiolkowski et al. (1988)
82	0.25	0.14	Gravel	Yoshida et al. (1988)

Table 8-27 Shear Wave Velocity Correlated to SPT N Value

Equation	Reference
$V_s = 116\left(N+0.3185\right)^{0.202}$	Jinan (1987)
$V_{s,1} = 61.89\left(N_{1,60CS}\right)^{0.36}$	Ulmer et al. (2020)
$V_{s,1}$ = normalized shear wave velocity = $V_s \cdot (P_a / \sigma'_v)^{0.25}$, and $N_{1,60cs} = N_{1,60}$ corrected for fine content	

8-8.2 Correlations with Cone Penetration Test.

Several correlations relating the shear wave velocity to the results of the cone penetration test have been developed and are summarized in Table 8-28. It should be noted that some cones are equipped with a geophone or accelerometer and can measure shear wave velocity directly.

Table 8-28 Correlations for Shear Wave Velocity with CPT results

Equation	Comments	Reference
$V_s = 134 + 0.0052 q_c$	Sands	Sykora and Stokoe (1983)
$V_s = 0.1 q_c$	Clays	Jaime and Romo (1988)
$V_s = 17.5 q_c^{0.33} \sigma'_v{}^{0.27}$	Sands	Baldi et al. (1989)
$V_{s1} = 102 q_{c1}^{0.23}$		Fear and Robertson (1995)
$V_s = (10.1 \log q_c - 11.4)^{1.67} \left(100 f_s / q_c\right)^{0.3}$		Hegazy and Mayne (1995)
$V_s = 14.1 q_c^{0.359} e^{-0.473}$	Clays	
$V_s = 3.18 q_c^{0.549} f_s^{0.025}$		
$V_s = 13.2 q_c^{0.192} \sigma'_v{}^{0.179}$	Sands	
$V_s = 12 q_c^{0.319} f_s^{-0.0466}$		
$V_s = 9.44 q_c^{0.435} e^{-0.532}$	Clays	Mayne and Rix (1995)
$V_s = 1.75 \cdot q_c^{0.627}$		
$V_s = 32.3 q_c^{0.089} f_s^{0.1219} z^{0.215}$		Piratheepan (2002)
$V_s = 11.9 q_c^{0.269} f_s^{0.109} z^{0.127}$	Clays	
$V_s = 25.3 q_c^{0.103} f_s^{0.029} z^{0.155}$	Sands	
$V_{s,1} = 0.0831 q_c^{0.103} \left(\sigma'_v / P_a\right)^{0.25} e^{1.788 I_c}$		Hegazy and Mayne (2006)
$V_s = 119 \log f_s + 18.5$		Mayne (2006)
$V_s = \left[10^{0.55 I_c + 1.68} \left(q_t - \sigma'_v / P_a\right)\right]^{0.5}$		Robertson (2009)
$V_{s,1} = 149 q_{c1}^{0.205}$		Karray et al. (2011)
$V_{s,1} = 16.88 \left(q_{c1NCS}\right)^{0.489}$		Ulmer et al. (2020)

V_s = shear wave velocity (m/s), $V_{s,1}$ = normalized shear wave velocity = $V_s \cdot (P_a/\sigma'_v)^{0.25}$,
q_c = cone tip resistance (kPa), q_{c1} = normalized cone tip resistance = $(q_c / P_a)\ (P_a/\sigma'_v)^n$
q_{c1NCS} = normalized cone tip resistance as detailed by Boulanger and Idriss (2014)
f_s = cone sleeve resistance (kPa), e = void ratio, z = depth of the soil layer,
σ'_v = effective vertical stress (kPa), I_c = soil index for estimating grain characteristics, and
n = 0.5 for I_c < 2.6, else 0.75.

8-9 SUGGESTED READING.

Topic	Reference
Soil Properties	Kulhawy, F. H. and Mayne, P. W. (1990). *Manual on estimating soil properties for foundation design (No. EPRI-EL-6800)*. Electric Power Research Inst., Palo Alto, CA; Cornell Univ., Ithaca, NY, Geotechnical Engineering Group.
Geotechnical Correlations	Carter, M. and Bentley, S. P. (2016). *Soil properties and their correlations*. John Wiley & Sons.
	Duncan, J. M., Horz, R. C., and Yang, T. L. (1989). *Shear Strength Correlations for Geotechnical Engineering, CGPR#4*, Center for Geotechnical Practice and Research, Blacksburg, VA, 93 pp.

8-10 NOTATION.

Symbol	Description
A	Empirical coefficient for Equation 8-37
a	CPT cone net area ratio, and empirical coefficient related to the steepness of the power function (Equation 8-15)
B	Foundation width or diameter, and empirical coefficient in Equation 8-45
b	Empirical coefficient related to the curvature of the power function
CBR	California Bearing Ratio
CBR_{soaked}	Soaked California Bearing Ratio
$CBR_{unsoaked}$	Unsoaked California Bearing Ratio
C_c	Compression index
C_{ec}	Modified compression index or compression ratio
C^*_c	Intrinsic compression index
CF	Clay-sized fraction
C_r	Recompression index
$C_{\varepsilon r}$	Modified recompression index or recompression ratio
C_u	Coefficient of uniformity
c_v	Coefficient of consolidation
C_α	Secondary compression index
$C_{\alpha\varepsilon}$	Modified secondary compression index or secondary compression ratio
D	Foundation embedment
DCP	Dynamic cone penetration index
D_{ji}	The particle size of the coarser sieve in Equation 8-41
D_r	Relative density
D_{si}	The particle size of the finer sieve in Equation 8-41
D_5	Particle-size diameter corresponding to 5% passing on the cumulative particle-size distribution curve

Symbol	Description
D_{10}	Particle-size diameter corresponding to 10% passing on the cumulative particle-size distribution curve
D_{60}	Particle-size diameter corresponding to 60% passing on the cumulative particle-size distribution curve
E	Young's modulus, and compactive effort index in Equation 8-44
e	Void ratio
E_D	Dilatometer modulus
E	Young's modulus, typically drained
e_L	Void ratio at a water content equal to the liquid limit
E_{PMF}	Young's modulus from pressuremeter
E_u	Undrained Young's modulus
e_0	Initial void ratio
e_{100}*	Intrinsic void ratio at 100 kPa
e_{1000}*	Intrinsic void ratio at 1000 kPa
f	Empirical coefficient for Equation 8-33
FC	Fines content
f_i	Fraction of particles (by mass) between two adjacent sieve sizes in Equation 8-41
f_s	CPT sleeve resistance
G	Shear modulus
GC	Gravel content
G_u	Undrained shear modulus
G_s	Specific gravity of solids
I_c	Soil index
I_v	Void index
$I_{v,ICL}$	Void index for the intrinsic compression line
$I_{v,SCL}$	Void index for the sedimentation compression line
K	Bulk modulus
k	Hydraulic conductivity
K_D	Dilatometer horizontal stress index
K_0	Coefficient of earth pressure at rest
LL	Liquid limit
m	Semi-empirical fitting parameter for Equation 8-20, and modulus number
M_{ds}	Constrained modulus
N	SPT N value. May be assumed to be equal to N_{60}
n	Porosity, number of datapoints, and coefficient for q_{c1}
NC	Normally consolidated
N_c	Empirical bearing capacity factor

Symbol	Description
N_k	Empirical bearing capacity factor
N_{kt}	Empirical bearing capacity factor
N_p	Slope of the σ'_v vs q_c plot
N_q	Bearing capacity number
N_{60}	SPT N value corrected for 60% hammer energy efficiency
$N_{1,60}$	N_{60} value corrected to an effective vertical overburden of 1 atm
$N_{1,60,cs}$	$N_{1,60}$ corrected for fine content
N'	SPT N value corrected for dynamic pore pressure effects
OC	Overconsolidated
OCR	Overconsolidation ratio
P_a	Atmospheric pressure
PI	Plasticity index
PL	Plastic limit
p_0	Pressure required to initiate movement of the dilatometer
q_c	Static CPT tip resistance
q_{c1}	Cone penetrometer tip resistance normalized to 1 atm overburden pressure.
$q_{c,NC}$	Static CPT tip resistance in normally consolidated sand
$q_{c,OC}$	Static CPT tip resistance in overconsolidated sand
q_d	Dynamic cone resistance
q_p	Static CPT net resistance
q_t	Cone penetrometer tip resistance corrected for pore pressure effects
R	Correction factor for overconsolidated static cone tip resistance
r^2	Coefficient of determination
s	Effective stress shear strength
S	Surface area factor for Equation 8-41
$S.D.$	Standard deviation
S_t	Sensitivity
s_u	Undrained shear strength
$s_{u,fv}$	Undrained shear strength from field vane tests
u or u_2	Pore pressure measured behind the cone tip
u_0	Hydrostatic initial pore pressure
V_s	Shear wave velocity
$V_{s,1}$	Normalized shear wave velocity
W	Weight of the field compactor in Equation 8-43
w	Water content
w_n	Natural water content
w_{opt}	Optimum water content referenced to a given standard
x	Empirical exponent for Equation 8-37 and empirical coefficient for Equation 8-45

Symbol	Description
y	Empirical coefficient for Equation 8-45
z	Depth below the soil layer
α	Empirical coefficient for Equation 8-34
β	Inclination of the failure wedge for foundation loading, exponent in Equation 8-9, and angle of repose
Δq_p	Change in static CPT cone net resistance
$\Delta\sigma'_v$	Change in vertical effective stress
ϕ'	Effective stress friction angle
ϕ'_{FS}	Fully softened friction angle
ϕ'_r	Residual friction angle
ϕ'_{sec}	Effective stress secant friction angle (stress dependent)
γ_d	Dry unit weight
$\gamma_{d,max}$	Maximum dry unit weight referenced to a given standard
γ_m	Moist unit weight
γ_w	Unit weight of the water
σ_v	Vertical total stress
σ_{vm}	Mean vertical total stress
σ_{v0}	Initial vertical total stress
σ'_{ff}	Effective normal stress on the failure plane at failure
σ'_p	Preconsolidation pressure or maximum past pressure
σ'_v	Vertical effective stress
ν	Poisson’s ratio

This Page Intentionally Left Blank

APPENDIX A. REFERENCES

Aas, G. 1980. Setninger av bygg på sand; sammenligning mellom effektivspenning parametere bestemt ved henholdsvis trykksondering og triaksialforsøk. [In Norwegian].

AASHTO (American Association of State Highway and Transportation Officials). 1991. *T-289 Standard Method of Test for Determining pH of Soil for Use in Corrosion Testing*. Washington D.C.: AASHTO.

AASHTO (American Association of State Highway and Transportation Officials). 2012. *T-288 Standard Method of Test for Determining Minimum Laboratory Soil Resistivity*. Washington D.C.: AASHTO.

AASHTO (American Association of State Highway and Transportation Officials). 2017. *LRFD Design Specifications*. Washington D.C.: AASHTO.

AASHTO (American Association of State Highway and Transportation Officials). 2018. *Standard Specification for Transportation Materials and Methods of Sampling and Testing*. Washington D.C.: AASHTO. 4855 pp.

Adikari, G. S. N. 1977. “Statistical Evaluation of Strength and Deformation Characteristics of Bangkok Clays.” *Asian Institute of Technology*.

Ahlvin, R. G., and Ulery, H. H. 1962. “Tabulated Values for Determining the Complete Pattern of Stresses, Strains, and Deflections Beneath a Uniform Circular Load on a Homogeneous Half Space.” *Highway Research Board Bulletin 342*.

Akin, M. K., Kramer, S. L., and Topal, T. 2011. “Empirical Correlations of Shear Wave Velocity (Vs) and Penetration Resistance (SPT-N) for Different Soils in an Earthquake-prone Area (Erbaa-Turkey).” *Engineering Geology*, 119(1), 1–17.

Al-Hashemi, H. M. B., and Bukhary, A. H. 2016. “Correlation Between California Bearing Ratio (CBR) and Angle of Repose of Granular Soil.” *Electronic journal of Geotechnical Engineering*, 21(17), 5655–5660.

Al-Khafaji, A. W. N., and Andersland, O. B. 1992. “Equations for Compression Index Approximation.” *Journal of Geotechnical Engineering*, 118(1), 148–153.

Alpan, I. 1964. “Estimating the Settlements of Foundations on Sands.” *Civil Engineering and Public Work Review*, 59(700).

Ameratunga, J., Sivakugan, N., and Das, B. M. 2016. *Correlations of Soil and Rock Properties in Geotechnical Engineering*. Springer.

American Lifelines Alliance. 2001. *Guidelines for the Design of Buried Steel Pipe.* American Society of Civil Engineers and Federal Emergency Management Agency, 83 pp.

Anderson, N., Croxton, N., Hoover, R., Sirles, P. 2008. “Geophysical Methods Commonly Employed for Geotechnical Site Characterization.” *Transportation Research Circular E-C130*, Transportation Research Board, Washington, DC.

Asaoka. 1978. “Observational Procedure of Settlement Prediction.” *Soils and Foundations*, 18(4), 87-101.

ASCE. 2001. *Design and Construction of Frost-Protected Shallow Foundations*. SEI/ASCE 32-01, https://doi.org/10.1061/9780784405642.

ASTM International. 2011. *D3999/D3999M-11e1 Standard Test Methods for the Determination of the Modulus and Damping Properties of Soils Using the Cyclic Triaxial Apparatus*. West Conshohocken, PA; ASTM International. (Withdrawn 2020)

ASTM International. 2011. *D3080/D3080M-11 Standard Test Method for Direct Shear Test of Soils Under Consolidated Drained Conditions*. West Conshohocken, PA; ASTM International. (Withdrawn 2020)

ASTM International. 2012. *D1557-12e1 Standard Test Methods for Laboratory Compaction Characteristics of Soil Using Modified Effort (56,000 ft-lbf/ft3 (2,700 kN-m/m3))*. West Conshohocken, PA; ASTM International.

ASTM International. 2012. *D4186/D4186M-12e1 Standard Test Method for One-Dimensional Consolidation Properties of Saturated Cohesive Soils Using Controlled-Strain Loading*. West Conshohocken, PA; ASTM International.

ASTM International. 2012. *D4554-12 Standard Test Method for In Situ Determination of Direct Shear Strength of Rock Discontinuities*. West Conshohocken, PA; ASTM International.

ASTM International. 2012. *D698-12e2 Standard Test Methods for Laboratory Compaction Characteristics of Soil Using Standard Effort (12 400 ft-lbf/ft3 (600 kN-m/m3))*. West Conshohocken, PA; ASTM International.

ASTM International. 2013. *D5311/D5311M-13 Standard Test Method for Load Controlled Cyclic Triaxial Strength of Soil*. West Conshohocken, PA; ASTM International.

ASTM International. 2013. *D6467-13e1 Standard Test Method for Torsional Ring Shear Test to Determine Drained Residual Shear Strength of Cohesive Soils*. West Conshohocken, PA; ASTM International.

ASTM International. 2014. *D2113-14 Standard Practice for Rock Core Drilling and Sampling of Rock for Site Exploration*. West Conshohocken, PA; ASTM International.

ASTM International. 2014. *D4220/D4220M-14 Standard Practices for Preserving and Transporting Soil Samples*. West Conshohocken, PA; ASTM International.

ASTM International. 2014. *D4452-14 Standard Practice for X-Ray Radiography of Soil Samples*. West Conshohocken, PA; ASTM International.

ASTM International. 2014. *D4546-14e1 Standard Test Methods for One-Dimensional Swell or Collapse of Soils*. West Conshohocken, PA; ASTM International.

ASTM International. 2014. *D7012-14e1 Standard Test Methods for Compressive Strength and Elastic Moduli of Intact Rock Core Specimens under Varying States of Stress and Temperatures*. West Conshohocken, PA; ASTM International

ASTM International. 2014. *D854-14 Standard Test Methods for Specific Gravity of Soil Solids by Water Pycnometer*. West Conshohocken, PA; ASTM International.

ASTM International. 2015. *D1556/D1556M-15e1 Standard Test Method for Density and Unit Weight of Soil in Place by Sand-Cone Method*. West Conshohocken, PA; ASTM International.

ASTM International. 2015. *D1587/D1587M-15 Standard Practice for Thin-Walled Tube Sampling of Fine-Grained Soils for Geotechnical Purposes*. West Conshohocken, PA; ASTM International.

ASTM International. 2015. *D2167-15 Standard Test Method for Density and Unit Weight of Soil in Place by the Rubber Balloon Method*. West Conshohocken, PA; ASTM International.

ASTM International. 2015. *D2850-15 Standard Test Method for Unconsolidated-Undrained Triaxial Compression Test on Cohesive Soils*. West Conshohocken, PA; ASTM International.

ASTM International. 2015. *D3282-15 Standard Practice for Classification of Soils and Soil-Aggregate Mixtures for Highway Construction Purposes*. West Conshohocken, PA; ASTM International.

ASTM International. 2015. *D4015-15e1 Standard Test Methods for Modulus and Damping of Soils by Fixed-Base Resonant Column Devices*. West Conshohocken, PA; ASTM International.

ASTM International. 2015. *D4044/D4044M-15 Standard Test Method for (Field Procedure) for Instantaneous Change in Head (Slug) Tests for Determining Hydraulic Properties of Aquifers*. West Conshohocken, PA; ASTM International.

ASTM International. 2015. *D5856-15 Standard Test Method for Measurement of Hydraulic Conductivity of Porous Material Using a Rigid-Wall, Compaction-Mold Permeameter*. West Conshohocken, PA; ASTM International.

ASTM International. 2015. *D6635-15 Standard Test Method for Performing the Flat Plate Dilatometer*. West Conshohocken, PA; ASTM International.

ASTM International. 2016. *D1196/D1196M-12(2016) Standard Test Method for Nonrepetitive Static Plate Load Tests of Soils and Flexible Pavement Components, for Use in Evaluation and Design of Airport and Highway Pavements*. West Conshohocken, PA; ASTM International.

ASTM International. 2016. *D1452/D1452M-16 Standard Practice for Soil Exploration and Sampling by Auger Borings*. West Conshohocken, PA; ASTM International.

ASTM International. 2016. *D1883-16 Standard Test Method for California Bearing Ratio (CBR) of Laboratory-Compacted Soils.* West Conshohocken, PA; ASTM International. doi: https://doi.org/10.1520/D1883-16

ASTM International. 2016. *D2166/D2166M-16 Standard Test Method for Unconfined Compressive Strength of Cohesive Soil*. West Conshohocken, PA; ASTM International.

ASTM International. 2016. *D3967-16 Standard Test Method for Splitting Tensile Strength of Intact Rock Core Specimens*. West Conshohocken, PA; ASTM International.

ASTM International. 2016. *D4253-16e1 Standard Test Methods for Maximum Index Density and Unit Weight of Soils Using a Vibratory Table*. West Conshohocken, PA; ASTM International.

ASTM International. 2016. *D4254-16 Standard Test Methods for Minimum Index Density and Unit Weight of Soils and Calculation of Relative Density*. West Conshohocken, PA; ASTM International.

ASTM International. 2016. *D4644-16 Standard Test Method for Slake Durability of Shales and Other Similar Weak Rocks*. West Conshohocken, PA; ASTM International.

ASTM International. 2016. *D4648/D4648M-16 Standard Test Methods for Laboratory Miniature Vane Shear Test for Saturated Fine-Grained Clayey Soil*. West Conshohocken, PA; ASTM International.

ASTM International. 2016. *D4959-16 Standard Test Method for Determination of Water Content of Soil by Direct Heating*. West Conshohocken, PA; ASTM International.

ASTM International. 2016. *D4971-16 Standard Test Method for Determining In Situ Modulus of Deformation of Rock Using Diametrically Loaded 76-mm (3-in.) Borehole Jack*. West Conshohocken, PA; ASTM International.

ASTM International. 2016. *D5084-16a Standard Test Methods for Measurement of Hydraulic Conductivity of Saturated Porous Materials Using a Flexible Wall Permeameter*. West Conshohocken, PA; ASTM International.

ASTM International. 2016. *D5607-16 Standard Test Method for Performing Laboratory Direct Shear Strength Tests of Rock Specimens Under Constant Normal Force*. West Conshohocken, PA; ASTM International.

ASTM International. 2016. *D5731-16 Standard Test Method for Determination of the Point Load Strength Index of Rock and Application to Rock Strength Classifications*. West Conshohocken, PA; ASTM International.

ASTM International. 2017. *D1140-17 Standard Test Methods for Determining the Amount of Material Finer than 75-µm (No. 200) Sieve in Soils by Washing*. West Conshohocken, PA; ASTM International.

ASTM International. 2017. *D2487-17e1 Standard Practice for Classification of Soils for Engineering Purposes (Unified Soil Classification System)*. West Conshohocken, PA; ASTM International.

ASTM International. 2017. *D2488-17e1 Standard Practice for Description and Identification of Soils (Visual-Manual Procedures)*. West Conshohocken, PA; ASTM International.

ASTM International. 2017. *D2937-17e2 Standard Test Method for Density of Soil in Place by the Drive-Cylinder Method*. West Conshohocken, PA; ASTM International.

ASTM International. 2017. *D4318-17e1 Standard Test Methods for Liquid Limit, Plastic Limit, and Plasticity Index of Soils*. West Conshohocken, PA; ASTM International.

ASTM International. 2017. *D4327-17 Standard Test Method for Anions in Water by Suppressed Ion Chromatography*. West Conshohocken, PA; ASTM International.

ASTM International. 2017. *D4394-17 Standard Test Method for Determining In Situ Modulus of Deformation of Rock Mass Using Rigid Plate Loading Method*. West Conshohocken, PA; ASTM International.

ASTM International. 2017. *D4395-17 Standard Test Method for Determining In Situ Modulus of Deformation of Rock Mass Using Flexible Plate Loading Method*. West Conshohocken, PA; ASTM International.

ASTM International. 2017. *D4491/D4491M-17 Standard Test Methods for Water Permeability of Geotextiles by Permittivity*. West Conshohocken, PA; ASTM International. https://doi.org/10.1520/D4491_D4491M-17.

ASTM International. 2017. *D4643-17 Standard Test Method for Determination of Water Content of Soil and Rock by Microwave Oven Heating*. West Conshohocken, PA; ASTM International.

ASTM International. 2017. *D6528-17 Standard Test Method for Consolidated Undrained Direct Simple Shear Testing of Fine Grain Soils*. West Conshohocken, PA; ASTM International.

ASTM International. 2017. *D6913/D6913M-17 Standard Test Methods for Particle-Size Distribution (Gradation) of Soils Using Sieve Analysis*. West Conshohocken, PA; ASTM International.

ASTM International. 2017. *D6938-17a Standard Test Methods for In-Place Density and Water Content of Soil and Soil-Aggregate by Nuclear Methods (Shallow Depth)*. West Conshohocken, PA; ASTM International.

ASTM International. 2017. *D7928-17 Standard Test Method for Particle-Size Distribution (Gradation) of Fine-Grained Soils Using the Sedimentation (Hydrometer) Analysis*. West Conshohocken, PA; ASTM International.

ASTM International. 2018. *D1586/D1586M-18 Standard Test Method for Standard Penetration Test (SPT) and Split-Barrel Sampling of Soils*. West Conshohocken, PA; ASTM International.

ASTM International. 2018. *C33/C33M-18 Standard Specification for Concrete Aggregates*. West Conshohocken, PA; ASTM International.

ASTM International. 2018. *D2573/D2573M-18 Standard Test Method for Field Vane Shear Test in Saturated Fine-Grained Soils*. West Conshohocken, PA; ASTM International.

ASTM International. 2018. *D4221-18 Standard Test Method for Dispersive Characteristics of Clay Soil by Double Hydrometer*. West Conshohocken, PA; ASTM International.

ASTM International. 2018. *D4427-18 Standard Classification of Peat Samples by Laboratory Testing*. West Conshohocken, PA; ASTM International.

ASTM International. 2018. *D4944-18 Standard Test Method for Field Determination of Water (Moisture) Content of Soil by the Calcium Carbide Gas Pressure Tester*. West Conshohocken, PA; ASTM International.

ASTM International. 2018. *D6951/D6951M-18 Standard Test Method for Use of the Dynamic Cone Penetrometer in Shallow Pavement Applications*. West Conshohocken, PA; ASTM International.

ASTM International. 2018. *D7263-09(2018)e2 Standard Test Methods for Laboratory Determination of Density (Unit Weight) of Soil Specimens*. West Conshohocken, PA; ASTM International.

ASTM International. 2019. *D2216-19 Standard Test Methods for Laboratory Determination of Water (Moisture) Content of Soil and Rock by Mass*. West Conshohocken, PA; ASTM International.

ASTM International. 2019. *D3213-19 Standard Practices for Handling, Storing, and Preparing Soft Intact Marine Soil*. West Conshohocken, PA; ASTM International.

ASTM International. 2019. *D4729-19 Standard Test Method for In Situ Stress and Modulus of Deformation Using the Flat Jack Method*. West Conshohocken, PA; ASTM International.

ASTM International. 2019. *D4829-19 Standard Test Method for Expansion Index of Soils*. West Conshohocken, PA; ASTM International.

ASTM International. 2019. *D4972-19 Standard Test Methods for pH of Soils*. West Conshohocken, PA; ASTM International.

ASTM International. 2019. *D8296-19 Standard Test Method for Consolidated Undrained Cyclic Direct Simple Shear Test under Constant Volume with Load Control or Displacement Control*. West Conshohocken, PA; ASTM International. doi: https://doi.org/10.1520/D8296-19

ASTM International. 2020. *D2435/D2435M-11(2020) Standard Test Methods for One-Dimensional Consolidation Properties of Soils Using Incremental Loading*. West Conshohocken, PA; ASTM International.

ASTM International. 2020. *D4647/D4647M-13(2020) Standard Test Methods for Identification and Classification of Dispersive Clay Soils by the Pinhole Test*. West Conshohocken, PA; ASTM International.

ASTM International. 2020. *D4719-20 Standard Test Methods for Prebored Pressuremeter Testing in Soils*. West Conshohocken, PA; ASTM International.

ASTM International. 2020. *D4767-11(2020) Standard Test Method for Consolidated Undrained Triaxial Compression Test for Cohesive Soils*. West Conshohocken, PA; ASTM International.

ASTM International. 2020. *D5778-20 Standard Test Method for Electronic Friction Cone and Piezocone Penetration Testing of Soils*. West Conshohocken, PA; ASTM International.

ASTM International. 2020. *D6429-20 Standard Guide for Selecting Surface Geophysical Methods*. West Conshohocken, PA; ASTM International.

ASTM International. 2020. *D6572-20 Standard Test Methods for Determining Dispersive Characteristics of Clayey Soils by the Crumb Test*. West Conshohocken, PA; ASTM International.

ASTM International. 2020. *D7181-20 Standard Test Method for Consolidated Drained Triaxial Compression Test for Soils*. West Conshohocken, PA; ASTM International.

ASTM International. 2020. *D7698-20 Standard Test Method for In-Place Estimation of Density and Water Content of Soil and Aggregate by Correlation with Complex Impedance Method*. West Conshohocken, PA; ASTM International.

ASTM STP 501. 1972. *Underwater Soil Sampling, Testing and Construction Control*. American Society of Testing and Materials, Philadelphia, PA.

ASTM STP 777. 1981. *Geotechnical Properties, Behavior, and Performance of Calcareous Soils*. American Society of Testing and Materials, Philadelphia, PA.

Athanasopoulos, G. A. 1995. “Empirical Correlations Vs -N SPT for Soils of Greece: A Comparative Study of Reliability.” *Proceedings of the 7th International Conference on Soil Dynamics and Earthquake Engineering*, 19–36.

Australian Drilling Industry Training Committee. 2015. *The Drilling Manual (5th ed)*. CRC Press/Taylor & Francis, Boca Raton, FL.

Ayadat, T., and Hanna, A. 2007a. “Identification of Collapsible Soil Using the Fall Cone Apparatus.” *Geotechnical Testing Journal*, 30(4), 312–323.

Ayadat, T., and Hanna, A. 2007b. “Prediction of collapse behaviour in soil.” *Revue Européenne de Génie Civil*, 11(5), 603–619.

Azzouz, A. S., Krizek, R. J., and Corotis, R. B. 1976. “Regression Analysis of Soil Compressibility.” *Soils and Foundations*, 16(2), 19–29.

Balasubramaniam, A. S., and Brenner, R. P. 1981. “Consolidation and Settlement of Soft Clay.” *Soft Clay Engineering,* E. W. Brand and R. P. Brenner, eds., Elsevier, 481–566.

Baldi, G., Bellotti, R., Ghionna, V., Jamiolkowski, M., and Lo Presti, D. C. F. 1989. “Modulus of Sands from CPT’s and DMT’s.” In *Proc. 12th Int. Conf. on Soil Mechanics and Foundation Engineering*, Rio de Janeiro, 165–170.

Baldi, G., Bellotti, R., Ghionna, V., Jamiolkowski, M., and Pasqualini, E. 1981. “Cone Resistance of a Dry Medium Sand.” In *Proc.10th Int. Conf. on Soil Mechanics and Foundation Engineering,* Stockholm, 427–432.

Bandyopadhyay, S.S. 1981. “Prediction of Swelling Potential for Natural Soils.” *Journal of Geotechnical Engineering*, 107(5): 658–691.

Barber, E.W. 1959. “Subsurface Drainage of Highways.” *Highway Research Board, Bulletin 209*, Highway Research Board, Washington, D.C.

Barron, R. A. 1948. “Consolidation of Fine-Grained Soils by Drain Wells.” *Transactions of ASCE*, Paper No. 2346, 718-743.

Bartholomew, C.L. and Haverland, M.L. 1987. *Concrete Dam Instrumentation Manual*. United States Department of the Interior, Bureau of Reclamation, Denver, CO.

Barton, N., Lien, R., and Lunde, J. 1974. “Engineering Classification of Rock Masses for the Design of Tunnel Support.” *Rock Mechanics*, 6(4), 189–236.

Bear, J. 1979. *Hydraulics of Groundwater*. McGraw-Hill, Inc., New York, NY, 574 pp.

Been, K., Jeffries, M. G., Crooks, J. H. A., and Rothenburg, L. 1987. “The Cone Penetration Test in Sands: Part II, General Inference of State.” *Geotechnique*, 37(3), 285–299

Begemann, H. K. S. 1974. “General Report for Central and Western Europe.” In *Proc. of the European Symposium on Penetration Testing*, Stockholm, 29–39.

Benson, C. H., and Trast, J. M. 1995. “Hydraulic Conductivity of Thirteen Compacted Clays.” *Clays and Clay Minerals*, 43(6), 669–681.

Benson, C. H., Zhai, H., and Wang, X. 1994. “Estimating the Hydraulic Conductivity of Compacted Clay Liners.” *Journal of Geotechnical Engineering*, 120(2), 366–387.

Bergdahl, U., Ottosson, E., and Malmborg, B. S. 1993. *Plattgrundläggning*. AB Svensk Byggtjänst och Statens geotekniska institute. [In Swedish].

Berney, E.S., Kyzar, J.D., Oyelami, L.O. 2012. *Device Comparison for Determining Field Soil Moisture Content*. USACE Report No. ERDC/GSL TR-11-42, United States Army Corps of Engineers, Vicksburg, MS.

Berney, E.S., Mejias-Santiago, M., Kyzar, J.D. 2013. *Non-nuclear Alternatives to Monitoring Moisture-Density Response in Soils*. USACE Report No. ERDC/GSL TR-13-6, United States Army Corps of Engineers, Vicksburg, MS.

Berney, E.S., Mejias-Santiago, M., Norris, D. 2016. *Validation Testing of Non-nuclear Alternatives to Monitoring Soil Density*. USACE Report No. ERDC/GSL TR-16-28, United States Army Corps of Engineers, Vicksburg, MS.

Bieniawski, Z. T. 1973. “Engineering Classification of Jointed Rock Masses.” *Transactions of the South African Institution of Civil Engineers*, 15, 335–344.

Bieniawski, Z. T. 1976. “Rock Mass Classification in Rock Engineering.” *Proc. Sym. on Exploration for Rock Engineering*, Ed. Z. T. Bieniawski, A. Balkema Rotterdam, 7-106.

Bieniawski, Z. T. 1990. *Tunnel Design by Rock Mass Classifications*, Update of Technical Report GL-79-19. Washington: Department of the Army U.S. Army Corps of Engineers.

Bieniawski, Z.T. 1989. *Engineering Rock Mass Classifications*. John Wiley & Sons, New York, NY.

Bjerrum, L. 1954. “Geotechnical Properties of Norwegian Marine Clays.” *Geotechnique*, 4(2), 49–69.

Bjerrum, L. 1972. “Embankments on Soft Ground, State-of-the-Art Report.” *Proc. of the Conference on Performance of Earth and Earth-supported Structures*, Lafayette, 1–54.

Bjerrum, L. 1973. “Problems of Soil Mechanics and Construction on Soft Clays and Structurally Unstable Soils.” *Proc. of the 8th Int. Conf. on Soil Mechanics and Foundation Engineering,* Moscow, 111–159.

Bjerrum, L., and Simons, N. E. 1960. “Comparison of Shear Strength Characteristics of Normally Consolidated Clays.” *Norwegian Geotechnical Institute*, 35, 13–22.

Boulanger, R. W., and Idriss, I. M. 2014. *CPT and SPT Based Liquefaction Triggering Procedures*. Report No. UCD/CGM-14/01, University of California at Davis, Davis, CA.

Bovis, M. J. 1985. “Earthflows in the Interior Plateau, Southwest British Columbia.” *Canadian Geotechnical Journal*, 22(3), 313–334.

Bowles, L. E. 1996. *Foundation Analysis and Design*. McGraw-Hill.

Bradley, N. and VandenBerge, D. R. 2015. *Beginner's Guide for Geotechnical Finite Element Analyses, CGPR #82*. Center for Geotechnical Practice and Research, Blacksburg, VA, 99 pp.

Brandon, T. L., Duncan, J. M., and Gardner, W. S. 1990. “Hydrocompression Settlement of Deep Fills.” *Journal of Geotechnical Engineering*, 116(10), 1536-1548.

Broch, E., and Franklin, J. A. 1972. “The Point-load Strength Test.” *International Journal of Rock Mechanics and Mining Sciences & Geomechanics Abstracts*, 9(6), 669–676.

Brown, P. 1969. “Numerical Analyses of Uniformly Loading Circular Rafts on Elastic Layers of Finite Depth.” *Geotechnique*, 19(2), 301-306.

Burgers, A. and Yoder, E.J. 1962. *Nuclear Moisture-Density Measurements in Construction Control*. Joint Highway Research Project, Indiana Department of Transportation and Purdue University, West Lafayette, Indiana

Burland, J. B. 1970. “Discussion, Session A.” *Proc. Conf. on In Situ Investigations in Soil and Rocks*, British Geotechnical Society, London, UK, 61-62.

Burland, J. B. 1990. “On the Compressibility and Shear Strength of Natural Clays.” *Géotechnique*, 40(3), 329–378.

Burland, J. B. and Burbridge, M. 1985. “Settlement of Foundations on Sand and Gravel.” *Proc. Institution of Civil Engineers, Part 1, Design and Contruction*, 78(1), 1325-1381.

Burland, J. B. and Wroth, C. P. 1974. “Settlement of Buildings and Associated Damage.” *SOA Review, Conf. Settlement of Structures*, Cambridge, 611-654.

Burmister, D. M. 1962. “Physical, Stress-Strain, and Strength Responses of Granular Soils.” *Sym. on Field Testing of Soils (STP 322)*, ASTM, Philadelphia, 67–97.

Butcher, A. P., McElmeel, K., and Powell, J. J. M. 1996. “Dynamic Probing and its Use in Clay Soils.” *Proc. of the Int. Conf. on Advances in Site Investigation Practice*, 383–395.

California Department of Water Resources. 2013. *ULE Special Testing Program, DWR Guidance Document*. California Department of Water Resources, Sacramento, CA.

Callanan, J. F., and Kulhawy, F. H. 1985. *Evaluation of Procedures for Predicting Foundation Uplift Movements*. Report EL-4107, Palo Alto, CA.

Carman, P. C. 1938. “The Determination of the Specific Surface of Powders.” *J. Soc. Chem. Ind. Trans.*, 57, 225.

Carman, P. C. 1956. *Flow of Gases Through Porous Media*. Butterworths Scientific Publications, London.

Carrier, W. D. 2003. “Goodbye, Hazen; Hello, Kozeny-Carman.” *Journal of Geotechnical and Geoenvironmental Engineering*, 129(11), 1054-1056.

Carrier, W. D., and Beckman, J. F. 1984. “Correlations Between Index Tests and the Properties of Remoulded Clays.” *Geotechnique*, 34(2), 211–228.

Carrillo, N. 1942. “Simple Two and Three Dimensional Case in the Theory of Consolidation of Soils.” *Journal of Mathematics and Physics*, 21(1-4), 1-5.

Carter, M., and Bentley, S. P. 2016. *Soil Properties and their Correlations*. John Wiley & Sons, Ltd.

Castellanos, B. A., Ritchie, J., and Brandon, T. L. 2021. *Estimating Fully Softened and Residual Shear Strength Parameters of Fine-Grained Soils*. Center for Geotechnical Practice and Research, Blacksburg, VA.

Chandler, R. J. 1969. “The Effect of Weathering on the Shear Strength Properties of Keuper Marl.” *Géotechnique*, 19(3), 321–334.

Chandler, R. J. 1970. “A Shallow Slab Slide in the Lias Clay near Uppingham, Rutland.” *Géotechnique*, 20(3), 253–260.

Chandler, R. J. 1988. “The In-Situ Measurement of the Undrained Shear Strength of Clays Using the Field Vane.” *Vane Shear Strength Testing in Soils: Field and Laboratory Studies, ASTM STP 1014*, A. F. Richards, ed., American Society for Testing and Materials, Philadelphia, 13–44.

Chapman, G. A., and Donald, I. B. 1981. “Interpretation of Static Penetration Tests in Sand.” *Proc. of the 10th Int. Conf. on Soil Mechanics and Foundation Engineering*, Stockholm, 455–458.

Chapuis, R. P. 2004. “Predicting the Saturated Hydraulic Conductivity of Sand and Gravel Using Effective Diameter and Void Ratio.” *Canadian Geotechnical Journal*, 41, 787-795.

Chen, F.H. 1975. *Foundations on Expansive Soils*. Elsevier Scientific Pub. Co., Amsterdam, New York, NY.

Cheng, Y. M., Hu, Y. Y., and Wei, W. B. 2007. “General Axisymmetric Active Earth Pressure by Method of Characteristics—Theory and Numerical Formulation.” *International Journal of Geomechanics*, 7(1), 1-15.

Christopher, B.R. and Fischer, G.R. 1991. “Geotextile Filtration Principles, Practices, and Problems.” *Proc. of the 5th GRI seminar on the topic of Geosynthetics in Filtration, Drainage, and Erosion Control*, Philadelphia, Pennsylvania, 1 – 17.

Clayton, C.R.I, Matthews, M.C., Simmons, N.E. 1995. *Site Investigation: Second Edition*.

Coduto, D. P., Yeung, M. C. R., and Kitch, W. A. 2011. *Geotechnical Engineering: Principles and Practices*. Prentice Hall.

Cokca, E. 2002. “Relationship Between Methylene Blue Value, Initial Soil Suction and Swell Percent of Expansive Soils.” *Turkish Journal of Engineering and Environmental Sciences*, 26: 521–529.

Cox, J. B. 1968. "A Review of the Engineering Characteristics of the Recent Marine Clays in South East Asia." *Research Report No. 6*.

Cozzolino, V. M. 1961. “Statistical Forecasting of Compression Index.” *Proc. of the 5th Int. Conf. on Soil Mechanics and Foundation Engineering*, Paris, France, 51–53.

D'Appolonia, D. J., Poulos, H. G., and Ladd, C. C. 1971. “Initial Settlement of Structures on Clay.” *Journal of the Soil Mechanics and Foundation Division*, 97(10), 1359-1377.

D’Appolonia, E., Alperstein, R., and D’Appolonia, D. J. 1967. “Behavior of a Colluvial Slope.” *Journal of Soil Mechanics and Foundations Division*, 93(4), 447–473.

Dakshanamurthy, V., and Raman, V. 1973. “A Simple Method of Identifying an Expansive Soil.” *Soils and Foundations*, 13(1), 97–104.

Davis, E. H., and Poulos, H. G. 1972. “Rate of Settlement Under Two and Three Dimensional Conditions.” *Geotechnique*, 22(1), 95-114.

Davis, R. O. and Selvadurai A. P. S. 1996. *Elasticity and Geomechanics*. Cambridge University Press, Cambridge, UK, 216 pp.

Day, R. W. 1990. “Differential Movement of Slab on Grade Structures.” *Journal of Performance of Constructed Facilities*, 4(4), 236-241.

Day, R. W. 1999. *Geotechnical and Foundation Engineering*. McGraw-Hill, New York, NY.

Decker, J. B., Rollins, K. M., and Ellsworth, J. C. 2008. “Corrosion Rate Evaluation and Prediction for Piles Based on Long-Term Field Performance.” *Journal of Geotechnical and Geoenvironmental Engineering*, 134(3), 341–351.

Deere, D.U. and Deere, D.W. 1988. “The Rock Quality Designation (RQD) Index in Practice.” *Proc., Rock Classification Systems for Engineering Purposes, ASTM STP 984, American Society for Testing and Materials*, Philadelphia, PA 91-101.

DeMello, V. F. B. 1971. “The Standard Penetration Test: A State-of-the-Art Report.” *Proc. of the 4th Panamerican Conference on Soil Mechanics and Foundation Engineering*, San Juan, PR, 1–86.

Dikmen, U. 2009. “Statistical Correlations of Shear Wave Velocity and Penetration Resistance for Soils.” *Journal of Geophysics and Engineering*, 6, 61–72.

Duncan, J. M. 1979. “Behavior and Design of Long-Span Metal Culverts.” *Journal of the Geotechnical Engineering Division*, 105(3), 399-418.

Duncan, J. M. and Chang C.-Y. 1970. “Nonlinear Analysis of Stress and Strain in Soils.” *Journal of the Soil Mechanics and Foundations Division*, 96(5), 1629-1653.

Duncan, J. M. and Wong, K. S. 1983. "Use and Mis-use of the Consolidated-undrained Triaxial Test for Analysis of Slope Stability During Rapid Drawdown." *Paper Prepared for 25th Anniversary Conference on Soil Mechanics*, Venezuela.

Duncan, J. M., and Buchignani, A. L. 1987. *Engineering Manual for Settlement Studies, CGPR #2*. Center for Geotechnical Practice and Research.

Duncan, J. M., and Mokwa, R. L. 2001. “Passive Earth Pressures: Theories and Tests.” *Journal of Geotechnical and Geoenvironmental Engineering*, 127(3), 248-257.

Duncan, J. M., Byrne, P., Wong, K. S., and Mabry, P. 1980. “Strength, Stress-Strain and Bulk Modulus Parameters for Finite Element Analyses of Stresses and Movements in Soil Masses.” *Report No. UCB/GT/80-01*, Univ. California-Berkeley, 77 pp. (Republished as CGPR #63, Center for Geotechnical Practice and Research, Virginia Tech, Blacksburg, VA).

Duncan, J. M., Horz, R. C., and Yang, T. L. 1989. *Shear Strength Correlations for Geotechnical Engineering*. Center for Geotechnical Practice and Research, Blacksburg, VA.

Duncan, J. M., O’Neil, B., Brandon, T. L., and VandenBerge, D. R. 2011. *Evaluation of Potential for Erosion in Levees and Levee Foundations, CGPR #64*. Center for Geotechnical Practice and Research, Virginia Tech, Blacksburg, VA, 36 pp.

Duncan, J. M., Wright, S. G., and Brandon, T. L. 2014. *Soil Strength and Slope Stability, 2nd ed*. Wiley, Hoboken, NJ.

Dunn, C. 2017. “Field Soils Testing.” *North Dakota DOT Training*. http://www.dot.nd.gov/divisions/materials/ttqp/soilstesting.pdf, (August, 2019)

Dunnicliff, J. 1993. *Geotechnical Instrumentation for Monitoring Field Performance*. John Wiley & Sons, New York, NY.

Elnaggar, H. A. and Krizek, R. J. 1970. “Statistical Approximation for Consolidation Settlement.” *Highway Research Record No. 323*, 87-96.

Erzin, Y., and Erol, O. 2004. “Correlations for Quick Prediction of Swell Pressures.” *Electronic Journal of Geotechnical Engineering*, 9(F): Paper No. 0476. available from www.ejge.com/2004/Ppr0476/Abs0476.htm.

Erzin, Y., and Erol, O. 2007. “Swell Pressure Prediction by Suction Methods.” *Engineering Geology*, 92(3–4): 133–145. doi:10.1016/j.enggeo.2007.04.002.

Fear, C. E., and Robertson, P. K. 1995. “Estimating the Undrained Strength of Sand: A Theoretical Framework.” *Canadian Geotechnical Journal*, 32(5), 859–870.

Feleke, G. G., and Araya, A. A. 2016. “Prediction of CBR Using DCP for Local Subgrade Materials.” *Proc. of the Int. Conf. on Transport and Road Research*, 1–30.

FEMA (Federal Emergency Management Agency). 2011. *Filters for Embankment Dams, Best Practices for Design and Construction*, 332 pp.

Fenning, P. J., and Hasan, S. 1995. “Pipeline Route Investigations Using Geophysical Techniques.” *Engineering Geology of Construction*, Geological Society Engineering Geology, Special Publication No. 10, M. Eddleston et al (Eds), pp. 229–233.

Ferrent, T. A. 1963. “The Prediction of Field Verification of Settlement on Cohesionless Soils.” *Proc. of the 4th Australia-New Zealand Conference on Soil Mechanics and Foundation Engineering*, 11–17.

FHWA (Federal Highway Administration). 1998. *Geotechnical Instrumentation*. Reference Manual FHWA HI-98-034, United States Department of Transportation, Federal Highway Association, Washington, DC.

FHWA. 1998. *Rock Slopes Reference Manual, FHWA-HI-99-007*. Washington, D.C.

FHWA. 1999. *Geotechnical Engineering Circular No. 4 Ground Anchors and Anchored Systems*, FHWA-IF-99-015. Washington, D.C.

FHWA. 2002. “Evaluation of Soil and Rock Properties.” *Geotechnical Engineering Circular No. 5. Publication No. FHWA-IF-02-034*. Federal Highway Administration, U.S. Department of Transportation, Washington, DC.

FHWA. 2003. “Application of Geophysical Methods to Highway Related Problems.” *Contract No. DTFH68-02-P-00083*. Federal Highway Administration, U.S. Department of Transportation, Washington, DC.

FHWA. 2006. “Soils and Foundations, Reference Manual – Volume I.” *Publication No. FHWA NHI-06-088*, Federal Highway Administration, U.S. Department of Transportation, Washington, DC.

FHWA. 2009. *Corrosion/Degradation of Soil Reinforcements for Mechanically Stabilized Earth Walls and Reinforced Soil Slopes*. National Highway Institute - Federal Highway Administration.

FHWA. 2009. *Technical Manual for Design and Construction of Road Tunnels – Civil Elements, FHWA-NHI-09-010*. Washington, D.C., 694 pp.

FHWA. 2009a. *Corrosion/Degradation of Soil Reinforcements for Mechanically Stabilized Earth Walls and Reinforced Soil Slopes, FHWA-NHI-09-087*. Washington, D.C.

FHWA. 2009b. *Design of Mechanically Stabilized Earth Walls and Reinforced Soil Slopes-Volume I and II, FHWA-NHI-10-024 and FHWA-NHI-10-025*. Washington, D.C.

FHWA. 2015. *Geotechnical Engineering Circular No. 7 Soil Nail Walls – Reference Manual, FHWA-NHI-14-007*. Washington, D.C.

FHWA. 2016. “Geotechnical Site Characterization.” *Geotechnical Engineering Circular No. 5. Publication No. NHI-16-072*. Federal Highway Administration, U.S. Department of Transportation, Washington, DC.

FHWA. 2017. *Geotechnical Engineering Circular No. 5 - Geotechnical Site Characterization*. U.S. Department of Transportation - Federal Highway Administration, Washington, DC.

FHWA. 2017. *Ground Modification Methods Reference Manual – Volume I, FHWA-NHI-16-027*, Geotechnical Engineering Circular 13, Washington D.C.

Filz, G., and Brandon, T. L. 1993. "Compactor Force and Energy Measurements," *ASTM Geotechnical Testing Journal*, Vol. 16, No. 4, December, pp. 442-449.

Foster, M., Fell, R., and Spannagle, M. 2000. “The Statistics of Embankment Dam Failures and Accidents.” *Canadian Geotechnical Journal*, 37(5), 1000-1024.

Frazer, R. A. and Wardle, L. J. 1976. "Numerical Analysis of Rectangular Rafts on Layered Foundations." *Geotechnique*, 26(4), 613-630.

Freeze, R.A. and Cherry, J.A. 1979. *Groundwater*, Prentice-Hall, Englewood Cliffs, NJ, 604 pp.

Fujiwara, T. 1972. “Estimation of Ground Movements in Actual Destructive Earthquakes.” *Proc. of the 4th European Symposium on Earthquake Engineering*, London, 125–132.

Fumal, T. E., and Tinsley, J. C. 1985. “Mapping Shear-Wave Velocities of Near-Surface Geologic Materials.” *Evaluating Earthquake Hazards in the Los Angeles Region -- An Earth-Science Perspective, U.S. Geological Survey Professional Paper 1360*, J. I. Ziony, ed., 127–149.

Gabr, M. A., Hopkins, K., Coonse, J., and Hearne, T. 2000. “DCP Criteria for Performance Evaluation of Pavement Layers.” *Journal of Performance of Constructed Facilities*, 14(4), 141–148.

Geological Society of London. 1977. “The Description of Rock Masses for Engineering Purposes.” *Quarterly Journal of Engineering Geology and Hydrogeology*, 10(4), 355–388.

George, J.T., Finley, R.E. and Riggins, M., 1999, January. "Determination of Rock Mass Modulus Using the Plate Loading Method." *9th ISRM Congress*. International Society for Rock Mechanics and Rock Engineering.

George, V., and Kumar, A. 2018. “Studies on Modulus of Resilience Using Cyclic Triaxial Test and Correlations to PFWD, DCP, and CBR.” *International Journal of Pavement Engineering*, 19(11), 976–985.

George, V., Nageshwar, C. R., and Shivashankar, R. 2009. “PFWD, DCP and CBR Correlations for Evaluation of Lateritic Subgrades.” *International Journal of Pavement Engineering*, 10(3), 189–199.

Gibson, R. E. 1953. “Experimental Determination of the True Cohesion and True Angle of Internal Friction in Clays.” *Proc. of the 3rd Int. Conf. in Soil Mechanics*, Zurich, 1, 126–130.

Gibson, R.E. and Anderson, W.F. 1961. “In-Situ Measurement of Soil Properties with the Pressuremeter.” *J. Civil Engineering and Public Works Review*, 56(658), London, 615-618.

Gielly, J., Lareal, P., and Sanglerat, G. 1969. “Correlations between In Situ Penetrometer Tests and the Compressibility of Soils.” *Proc. of the Conferences on In Situ Investigations of Soils and Rocks*, London, 167–172.

Giroud, J.-P. 1972. “Settlement of Rectangular Foundation on Soil Layer.” *Journal of the Soil Mechanics and Foundations Division*, 98(SM1), 149-154.

Giroud, J.P. 2010. “Development of Criteria for Geotextile and Granular Filters.” *Proc. of the 9th Int. Conf. on Geosynthetics*, Guaruja, Brazil, Vol. 1, 45–64.

Goldberg, G. D., Lovell, C. W., and Miles, R. D. 1979. “Use the Geotechnical Data Bank.” *Transportation Research Record*, 702, 140–146.

Goodman, R. 1970. *The Deformability of Joints*. Determination of the In Situ Modulus of Deformation of Rock, ASTM International, West Conshohocken, PA., 174-196.

Goodman, R.E. 1989. *Introduction to Rock Mechanics. 2nd Ed.* John Wiley & Sons, New York.

Griffiths, D. V., and P. A. Lane. 1999. “Slope Stability Analysis by Finite Elements.” *Geotechnique 49*, No. 3, pp. 387-403.

Hamel, J. V. 1970. *Stability of Slopes in Soft, Altered Rocks*. Ph.D. dissertation, University of Pittsburgh.

Hansbo, S. 1957. “A New Approach to the Determination of the Shear Strength of Clay by the Fall-Cone Test.” *Royal Swedish Geotechnical Institute Proceedings*, 14, 1–46.

Hansbo, S. 1979. “Consolidation of Clay by Band-Shaped Prefabricated Drains.” *Ground Engineering*, 12(5), 16-25.

Hara, A., Ohta, T., Niwa, M., Tanaka, S., and Banno, T. 1974. “Shear Modulus and Shear Strength of Cohesive Soils.” *Soils and Foundations*, 14(3), 1–12.

Harr, M. E. 1977. “Chapter 5 – Analysis of flow systems.” *Mechanics of Particulate Media*, McGraw Hill, New York, NY, 142-183.

Harrison, J. A. 1986. “Correlation of CBR and Dynamic Cone Penetrometer Strength Measurement of Soils.” *Australian Road Research1*, 16(2), 130–136.

Hasancebi, N., and Ulusay, R. 2007. “Empirical Correlations Between Shear Wave Velocity and Penetration Resistance for Ground Shaking Assessments.” *Bulletin of Engineering Geology and the Environment*, 66(2), 203–213.

Hatanaka, M., and Uchida, A. 1996. “Empirical Correlations Between Penetration Resistance and Internal Friction Angle of Sandy Soils.” *Soils and Foundations*, 36(4), 1–9.

Hazen, A. 1892. “Some Physical Properties of Sands and Gravels, with Special Reference to Their Use in Filtration.” *24th Annual Report, Massachusetts State Board of Health*, Pub. Doc. No. 34, 539-556.

Hazen, A. 1911. “Discussion of ‘Dams on Sand Foundations: Some Principles Involved in Their Design, and the Law Governing the Depth of Penetration Required for Sheet-Piling.’” *Transactions of the American Society of Civil Engineers*, 73(3), 190–207.

Hegazy, Y. A., and Mayne, P. W. 1995. “Statistical Correlations Between Vs and CPT Data for Different Soil Types.” *Proc. of the Int. Sym. on Cone Penetration Testing CPT95*, Spon Press, Linkoping, Sweden, 173–178.

Hegazy, Y. A., and Mayne, P. W. 2006. “A Global Statistical Correlation Between Shear Wave Velocity and Cone Penetration Data.” *Site and Geomaterial Characterization* (GeoShanghai International Conference), 243–248.

Helenelund, K. V. 1951. “On Consolidation and Settlement of Loaded Soil Layers.” Ph.D. Dissertation, Finland Technical Institute.

Hemphill, G.B. 2012. *Practical Tunnel Construction*. John Wiley & Sons.

Hill, S., Skempton, A. W., and Petley, D. J. 1967. “The Strength Along Structural Discontinuities in Stiff Clays.” *Proc. of the Geotechnical Conference Oslo 1967 on Shear Strength Properties of Natural Soils and Rocks*, 2, 29–46.

Hoek, E. 2007. *Practical Rock Engineering*. RocScience Inc., Toronto, ON.

Hoek, E. and Bray, J. 1981. *Rock Slope Engineering, 3rd Ed*. The Institution of Mining and Metallurgy, London.

Holden, J. C. 1976. “The Determination of Deformation and Shear Strength Parameters for Sands using the Electrical Friction-cone Penetrometer.” *Norwegian Geotechnical Institute*, 110, 55–60.

Holtz, R. D., and Holm, G. 1973. *Belastningsförsök på Svartmocka*. [In Swedish]. Stockholm.

Holtz, R. D., and Kovacs, W. D. 1981. *An Introduction to Geotechnical Engineering*. Prentice Hall.

Holtz, R. D., Kovacs, W. D., and Sheahan, T. C. 2011. *An Introduction to Geotechnical Engineering, 2nd Ed*. Prentice Hall, Upper Saddle River, NJ, 853 pp.

Hough, B. K. 1957. *Basic Soils Engineering*. The Ronald Press Company, New York, 114-115.

Hough, B. K. 1969. *Basic Soil Engineering*. 2nd ed., The Ronald Press Company, New York.

Houlsby, A.C. 1976. “Routine Interpretation of the Lugeon Water-Test.” *J. Engineering Geology*, 9, 303-313.

Hutchinson, J. N. 1967. “Written Discussion.” *Proc. of the Geotechnical Conference Oslo 1967 on Shear Strength Properties of Natural Soils and Rocks*, 2, 183–184.

Hutchinson, J. N. 1969. “A Reconsideration of the Coastal Landslides at Folkestone Warren, Kent.” *Géotechnique*, 19(1), 6–38.

ICC (International Code Council). 2018. *International Building Code*. International Code Council.

ICOLD (International Commission on Large Dams). 2014. “Internal Erosion of Existing Dams, Levees and Dykes, and Their Foundations.” *Bulletin 164*, Volume 1: Internal Erosion Processes and Engineering Assessment, Eds. Bridle, R. and Fell, R., International Commission on Large Dams, Paris.

Imai, T. 1977. “P-and S-wave Velocities of the Ground in Japan.” *Proc. of the 9th Int. Conf. on Soil Mechanics and Foundation Engineering*, 127–132.

Imai, T., and Tonouchi, K. 1982. “Correlation of N-value with S-wave Velocity and Shear Modulus.” *Pro. of the 2nd European Symposium on Penetration Testing*, Amsterdam, 67–72.

Imai, T., and Yoshimura, Y. 1975. “The Relation of Mechanical Properties of Soils to P and S-Wave Velocities for Ground in Japan.” *Technical Note OYO Corporation*.

Imai, T., Fumoto, H., and Yokota, K. 1975. “The Relation of Mechanical Properties of Soil to P and S-Wave Velocities in Japan” [In Japanese]. *Proc. of 4th Japan Earthquake Engineering Symposium*, 89–96.

Iwasaki, K., and Kamei, T. 1994. “Evaluation of In Situ Strength and Deformation Characteristics of Soils Using Flat Dilatometer.” *Doboku Gakkai Ronbunshu*, 1994(499), 167–175.

Iyisan, R. 1996. “Correlations Between Shear Wave Velocity and in-situ Penetration Test Results” [In Turkish]. *Teknik Dergi (Digest)*, 7, 1187–1199.

Jafari, M. K., Shafiee, A., and Razmkhah, A. 2002. “Dynamic Properties of the Fine Grained Soils in South of Tehran.” *Journal of Seismology and Earthquake Engineering*, 4(1), 25–35.

Jaime, A., and Romo, M. P. 1988. “Mexico Earthquake of September 19, 1985 - Correlations Between Dynamic and Static Properties of Mexico City Clay.” *Earthquake Spectra*, 4(4), 787–804

Jamiolkowski, M., Ghionna, V., Lancellotta, R., and Pasqualini, E. 1988. “New Correlations of Penetration Tests for Design Practice.” *Proc. of the 1st Int. Sym. on Penetration Testing*, Orlando, FL, 263–296.

Jamiolkowski, M., Ladd, C. C., Germaine, J. T., and Lancellotta, R. 1985. “New Developments in Field and Laboratory Testing of Soils.” *Proc. of the 11th Int. Conf. on Soil Mechanics and Foundation Engineering*, 1, 57–154.

Janbu, N. 1963. “Soil Compressibility as Determined by Oedometer and Triaxial Tests.” *Proc. of the 3rd European Conference on Soil Mechanics and Foundation Engineering*, Wiesbaden, 19–25.

Janbu, N. 1985. “Soil Models in Offshore Engineering.” *Geotechnique*, 35(3), 241–281.

Janbu, N., and K., S. 1974. “Effective Stress Interpretation of In Situ Static Penetration Tests.” *Proc. of the European Symposium on Penetration Testing*, Stockholm, 181–193.

Jimenez Salas, J. A. 1948. “Soil Pressure Computations: A Modification of Newmark's Method.” *Proc. 2nd Int. Conf. on Soil Mechanics and Foundation Engineering*, Rotterdam.

Jinan, Z. 1987. “Correlation Between Seismic Wave Velocity and the Number of Blow of SPT and Depth.” *Selected Papers from the Chinese Journal of Geotechnical Engineering*, 92–100.

Johnson, L.D. 1978. *Predicting Potential Heave and Heave with Time in Swelling Foundation Soils*. Technical Report S-78-7, U.S. Army Engineer Waterways Experiment Station, Vicksburg, MS.

Johnson, L.D., and Snethen, D.R. 1978. “Prediction of Potential Heave of Swelling Soil.” *Geotechnical Testing Journal*, 1(3): 117–124. doi:10.1520/GTJ10382J.

Kahl, H., Muhs, H., and Meyer, W. 1968. “Ermittlung der Grösse und des Verlaufs des Spitzendrucks bei Drucksondierungen in Ungleischförmigen Sand-Kies-gemischen und in Kies.” [In German]. *Mitteilungen DEGEBO*, 21, 1–36.

Kamei, T., and Iwasaki, K. 1995. “Evaluation of Undrained Shear Strength of Cohesive Soils Using a Fat Dilatometer.” *Soils and Foundations*, 35(2), 111–116.

Karlsson, R., and Viberg, L. 1967. “Ratio c/p’ in Relation to Liquid Limit and Plasticity Index, with Special Reference to Swedish Clays.” *Proc. of the Geotechnical Conference Oslo 1967 on Shear Strength Properties of Natural Soils and Rocks*, 1, 43–47.

Karray, M., Lefebvre, G., Ethier, Y., and Bigras, A. 2011. “Influence of Particle Size on the Correlation Between Shear Wave Velocity and Cone Tip Resistance.” *Canadian Geotechnical Journal*, 48(4), 599–615.

Kayabali, K. 1996. “Soil Liquefaction Evaluation Using Shear Wave Velocity.” *Engineering Geology*, 44(1–4), 121–127.

Kenney, T. C. 1967. “The Influence of Mineral Composition on the Residual Shear Strength of Natural Soils.” *Proc. of the Geotechnical Conference Oslo 1967 on Shear Strength Properties of Natural Soils and Rock*s, Oslo, Norway, 1, 123–129.

Kenney, T. C. 1959. “Discussion of Geotechnical Properties of Glacial Lake Clays.” *Journal of the Soil Mechanics and Foundations Division*, 85(SM1), 67–79.

Kenney, T. C., Lau, D., and Ofoegbu, G. I. 1984. “Permeability of Compacted Granular Materials.” *Canadian Geotechnical Journal*, 21(4), 726-729.

Kerisel, J. 1961. “Fondations Profondes en Milieu Sableux.” [In French]. *Proc. of the 5th Int. Conf. on Soil Mechanic*s, Paris, France, 73–83.

Kezdi, A. 1974. *Handbook of Soil Mechanics Vol. 1: Soil Physics*. Elsevier, Hungary.

Kiku, H., Yoshida, N., Yasuda, S., Irisawa, T., Nakazawa, H., Shimizu, Y., Ansal, A., and Erkan, A. 2001. “In Situ Penetration Tests and Soil Profiling in Adapazari, Turkey.” *Proc. of the ICSMGE/TC4 Satellite Conference on Lessons Learned from Recent Strong Earthquakes*, 259–265.

Kirkham, D. 1950. “Seepage into Ditches in the Case of a Plane Water Table and an Impervious Substratum.” *Transactions, American Geophysical Union*, 31.3, 425-430.

Kirkham, D. 1960. “Seepage into Ditches from a Plane Water Table Overlying a Gravel Substratum.” *Journal of Geophysical Research*, 65(4), 1267-1272.

Kleyn, E. G., and Van Heerden, M. J. J. 1983. “Using DCP Soundings to Optimize Pavement Rehabilitation.” *Proc. of the Annual Transportation Convention*, 3, 319–334.

Koerner, R. 2012. *Designing with Geosynthetics, 6th Ed*. Xlibris Corp.

Komornik, A., and David, D. 1969. “Prediction of Swelling Pressure of Clays.” *Journal of the Soil Mechanics and Foundations Division*, 95(1): 209–226.

Koppula, S. D. 1981. “Statistical Estimation of Compression Index.” *Geotechnical Testing Journal*, 4(2), 68–73.

Kozeny, J. 1927. “Ueber kapillare Leitung des Wassers im Boden.” [In Swedish]. Wien, Akad. Wiss., 136(2a), 271.

Kulhawy, F.H. and Mayne, P.W. 1990. *Manual for Estimating Soil Properties for Foundation Design*. Report EL-6800, Electric Power Research Institute, Palo Alto, CA.

Ladd, C. C. 1991. "Stability evaluation during staged construction." *ASCE, Journal of Geotechnical Engineering*, 117, 540-615.

Ladd, C. C., and DeGroot, D. J. 2004. “Recommended Practice for Soft Ground Site Characterization: Arthur Casagrande Lecture.” *Proc. of the 12th Panamerican Conference on Soil Mechanics and Geotechnical Engineering*, 3–57.

Ladd, C. C., and Foott, R. 1974. “New Design Procedure for Stability of Soft Clays.” *Journal of the Geotechnical Engineering Division*, 100(GT7), 763–786.

Ladd, C. C., Foott, R., Ishihara, K., Schlosser, F., and Poulos, H. G. 1977. “Stress-Deformation and Strength Characteristics.” *Proc. of the 9th Int. Conf. on Soil Mechanics and Foundation Engineering*, Tokyo, Japan, 421–494.

Lambe, T. W., and Whitman, R. V. 1969. *Soil Mechanics*. John Wiley & Sons.

Larson, E. 1980. “Undrained Strength in Stability Calculation of Embankments and Foundation on Soft Clays.” *Canadian Geotechnical Journal*, 17(4), 591–602.

Lauffer, H. 1997. “Rock Classification Methods Based on the Excavation Response.” *Felsbau*, 15(3), 179–182.

Lee, S. H. H. 1990. “Regression Models of Shear Wave Velocities.” *J Chinese Insti Eng*, 13, 519–532.

Leonards, G. 1976. “Estimating Consolidation Settlements of Shallow Foundations on Oversonsolidated Clay.” *Special Report - Transportation Research Board, National Research Council.*, 163, 13-16.

Leroueil, S., Tavenas, F., and Le Bihan, J. 1983. “Propriétés Caractéristiques des Argiles de l’est du Canada.” [In French]. *Canadian Geotechnical Journal*, 20(4), 681–705.

Livneh, M. 1989. “Validation of Correlations Between a Number of Penetration Tests and In Situ California Bearing Ratio Tests.” *Transportation Research Record*, 1219, 56–67.

Lo, Y. K. Y., and Lovell, C. W. 1982. “Prediction of Soil Properties from Simple Indices.” *Transportation Research Record*, 873, 43–49.

Loudiere, D., Fayoux, D., Houis, J., Perfetti, J., and Sotton, M. 1983. “The Use of Geotextiles in French Earth Dams.” *Water Power and Dam Construction*, January, 19-2.

Luettich, S.M., Giroud J.P, and Bachus, R.C. 1992. “Geotextile Filter Design Guide.” *Geotextiles and Geomembranes*, Vol 11, Issues 4-6, pp355-370.

Lumb, P., and Holt, J. K. 1968. “The Undrained Shear Strength of a Soft Marine Clay from Hong Kong.” *Geotechnique*, 18(1), 25–36.

Lunne, T., and Christoffersen, H. P. 1985. “Interpretation of Cone Penetrometer Data for Offshore Sands.” *Norwegian Geotechnical Institute*, 156, 1–12.

Lunne, T., and Kleven, A. 1982. “Role of CPT in North Sea Foundation Engineering.” *Norwegian Geotechnical Institute*, 139, 1–14.

Lunne, T., Robertson, P. K., and Powell, J. J. M. 1997. *Cone Penetration Testing in Geotechnical Practice*. Blackie Academic and Professional.

Lutenegger, A. and Hallberg, G. 1981. *Borehole Shear Test in Geotechnical Investigations*. STP740, Laboratory Shear Strength of Soil, R. Yong, R. and Townsend, F. eds., ASTM International, West Conshohocken, PA, 566-578.

Maheswari, R. U., Boominathan, A., and Dodagoudar, G. R. 2010. “Use of Surface Waves in Statistical Correlations of Shear Wave Velocity and Penetration Resistance of Chennai Soils.” *Geotechnical and Geological Engineering*, 28(2), 119–137.

Marchetti, S. 1980. “In Situ Tests by Fat Dilatometer.” *Journal of the Geotechnical Engineering Division*, 106(GT3), 299–321.

Marchetti, S. 1997. “The Flat Dilatometer: Design Applications.” *Proc. of the 3rd Geotechnical Engineering Conference at Cairo University*, Cairo, ed., 421–448.

Marchetti, S., Monaco, S., Totani, G., Calabrese. M. 2006. "The Flat Dilatometer Test in Soil Investigations." ISSMGE Committee TC102. *Proc. 2nd Int. Conf. on Flat Dilatometer, In-Situ Soil Testing*, Fairfax, VA.

Marinos, P. G., Marinos, V., and Hoek, E. 2007. “The Geological Strength Index (GSI): A Characterization Tool for Assessing Engineering Properties for Rock Masses.” *Proc. of The International Workshop on Rock Mass Classification in Underground Mining*, 87–94.

Marsland, A.R. 1953. “Model Experiments to Study the Influence of Seepage on the Stability of a Sheeted Excavation in Sand.” *Geotechnique*, 3(6), 223-241.

Marston. A and Anderson, A. O. 1913. “The Theory of Loads on Pipes in Ditches and Tests of Cement and Clay Drain Tile and Sewer Pipe.” *Bulletin No. 31*, Iowa Eng. Experiment Station, Ames, IA.

Mayne, P. W. 1985. “Stress Anisotropy Effects on Clay Strength.” *Journal of Geotechnical Engineering*, 111(3), 356–366.

Mayne, P. W. 2006. “The Second James K. Mitchell Lecture Undisturbed Sand Strength from Seismic Cone Tests.” *Geomechanics and Geoengineering: An International Journal*, 1:4, 239–257.

Mayne, P. W. 2007. *Cone Penetration Testing State-of-Practice*. NCHRP Project 20-05.

Mayne, P. W., and Rix, G. J. 1995. “Correlations Between Shear Wave Velocity and Cone Tip Resistance in Natural Clays.” *Soils and Foundations*, 35(2), 107–110.

Mayne, P.W. 2012. "SOA Report: Geotechnical Site Characterization in the Year 2012 and Beyond." *State-of-the-Art and Practice in Geotechnical Engineering*, GSP 226, GeoCongress 2012, Oakland, CA, ASCE Press, Reston, VA.

McCook. 2010. “Empirical Estimates of Permeability for Earth Dam Projects.” Webinar presentation. American Society of Dam Safety Officials, Lexington, KY.

McCormack, D.E., and Wilding, L.P. 1975. “Soil Properties Influencing Swelling in Canfield and Geeburg Soils.” *Soil Science Society of America Journal*, 39(3): 496–502. doi:10.2136/sssaj1975.03615995003900030034x.

McGuire, Michael; Filz, G. M.; and Brandon, T. L. 2009. *The Emergence of Intelligent Compaction in U. S. Practice, CGPR Report No. 53*, Center for Geotechnical Practice and Research, Virginia Tech, 69 pp.

Mehta, M.R. and Veletsos, A.S. 1959 "Stresses and Displacement in Layered Systems." *Structural Research Series No. 178*, University of Illinois, Urbana, IL.

Melzer, K. J. 1968. “Sondenuntersuchungen in Sand.” [In German]. *Mitteilungen der Vereinigung der Grosskesselbetreiber*, 43, 1–345.

Merritt, A. H., and Coon, R. F. 1970. “Predicting in Situ Modulus of Deformation Using Rock Quality Indexes.” *Determination of the In Situ Modulus of Deformation of Rock, ASTM STP 477*, 154–173.

Mesri, G. 1973. “Coefficient of Secondary Compression.” *Journal of Soil Mechanics and Foundation Division*, 99(1), 123-137.

Mesri, G. 1975. “Discussion on ‘New design procedure for stability of soft clays.’” *Journal of the Geotechnical Engineering Division*, 101(GT4), 409–412.

Mesri, G. and Castro, A. 1987. “C_α/C_c Concept and K_0 during Secondary Compression.” *Journal of Geotechnical Engineering*, 113(3), 230-247.

Mesri, G., and Godlewski, P. M. 1977. “Time- and Stress-compressibility Interrelationship.” *Journal of the Geotechnical Engineering Division*, 103(5), 417-430.

Meyerhof, G. G. 1956. “Penetration Tests and Bearing Capacity of Cohesionless Soils.” *Journal of the Soil Mechanics and Foundations Division*, 82(1), 1–19.

Meyerhof, G. G. 1965. “Shallow Foundations.” *Journal of the Soil Mechanics and Foundations Division*, 91(SM1), 21-31.

Meyerhof, G. G. 1976. “Bearing Capacity and Settlement of Pile Foundations.” *Journal of the Geotechnical Engineering Division1*, 102(3), 197–228.

Mitachi, T., and Kitago, S. 1976. “Change in Undrained Shear Strength Characteristics of Saturated Remolded Clay Due to Swelling.” *Soils and Foundations*, 16(1), 45–58.

Mitchell, J. K. 1981. “Soil Improvement: State-of-the-Art Report.” *Proc. of the 10th Int. Conf. on Soil Mechanics and Foundation Engineering*, Stockholm, 509–565.

Mitchell, J. K. 1993. *Fundamentals of Soil Behavior*. John Wiley and Sons, Inc., New York.

Mitchell, J. K., and Gardner, W. S. 1975. “In-Situ Measurement of Volume Change Characteristics.” *Proc. of the ASCE Specialty Conference on In Situ Measurement of Soil Properties*, Raleigh, NC, 279–345.

Molinda, G. M., and Mark, C. 1994. *Coal Mine Roof Rating (CMRR): A Practical Rock Mass Classification for Coal Mines*. Vol. 9387, United States Department of Interior, Bureau of Mines.

Moran, Proctor, Mueser, and Rutledge 1958. *Study of Deep Soil Stabilization by Vertical Sand Drains*. Bureau of Yards and Docks, Department of the Navy.

Morgenstern, N. R., and Price, V. E. 1965. "The Analysis of the Stability of General Slip Surfaces." *Geotechnique*, 15(1), 79–93.

Moser, A. P. 1990. *Buried Pipe Design*. McGraw-Hill Inc.

Muhs, H., and Weiss, K. 1971. “Untersuchung von Grenztragfähigkeit und Setzungsverhalten Flachgegründeter Einzelfundamente in Ungleichförmigen Nichtibindigen Boden.” [In German]. *Mitteilungen DEGEBO*, 26, 1–39.

NAVFAC. (1982). *Foundations and Earth Structures Design Manual 7.2.* Department of the Navy Naval Facilities Engineering Command, Alexandria, VA.

NAVFAC. (1983). *Soil Dynamics and Special Design Aspects Design Manual 7.3.* Department of the Navy Naval Facilities Engineering Command, Alexandria, VA.

Nayak, N.V. 1979. *Foundation Design Manual*. Dhanpat Rai and Sons, Delhi, India.

Nayak, N.V., and Christensen, R.W. 1971. “Swelling Characteristics of Compacted, Expansive Soil.” *Clays and Clay Minerals*, 19(4): 251–261. doi:10.1346/CCMN.1971.0190406.

Nazzal, M. 2003. “Field Evaluation of In Situ Test Technology for QC/QA Procedures During Construction of Pavement Layers and Embankments.” Louisiana State University.

NCHRP (National Cooperative Highway Research Program). 2001. *Guide for Mechanistic-Empirical Design of New and Rehabilitated Pavement Structures*.

NCHRP (National Cooperative Highway Research Program). 2018. *Manual on Subsurface Investigations*. National Cooperative Highway Research Program Publication No. CRP Project 21-20. Transportation Research Board, National Academies of Science Engineering, and Medicine, Washington, DC.

Nelson, J., and Miller, D. J. 1992. *Expansive Soils: Problems and Practice in Foundation and Pavement Engineering*. John Wiley & Sons.

Newmark, N. M. 1942. “Influence Charts for Computation of Stress in Elastic Foundations.” *Engineering Experiment Station Bulletin Series,* No. 338, University of Illinois at Urbana Champaign, College of Engineering.

Nishida, Y. 1956. “A Brief Note on the Compression Index of Soil.” *Journal of the Soil Mechanics and Foundations Division*, 82(3), 1–14.

NOAA (National Oceanic and Atmospheric Administration). 1978. *Geodetic Bench Marks. U.S. Department of Commerce - National Oceanic and Atmospheric Administration*.

Nonveiller, E. 1967. “Shear Strength of Bedded and Jointed Rock as Determined from the Zalesina and Vajont slides.” *Proc. of the Geotechnical Conference Oslo 1967 on Shear Strength Properties of Natural Soils and Rocks*, 1, 289–294.

NRC (Nuclear Regulatory Commission). 1996. *Working Safely with Nuclear Gauges*. Report No. NUREG/BR-0133, United States Nuclear Regulatory Commission.

NRCS (Natural Resources Conservation Service). 2002. “Rock Material Field Classification System.” *Part 631 Geology National Engineering Handbook*, 12-1-12–12.

NYDOT (New York State Department of Transportation). 2013. *Geotechnical Design Manual*. New York State Department of Transportation, Albany, NY.

O'Neil, M.W., and Ghazzally, O.I. 1977. "Swell potential related to building performance." *Journal of the Geotechnical Engineering Division*, 103(12): 1363–1379.

Ohba, S., and Toriumi, I. 1970. "Dynamic Response Characteristics of Osaka Plain." *Soils Foundations*, 13(4), 61–73.

Ohsaki, Y., and Twasaki, R. 1973. "On Dynamic Shear Moduli and Poisson's Ratio of Soil Deposits." *Soils and Foundations*, 13(4), 61–73.

Ohta, Y., and Goto, N. 1978. "Empirical Shear Wave Velocity Equations in Terms of Characteristics Soil Indexes." *Earthquake Engineering & Structural Dynamics*, 6, 167–187.

Ohya, S., Imai, T., and Matsubara, M. 1982. "Relationships Between N Value by SPT and LLT Pressuremeter Results." *Proc. of the 2nd European Symposium on Penetration Testing*, Amsterdam, 125–130.

Olson, R. E. 1977. "Consolidation Under Time Dependent Loading." *Journal of the Geotechnical Division*, 103(GT1), 55-60.

Osterberg 1972. Personal communication cited in Azzouz et al. 1976.

Paikowsky, S. G., Palmer, C. J., and Rowles, L. E. 2006. "The Use of Tactile Sensor Technology for Measuring Soil Stress Distribution." *Proc. GeoCongress 2006–Geotechnical Engineering in the Information Technology Age*, ASCE, Atlanta.

Parcher, J. V., and Means, R. E. 1968. *Soil Mechanics and Foundations*. Charles E. Merrill, Columbus, OH.

Parkin, A., Holden, J., Aamot, K., Last, N., and Lunne, T. 1980. *Laboratory Investigations of CPT's in Sand*. Report 52108-9.

Parry, R. H. 2004. *Mohr Circles, Stress Paths and Geotechnics*. CRC Press.

Parry, R. H. G. 1977. "Estimating Bearing Capacity in Sand from SPT Values." *Journal of the Geotechnical Engineering Division*, Raleigh, NC, 1014–1019.

Parry, R.H.G. 1971. "A Direct Method of Estimating Settlements in Sand for SPT Values." *Proc. Sym. on the Interaction of Structure and Foundation*, Birmingham, 29-32.

Patel, R. S., and Desai, M. D. 2010. "CBR Predicted by Index Properties of Soil for Alluvial Soils of South Gujarat." *Proc. of the Indian Geotechnical Conference*, 79–82.

Pavlovsky, N. N. 1956. *Collected Works*. Akad. Nauk USSR, Leningrad.

Peck, R. B. 1969. "Deep Excavation and Tunneling in Soft Ground." *Proc. of the 7th Int. Conf. on Soil Mechanics and Foundation Engineering, Mexico: State-of-the-Art Report*, 225-325.

Peck, R. B. and Reed, W. C. 1954. "Engineering Properties of Chicago Subsoils." *Engineering Experiment Station Bulletin,* No. 423, University of Illinois.

Peck, R.B, Hansin, W.E, and Thornburn, T.H. 1974. *Foundation Engineering, 2nd Ed*. John Wiley & Sons, Inc., New York, 514p.

Peck, R.B. 1969. "Advantages and Limitations of the Observational Method in Applied Soil Mechanics." *9th Rankine Lecture, Geotechnique*, 19, 171-187.

Peck, R.B. 1972. *Observation and Instrumentation*. United States Department of Transportation, Publication No. 131, Federal Highway Administration, Highway Focus 4(2), 1-5.

Peck, R.B., and Bazarra, A.R.S. 1969. "Discusion to Settlement of Spread Footings on Sand." *JSMFE (ASCE)*, 95 (SM3), 905-909.

Piratheepan, P. 2002. "Estimating Shear-Wave Velocity from SPT and CPT Data." M.S. thesis, Clemson University.

Pitilakis, K. D., Anastasiadis, A., and Raptakis, D. 1992. “Field and Laboratory Determination of Dynamic Properties of Natural Soil Deposits.” *Proc. of 10th World Conference on Earthquake Engineering*, 1275–1280.

Polshin, D. E. and Tokar, R. A. 1957. “Maximum Allowable Non-uniform Settlement of Structures.” *Proc. 4th Int. Conf. on Soil Mechanics and Foundation Engineering*, Butterworth’s, London, Vol. 1, 402-405.

Potts, D. M. and L. Zdravkovic. 1999. *Finite Element Analysis in Geotechnical Engineering: Vol. 1 Theory and Application*. ICE Publishing, 500 pp.

Potts, D. M. and L. Zdravkovic. 2001. *Finite Element Analysis in Geotechnical Engineering: Vol. 2 Theory and Application*. ICE Publishing, 500 pp.

Poulos, H. G. 1975. “Settlement of Isolated Foundations.” *Soil Mechanics - Recent Developments*, S. Valliappan, S. Hain, and Lee, I. K., eds., William H. Sellent Pty, Zetland, 181–212.

Poulos, H. G. 1988. *Marine Geotechnics*. Taylor & Francis Ltd.

Poulos, H. G., and Davis, E. H. 1974. *Elastic Solutions for Soil and Rock Mechanics*. John Wiley and Sons, 424 pp.

Poulos, H. G., and Davis, E. H. 1980. *Pile Foundation Analysis and Design*. John Wiley & Sons, New York, New York.

Randolph, M., and Gourvenec, S. 2011. *Offshore Geotechnical Engineering*. CRC Press.

Ranganathan, B.V. & Satyanarayana, B. 1965. “A Rational Method of Predicting Swelling Potential for Compacted Expansive Clays.” *Proc. 6th Int. Conf. on Soil Mechanics and Foundation Engineerin*g, ISSMGE, London, 1, 92–96.

Rao, B. H., Venkataramana, K., and Singh, D. N. 2011. “Studies on the Determination of Swelling Properties of Soils from Suction Measurements.” *Canadian Geotechnical Journal*, 48(3), 375-387.

Rendon-Herrero, O. 1983. “Closure of Universal Compression Index Equation.” *Journal of Geotechnical Engineering*, 109(5), 755–761.

Ricceri, G. and Soranzo, M. 1985. “An Analysis on Allowable Settlement of Structures.” *Riv. Ital. Geotec*., 4, 177-188.

Ricceri, G., Simonini, P., and Cola, S. 2002. “Applicability of Piezocone and Dilatometer to Characterize the Soils of the Venice Lagoon.” *Geotechnical and Geological Engineering*, 20(2), 89–121.

Robertson, P. K. 2009. “Interpretation of Cone Penetration Tests - A Unified Approach.” *Canadian Geotechnical Journal*, 46(11), 1337–1355.

Robertson, P. K., and Cabal, K. L. 2014. *Guide to Cone Penetration Testing for Geotechnical Engineering*. Gregg Drilling & Testing, Inc.

Robertson, P. K., and Campanella, R. G. 1983. “Interpretation of Cone Penetration Tests. Part I: Sand.” *Canadian Geotechnical Journal*, 20(4), 718–733.

Robertson, P. K., and Campanella, R. G. 1984. *Guidelines for Use and Interpretation of the Electronic Cone Penetration Test*. Hogentogler & Company, Inc.

Robertson, P.K. 2009. "Cone Penetration Testing: A Unified Approach." *J., Canadian Geotechnical Journal*, 46(11), 1337–1355.

Roscoe, K. H., Schofield, A. N., Wroth, C. P., and Henkel, D. J. 1958. “Discussion: On the Yielding of Soils.” *Géotechnique*, 8(3), 22–53.

Rowland, S.; Duebendorfer, E.; and Schiefelbein, I. 2007. *Structural Analysis & Synthesis – A Laboratory Course in Structural Geology, 3rd Ed*. Blackwell, Malden, MA.

Saada, A. S. and Townsend, F. C. 1981. "State of the Art: Laboratory Strength Testing of Soils," *Laboratory Shear Strength of Soils, ASTM STP 740*, R. N. Yong and F. C. Townsend, Eds., ASTM, pp. 7-77.

Sabatini, P. J., Bachus, R. C., Mayne, P. W., Schneider, J. A., and Zettler, T. E. 2002. *Geotechnical Engineering Circular No. 5: Evaluation of Soil and Rock Properties*. Federal Highway Administration.

Sakai, Y. 1968. *A Study on the Determination of S-Wave Velocity by the Soil Penetrometer.* [In Japanese].

Salem, A. M., and Krizek, R. J. 1976. “Stress-Deformation-Time Behaviour of Dredgings.” *Journal of the Geotechnical Engineering Division*, 102(GT2), 139–157.

Salgado, R. 2008. *The Engineering of Foundations*. McGraw Hill, Boston, p. 882.

Santi, P. M. 1998. “Improving the Jar Slake, Slake Index, and Slake Durability Tests for Shales.” *Environmental & Engineering Geoscience*, IV(3), 385–396.

SCDOT (South Carolina Department of Transportation). 2010. *Geotechnical Design Manual*. South Carolina Department of Transportation, Columbia, SC.

Schmertmann, J. H. 1970. “Static Cone to Compute Static Settlement Over Sand.” *Journal of Soil Mechanics and Foundations Division*, 96(SM3), 1011-1043.

Schmertmann, J. H. 1975. “Measurement of In Situ Shear Strength.” *Proc. of the ASCE Specialty Conference on In Situ Measurement of Soil Properties*, 2, 57–138, 341–355.

Schmertmann, J. H. 1978. *Guidelines for Cone Penetration Test: Performance and Design*. Washington, DC.

Schmertmann, J. H., Hartman, J. P., and Brown, P. R. 1978. “Improved Strain Influence Factor Diagrams.” *Journal of the Geotechnical Engineering Division*, 104(8), 1131-1135.

Schneider G.L. and Poor, A.R. 1974. “The Prediction of Soil Heave and Swell Pressures Developed by an Expansive Clay,” *Research Report, No: TR-9-74*, Construction Research Center, Univ. Of Texas.

Schofield, A. N., and Wroth, C. P. 1968. *Critical State Soil Mechanics*. Mcgraw Hill Book Co Ltd.

Schultz, E., and Sherif, G. 1973. “Prediction of Settlement from Evaluated Settlement Observations for Sand.” *Proc. 8th ICSMFE*, Moscow, Vol. 1.3, 225-230.

Seed, H. B., and Idriss, I. M. 1981. “Evaluation of Liquefaction Potential Sand Deposits Based on Observation of Performance in Previous Earthquakes.” *ASCE National Convention (MO)*, 481–544.

Seed, H.B., Woodward, R.J., and Lundgren, R. 1962. “Prediction of Swelling Potential for Compacted Clays.” *Journal of the Soil Mechanics and Foundation Engineering Division*, 88(3): 53–87.

Sehn, A.L. 1990. *Experimental Study of Earth Pressures on Retaining Structures*. Ph.D. Dissertation, Virginia Tech, 347 pages.

Sherard, J.L., Dunnigan, L.P. and Talbot, J.R. 1984. “Basic Properties of Sand and Gravel Filters.” *Journal of Geotechnical Engineering*, 110(6), 684-700.

Shibata, T. 1970. *The Relationship Between the N-value and S-Wave Velocity in the Soil Layer*. Kyoto, Japan.

Shioi, Y., and Fukui, J. 1982. “Application of N-Value to Design of Foundations in Japan.” *Proc. of the 2nd European Symposium on Penetration Testing*, Amsterdam, 159–164.

Singh, D., Reddy, K. S., and Yadu, L. 2011. “Moisture and Compaction Based Statistical Model for Estimating CBR of Fine Grained Subgrade Soils.” *International Journal of Earth Sciences and Engineering*, 4(6), 100–103.

Sirles, P. 2006. *Use of Geophysics for Transportation Projects*. National Cooperative Highway Research Program Synthesis 357, Transportation Research Board, Washington, DC.

Skempton, A. W. 1944. “Notes on the Compressibility of Clays.” *Quarterly Journal of the Geological Society of London*, 100, 119-135.

Skempton, A. W. 1957. “Discussion on the Planning and Design of the New Hong Kong Airport.” *Proc. of the ICE*, 7(2), 307–307.

Skempton, A. W. 1964. “Long-term Stability of Clay Slopes.” *Géotechnique*, 14(2), 77–102.

Skempton, A. W. 1985. “Residual Strength of Clays in Landslides, Folded Strata and the Laboratory.” *Géotechnique*, 35(1), 3–18.

Skempton, A. W. and MacDonald, D. H. 1956. “The Allowable Settlement of Buildings.” *Proc. Institution of Civil Engineers*, 5(6), 727-769.

Skempton, A. W., and Northey, R. D. 1952. “The Sensitivity of Clays.” *Geotechnique*, 3(1), 30–53.

Skempton, A. W., Schuster, R. L., and Petley, D. J. 1969. “Joints and Fissures in the London Clay at Wraysbury and Edgware.” *Géotechnique*, 19(2), 205–217.

Skinner, E. H. 1988. “A Ground Support Prediction Concept: The Rock Structure Rating (RSR) Model.” *Rock Classification Systems for Engineering Purposes, STP 984*, 35–51.

Slichter, C.E. 1905. “Field Measurements of the Rate of Movement of Underground Water,” *Water-Supply and Irrigation Paper No. 140*, U.S. Geological Survey, Department of the Interior, Series 0, Underground Waters, 43.

Smith, R. B., and Pratt, D. N. 1983. “A Field Study of In Situ California Bearing Ratio and Dynamic Cone Penetrometer Testing for Road Subgrade Investigations.” *Australian Road Research*, 13(4), 285–294.

Sowers, G. F. 1970. *Introduction to Soil Mechanics and Foundations, 3rd Ed*. The Macmillan Company, Collier-Macmillan Ltd., London, 102.

Sowers, G. F. 1979. *Introductory Soil Mechanics and Foundations: Geotechnical Engineering*. Macmillan & Co, New York, New York.

Spangler, M. G. 1948. “Underground Conduits - An Appraisal of Modern Research.” *Transactions of ASCE*, 113, 316-374.

Spencer, E. 1967. "A Method of Analysis of the Stability of Embankments Assuming Parallel Inter–slice Forces." *Geotechnique*, 17(1), 11–26.

Sridharan, A., and Gurtug, Y. 2004. “Swelling Behaviour of Compacted Fine-grained Soils.” *Engineering Geology*, 72(1–2): 9–18. doi:10.1016/S0013-7952(03)00161-3.

Stark, T. D., and Hussain, M. 2013. “Empirical Correlations: Drained Shear Strength for Slope Stability Analyses.” *J. Geotech. Geoenviron. Eng.*, 139(6), 853–862.

Stroud, M. A. 1974. “The SPT in Insensitive Clays and Soft Rocks.” *Proc. of the European Symposium on Penetration Testing*, Stockholm, 367–375.

Stroud, M. A., and Butler, F. G. 1975. “The Standard Penetration Test and the Engineering Properties of Glacial Materials.” *Proc. of the Sym. on the Engineering Behaviour of Glacial Materials*, 117–128.

Sykora, D. E., and Stokoe, K. H. 1983. “Correlations of In-Situ Measurements in Sands of Shear Wave Velocity.” *Soil Dynamics and Earthquake Engineering*, 20, 125–136.

Tan, C. and Duncan, J. M. 1991. “Settlement of Footings on Sands-Accuracy and Reliability.” *Proc. Geotechnical Engineering Congress 1991*, 446-455.

Terzaghi, K. 1943. *Theoretical Soil Mechanics*. John Wiley and Sons, New York, NY.

Terzaghi, K. 1946. “Rock Defects and Loads on Tunnel Supports.” *Rock Tunneling with Steel Supports*, Ed. R. V. Proctor and T. White, Commercial Shearing Inc., Youngstown, OH.

Terzaghi, K. 1950. “Geologic Aspects of Soft Ground Tunneling.” *Applied Sedimentation*, Ed. R. Task and D. Parker, John Wiley and Sons, New York, NY, 193-209.

Terzaghi, K. and Peck, R. B. 1967. *Soil Mechanics in Engineering Practice, 2nd Ed.* John Wiley & Sons, Inc., New York.

Terzaghi, K., Peck, R. B., and Mesri, G. 1996. *Soil Mechanics in Engineering Practice, 3rd Ed.* John Wiley & Sons, Inc., New York.

Thakur, V.K.S., and Singh, D.N. 2005. “Rapid Determination of Swelling Pressure of Clay Minerals.” *Journal of Testing and Evaluation*, 33(4): 239–245. doi:10.1520/JTE11866.

Tiwari, B., and Ajmera, B. 2010. “A New Correlation Relating the Shear Strength of Reconstituted Soil to the Proportions of Clay Minerals and Plasticity Characteristics.” *Applied Clay Science*, Fullerton, 53(1), 88.

Tobar, T. and Meguid, M. A. 2010. "Comparative Evaluation of Methods to Determine the Earth Pressure Distribution on Cylindrical Shafts: A Review." *Tunnelling and Underground Space Technology*, 188-197.

Tschebotarioff, G. P. 1973. *Foundations, Retaining and Earth Structures*. Mcgraw Hill Book Co Ltd, New York, New York.

Tunbridge, L. 2017. "Hydraulic Conductivity Determination by Lugeon Test – Testing in Practice." *Proc. Workshop on Drainage of Large Rockslides*, Oslo, Norway.

TXDOT (Texas Department of Transportation). 2014. “Test Procedure for Determining Potential Vertical Rise.” *TXDOT Designation: TEX-124-E*, 10 pp.

Ulmer, K. J., Green, R. A., and Rodriguez-Marek, A. 2020. “A Consistent Correlation between V_s, SPT, and CPT Metrics for Use in Liquefaction Evaluation Procedures.” *Geo-Congress 2020, American Society of Civil Engineers*, Reston, VA, 132–140.

United States Department of the Army. 1984. *Engineering and Design - Pavement Criteria for Seasonal Frost Conditions - Mobilization Construction - EM 1110-3-138*.

USACE (United States Army Corps of Engineers). 1947. *Soil Mechanics Fact Finding Survey Progress Report: Cooperative Triaxial Shear Research Program of the Corps of Engineers: Pressure Distribution Theories, Earth Pressure Cell Investigations and Pressure Distribution Data*. Review prepared by Donald W. Taylor, Mississippi River Commission, Vicksburg, Miss., U.S. Army Engineer Waterways Experiment Station, 332 pages.

USACE. 1952. *Soil Mechanics Design, Seepage Control, Engineering Manual No. 1110-2-1901*. Civil Works Construction, Part CXIX.

USACE. 1956. *Investigating Underseepage and Its Control, Lower Mississippi River Levees, Technical Memorandum 3-424*. Waterway Experiment Station, Vicksburg, MS.

USACE. 1970. *Laboratory Soils Testing*.

USACE. 1984. *Engineering and Design - Pavement Criteria for Seasonal Frost Conditions - Mobilization Construction - EM 1110-3-138*.

USACE. 1986. *Engineering and Design, Seepage Analysis and Control for Dams, Engineering Manual, EM 1110-2-1901*. Office of the Chief of Engineers, Washington, D.C.

USACE. 1987. *Instrumentation for Concrete Structures*. Engineering Manual, EM 1110-2-4300. United States Army Corps of Engineers. Washington, DC.

USACE. 1990. *Settlement Analysis, EM- 1110-1-1904*. U. S. Army Corps of Engineers.

USACE. 1993. *Seepage Analysis and Controls for Dams*. U.S. Army Corps of Engineers.

USACE. 1995a. *Geophysical Exploration for Engineering and Environmental Investigations*. Engineer Manual 1110-1-1802, United States Army Corps of Engineers, Washington, DC.

USACE. 1995b. *Instrumentation of Embankment Dams and Levees*. Engineering Manual 1110-2-1908, United States Army Corps of Engineers, Washington, DC.

USACE. 2000. *Design and Construction of Levees, Engineering Manual 1110-2-1913*. Office of the Chief of Engineers, Washington, D.C.

USACE. 2003. *EM 1110-2-1902, Engineering and Design – Slope Stability. Department of the Army, U. S. Army Corps of Engineers*. Washington, DC. 204 pages.

USBR (United States Department of Interior Bureau of Reclamation). 2014. *Embankment Dams. Design Standards No. 13*, Denver Colorado.

USBR. 1998. *Earth Manual, Part 1, 3rd Ed*. Earth Sciences and Research Laboratory, Technical Service Center, Denver, CO., 348 pages

USBR. 2011. *Design Standards No. 13, Chapter 4: Stability Analyses*. U.S. Department of the Interior, Technical Service Center. October 2011, 159 pages.

USGS (United States Geological Survey). 2014. *Karst in the United States: A Digital Map Compilation and Database*. U.S. Department of the Interior, U.S. Geological Survey.

Valentine, R. J. 2013. *An Assessment of the Factors that Contribute to the Poor Performance of Geosynthetic-Reinforced Earth Retaining Walls, Proceedings of the International Symposium on Design and Practice of Geosynthetic-Reinforced Soil Structures.* Bologna, Italy, editors Ling, Gottardi, Cazzuffi, Han and Tatsuoka, DEStec Publications, pp. 318-327.

Van Der Merwe, D.H. 1964. “The Prediction of Heave from the Plasticity Index and Percentage Clay Fraction of Soils,” *Civil Engineers in South Africa*, 6, 337–42.

Vanapalli, S. K. and Lu, L. 2012. “A State-of-the-art Review of 1-D Heave Prediction Methods for Expansive Soils.” *International Journal of Geotechnical Engineering*, 6, 15-41.

VandenBerge, D. R., Duncan, J. M., and Brandon, T. L. 2014. *Rapid Drawdown Analysis using the Finite Element Method, CGPR #79*. Center for Geotechnical Practice and Research, Virginia Tech, Blacksburg, VA, 305 pp.

Veismanis, A. 1974. “Laboratory Investigation of Electrical Friction-Cone Penetrometers in Sand.” *Proc. of the European Symposium on Penetration Testing*, Stockholm, 407–419.

Vidalie, J.-F. 1977. *Relations entre les Propriétés Physico-Chimiques et les Caractéristiques Mécaniques des Sols Compressibles [Relations between the Physico-Chemical Properties and the Mechanical Characteristics of Compressible Soils]*. [In French]. *Rapport de Recherche,* No.65.

Vijayavergiya, V.N. & Ghazzaly, O. I. 1973. “Prediction of Swelling Potential for Natural Clays.” *Proc. of the 3rd Int. Conf. on Expansive Soils*, Haifa, Israel, 1, 227-236.

Villet, W. C. B., and Mitchell, J. K. 1981. “Cone Resistance, Relative Density and Friction Angle.” *Sym. on Cone Penetration Testing and Experience, Geotechnical Engineering Division, ASCE*, 178–208.

Voight, B. 1973. “Correlation Between Atterberg Plasticity Limits and Residual Shear Strength of Natural Soils.” *Géotechnique*, 23(2), 265–267.

Wahls, H. E. 1981. “Tolerable Settlement of Buildings.” *Journal of the Geotechnical Engineering Division*, 107(11), 1489-1504.

Webb, D. L. 1969. “Settlement of Structures on Deep Alluvial Sandy Sediments in Durban, South Africa.” *Proc. of the Conf. on the In Situ Behavior of Soils and Rocks*, 181–188.

Webster, S.L., Grau, R.H., Williams, T.P. 1992. *Description and Application of Dual Mass Dynamic Cone Penetrometers*. Report from U.S. Army Corps of Engineers, Waterways Experiment Station, Vicksburg, MS.

Weston, D. J. 1980. “Expansive Roadbed, Treatment for Southern Africa.” *Proc. 4th Int. Conf. on Expansive Soils*, 1: 339-360.

White, D. J., Vennapusa, P., Tutumluer, E., Vavrik, W., Moaven, M., and Gillen, S. 2018. “Spatial Verification of Modulus for Pavement Foundation System.” *Transportation Research Record*, 2672(52), 333–346.

Whitman, R. V., and Bailey, W. A. 1967. "Use of Computers for Slope Stability Analyses." *ASCE, Journal of the Soil Mechanics and Foundations Division*, 93(4), 475–498.

Williamson, D., and Kuhn, C. R. 1988. “The Unified Rock Classification System.” *Rock Classification Systems for Engineering Purposes, STP984*, 7–16.

Windle, D. and Wroth, C.P. 1977. *The Use of a Self-boring Pressuremeter to Determine the Undrained Properties of Clays*. Ground Engineering, London.

Wolff, T. F. 1989. “Pile Capacity Prediction Using Parameter Functions.” *Predicted and Observed Axial Behavior of Piles: Results of a Pile Prediction Symposium*, ASCE, 96–106.

Wright, S. G. 2013. “2013 H. Bolton Seed Lecture: Slope Stability Calculations.” Accessed December 23, 2020. https://www.youtube.com/watch?v=Q_6aOU7msBM.

Wroth, C. P., and Wood, D. M. 1978. “The Correlation of Index Properties with some Basic Engineering Properties of Soils.” *Canadian Geotechnical Journal*, 15(2), 137–145.

Yang, H., D.J. White, V.R. Schaefer. 2006. "In Situ Borehole Shear Test and Rock Borehole Shear Test for Slope Investigation." *Site and Geomaterial Characterization (GSP 149, GeoShanghai)*, pp. 293–298.

Yashas, S., Harish, S., and Muralidhara, H. R. 2016. “Effect of California Bearing Ratio on the Properties of Soil.” *American Journal of Engineering Research*, 5(4), 28–37.

Yildirim, B., and Gunaydin, O. 2011. “Estimation of California Bearing Ratio by Using Soft Computing Systems.” *Expert Systems with Applications*, 38(5), 6381–6391.

Yoshida, Y., Ikemi, M., and Kokusho, T. 1988. “Empirical Formulas of SPT Blow Counts for Gravelly Soils.” *Proc. of the 1st Int. Sym. on Penetration Testing*, 2, 381–387.

Zeigler, T.W., 1972. *In Situ Tests for the Determination of Rock Mass Shear Strength.* U.S. Army Engineer Waterways Experiment Station, Soils and Pavements Laboratory.

APPENDIX B. LIST OF COMPUTER PROGRAMS

Table B-1 List of Computer Programs

Name	Company	Application	Website
FOSSA	ADAMA Engineering Inc.	Assessing stresses and settlements under embankment and footings acting on horizontal ground surfaces	http://www.geoprograms.com/
GeoCoPS	ADAMA Engineering Inc.	Interactive program for the design of geosynthetic tubes	http://www.geoprograms.com/
MSEW	ADAMA Engineering Inc.	Design and analysis of mechanically stabilized earth walls	http://www.geoprograms.com/
Reslope	ADAMA Engineering Inc.	Interactive, design-oriented, program for geosynthetic-reinforced slopes	http://www.geoprograms.com/
ReSSA+	ADAMA Engineering Inc.	Assessing the rotational and translational stability of reinforced slopes and walls	http://www.geoprograms.com/
ADINA	ADINA R&D Inc.	Stress analysis of solids (2D and 3D) and structures in statics and dynamics	http://www.adina.com/
AEC Slope	AEC Logic Pvt. Ltd	Analyzing stability of slopes for road, railways, river training works, canal embankment, dams etc.	http://www.aeclogic.com/
gINT Professional	Bentley System Inc.	Reporting and managing subsurface data, including borehole logs, well logs, CPT data, and geophysical logs.	https://www.bentley.com/
FB-Deep	Bridge Software Institute	Static axial capacity program used for drilled shafts and driven piles	https://bsi.ce.ufl.edu/
FB-MultiPier	Bridge Software Institute	Nonlinear finite element analysis program capable of analyzing multiple bridge pier structures interconnected by bridge spans.	https://bsi.ce.ufl.edu/
Bearing Pile designer	CADS	Used to select a suitable pile type for known soil strata by investigating the effects of soil parameters and different pile types. Allows the bearing capacity of individual piles and groups of piles of various lengths and types to be checked, including bored piles, continuous flight auger (CFA) piles, driven cast in place, driven tubular steel, driven steel H piles and driven precast piles.	https://cads.co.uk/
Piled Wall Suite	CADS	Analysis and design of embedded walls in concrete or steel. Includes analysis and design for sheet piles, king piles, contiguous and secant bored piles and diaphragm walls	https://cads.co.uk/
RC Pad Base Designer	CADS	Designing and checking of bases. Can be used stand-alone or as part of the CADS integrated analysis, design, and detailing solution.	https://cads.co.uk/
RC Pile cap designer	CADS	Pile Cap Designer software that automatically produces a selection of suitable designs to BS 8110 and EC2 for pile caps with 2-9 piles supporting circular or rectangular columns	https://cads.co.uk/
Reslope	CADS	Slope stability software package for calculating the factor of safety of earth slopes. Uses Bishop's simplified method and circular slip surfaces.	https://cads.co.uk/

Name	Company	Application	Website
AWALL	Callide Technologies Inc	The AWall CAD Tool allows a user to accurately represent the Plan and Elevation views of a retaining wall on their grading plan	http://www.ctiware.com/
VESPA2MSE	Callide Technologies Inc	Design and drawing of mechanically stabilized earth retaining walls.	http://www.ctiware.com/
Mfield	Canary System Inc.	Mobile application designed to bridge the gap between data collection and observations in the field, and the hosted project database.	http://canarysystems.com/
IS GeoMassi	CDM Dolmen and omnia IS srl	Performs for calculation of three-dimensional boulders falling on a slope using the "Lumped Mass hybrid" method associated with a statistical analysis.	https://www.cdmdolmen.it/
IS GeoPendii	CDM Dolmen and omnia IS srl	Stability analysis of slopes in loose terrain based on limit equilibrium methods.	https://www.cdmdolmen.it/
IS GeoRocce	CDM Dolmen and omnia IS srl	Classification of the quality of rock masses using the most widespread theories in the geo-mechanical field.	https://www.cdmdolmen.it/
IS Geostrati	CDM Dolmen and omnia IS srl	Numerical interpretation and graphic representation of the results of SPT, DP (Dynamic Probing), and CPT tests performed on project sites.	https://www.cdmdolmen.it/
IS Muri	CDM Dolmen and omnia IS srl	Finite element analysis, according to the NTC 2018 and Eurocode, of inland walls with constant or variable section, with buttresses, teeth, poles, and tie rods.	https://www.cdmdolmen.it/
IS Paratie	CDM Dolmen and omnia IS srl	Designing flexible containment structures for which the soil-structure interaction is analyzed in the nonlinear field with hysteresis taking into account the deformability of the face.	https://www.cdmdolmen.it/
IS ProGeo	CDM Dolmen and omnia IS srl	Geotechnical modules useful for the rough design of structures in contact with the ground.	https://www.cdmdolmen.it/
IS PL	CDM Dolmen and omnia IS srl	Complete analysis of piles.	https://www.cdmdolmen.it/
IS Plinti	CDM Dolmen and omnia IS srl	Analysis and design of surface foundations.	https://www.cdmdolmen.it/
MasterKey: Retaining wall	Civil and Structural Computer Services Limited	Designing retaining walls with full control over the design process.	https://www.masterseries.com/
AllPile	Civiltech, Inc.	Windows-based analysis program that handles virtually all types of piles, including steel pipes, H-piles, pre-cast concrete piles, auger-cast piles, drilled shafts, timber piles, jetted piles, tapered piles, piers with bell, micropiles (minipiles), uplift anchors, uplift plate, and shallow foundations.	https://civiltech.com/
Liquefy Pro	Civiltech, Inc.	Liquefaction analysis and settlement analysis due to liquefaction.	https://civiltech.com/

Name	Company	Application	Website
Shoring Suit	Civiltech, Inc.	Design and analysis tool containing four modules for shoring, earth pressure, surcharge, and heave.	https://civiltech.com/
Super Log	Civiltech, Inc.	Generating boring log and test pit graphical reports for field drilling and geotechnical investigation.	https://civiltech.com/
Galena	Clover Associates	Slope stability analysis.	http://www.galenasoftware.com/
CPT Tool 3.2	Datgel Pty Ltd	Analysis of CPT data.	https://www.datgel.com/
DGD Tool 4	Datgel Pty Ltd	Geotechnical *in situ* and lab result storage and reporting, including logs for boreholes, test pits, DCPs and vibrocores, and a large range of summary graphs, histograms, fence, table, and map reports.	https://www.datgel.com/
Datgel Lab and In Situ Tool 3	Datgel Pty Ltd	Analysis of laboratory and *in situ* tests.	https://www.datgel.com/d
DC Bearing	DC Software	Analysis of bearing capacity in accordance with Eurocode 7.	https://www.dc-software.de/
DC Cantilever	DC Software	Analysis of cantilever walls in accordance with Eurocode 7.	https://www.dc-software.de
DC Footing	DC Software	Analysis and design of single, block and sleeve footings, rectangular, strip and circular footings according to Eurocode 7.	https://www.dc-software.de
DC Gabion	DC Software	Design and analysis of gabions and supporting structures of layered blocks and concrete stack stones.	https://www.dc-software.de
DC Geotex	DC Software	Analysis of reinforced earth with geosynthetics in accordance with Eurocode 7.	https://www.dc-software.de
DC Inflit	DC Software	Analysis of infiltration.	https://www.dc-software.de/
DC Integra 3D	DC Software	3D display of foundation pits with exact wall geometry and automatic generation of slope intersections.	https://www.dc-software.de/
DC Lamellae	DC Software	Stability analysis of diaphragm wall lamellae.	https://www.dc-software.de/
DC Nail	DC Software	Analysis of soil nailing in accordance with Eurocode 7.	https://www.dc-software.de/
DC Pile	DC Software	Analysis and design of piles.	https://www.dc-software.de/
DC Settlement	DC Software	Settlement analysis according to Eurocode 7.	https://www.dc-software.de
DC Slope	DC Software	Slope stability analysis according to Eurocode 7.	https://www.dc-software.de
DC Underpinning	DC Software	Analysis and design of underpinning and retaining walls.	https://www.dc-software.de/
DC Bore	DC Software	Bore well logs, layer specifications, well, and gauge sinking.	https://www.dc-software.de/
DC Cone	DC Software	Conducting and interpreting CPT data.	https://www.dc-software.de/
DC Cons	DC Software	Data reduction of Atterberg limits according to DIN 18 122 / SN 670 345 / OENORM B 4411 /CEN ISO/TS 17892-12.	https://www.dc-software.de/
DC Lime	DC Software	Determination of lime content according to DIN 18 129.	https://www.dc-software.de/
DC Load	DC Software	Conduction and interpretation of plate load testing.	https://www.dc-software.de/
DC Pump	DC Software	Pump test graphics and evaluation.	https://www.dc-software.de/

Name	Company	Application	Website
DC Shear	DC Software	Shear strength test according to DIN 18 137 and interpretation of results.	https://www.dc-software.de/
DC Sieve	DC Software	Sieve and sedimentation analysis.	https://www.dc-software.de/
DeepFND	Deep Excavation LLC	Analysis and design of deep foundation.	http://www.deepexcavation.com/
DeepEX	Deep Excavation LLC	Geotechnical and structural design for many wall types that include soldier pile walls, sheet pile walls, and diaphragm walls with multiple sections of reinforcement. Can also perform slope stability analysis with soil nailing.	http://www.deepexcavation.com/
Deviate VR	Deep Excavation LLC	Inspecting pile installation records in three dimensions or using virtual reality.	http://www.deepexcavation.com/
Helixpile	Deep Excavation LLC	Design and analysis of helical piles.	http://www.deepexcavation.com/
HoloDeepex	Deep Excavation LLC	Full design-visualization program for deep excavations.	http://www.deepexcavation.com/
Snail Plus	Deep Excavation LLC	Soil nail analysis software. Follows the FHWA methodology for the design of soil nail walls.	http://www.deepexcavation.com/
Trench	Deep Excavation LLC	Evaluating the stability of slurry supported trenches and panels for 2D and 3D analyses.	http://www.deepexcavation.com/
TriAxial PRO	Deep Excavation LLC	Processing triaxial test data.	http://www.deepexcavation.com/
Deltares Geotechnical Softwares	Deltares	Package of eight design software: namely D-Foundations, D-Geo Pipeline, D-Geo Stability, D-Pile Group, D-Settlement, MWell, MSeep and D-Sheet Piling	https://www.deltares.nl/
Delft3D Flexible Mesh Suite	Deltares	Simulation of storm surges, hurricanes, tsunamis, detailed flows and water levels, waves, sediment transport and morphology, and water quality and ecology. Capable of handling the interactions between these processes.	https://www.deltares.nl/
D-Foundations	Deltares	Design of foundations following Eurocode 7 and Dutch and Belgian annexes.	https://www.deltares.nl/
D-Geo Pipelines	Deltares	Design of a pipeline installation in a trench and trenchless installation, using the micro tunneling technique or the Horizontal Directional Drilling (HDD) technique.	https://www.deltares.nl/
D Geostability	Deltares	Slope stability analysis.	https://www.deltares.nl/
D Pile Groups	Deltares	Three-dimensional behavior of single piles and pile groups, interacting via the pile cap and the soil, as a function of loading.	https://www.deltares.nl/
D Settlement	Deltares	Settlement analysis, offering accurate and robust models, capturing consolidation, creep, submerging, drains, staged loading, and unloading and reloading	https://www.deltares.nl/
D- sheet piling	Deltares	Design retaining walls and horizontally loaded piles.	https://www.deltares.nl/

Name	Company	Application	Website
M Seep	Deltares	Simulation of two-dimensional stationary groundwater flow in a cross section of layered soil structures or in one phreatic aquifer, composed of different material areas.	https://www.deltares.nl/
M Well	Deltares	Groundwater modeling to analyze time-dependent hydrogeological problems, such as dewatering, in multilayer soil profiles.	https://www.deltares.nl/
Diana	Diana FEA	Finite element software package for structural, geotechnical, tunneling, earthquake disciplines, and oil & gas engineering.	https://dianafea.com/
Foundation3D 2018	Dimensional Solutions, Inc	Designing foundations for industrial equipment such as horizontal exchangers, horizontal vessels, vertical vessels, fractionation towers, air filters, pipe racks and other plant supports or simply any structure that needs a simple spread or combined footing.	https://www.dimsoln.com/
Mat3D 2018	Dimensional Solutions, Inc	Design of soil and pile supported, multi-load point mat foundations.	https://www.dimsoln.com/
DSAnchor	Dimensional Solutions, Inc	Designing anchors for concrete foundations.	https://www.dimsoln.com/
Shaft3D	Dimensional Solutions, Inc	Design and analysis of drilled shafts or caisson type foundations.	https://www.dimsoln.com/
SoFA	Dr. Konstantinos Nikolaou	Shallow foundation analysis, including settlement calculations and static and seismic bearing capacity.	http://sofasoftware.weebly.com/
APILE	Ensoft Inc.	Axial capacity, as a function of depth, of a driven pile in clay, sand, or mixed-soil profiles.	https://www.ensoftinc.com/
DynaMat	Ensoft Inc.	Equivalent dynamic stiffness and damping of machine foundations using a three-dimensional hybrid method.	https://www.ensoftinc.com/
DynaN	Ensoft Inc.	Dynamic response of both shallow and deep foundations under harmonic, transient, and random loadings using the improved Novak's method.	https://www.ensoftinc.com/
DynaPile	Ensoft Inc.	Dynamic stiffness of single piles or pile groups.	https://www.ensoftinc.com/
GeoMat	Ensoft Inc.	Analysis of mats or structural slabs supported on soils.	https://www.ensoftinc.com/
GROUP	Ensoft Inc.	Analysis of pile groups subjected to both axial and lateral loadings.	https://www.ensoftinc.com/
LPILE	Ensoft Inc.	Analysis of a pile under lateral loading using the p-y method.	https://www.ensoftinc.com/
PileGPw	Ensoft Inc.	Distribution of load and axial deformation of the piles within a pile group.	https://www.ensoftinc.com/
PYWALL	Ensoft Inc.	Flexible retaining wall systems considering the soil-structure interaction using the beam-column model.	https://www.ensoftinc.com/
SETOFF	Ensoft Inc.	Settlement calculation for shallow and deep foundations.	https://www.ensoftinc.com/
SHAFT	Ensoft Inc.	Axial capacity and the short-term, load-settlement curves of drilled shafts or bored piles in various types of soils.	https://www.ensoftinc.com/

Name	Company	Application	Website
STABLPRO	Ensoft Inc.	2-D slope stability analysis using limit equilibrium method.	https://www.ensoftinc.com/
TZPILE	Ensoft Inc.	The t-z method to estimate the displacement as a function of load for driven piles and drilled shafts.	https://www.ensoftinc.com/
Walls Retain	Fides DV	Analysis and design of retaining walls.	http://www.fides-dvp.eu/
Fides geostability	Fides DV	Stability computations in geotechnics using kinematic element analysis methods (KEA).	http://www.fides-dvp.eu/
FIDES Groundslab	Fides DV	Interactive generation and calculations of elastic semi-infinite space model.	http://www.fides-dvp.eu/
FIDES-WinTube-3D	Fides DV	Interactive graphical preprocessing for tunneling and geotechnical models for SOFiSTiK solvers.	http://www.fides-dvp.eu/
Geo5	Fine	Geotechnical analysis based on analytical and finite element methods.	https://www.finesoftware.eu/
AnAqSim	Fitts Geosolutions LLC	Simulation and prediction of groundwater conditions and groundwater/surface-water interactions. Alternative to MODFLOW.	http://www.fittsgeosolutions.com/
SCALE	Fitzroy System Ltd.	Bundle software for structural design with foundation design components.	https://fitzroy.com/
LUCID	Fitzroy System Ltd.	It is a bundle software for structural design and useful for design of different type of foundations and retaining walls.	https://fitzroy.com/
Strata Explorer	GAEA Technologies Ltd.	Application suite for subsurface mapping and data management to evaluate contaminants, soil and rock properties, minerals, oil and gas deposits, and oil sands. It is ideal for the environmental, geotechnical, mining, oil sands, and petroleum industries.	http://gaea.ca/
WinLog RT	GAEA Technologies Ltd.	Creation of boring and well logs and managing boring and well data.	http://gaea.ca/
Winsieve	GAEA Technologies Ltd.	Creation of grain-size analysis charts in several standard or custom formats.	http://gaea.ca/
Reactiv	Geocentrix Ltd.	Design of reinforced slopes in a wide variety of soil types, using reinforced soil or soil nails.	http://www.geocentrix.co.uk/
ReWard	Geocentrix Ltd.	Design of embedded retaining walls, incorporating several UK and international design standards including BS 8002 and Eurocode 7.	http://www.geocentrix.co.uk/
Repute	Geocentrix Ltd.	Onshore pile design and analysis.	http://www.geocentrix.co.uk/
Geogiga Seismic Pro	Geogiga Technology corp.	Seismic data processing and interpretation software.	http://www.geogiga.com/
CPeT IT	Geologismiki	Interpretation of Cone Penetration data.	http://geologismiki.gr/
Cliq	Geologismiki	Cone Penetration Based soil liquefaction software that for CPT data interpretation, factor of safety, liquefaction potential index and post-earthquake displacements (both vertical and lateral).	https://geologismiki.gr/
LiqSvs	Geologismiki	Liquefaction analysis that accepts SPT and V_s field data.	https://geologismiki.gr/
SPAS	Geologismiki	Seismic signal processing and seismic analysis.	https://geologismiki.gr/

Name	Company	Application	Website
LiqIT	Geologismiki	Assessment of liquefaction potential based on commonly used field data.	https://geologismiki.gr/
StoneC	Geologismiki	Vibro-replacement and design of stone columns.	https://geologismiki.gr/
SteinP 3DT	Geologismiki	Settlement calculation taking into consideration the influence of nearby footing elements.	https://geologismiki.gr/
SteinN Pro	Geologismiki	Preliminary settlement analysis below a rectangular footing.	https://geologismiki.gr/
BLogPro	Geologismiki	Creation of simple soil borehole logs.	https://geologismiki.gr/
SPTCorr	Geologismiki	Estimation of various soil properties from the Standard Penetration Test blow count.	https://geologismiki.gr/
GEODelp	GEOS	Prediction of settlement from *in situ* measurements.	http://www.geos-ic.com/
GEO Fond	GEOS	Calculation of settlement under embankments and dimensioning of shallow and deep foundation.	http://www.geos-ic.com/
GEOMUR	GEOS	Design of retaining walls and analysis of internal and external stability.	http://www.geos-ic.com/
GEOSpar	GEOS	Design of nailed wall cladding and calculation of steel section and support plates.	http://www.geos-ic.com/
GEO Stab	GEOS	Slope stability, calculation of general stability of supports, and dimensioning reinforced floor and nailed walls.	http://www.geos-ic.com/
RIDO	GEOS	Calculation of elastoplastic equilibria and dimensioning of retaining screens.	http://www.geos-ic.com/
Z-soil	GEOS	2-D and 3-D finite element numerical simulation and geotechnical calculation of simple and complex structures.	http://www.geos-ic.com/
AIR/W	Geoslope	Finite element simulation of air transfer in mine waste and other porous media.	https://www.geoslope.com/
CTRAN/W	Geoslope	Finite element simulation of solute and gas transfer in porous media.	https://www.geoslope.com/
Quake/W	Geoslope	Finite element simulation of earthquake liquefaction and dynamic loading.	https://www.geoslope.com/
SEEP/W	Geoslope	Finite element simulation of groundwater flow in porous media.	https://www.geoslope.com/
SIGMA/W	Geoslope	Finite element simulation of stress and deformation in earth and structural materials.	https://www.geoslope.com/
SLOPE/W	Geoslope	2-D slope stability analysis using limit equilibrium method.	https://www.geoslope.com/
TEMP/W	Geoslope	Finite element simulation of heat transfer and phase change in porous media.	https://www.geoslope.com/
Geo Studio	Geoslope	Integrated suite for simulation of slope stability, ground deformation, and heat and mass transfer in soil and rock.	https://www.geoslope.com/
ILA	GeoSoft	Slope stability analysis, including features for retaining system designing	https://www.geoandsoft.com/
CE.CA.P	GeoSoft	Analysis and design of foundations	https://www.geoandsoft.com/
DIADIM	GeoSoft	Solution of dimensioning problems and verification through finite difference model.	https://www.geoandsoft.com/
INSITU	GeoSoft	Interpretation of static and dynamic geotechnical *in situ* tests.	https://www.geoandsoft.com/
VERCAM	GeoSoft	Analysis and design of retaining, gravity and in concrete walls.	https://www.geoandsoft.com/

Name	Company	Application	Website
LIQUITER	GeoSoft	Determination of safety factors pertaining to the liquefaction of incoherent saturated terrains subjected to earthquake phenomena.	https://www.geoandsoft.com/
CLUSTAR	GeoSoft	Computerized structural geology data collection and analysis, which recognizes the discontinuity sets of a rock mass through hierarchical and non-hierarchical clustering procedures derived from the multivariate analysis.	https://www.geoandsoft.com/
ROTOMAP	GeoSoft	3-D model for rock fall analysis and the design of rock fall protective systems.	https://www.geoandsoft.com/
ROCK3D	GeoSoft	Stability analysis of removable blocks on planar rock slopes.	https://www.geoandsoft.com/
Load cap	Geostru	Computation of bearing capacity on rocky or loose soils and analysis of soil reinforced with geogrid.	https://www.geostru.eu/
GDW	Geostru	Design and analysis of gabion walls, simple concrete weirs, and gabion weirs in static and seismic conditions.	https://www.geostru.eu/
GFAS	Geostru	Mechanical analysis of soil using the finite element method.	https://www.geostru.eu/
Pile and Micropile	Geostru	Calculation of the bearing capacity of the foundation terrain of a pile or micropile (Screw-piles).	https://www.geostru.eu/
MDC	Geostru	Design and analysis of reinforced concrete retaining walls resting either on their own foundation or on piles, optionally supported by tiebacks.	https://www.geostru.eu/
SPW	Geostru	Design and analysis of sheet pile walls, drilled piles, and diaphragm walls.	https://www.geostru.eu/
Rock Plane	Geostru	Evaluation of localized instability rocky elements affected by seismic movements and/or by presence of water pressures within intersurface fractures.	https://www.geostru.eu/
Down Hole	Geostru	Processing borehole seismic tests.	https://www.geostru.eu/
Dynamic Probing	Geostru	Interpretation of Dynamic Penetration test.	https://www.geostru.eu/
Adamas	Geosysta Ltd.	Integrated data management system for geotechnical data.	http://geosysta.com/
Drillysis	Geosysta Ltd.	Borehole logging application.	http://geosysta.com/
WALLAP	Geosolve	Stability analysis of cantilevered and propped cantilever retaining walls.	http://www.geosolve.co.uk/
Slope	Geosolve	Slope stability analysis.	http://www.geosolve.co.uk/
GWALL	Geosolve	Analysis of retaining wall problems including gravity walls and cantilever wall with bases.	http://www.geosolve.co.uk/
ELPLA	Geotec Software	Analysis of single piles, pile groups, and piled raft foundation.	https://www.elpla.com/
GeoSuite	Geotechnical Software and Services	Comprehensive geotechnical software package	http://geoadvanced.com/
GeoLiqu	Geotechnical Software and Services	Soil liquefaction analysis, including liquefaction potential, seismic settlement (dry and saturated) and lateral spreading based on standard penetration test (SPT) data, cone penetration test (CPT) data and shear wave velocity (Vs) data profiles.	http://geoadvanced.com/

Name	Company	Application	Website
GeoComp	Geotechnical Software and Services	Calculation of compression deformation utilizing Standard Penetration test (SPT), cone penetration test (CPT), and shear wave velocity (V_s) data.	http://geoadvanced.com/
GeoBP	Geotechnical Software and Services	Bearing capacity analysis of soil.	http://geoadvanced.com/
GeoEP	Geotechnical Software and Services	Calculation of static and seismic lateral earth pressures, utilizing trial wedge method, for surface configurations such as level, ascending and/or descending or stepped surfaces.	http://geoadvanced.com/
GGU 3D SSFLOW	GGU Soft	Simulation of steady-state groundwater flow in three-dimensional groundwater systems using finite element methods.	https://www.ggu-software.com/
GGU 3D Transient	GGU Soft	Analysis of transient groundwater flow using the finite element method based on a 3-D groundwater system analyzed using GGU 3D SSFLOW.	https://www.ggu-software.com/
GGU-Axpile	GGU Soft	Bored and driven pile calculations and graphical representation of results.	https://www.ggu-software.com/
GGU Consolidate	GGU Soft	Analysis of 1-D consolidation processes in single-layered systems (analytical), multi-layered systems (numerical), and single- or multi-layered systems with vertical drains.	https://www.ggu-software.com/
GGU Elastic	GGU Soft	Analysis of plane and axis-symmetrical deformation using the finite element method.	https://www.ggu-software.com/
GGU Retain	GGU Soft	Analysis of retaining walls based on the Recommendations of the German Working Group for Excavations and for Waterfront Structures (EAB + EAU).	https://www.ggu-software.com/
GGU Settle	GGU Soft	Settlement analysis of triangular and rectangular foundations, including mutual influence of neighboring foundations.	https://www.ggu-software.com/
GGU Slab	GGU Soft	Analysis of elastically-supported slabs based on the modulus of subgrade reaction and constrained modulus methods using the finite element method.	https://www.ggu-software.com/
GGU Stability	GGU Soft	Slope stability analysis and analysis of soil nailing and reinforced earth walls. Nailing can consist of anchors, soil nails, geosynthetics (reinforced earth), or injection piles.	https://www.ggu-software.com/
GGU Trench	GGU Soft	Analysis of diaphragm wall stability in accordance with DIN 4126	https://www.ggu-software.com/
GGU-Underpin	GGU Soft	Analysis and design of underpinning.	https://www.ggu-software.com/
BorinGS	Gookin Software	Creation and management of boring logs.	http://www.gookinsoftware.com/
FSCONSOL	GWP Geo software Inc.	Determination of the rate and magnitude of consolidation of soil slurries, such as mine tailings, deltaic deposits, and other soft soils.	http://www.fsconsol.com/
FTG	Inducta Pty. Ltd.	Design of pad and strip footings.	https://www.inducta.com.au/
PileAXL	Innovative Geotechnics Pty Ltd, Australia	Analysis of single pile behavior under axial loading applied at the pile head for both onshore and offshore engineering problems.	https://www.pilegroups.com/

Name	Company	Application	Website
PileSuite	Innovative Geotechnics Pty Ltd, Australia	Deep foundation analysis and design for both onshore and offshore projects.	https://www.pilegroups.com/
PileGroup	Innovative Geotechnics Pty Ltd, Australia	Finite element simulation of deformations and loads of pile groups subject to general 3-D loading, such as axial and lateral forces and moments applied on the pile caps.	https://www.pilegroups.com/
PileLAT	Innovative Geotechnics Pty Ltd, Australia	Finite-element simulation of laterally loaded piles (single piles mainly under lateral loading) based on automatically generated nonlinear p-y curves for various soil and rock types.	https://www.pilegroups.com/
PileROC	Innovative Geotechnics Pty Ltd, Australia	Prediction of settlement for piles socketed into rock under compressive axial loading and estimates of ultimate and factored axial capacities for a range of socket lengths.	https://www.pilegroups.com/
Geo Tec B	Interstudio S.r.1	Analysis of stratified slopes in the presence of water and loads.	http://en.interstudio.net/
3DEC	Itasca Consulting Group	3-D simulation for advanced geotechnical analysis of soil, rock, ground water, structural support, and masonry using the distinct element method.	https://www.itascacg.com/
FLAC	Itasca Consulting Group	2-D finite difference simulation for advanced geotechnical analysis of soil, rock, groundwater, and ground support.	https://www.itascacg.com/
FLAC3D	Itasca Consulting Group	3-D finite difference simulation for advanced geotechnical analysis of soil, rock, groundwater, and ground support.	https://www.itascacg.com/
PFC	Itasca Consulting Group	Distinct Element Method (DEM) for advanced, fast multi-physics simulation.	https://www.itascacg.com/
UDEC	Itasca Consulting Group	2-D simulation of the quasi-static or dynamic response to loading of media containing multiple, intersecting joint structures using the distinct element method.	https://www.itascacg.com/
FLAC/Slope	Itasca Consulting Group	Slope stability analysis.	https://www.itascacg.com/
CESAR- LPCP	itech-soft	Simulation of stability and deformation using the finite element method in 2-D and 3-D.	http://www.cesar-lcpc.com/
Lean Wall	Javasoft	Design of concrete or masonry leaning walls.	https://javasoft-softwares.com/
Retain Wall	Javasoft	Design of concrete or masonry retaining walls.	https://javasoft-softwares.com/
Key Wall Pro	Key wall Retaining wall system Inc	Design and analysis of gravity walls and soil reinforced wall sections for all Keystone structural units and most common soil reinforcement materials.	http://keystonewalls.com/
HoleBaseSI	Keynetix Ltd	Geotechnical knowledge management system for inclusion of geotechnical data within the BIM process.	https://www.keynetix.com/
Twall Design	LG Soft	External stability analysis of reinforced concrete cantilever walls (sliding, overturning and bearing capacity) under both static and seismic conditions.	https://www.dec.uc.pt/

Name	Company	Application	Website
Limit state GEO	LimitSTATE Ltd	Geotechnical stability analysis using the limit state approach to determine the critical failure mechanism.	http://www.limitstate.com/
Midas GTS	MIDAS IT	Finite element simulation of deep foundations, excavations, complex tunnel systems, seepage, consolidation, embankments, dynamic conditions, and slope stability analysis.	http://midasgtsnx.com/
4D Geotechnical Hazard assesment	Mira Geoscience Ltd.	Quantitative forecasting of geotechnical hazard for design or real time monitoring applications.	http://www.mirageoscience.com/
GSLOPE	Mitre Software Cooperation	Limit equilibrium slope stability analysis of existing natural slopes, unreinforced man-made slopes, or slopes with soil reinforcement.	http://www.mitresoftware.com/
GTILT	Mitre Software Cooperation	Management of slope inclinometer data.	http://www.mitresoftware.com/
EDIPLIN	Newsoft SAS	Design and verification of foundation of reinforced concrete poles.	https://www.newsoft-eng.it/
FEQDrain	NISEE - University of California, Berkeley	Analysis of earthquake generation and dissipation of pore water pressure in layered sand deposits with vertical drains.	https://nisee.berkeley.edu/
NovoCPT	Novo Tech Software Inc.	CPT interpretation.	http://www.novotechsoftware.com/
Novoformula	Novo Tech Software Inc.	Geotechnical correlations.	http://www.novotechsoftware.com/
NovoLiq	Novo Tech Software Inc.	Soil liquefaction analysis.	http://www.novotechsoftware.com/
Vislog	Novo Tech Software Inc.	3-D soil profile visualization.	http://www.novotechsoftware.com/
Frew	Oasys Ltd	Embedded retaining wall analysis.	https://www.oasys-software.com/
Greta	Oasys Ltd	Stability analysis for gravity retaining walls.	https://www.oasys-software.com/
PDisp	Oasys Ltd	Soil settlement calculation and displacement analysis.	https://www.oasys-software.com/
Piles	Oasys Ltd	Calculation of load capacity and settlement for single piles.	https://www.oasys-software.com/
Safe	Oasys Ltd	2-D finite element simulation in plane stress, plane strain, or axial symmetry.	https://www.oasys-software.com/
Siren	Oasys Ltd	Seismic site response analysis.	https://www.oasys-software.com/
Slope	Oasys Ltd	2-D slope stability analysis.	https://www.oasys-software.com/
Xdisp	Oasys Ltd	Prediction of ground movement, settlement, and assessment of building and utility damage.	https://www.oasys-software.com/
Alp	Oasys Ltd	Analysis of laterally loaded piles.	https://www.oasys-software.com/
Seisopt 2D	Optim Software	Creation of detailed velocity models from surface refraction array data using a proprietary simulated annealing optimization algorithm.	http://www.optimsoftware.com/
Seisopt Remi	Optim Software	Implementation of the Refraction Microtremor (ReMi) method to measure the *in situ* shear wave velocity profile.	http://www.optimsoftware.com/
Optum G2	Optum Comput. Engineering	2-D finite element simulation for geotechnical stability and deformation analysis in plane strain or axisymmetry.	https://optumce.com/

Name	Company	Application	Website
Optum G3	Optum Comput. Engineering	3-D finite element simulation for geotechnical stability and deformation analysis in plane strain or axisymmetry.	https://optumce.com/
SPW911	Pile Buck	Sheet pile design.	http://www.pilebuck.com/
GRLWEAP	Pile Dynamics Inc.	1-D wave equation analysis to simulate motions and forces in a pile when driven by either an impact or vibratory hammer.	https://www.pile.com/
Pile Driving Analyzer	Pile Dynamics Inc.	Dynamic load testing and pile driving monitoring.	https://www.pile.com/
CAPWAP	Pile Dynamics Inc.	Simulation of static load test in compression and tension, prediction of load displacement behavior, and determination of stresses at each depth along the pile.	https://www.pile.com/
Thermal Integrity Profiler	Pile Dynamics Inc.	Quality control or assessment of drilled shafts/bored piles, auger cast in place (ACIP)/continuous flight auger (CFA) or drilled displacement piles, slurry walls, barrettes, soil nails, and jet grouted columns.	https://www.pile.com/
PDI TOMO 3D	Pile Dynamics Inc.	3-D tomography imaging tool for analyzing wave speeds to yield a wave speed of entire shaft volume.	https://www.pile.com/
PDA-DLT	Pile Dynamics Inc.	Dynamic load testing for drilled shafts.	https://www.pile.com/
Plaxis 2D	Plaxis	2-D finite element simulation with add-ons for ground water flow, dynamic loading, and thermal analysis of soils and rocks.	https://www.plaxis.com/
Plaxis 3D	Plaxis	3-D finite element simulation with add-ons for ground water flow, and dynamic loading of soils and rocks.	https://www.plaxis.com/
Geo Program	Presta Shop	Complete geotechnical analysis.	http://www.programgeo.it/
Various books and software for soil mechanics	Prof. Arnold Verruijt (Deflt University of Technology)	Analysis of sheet pile walls in layered soils, slope stability, piles, groundwater flow, and finite element simulation of steady and non-steady groundwater flow.	http://geo.verruijt.net/
PROKON	Prokon Software Consultants	Structural design that is useful for slope stability analysis, rock stability and capacity analyses and pile capacity analysis.	https://www.prokon.com/
Geotech Masters	Q System Engineering LLC	Analysis and design of foundations and piles.	http://qsystemsengineering.net/
Retain Pro 10	Retainpro Software div. ENERCAL, Inc.	Design and analysis of earth retaining structures.	https://retainpro.com/
CPillar	Rocscience	Evaluation of the stability of surface or underground crown pillars, and laminated roof beds.	https://www.rocscience.com/
Dips	Rocscience	Stereographic projection.	https://www.rocscience.com/
Examine	Rocscience	Stress analysis and data visualization tool for underground excavations in rock.	https://www.rocscience.com/
RocData	Rocscience	Analysis of rock and soil strength data, and determination of strength envelopes and other physical parameters.	https://www.rocscience.com/
RocFall	Rocscience	2-D statistical analysis to assist with assessment of slopes at risk for rock falls.	https://www.rocscience.com/

Name	Company	Application	Website
RocPlane	Rocscience	Planar rock slope stability analysis and design.	https://www.rocscience.com/
RocSupport	Rocscience	Estimation of support requirements of tunnels in weak rock.	https://www.rocscience.com/
RocTopple	Rocscience	Toppling analysis and support design for rock.	https://www.rocscience.com/
RS2	Rocscience	2-D finite element simulation.	https://www.rocscience.com/
RS3	Rocscience	3-D finite element simulation.	https://www.rocscience.com/
RSPile	Rocscience	Pile analysis.	https://www.rocscience.com/
Settle	Rocscience	3-D soil settlement analysis.	https://www.rocscience.com/
Slide2	Rocscience	2D slope stability analysis using limit equilibrium method and finite element seepage analysis.	https://www.rocscience.com/
Slide3	Rocscience	3-D slope stability analysis	https://www.rocscience.com/
SWedge	Rocscience	Evaluation of the geometry and stability of surface wedges in rock slopes.	https://www.rocscience.com/
UnWedge	Rocscience	3-D stability analysis and visualization program for underground excavations in rock containing intersecting structural discontinuities.	https://www.rocscience.com/
ELK	Sharper Geo	Analysis of *in situ* tests and slope stability.	http://www.sharpergeo.com/
SVDesigner	Soil Vision system Ltd	3-D conceptual modeler and visualization tool for the geotechnical and hydrogeological fields.	https://soilvision.com/
SVseismic	Soil Vision system Ltd	Dynamic analysis by the finite element direct time step-by-step integration method.	https://soilvision.com/
SVslope	Soil Vision system Ltd	3-D slope stability analysis.	https://soilvision.com/
SVsoils	Soil Vision system Ltd	Estimation and mathematical representation of soil constitutive models for subsequent numerical modeling.	https://soilvision.com/
SVflux	Soil Vision system Ltd	1-D, 2-D, and 3-D finite element simulation of groundwater.	https://soilvision.com/
SVsolids	Soil Vision system Ltd	Determination of the stress state and deformation of soils under various loading conditions and solving stress-deformation problems.	https://soilvision.com/
TSLOPE 3D	TAGA Engineering Software Ltd.	3-D slope stability analysis.	https://tagasoft.com/
CASTeR	Technology Development Center	Generation of soil test reports.	http://www.tdcindia.com/
GTeCS	Technology Development Center	Analysis of slope stability, bearing capacity, pile capacity, settlement, and under-reamed pile capacity.	http://www.tdcindia.com/
TensarSoils	Tensar International Corporation	Analysis and design of retaining walls.	https://www.tensarcorp.com/
Dimensions	Tensar International Corporation	Calculation of bearing capacity and projected settlement beneath shallow foundations.	https://www.tensarcorp.com/
Foxta V3	Terrasol	Design of shallow, deep, and raft foundations.	https://www.terrasol.fr/

Name	Company	Application	Website
K-REA V4	Terrasol	Design of retaining walls using the subgrade reaction method, including diaphragm walls, sheetpile walls, and soldier pile walls.	https://www.terrasol.fr/
Straticad	Terrasol	Semi-automatic processing of geotechnical data within drawings and their display in 2-D and 3-D.	https://www.terrasol.fr/
Talren V5	Terrasol	Slope stability analysis, including stability of geotechnical structures, reinforcement, natural slopes, cut or fill slopes, earth dams, and dikes.	https://www.terrasol.fr/
Unipile 5.0	UniSoft GS	Analysis of piles and pile groups.	https://www.unisoftgs.com/
Unisettle 4.0	UniSoft GS	Stress and settlement calculations involving complex load combinations and site conditions.	https://www.unisoftgs.com/
UTEXAS	University of Texas at Austin	2-D slope stability analysis using limit equilibrium method.	http://www.ce.utexas.edu/prof/wright/UTEXASED4/UTEXASED4%20Home.htm
SigmaSpectra	University of Texas at Austin	Selection of suites of earthquake ground motions from a library of ground motions such that the median of the suite matches a target response spectrum at all defined periods.	https://github.com/arkottke/sigmaspectra
Strata	University of Texas at Austin	1-D linear-elastic and equivalent-linear site response analyses using time series or random vibration theory ground motions.	https://github.com/arkottke/strata
SLAMMER	University of Texas at Austin	Sliding-block analyses to evaluate seismic slope performance.	https://pubs.usgs.gov/tm/12b1/
MODFLOW	USGS	Simulation and prediction of groundwater conditions and groundwater/surface-water interactions. MODFLOW is the USGS's modular hydrologic model.	https://water.usgs.gov/ogw/modflow/
HYDRO-THERM	USGS	Simulation of multi-phase groundwater flow and associated thermal energy transport in three dimensions.	https://volcanoes.usgs.gov/software/hydrotherm/
VERSAT-P3D	Wutec Geotechnical International, B.C., Canada	Finite element simulation for quasi-3D nonlinear dynamic analyses of single piles and pile groups in the frequency and time domains.	http://www.wutecgeo.com/
VERSAT-2D	Wutec Geotechnical International, B.C., Canada	Software package (VERSAT-2D Processor, VERSAT-S2D and VERSAT-D2D) for 2-D finite element simulation of stresses, deformations, and soil-structure interactions for static loading and dynamic analyses of earth structures subjected to dynamic loads from earthquakes, machine vibration, waves, or ice action.	http://www.wutecgeo.com/

This Page Intentionally Left Blank

APPENDIX C. SYMBOLS USED IN GEOTECHNICAL ENGINEERING

One potentially confusing aspect of geotechnical engineering is the lack of standardization used for common engineering parameters. Different symbols were adopted at the various U.S. and overseas universities, as well as organizations such as NGI, USBR, and USACE, who were involved in the early years of soil mechanics. As an example, when presenting the results of the compression curve of a conventional consolidation test, the symbols used for the x-axis (vertical effective stress) include: p, p', σ'_v, $\overline{\sigma}_v$, and others. The purpose of this Appendix is not to offer suggestions for standardization, but to provide a listing of the different symbols that have been used historically in the geotechnical literature to be used as a cross-reference when consulting old figures, papers, and texts.

Table C-1 Symbols Used in Geotechnical Engineering

Symbol	Description
a	Isotropic transformation factor for flow nets
a	CPT net area ratio used for pore pressure corrections
a	Acceleration
a	Strength parameter used with a power function for nonlinear failure envelope
a	Attraction
A	Cross sectional area of the flow region perpendicular to the flow direction
A	Skempton pore pressure parameter
$\bar{A}$	Skempton pore pressure parameter
ACU	Anisotropically consolidated-undrained triaxial test
$\bar{A}_f$	Skempton pore pressure parameter at failure
a_v	Coefficient of compressibility
b	Strength parameter used with a power function for nonlinear failure envelope
B	Width of a foundation, loaded area, or tunnel
B	Skempton's pore pressure parameter
$\overline{B}$	Skempton's pore pressure parameter
B_c	Diameter of a flexible pipe
B_d	Width of trench in pipe loading calculations
B_t	Bulk modulus of soil
c	Total stress cohesion intercept (sometimes undrained shear strength)
c'	Effective stress cohesion intercept.
C	Number of surfaces on which pullout resistance is mobilized
$C_{\alpha\varepsilon}$	Modified secondary compression index or secondary compression ratio
CAU	Anisotropically consolidated undrained triaxial test
CBR	California Bearing Ratio
CBR_{soaked}	Soaked California Bearing Ratio
$CBR_{unsoaked}$	Unsoaked California Bearing Ratio
C_c	Compression index

Symbol	Description
C_c	Coefficient of curvature for grain-size distribution curve.
C^*_c	Intrinsic compression index
$C_{c\varepsilon}$	Modified compression index
c_{CU}	Total stress cohesion intercept from CU triaxial test
C_d	Load coefficient in pipe loading calculations
CF	Clay-sized fraction
c_h	Coefficient of consolidation in horizontal direction
CIU	Isotropically consolidated-undrained triaxial test
C_r	Recompression index
$C_{r\varepsilon}$	Modified recompression index
CRR	Cyclic resistance ratio
C_s	Swelling index, often used as a synonym for recompression index
CSR	Cyclic stress ratio
C_t	Creep factor for coarse-grained settlement methods
C_u	Coefficient of uniformity for grain-size distribution curve
C'_u	Linear coefficient of uniformity (geotextile design)
c_v	Coefficient of consolidation in vertical direction
$C_{\varepsilon c}$	Modified compression index
$C_{\varepsilon r}$	Modified recompression index
$C_{\varepsilon\alpha}$	Modified coefficient of secondary compression
d	Distance between the loaded points
d	Y-intercept of the failure envelope (*K_f-line*) in MIT stress path space (p vs q)
d'	Y-intercept of the failure envelope (*K_f-line*) in MIT stress path space (p' vs q)
d_c	Effective drainage diameter
d_w	Equivalent diameter of well or PVD
D	Diameter of the lab or field vane
D	Diameter
D	Outer diameter of pipe
D	Foundation embedment
D	Damping ratio
D_5	Particle-size diameter corresponding to 5% passing on the cumulative particle-size distribution curve
D_{10}	Particle-size diameter corresponding to 10% passing on the cumulative particle-size distribution curve
D_{15}	Particle-size diameter corresponding to 15% passing on the cumulative particle-size distribution curve
D_{30}	Particle-size diameter corresponding to 30% passing on the cumulative particle-size distribution curve
D_{60}	Particle-size diameter corresponding to 60% passing on the cumulative particle-size distribution curve
DCP	Dynamic cone penetrometer or DCP penetrometer index
D_e	equivalent core diameter
D_r	Relative density

Symbol	Description
DSS	Direct simple shear test
D'_x	Particle size for which X% of the soil is finer for linearized particle distribution (geotextile design)
D_xB	Particle size for which X% of the soil is finer for a base soil
D_xF	Particle size for which X% of the soil is finer for a filter material
e	Void ratio
e_0	Initial void ratio
e^*_{100}	Intrinsic void ratio at 100 kPa
e^*_{1000}	Intrinsic void ratio at 1000 kPa
e_f	Final void ratio or void ratio at failure
e_L	Void ratio at a water content equal to the liquid limit
e_{max}	Maximum index void ratio
e_{min}	Minimum index void ratio
E	Elastic modulus our Young's Modulus
E	Compactive effort index
E'	Equivalent modulus
E_a	Active earth pressure force
E_D	Dilatometer modulus
E_i	Initial tangent modulus
EI	Expansion index
E_m	Modulus of elasticity of mat
E_P	Pressuremeter modulus
E_s	Modulus of elasticity of soil
ESP	Effective stress path (MIT p' vs q stress path space)
E_u	Undrained Young’s modulus
F	Factor of safety
F	Percentage passing a No. 200 (75 µm) sieve (only considering the particles passing a 3-inch sieve)
F	Size correction factor
F^*	Pullout resistance factor
FC	Fine contents
f_i	Fraction of particles between two adjacent sieve sizes (Kozeny-Carman equation)
F_n	Radial drainage factor related to drain spacing
F_r	Radial drainage factor related to well resistance
F_r	Factor of safety for geosynthetic strength
FR	Cone penetration test friction ratio
f_s	Cone penetrometer friction sleeve resistance
F_s	Radial drainage factor related to soil disturbance (smear)
FS	Factor of safety
FS_g	Factor of safety for geotextile permeability
F_w	Factor of safety against wedge failure
G	Shear modulus

Symbol	Description
GC	Gravel Content
GI	group index
G_s	Specific gravity of solids
GSI	Geological Strength Index
G_u	Undrained shear modulus
H	Height
H	Depth of soil cover or vertical distance between ground surface and tunnel roof
H	Initial thickness in settlement
H_{dr}	Drainage path length
H_i	Thickness of each soil layer (may be listed without subscript)
H_i	Average height of the slice in slope stability analysis
H_i	Initial height of the test specimen
h_l	Head loss across flow region
h_p	Pressure head
h_t	Total hydraulic head
H_t	Tunnel height
H_t	Total thickness of transformed soil system
h_v	Velocity head
h_z	Elevation head
i	Hydraulic gradient
I	Influence factor for change in stress calculations
I_1	First stress invariant
I_c	Soil index
ICU	Isotropically consolidated-undrained triaxial test
I_D	Dilatometer material index
I_s	Uncorrected point load strength index
$I_{s(50)}$	Size corrected point load strength index
I_v	Void index
$I_{v,ICL}$	Void index for the intrinsic compression line
$I_{v,SCL}$	Void index for the sedimentation compression line
I_z	Schmertmann strain influence factor
I_{zp}	Schmertmann peak influence factor
k	Hydraulic conductivity or permeability
K	Wedge factor
K	Bulk modulus
K_0	Coefficient of lateral earth pressure at rest
K_0-$line$	Line through p’ and q (MIT) for at-rest conditions
K_a	Active earth pressure coefficient
K_b	Bulk modulus parameter for Duncan-Chang model
K_c	Anisotropic consolidation stress ratio = $\sigma'_{1c} / \sigma'_{3c}$
K_D	Dilatometer horizontal stress index

Symbol	Description
K_f-*line*	Failure envelope in MIT stress path space (p'_f vs. q_f)
k_g	Hydraulic conductivity of geotextile across plane of fabric
k_h	Hydraulic conductivity in horizontal direction
K_m	Mat stiffness factor
K_p	Passive earth pressure coefficient
k_s	Coefficient of subgrade reaction
k_s	Hydraulic conductivity of the disturbed zone
K_{ur}	Unload-reload modulus parameter Duncan-Chang model
k_v	Hydraulic conductivity in horizontal direction
l	Distance between two points along a structure
L	Length
L	Longest dimension of a foundation or loaded area
L	Length of flow path
L_e	Length of reinforcement embedded behind the trial failure surface
LI or I_L	Liquidity index
LIR	Load Increment Ratio for consolidation test
LL	Liquid limit
L_m	maximum distance water must flow through a vertical drain
m	Modulus number
$MARV$	Minimum average roll value used for various properties of geosynthetics
M_{ds}	Constrained modulus
MSE	Mechanically stabilized earth
m_v	Coefficient of volume compressibility
n	Porosity
n	Vertical drain spacing ratio
N	Standard Penetration Test blow count (blows/ft). Often assumed to be N_{60}
N'	Average Standard Penetration Test value
N_1	Standard Penetration Test blow count normalized to overburden pressure of 1 tsf
$N_{1,60}$	Standard Penetration Test blow count corrected for 60% of hammer energy and normalized to an overburden pressure of 1 tsf.
$N_{1,60,cs}$	SPT blow count corrected for 60% of hammer energy and fines content, and normalized to an overburden pressure of 1 tsf.
N_{60}	SPT blow count corrected for 60% of hammer energy
N_c	Bearing capacity factor
NC	Normally consolidated
N_{crit}	Undrained stability factor
N_d	Number of equipotential (head) drops in the flow net
N_f	Number of flow channels in the flow net
N_k	Bearing capacity factor used for reduction of CPT data in fine-grained soil
N_{kt}	Bearing capacity factor used for reduction of CPT data in fine-grained soil
N_q	Bearing capacity factor
N'_{silty}	Standard Penetration Test blow count for saturated silty sands

Symbol	Description
O_{95}	Geotextile apparent opening size
OC	Overconsolidated
OCR	Overconsolidation ratio
p	MIT stress path parameter = $(\sigma_1 + \sigma_3)/2$ or $(\sigma_v + \sigma_h)/2$
p'	MIT stress path parameter = $(\sigma'_1 + \sigma'_3)/2$ or $(\sigma'_v + \sigma'_h)/2$
p_0	Pressure required to initiate movement of the dilatometer
p_0	Pressuremeter liftoff pressure
P_a	Atmospheric pressure
p_a	Tunnel air pressure
P_c	Maximum past pressure or preconsolidation pressure
p_f	MIT stress path parameter p at failure
p_f	Inflection point in pressuremeter curve assumed to delineate the change from pseudo elastic to plastic response and the point where creep may be expected
p'_f	MIT stress path parameter p' at failure
PI	Plasticity index
p_L	Pressuremeter limit pressure where the curve becomes asymptotic on a pressure versus volume curve
PL	Plastic limit
P_p	Maximum past pressure or preconsolidation pressure
P'_p	Maximum past pressure or preconsolidation pressure
p_r	Pressuremeter yield point during the reloading portion of an unload–reload cycle where recompression ends and the soil reinitiates plastic shearing
P_r	Geosynthetic reinforcement's resistance to pullout
PSR	Principal stress ratio
p_u	Pressuremeter minimum pressure during unloading during the unload–reload cycle
q	Volumetric flow rate
q	MIT stress path parameter = $(\sigma_1 - \sigma_3)/2$ or $(\sigma_v - \sigma_h)/2$
Q	Rock tunneling quality index
Q	Quantity of flow
Q	Unconsolidated-undrained (UU) triaxial test
q_0	Applied pressure or load
q_0	Applied stress at the base of the foundation or structure
$q_{0\text{-}net}$	Net vertical stress applied by the structure
q_c	Cone penetrometer tip resistance or cone bearing (not corrected for pore pressure effects)
q_{c1}	Cone penetrometer tip resistance or cone bearing normalized to an overburden pressure of 1 tsf
q_d	Dynamic cone resistance
q_f	Applied stress following removal of surcharge
q_f	MIT stress path parameter q at failure
q_s	Surcharge load
q_t	Cone penetrometer tip resistance corrected for pore pressure effects
q_u	Unconfined compressive strength
q_w	Discharge capacity of the drain

Symbol	Description
r	Horizontal distance from centerline of a foundation
R	Radius of influence in well design
R	Correction factor for overconsolidated static CTP cone tip resistance
R	Isotropically consolidated undrained triaxial test with pore water pressure measurements.
R	Isotropically consolidated undrained triaxial test without pore water pressure measurements.
RC	Relative compaction
R_f	Reduction factor for Duncan-Chang model
RF_{CR}	Reduction factor for creep
RF_D	Reduction factor for durability
RF_{ID}	Reduction factor for installation damage
RMR	Rock mass rating
RQD	Rock Quality Designation
r_u	Pore pressure coefficient
s	Ratio of the disturbed zone diameter to the diameter of the drain
s	Settlement
s	Shear strength
S	Degree of saturation
S	Surface area factor for grain shape (Kozeny-Carman equation)
S	Seepage force
s_c	Primary consolidation settlement
SRF	Strength reduction factor
s_s	Secondary compression settlement
s_{su}	Undrained steady state shear strength
S_t	Sensitivity
$S_{t,fv}$	Sensitivity measured using field vane shear apparatus
s_u	Undrained shear strength for a $\phi = 0$ envelope = $(\sigma_{1f} - \sigma_{3f})/2$
$s_{u,fv}$	Undrained shear strength determined using field vane apparatus
$s_{ur,fv}$	Remolded undrained shear strength determined using field vane apparatus
t	Thickness
t	Stand up time for tunneling in raveling soils
t	Time after start of consolidation
t	Time
T	Elapsed time between excavation and completion of permanent structure
T	Temperature
T	Time factor in consolidation theory
t_{50}	Time for 50% consolidation to be achieved
t_{90}	Time for 90% consolidation to be achieved
T_{all}	Geosynthetic's long-term tensile strength
t_g	Geotextile thickness
t_m	Thickness of mat
T_{max}	Maximum net torque for vane shear test

Symbol	Description
t_p	Time required to finish primary consolidation
T_r	Time factor for radial consolidation
T_{res}	Residual torque reading for vane shear test
TSP	Total stress path (MIT)
(T-u_s)SP	Total stress path – static pore water pressure (MIT)
T_{ULT}	Ultimate tensile strength of the geosynthetic based on the MARV
T_v	Time factor for vertical drainage
u	Pore water pressure
U	Uplift force applied by water at the failure plane
$\overline{U}$	Degree of consolidation
u_0	Initial pore water pressure
u_2	Cone penetrometer pore water pressure for sensing element located directly behind cone tip
u_a	Pore air pressure
$\overline{U}_c$	Combined degree of consolidation
UC	Unconfined compression test
$\overline{U}_{fs}$	Degree of consolidation following surcharge application
$\overline{U}_r$	Degree of radial consolidation
USR	Undrained strength ratio = s_u/σ'_v
USR_{NC}	Undrained strength ratio for normally consolidated conditions
UU	Unconsolidated-undrained triaxial test
u_x	Excess pore water pressure
U_z	Degree of compression
$\overline{U}_z$	Average degree of consolidation
v	Specific volume = $1 + e$
V	Total volume
V	Total volume (phase relationships)
V_0	Initial calculated volume within the uninflated membrane for pressuremeter
V_a	Volume of air (phase relationships)
v_d	Discharge velocity
v_s	Seepage velocity
V_s	Volume of solids (phase relationship)
V_s	Shear wave velocity
V_{s1}	Normalized shear wave velocity
V_v	Volume of voids (phase relationship)
V_w	Volume of water (phase relationships)
w	Water content (gravimetric)
W	Width of the system perpendicular to the page
W	Weight
W	Total weight (phase relationships)
w_0	Initial water content

Symbol	Description
W_c	Flexible pipe load
W_d	Rigid pipe load
w_f	Final water content
W_i	Weight of each slice (limit equilibrium slope stability analysis)
w_L	Liquid limit
w_n	Natural water content
w_{opt}	Optimum water content
w_p	Plastic limit
W_p	Prism load on pipe
W_s	Weight of solids (phase relationships)
W_T	Total weight of sample (phase relationships)
W_w	Weight of water (phase relationships)
y	Height of the flow region
z	Depth along vertical drain
z	Elevation of a point of interest above the elevation datum
z	Depth below the soil layer
z_{crit}	Critical depth for unsupported shafts in clay soils
z_i	Layer thickness for settlement calculations
z_p	Depth below an applied load
α	Angle between the major principal plane and the plane of interest
α	Settlement correction factor
α	Dip direction or dip azimuth
α	Scale correction factor to account for nonlinear stress reduction
α	Slope of the failure line (K_f) in MIT *p* - *q* space
α'	Slope of the failure line (K_f) in MIT *p'* - *q* space
β_α	Empirical or semi-empirical coefficient relating *k* to D_α
δ	Effective soil-geosynthetic interface friction angle
Δe	Change in void ratio
ΔH	Change in layer thickness
ΔH	Change in height
Δh_L	Total head loss for one equipotential drop on a flow net
δ_L	Angular distortion
Δ_L	Deflection ratio
δ_{max}	Differential settlement
Δq_p	Change in cone tip resistance
$\Delta\sigma$	Change in applied stress
$\Delta\sigma'_v$	Change in vertical effective stress
$\Delta\sigma_d$	Change in deviatoric stress or change in principal stress difference = $\Delta\sigma_1$ - $\Delta\sigma_3$
$\Delta\sigma_v$	Change in total vertical stress
Δu	Change in pore water pressure
ε_a	Vertical or axial strain

Symbol	Description
ε_{crit}	Critical strain for structural distress
$\dot{\varepsilon}$	Strain rate
ε_h	Horizontal strain
ε_r	Radial strain
ε_{vol}	Volumetric strain
ε_v	Volumetric strain
ε_v	Vertical strain
ϕ	Total stress friction angle
ϕ'	Effective stress friction angle
ϕ_{UU} *or* ϕ_U	Total stress friction angle from UU triaxial test (S < 100%)
$\overline{\phi}$	Effective stress friction angle
ϕ_{CU}	Total stress friction angle from CU triaxial test
ϕ'_{FS}	Fully softened friction angle
$\overline{\phi}_{FS}$	Fully softened friction angle
ϕ'_{RES}	Residual friction angle
$\overline{\phi}_{RES}$	Residual friction angle
ϕ'_R	Residual friction angle
$\overline{\phi}_R$	Residual friction angle
ϕ'_{SEC}	Effective stress secant friction angle (stress dependent)
$\overline{\phi}_{SEC}$	Effective stress secant friction angle (stress dependent)
γ	Unit weight
γ	Shear strain
γ'	Effective unit weight
γ_b	Buoyant unit weight
γ_d	Dry unit weight
$\gamma_{d\text{-}max}$	Maximum dry unit weight
γ_m	Moist unit weight
γ_{SAT}	Saturated unit weight
γ_T	Total, wet, or moist unit weight
γ_w	Unit weight of water
$\dot{\gamma}$	Shear strain rate
λ	Ratio of the circumferential stress to the vertical stress in circular openings
μ	Coefficient of friction
μ'	Coefficient of friction for trench backfill
μ_0	Influence factor associated with embedment of load
μ_1	Influence factor associated with geometry and Poisson's ratio
μ_R	Vane correction factor
ν	Poisson's ratio
ν_m	Poisson's ratio of mat

Symbol	Description
θ	Volumetric moisture content
σ	Total normal stress
σ'	Effective normal stress
$\overline{\sigma}$	Effective normal stress
σ_1	Total major principal stress
σ'_1	Effective major principal stress
$\overline{\sigma}_1$	Effective major principal stress
$\sigma'_{1,con}$	Effective major consolidation stress
$\overline{\sigma}_{1,con}$	Effective major consolidation stress
σ_2	Total intermediate principal stress
σ'_2	Effective intermediate principal stress
$\overline{\sigma}_2$	Effective intermediate principal stress
σ_3	Total minor principal stress
σ'_3	Effective minor principal stress
$\overline{\sigma}_3$	Effective minor principal stress
$\sigma'_{3,con}$	Effective minor consolidation stress
$\overline{\sigma}_{3,con}$	Effective minor consolidation stress
σ'_c	Consolidation stress
$\overline{\sigma}_c$	Consolidation stress
σ_{cell}	Cell pressure for triaxial test
σ_d	Principal stress difference or deviatoric stress
$\sigma_1 - \sigma_3$	Principal stress difference or deviatoric stress
σ'_{fc}	Effective normal stress on the failure plane during consolidation
$\overline{\sigma}_{fc}$	Effective normal stress on the failure plane during consolidation
σ_{ff}	Total normal stress on failure plane at failure
σ'_{ff}	Effective normal stress on failure plane at failure
σ_h	Total horizontal stress
σ'_h	Effective horizontal stress
$\overline{\sigma}_h$	Effective horizontal stress
σ'_m	Mean effective stress
$\overline{\sigma}_m$	Mean effective stress
σ'_N	Effective normal stress on failure surface
$\overline{\sigma}_N$	Effective normal stress on failure surface
σ'_p	Maximum past pressure or preconsolidation stress
$\overline{\sigma}_p$	Maximum past pressure or preconsolidation stress
σ'_{crit}	Critical confining stress
σ'_{ps}	Effective stress after perfect sampling
σ'_p	Effective stress after perfect sampling
σ_t	Interior tunnel pressure from compressed air or breasting

Symbol	Description
σ_v	Total vertical stress
σ'_v	Vertical effective stress
$\overline{\sigma}_v$	Vertical effective stress
σ_{v0}	Initial vertical total stress
σ'_z	Vertical effective stress
σ_{z0}	initial geostatic vertical total stress
σ'_{z0}	Initial or *in situ* vertical effective stress
σ'_{zp}	Initial vertical effective stress at depth of Schmertmann peak influence factor
τ	Shear stress
τ_{cyc}	Applied peak cyclic shear stress
τ_f	Shear stress at failure
τ_{ff}	Shear stress on the failure surface at failure
τ_{eq}	Shear stress required for equilibrium
ω	Tilt angle due to differential settlement
ψ	Matric suction
Ψ	Dip
Ψ_g	Geotextile permittivity, provided by manufacturers or from testing (ASTM D4491)

Table C-2 Acronyms and Abbreviations

Term	Definition
2-D or 2D	Two dimensional
3-D or 3D	Three dimensional
AASHTO	American Association of State Highway and Transportation Officials
ACU	Anisotropically consolidated undrained
AMTS	Automated total station
AR	Augmented reality
BLM	U.S. Bureau of Land Management
BPT	Becker penetration test
CB	Cement-bentonite
CD	Consolidated drained
CU	Consolidated undrained
CK_0U	K_0 consolidated undrained
CPMT	Cone pressuremeter
CPT	Cone penetration test
CPTu	Piezocone test
CRS	Constant rate of strain (consolidation test)
CYCDSS	Cyclic direct simple shear
DCP	Dynamic cone penetration
DMT	Flat plate dilatometer test
DOT	Department of Transportation
DPI	Dynamic cone penetration index
DPT	“Dutch” cone penetrometer test
DSS	Direct simple shear
DST	Direct shear test
DTM	Digital terrain model
EDG	Electrical density gauge
EIS	Electrical impedance spectroscopy
EROS	Earth Resources Observation System
FDM	Finite difference method
FEA or FEM	Finite element analysis or method
FEMA	Federal Emergency Management Agency
FERC	Federal Energy Regulatory Commission
FHWA	Federal Highway Administration
GIS	Geographic information system
GPS	Global positioning system
HCMM	Heat Capacity Mapping Mission
ICL	Intrinsic compression line for remolded clays (Burland 1990)
ICOLD	International Committee on Large Dams

Term	Definition
ICU	Isotropically consolidated undrained
ID	Inside diameter
ISO	International Organization for Standardization
ISRM	International Society for Rock Mechanics
IST	Impact soil tester
LEL	Lower explosive limit
LFD	Lightweight falling deflectometer
LIDAR	Light detection and ranging
LIR	Load increment ratio
LPT	Large penetration test
LVDT	Linear pvariable displacement transducer
M-DI	Moisture-density indicator
MEMS	Micro-electro-mechanical
MSE	Mechanically stabilized earth
MSW	Municipal solid waste
NAIP	National Agriculture Imagery Program
NCIC	National Information Center
NCHRP	National Cooperative Highway Research Program
NCRS	National Resources Conservation Service
NDG	Nuclear density gauge
NFS	Not frost-susceptible
NP	Nonplastic
NRC	Nuclear Regulatory Commission
OD	Outside diameter
OSHA	Occupational Safety and Health Administration
PFS	Possibly frost-susceptible
PLT	Plate load test
PMT	Pressuremeter test
RMR	Rock mass rating
RTD	Resistance temperature device
SAR	Synthetic aperture radar
SB	Soil-bentonite
SBPMT	Self-boring pressuremeter
SBT	Soil behavior type
SCB	Soil-cement-bentonite
SCL	Sedimentation compression line for natural clays (Burland 1990)
SCPTu	Seismic piezocone test
SDG	Soil density gauge
SLAR	Side-looking airborne radar

Term	Definition
SPT	Standard Penetration Test
SS	Surface stiffness
TVA	Tennessee Valley Authority
UAV	Unmanned aerial vehicle
UEL	Upper explosive limit
USACE	United States Army Corps of Engineers
USBR	United Stated Bureau of Reclamation
USCS	Unified Soil Classification System
USDA	United State Department of Agriculture
USEPA	United States Environmental Protection Agency
USFS	United States Forest Service
USGS	United States Geological Survey
UU	Unconsolidated undrained
VST	Vane shear test

This Page Intentionally Left Blank

APPENDIX D. GLOSSARY

Active zone – The near-surface zone affected by seasonal variation in water content. Also, zone within a soil mass subjected to active earth pressure conditions.

Activity of clay – The ratio of plasticity index to percent by weight of the total sample that is smaller than 0.002 mm in grain size. This property can be correlated with the type of clay mineral.

Adobe – Sandy clays and silts of medium plasticity usually found in the semiarid regions of the southwestern United States. The name is also applied to some high plasticity clays with high clay content and high swell and shrink potential usually found in the western United States.

Aeolian soil – Material transported and deposited by wind.

Aquiclude – A relatively impervious rock or soil layer underlying or overlying an aquifer.

Aquifer – Relatively permeable rock or soil stratum that can store and easily transmit water. Also used for the sand layer often found beneath levees in the lower Mississippi Valley.

Alluvial soils – Materials transported and deposited by running water.

Anisotropic soil – A soil mass having different properties in different directions, often referring to strength or permeability characteristics.

As-compacted – Condition of the soil after compaction is completed.

Azimuth – Is the angle of a feature measured from North at 0° in a spherical coordinate system.

Baby poop – Very soft clay located just above limestone in karst. Frequently orange and formed by dissolution.

Back-packing – Any material (commonly granular) that is used to fill the empty space between the lagging of a wall system and a rock surface.

Backswamp – The prolonged accumulation of floodwater sediments in flood basins bordering a river; materials are generally clays but tend to become siltier near the riverbank

Balanced load – See Compensated foundation

Bank-run sand and gravel – Raw material excavated from a borrow pit, but not sorted or separated into specific grades.

Bedding – Planes of dissimilar materials caused by deposition normally encountered in sedimentary rocks.

Bentonite – High plasticity clay consisting of mostly montmorillonite, resulting from the weathering of volcanic ash mainly in the presence of water. It is normally hard when dry but swells considerably when wet. This clay is commonly used with water as drilling mud and as liner in landfills.

Black cotton soil – Black expansive soil commonly encountered in India. The name originates from the fact that this soil is common in areas where the main crop is cotton.

Blocky – Adjective for soils that can be broken down into small angular lumps which are difficult to break down further.

Blow sand – Wind-driven or drifted sands.

Blue marl – Name given to a bluish-green clay from the Miocene that can be found along the fall line from Richmond, VA, into Maryland. This soil is considered to be acidic, usually with a pH less than 4.0, which can affect water quality and prevent plant or aquatic life.

Bog – Wetland covered with peat with a high water table that accumulates dead plants, usually mosses, and mainly sphagnum. It is generally nutrient poor and acidic.

Boney ground – Ground containing significant amounts of large gravel, cobbles, and boulders.

Borehole jack – An *in situ* test device used to estimate the deformability of rocks. Equipment description and operating procedures are presented in ASTM D4971.

Boulder – Rock particles that have a greatest dimension of at least 12 inches.

Boulder clay – Geological term used to designate clays formed from glacial drift that has not been subjected to the sorting action of water and therefore contains particles from boulders to clay sizes. Boulder clays are also called tills.

Boundary condition – Physical parameters assigned to the edges or boundaries of the domain in numerical analysis. Examples are constant total head boundaries in FE seepage analysis or restrained displacement boundaries in FE stress analysis.

Breaker run – Crushed rock with large particles refers to large broken stone obtained as part of quarrying or mining activities.

Buckshot – Term applied to clays of the southern and southwestern United States that cracks into small, hard, relatively uniform sized lumps on drying. The lumps are similar to the size of buckshot and the soil is very sticky when wet.

Bull's liver – An inorganic silt or silty sand usually encountered in the New York City area. The name Bull's liver comes from its red color and jelly-like behavior when it is subjected to vibration.

Bull's tallow or Bull tallow clay – Tan or gray high plasticity clay typically found in relatively thin layers directly above partially weathered rock or rock in the Charlotte, NC, area. This clay normally has high shrink and swelling potential.

Caliche – Sedimentary rock from arid and semiarid climate in which soil particles, such as gravel, sand, clay, and silt, are cemented and coated by carbonate (often calcium or magnesium carbonate). The level of cementation varies significantly within a deposit. The soil has light coloration often exhibits light colored concretions of various sizes depending on the level of development of the soil profile. The consistency of caliche varies from soft rock to firm soil.

Capillary stresses – Pore water pressures less than atmospheric values produced by surface tension of pore water acting on the meniscus formed in void spaces between soil particles.

Channel fill – Deposits laid down in abandoned meander loops isolated when rivers shorten their courses; composed primarily of clay. However, silty and sandy soils are found at the upstream and downstream ends

Chip – Name given to crushed angular rock fragments smaller than a few centimeters.

Clay – Soil particles passing a No. 200 (75-µm) sieve that exhibit plasticity (putty-like properties) within a range of water contents, and considerable strength when air dried. For classification of clayey soils, refer to Section 1-3.3.

Clay size fraction – The portion of the soil which is finer than 0.002 mm. This is not a viable measure of the plasticity of the material or its characteristics as a clay.

Coarse-grained soils – Soils that contain 50% or more particles retained on a No. 200 (75 µm) sieve.

Cobbles – Rock particles that pass through a 12-inch square opening sieve but are retained on a 3-inch square opening sieve.

Coffee grounds – Soil formed from freshwater marshes that has been dry for decades and has decomposed to the point that is black and inert with little to no plasticity. It is black and granular even when wet.

Colluvial soils – Material transported and deposited by gravity, often found in the vicinity of slopes.

Colluvium – Loose soil deposited at the bottom of a slope.

Compacted – Soil specimen formed by compaction in a mold at a given water content and relative compaction usually referred to a given compaction standard.

Compensated foundation – Method used to support heavy structures over compressible strata. In this approach, the weight of the structure is balanced, completely or partially, by soil that is permanently excavated from the building footprint.

Compression index – Parameter which quantifies the compressibility of normally consolidated soil in one-dimensional compression. Normally, it is the log-linear slope of the compression curve defined by void ratio (y-axis) and the logarithm of vertical effective stress (x-axis).

Cone Penetration Test (CPT) – An *in situ* test that utilizes a standard cone-shaped instrument that is pushed at a standard constant rate from the ground surface to obtain a continuous record of the penetration resistance of the cone tip and the frictional resistance of the soil acting on the friction sleeve of the probe. Testing is currently conducted in accordance with ASTM D5778.

Consolidation tests – Tests in which the volume change of the soil is determined for a change in applied stress, normally for one-dimensional compression.

Coquina – Soft, porous sedimentary rock, mainly limestone, composed largely of shells, coral, and fossils cemented together, with particles averaging 0.079 in (2 mm) or greater in size.

Compression curve – Curve relating the void ratio or strain to the effective stress applied (usually in log scale).

Critical depth – The depth over which soil compression caused by changes in stress contributes to significant surface settlement. The critical depth in fine-grained soils corresponds to the depth at which the change in stress is less than 10% of the existing vertical effective stress. In coarse-grained soils, the critical depth occurs when the change in stress is less than 20% of the existing vertical effective stress. Critical depth can also be used to refer to the depth from the ground surface for which no support is required for vertical shafts in clay.

Cyclic Stress Ratio (CSR) – Amplitude of the cyclic shear stress imposed by an earthquake normalized by the initial effective vertical stress. In a cyclic triaxial test, this is equal to one-half of the applied cyclic deviator stress divided by the isotropic consolidation stress.

Deflection ratio – The maximum expected deviation from uniform settlement divided by the overall length of the structure, which is an approximate measure of the curvature caused by settlement.

Deltaic – Deposits formed at the mouths of rivers, which result in extension of the shoreline.

Desert varnish – Also called patina, rock varnish, or rock rust, is thin, dark red to black mineral coating found on pebbles and rocks surfaces in arid regions.

Desiccation – The process of shrinkage or consolidation of the fine-grained soil produced by increase of effective stresses in the grain skeleton accompanying the development of capillary stresses in the pore water. Desiccation is often a result of soil drying.

Dewatering – Process where water is pumped from a foundation excavation or pumped from a pervious soil stratum with the purpose of lowering the water table.

Diatomaceous earth – Soft, siliceous sedimentary rock that usually crumbles into powder. When crumbled, the particles are silty and contain large amounts of diatoms, the siliceous skeletons of minute marine or freshwater organisms.

Differential settlement – Difference in vertical displacement between horizontally spaced points. Often, difference in settlement between structural elements, such as footings or columns.

Dip – Angle that the surface of the rock forms with a horizontal plane.

Dissipate – Increase or decrease of pore water pressure in order to achieve an equilibrium condition. Can also refer to the decrease in the magnitude of a value with depth, such as the dissipation of stress increase with depth.

Dispersive clays – Clays containing a high percentage of dissolved sodium in the pore water, such that when exposed to water, are very susceptible to erosion.

Distortion – The slope of the expected settlement profile or the ratio of the settlement between two points to the distance separating the points.

Disturbed specimen – Soil specimen obtained without care taken to preserve the volume or structure of the soil. Disturbed specimens are used for index tests, and are not used for strength or compressibility tests.

Double Drainage – Condition when the excess pore water pressure can drain from the top and bottom boundaries of the laboratory test specimen or from a layer of clay *in situ*.

Dune sands – Mounds, ridges, and hills of uniform fine sand characteristically exhibiting rounded grains

Dynamic cone penetration (DCP) – An *in situ* test performed by driving a standard-sized cone into the ground using a drop hammer. This test is detailed in ASTM D6951.

Effective diameter – The grain size that has the primary influence on the average pore size of the soil, which is typically selected as the grain size corresponding to 5 to 20% passing on the cumulative particle-size distribution curve.

Effective Stress – The net stress across points of contact of soil particles, generally considered as equivalent to the total stress minus the pore water pressure.

Ejecta – Loose deposits of volcanic ash, lapilli, bombs, etc.

Elevation head – measure of potential energy of water defined by the vertical distance of the water surface from a datum.

Equalization – Action of letting something reach equilibrium.

Equipotential line – Lines or curves define points of constant total head.

Equivalent Fluid Pressure – Horizontal pressures of soil, or soil and water in combination, which increase linearly with depth and are equivalent to those that would be produced by a heavy fluid of a selected unit weight.

End of Primary Consolidation (EOP) – When all the excess pore pressure in the soil created by the increase in stress is dissipated and the soil enters into secondary compression.

Estuarine – Mixed deposits of marine and alluvial origin laid down in widened channels at mouths of rivers and influenced by tide of body of water into which they are deposited

Excess Pore Pressures – Increment of pore water pressures greater than hydrostatic values, produced by application of normal stresses or shear stresses.

Exit Gradient – The hydraulic gradient (difference in head at two points divided by the distance between them) at the point where water exits soil. Exit gradients are often used as an indicator of erosion at the downstream toe of dams and levees.

Expansion Index – Percent swell multiplied by 10 for the ASTM D4829 test.

Extraction wells – Pumped wells that withdraw groundwater or contaminated groundwater from an aquifer.

Fibric peat – Peat in which the original plant fibers are slightly decomposed and contain 67% or more fibers.

Field Boring Log – Logged information of a boring prepared during the drilling process. A typical field log includes all the relevant information for the boring that was completed, including a unique boring identification number, date of drilling, personnel on-site, boring advancement method (i.e., auger, rotary wash, direct push, sonic), depths where samples were obtained, type of samples (i.e., split-barrel and Shelby tube), hammer type, raw SPT N-values, water level observations, and preliminary estimates of stratigraphy. If available, the global positioning system (GPS) coordinates should be included. The field log provides a unique designation of each recovered sample, whether disturbed or undisturbed, as well as a field visual classification of the sample in accordance with ASTM D2488.

Fill – Any constructed soil deposit. It can range from soils that are free of organic matter and that are carefully compacted (controlled fill) to heterogeneous accumulations of rubbish and debris (uncontrolled fill).

Final boring log – Official engineering record of the drilling and sampling efforts that is prepared using the information from the field boring log, and lab and field test results.

Fine-grained soils – Soils that contain 50% or more particles passing a No. 200 (75 µm) sieve.

Finite difference method (FDM) – Numerical method that approximates derivatives by finite differences to solve differential equations with geotechnical applications, including consolidation, seepage, and stress-deformation analysis. In many cases, a physical body (e.g., soil mass, retaining wall, etc.) is discretized by dividing the geometry into small regions where properties are be assumed to be uniform.

Finite element method (FEM) – Numerical method in which a physical body (e.g., soil mass, retaining wall, etc.) is discretized by dividing the geometry into small areas, called elements, where properties are be assumed to be uniform. Adjacent elements in the body are connected at nodes. Global equations are developed to relate the elements, the constitutive theory assigned to the elements, and the selected boundary conditions. FEM is commonly used to solve stress-deformation and seepage problems in geotechnical engineering.

Fissured – Soils that break along predetermined surfaces with little resistance. Fissuring in soils may be an indicator of overconsolidation.

Flat plate dilatometer (DMT) or Marchetti Dilatometer – An *in situ* test that utilizes a device consisting of a robust steel blade that is pushed into the ground and then periodically stopped to allow the controlled measured inflation of a flexible steel membrane. The testing procedures are presented in ASTM D6635.

Floating foundation – see compensated foundation.

Floodplain – Deposits laid down by a stream that within a portion of its valley is subject to inundation by floodwaters

Flow banding – Layering that is sometimes seen in rocks formed from magma.

Flow line – Paths that water particles take when flowing through a soil. Flow lines are an element of flow nets.

Flow net – Graphical solution to the La Place equation used to show the spacial variation of total head. Flow nets are used for seepage calculations in geotechnical engineering.

Flow slide – Shear failure in which a soil mass moves over a relatively long distance in a fluid-like manner, occurring rapidly on flat slopes in loose, saturated, uniform sands, saturated silts, or in highly sensitive clays.

Foliation – Laminated structure of the minerals in a rock created by deformation.

Free swell – Condition in which the soil is allowed to swell with no confining stress being applied.

Full scale – Loading condition for a sensor where the maximum design load is applied.

Fuller's earths – Soils having the ability to absorb fats or dyes. These soils have the capability to decolorize oil or other liquids without chemical treatment. They are usually high plasticity sedimentary clays.

Fully softened shear strength – The drained shear strength of a clay in its normally consolidated state.

Glacial soils – Material transported and deposited by glaciers, or by meltwater from glaciers.

Glacial till – An accumulation of debris, deposited beneath, at the side (lateral moraines), or at the lower limit of a glacier (terminal moraine). Material lowered to the ground surface in an irregular sheet by a melting glacier is known as a ground moraine. See also Boulder Clay.

Glacio-fluvial deposits – Coarse- and fine-grained material deposited by streams of meltwater from glaciers. Material deposited on the ground surface beyond the terminal edge of a glacier is known as an outwash plain. Gravel ridges are known as kames and eskers. Depressions are known as kettles and can be filled with peat.

Glacio-lacustrine deposits – Material deposited within lakes by meltwater from glaciers, consisting of clay in central portions of lake and alternate layers of silty clay or silt and clay (varved clay) in peripheral zones.

Glassified sand – Granular deposits at the ground surface occurring after an intense forest fire.

Goodman jack – See Borehole jack.

Goonies – Cobbles found floating in a soil matrix.

Gravel – Soil particles that pass through a 3-inch square opening sieve but are retained on a No. 4 (4.75 mm) sieve. Gravels can be divided into: (1) coarse gravels, gravel particles that are retained on a ¾-inch square opening sieve, and (2) fine gravels, gravel particles that pass through a ¾-inch square opening sieve.

Grove sand – See Sugar sand

Gumbo – Fine-grained, highly plastic clay of the Mississippi Valley. It has a sticky, greasy feel and forms large shrinkage cracks on drying.

Gyp or gip soil – Gypsum soil (or soil containing gypsum) or caliche soil.

Hardpan – Soil layers that have become hard as rock due to cementing minerals, and do not become plastic when mixed with water, and are relatively impervious. It has also been applied to any hard or overconsolidated layer that is hard to excavate. Because of this ambiguity, Sower (1979) recommends that engineers should avoid this term because many lawsuits have centered about definition. The name implies a condition of a soil rather than a type of soil.

Hillwash – Fine colluvium consisting of clayey sand, sand silt, or clay.

Hogging – Manifestation of differential settlement in a structure that results in concave downward shape.

Homogeneous soil – Soils with the same color, appearance, and properties from point to point. No soil deposit is truly homogeneous.

Humus – Brown or black material formed by the partial decomposition of vegetable or animal matter. It is the organic portion of soil.

Hydraulic conductivity – Discharge velocity of water through a unit area under a unit hydraulic gradient. Can also be viewed as a coefficient of proportionality relating seepage velocity to hydraulic gradient. Often called permeability in geotechnical engineering practice.

Hydraulic gradient – Head loss divided by the length over which the head loss occurs.

Hydraulic head or Total head – Measure of potential energy calculated as the sum of the elevation head, velocity head, and pressure head.

Hydrodynamic Lag Time – See Lag Time.

Hydrostatic – Condition of equilibrium of fluids for no-flow conditions. Also referred to a condition where stresses or pore water pressures are equal in all directions.

Hydrostatic pore pressures – Pore water pressures or groundwater pressures exerted under conditions of no flow where the magnitude of pore pressures increase linearly with depth below the ground surface.

Igneous rocks – Rocks formed from the cooling and solidification of magma.

Inherent anisotropy – Variation of shear strength as a function of the direction of the failure plane. It is the result of significant differences in the soil structure which occur during the formation of the soil.

Intact sample – See Undisturbed sample.

Isotropic soil – A soil mass having essentially the same properties in all directions, referring primarily to stress-strain or permeability characteristics.

Isotropic – Equal in all directions.

Kaolin – White or pink clay of low plasticity. It is composed largely of minerals of the kaolinite family.

Karst – Terrain usually formed from the dissolution of rocks such as limestone, dolomite, and gypsum. It normally contains an underground drainage system composed of sinkholes and caves.

Lacustrine – Material deposited within lakes (other than those associated with glaciation) by waves, currents, and organo-chemical processes; deposits consist of unstratified organic clay or clay in central portions of the lake and typically grade to stratified silts and sands in peripheral zones

Lag time – Time required for an instrument to respond to a change in input.

Laminated – Layering consisting of different materials or material colors of less than ¼ inch in thickness.

Lamination – Sequence of fine layers in a small scale (usually less than one centimeter in thickness) normally observed in sedimentary rocks.

Landslide deposits – Considerable masses of soil or rock that have slipped down, more or less as units from their former position on steep slopes.

Laterites – Residual soils rich in iron formed in hot and humid climates (tropical regions). The cementing action of iron oxides and hydrated aluminum oxides makes dry laterites extremely hard. The high content of iron oxide makes many laterites to be rusty-red. Laterites are usually developed after significant weathering of the parent rock.

Ledge – Colloquial name for bedrock in Vermont and New Hampshire.

Lens or Lensed – Small pockets of dissimilar soil scattered throughout the mass of a clay.

Load increment ratio (LIR) – Variable used to quantify the change in load to a test specimen. Defined as the ratio of the change in stress to the current stress. A load increment ratio of unity indicates that the load was doubled.

Loam – Low plasticity sandy silt or silty sand mixed with organic matter that is well suited to tilling. Mainly applies to the uppermost soil layer and should not be used to describe deep deposits of parent materials. Major soil type in the USDA system. Not

considered a USCS soil type in conventional geotechnical engineering (ASTM D2487 and D2488).

Loess – A wind deposited, calcareous, unstratified deposit of silts or sandy or clayey silt traversed by a network of vertical tubes formed by the decay of root fibers. Loess slopes have the ability to withstand vertical cuts.

Lugeon – Flow of one liter of water per meter per minute under a pressure of 10 bars (145 psi) in a constant head double packer test.

Marine soils – Material transported and deposited by ocean waves and currents in shore, near shore, and offshore areas.

Marl – Calcium carbonate or lime-rich sedimentary rock. It is mainly composed of a mixture of sand, silt, and/or clay. Marls are often light to dark gray or greenish in color and sometimes contain colloidal organic matter.

Matric suction – Difference between pore air pressure minus pore water pressure. Often used in the characterization of partially saturated soils.

Maximum past pressure – See Preconsolidation pressure.

Metamorphic rocks – Rocks transformation by heat, pressure, or both. This transformation can alter the physical and chemical properties of the rock.

Minimally disturbed sample – See undisturbed sample.

Modified compression index – Parameter which quantifies the compressibility of normally consolidated soil in one-dimensional compression. Normally, it is the log-linear slope of the compression curve defined by axial (y-axis) and the logarithm of vertical effective stress (x-axis).

Modified recompression index – Parameter which quantifies the compressibility of overconsolidated soil in one-dimensional compression. Normally, it is the log-linear slope of the compression curve defined by axial (y-axis) and the logarithm of vertical effective stress (x-axis). Normally obtained by a rebound-reload loop in a consolidation test. Also called the modified swelling index.

Montmorillonite – A group of very small clay minerals with extreme swelling and shrinking properties. Normally results from volcanic or hydrothermal activities.

Mucks – Peat deposits which have advanced in decomposition to such extent that the botanical character is no longer evident.

Muskeg – North American term for peat. According to Sowers (1979), the bogs in which the peat forms are often called *muskegs*.

Nominally disturbed sample – See Undisturbed sample.

Normal consolidation or normally consolidated – Condition of a soil where the current effective stress is the maximum effective stress ever realized, and all excess pore pressures have been dissipated.

Nested piezometers – Multiple standpipe piezometers that are installed in a single boring with an impervious seal separating the different measurement zones.

Neutral stress – Synonym for pore water pressure. This is a term that is normally used in older geotechnical literature.

One-dimensional compression test – A compression test, normally a consolidation test, in which the soil specimen is confined laterally and deformation occurs in the same direction as the vertically applied load.

Open standpipe piezometer – Type of standpipe piezometer, similar to an open well, except that the screen extends only across a specific stratum of interest. Seals are installed above and below this zone to only allow water to enter from the stratum of interest.

Open well piezometer – Type of standpipe piezometer with a full-length screen and a surficial seal that is best suited to relatively homogeneous soil profiles. In layered soils, the measured groundwater level will correspond to the layer with the highest total head.

Organic soils – Soil material containing enough organic or vegetable matter as to influence the engineering properties. .

Osmotic pressure – Pressure in a solution that is the product of the molar concentration of the solute solution, the universal gas constant, and the temperature, in degrees Kelvin.

Overconsolidation – The condition that exists if a soil deposit has been fully consolidated under an effective stress greater than the existing effective stress.

Peat – Organic soil derived from decomposing plant material, normally sedimented in an anaerobic environment. Peats are considered to have less than 25% ash (mineral components) per dry weight.

Perched water table – Spatially limited unconfined water table, separated from the main groundwater regime, caused by the presence of a low permeability layer.

Piedmont soils – Alluvial deposits at the foot of hills or mountains; extensive plains or alluvial fans

Piezocone test (CPTu) – Cone penetration test where the pore pressures behind the tip of the cone are measured during penetration.

Piezometer – A device installed for measuring the pressure head of pore water at a specific point within the soil mass.

Pinnacle – Is an individual and isolated column of rock, often associated with karst terrain.

Piping – The movement of soil particles as the result of unbalanced seepage forces produced by percolating water, leading to the development of boils or erosion channels.

Pit run sand and gravel – See bank run.

Plane strain – A strain boundary condition where strains are only allowed in two directions. Plane strain boundary conditions often result in a three-dimensional stress state. Many geotechnical engineering analyses that are performed in two-dimensions assume that plane strain boundary conditions exist in the third dimension.

Plastic equilibrium – The state of stress of a soil mass that has been loaded and deformed to such an extent that its ultimate shearing resistance is mobilized at one or more points. Solutions employing plastic equilibrium assume full mobilization of the soil's shear strength within a soil mass or along a specified failure surface.

Pluff Mud – Colloquial term for a very soft, odorous mud encountered in South Carolina.

Point bar – Alternating deposits of arcuate ridges and swales (lows) formed on the inside or convex bank of river bends. The ridge deposits consist primarily of silt and sand, while swales are often clay filled

Positive cutoff – The provision of a line of tight sheeting or a barrier of impervious material extending downward to an essentially impervious lower boundary to intercept completely the path of subsurface seepage.

Preconsolidation pressure – Maximum effective stress, under conditions of full pore pressure dissipation, that has been applied to a soil in the past. Synonym for maximum past pressure.

Prefabricated vertical drain (PVD) – Plastic strip, normally encased in a filter fabric, that can be inserted into the soil by a mandrill to facilitate the dissipation of excess pore water pressures.

Pressure head – Synonym for piezometric head. Component of total head that is equal to the water pressure divided by the unit weight of water.

Primary consolidation – The time-dependent compression of a soil under the application of a stress that occurs while excess pore pressures dissipate with time.

Pumice – Porous rock associated with lava flows. May be mixed with nonvolcanic sediments.

Pyroclastic soils – Soil-like material ejected from volcanoes and transported by gravity, wind and air.

Radial consolidation – Consolidation of a soil mass where pore water pressures are dissipated laterally or radially. Radial consolidation occurs when the drainage boundary is cylindrical (stone column) or a strip or line (PVD).

Recompression index – Parameter which quantifies the compressibility of overconsolidated soil in one-dimensional compression. Normally, it is the log-linear slope of the compression curve defined by void ratio (y-axis) and the logarithm of vertical effective stress (x-axis). Normally obtained by a rebound-reload loop in a consolidation test. Also called the *swelling index.*

Reconstituted – Soil sample formed for laboratory testing at a given density and water content. This term is mainly used for coarse-grained test specimens.

Recycled concrete aggregate (RCA) – Recycled road or structural concrete. The concrete is usually processed and screened. The processing consists of crushing the concrete into smaller pieces. Any leftover steel is removed using a magnet. This type of material can serve as a replacement for natural stone aggregates.

Recycled or reclaimed asphalt pavement (RAP) – Excavated and processed asphalt concrete from road wearing surface. When properly processed, it consists of high-quality and well-graded aggregates coated by asphalt cement.

Recycled or reclaimed asphalt shingles (RAS) – Recycled shingles that are used as aggregate for hot mix asphalt. Depending on the quality, this can reduce the cost of the new asphalt mix and the amount of fine aggregate used in the mix.

Recycled pavement material (RPM) – Pulverized mixture of asphalt and base course material usually forming a broadly graded material.

Relative density – Parameter used to quantify the density of a soil relative to the loosest and densest states. It is calculated as the ratio of the difference between the maximum void ratio and current void ratio to the difference between the maximum and minimum void ratios.

Remolded – Soil sample mixed to a given water content to achieve a desired consistency. This term is mainly used for fine-grained soils.

Residual shear strength – The lowest drained shear strength of a soil that is achieved by shear displacement along a failure plane until particle alignment is achieved. This term is normally reserved for fine-grained soils. Residual conditions are often associated with slickensides forming on the failure plane.

Residual soil – Material formed by disintegration of underlying parent rock or partially indurated material.

Response to wetting tests – Tests in which the volume change of the soil is measured as the soil is given access to water or if the water content is reduced by drying.

Riprap – Boulder-size material normally place to strengthen structures against scour, wave action, and ice erosion.

Rippability – The characteristic of dense and/or rocky soils that can be excavated by ripping with a rock rake or ripper.

Riverjack – Alluvial cobbles and boulders.

Rock – Natural solid mineral or aggregate of minerals which is normally classified by the way it was formed.

Rock borehole shear test – *In situ* method to measure the strength of relatively weak rock or rock that is easily disturbed upon drilling and coring (e.g., weathered rock, fractured rock, shale, etc.). This test is a modification of the Iowa borehole shear test originally developed for soil.

Rock dirt combination (RDC) – Local term used in the Harrisonburg, VA, area to describe material from a quarry consisting of a mixture of overburden soil and rock.

Rock flour – Fine-grained soil, normally with silt-sized particles, formed by the grinding of bedrock by glaciers or by drilling. Rock flour normally classifies as a nonplastic silt.

Rock mass – A large body containing rock in intact and weathered conditions accompanied by structural discontinuities like fault, joints, etc., which can be interbedded with soil material.

Rock Quality Designation (RQD) – Calculated parameter used to quantify the quality of a rock core. It is equal to the total length of recovered core pieces greater than 4 inches in length divided by the recorded core run.

Rock Mass Rating (RMR) – Rock classification system based on uniaxial compressive strength, RQD, spacing and properties of the joints, and groundwater conditions.

Sagging – Manifestation of differential settlement in a structure that results in concave upward shape.

Sand – Soil particles that pass through a No. 4 (4.75 mm) sieve and are retained on a No. 200 (75 µm) sieve. Sands can be divided into: (1) coarse sands, sand particles that are retained on a No. 10 (2.00 mm) sieve, (2) medium sands, sand particles that pass through a No. 10 (2.00 mm) sieve and are retained on a No. 40 (425 µm) sieve, and (3) fine sands, sand particles that pass through a No. 40 (425 µm) sieve.

Secondary compression – Time dependent settlement of soil at constant effective stress. Normally considered to be a result of particle rearrangement.

Shale – Fine-grained sedimentary rock made of silt and clay particles. Shale usually breaks along planes of weakness and can slake when subjected to wet-dry cycles.

Shape factor – Ratio of the number of flow channels in a flow net to the number of equipotential drops.

Shore deposits – Deposits of sands and/or gravels formed by the transporting, erosion, and sorting action of waves on the shoreline.

Shot rock – Material from a rock quarry that has not been sorted or screened. It includes everything (from fine sand to small boulders) that can be loaded after a quarry blast. It is also a name given to riprap, although riprap is typically sorted and graded.

Sedimentary rocks – Rocks formed by the accumulation and cementation of smaller particles.

Seismic CPT (SCPT) – Cone penetration test where the cone contains a geophone or accelerometer in order to measure the shear wave velocity. A seismic source is applied at the ground surface in the vicinity of the cone hole.

Settlement – Vertical deformation of a foundation element (footing, mat, or pile). Can also be used to describe the compression of a soil layer under an applied change in stress.

Silt – Nonplastic or slightly plastic soil particles passing a No. 200 (75-µm) sieve that exhibit little or no strength when air dried. Silt-sized soils are normally considered to be larger than 0.002 mm. For classification of silty soils, refer to ASTM D2487.

Size-corrected Point Load Strength Index – Strength obtained from a point load test where the data have been corrected for the size of the test specimen.

Smear – Alignment of clay particles along a shear surface that creates a thin layer of low hydraulic conductivity.

Specific surface area – Surface area of soil particles, usually expressed as the area (units of L^2) per gram.

Slickenside – Condition of a shear surface where considerable displacement has taken place. The clay particles align in the direct of shear, and the shear surface is usually polished, glossy, or sometimes striated.

Slickensided clay – Clay that has experienced repeated or accumulated displacement along a fissure or a failure plane causing the surface to be smooth and shiny.

Split Cylinder Test – A test used to determine the tensile strength of rock cores in which the test specimen is loaded diametrically via hardened steel end platens.

Splitting tensile strength – Tensile strength obtained from a split cylinder test.

Staged – Condition where loading or shearing is performed in incremental stages.

Standard Penetration Resistance – The number of blows of a 140-pound hammer, falling 30 inches, required to advance a 2-inch O.D., split barrel sampler 12 inches in a soil mass.

Standard Penetration Test – An *in situ* test that measures resistance to the penetration of a standard, thick-walled drive sampler in an open borehole using a drop hammer. This test proceeds by driving a thick-walled, split-barrel (a.k.a., split spoon) sampler into the ground using incremental blows from a drop hammer. The sampler is driven a total of 18 inches into the ground. The procedure is presented in ASTM D1586.

Standpipe piezometer – Watertight pipe with a screened section installed in a borehole with one or more seal to allow long-term measurement of groundwater levels. The term is used to refer to both open wells and open standpipe piezometers.

Stone – Gravel-size particles manufactured by crushing rock.

Stratified – Earth materials with layers of different material or color of at least ¼ inch in thickness.

Stress path triaxial test – Triaxial test in which both the vertical and horizontal stresses, and possibly the pore water pressure, are varied systematically to follow prescribed loading paths.

Strike – Line representing the linear feature of the intersection of a rock surface with the horizontal plane.

Sugar sand – Local name used for specific types of sands in various places. It is a fine sandy soil in New Jersey. In Kansas, it refers to a type of granular calcite found in Ness and Hodgeman counties. In Florida, it refers to a fine sand that does not hold water or nutrients very well.

Surcharge – Fill or other material used to apply a temporary stress to a compressible soil layer. The fill is removed after a predetermined amount of compression or consolidation has occurred.

Swelling index – See recompression index.

Talus - Deposits created by gradual accumulation of unsorted rock fragments and debris at the base of cliffs or slopes.

Terrace – Relatively narrow, flat-surfaced, river-flanking remnants of floodplain deposits formed by entrenchment of rivers.

Till – See Boulder Clay.

Tilt – Outward rotational displacement of a retaining wall or other structure.

Time curve – See Time-deformation curve.

Time-deformation curve – A plot relating the deformation of a foundation element or laboratory test specimen as a function of time after being subjected to a change in stress.

Tire derived aggregate (TDA) – Lightweight construction material obtained by shredding or chipping scrap tires. The particle size usually ranges from 0.5 inches to 12 inches. TDA has been used in a wide range of projects, including lightweight embankment fill, landslide repair or stabilization, retaining wall backfill, roads, vibration mitigation, among others.

Topsoil – Upper and outermost layer of soil that supports plant life. Usually contains considerable organic matter.

Total stress – At a point in a soil mass, the sum of the net stress across contact points of soil particles (effective stress) plus the pore water pressure at the point.

Trap – Dark-colored, fine-grained, non-granitic intrusive rock. The most common trap rock is basalt, but also includes peridotite, diabase, and gabbro.

Triaxial permeameter – Pressure chamber holding a cylindrical soil test specimen in a flexible membrane used to perform hydraulic conductivity tests. Also called a *flexible wall permeameter*.

Tuff – Soft porous rock composed of consolidated volcanic ash.

Uncorrected Point Load Strength Index – Strength obtained from a point load test that has not been corrected for the size of the test specimen.

Underconsolidation – Condition that exists if a soil deposit is not fully consolidated under the existing overburden pressure and excess hydrostatic pore pressures exist within the material.

Velocity head – One of the three components of total head, equal to the flow velocity squared divided by twice the acceleration of gravity. Flow velocity in earth materials is often slow enough (laminar flow) that the influence of the velocity head can be ignored.

Vertical drains – Drainage conduits, such as stone columns or prefabricated vertical drains, that are used to allow radial dissipation of pore water pressures and accelerate consolidation.

Virgin compression – Compression of a soil at stresses in excess of the preconsolidation pressure or maximum past pressure.

Water Level Indicator - An electrical device used to measure the distance from the ground surface or top of the casing to the top of the water surface in open pipe piezometers. Graduations on the electrical cable are used to measure the depth to the water surface.

Well resistance – Resistance to flow in a prefabricated vertical drain.

Undisturbed Specimen – Soil sample taken with a thin-walled sampler or block sample with special attention given to maintaining the volume, density, soil structure, and water content. Undisturbed is often written in quotes since no soil sample can be truly "undisturbed." Recently, this term has been replaced with the term *intact specimen*.

Varved Silt or Clay – A fine-grained glacial lake deposit with alternating thin layers of silt or fine sand and clay, formed by variations in sedimentation from winter to summer during the year.